Modelling effects of structure in soft natural clays

by

Béatrice Anne Baudet

A dissertation submitted for the

Degree of Doctor of Philosophy

City University, London

Department of Civil Engineering

Geotechnical Engineering Research Centre

May 2001

TABLE OF CONTENTS Page

LIST OF TABLES

LIST OF FIGURES

ACKNOWLEDGEMENTS

I would firstly like to thank Dr Sarah Stallebrass for her trust, help and support throughout these years. She showed me the real meaning of research, and I shall follow her example when supervising research projects myself. I would thank her also for being supportive outside university by being a friend.

I am very grateful to Prof. Sebastiano Rampello and Dr Luigi Callisto for providing data for Pisa clay, Prof. John Atkinson for data for Bothkennar clay, and Dr Matthew Coop for data for Sibari clay. Dr Federica Cotecchia also contributed to my research by giving helpful advice and making results of her research available to me before it was published.

I would also like to thank the Geotechnical Engineering Research Centre for giving me a grant during these three years, and Prof. John Atkinson and Prof. Neil Taylor for their availability and good advice.

I could not express too many thanks to my dear Matthew, who advised me, supported me and had to deal with all the hidden sides of a PhD (anxious evenings, panic crises...). Thank you also for being so trustful and forceful; I would not have achieved my ambition without you.

I would like to thank all those who made the research group so lively and friendly, those who only spent a few months, and those who remained during all these years. In particular, thanks go to Andrew, Pete and Ulrich for sharing the same moments of happiness as well as anxiety. We have developed during these years friendships that are, I hope, inextinguishable.

I am also grateful to Dr Paul Lévêque who, by giving me beautiful books on geology before he died, helped me to decide whether to take on geotechnics or hydraulics at Glasgow. This was the real starting point of my career in geotechnics.

Finally, and not least, I would like to thank my family for being so loving and supportive throughout the years, for their advice in the turning points of my career and for their trust.

DECLARATION

I grant powers of discretion to the University Librarian to allow this dissertation to be copied in whole or in part without further reference to me. This permission covers only single copies made for study purposes, subject to normal conditions of acknowledgement.

ABSTRACT

Geological processes give natural clays a different structure to that of clays that are reconstituted in the laboratory. In soft clays, this structure often breaks down under loading; this is called destructuration. This project aimed to develop a model to predict destructuration in soft natural clays. An understanding of the main characteristics of the behaviour of these clays was detained from data reported in the literature. Existing frameworks that describe the behaviour of these clays were reviewed, and basic concepts proposed to model structured soils.

The Sensitivity framework (Cotecchia & Chandler, 2000) uses sensitivity as a parameter that can represent structure in both volumetric and stress space before significant destructuration takes place. Study of the behaviour of three soft clays with low to medium sensitivities; Sibari, Bothkennar and Pisa clays, demonstrated that sensitivity changes in parallel with destructuration during both volumetric compression and undrained shearing such that there is a single expression that directly relates change in normalised sensitivity to change in damage strain, where the increment of damage strain is the magnitude of the vector of plastic strain increment.

This destructuration law was used to extend an existing model, the Three-surface kinematic hardening (3-SKH) model which was developed by Stallebrass & Taylor (1997) for reconstituted clays. The new model requires only three new parameters to represent structure and its degradation that can each be derived from data from a single isotropic compression test. They are: the initial sensitivity, which represents the initial degree of structure in the natural clay; the ultimate sensitivity, which represents the stable elements of structure in the clay; and the parameter k, which controls the rate of destructuration with plastic strains. The other parameters used are the same as in the 3-SKH model and are derived from data from tests on the corresponding reconstituted clay.

The model was evaluated against data from tests on Bothkennar and Pisa clay. Qualitatively, the model could predict the important features of behaviour observed in these clays. Quantitatively, results of analyses showed that determining initial sensitivity in a consistent way by using the Sensitivity framework leads to predicted values of undrained shear strength within 10 to 20% of the experimental values. Typically destructuration was correctly predicted in analyses simulating volumetric compression, but it was over-predicted by about 15 to 25% in analyses simulating undrained tests. This could be improved in some cases by using an ultimate sensitivity greater than unity in analyses simulating tests on specimens that are likely to have stable elements of structure arising from fabric. Structural anisotropy seemed to influence the behaviour of Pisa clay, and a model including structural anisotropy may improve predictions on such soils. The main limitation of the current research is the difficulty in determining the initial stress state and sensitivity to be used in the analyses; improvement of this should be the prime aim of further work.

LIST OF SYMBOLS

b	variable representing the degree of bonding – Gens & Nova (1993)
b_1	scalar measure of degree of approach of history surface to bounding surface - 3-SKH model (Stallebrass, 1990)
b_1	scalar measure of degree of approach of history surface to sensitivity surface - S3-SKH model
b_2	scalar measure of degree of approach of yield surface to history surface - 3-SKH model (Stallebrass, 1990) and S3-SKH model
b_{1max}	maximum value of b_1
b_{2max}	maximum value of b_2
e	void ratio
e_L	void ratio at the liquid limit
e_0	*in situ* void ratio
e_{100}^*	void ratio obtained from a one-dimensional curve of the reconstituted clay at a value of vertical effective stress equal to 100 kPa – Burland (1990)
e_{1000}^*	void ratio obtained from a one-dimensional curve of the reconstituted clay at a value of vertical effective stress equal to 1000 kPa – Burland (1990)
f	defines a function
h	variable represenbting a measure of damage – Gens & Nova (1993)
h	hardening function - 3-SKH model (Stallebrass, 1990) and S3-SKH model
h_0	hardening function when the current stress state lies on the bounding surface – 3-SKH model (Stallebrass, 1990)
h_0	hardening function when the current stress state lies on the sensitivity surface – S3-SKH model
k	parameter controlling the rate of destructuration with plastic strain – S3-SKH model
k	parameter controlling the rate of destructuration with plastic strain – Rouainia & Muir Wood (2000)
m	stiffness constant defined by Viggiani & Atkinson (1995)
n	stiffness constant defined by Viggiani & Atkinson (1995)
$\mathbf{n_h}$	outward normal to the history surface – S3-SKH model
$\mathbf{n_y}$	outward normal to the yield surface – S3-SKH model
p	mean effective stress – Rouainia & Muir Wood (2000)
p_c	parameter representing the preconsolidation pressure for the reconstituted clay – Tamagnini & D'Elia (1999)
p_e	equivalent pressure: value of p' at the point on the normal compression line of the reconstituted clay at the same specific volume – Rouainia & Muir Wood (2000)
p_l	limiting value of mean effective stress below which deformations are elastic – Tamagnini & D'Elia (1999)
p_m	parameter representing the bond strength of the natural soil – Tamagnini & D'Elia (1999)
p'	mean effective pressure
p_a'	mean effective pressure at the centre of the history surface – 3-SKH model (Stallebrass, 1990) and S3-SKH model
p_b'	mean effective pressure at the centre of the yield surface – 3-SKH model (Stallebrass, 1990) and S3-SKH model
p_c'	preconsolidation pressure: mean effective stress at the intersection (larger value) of the state boundary surface with an elastic wall
p_{cs}'	mean effective stress at critical state
p_e'	equivalent pressure: value of p' at the point on the normal compression line of the reconstituted clay at the same specific volume – Callisto (1996)
p_{iy}'	equivalent pressure: value of p' at the intersection of the isotropic compression curve of the natural clay and an elastic wall

p_k' equivalent pressure: value of p' at the point on the normal compression line of the reconstituted clay at the same specific volume – Allman & Atkinson (1992)

p_{K0NC}' equivalent pressure: value of p' on the one-dimensional compression curve of the natural clay at the same specific volume – Cotecchia & Chandler (2000)

p_{koy}' equivalent pressure: value of p' at the intersection of the one-dimensional compression curve of the natural clay and an elastic wall

p_0' mean effective pressure at the centre of the yield surface – Modified Cam Clay model (Roscoe & Burland, 1968)

p_0' mean effective pressure at the centre of the bounding surface - 3-SKH model (Stallebrass, 1990)

p_0' mean effective pressure at the centre of the sensitivity surface – S3-SKH model

p_r' reference pressure – Viggiani & Atkinson (1995)

p_{SCC}' equivalent pressure: value of p' on the sedimentation compression curve at the same volume – Callisto (1996)

p_β' component of the vector $\underline{\beta}$

p_γ' component of the vector $\underline{\gamma}$

p_e^* equivalent pressure: value of p' at the point on the normal compression line of the reconstituted clay at the same specific volume -

p_{ie}^* equivalent pressure: value of p' at the intersection of the isotropic compression line of the reconstituted clay with an elastic wall

p_{if}^* equivalent pressure: value of p' at the intersection of the line representing the isotropic stable states of the natural clay with an elastic wall

p_{iy}^* equivalent pressure: value of p' on the isotropic compression curve of the reconstituted clay at the same specific volume as the specific volume at the point of isotropic gross yield – Cotecchia & Chandler (2000)

p_{koe}^* equivalent pressure: value of p' on the one-dimensional compression curve of the reconstituted clay at the same specific volume as the specific volume at the point of one-dimensional gross yield – Cotecchia & Chandler (2000)

q deviatoric stress – Rouainia & Muir Wood (2000)

q' deviatoric stress

q_a' deviatoric stress at the centre of the history surface - 3-SKH model (Stallebrass, 1990) and S3-SKH model

q_b' deviatoric stress at the centre of the yield surface - 3-SKH model (Stallebrass, 1990) and S3-SKH model

q_{cs}' deviatoric stress at critical state

q_{peak} deviatoric stress at the apex of the state boundary surface of a natural clay – Cotecchia & Chandler (2000)

q_β' component of the vector $\underline{\beta}$

q_γ' component of the vector $\underline{\gamma}$

q_{peak}^* deviatoric stress at the apex of the state boundary surface of a reconstituted clay – Cotecchia & Chandler (2000)

r ratio of the size of the structure surface to the reference surface - structure model (Rouainia & Muir Wood, 2000; Gajo & Muir Wood, 2001)

r_0 initial degree of structure - Rouainia & Muir Wood (2000)

s parameter representing current sensitivity – S3-SKH model

s_f parameter representing the ultimate sensitivity – S3-SKH model

s_0 parameter representing the initial sensitivity – S3-SKH model

u excess pore water pressure

v specific volume

v_k logarithm of the specific volume on a swelling line of a reconstituted soil when $p' \leftarrows 1$kPa

v_n normalised specific volume defined by Coop & Cotecchia (1995)

w water content

w_c water content

w_P plastic limit

w_L liquid limit

A stiffness constant defined by Viggiani & Atkinson (1995)
A parameter controlling the relative influence of plastic volumetric and shear strain on destructuration in the structure model by Rouainia & Muir Wood (2000)
C_c compression index defined as the gradient of the one-dimensional compression curve of the natural clay in a plot of e against $\log\sigma_v'$
C_c^* compression index defined as the gradient of the one-dimensional compression curve of the reconstituted clay in a plot of e against $\log\sigma_v'$
C_{ur} undrained shear strength of the reconstituted clay – Leroueil *et al.* (1983)
C_u undrained shear strength – Leroueil *et al.* (1983)
CIP isotropically consolidated constant p' test – Lagioia & Nova (1995)
CIU isotropically consolidated undrained test – Lagioia & Nova (1995)
CSL* critical state line of the reconstituted clay
CSL critical state line of the natural soil
G shear modulus
G_e' elastic shear modulus - 3-SKH model (Stallebrass, 1990) and S3-SKH model
G_0 elastic shear modulus - Rampello & Silvestri (1993)
G_{max} elastic shear modulus – Shibuya *et al.* (2000)
H_1, H_2 hardening functions - 3-SKH model (Stallebrass, 1990) and S3-SKH model
I_L liquidity index
I_{LC} liquidity index – Leroueil *et al.* (1983)
I_v void index defined by Burland (1990)
ICL intrinsic compression line representing the states of the normally consolidated reconstituted soil
K' bulk modulus
K_0 coefficient of earth pressure at rest
LI liquidity index
LL liquid limit
LSP length of stress path calculated along a given stress path in q'-p' plane
M critical state friction coefficient
$MI(G)$ Metastability Index – Shibuya *et al.* (2000)
N logarithm of the specific volume of isotropically normally consolidated reconstituted soil when $p' \leftarrows 1$kPa
N_0 logarithm of the specific volume of one-dimensionally normally consolidated reconstituted soil when $p' \leftarrows 1$kPa
NCL* one-dimensional normal compression line of the reconstituted clay
iso-NCL* isotropic compression line of the reconstituted clay
OCR overconsolidation ratio defined as the maximum previous vertical effective stress divided by the current vertical effective stress
PI plasticity index
PL plastic limit
R ratio of the size of the yield surface to the reference surface - structure model (Rouainia & Muir Wood, 2000)
R ratio of the size of the yield surface to the bounding surface - structure model (Gajo & Muir Wood, 2001)
R_0 overconsolidation ratio
S ratio of the size of the yield surface to the history surface - 3-SKH model (Stallebrass, 1990) and S3-SKH model
S_t strength sensitivity defined by Terzaghi (1944)
S_t initial sensitivity in normalised plots
S_{tc} value of sensitivity at the end of creep – (Fig. 3.3.6)
S_u undrained shear strength of the natural soil
S_u^* undrained shear strength of the reconstituted soil
S_σ stress sensitivity defined by Cotecchia & Chandler (2000)

SBS	state boundary surface of a natural clay
SBS*	state boundary surface of a reconstituted clay
SCL	sedimentation compression line, representing in e-logσ_v' or in ln$v$-lnp' the states of the soil in the ground
T	ratio of the size of the history surface to the bounding surface - 3-SKH model (Stallebrass, 1990)
T	ratio of the size of the history surface to the sensitivity surface – S3-SKH model
W	work done during a test, equivalent to the strain energy released by the soil when loaded
Y	gross yield point
Y_3	gross yield point – Smith *et al.* (1992)
YSR	yield stress ratio defined as the vertical effective stress at which the soil yields in one-dimensional compression divided by the current vertical effective stress
β	parameter defining the rotation of the bounding surface of a natural clay – Gajo & Muir Wood (2001)
β	the vector joining the conjugate points on the history and bounding surfaces – 3-SKH model (Stallebrass, 1990)
β	the vector joining the conjugate points on the history and sensitivity surfaces – S3-SKH model
δ	designs a small variation of the parameter
Δ	designs a variation of the parameter
ε	strain
ε_a	axial strain
ε_n	natural strain
ε_r	radial strain
ε_s	shear strain
ε_v	volumetric strain
ε_s^e	elastic shear strain
ε_v^e	elastic volumetric strain
ε_s^p	plastic shear strain
ε_v^p	plastic volumetric strain
ε^p	damage strain
γ	the vector joining the two conjugate points on the yield and history surfaces - 3-SKH model (Stallebrass, 1990) and S3-SKH model
η	stress ratio q'/p'
κ	gradient of a swelling line in ln$v$-lnp' plane
λ	gradient of the normal compression line in ln$v$-lnp' plane
ν	Poisson's ratio
σ	total stress
σ_a	total axial stress
σ_r	total radial stress
σ'	effective stress
σ_a'	axial effective stress
σ_c'	cell pressure
σ_c'	preconsolidation pressure in the oedometer
σ_h'	horizontal effective stress
σ_{ho}'	horizontal effective stress *in situ*
σ_n'	normal effective stress
σ_p'	vertical preconsolidation stress
σ_r'	radial effective stress
σ_v'	vertical effective stress
σ_{vc}'	vertical preconsolidation stress of a natural soil
σ_{vo}'	vertical effective stress *in situ*

σ_{vy}'	vertical effective stress at gross yield for a natural soil
σ_1'	axial effective stress
σ_3'	radial effective stress
σ_e^*	equivalent pressure: value of σ' on the intrinsic compression curve at the same specific volume
σ_{ey}^*	equivalent pressure: value of σ' on the intrinsic compression curve at the same specific volume – Cotecchia & Chandler (2000)
σ_{vc}^*	vertical preconsolidation stress of a reconstituted soil
σ_{vy}^*	vertical effective stress at gross yield for a reconstituted soil
τ	shear stress
ψ	exponent in the hardening modulus - 3-SKH model (Stallebrass, 1990) and S3-SKH model
Φ'	angle of friction
Γ	logarithm of the specific volume of the soil at critical state when $p \leftarrows 1$kPa

CHAPTER 1 INTRODUCTION

1.1 BACKGROUND TO THE PROJECT

In recent years detailed experimental studies of both soft and stiff natural clays have emphasised that soil structure, which is defined in Section 1.5, should be of the same importance as stress state and stress history in a framework for natural clays (Leroueil & Vaughan, 1990; Burland, 1990). Natural structure generally gives extra strength to natural clays, but this structure is often unstable and breaks down under loading, in particular in soft clays. This process is termed destructuration. Destructuration has severe implications for the amount of settlement and for the stability of geotechnical structures built on these soils. It is thus critical to include structure in a model for soft natural clays. This model should be able to predict the behaviour at small strains, up to 1%, that defines the strength and stiffness of the natural soil, the onset of destructuration and the reduction in strength when reaching large strains. A number of numerical models based on the critical state theory exist that can successfully predict the behaviour of reconstituted clays. These models include advanced features of behaviour such as stiffness non-linearity, stress-induced anisotropy and/or the effect of recent stress history. A model for soft natural clays would need to include these features as well as structure.

1.2 AIMS & OBJECTIVES

1.2.1 Aims

The aims of this project are;

To determine whether a single parameter can be used to represent structure and its degradation under loading.

To establish what controls the degradation of structure and hence derive an expression to describe this process which uses few parameters that each can be derived from standard laboratory tests.

To evaluate whether a model including structure and degradation of structure is sufficient to predict the destructuration of these clays.

1.2.2 Objectives

The aims listed above are achieved by;

1. Showing that sensitivity is a good parameter to represent structure, based on the Sensitivity framework proposed by Cotecchia & Chandler (2000)
2. Developing an expression to describe structure degradation under shearing and compression, drained or undrained, which uses only three parameters, including sensitivity, that are all soil properties and can be derived from a single isotropic compression test.
3. Using this destructuration law to extend an existing model, the Three-surface kinematic hardening (3-SKH) model, which was developed by Stallebrass & Taylor (1997) for reconstituted and stable stiff clays i.e. stiff clays with stable forms of structure.
4. Carrying out a parametric study to validate the model and demonstrate its potential to reproduce the observed behaviour of soft natural clays described in the literature.
5. Comparing the predicted response from the new model to triaxial test data available from the literature.
6. Assessing whether the pattern of stress-strain response predicted by the model is qualitatively similar to that observed in drained and undrained tests on soft natural clays and described in Sections 2.3 and 2.4.
7. Assessing the ability of the model to predict with sufficient accuracy the undrained shear strength of the soil using parameters to control the destructuration that are derived from volumetric compression data only. In undrained compression tests, it is expected that during the experiments localisation phenomena occurred in the specimens after reaching peak strength. The comparison between the amount of destructuration predicted by the model and computed from test data will therefore be more complex, as is explained in Section 1.3.3.

1.3 BASIC METHODOLOGY

This section describes the methodology that has been chosen to achieve the objectives listed above. The effects of sample disturbance and localisation are also discussed in view of the necessity to compare predicted and experimental data in order to evaluate the new model.

1.3.1 Methodology

The aims outlined above require the development and evaluation of a simple constitutive model to simulate the breakdown of structure in soft natural clays. Ideally, this model should be comparatively easy to use but still should significantly improve predictions of the behaviour of soft natural clays.

Much work has already been published on soft natural clays, and therefore during this project existing data will be used as much as possible. In particular, several frameworks have been proposed in recent years to describe the behaviour of structured natural clays (Leroueil &

Vaughan, 1990; Burland, 1990; Kavvadas & Anagnostopoulos, 1998; Cotecchia & Chandler. 2000). These frameworks will be reviewed and compared, bearing in mind the aim of identifying a single parameter to quantify structure. The Sensitivity framework (Cotecchia & Chandler, 2000), which proposes sensitivity as a parameter to represent structure in both volumetric and stress space, will be applied to the behaviour of three soft natural clays; Sibari, Bothkennar and Pisa clays. Experimental data for these clays were available from the literature (Coop & Cotecchia, 1995; Allman, 1992; Smith, 1992; Callisto, 1996; Rampello *et al.*, 1996). The three clays, which have low to medium sensitivities, each have different types of structure: Sibari has a stable structure under loading, while Bothkennar and Pisa clays have unstable structures. They therefore should display a range of behaviour typical of clays that have low to medium sensitivities.

A destructuration law will be derived from observations of experimental results on Bothkennar and Pisa clays. This law will be used to extend an existing model, the Three-surface kinematic hardening (3-SKH) model, which was initially developed by Stallebrass (1990) for reconstituted clays and stable stiff clays. The new model will be developed following basic concepts that were originally proposed by Gens & Nova (1993) to model bonded soils, and were later applied to the development of a number of constitutive models for these soils (Gajo & Muir Wood, 2001; Kavvadas & Amorosi, 2000; Rouainia & Muir Wood, 2000; Tamagnini & d'Elia, 1999).

Model predictions will be compared to experimental results obtained from a range of tests that were performed on natural Bothkennar clay by Smith (1992) and Allman (1992), and on natural Pisa clay by Callisto (1996) and Rampello *et al.* (1996). This comparison requires the consideration of two factors that may affect results obtained in the laboratory. Firstly, disturbance is likely to have occurred in the soft clay samples during sampling, transportation, storage, preparation and installation in the apparatus. Secondly, localisation may have taken place in the specimens during the tests, leading to erroneous measurements of strain during these tests. The possible effects of sample disturbance and localisation on the measured behaviour of the samples are described below.

1.3.2 Sample disturbance

The process of sampling usually involves removing a block of soil from the ground, storing it, transporting it to the laboratory, trimming a test specimen and installing the specimen in the apparatus. This process causes the structure in soft clays to change, which is called disturbance. Interpretation of laboratory tests requires an assessment to be made of the effects of disturbance prior to testing. These effects include both a reduction of the mean effective stress in the sample

and of the apparent preconsolidation pressure. In the laboratory, disturbance then affects the behaviour in different ways, depending on the type of test that is undertaken.

In Chapter 3 the behaviour of three soft natural clays, Bothkennar, Pisa and Sibari clay, will be examined. Bothkennar clay was sampled using the piston, Laval and Sherbrooke methods. Pisa clay was sampled using the Laval method (1993 tests) and Sibari clay was sampled using the Osterberg piston sampler. Hight *et al.* (1992b) carried out a comparative study of the different methods of sampling the Bothkennar soft clay. They found that the Sherbrooke sampler produced slightly higher quality samples than the Laval sampler, although there was no difference in the small strain characteristics of soil sampled using the two methods. Both the Sherbrooke and the Laval samplers produced samples superior to those from displacement piston sampling. However even with Sherbrooke and Laval samplers some disturbance occurred, causing a reduction of the mean effective stress and of the preconsolidation pressure. After sampling, transportation from the site was accompanied by further reduction of the mean effective stress. Specimen preparation methods also caused additional disturbance, with reduction of the mean effective stress and of the apparent preconsolidation pressure.

The way in which sampling affects observed behaviour varies with the type of laboratory test. To estimate the undrained shear strength of a clay in the field the specimen of clay tested in the laboratory should have the same water content and the same mean effective stress that exist *in situ*. If the sample has been destructured during sampling, it is usually not possible to duplicate both conditions in the laboratory. Two approaches are then possible: (1) to keep the water content of the laboratory specimen equal to that desired and carry out an unconsolidated undrained test, or (2) to make the effective stresses in the laboratory specimen equal to those desired and run a consolidated undrained test. The strengths measured by the two tests are usually different. In unconsolidated undrained tests, both the effects of the reduction of the mean effective stress and of the apparent preconsolidation pressure are apparent. In consolidated tests, only the effects of the reduction in apparent preconsolidation pressure are evident. Reconsolidation to the estimated *in situ* stress does not generally seem to cause significant additional disturbance (Hight *et al.*, 1992b).

As a result, it will be difficult to estimate the *in situ* state of the clay, that is its apparent preconsolidation pressure and void ratio, and its degree of structure in the ground. This has implications for modelling soft natural clays, in particular if boundary value problems have to be simulated. This problem will be discussed in Sections 4.4.2 and 5.4.2.

1.3.3 Localisation

Comparisons between data obtained from numerical analyses and from laboratory tests must be carried out with caution. Often specimens in the laboratory are subjected to non-uniform stresses and strains during testing, due for example to end restraint or bedding. The formation of shear planes, common in overconsolidated specimens of clay, causes localised strain-softening in the specimen and measurements of axial strain, local or overall, will be erroneous even when the gauges happen to be located across the shear band. In the following the formation of shear planes in soft clays is discussed.

Burland (1990) has shown, using data from triaxial compression tests on stiff Todi clay, that the formation of the failure plane coincides with peak strength. After peak, the curve of deviator force versus overall axial strain falls steeply to a well defined plateau (see Figure 1.3.1). The excess pore pressure changes stop suddenly, shortly after the peak strength is reached. Prior to the peak strength, the local strains are less than the overall strains. After the peak strength is reached the local axial strains decrease as a result of the unloading process since neither of the gauges was located across the developing shear plane. The post-rupture deformation consists of near-rigid body sliding on the failure plane with very slight axial extension in the surrounding clay. Atkinson (2000) associated the formation of shear planes with local drainage. He found that the soil in these planes dilated and weakened. He also showed that the effect of shear bands in undrained tests is to lower the peak strength (path CDE in Figure 1.3.2).

Leroueil *et al.* (1990) noted that a normally consolidated specimen undergoing triaxial compression generally deforms in the shape of a barrel; that the strains are relatively homogeneous and the concepts of critical states can be applied. Smith (1992), who performed tests on three soft clays, reported that pure slip plane failures are rare for these soils, and that the formation of any slip plane is usually accompanied by some bulging as well, or necking in extension. However, Burland (1990) reported that the formation of rupture planes was observed during tests carried out at Imperial College on normally consolidated specimens of kaolin. There is further evidence from triaxial compression tests performed on Leda clay, a soft clay from Canada, that normally consolidated clays develop localised planes when sheared (Mitchell, 1970). Mitchell carried out a series of undrained compression tests on Leda clay, and compared the modes of failure and stress-strain behaviour observed. The tests are summarised in Table 1.3.1. It is obvious from these data that strain-softening of the clay is associated with the formation of shear planes, but when little or no softening occurs, the specimen bulges. More recently, a study of the behaviour of normally consolidated Bothkennar clay showed that some shear planes had developed in the Sherbrooke specimens (Hight *et al.*, 1992b). Ramanatha Iyer (1975) also observed the formation of failure planes in Drammen clay, a sensitive clay from

Norway. However, it is not certain to what extent the strain-softening observed in soft natural clays is always associated with the formation of shear planes. One effect of the formation of shear planes is that the true strains are always significantly under-estimated since post-rupture strains are concentrated in the shear zone. As a result, assuming the stresses are calculated correctly, stress-strain curves may show a steep reduction in deviatoric stress with shear strain, which in reality may not be so steep (see Figure 1.3.3). In this dissertation it will be assumed that the post-peak effect of localisation on the behaviour of soft natural clays is less than on the post-peak behaviour of stiff clays, so that the amount of destructuration observed in laboratory tests can be measured reliably.

1.4 THEORETICAL FRAMEWORK

The new model proposed in this dissertation is extended from an existing model developed for reconstituted and stable stiff clays, the 3-SKH model (Stallebrass & Taylor, 1997). The 3-SKH model is an elasto-plastic kinematic hardening model developed as an extension of the Modified Cam Clay model within the framework of Critical State soil mechanics. The usual method of characterising structure is to establish similarities and differences between the behaviour of natural and reconstituted clays (Leroueil & Vaughan, 1990; Burland, 1990; Cotecchia & Chandler, 2000). To highlight the similarities between natural and reconstituted behaviour, the description and analysis of the predicted and experimental data will be based on the theory of Critical State soil mechanics of which the principal assumptions are given in Section 1.4.2. In addition, a number of methods have been proposed to normalise the behaviour of natural soils so that the effect of structure is highlighted (Burland, 1990; Coop & Cotecchia, 1995). These methods are reviewed in Section 1.4.3.

1.4.1 Interpretation of data

The experimental data taken from the literature and used in this dissertation are mostly data from triaxial tests. The numerical model presented in this dissertation is therefore confined to the triaxial plane. The state of the soil is described by the stress invariants, p' and q', and the specific volume v (Schofield & Wroth, 1968). The stress parameters are defined as;

$$p' = \frac{\sigma'_a + 2\sigma'_r}{3} \tag{1.4.1}$$

$$q' = \sigma'_a - \sigma'_r \tag{1.4.2}$$

where σ_a' and σ_r' are the axial and radial effective stresses.

The specific volume v is the volume in space occupied by unit volume of soil grains. The corresponding parameters for volumetric strain, ε_v, and shear strain, ε_r, are;

$$\varepsilon_v = \varepsilon_a + 2\varepsilon_r \tag{1.4.3}$$

$$\varepsilon_s = \frac{2}{3}(\varepsilon_a - \varepsilon_r) \tag{1.4.4}$$

where ε_a and ε_r are the axial and radial strains. The volumetric and shear strains in the experiments will be calculated as natural strains, which are more appropriate to compare with the strains computed in the analyses which always use current dimensions. The expression relating natural strains, ε_n, to ordinary strains, ε, is;

$$\varepsilon_n = -\ln(1-\varepsilon) \tag{1.4.5}$$

1.4.2 Critical State soil mechanics

This section reviews the behaviour of reconstituted clays in the context of the Critical State soil mechanics. The main assumptions used in this dissertation concerning the behaviour of reconstituted clays are listed below;

- The state of the soil, described by the parameters p', q' and v (Schofield & Wroth, 1968), always lies within or on a unique state boundary surface.
- In the ln$v$-lnp' plane (Butterfield, 1979), the locus of isotropically consolidated states for reconstituted clays, which is called here the isotropic intrinsic compression line, is assumed to be a straight line of the form;

  $$\ln v = N - \lambda \ln p' \tag{1.4.6}$$

  where N is the natural logarithm of the specific volume on the isotropic compression line at $p' \fallingdotseq 1$kPa (see Figure 1.4.1). A swelling line passing through the point (p', v) is described by the equation;

  $$\ln v = v_k - \kappa \ln p' \tag{1.4.7}$$

  where v_k is the natural logarithm of the specific volume on the swelling line at $p' \fallingdotseq 1$kPa.
- All soils ultimately reach a critical state, defined by Schofield & Wroth (1968) as a unique state of constant volume and effective stress. For a given specific volume the critical state

occurs at a unique stress, and the locus of critical states in ln$v$-q'-p' space coincides with lines with equations;

$$q' = \pm Mp' \tag{1.4.8}$$

$$\ln v = \Gamma - \lambda \ln p' \tag{1.4.9}$$

where Γ is the natural logarithm of the specific volume on the critical state line at $p' = 1$kPa. Schofield and Wroth (1968) described the critical state as "flow of the soil like a frictional fluid", with the energy dissipated as friction. The gradient of the critical state line in q'-p' plane, M, is a simple constant modelling frictional behaviour at the macroscopic scale. It defines the deviator stress, q_{cs}', needed to keep the soil flowing at the critical state for a given mean effective stress, p_{cs}'.

- The region extending from a swelling line to the state boundary surface is defined as an elastic wall. In the theory of Critical State soil mechanics, the response of the soil on an elastic wall is considered to be purely elastic, and after reaching the state boundary surface to be a less stiff combination of elastic and plastic behaviour. In the Modified Cam Clay model (Roscoe & Burland, 1968), the projection of the state boundary surface on an elastic wall is elliptical (see Figure 1.4.2), with equation;

$$\left(p' - p'_0\right)^2 + \frac{q'^2}{M^2} = p'_0{}^2 \tag{1.4.10}$$

where p'_0 is the centre of the yield locus. The flow rule is then expressed as;

$$\frac{\delta\varepsilon_v^p}{\delta\varepsilon_s^p} = \frac{2M}{M^2 - \eta^2} \tag{1.4.11}$$

where $\delta\varepsilon_v^p$ and $\delta\varepsilon_s^p$ are increments in plastic volumetric and shear strain respectively, and η is a stress ratio equal to q'/p'.

1.4.3 Normalisation

The state of a soil is usually described by stress, volume and stress history, and when the soil is natural, also by structure. The process of normalisation brings more consistency to data from a given soil. Discrepancies between data from a given soil may be due to differences in preconsolidation pressures with depth, in composition or in structure. By taking account of these factors the main features of behaviour of the soil can be highlighted. The methods described below explain how to normalise with respect to these three factors.

The first normalisation takes account of the different depths of soil samples leading to different preconsolidation pressures, and was originally proposed by Parry (1960) for reconstituted clays. The state boundary surface of a reconstituted soil is unique, defined in this case in q'-p'-v space, and delimits the space for all possible states. The projection of the state boundary surface on an elastic wall is called the bounding surface, and is usually plotted in the q'-p' plane. At different depths the stress state of the soil lies on different elastic walls corresponding to different void ratios and different preconsolidation pressures, that is different sizes of bounding surface. By dividing the deviatoric stress, q', and mean effective stress, p', by the equivalent preconsolidation pressure p_e^* shown in Figure 1.4.3, the effect of volume is accounted for. In the normalised plane q'/p^*_e-p'/p^*_e all the bounding surfaces define a unique surface, the state boundary surface. This first method of normalisation has some variants, as the equivalent pressure can be calculated in different ways. In this dissertation, rather than using an equivalent pressure at the current volume as in Figure 1.4.3, the equivalent pressure p^*_{ie} will refer to the mean effective stress at the intersection of an elastic wall and the intrinsic isotropic compression line shown in Figure 1.4.4. This makes it possible to compare sizes of state boundary surfaces directly in the normalised stress space.

The second normalisation takes account of composition (unit weight, grading, Atterberg limits). It was proposed by Burland (1990), following the method described by Skempton (1970) which used the liquidity index. Burland defined the void index, I_v, a normalised void ratio, as;

$$I_v = \frac{e - e^*_{100}}{e^*_{100} - e^*_{1000}} \qquad (1.4.11)$$

where e^*_{100} and e^*_{1000} are the void ratios obtained from a one-dimensional compression curve for the reconstituted clay in the e-lnσ'_v plane at values of mean effective stress equal to 100kPa and 1,000kPa respectively (Figure 1.4.5). In the normalised I_v-lnσ'_v plane, the one-dimensional compression curves of all reconstituted clays plot on a unique line, the intrinsic compression line. Figure 1.4.6 shows one-dimensional compression curves obtained from tests on natural samples from the Upper clay (sub-layer B1) underneath the Tower of Pisa, plotted in the I_v-lnσ'_v plane. The compression curves plot to the right of the intrinsic compression line, showing the difference in structure between natural and reconstituted clays. The sedimentation compression line (SCL) was defined by Burland to represent the state in the ground for clays of medium sensitivity (4-6). Burland showed that for a range of clays, with liquid limits between 25% for Lower Cromer Till to 136% for Whangamarino clay, there is a direct relationship between the void ratio at the liquid limit, e_L, and the intrinsic constants of compressibility e^*_{100} and $C^*_c = \left(e^*_{100} - e^*_{1000}\right)$, as is illustrated in Figure 1.4.7. Coop & Cotecchia (1995) have

demonstrated using data from Sibari clay that this relationship is not valid for all clays, and therefore it should be determined specifically for a given site.

This normalisation I_v-lnσ'_v was proposed by Burland on the basis of oedometer test data. Coop & Cotecchia (1995) identified some disadvantages in this method. A particular problem is that soils with different values of K_0 cannot be compared rigorously as the vertical effective stress σ'_v is not an invariant. They presented a redefinition of this type of normalisation which uses compression data in the ln$v$-lnp' plane after Butterfield (1979). The parameter v_n was defined, as;

$$v_n = \exp\left(\frac{\ln(v) - N_0}{\lambda}\right) \tag{1.4.12}$$

where λ is the slope of the one-dimensional line in the ln$v$-lnp' plane and N_0 is the natural logarithm of the specific volume on the one-dimensional compression line at $p' \leftrightharpoons 1$kPa, both defined by the reconstituted soil. In the lnv_n-lnp' plane, the one-dimensional compression curves of all reconstituted clays again plot on a unique intrinsic compression line. The main advantage to this new normalisation is that isotropic normal compression curves can also be plotted on this graph. They form a unique line for the reconstituted clays that we will call the isotropic intrinsic compression line. Figure 1.4.8a shows one-dimensional compression curves obtained from tests on reconstituted and natural Sibari clay samples that were retrieved from different depths, in the e-lnσ_v' plane. The compression curves of both reconstituted and natural samples all plot at different locations in the volumetric space. Figures 1.4.8b and 1.4.8c show these curves after normalising for composition, in the lnv_n-lnp' plane. The values of λ and N_0 used by Coop & Cotecchia for the natural samples were derived from test data on the corresponding reconstituted samples. The compression curves of the reconstituted samples plot on the intrinsic compression line. The compression curves of the natural samples plot to the right of the intrinsic compression line, highlighting the differences between natural and reconstituted structure.

This third method of normalising will be used in the dissertation. For the natural samples of Bothkennar clay the corresponding samples of reconstituted clay were not available, hence for this soil a relationship between the void ratio at liquid limit, e_L, and the parameters λ, N_0, and N has been investigated. Figure 1.4.9 shows values of the compression parameters λ and N_0 for reconstituted Sibari and Bothkennar clays, plotted against the void ratio at liquid limit e_L. The data points for Sibari clay plot on a straight line, demonstrating that there is a linear relationship between e_L and λ, and e_L and N_0. One-dimensional compression test data from reconstituted Bothkennar clay samples were available for only two different depths. Following Coop & Cotecchia (1995), it was assumed that the relationship between e_L and λ, and e_L and N_0 is linear and site specific, thus a straight line was drawn between the two points obtained as shown in

Figure 1.4.9. Empirical equations were derived from these lines which were used to compute the values of λ and N_0 for other depths corresponding to different values of liquid limit. For the natural samples of Pisa clay, the corresponding reconstituted samples were available and the values of λ and N_0 could be derived directly from volumetric compression test data. The values of N were calculated assuming a constant ratio between the preconsolidation pressure on the one-dimensional and one the isotropic compression lines.

A method of normalising for structure in stress space has been proposed by Cotecchia & Chandler (2000) and will be described in Section 2.3.5.

1.5 TERMINOLOGY

Different vocabulary has been used in the literature to describe clays and some aspects of their behaviour. This section aims to clarify the terminology used in this dissertation.

1.5.1 Soft clays

The generic term "soft clay" is used to describe normally consolidated or lightly apparent overconsolidated soil with a low undrained shear strength (S_u < 50kPa). The clays examined here mainly fit these characteristics, but some soft natural clays have an overconsolidation ratio of up to 4, for example when they have been subjected to thixotropic hardening, or they have an undrained shear strength slightly higher than 50kPa.

1.5.2 Remoulded, reconstituted, intrinsic, destructured, structure-less, unbonded

Many advances in soil mechanics have stemmed from carefully controlled laboratory tests. These tests had as their objective a better understanding of the behaviour of the soil during one-dimensional or isotropic compression, and drained or undrained shearing. In order to create homogeneity between the responses of the different samples tested, the soil was often reworked at water contents below the liquid limit. This is the process of "remoulding". It was recognised more recently that this procedure was not rigorous enough to ensure a consistent comparison between the responses of the samples and to draw conclusions from them. Burland (1990) suggested a standardised procedure, which consists of mixing the clay thoroughly at a water content equal to or greater than the liquid limit (1.25 w_L) without previously air drying or oven drying. The clay is then consolidated, preferably under one-dimensional conditions. He called a soil that has followed this procedure "reconstituted", and he called its properties "intrinsic" properties, as they refer to the inherent properties of the soil that are independent of its natural state. Fearon & Coop (2000) showed that soils that have been reconstituted using high- energy

methods, such as mincing may have different characteristics to those created following the method proposed by Burland,. They suggested that the meaning of the term "intrinsic" suggested by Burland may need to be reviewed as the intrinsic behaviour seems to be highly dependent on the method used. Kavvadas & Anagnostopoulos (1998) differentiated between destructured and reconstituted or remoulded, arguing that when a soil is reconstituted it does not necessarily reach its intrinsic properties. They qualified this state of the soil as "destructured", as opposed to "structured" for the natural soil. The adjectives "structure-less" and "unbonded" are sometimes used to refer to the clay in which all the structure has been removed (Gens & Nova, 1993; Rouainia & Muir Wood, 2000). However these adjectives have been criticised by researchers who state that structure is present even in reconstituted clays (Cotecchia & Chandler, 2000).

In the following, the term "reconstituted" will be used to describe clays that have been reworked in the laboratory, except in the legends of some figures from the literature where the authors have used the term "destructured". The term "intrinsic" will apply to any feature of a reconstituted soil, and an asterisk will be used to denote an intrinsic property (for example NCL^* for the intrinsic normal compression line).

1.5.3 Natural, intact, undisturbed, structured

In the literature, a variety of terms is used to describe the *in situ* state of the clay. Authors usually use the adjectives "natural", "intact", "undisturbed" or "structured" to describe the clay in the ground or after it has been sampled using a high quality sampler such as the Laval or Sherbrooke methods. In the following, a clay *in situ* or having been retrieved from the ground with a very high quality sampler will be described as "natural", as opposed to "reconstituted", except in the legend of figures from the literature where the authors have sometimes used a different terminology.

1.5.4 Structure

Structure has been defined as the arrangement of particles in the clay, termed *fabric*, and the resistance of this fabric to alteration by physical, chemical, or electrical means, termed *bonding* (Lambe & Whitman, 1969). It is assumed in this dissertation that fabric is a stable element of structure that cannot be removed under loading or in some cases even by reconstitution. Bonding is considered to be the unstable element of structure, which can break down under loading. The effects of fabric and bonding are combined in most clays, but typically in soft natural clays the effect of bonding dominates the behaviour, which makes these clays unstable. The development of fabric and bonding is dependent on the physico-chemical environment such

as chemistry, pressure, temperature, organic content, and on the mechanical boundaries such as the consolidation strain path and the deposition and consolidation rate (Mitchell, 1982). A classification of the different types of structure will be reported in Section 2.2.1. The definitions of structure given above (Lambe & Whitman, 1969; Mitchell, 1982) make it clear that structure may also exist in reconstituted material. In general, the structure is different in natural and reconstituted soils, and it is this difference that is responsible for the differences observed in their behaviour.

1.5.5 Yield, gross yield and destructuration

"Yield" strictly marks the limit of recoverable deformation. However in most tests the true yield is not identified and only a significant change in the stress-strain response can be detected at larger strains. This is referred to as "gross yield" (Hight *et al.*, 1992; Cotecchia & Chandler, 2000). In this work, gross yield is defined as the point where the stress state reaches a limit state curve. Reconstituted clays reach gross yield on the state boundary surface. In structured natural clays, gross yield is associated with a disruption of structure, otherwise called "destructuration", and the gross yield locus is regarded as a domain separating stress states which do not significantly alter the structure from those which cause destructuration. Post-gross yield deformation is a consequence of both the breaking of the inter-particle bonds, and the irreversible re-arrangement of the particles even if the underline fabric is not significantly altered. While gross yield is a macroscopically observed phenomenon characterised by a marked change in stiffness, the destructuration occurring at the particle scale can be observed to some extent by using scanning electron microscopy (S.E.M.) or examining porosimetry (e.g. Delage and Lefebvre, 1984).

In the following, the term "gross yield" will be used to define the point where the soil stress reaches the limit state curve, which corresponds to the locus of normally consolidated states for reconstituted clays, and to the locus marking the start of significant destructuration for natural clays. "Destructuration", which starts at "yield" with the onset of plastic deformation and becomes significant at gross yield, will describe the breakage of bonds and the progressive rearrangement of the particles under loading.

CHAPTER 2 LITERATURE REVIEW

2.1 INTRODUCTION

This chapter describes the effects of structure on the behaviour of soft natural clays. These effects have been identified both in compression and shearing tests, drained and undrained. Since different loading and drainage paths involve different mechanisms, until now structure has been quantified using different methods for volumetric compression and shearing of soils. In order to be used in a constitutive model, a parameter representing structure must be valid for all stress paths. Thus the following review is carried out with an underlying aim, which is to find and evaluate an appropriate parameter to quantify structure that can subsequently be used in constitutive equations.

The effects of structure on the behaviour of natural soils have been widely investigated and are reported in the literature. In particular, natural soils have been examined in terms of similarities and differences to reconstituted soils, and a number of research programmes have aimed to bring coherence to the description of the many aspects of their behaviour, which has caused several frameworks to be proposed (Leroueil & Vaughan, 1990; Burland, 1990; Cotecchia & Chandler, 2000). This approach is most critical for constitutive modelling as it results in a basis for extending an existing model developed for reconstituted clays to predict the behaviour of natural clays.

In the following, Sections 2.2 to 2.4 examine the different types of structure reported in the literature, their effects on the behaviour of soft natural clays, and the processes involved in destructuration. Then Section 2.5 reviews the existing frameworks for natural structured soils and investigates how they apply to soft natural clays, with particular emphasis on the Sensitivity framework presented by Cotecchia & Chandler (2000). Finally, Section 2.6 evaluates the way structure and destructuration have been modelled in existing constitutive models for natural soils.

2.2 NATURAL STRUCTURE IN SOFT NATURAL CLAYS

One of the difficulties encountered when studying natural clays is the great variability of their structure. The conditions during deposition, such as the salinity of the water, temperature and current, and processes occurring after deposition, such as mechanical unloading caused by erosion or rising of the water level, creep, thixotropy and cementing, all contribute to this variability. Some classifications for structure have been proposed, which mainly distinguish between structure occurring in normally consolidated clays and that occurring in overconsolidated clays. This dissertation concerns the type of structure that occurs in normally

consolidated or soft clays. However all types are reported here since soft clays can be found in apparently overconsolidated states due to thixotropic hardening or ageing.

2.2.1 Classification of structure

Two of the most recent and complete classifications have been proposed by Kavvadas & Anagnostopoulos (1998) and by Cotecchia & Chandler (2000). Their respective approaches present similarities and differences.

Cotecchia & Chandler (2000) give a definition of structure similar to that of Lambe & Whitman (1969), as reported in Section 1.6. Structure is therefore considered as the combination of fabric (the arrangement of the soil component particles) and bonding (inter-particles forces which are not of a purely frictional nature). According to this definition, any clay has a structure, including reconstituted clays. Kavvadas & Anagnostopoulos (1998) define structure differently. They consider that a soil is in a structured state when its properties deviate from the intrinsic (structure-less) properties. According to them a soil is in an "intrinsic" state if it has been reconstituted "recently", that is in the last few hours, so that ageing did not have time to occur. They differentiate between reconstituted and intrinsic states, on the base that reconstituted states correspond to various degrees of destructuration but are not completely structure-less. They also postulate that according to their definition, even recently overconsolidated clays are structured, since overconsolidation causes a deviation from the intrinsic properties. The definition for "intrinsic" given by Kavvadas & Anagnostopoulos is not very practical for use on existing data since it is not possible to check rigorously which data should be considered as intrinsic. Laboratory tests on reconstituted clays are well controlled and repeatable, therefore they should form a reliable basis for comparison. Thus it seems more logical to examine the effects of natural structure by comparing the behaviour of natural clays to that of reconstituted clays. The adjective "intrinsic" should refer to properties of reconstituted clays, independent of the fact that reconstituted clays also have a structure.

The classifications proposed by both sets of researchers take account of geological history. Types of structure can be gathered into two main groups. These types of structure are common to Cotecchia & Chandler and Kavvadas & Anagnostopoulos, and refer to the time when structure developed, that is before or after sedimentation. In addition, Kavvadas & Anagnostopoulos postulated that overconsolidation and leaching also are causes of structure development.

The first type of structure includes all structures that develop during and after deposition solely as a result of one-dimensional consolidation (sedimentation). The soil develops structure before the end of sedimentation, and becomes stiffer due to inter-particle bonds that carry stresses due to loading without a significant reduction in the void ratio. The

compressibility is significantly reduced and, for any increase of the overburden pressure due to the deposition of new sediments, the soil follows an almost horizontal path (FI in Figure 2.2.1) to a final state (I) located above the intrinsic compression line. Cotecchia & Chandler (2000) termed this type of structure *sedimentation* structure, and Kavvadas & Anagnostopoulos (1998) called it *concurrent* structure. *In situ,* normally consolidated clays from deposition follow their *sedimentation compression curve* in a plot of void ratio against vertical effective stress, as originally defined by Terzaghi (1941). For clays with a sedimentation structure the sedimentation compression line is the locus of gross yield points obtained during one-dimensional compression tests performed on samples from different depths in the laboratory. According to Cotecchia & Chandler (2000), the sedimentation compression curves of a natural clay and the same clay reconstituted are offset in volumetric space despite both clays having identical mineralogical composition (Fig. 2.2.2 (a)). The different positions of the curves are the result of the differences in their sedimentation structures. This structure is present only in normally consolidated clays, natural and reconstituted, and can encompass many different fabrics and degrees of bonding. According to Kavvadas & Anagnostopoulos (1998), intrinsic and sedimentation compression lines are only parallel in the e-lnp' plane if the structure developed progressively. In this case, soil elements in deeper elevations acquired a certain amount of structure earlier than soil elements in shallower elevations. As a result the bond strength is larger in deeper strata. If the structure developed through the whole deposit in a relatively short period of time, any further increase in bond strength due to the accumulation of additional sediments has been undertaken similarly by all soil elements. In this case the sedimentation compression line is offset to the right of the intrinsic compression line by a constant amount, equal to the length of (FI) in Figure 2.2.1. In an e-p' plot with a linear stress axis the two lines will be parallel (Fig. 2.2.3 (a)), whereas they will converge in the e-lnp' plane (Fig. 2.2.3 (b)).

The sedimentation or concurrent structure can be modified by some geological processes subsequent to normal consolidation. These processes might be simple geological unloading, for example due to erosion or a rising water table, or, additionally, creep, thixotropy, post-depositional bonding, or more generally diagenesis. Geological unloading is usually referred to as overconsolidation, and the past maximum pressure as the preconsolidation pressure. This type of structure is termed *post-sedimentation* structure (Cotecchia & Chandler, 2000; Kavvadas & Anagnostopoulos, 1998). According to Cotecchia & Chandler (2000), clays with a post-sedimentation structure due only to overconsolidation return to their sedimentation structure when reloaded to their preconsolidation pressure (Fig. 2.2.2 (b)). For clays that have a post-sedimentation structure due to processes other than overconsolidation, gross yield occurs to the right of the sedimentation compression curve (Fig. 2.2.2 (c)). According to Kavvadas & Anagnostopoulos (1998), overconsolidation is in itself a process causing structure development,

because the magnitude of the inter-particle bonding is related to the equivalent stress on the sedimentation compression line and not to the current stress level, and is controlled by the stress history (typically the maximum preconsolidation pressure). This corresponds to stress path OB in Figure 2.2.1, with the final state (B) away from the intrinsic compression line. Therefore they feel that even recently overconsolidated clays have a structure. This is different from the approach followed by Cotecchia & Chandler (2000) who describe the post-sedimentation structure caused by overconsolidation as reversible. They present experimental evidence, using test data on reconstituted Pappadai clay (Cotecchia, 1996), that overconsolidated reconstituted clays reach gross yield on their normal compression line, and that their flow rule is linear, implying that their behaviour is frictional only. Destructuration is generally defined as an irreversible process involving the breaking of inter-particle bonds, therefore the evidence of reversibility of structure in overconsolidated reconstituted clay presented by Cotecchia implies that overconsolidation is not a cause of structure development. However overconsolidation can be a cause of structure degradation, as experimental evidence shows that when natural clays are swelled back to reach high levels of overconsolidation, the slope of the swelling line of the natural clay rises to reach the value of the slope of that of the reconstituted clay. This is called "swell sensitivity" (Schmertmann, 1969) and proves that swelling to a high level of overconsolidation can lead to an irreversible change in structure.

Kavvadas & Anagnostopoulos (1998) postulate that leaching is also a process in the development of structure. Leaching, which changes the composition of the soil such that the liquid limit changes, leads to a reduction in the shear resistance in the reconstituted state (Skempton & Northey, 1952). This also increases the sensitivity, because this has the effect of moving the intrinsic compression line towards lower values of void ratio whereas the current state of the soil is unchanged. In fact, Skempton & Northey (1952) considered leaching to be a cause of the formation of "quick clays", for which the reconstituted strength is so low that they become almost liquid following a slight disturbance. The structure which is referred to here is different from the other types of structure as it does not relate to added bond strength in the natural clay, but to reduced strength in the reconstituted clay. It therefore does not fit in the classification given by Cotecchia & Chandler, but is still worthwhile considering since it causes an increase in sensitivity and is likely to have happened in many soft natural clays.

Despite some major discrepancies, these two classifications have a common aim which is to interpret the position of the *in situ* state of natural soils in volumetric space. From the point of view of modelling, both sets of researchers agree that it is the distance of the yield stress from the intrinsic compression line that controls compression and strength behaviour. The implications for modelling of these two classifications will be examined in Sections 2.5.1 and 2.5.2 where they are used in frameworks to interpret the main features of the behaviour of natural soils.

2.2.2 Stability of structure

Natural structure is either stable, when it does not change under loading, or metastable, when it changes under loading. Clays with a stable structure are those which tend to have a compression behaviour that lies parallel to and above the intrinsic compression line after gross yield, with little tendency to converge. During shearing, the behaviour is predominantly frictional with again little tendency to strain-soften towards the intrinsic critical state line. Clays with a metastable structure are those which show marked convergence of the compression curve with the intrinsic compression line after gross yield, and strain-soften during shearing towards the intrinsic critical state line as the structure breaks down.

Often for soft clays the conditions of deposition of the clay determine the stability of its structure. A clay deposited rapidly has a more densely packed fabric, leading to more stability. A clay deposited more slowly usually has a very open fabric, due to electrical, chemical or physical bonds developed between the clay particles during deposition (Skempton & Northey, 1952). These bonds are usually unstable and break down under loading. However the behaviour of metastable clays can be influenced both by bonding and fabric. In this case the clay becomes stable before reaching the intrinsic state. Experimental evidence of stable structures has been reported in the literature, notably on stiff clays such as Boom clay (Coop *et al.*, 1995), but also on soft clays such as Sibari clay, a soft layered clay from Southern Italy (Coop & Cotecchia, 1995). The behaviour of clays with a stable structure is typical of reconstituted clays but within a larger state boundary surface. Ingram (2000) has demonstrated that the behaviour of these soils can be predicted using classical advanced models for reconstituted soils and the appropriate state boundary surface. A model for soft natural clays should include all aspects of structure, that is the relative effects of fabric and bonding. It will be shown in Section 4.4 that this can be achieved with very few added parameters.

2.3 EFFECTS OF STRUCTURE ON THE BEHAVIOUR OF SOFT CLAYS

2.3.1 State boundary surface and gross yield curve

The most obvious effect of structure is that it allows natural soils to exist at higher void ratios than reconstituted soils under the same effective stress. Leroueil & Vaughan (1990) defined a structure-permitted space for natural soils, delimited in volumetric space by the compression curve of the intact soil and the intrinsic normal compression line (Fig. 2.3.1). Similarly, the natural soil is able to sustain a higher effective stress than the reconstituted soil at the same void ratio. This implies that the natural soil has a state boundary surface larger than that of the reconstituted clay. Tavenas & Leroueil (1985) demonstrated that structure produces an increase

in the size of the normalised gross yield curve, as shown in Figure 2.3.2 for four soft natural clays. One of the processes of structure formation is ageing. Drained "creep", which is characterised by a reduction in specific volume under constant pressure causes an increase in the size of the gross yield surface, but not in the size of the state boundary surface. The relationship between ageing and creep in the literature is ambiguous, although creep is certainly a component of ageing. Because ageing may be associated with the formation of structure, it may also be related to an increase in the size of the state boundary surface. The effects of ageing and creep on the behaviour of reconstituted clays are reported below, and the apparent anisotropy of the gross yield surface of natural clays is examined.

In 1967, Bjerrum was the first to propose a model for the effects of ageing on the behaviour of clays. He suggested that the ageing of a clay under a constant effective stress leads to a reduction of void ratio due to secondary deformation, and that it is possible to define one-dimensional curves for different consolidation times in the oedometer (Fig. 2.3.3a). This was verified by test data from samples of Norwegian Drammen clay consolidated for different times of up to 30 days (Fig. 2.3.3b). Although the different compression curves for different loading rates correspond to different sizes of boundary surface, after creep has occurred the soil state always returns to the same compression line or boundary surface providing the loading rate is the same as that used before.

Ten years later, and supported by data on Champlain clay, Tavenas & Leroueil (1977) have suggested that ageing produces not only an increase in preconsolidation pressure, but also an expansion of the entire gross yield curve (Fig. 2.3.4). Because the investigation of ageing involves such long periods of time, no additional significant data were available in 1990 and Leroueil *et al.* were still using the hypothesis proposed by Bjerrum to describe the effects of ageing on the behaviour of soft natural clays (Figure 2.3.5).

In 1992, Allman & Atkinson investigated the effects of ageing on Bothkennar clay for shorter periods of time. Reconstituted specimens were one-dimensionally compressed to normally consolidated states, and left to rest for periods of up to 200 hours (about 8 days) before shearing at constant mean effective stress. Specimen B49 in Figure 2.3.6a was sheared immediately after drained compression. Specimen B33 was sheared after a period of rest of about 20 hours and specimen B70 after about 200 hours. A fourth specimen B55 was overconsolidated by unloading from a state close to the K_0 normal compression line. They found that even after a period of rest of only 20 hours (B33), the aged specimen behaved like a lightly overconsolidated specimen, with a higher stiffness at the start of shearing as seen from the steeper stress paths (Fig. 2.3.6b). The normalised paths seem to show that in this case there has been no increase in the size of the state boundary surface due to ageing. Jardine (1985) had obtained similar results on reconstituted specimens of Magnus clay left to rest for 20 days (Fig. 2.3.7). In stress space, the effects of ageing can be interpreted as a move to a new elastic wall

(path (OA) in Fig. 2.2.1), thus an increase in the size of the gross yield surface. These data were not normalised and so it cannot be seen if the ageing has influenced the size of the state boundary surface.

Numerous papers have proved that the shape of the gross yield curve, with gross yield defined as in Section 1.6, is affected by structural anisotropy (Tavenas & Leroueil., 1977; Graham & Li, 1985; Smith *et al.*, 1992; Callisto, 1996), for example the gross yield curve of Saint-Alban clay is given in Figure 2.3.8. By normalising the gross yield curve by an equivalent pressure on the normal compression line of the reconstituted clay, researchers showed that the shape of the state boundary surface is also anisotropic (see Figures 2.3.8 to 2.3.11). Structural anisotropy generally results in the shape of the stress-strain curves and undrained stress paths of specimens that have been consolidated anisotropically being different from those for specimens that have been consolidated isotropically. Figures 2.3.12 and 2.3.13 show the isotropic and K_0 compression curves for Saint-Alban clay and Bothkennar clay. Both clays are initially much less stiff in isotropic compression, they have a poorly defined isotropic gross yield, and the isotropic compression curves cross the K_0 compression curves at large strains. Cotecchia & Chandler (2000) attributed this to the fact that sensitive clays possess a structure that is disturbed by the imposition of isotropic stresses on initially anisotropic specimens. They suggested that models for natural soils should take account of structural anisotropy. However the interpretation of the shape of the gross yield curve should be taken with caution. Its apparent anisotropy can be due to stress-induced anisotropy. Numerical models including kinematic hardening for example, while using an isotropic state boundary surface, may still be able to reproduce an anisotropic gross yield curve by simulating the right stress history.

2.3.2 Undrained shear strength

As a consequence of the larger size of the state boundary surface, the undrained shear strength of a natural clay is higher than that of the clay when reconstituted. This difference in strengths is usually quantified by *sensitivity*, S_t, which is defined as;

$$S_t = \frac{S_u}{S_u^*} \tag{2.3.1}$$

where S_u is the undrained shear strength of the natural clay, and S_u^* is the undrained shear strength of the reconstituted clay at the same water content. This quantity was first introduced by Terzaghi (1944), and is the most commonly used measure of natural structure. However it does not take account of destructuration, of which one of the aspects is the reduction in shear strength with plastic strain. As no recent data comparing the response of natural and reconstituted specimens during undrained shearing are available, the effects of structure and

destructuration on the shear strength of clays have been illustrated by Figures 2.3.14 and 2.3.15. It must be noted that, as was explained in Section 1.6, the terminology used in this dissertation is different from that used by some authors. Skempton & Northey (1952) compared the stress-strain curves obtained on natural and reconstituted specimens of Shellhaven clay (referred to as undisturbed and remoulded respectively in Figure 2.3.14). Tavenas & Leroueil (1977) compared the curves obtained during undrained shearing on intact and destructured specimens of three soft clays, where the destructured specimens refer to natural specimens that have been consolidated to stresses beyond gross yield before shearing (see Figure 2.3.15). The curves for the natural specimens show a higher peak deviatoric stress than the destructured specimens. The curves for destructured Saint-Alban and Bäckebol clays are unusual for soft clays as they show peaks. In fact the specimens had been overconsolidated to ratios up to 4 before shearing in order to match the high level of apparent overconsolidation in the natural specimens, due to ageing and thixotropic hardening. The difference between the values of peak strength in the natural and destructured specimen is quantified by sensitivity. After reaching its peak strength, the natural clay strain-softens as destructuration occurs in the specimen. Its shear strength reduces with plastic strain to values as low as the values of shear strength for the reconstituted soil in some cases. This reduction in shear strength occurs in most soft natural clays, thus it is critical that it is simulated in models for such clays. Destructuration will be described in more detail in Section 2.4.

2.3.3 Pre-failure deformation

Another effect of structure is to cause the natural soil to have a higher small strain stiffness than the remoulded soil. Some authors have suggested that these differences in stiffness could be used to quantify structure (Shibuya *et al.*, 2000). Since there are not much data available for soft natural clays, work undertaken on stiff clays is also included in this section as it gives more insight into the different values of shear modulus in natural and reconstituted samples and their implications for modelling.

Shibuya *et al.* (2000) performed a series of laboratory bender element tests on natural and reconstituted specimens from soft Ariake and Bangkok clays. The natural specimens were recovered from a wide range of depths, and re-consolidated to *in situ* stresses before testing. Results of the tests are plotted as liquidity index, I_L, against shear modulus, G_{max}, as shown in Figure 2.3.16. The curve for the reconstituted clay plots as a straight line, β^*-β^*. For a given value of liquidity index, the natural soil has a higher small strain stiffness than the reconstituted soil. Similarly, for a given value of shear modulus, the natural soil has a higher liquidity index than the reconstituted soil. Shibuya *et al.* (2000) established that this difference in liquidity

index quantifies the degree of structure. They termed this difference the Metastability Index, *MI(G)*.

Rampello & Silvestri (1993) obtained similar results by examining the small strain undrained stiffness of stiff overconsolidated Vallericca clay, which behaves like a clay with a stable structure during drained compression to very high stresses so that the compression curves of the natural and reconstituted soils are substantially parallel. They took the comparison further by investigating the dependence of the elastic stiffness (here denoted G_0) on the mean effective stress and the void ratio (Fig. 2.3.17). They plotted values of shear modulus against mean effective stress, normalised firstly by the equivalent pressure on the intrinsic isotropic normal compression line and then also by an equivalent pressure on the appropriate normal compression line for each set of specimens, either natural or reconstituted (Fig. 2.3.18). The latter normalisation accounts for the position of the natural compression curve relative to the reconstituted. Using this normalisation, the stiffness data from the natural Vallericca clay were then found to fall very close to the reconstituted data, showing that the stiffnesses of natural and reconstituted clay are the same when stress and state related to the appropriate state boundary surface are accounted for. Cotecchia (1996) made similar comparisons of stiffness for Pappadai clay, and Coop *et al.* (1995) for Boom clay, both clays having a stable structure.

2.3.4 Critical state

Experimental evidence has shown that in volumetric space a critical state line exists for a natural clay, which is usually different from that of the corresponding reconstituted clay.

Cotecchia (1996) found that for stiff Pappadai clay, failure points plot in the v-lnp' plane on a straight line between the intrinsic and natural isotropic compression lines of the clay. The natural and intrinsic isotropic compression lines are not parallel to each other, but the critical state line proposed for the natural clay plots parallel to the isotropic compression line of the natural clay (Fig. 2.3.19). The spacing between the isotropic compression line and the critical state line is about the same for the natural and for the reconstituted clay.

Smith *et al.* (1992) identified failure points for Bothkennar, reached during drained probe tests, which define a line plotting between the sedimentation compression curve of the natural clay and its intrinsic compression curve (line CC′ in Fig. 2.3.20). Unlike Pappadai clay, the proposed critical state line is neither parallel to the intrinsic nor the sedimentation compression curve. However the authors suggest that none of the specimens quite reached a critical state.

Graham and Li (1985) performed undrained shear tests on natural specimens of Winnipeg clay. They observed that only small reductions in strength occurred after reaching the peak value of deviator stress, and considered these points to be close to critical state. When

plotted in the volumetric plane, these values give a critical state line parallel to the sedimentation compression curve and the intrinsic compression curve, but in between these lines (Fig. 2.3.21). Similarly to the data from Pappadai clay, the spacing between the normal compression and critical state line is the same for the natural and reconstituted clay.

Coop & Cotecchia (1995) investigated the effect of layering on the behaviour of clays using data by Best (1994) who performed a series of laboratory tests on artificially layered soils. Layered specimens were created, which were constituted of one layer of silica sand and one of reconstituted plastic clay, with different proportions of clay to sand. Some mixed specimens were also created with the same proportions of sand and clay, but mixed together, to define the intrinsic behaviour of the soil. The results show that in one-dimensional compression, the layering causes an offset of the compression curve of the layered soil with respect to the intrinsic compression curve, but there is no convergence between them even at large strains (Fig. 2.3.22). Shearing data, drained and undrained, normalised by volume, defined a stable state boundary surface much larger than the intrinsic surface. The specimens also reached a critical state in volumetric space well to the right of the intrinsic critical state line. Therefore both in compression and shearing the layering provided a very stable form of macro-structure and the behaviour of the layered soil was offset volumetrically from the intrinsic behaviour. This simple example of layering indicates that fabric might give rise to stable forms of structure, as will be discussed later.

The effects of a stable structure seen for a layered soil are consistent with the offset of the critical state line for the natural specimens of Pappadai clay with respect to that of the reconstituted clay, but with a constant spacing between normal compression and critical state line. Results from tests on Bothkennar and Winnipeg clay must be reviewed with more caution, as both clays have metastable structures. In particular tests on Winnipeg clay, even if they give results consistent with the behaviour of layered soils, only reached 15% strain. For Bothkennar clay some fabric may exist (see Section 3.2.1), that would play the same role as layering in the large strain behaviour of the clay.

In the stress plane q'-p', the values of friction coefficient M have been found to be slightly different for the natural and reconstituted clay (Cotecchia, 1996; Callisto, 1996). By plotting the flow rules for the natural Pappadai clay, Cotecchia found that, like the reconstituted clay, the natural clay exhibits a frictional behaviour at large strains, but with a friction parameter M greater than that of the reconstituted clay, due to structure. This may be because the linear stress dilatancy relationship found for Pappadai clay, which is derived from the strain energy dissipation equation, is an approximation of a more complex relationship that includes energy dissipation due to both friction and destructuration. Nevertheless, the values of M found by Cotecchia and Callisto for the natural and reconstituted specimens they tested differ by only 9% to 14%. Leroueil *et al.* (1979) found that for Saint-Alban clay, the large strain strengths for the

natural and reconstituted clay plot in a narrow band. Comparatively, it seems that it is the volumetric offset of the critical state line for clays due to an effect of fabric that will cause the largest difference in behaviour between natural and reconstituted clay.

2.4 DESTRUCTURATION

Destructuration describes the process that combines the breaking of inter-particle bonds and the irreversible re-arrangement of particles, which occurs in natural soils with metastable structure with plastic strain, as defined in Section 1.6. Natural soils with stable structure do not undergo destructuration. Destructuration, occuring at the particle scale, can either be deduced from macroscopical observations, or be observed to some extent by using scanning electron microscopy (S.E.M.) or examining porosimetry (e.g. Delage and Lefebvre, 1984). As was noted in Section 1.6, the onset of significant destructuration is usually associated with gross yield. Gross yield, which is a state at which soil stiffness falls significantly and thus plastic strains become substantially larger, has been recognised by several authors as a result of the degradation of structure (Hight *et al.*, 1992; Cotecchia & Chandler, 2000). It is usually relatively abrupt and easily identified. The gross yield curve is regarded as a domain separating stress states which do not significantly alter the structure from those which cause destructuration. The onset of destructuration and its subsequent effects have been identified for a great range of natural clays both in volumetric compression and shearing tests. The following discussion presents data from tests on a selection of soft natural clays presented in the literature, where particularly useful tests were performed and which have been interpreted by the authors in a helpful way.

Graham & Li (1985) studied the behaviour of Winnipeg clay in one-dimensional compression. The data are plotted in the compression plane v-lnσ_l', with σ_l' equivalent to the vertical effective stress σ_v'. The compression curve for the specimen of reconstituted clay follows the normal compression line. The specimens of natural clay show a different behaviour. Once they have reached gross yield, they decrease in volume at a rate greater than that associated simply with the sedimentation compression curve (Fig. 2.4.1). The post-yield compression index, C_c, defined as the slope of the compression curve in e-lnσ_v' space, is larger after gross yield than the compression index determined from the sedimentation compression curve. For Winnipeg clay, C_c was observed to be equal to 1.08 immediately following gross yield for the compression curve of the natural clay, instead of 0.7 for the sedimentation compression line. There must therefore be a component of structure that contributes to the strength of the soft clay up to a threshold stress after which the structure is disrupted. Graham & Li suggested that the unexpectedly abrupt gross yield observed was probably due to the breakdown of cementation.

Burland (1990) reported in his Rankine lecture similar results on a large number of natural soft clays from different origins (Italy, Great Britain, Canada, France, Norway, Indonesia). Figures 2.4.2 and 2.4.3 show typical compression curves for specimens of two natural soft clays. Bothkennar clay and Leda clay, and for the corresponding specimens of reconstituted clay. It seems that for the natural metastable clays gross yield in compression is associated with a marked increase in compressibility. The compression curve converges slowly towards the sedimentation curve for the reconstituted clay. Callisto (1996) obtained similar results on natural specimens of Pisa clay (Fig. 2.4.4). He called gross yield states "conditions of destructuration". The convergence of the compression curve of the natural clay towards the intrinsic compression curve indicates that following large post-yield strains the clay tends to a mechanical behaviour similar to that of the reconstituted soil.

Clays with a stable structure for example due to layering follow a line parallel to the compression curve for the reconstituted clay, roughly coinciding with their sedimentation compression curve. This is illustrated by Figure 2.4.5 (a) which shows compression curves for Sibari clay, a clay with a stable structure from Southern Italy. This is even clearer after normalising the compression data using v_n as defined in Section 1.6 (Fig. 2.4.5 (b)). The normalisation highlights the stable natural structure of the clay, as the compression curves for the natural clay lie outside the intrinsic compression line but remain parallel to it, even at very large stresses. Cotecchia & Coop (1995) observed that the Sibari clay was layered, which is why they had simulated the effects of layering with the simple two-layer model. As for the model soil, the naturally layered fabric gave rise to a stable structure.

Cotecchia (1996) used scanning electron microscopy to examine the changes in the microstructure of both natural and reconstituted Pappadai clay during one-dimensional compression in an oedometer. She found that in the natural stiff clay, gross yield weakens the clay bonding and makes the fabric chaotic, erasing the initial fabric present before yield. Beyond gross yield the compression of the clay gave rise to a regular and resistant fabric. In the normally consolidated reconstituted clay the compression resulted in a non-uniform densification, which did not necessarily give rise to an orientated fabric. The structures of the natural stiff clay and of the reconstituted clay were found to remain different beyond gross yield up to very high stresses, with the structural differences tending to diverge with compression rather than to become similar. Even if the Pappadai clay is homogeneous, again the effects of fabric are a stable form of structure, even though in this case it is a micro-fabric.

A series of drained probing tests, rectilinear in the q'-p' stress plane and radiating from the estimated *in situ* state of the soils, was performed on Pisa clay (Callisto, 1996) and Bothkennar clay (Smith, 1992). The stress paths are shown in Figure 2.4.6. In all cases, the tests were carried out to large strains but did not seem to reach the critical state. The stress paths, normalised with respect to the equivalent pressure on the intrinsic normal compression curve

(see Figure 1.7.1), reach states for which an outer surface can be defined. On reaching this surface, the paths bend inside it (Fig. 2.4.7). Unlike the reconstituted clay, the normalised stress paths do not reach a state boundary surface and remain on it. Therefore the behaviour of natural Pisa and Bothkennar clays cannot be normalised in a classic manner. The outer surface has been identified as the *destructuration surface* or *structure surface*. Callisto (1996) plotted contours of strain energy, using the equations of the work done per unit volume:

$$W = \int \left(p'.\delta\varepsilon_v + q'.\delta\varepsilon_s \right) \tag{2.4.1}$$

and the length of the stress path:

$$LSP = \int \sqrt{\left(\delta p'^2 + \delta q'^2 \right)} \tag{2.4.2}$$

on a plot showing the destructuration surface determined experimentally for Pisa clay. He found that for Pisa clay the destructuration surface coincides with the contour of constant strain energy W=2kJ/m^3 (Fig. 2.4.8), where the energy is defined as the work done to achieve volumetric and shear deformations. Callisto suggested that the start of destructuration should be associated with a threshold in energy. In fact, as strain energy is dependent on both stresses and strains, a significant change in the stress-strain response, such as occurs at gross yield, should lead to a significant change in strain energy. Tavenas *et al.* (1979) previously found that for four sensitive clays the gross yield loci coincided approximately with contours of strain energy between 0.5kJ/m^3 and 2kJ/m^3 (Figs. 2.4.9 and 2.4.10). Leroueil and Vaughan (1990) also suggested that the gross yield of structure should be considered as a function of strain or strain energy.

The response of the natural clay during undrained shearing is linked to the procedure used to reconsolidate the specimen before shearing. For specimens reconsolidated anisotropically to a stress state before gross yield, the stress paths in undrained compression seem to show an increase in deviatoric stress q' at approximately constant mean effective stress p' until they reach a peak deviatoric stress. Then they bend sharply and move inwards along a line of constant stress ratio close to the value of the critical state ratio M for the reconstituted clay. Patterns of behaviour similar to this have been found for a number of clays from different origins and locations (Allman & Atkinson, 1992; Smith *et al.*, 1992; Callisto, 1996; Tavenas & Leroueil, 1977; Shibuya *et al.*, 2000). Typical stress paths are shown in normalised stress space in Figures 2.4.11 and 2.4.12, and in the q'-p' plane in Figures 2.4.13 to 2.4.15. They show a behaviour different to that of normally consolidated reconstituted clays, which would strain-harden rather than strain-soften. Specimens sheared in extension seem to reach a critical state

line in the q'-p' plane with a stress ratio which is also very close to the intrinsic critical stress ratio in extension (Smith, 1992; Callisto, 1996).

Specimens reconsolidated anisotropically to a stress state beyond yield are seen to be much less brittle in compression (Fig. 2.4.16), with a lower stress ratio at peak deviatoric stress. The stress paths again move inwards along the same constant stress ratio line as the specimens that were reconsolidated to stresses before gross yield (Smith, 1992). When normalised with respect to the equivalent pressure on the intrinsic normal compression line, the stress paths seem to move towards the intrinsic critical state line, but it is not clear if they eventually reach it even if the specimens are sheared to large strains (Allman & Atkinson, 1992). The strain-softening behaviour that occurs post-peak indicates a reduction in shear strength, caused by the degradation of structure.

To summarise, destructuration is identifiable at the macroscopic scale as a marked decrease in stiffness and strength. It is associated with gross yield in drained tests, or peak deviatoric stress in undrained tests. When normalising stress paths of natural clays with respect to volume, the gross yield and peak points define an outer surface, called a structure surface, which represents states where significant destructuration begins. At these states normalised stress paths generally move inside the structure surface. In numerical models for reconstituted soils the change in size of the bounding surface of normally consolidated clays is governed by volumetric hardening. Normalised stress paths define a state boundary surface which they do not move inside at large strains. The data for natural clays show that destructuration causes natural specimens to strain-soften, such that their state boundary surface cannot be identified by normalising by volume only. Therefore the size of the bounding surface cannot be related solely to changes in the current elastic wall, but also to destructuration. Thus the state boundary surface is not stable in q'-p'-v space unlike that of the reconstituted clay, but decreases in size with destructuration.

2.5 EXISTING FRAMEWORKS FOR THE BEHAVIOUR OF NATURAL CLAYS

Recently a lot of work has been undertaken to bring coherence to the behaviour of natural soils in the same way as Critical State Soil Mechanics provided a framework for the behaviour of reconstituted clays. The effects of structure have been characterised (for example Burland, 1990; Leroueil & Vaughan, 1990), and the causes of structure have been investigated (Cotecchia, 1996; Cotecchia & Chandler, 2000; Kavvadas & Anagnostopoulos, 1998). All this research agrees that even if the origins of structure are complex, its effects can be described in a simple and general way. The literature reports frameworks for weak rocks and a wide range of natural clays, both stiff and soft. The aim of this dissertation is to model the effects of structure

in soft natural clays, therefore the following review will highlight the aspects of these frameworks which are specific to soft natural clays, and distinguish between frameworks that quantify structure and frameworks that are qualitative.

2.5.1 Qualitative frameworks

It has been seen above that structure allows natural soils to exist at states outside the permissible space for reconstituted soils delimited by the state boundary surface for the reconstituted soil. As noted earlier, Leroueil & Vaughan (1990) defined the space enclosed between the intrinsic normal compression line and the compression curve of the natural soil "structure-permitted" space. Burland (1990) introduced a new normalisation to highlight the effects of structure in volumetric space on natural soils. The new normalising parameter was the void index, I_v, as defined in Section 1.6. In a normalised plot of the void index, I_v, against the logarithm of the mean effective stress, p', the one-dimensional normal compression lines of reconstituted clays all coincide, forming a unique line called the intrinsic compression line (ICL) (Fig. 2.5.1), as reported in Section 1.6. On the same graph Burland (1990) also plotted *in situ* stress states of a range of stiff and soft clays of medium sensitivity (values between 4 and 6) as defined by Equation 2.3.1. The data defined a relatively narrow band, and the regression line through the data was termed the Sedimentation compression line (SCL). For these normally consolidated medium sensitivity clays the sedimentation compression line represents an approximation to the state of the soil in the ground. Kavvadas & Anagnostopoulos (1998) defined their framework using a standard *e-lnp'* plot (Fig. 2.5.2). They chose the same terminology as Burland (1990), and called the normal compression line of the structure-less clay, as opposed to the reconstituted clay for Burland, the intrinsic compression line, and the line representing the state in the soil at deposition the sedimentation compression line. This sedimentation compression line is different from that of Burland as it does not represent the *in situ* states of clays of medium sensitivity but refers to the specific sedimentation compression line of the clay examined. Kavvadas & Anagnostopoulos also defined a *bond strength line*, which is distinct from the sedimentation compression line, and represents the compression curve of clays that have a post-sedimentation structure such that they yield to the right of their sedimentation compression line. The bond strength line is similar to the line delimiting the structure-permitted space in the framework presented by Leroueil & Vaughan (1990). Assuming normally consolidated natural clays have no post-sedimentation structure they would reach gross yield on the sedimentation compression line defined by Kavvadas & Anagnostopoulos, which constitutes a lower limit to the bond strength envelope.

The three frameworks have common principles, notably the significance of the position of the *in situ* state in volumetric space with respect to the intrinsic compression line. Burland

(1990) established that clays whose *in situ* states lie close to or on the sedimentation compression line, that is of medium sensitivity, show a marked yield when compressed volumetrically to a state near the sedimentation compression line, with a large increase in compressibility, such that the state of the soil converges towards the intrinsic compression line at large strain. Conversely, clays whose *in situ* states lie close to or on the intrinsic compression line have one-dimensional compression curves which are essentially parallel to the intrinsic compression line. This is illustrated in Figure 2.5.3 with data from tests on soil from the Mississippi Delta (Burland, 1990). Figure 1.7.4 also shows that specimens of Pisa clay, which is of medium sensitivity with an *in situ* state close to the sedimentation compression line, when compressed one-dimensionally show a larger increase in compressibility post-gross yield than those whose *in situ* state is close to the intrinsic compression line. Consequently, it appears that clays with a high degree of structure (*in situ* state far from the intrinsic compression line) have a metastable structure, while clays with a low degree of structure (*in situ* state close to or on the intrinsic compression line) have a more stable structure.

Leroueil & Vaughan (1990) established that large compression strains develop when yield occurs in structure-permitted space, and that they depend on the difference in void ratio between the yield point and the curve delimiting the structure-permitted space (the compression curve of the bonded material in Figure 2.3.1). They then demonstrated that for normally consolidated clays there exists a relationship between compressibility post-gross yield C_c, initial void ratio e_0 and sensitivity S_t, as is illustrated in Figure 2.5.4 (Leroueil *et al.*, 1983). The graph shows that the higher the sensitivity, the greater the post-gross yield compressibility for a given initial void ratio. It must be assumed that Leroueil *et al.* have not included clays with stable structure in their study, which will have the same compressibility as the reconstituted soil irrespective of sensitivity. Their statement implies that for metastable natural clays the compressibility post-gross yield C_c is not directly related to the intrinsic compressibility C_c^*, which is related to liquid limit only, but is dependent on structure as well as index properties. Thus the intrinsic compressibility C_c^* is a limiting value for C_c. This quantifies the principle proposed by Burland that the position of the *in situ* state in volumetric space with respect to the intrinsic compression line defines the degree of sensitivity of the soil. Furthermore, the graph shown in Figure 2.5.4 relates sensitivity, determined in terms of undrained shear strength, to the volumetric response of metastable natural clays. This has already been done successfully by several researchers, and some useful frameworks that have stemmed from their work are reported in the following section.

2.5.2 Quantitative frameworks

This section reviews frameworks that use sensitivity as a means to quantify structure. The first framework for soft natural clays that included sensitivity as a parameter representing structure was proposed by Skempton & Northey (1952). The differences in the mechanical behaviour of different clays had already been recognised to be due to the differences in both their composition and their structure. Skempton & Northey (1952) tried to normalise the response of the clay in compression with respect to its composition. The composition of the soil was taken into account by means of the Atterberg limits, more particularly the liquidity index (LI). The liquidity index is given by the expression after Terzaghi (1936):

$$LI = \frac{\omega - PL}{LL - PL} \tag{2.5.1}$$

where ω denotes the water content, and LL and PL denote the liquid and plastic limits of the soil. When the water content equals the liquid limit, LI=1, and when the water content equals the plastic limit, LI=0. Skempton & Northey (1952) plotted *in situ* states measured in the field for sixteen clays, the curves (or points, where the data is limited) relating liquidity index to effective consolidation pressure. The clays were normally consolidated, and it will be assumed that their behaviour is affected by sedimentation structure only; and hence the curves shown correspond to the sedimentation compression curves of the clays (Fig. 2.5.5). On the same plot, Skempton & Northey reported the normal compression curves for three of these clays reconstituted to form a slurry and one-dimensionally compressed in the laboratory. When normalised in this way the three sets of data plotted within a narrow band. Thus, as might be expected, once normalised with respect to the liquidity index, reconstituted clays show approximately the same response in compression. This reflects the fact that clays reconstituted in the laboratory undergo similar deposition and consolidation conditions, and has also been highlighted by other methods of normalising that are reported in Section 1.6, such as the use of the void index by Burland (1990). If the influence of composition on the compression behaviour of natural normally consolidated clays can be normalised by the liquidity index, any other differences observed in the compression behaviour must be caused by sedimentation structure. Fig. 2.5.5 shows that the sedimentation compression curves for the natural clays plot to the right of the curve for the reconstituted clays. Skempton & Northey studied the position of these curves with respect to the sensitivities of the undisturbed clays, where sensitivity is determined in terms of undrained strength (see Section 2.3.2). They found that for clays with a sedimentation structure as defined by Cotecchia & Chandler (2000), a definite correlation exists between sensitivity determined *in situ* using the vane apparatus, and the liquidity index for any

given pressure. The greater the difference in liquidity index with respect to the equivalent value on the curve for the reconstituted clay, the higher the sensitivity.

The relationship between sensitivity, liquidity index and consolidation pressure was further investigated and confirmed by Houston & Mitchell (1969) using test data from clays with a sedimentation structure. A schematic diagram of the framework proposed by Houston & Mitchell (1969) is shown in Figure 2.5.6. More recently, Cotecchia & Chandler (2000) have used data presented in the paper by Skempton (1970) to investigate the correlation between the location of the *in situ* state of the clay in LI-σ_v' space and the sedimentation sensitivity (S_u/S_u^*) of the clay (Fig. 2.5.7 (a)). They identified sedimentation compression curves that plot close to each other for similar sensitivities. Despite some scatter, which they attributed to errors in evaluating the sensitivity or water content, they were able to extrapolate the sedimentation compression curves corresponding to different values of sensitivity from the data and these are plotted as dashed lines in Figure 2.5.7 (b). Cotecchia & Chandler (2000) concluded that clays of different origins and sedimentation structures but equal sensitivity have the same sedimentation compression curve. Following Burland (1990), they replotted the compression curves on a graph relating the void index to the vertical effective stress. The resulting curves plotted in a band of parallel lines corresponding to contours of equal sensitivity. Data from Skempton & Northey (1952), Skempton (1970) and Burland (1990) suggest that, assuming very little destructuration occurs before gross yield, sedimentation sensitivity and the ratio of the yield vertical stress on the sedimentation compression curve to the equivalent pressure on the intrinsic compression curve are equal. This equality has been assumed by Cotecchia (1996) in the sketch shown in Fig. 2.5.8. This constitutes the "Sensitivity framework" for natural clays with a sedimentation structure (Cotecchia & Chandler, 2000). The bottom line represents the contour of sensitivity equal to unity, and is the unique sedimentation compression curve for all reconstituted clays, called the intrinsic compression line by Burland (1990). The other lines plot with increasing values of sensitivity: for a given value of void index the greater the vertical stress representing the sedimentation state of the soil, the higher the sensitivity, which is consistent with data from Houston & Mitchell (1969). Therefore a framework is available for natural clays, which links the *strength sensitivity* of a clay, defined as S_u/S_u^* as in Section 2.3.2, to the location of its sedimentation compression curve in the I_v-σ_v' plane. For clays with a sedimentation structure, generally normally consolidated clays, the sedimentation compression lines represent the locus of gross yield stresses, σ_{vy}' on Figure 2.5.8. Cotecchia & Chandler (2000) defined the ratio of σ_{vy}' to the equivalent stress σ_{ey}^* on the intrinsic compression line (ICL) as the *stress sensitivity* $S_\sigma = \sigma_{vy}' / \sigma_{ey}^*$. They therefore suggested that the stress sensitivity is, for all practical purposes, numerically equal to the strength sensitivity S_t, so that $S_t = S_\sigma = \sigma_{vy}' / \sigma_{ey}^*$. They then demonstrated that the behaviour of clays with a post-sedimentation structure is also in

accordance with the Sensitivity framework shown in Figure 2.5.8. For these clays the constant S_t lines in the figure are the loci of the gross yield points of clay specimens of equal strength sensitivity S_t compressed one-dimensionally.

Cotecchia & Chandler (2000) also showed that natural clays sheared from normally consolidated states exhibit their peak undrained strength at the apex of a state boundary surface, with a strength q_{peak} as shown in Figure 2.5.9. They then redefined strength sensitivity S_t as the ratio of the deviatoric stress at the apex of the state boundary surface of the natural clay to the corresponding deviatoric stress at the apex of the state boundary surface of the reconstituted clay at the same specific volume. The equality of S_t and S_σ $(= \sigma_{vy}' / \sigma_{ey}^* = p_{K0y}' / p_{K0y}^* = p_{iy}' / p_{iy}^*)$ implies that there is geometric similarity between the state boundary surface of the natural clay and that of the corresponding reconstituted clay, and that the ratio between the sizes of the state boundary surfaces is the same for clays of equal strength sensitivity S_t. This is supported by test data on Winnipeg clay (Graham & Li, 1985; see Figure 2.3.9).

Cotecchia & Chandler (2000) normalised the test data further to account for the influence of composition on both specific volume and strength, by taking the friction coefficient M as a normalising factor for the effects of soil composition on soil strength, and using the void index as defined by Burland (1990). They proposed that the state boundary surface in I_v-q'/M-p' space should be the same for clays of different composition and structure, but equal strength sensitivity, as shown in Figure 2.5.10. This statement refers to the position of the state boundary surface before significant destructuration occurs, assuming that very little structure degradation takes place before gross yield. From the data presented in Section 1.3, it can be seen that this normalisation will not work after gross yield, when different natural clays will have different rates of destructuration. Also, this proposal by Cotecchia & Chandler does not take account of structural anisotropy that may occur in natural clays. The following section investigates the application of the Sensitivity framework to natural clay data.

2.5.3 Application of the Sensitivity framework to natural clay data

Cotecchia & Chandler (2000) have demonstrated the equivalence between strength sensitivity, S_t, and stress sensitivity, S_σ. They then used this correlation to normalise test data from natural clay specimens and thus postulate that there is a single normalised state boundary surface which applies to all clays.

The Sensitivity framework implies that the size of the gross yield curves obtained from natural samples of a clay of given sensitivity S_t are in a constant ratio to the size of the curves obtained from tests on the corresponding reconstituted samples. Consequently the gross yield curves obtained from natural and reconstituted samples of a given clay of sensitivity S_t should

form a unique curve in the $q'/S_t p_e^*$ versus $p'/S_t p_e^*$ plane, where p_e^* is the normalising factor for volume, and S_t is the normalising factor for structure. In the context of the Sensitivity framework, similar samples from different depths are assumed to have a single sedimentation compression line, thus to have constant S_t. That means that their gross yield curves can be normalised solely with respect to volume. Cotecchia & Chandler (2000) further normalised the deviatoric stress by composition by means of the intrinsic strength parameter M. Then the gross yield curves of clays of different structure and composition should all reduce to a unique curve in the $q'/MS_t p_e^*$ versus $p'/S_t p_e^*$ plane, with $S_t = S_\sigma = p_{iy}'/p_{iy}^* = p_{K_0 y}'/p_{K_0 y}^*$ (see Figure 2.5.11).

Cotecchia & Chandler applied this normalisation to data from natural clays. They first demonstrated the applicability of the normalisation to data from Sibari clay, which is a layered soft clay with a stable structure, of sensitivity around 2.5-3.5. Shear test data obtained from Sibari clay specimens retrieved from a wide range of depths are shown in Figure 2.5.12 (Coop & Cotecchia, 1995). The specimens were K_0-consolidated to a stress beyond yield and then sheared, either drained or undrained. The stresses have been normalised by the equivalent pressure on the intrinsic normal compression line, p_e^*, and the deviatoric stress has further been normalised by the strength parameter M to take account of the varying composition with depth. For each natural specimen the data from the corresponding reconstituted test are shown. The normalised stress paths followed by the natural specimens do not describe or fall within a unique state boundary surface, due to their different structures. For each specimen, Cotecchia & Chandler calculated the strength sensitivity S_t as the ratio of the peak deviatoric stress of the natural specimen to that of the corresponding reconstituted sample (q_{peak}/q_{peak}^*). They found that these values of sensitivities, plotted against the corresponding values of stress sensitivities S_σ computed from the K_0-consolidation tests, are a close fit to the linear relationship $S_t = S_\sigma$ (Figure 2.5.13). Cotecchia & Chandler then normalised the test data shown in Figure 2.5.12 using S_t, p_e^* and M, as discussed above. The resulting curves are shown in Figure 2.5.14. The stress paths for the normally consolidated natural specimens now plot close to the curves representing the state boundary surface of the reconstituted clay. Although some second order effects of structure are still visible, the normalisation has accounted for the majority of the effect of structure on the behaviour of the stable Sibari clay, demonstrating that it can be described by the Sensitivity framework.

Cotecchia & Chandler also verified the approximate equality of strength and stress sensitivity for Pappadai clay, a stiff clay with a quasi stable structure, and for the soft metastable Bothkennar clay. They plotted gross yield data from shear tests on Bothkennar and Pappadai clays, as well as a stress path from a reconstituted specimen of Pappadai clay, all again normalised by S_t, p_e^* and M, to show the general applicability of the proposed normalisation. The gross yield states of both clays were found to plot in a narrow band, except at states near the

isotropic axis where the data point for Bothkennar clay suggests that there may be a hook in the gross yield curve of the soft clay (Fig. 2.5.15). Cotecchia & Chandler attributed the shape of the gross yield curve of Bothkennar clay to the fact that soft clays are more sensitive and more easily disturbed by the imposition of isotropic stresses on initially anisotropic samples. This hypothesis cannot be justified by the data shown on Figure 2.5.15 only, where there is only one data point that plots away from the normalised gross yield curve determined for Pappadai clay. In addition, this data point represents a gross yield point that is poorly defined by the isotropic compression curve of Bothkennar clay, as has been seen in Figure 2.3.13. However, Figure 2.3.10 shows more data points which support an assumption that the normalised gross yield curve of Bothkennar clay has an anisotropic shape. Thus if structural anisotropy is present it may not be possible to find a normalisation that will give a unique normalised state boundary surface for all clays.

Cotecchia & Chandler (2000) successfully demonstrated that the behaviour of clays with a stable structure such as Sibari clay is described by the Sensitivity framework. The behaviour of Pappadai clay, with a quasi stable structure, and Bothkennar clay, with a metastable structure, is also described by the Sensitivity framework, but up to gross yield only. Until this point little destructuration occurs and sensitivity can be assumed to be constant in both stiff and soft clays. But beyond gross yield, when significant destructuration takes place, the normalisations proposed are no longer applicable. The reduction in sensitivity associated with destructuration must be taken into account. In terms of modelling, the Sensitivity framework can be used to define the size of the state boundary surface of the natural clay with respect to that of the reconstituted clay. The equivalence between strength and stress sensitivity up to gross yield indicates that up to that point the state boundary surfaces of the natural and reconstituted clay are of similar shape, with a size-ratio equal to sensitivity. However this equivalence has not been proven for states beyond gross yield. In order to find a single parameter to represent structure for all stress paths, it will be necessary to establish the correlation between strength and stress sensitivity beyond gross yield. This will be investigated in Chapter 3.

2.6 EXISTING MODELS FOR SOFT CLAYS

2.6.1 Introduction

The objective of the research is to extend the 3-SKH model (Stallebrass, 1990) so that it is able to simulate the behaviour of natural soft clays. Therefore, the following review does not include models developed to predict the behaviour of clays at small strains as this is already a feature of the 3-SKH model. The models that are of interest for this work are those that have been

developed or modified to simulate one or more forms of structure. Before reviewing existing models it is important to clarify the terminology used in the literature to describe constitutive models. As the techniques for measuring small strains in the laboratory improved, it became clear that deformations that were traditionally described as elastic and recoverable were certainly elasto-plastic. The extent of truly elastic deformation for most soils is very small, although Smith *et al.* (1992) suggested that large-scale changes in particle packing are delayed until the stress state reaches what would previously have been described as the yield surface. It is this type of traditional yield surface that is referred to in many constitutive models. However, in these models, the yield surface defines the boundary between elastic and plastic deformations, whereas experimentally yield often only describes a significant change in the response of the soil. Most of the time, determination of yield is indeed the determination of gross yield, and it is achieved by fitting a bilinear relationship to the stress-strain curves obtained in the laboratory, and hence it involves a large amount of subjectivity. Multi-surface models allow for plastic deformations within the traditional yield surface. In these models, the gross yield surface has been renamed the distinct-yield surface, the limit surface, the outer surface or the bounding surface according to the model, and an inner surface representing the true elastic region is referred to as the yield surface. In the following, yield surface will refer to the boundary between elastic and plastic behaviour in the model.

2.6.2 Basic concepts used to model bonded soils

In the development of constitutive models for bonded soils in recent years, various approaches have been proposed. Oka *et al.* (1989) presented a constitutive model for soft natural clays in which damage to the structure is contained in the plastic formulation. Structure is modelled as extra strength that reduces with plastic straining to the strength of the "unstructured" material (due to frictional resistance only). By contrast, Chazallon & Hicher (1995) expressed damage as a change to the elastic properties. The model combines plasticity and damage but avoids coupling them by distinguishing between the grains and the cemented matrix at the microscopic scale. The mechanical behaviour of the grains is modelled by an elasto-plastic law, and the behaviour of the cemented matrix by an elastic model which takes into account the damage spreading inside the material and the degradation of the bonds by means of a damage law. The amount of bonding is linked to an isotropic damage variable that depends on a damage energy release rate that is thermodynamically acceptable.

The concepts underpinning the extension of classical hardening plasticity to bonded materials were first laid out by Gens & Nova (1993). Leroueil & Vaughan (1990) noted that similar patterns of behaviour are observed in materials with bonds of geological origin, in artificially cemented soils and in grouted sands, some patterns even extending to soft natural

clays. Following this work, Gens & Nova (1993) selected two basic features of the behaviour of bonded materials which should be modelled. Firstly, they recognised that the role played by yield is fundamental to the behaviour of natural materials, in particular the onset of destructuration, and secondly that the observed behaviour of bonded material needs to be considered with respect to the behaviour of the equivalent unbonded material. They also defined the effect of bonding on the initial elastic domain by using a larger yield surface, and allowing for tensile strength and true cohesion (Figure 2.6.1). The increased yield stress and tensile strength are directly proportional to the yield stress of the unbonded material by factors equal to functions of the degree of bonding, *b* (Figure 2.6.2).

The effects of bonding are described through the introduction of bond-related internal variables. Bond degradation is modelled using hardening laws linking changes in these bond-related internal variables to plastic strain rate. Yield locus changes are controlled by conventional volumetric hardening associated with bond degradation. The evolution of the yield surface when hardening of the unbonded material dominates with respect to decrease in bonding is shown in Figure 2.6.3a. Figure 2.6.3b shows the change in the yield surface when the rate of decrease in bonding has become sufficient for the yield locus to be shrinking despite volumetric hardening with plastic strain. In the general formulation of the model the degree of bonding, *b,* is defined as a function of the measure of damage, *h,* (Figure 2.6.4), where the quantity *h* is a function of both plastic volumetric and shear strain. An example of the capability of the model to predict the isotropic compression of bonded materials is given in Figure 2.6.5, where a simple formulation of the damage function has been used in order to evaluate the approach.

Lagioia & Nova (1995) used these constitutive laws to develop a model for soft rocks. The model requires 13 parameters, of which the majority can be derived by back-analysis from isotropic compression test data. The model was evaluated by simulating a range of tests that had been performed on calcarenite specimens in the laboratory; a drained constant p′ test and an undrained compression test in the triaxial apparatus, and a one-dimensional compression test in the oedometer. Figures 2.6.6 and 2.6.7 show a comparison of the model predictions and experimental data for the different tests. Qualitative and quantitative accuracy is generally satisfactory. The model was able to reproduce the marked gross yield in one-dimensional compression, with a destructuration phase at constant stress which corresponds to the transition from a rock-like to a soil-like material (Fig. 2.6.6), and the strain-softening in drained and undrained shearing tests (Fig. 2.6.7). As was shown in Chapter 2, destructuration in soft natural clays manifests itself in drained compression tests by a marked gross yield associated with an increase in compressibility, and in shearing tests by strain-softening associated with contraction.

The basic concepts proposed by Gens & Nova (1993) can be applied to the modelling of soft clays. In particular, the approach they followed is consistent with a methodology that extends a base model to allow it to predict the behaviour of a wider range of soils. The concept

of associating plastic hardening with bond degradation is also a good base for modelling natural bonded soils. The model proposed by Gens & Nova (1993) was not able to predict advanced features of soil behaviour, such as non-linearity, stress-induced anisotropy or the effect of recent stress history, but their methodology is simple and clear enough to apply to existing more sophisticated soil models. A key issue that was not addressed by Gens & Nova is the determination of the relationship between destructuration and plastic strain, or the destructuration law. This is an important issue that distinguishes between types of bonded soils. In the following, models that have been proposed in recent years for bonded soils are reviewed. These models have been developed from existing models for reconstituted clays. Their approach is either to include effects of structure in an existing bounding surface, or to add an extra structure surface to the model. The models have been developed within the framework of Critical State Soil Mechanics.

2.6.3 Models developed within the Critical State framework

Various sophisticated models have been developed recently within the framework of Critical state soil mechanics to predict the behaviour of natural clays. These models are mainly a direct application of the concepts outlined by Gens & Nova (1993). The models include advanced features of soil behaviour such as non-linearity and sometimes structural anisotropy. The following review focuses on the four most complete models that have been developed recently for natural clays. Other models that have been proposed recently only deal with volumetric compression of the natural soil and are not rigorously derived in the Critical state framework (for example Liu & Carter, 2000; Nagaraj *et al.*, 1998).

In all the models, the effects of structure are simulated in part by an increase in the size of the bounding surface defined in the model. This is achieved in two different ways. Either extra strength (bond strength) is added to the reconstituted material (Gajo & Muir Wood, 2001; Rouainia & Muir Wood, 2000; Tamagnini & d'Elia, 1999), which is usually referred to as the "unstructured" or "unbonded" material. Alternatively the gross yield curve of the natural soil is simply determined directly in the laboratory, for example the bond strength envelope shown in Figure 2.6.8 (Kavvadas & Amorosi, 2000). In addition, Rouainia & Muir Wood (2000) included the bounding surface of the reconstituted clay in the model, which they called the *reference* surface (Figure 2.6.9). Tamagnini & D'Elia (1999) expressed the preconsolidation pressure of the natural clay, which defines the size of the bounding surface, as the sum of the preconsolidation pressure for the reconstituted clay, p_c, and the bond strength, p_m (Figure 2.6.10).

Gajo & Muir Wood (2001) and Rouainia & Muir Wood (2000) described the size of the bounding surface of the natural clay as the size of the bounding surface of the reconstituted clay

multiplied by the degree of structure, r. This approach is similar to the method proposed by Ingram (2000) to model the behaviour of stable stiff natural clays and is an application of the Sensitivity framework (Cotecchia & Chandler, 2000). Predictions for the natural soil are made using a larger state boundary surface defined by calculating the preconsolidation pressure at the intersection of an elastic wall and the natural normal compression line. For stable clays, this preconsolidation pressure is equal to the preconsolidation pressure of the reconstituted clay multiplied by sensitivity. Some authors (Tamagnini & D'Elia, 1999; Kavvadas & Amorosi, 2000) also include a tensile strength in the size of the bounding surface, so that the origin of the stress plane is inside the bounding surface. However this does not seem relevant for soft clays.

In these models, destructuration is a function of plastic strain. The three models referred to above allow destructuration to start inside the bounding surface, by using kinematic hardening plasticity (Gajo & Muir Wood, 2001; Kavvadas & Amorosi, 2000; Rouainia & Muir Wood, 2000) or a bounding plasticity mapping rule (Tamagnini & D'Elia, 1999). The size of the elastic region is always difficult to measure directly, therefore some assumptions must be made. Tamagni & D'Elia (1999) fixed a limiting value of mean effective stress p_l below which deformations are elastic, typically 1kPa. Rouainia & Muir Wood (2000) expressed the size of the yield surface as a constant ratio, R, of the size of the reference surface. This approach assumes that the size of the elastic region is independent of structure, and thus remains the same as that of the reconstituted material. By contrast, Kavvadas & Amorosi (2000) expressed the size of the yield surface as a constant ratio of the size of the bounding surface or bond strength envelope of the natural clay. This last approach, which was later adopted by Gajo & Muir Wood (2001), is in agreement with the work carried out by Ingram (2000), who used the Three-surface kinematic hardening model (Stallebrass & Taylor, 1997) to evaluate predictions of the behaviour of stiff natural clays. He found that using larger bounding and inner surfaces gives improved predictions of the small strain response, which is related to the size of the inner surfaces. Also near failure, the state of the soil, whether it is wet or dry of critical state, defines if the behaviour on approaching failure is associated with contraction or dilation. The derivation of the constitutive equations is more straightforward if yield and destructuration are associated by having the size of the plastic yield surface also dependent on the degree of structure.

The hardening rules used by the four models are very similar in concept. Following Gens & Nova (1993), the hardening laws consist of two competing terms. The first term is either the isotropic hardening of the Modified Cam Clay model (Gajo & Muir Wood, 2001; Kavvadas & Amorosi, 2000; Rouainia & Muir Wood, 2000) or similar to the hardening law proposed by Nova (1977) (Tamagnini & D'Elia, 2000). The second term controls the decrease of the structure-related hardening parameters with a damage strain, which is a function of plastic strain. All four models assume that the degree of structure decreases exponentially with damage strain. The damage strains are expressed in a general way, so that volumetric and shear plastic

strains have different influences on the degradation of structure. Gajo & Muir Wood (2001), Rouainia & Muir Wood (2000) and Tamagnini & D'Elia (1999) ensured a monotonic decrease of structure by making the damage strain a function of absolute values of the plastic strains. Furthermore, in all three models, for deformation inside the bounding surface decay of stiffness is related in some way to the distance of the current stress to the bounding surface.

The four models also include some aspects of structural anisotropy. Tamagnini & D'Elia (1999) use different stress ratios at critical state in compression and extension. In the model proposed by Kavvadas & Amorosi (2000), the bond strength envelope is not necessarily circular in the deviatoric hyper-plane, and therefore it can describe shear strength anisotropy by independently controlling the shear strength in various modes of deformation (triaxial, plane strain, simple shear, etc). This is a more sophisticated form of that by Tamagnini & d'Elia. In addition, the models proposed by Kavvadas & Amorosi and by Rouainia & Muir Wood can account for bond-induced anisotropy; for example bonds may degrade more easily in extension than in compression, or by shearing along a specific plane. This is achieved by introducing an eccentricity along the q'-axis (bounding surface not centred on the isotropic p′-axis), and the anisotropy can be expressed as the ratio of the deviatoric stress at the centre of the bounding surface to the mean effective stress. This ratio has been termed the *primary anisotropy tensor* by Kavvadas & Amorosi (2000). In the model by Rouainia & Muir Wood (2000), the primary anisotropy tensor is a simple function of the degree of bonding, and is equal to zero when the degree of bonding is unity (for instance for reconstituted soils). In the model proposed by Kavvadas & Amorosi (2000), the primary anisotropy changes only during plastic deformation from material states on the bond strength envelope, when loading is not along a stabilised radial stress path. The model proposed by Gajo & Muir Wood (2001) simulates a large initial anisotropy of structure and subsequent reduction due to destructuration. Anisotropy and destructuration are modelled by using a hardening rule which is both rotational and kinematic. The rotational hardening relationship is defined such that the rotation, represented by the length β in Figure 2.6.11, decreases with destructuration.

The models use the same number of parameters as many advanced models, typically between 10 and 13, with between 3 and 5 parameters to represent structure. The model proposed by Rouainia & Muir Wood (2000) is sensitive to changes in the values of the parameters, as is illustrated for an undrained triaxial compression test in Figure 2.6.12. The parameters related to structure in Figure 2.6.12 are: the parameter A, which controls the proportion of shear strain in the damage strain function, where A=1 if destructuration is dependent on shear strain only and A=0 if destructuration depends on volumetric strain only, if A=0, the parameter k, which controls the rate of destructuration with damage strain, and the parameter r_0, which represents the initial degree of structure. An increase in r_0 of 30% causes an increase in undrained shear strength of 30%. Changing the value of A from 0.494 to 1 does not have much effect as shear

strains dominate deformation during undrained shearing. Dividing the value of k by 10 leads to an increase of undrained shear strength of about 15%, and a stiffer behaviour up to peak strength.

Rouainia & Muir Wood used an optimisation procedure to find the best set of parameters. They then carried out analyses of undrained compression tests for isotropic and anisotropic stress histories at different preconsolidation levels and for different degrees of overconsolidation. Predicted and experimental data are shown in Figures 2.6.13, 2.6.14 and 2.6.15, the experimental data being obtained from tests on a low sensitivity clay from Sweden, Norrköping clay. The patterns of behaviour are generally well captured in terms of stress path and peak strength, even if the peak strengths tend to be over-predicted by up to 15% in Figures 2.6.13 and 2.6.15. However all the simulations shown in Figure 2.6.14a, and in particular analysis *CAU5*, under-predicted the initial value of shear modulus, resulting in the peak occurring at higher strains than in the experiment. In some simulations the destructuration post-peak strength is over-predicted by up to 25%, for example analyses *CIU7* and *CAU2*. Analyses of drained tests were then carried out using the same parameters. Predicted and experimental data compare well as the model differentiates between isotropically and anisotropically consolidated specimens (Figure 2.6.16).

In the models proposed by Tamagnini & D'Elia (1999) and Kavvadas & Amorosi (2000) the effects of volumetric and shear plastic strains on destructuration are uncoupled, therefore the parameters related to each strain can be determined from the appropriate laboratory test (for example isotropic compression, or undrained shearing if neglecting the small amount of plastic volumetric strains). Predicted data for undrained compression tests at different overconsolidation levels, and for a drained test, using the model proposed by Kavvadas & Amorosi (2000), are shown in Figures 2.6.17, 2.6.18 and 2.6.19. The experimental data were obtained from tests on stiff Vallericca clay. The model manages to reproduce the main features of the behaviour of the clay, combining strain-softening and dilation inside the bond strength envelope with significant degradation of structure after reaching it. The undrained shear strength of the clay is predicted within 10% of the experimental value. Also, post-peak there is a very good match between predicted and experimental data, with an error of less than 10%. However these results cannot be compared directly to results obtained using the model by Rouainia & Muir Wood (2000) since the data used in this case are from a stiff clay, in which not much destructuration occurs, while Rouainia & Muir Wood (2000) evaluated their model using data from a soft clay.

Gajo & Muir Wood (2001) evaluated the potential of rotational hardening in modelling the evolution of structural anisotropy in natural clays by simulating a series of drained probes and undrained triaxial compression tests that were performed by Smith (1992) on natural Bothkennar clay specimens. The majority of the parameters were determined by trial and error.

Figure 2.6.20 shows a comparison of model predictions when the bounding surface cannot rotate and when it has a variable inclination, with experimental data for gross yield curves obtained during drained probes radiating from the *in situ* stress point. At the beginning of the analysis, when significant destructuration has not started yet, the prediction using a rotated surface is better than that using a non-rotated surface. At large strains, destructuration has caused the predicted anisotropy of the bounding surface to reduce, and the predicted gross yield curves using rotated and non-rotated surfaces are approximately the same. Figure 2.6.21 shows that destructuration and structural anisotropy are successfully combined to give a good prediction of the normalised behaviour of Bothkennar clay during the drained probes. Figure 2.6.22 shows a comparison of model prediction and experimental data for stress paths obtained during undrained triaxial compression and extension tests on natural Bothkennar clay specimens. Simulation of intact specimens SCU1 and SCU3 shows good agreement with the test data, while the prediction of stress paths for specimens that had been isotropically and K_0-compressed beyond gross yield before shearing are less successful. The model proposed by Tamagnini & D'Elia (1999) was not validated against laboratory test data.

2.6.4 Conclusions

The four models presented above are simple extensions of existing models. They show that adding a component to the hardening modulus that causes the size of the bounding surface to reduce with both plastic volumetric and shear strains is sufficient to improve predictions of the behaviour of sensitive clays. However all four models, which include advanced features of the behaviour of natural soils such as non-linearity and structural anisotropy, still have not determined a simple expression for damage strain. The general functions they propose can be defined by parameters that are not soil properties, which will make the models complex to use in finite element analyses as they will require many sets of parameters for different stress paths. To illustrate the capabilities of their models the authors used data from tests which highlight the effects of destructuration, such as undrained compression tests and drained probing tests. Qualitatively, the models are able to reproduce the patterns of behaviour due to destructuration that are observed in tests on sensitive clays, in particular strain-softening during undrained compression tests and reversal in normalised stress path direction during drained probing tests. Quantitatively, the model by Rouainia & Muir Wood (2000), which was evaluated against test data from a soft clay, achieve a rather good match between the predicted and experimental values of undrained shear strength of the soil, with an accuracy of about 15%. Post-peak strength the predicted destructuration was within 25% of the experimental results, but it must be remembered that a direct comparison with the experimental results may not be valid due to the possibility of localisation occurring in the specimens during the experiments. In the evaluation

of the model presented in Chapter 5 data from undrained compression tests and drained probing tests will also be mainly used to assess qualitatively and quantitatively the new model. Since in the new model the parameters used to describe destructuration will be derived from isotropic compression tests only, it will be expected that there will be a good match between predicted response and experimental results from volumetric compression tests. However it will be critical to measure the accuracy with which the undrained shear strength of the clay is predicted. In analyses simulating undrained compression tests it will be considered that post-peak a direct comparison between the predicted decrease in strength and experimental results may not be valid due to the possible occurrence of localisation in the specimens. Gajo & Muir Wood (2001), Rouainia & Muir Wood (2000) and Kavvadas & Amorosi (2000) suggested representing bond-induced (structural) anisotropy by introducing a deviatoric component in the bounding surface. It is not clear from their results that this improves predictions significantly. Finally, since soft clays reach large strains at relatively low changes of stresses, it appears that in such clays it is critical to model correctly the behaviour at large strains. This will be achieved in Section 4.2.4 by assessing the capability of the base model to simulate the behaviour of reconstituted specimens of three soft clays at large strain in both drained and undrained tests. There will not be the problem of localisation as the soft reconstituted clays are strain-hardening.

2.7 SUMMARY

The literature review presented in this chapter has emphasised the need to integrate structure in a model to predict the behaviour of soft natural clays. Structure has been quantified in terms of stiffness, with the metastability index *MI(G)*, or in terms of strength, with the strength sensitivity S_t or the stress sensitivity S_σ. The onset of significant destructuration has been identified as corresponding to gross yield. In stable clays, the differences in stiffness or strength due to structure are taken into account by normalising with respect to volume on the normal compression line of the natural clay. State, and in particular the size of the state boundary surface, seem to be the critical factor controlling the behaviour of the soil. It is therefore important to consider the appropriate state boundary surface when modelling the behaviour of natural soils. Cotecchia & Chandler (2000) have demonstrated that the state boundary surfaces of the natural and reconstituted clay have similar shapes, and that the ratio of their sizes is equal to the value of sensitivity. In their Sensitivity framework, Cotecchia & Chandler postulated that stress sensitivity is equivalent to strength sensitivity for initial states prior to gross yield. Sensitivity in its general sense appears to be a good parameter to represent structure in natural clays prior to gross yield, both in compression and shearing. Of the three constitutive models that have been reviewed, only the model by Rouainia & Muir Wood (2000) uses a parameter to represent structure that can be associated with sensitivity. Experimental evidence shows that

post-gross yield the size of the bounding surface of the natural clay changes with both volume and destructuration. Existing models for structured clays can reproduce these effects as observed in the laboratory, but they still use general expressions for the destructuration law. If the long-term objective is to use the model for finite element analyses, a single function must be defined for the destructuration law, which uses only soil properties as parameters.

In the next chapter it will be demonstrated that current sensitivity, which represents both strength and stress sensitivity under loading, is a good parameter to use in constitutive equations to represent structure, pre- and post-gross yield. The application of the Sensitivity framework (Cotecchia & Chandler, 2000) to the behaviour three soft clays from different origins and locations will be examined and test data from these clays will be used to derive a simple expression for damage strain.

CHAPTER 3 SENSITIVITY: A PARAMETER TO REPRESENT STRUCTURE

3.1 INTRODUCTION

This chapter links the behaviour of soft natural clays observed in laboratory element tests and reviewed in Chapter 2, to the formulation of a destructuration law using sensitivity as a key parameter. Experimental evidence showed in Section 2.3.1 that the behaviour of soft natural clays may be affected by structural anisotropy. The present project is focused on the general effects of destructuration and mainly concerned with providing a simple model. Therefore in the following, the interpretation of data to derive a destructuration law will not allow for possible effects of structural anisotropy.

As noted in Section 2.2, the main difficulty when modelling structure and destructuration is the great variability of natural clays, caused by the different processes to which they were subjected during and after deposition. To develop a single model that can simulate the behaviour of a wide range of soft natural clays, it is therefore necessary to determine an expression for the degradation of structure that describes the mechanical behaviour of the soil at the macro level. The aim of this chapter is to determine a destructuration law that uses as few parameters as possible which are soil properties. In existing models for structured clays, destructuration is simulated by the reduction of the size of the bounding surface defined in the model, with damage strain. It was seen in Section 2.6.3 that this is achieved by applying a damage-type function either to the preconsolidation pressure determining the size of the bounding surface (Tamagnini and d'Elia, 1999; Kavvadas and Amorosi, 2000) or to the variable representing current structure, defined as the ratio of the size of the bounding surface of the natural clay to that of the reconstituted clay (Rouainia and Muir Wood, 2000). This damage function uses a damage strain as a variable, which is usually a general function of plastic volumetric and shear strains.

In Section 2.5.3 it was shown that sensitivity is a measure of natural structure, which is valid up to gross yield in both stress and volumetric space. In this chapter, it will be demonstrated that the current sensitivity for a given applied stress is a good parameter to use to represent the changing level of structure after gross yield or peak strength, and that it depends on the initial value of natural sensitivity and on the magnitude of plastic strain only. This will be shown by first investigating whether the Sensitivity framework as described in Section 2.5.2 (Cotecchia & Chandler, 2000) can account for the behaviour of three soft clays that were deposited under different conditions. These clays are Bothkennar clay, Pisa clay and Sibari clay. Because of their different origins and structures, they display a range of behaviour that is typical of clays of low to medium sensitivity. They will be referred to as *reference* clays. Sibari clay

has a stable structure, while Bothkennar and Pisa clays have metastable structures. Cotecchia and Chandler (2000) showed that clays with a stable structure follow similar behaviour pre- and post-gross yield, unlike clays with metastable structures (see Section 2.5.3). The use of the Sensitivity framework to describe the behaviour of the three reference clays pre-gross yield will be presented in Section 3.2, and the limitations of the framework when used to describe the behaviour of the metastable clays post-gross yield will be investigated in Section 3.3. This will lead to the formulation of an expression describing the current value of damage strain in Section 3.4. It will be shown that for clays with a low to medium sensitivity there is a unique expression for damage strain that is valid for all clays within this range of sensitivities despite their variable nature, and this expression should include both shear and volumetric strain.

3.2 APPLICATION OF THE SENSITIVITY FRAMEWORK TO THE BEHAVIOUR OF THREE REFERENCE CLAYS

The physical and mechanical properties of the clay soils that are encountered today are the result of the succession and the interaction of geological processes. The characteristics of the environment of deposition, such as salinity, temperature, current, volume and type of solid deposit, have had a direct effect on the lithology of clay deposits. After formation, the deposits have been subjected to consolidation, erosion, or other geological modifications *in situ*. Thus the nature and properties of clay deposits are extremely variable depending on geographical location and geological history. In the next section, the three reference clays are described. They have been chosen not only because a wide range of test data are available, but also because of their different geological and loading histories. In the following description, their similarities and differences will be highlighted in terms of conditions of deposition, rate of sedimentation, mineralogy, organic content, bonding and soil properties. From these observations a first estimate of the expected response of these soils to loading can be made that is derived from soil properties and history only. The link between soil properties and history, and the behaviour observed in laboratory element tests, will then be checked in Sections 3.2.2 and 3.3.

3.2.1 Description of the reference clays

(i) Bothkennar clay

The first reference clay is Bothkennar clay. This soft clay deposit is situated at Bothkennar on the edge of the River Forth, approximately midway between Edinburgh and Glasgow, Scotland. The soft clay sequence is formed of the Claret and Letham beds (Fig. 3.2.1). The Claret beds were deposited at a time of higher sea level, between 5000 and 3000 BP, by tidal transport in an

offshore, shallow environment. The average rate of deposition was about 8mm/year. Within the sequence, three principal facies can be identified: a bedded facies, in which the primary sedimentary layering remains visible, a mottled facies, in which the bedding has been partially or totally destroyed by bioturbation, and a laminated facies, in which numerous silt laminae are present, closely spaced. The differences between the facies are attributed to variations in the rate of deposition. While the sedimentary structures are recorded by the bedded facies, locally more energetic wave and current conditions gave rise to the laminated facies. Reduced rates of sedimentation at times allowed burrowing organisms to rework the sediment and so to produce the mottled facies.

Paul *et al.* (1992) found that different soil microstructures correspond to the different facies by examination under a Scanning Electron Microscope. The bedded facies has an open structure based on regions of clay particles arranged in a general honeycomb pattern (Fig. 3.2.2 (a)). Many silt particles float in the clay matrix, and occasional local bonding occurs between the silt particles (Fig. 3.2.2 (b)). By contrast the mottled facies shows evidence of biogenic disturbance, with the clay particles organised in an open boxwork whose domain structure is relatively poorly developed (Fig. 3.2.3). In this facies, silt particles are less frequent and are not usually bonded.

Below 3.5m, the clay has an apparent overconsolidation of 1.4-1.6, of which only a maximum of 1.25 can be attributed to mechanical overconsolidation by erosion or groundwater lowering. The principal clay mineral in the Bothkennar deposit is illite. The Bothkennar clay has a significant organic content of between 3% and 8%, due to the presence of a residue of marine organisms that have attached themselves to the clay (Paul *et al.*, 1992). The plastic limit is typically 25%. The liquid limit is generally 65-80% from below the crust down to a depth of 12m, and then gradually decreases to about 50% just above the sand (Fig. 3.2.4a), leading to a plasticity index varying between 25% and 55%. The sensitivity of the clay also varies with the facies. Figure 3.2.4b shows a profile of sensitivity against depth, based on BS fall cone tests performed in the laboratory by Hight *et al.* (1992). The value of sensitivity was found to vary between 5 and 15, with peak values around depths of 8m and 12-14m.

(ii) Pisa clay

The second reference clay is Pisa clay. This is the Upper Clay, often named Pancone clay, of the subsoil underneath the Tower of Pisa, Central Italy. The sub-layers B1 and B3 will be examined particularly (Fig. 3.2.5). The clay was deposited in shallow brackish-water lagoon environment, about 5,000 BC, at an average rate of deposition of the soil of 2.5 mm/year (Skempton, 1970). Some erosion of about 50 kPa occurred, which caused the clay to be overconsolidated to a ratio around 1.7 in sub-layer B1 and around 1.3 in sub-layer B3. The clay fraction is high, at 60%, the

liquid limit is about 80%, and the plastic limit is approximately constant and equal to 25%. Consequently the plasticity index has a value varying between 40 and 50% (Fig. 3.2.6). The principal clay minerals in Pisa clay are illite, vermiculite, and some kaolinite. In the deposit the calcium carbonate content is about 10%. The sensitivity of Pisa clay is usually measured as 5 in the vane shear apparatus, and can be considered constant throughout the homogeneous sub-layers B1 and B3.

(iii) Sibari clay

The last reference clay is Sibari clay, which was retrieved from the deep sediments forming the subsoil of the Sibari plain, Southern Italy. These coastal and alluvial sediments were deposited in the last 10,000 years in a transitional environment, leading to the deposit having a complex stratigraphy. This is particularly obvious from the interbedding of soils of different grading, with silt and sand strata within the silty clays (Fig. 3.2.7). The average rate of deposition has been about 10mm/year. The clay is mainly normally consolidated. Despite the variability of the soil the plastic limit is almost constant at 22%, while the liquid limits reflect the variations in clay fraction (Fig. 3.2.8). The principal clay minerals present in the soils are illite and chlorite. There is a progressive increase in the carbonate content with depth. The average value of carbonate content is less than 1%, but it can reach some peak values of 13% in the peat strata. A fairly low organic content of 0.63% was measured for all the specimens used for the experiments (Coop & Cotecchia, 1995). The sensitivity of Sibari clay was found to be equal to 2.5-3.5 from triaxial test data on samples from a wide range of depths (Coop & Cotecchia, 1995).

(iv) Summary

The main features of the three reference clays are summarised in Table 3.2.1. The three clays have a lot of similarities: they are all of Post-Glacial age, they have plastic limits of the same order, and their predominant clay mineral is illite. The main difference between the three clays is the variety of rates of sedimentation they were deposited under, which also varied during their history. This variability in rates of deposition is critical to the development of structure and to the subsequent mechanical properties of the clay. In clays deposited rapidly, bonding has not had time to develop and particles show a preferred orientation or fabric. In clays deposited slowly, bonding, which has had time to develop, dominates the behaviour. Pisa clay was deposited at a uniform slow rate (2.5mm/year), whereas the Bothkennar deposit was formed under variable rates of sedimentation, leading to different facies in the clay. It is expected that these different facies will have different responses to loading. Experimental evidence shows that

natural samples retrieved from the mottled facies have a higher value of undrained shear strength normalised by vertical effective stress, than those retrieved from the bedded facies (Hight *et al.*, 1992b). In the same way, natural samples retrieved from the bedded facies have a higher normalised undrained shear strength than the laminated facies. Hight *et al.* (1992b) attributed these facts to higher degrees of structure in the mottled and bedded facies. Sibari clays, which were deposited much more rapidly (10mm/year), and in a transitional environment, are expected to have a stable behaviour due to the dominant effects of their fabric with little evidence of bonding.

3.2.2 Behaviour of the reference clays

Cotecchia & Chandler (2000) divided the behaviour of natural clays into pre- and post-gross yield behaviour. Clays with a stable structure will have the same pre- and post-gross yield behaviour, while clays with a metastable structure will not. Cotecchia & Chandler demonstrated that by normalising with respect to both volume and stress sensitivity, with stress sensitivity defined as in the Sensitivity Framework (see Section 2.5.2), the significant effects of structure on the behaviour of stable natural clays can be accounted for. After this normalisation, the normalised state boundary surface of the natural clay is close to that of the reconstituted clay. The sensitivity of natural stable clays can be assumed to remain constant under loading, and when this is known the behaviour of these clays can be described by stress, volume and stress history only, like reconstituted clays. Thus the behaviour of clays with a stable structure is described by a Sensitivity framework in which clays can be distinguished by a constant value of sensitivity.

This first paragraph examines the behaviour of Sibari clay, and shows similar results to those presented by Cotecchia & Chandler (2000), who demonstrated the application of the Sensitivity framework to the behaviour of Sibari clay (Section 2.5.3). Figure 3.2.9 shows normalised stress paths obtained from drained (constant p') and undrained tests performed on natural and reconstituted specimens of Sibari clay, replotted from Coop & Cotecchia (1995) but using a different normalising equivalent pressure. Here the stress paths have been normalised with respect to volume by the equivalent pressure at the intersection of an elastic wall and the intrinsic isotropic normal compression line, which was proposed in Section 1.7. By projecting the behaviour of the clay on an elastic wall, this normalisation allows more useful interpretation and comparison of the bounding surface of the natural and reconstituted clay for modelling. The samples of Sibari clay were retrieved from different depths, were K_0-consolidated to a stress post-gross yield and then sheared from a normally consolidated state. Details of the tests are given in Table 3.2.2. A further normalisation by the friction coefficient M was required for the deviatoric stresses to account for composition. The stress paths for the reconstituted clay define

a single state boundary surface, and reach failure on the intrinsic critical state line on the state boundary surface. The stress paths described by the natural specimens lie well outside the intrinsic state boundary surface, and do not form a unique surface. They have different stress sensitivities, which are calculated using the Sensitivity framework defined in Section 2.5.2, due the variability in nature and structure of the deposit with depth. By further normalising the data with respect to the appropriate values of stress sensitivity, the stress paths fall within the range of paths defining the intrinsic state boundary surface, as is shown in Fig. 3.2.10. This confirms that Sibari clay has a stable structure due to its layering, as was demonstrated by Coop & Cotecchia (1995). Its stress sensitivity remains constant with plastic strain, that is Sibari clay behaves like a reconstituted clay but with a larger state boundary surface, the volumetric and stress offset being a consequence of structure. Thus, as with other stable clays, the behaviour of Sibari clay pre- and post-gross yield can be described by the Sensitivity framework.

Figure 3.2.11 shows normalised stress paths obtained from undrained tests performed on natural and reconstituted specimens of Bothkennar clay. Details of the tests are given in Table 3.2.3. The natural specimens have been reconsolidated to *in situ* stresses except specimens LUD1 and SUD2 that were compressed, anisotropically and isotropically respectively, to stresses greater than the gross yield stresses. The specimens reconsolidated to *in situ* stresses were compressed isotropically to a value of p' equal to the value of *in situ* horizontal effective stress, then the vertical effective stress was increased to reach its *in situ* value. The reconstituted specimens were consolidated and swelled back to different levels of overconsolidation. As above, the stress paths have been normalised for volume, by the equivalent pressure proposed in Section 1.7, and for composition, by the friction coefficient M. The stress paths for the reconstituted specimens are inside the intrinsic state boundary surface which was found to have a shape similar to the Modified Cam Clay state boundary surface, and reach failure on the intrinsic critical state line on this surface. The stress paths for the natural specimens, taken from different depths, lie outside the intrinsic state boundary surface. They do not form a unique state boundary surface, as the natural samples have been retrieved from different facies in the clay sequence. When the data are further normalised by the value of sensitivity at the start of shearing, the stress paths fall within a single state boundary surface (Fig. 3.2.12). Sensitivity has been calculated as the stress sensitivity by using the Sensitivity framework when data were available, otherwise by using the strength sensitivity as defined by Equation 2.3.1 and assuming that strength and stress sensitivity were equivalent up to gross yield. The stress path of the reconstituted specimen B51, which was normally consolidated before shearing, starts from the K_0 normal compression line on the normalised state boundary surface, and follows this surface to the critical state line. The stress paths of the two other reconstituted specimens B71 and B72, which were swelled to different levels of overconsolidation before shearing, rise at almost constant mean effective stress to reach a peak

deviatoric stress on the normalised state boundary surface, then they follow this surface to the critical state line. Natural clays with a stable structure would show behaviour similar to that of the reconstituted clays. However the end points of the stress paths for the natural Bothkennar clay are inside the normalised state boundary surface, emphasising that the clay has a metastable structure which is undergoing destructuration during shearing. The stress points corresponding to peak deviatoric stresses or gross yield are very close to the normalised state boundary surface, indicating that up to the peak, the amount of destructuration occurring is not significant.

Figure 3.2.13 shows normalised stress paths obtained from drained tests performed on natural and reconstituted specimens from Pisa clay (data from Callisto, 1996). For each set of specimens, the tests consisted of four drained probes, starting from the estimated *in situ* state and loaded by a stress path in a constant direction. The tests, summarised in Table 3.2.4, are described by a letter (A for natural, R for reconstituted) and the angle of direction of the stress path to the horizontal. As above, the stress paths have been normalised with respect to volume and composition. The *in situ* stress state for the reconstituted clay lies within the intrinsic state boundary surface which again has a shape similar to that defined in the Modified Cam Clay soil model. The end states of the normalised stress paths R0 and R30 are close to the intrinsic isotropic and K_0- normal compression lines on the state boundary surface, as would be expected in the Critical state framework. Also, stress path R60 approaches failure on the intrinsic critical state line on the state boundary surface. It is suspected that shear planes developed during test R90, causing the specimen to strain-soften, which would explain the apparent failure of the specimen before reaching the critical state point. The *in situ* stress state for the natural clay lies outside the intrinsic state boundary surface. The stress paths, unlike those of the reconstituted specimens, do not reach end points on a surface representing the locus of stable states or the state boundary surface. The stress paths reverse in direction and tend to states closer to the intrinsic state boundary surface. The maximum stress states at which the stress paths reverse in direction have been identified as gross yield points (Callisto, 1996), and the normalised gross yield curve obtained has a shape similar to that of the intrinsic state boundary surface. After normalising by the stress sensitivity, determined from isotropic compression test data obtained from tests performed on a sample from the same sub-layer, the *in situ* stress states of the natural and reconstituted samples coincide, as is shown in Fig. 3.2.14. If the stress sensitivity used is correct, this implies that the natural and reconstituted samples are at the same state with respect to the state boundary surface at the start of shearing, and that very little destructuration occurred during the reconsolidation stage. Figure 3.2.15 shows points representing the magnitude of accumulated plastic strain during the drained probes. The structure surface defined by the normalised stress paths coincides with the contour of magnitude of accumulated plastic strain equal to 5%. This indicates that destructuration must have occurred before gross yield, causing the size of the state boundary surface to reduce. The surface defined by the stress points where

the normalised stress paths reverse in direction is well within the normalised state boundary surface for the reconstituted clay (Fig. 3.2.14). The value of sensitivity used in the normalisation is therefore too high. The value of sensitivity has reduced before gross yield, and the outer surface defined for the natural clay corresponds to the shrunk state boundary surface, for which the size is represented by the reduced value of sensitivity.

3.2.3 Summary

For the three reference clays, normalisation with respect to volume and composition only is not sufficient. Structure must be taken into account. The normalisation proposed by Cotecchia & Chandler (2000) in Section 2.5.3, which is based on the Sensitivity Framework, can be applied to Sibari clay which has a stable structure. Normalised with respect to both volume and structure, the natural Sibari clay behaves like the reconstituted clay, within a normalised state boundary surface close to the intrinsic surface. The normalisation allows for the volumetric offset resulting from the layering of the clay. Ingram (2000) successfully used a similar approach to account for stable structure in modelling the behaviour of the stiff overconsolidated Oxford and Boom clays.

The clays from Bothkennar and Pisa have a metastable structure. When normalised with respect to volume and structure, the stress paths of the natural clay fall within or on the normalised state boundary surface. For natural Bothkennar clay specimens the gross yield points are close to this curve, showing that up to gross yield only a small amount of destructuration takes place. For Pisa clay contours of magnitude of plastic strain increment indicate that some destructuration has occurred before gross yield. It also shows that the destructuration occurred in parallel with a reduction in stress sensitivity. Therefore clays with a metastable structure cannot always be described by the Sensitivity framework which states that such clays have a stress sensitivity that is quasi constant up to gross yield, and equivalent to strength sensitivity.

Cotecchia & Chandler (2000) established that natural and intrinsic state boundary surfaces have similar shapes (Section 2.3.3). Therefore the value of stress sensitivity determined according to the Sensitivity framework gives a good estimation of the ratio of the size of the state boundary surface of the natural clay to that of the reconstituted clay up to gross yield. Existing models assume that the onset of destructuration corresponds to plastic yield. In kinematic and bounding plasticity models, which simulate the start of plastic deformations within the state boundary surface, destructuration starts inside the state boundary surface (Kavvadas and Amorosi, 2000; Rouainia and Muir Wood, 2000). The onset of significant destructuration occurs as the stress state approaches the bounding surface, with the stiffness decaying dramatically, and this stress state is recognised as gross yield to match experimental

evidence. In the following section, the behaviour of natural clays post-gross yield is investigated.

3.3 BEHAVIOUR POST-GROSS YIELD

3.3.1 Effects of metastable structure on the behaviour of soft natural clays post-gross yield

It has been seen above that while Sibari clay, which has a stable structure, behaves in the same way both pre- and post-gross yield, Bothkennar and Pisa clays do not. Their behaviour cannot be normalised in the way proposed above, which assumes a constant stress sensitivity pre- and post-gross yield. Instead, the normalised stress paths show a sharp bend at gross yield and tend towards a stable state inside the normalised state boundary surface. This is visible both in volumetric and stress space.

Figures 3.3.1, 3.3.2 and 3.3.3 show compression curves for the three reference clays in a normalised plot of the logarithm of v_n, defined as in section 1.7, against the logarithm of the mean effective stress p'. At large strains, the compression curves for Sibari clay remain parallel to the intrinsic normal compression line, but offset to the right. According to the Sensitivity framework, this means that the stress sensitivity remains constant with plastic volumetric straining. After gross yield, the compression curves of Bothkennar and Pisa clays fall below the natural normal compression line and some of them converge towards a line of stable states. According to the Sensitivity framework, this indicates that stress sensitivity is reducing with plastic volumetric strain. The metastable structure of the clays is disturbed and changes with plastic volumetric strain. The size of the state boundary surface of the natural clay projected on successive elastic walls becomes closer to that of the reconstituted clay as the soil is compressed, as is illustrated in Figure 3.3.4. What this diagram cannot show is the effect of plastic strains during shearing which causes a reduction in size of the state boundary surface of the natural clay towards the intrinsic state boundary surface.

In stress space, the paths from drained and undrained tests performed on Sibari clay, normalised as described above, follow the normalised state boundary surface to the intrinsic critical state line (Fig. 3.2.10). Therefore even at large strains the offset of the natural state boundary surface is constant and of magnitude similar to the value of stress sensitivity. For stable clays such as Sibari clay, stress sensitivity remains constant with both plastic volumetric and shear strains, and is equivalent to the strength sensitivity even post-gross yield or post-peak. For metastable clays such as Bothkennar and Pisa clay, the normalisation proposed by Cotecchia & Chandler (2000) is not valid after gross yield. This is shown in Figs. 3.2.12 and 3.2.14, where the drained and undrained stress paths, normalised with respect to both volume

and initial stress sensitivity at the start of shearing, fall below the normalised state boundary surface after gross yield. Figure 3.3.5 shows normalised stress paths of undrained tests performed on natural Bothkennar clay specimens, SUD2 and LUD1, that have been reconsolidated beyond yield, isotropically and anisotropically respectively, before shearing. The stress paths have been normalised by volume (equivalent pressure p_{ie}^{*}) and by the initial stress sensitivity (S_t) at the start of consolidation, defined as the ratio of the mean effective stress at gross yield to the equivalent pressure on the corresponding intrinsic normal compression line. Both specimens have been allowed to creep before shearing (see Figure 3.3.6), thus they are inside the state boundary surface at the start of the shearing stage. In Figure 3.3.5, the stress paths followed by both specimens start well inside the initial state boundary surface, due to the effect of creep and to the significant amount of destructuration that occurred during the consolidation stage. The consolidation curves of both tests are shown in Figure 3.3.6. For each specimen the stress sensitivity at the end of creep can be calculated by extrapolating the compression curves of the natural clay down to the value of specific volume reached after creep. This is illustrated in Figure 3.3.6 for specimen SUD2 for which the stress sensitivity can be calculated directly from the compression curve. For specimen LUD1, which was compressed one-dimensionally, the stress sensitivity at the end of creep was calculated using an isotropic preconsolidation pressure that was determined assuming that the shape of the state boundary surface for the natural clay is similar to that of the Modified Cam Clay model.

Figure 3.3.7 shows the stress paths followed by specimens SUD2 and LUD1, normalised with respect to volume and stress sensitivity, using the reduced value of sensitivity at the end of creep (S_{tc}). With such a normalisation the difference between the natural current and intrinsic state boundary surfaces is accounted for. The stress paths followed by specimens SUD2 and LUD1 start inside the normalised state boundary surface due to the effect of creep. The stress path followed by specimen LUD1 reaches peak strength on the normalised state boundary surface then, unlike stable clays, it bends and goes towards a critical state well inside the normalised state boundary surface. Both tests being undrained, if destructuration were dependent on volumetric strain only, the stress paths would move towards a critical state on the normalised state boundary surface. Since the stress paths clearly go inside the normalised state boundary surface, the behaviour of the natural specimens cannot be normalised for volume, therefore plastic shear strain must cause destructuration as well. The strain-softening occurring post-peak strength implies that the value of strength sensitivity, defined as the ratio of the current shear strength of the natural clay to that of the reconstituted clay, is reducing with plastic shear strain.

In plasticity theory, critical state occurs at the apex of the plastic potential contour, where the increment in plastic volumetric strain is equal to zero. In soils with an associated flow, the yield surface and plastic potential contour are coincident, and critical state occurs at

the apex of the yield surface. If a state boundary surface is normalised for volume, the critical state should occur at the apex of the normalised state boundary surface. Isotropic compression tests have already shown that destructuration occurs with plastic volumetric strain. If natural clays are assumed to follow the normality rule, then they should reach critical state on the state boundary surface. This implies that during undrained compression, if the normalised stress paths reach the state boundary surface at the peak deviatoric stress, they stay on it and as the samples are strain-softening the size of the surface decreases at constant specific volume. Thus during undrained shearing the reduction in size of the state boundary surface must be predominantly due to plastic shear strain.

To summarise, there is experimental evidence that in isotropic compression, the value of current stress sensitivity reduces after gross yield as the compression curve of the natural soil converges towards a line equal to or parallel to the isotropic intrinsic compression line. Also, that during undrained shearing, the value of current strength sensitivity reduces as the shear strength decreases after reaching a peak value. Thus sensitivity, which changes in parallel to destructuration and tends to an asymptotic value representing stable states, appears to be a good parameter to represent natural structure and its subsequent changes with plastic strain. The Sensitivity framework (Cotecchia and Chandler, 2000) assumes that very little destructuration occurs before gross yield, and that stress sensitivity and strength sensitivity are equivalent up to gross yield, that is, whilst the value of sensitivity is approximately constant. However the equivalence has not been proven after gross yield, when sensitivity is reducing significantly. There are no available data to verify this hypothesis, but the reasonableness of assuming the equivalence between stress and strength sensitivity post-gross yield will be assessed in the next section. This will allow to determine whether sensitivity can be used as a single parameter to describe destructuration during both volumetric compression and undrained shearing. Also, by assuming the equivalence between stress and strength sensitivity post-gross yield, the effect of destructuration is represented as a change in size of the state boundary surface with plastic volumetric and shear strain, but not a change in shape. This makes it possible to isolate the effects of structure into a single feature, which is the size of the state boundary surface, and to express these effects as the ratio of the size of the state boundary surface of the natural clay to that of the corresponding reconstituted clay. The implementation of this approach into an existing model will be comparatively easy, and structure will be represented by a parameter, sensitivity, that has been defined rigorously.

Given this assumption, the following section investigates which simple function of plastic volumetric and shear strain is appropriate for use in a destructuration law. To do so, it is assumed that during isotropic compression the natural clay lies on the state boundary surface post-gross yield. It is also assumed that during undrained shearing the stress state of the natural clay lies on the state boundary surface post-peak strength.

3.3.2 Characterisation of destructuration

The previous section showed that both plastic volumetric and shear strains cause destructuration, leading to a reduction in sensitivity. There is experimental evidence that the onset of significant destructuration is coincident with contours of strain energy as defined in Section 2.4 (Tavenas *et al.*, 1979; Callisto, 1996). Therefore destructuration should depend on both stress state and plastic strain. In constitutive models in which flow is associated, the vector of plastic strain increment is always linked to the current stress state. Thus strain energy is directly related to the magnitude of the vector of plastic strain increment, and indirectly to its direction thus the onset of significant destructuration may be associated with the magnitude and direction of the vector of plastic strain increment.

Existing models simulate the effects of structure and degradation of structure in the size of a bounding surface (see section 2.4). In these models, the size of the bounding surface is governed by two competing terms, the Modified Cam-Clay hardening rule, which causes the surface to expand or contract with plastic volumetric strain, and a destructuration law which causes the size of the bounding surface to reduce with a damage strain. This damage strain is usually a general function of plastic volumetric and shear strain, and is defined by several parameters that need to be determined by a number of different tests. As a result, the bounding surface normalised by volume only does not describe a unique state boundary surface. The size of the state boundary surface changes with both plastic volumetric and shear strain. In addition, existing models assume that the state boundary surface of the natural clay will always reduce to that of the reconstituted clay in the limiting case of infinite plastic strain. As was seen in the example of Bothkennar clay in Figure 3.3.2, as the clay destructures in some cases it does not appear that it will ever reach the intrinsic state and in this case it therefore seems to have some stable elemenst of structure as well as metastable. In the following the causes of destructuration are investigated in order to find an appropriate expression to be used in a damage function. It is accepted that this will be some function of plastic strain. The limiting conditions are also investigated, particularly at large strain to try to define what controls the limiting size of the state boundary surface.

(i) Defining an appropriate damage strain

In order to establish an appropriate damage function, the relationship between plastic strain and a measure of change in sensitivity must be investigated.

The simplest form of destructuration law would consist of a damage function that was dependent only on plastic volumetric strain. In that case, the combination of the hardening rule with the destructuration law would give a simple function of plastic volumetric strain governing

all changes in the size of the bounding surface. Also, the state boundary surface would be stable, but of a shape in q'-p'-v space different to that of the state boundary surface of the reconstituted clay. However destructuration occurs in undrained shearing, where plastic volumetric strains are very small, as well as in isotropic compression, where they dominate. Therefore it seems unlikely that the same function could successfully describe degradation of structure in terms of plastic volumetric strain for both loading paths. Table 3.3.1 shows the magnitudes of plastic volumetric strain, $\Delta\varepsilon_v^p$, and plastic shear strain, $\Delta\varepsilon_s^p$, occurring post-gross yield, or post-peak, in isotropic and K_0 compression tests, drained probes and undrained shearing tests, performed on Pisa clay and Bothkennar clay. The magnitudes of plastic strain were derived by calculating the total volumetric and shear strains, directly from the test data and then subtracting elastic volumetric and shear strains computed assuming isotropic elasticity (Graham and Houlsby, 1983). The quantity $\Delta\varepsilon^p$ is also shown in the table, and represents the modulus of the vector of increment of plastic strain, calculated as;

$$\Delta\varepsilon^p = \sqrt{\Delta\varepsilon_v^{p^2} + \Delta\varepsilon_s^{p^2}} \tag{3.3.1}$$

In the following, $\Delta\varepsilon^p$ will be referred to as the plastic strain increment. It is assumed that post-gross yield, or post-peak, the stress state lies on the state boundary surface. Therefore for each stress point (p',q') post-gross yield or post-peak, sensitivity can be calculated as the ratio of the preconsolidation pressure, p_c', corresponding to the mean effective stress at the intersection of the state boundary surface with an elastic wall, to the equivalent pressure, p_{ie}^*, defined earlier and also shown in Figure 3.3.8. The values of change in sensitivity, Δs, are also shown in Table 3.3.1. It should be noted that this approach can only be used on data that result from stress paths that cause the bounding surface to expand in spite of destructuration. The figures in Table 3.3.1 show that destructuration occurs in isotropic compression, drained and undrained shearing. It was seen in Section 2.5.1 that the rate of change is proportional to the initial sensitivity. Therefore, as all tests were performed on different samples, particularly samples from Bothkennar clay retrieved from different facies, the reduction in sensitivity should be related to the initial value of sensitivity in the sample. For that purpose change in sensitivity has been normalised with respect to the value of sensitivity at gross yield or peak, and this quantity is shown in Table 3.3.1 as $\Delta s/s_0$. The relative influence of volumetric and shear strain on destructuration is examined by calculating the rates of change of normalised sensitivity with plastic volumetric strain, plastic shear strains, and plastic strain increment respectively, where plastic strain increment has been defined as in Equation 3.3.1. For example the rate of change of

normalised sensitivity with plastic volumetric strain is calculated as $\frac{1}{s_0}\frac{\Delta s}{\Delta \varepsilon_v^p}$. The values obtained for the different tests on Bothkennar and Pisa clay are shown in the last three columns of Table 3.3.1.

The data analysed for Pisa clay were obtained from a specimen compressed isotropically from an isotropic state (test 19B), three specimens subjected to drained probes (tests A0, A30 and A90 respectively), and a specimen sheared undrained (test AUC), all performed by Callisto (1996). In these tests, the reduction in sensitivity varies from 3% for the test on specimen A0 to 50-55% for the tests on specimens AUC and 19B. This variation seems to be related to the change in plastic strain achieved during the test (4% plastic volumetric strain for the test on specimen A0 against 32% for the test on specimen 19B). As expected, in the test on specimen 19B there was no plastic shear strain (pure compression), but 32% plastic volumetric strain, whilst only 1% plastic volumetric strain occurred during the test on specimen AUC (undrained), but 27% plastic shear strain. This leads to an infinite value of rate of change in s/s_0 with plastic shear strain, and a small value for the rate of change of s/s_0 with plastic volumetric strain (-1.8), for the test on specimen 19B. By contrast, for the test on specimen AUC the rate of change of s/s_0 with plastic volumetric strain is large (-50.5) but the rate of change of s/s_0 with plastic shear strain is small (-1.9). Similarly, for the test on specimen A90 (constant p′) the rate of change of s/s_0 is large with plastic volumetric strain (-54.5) and small with plastic shear strain (-1.8). Therefore change in sensitivity must be dependent on both plastic volumetric and shear strains. Plastic strain increment combines both strains, and is formulated so that plastic volumetric and shear strains have the same influence on destructuration. The values of rate of change in s/s_0 with plastic strain increment show good agreement for all tests except the test on specimen A0. This can be attributed to the simplistic approach applied to little data, which is meant to give a clear but approximate indication of the various influences of plastic strain on the destructuration process. However for all other tests, including the test on specimen A30 in which similar magnitudes of plastic volumetric and shear strain occur, the rates obtained vary very little, between -1.4 and -1.9. This is illustrated in Figure 3.3.9. In particular, Figure 3.3.9c shows change in normalised sensitivity plotted against change in plastic strain, with a best fit line to the data points. The correlation coefficient is equal to 0.99, confirming that direct proportionality exists between increment of change in normalised sensitivity and increment of plastic strain, which is equivalent to an exponential relationship between sensitivity and plastic strain. Figure 3.2.15, in which the structure surface was shown to coincide with the contour of plastic strain increment equal to 5%, also demonstrates that plastic strain increment forms an appropriate damage strain for Pisa clay.

The data analysed for Bothkennar clay were obtained from a range of specimens subjected to tests, such as isotropic and anisotropic compression from an initial isotropic state, drained probes and undrained compression tests. The reduction in sensitivity varies from 14% to 62%. As expected, no plastic shear strain occurred during the isotropic test on specimen SUD2 and very little plastic shear strain occurred during test on specimen LCD0, which was compressed from an anisotropic state, whilst very little plastic volumetric strain occurred during the undrained tests on specimens SH13, L23 and SH5. During the tests on specimens LCD55, LCD70 and B86, both volumetric and shear strains would have influenced destructuration. Values for the rate of change in s/s_0 with plastic volumetric strain and with plastic shear strain separately vary over a large range, between about -1 and -177, due to the different modes of loading, as was noticed for Pisa clay. For example, for the undrained test on specimen L23, the rate of change of normalised sensitivity with plastic volumetric strain is very large (-78) but the rate of change of normalised sensitivity with plastic shear strain is small (-1.7), in contrast for test on specimen LCD0 (isotropic compression) the rate of change of normalised sensitivity with plastic volumetric strain is small (-2), but very large with respect to plastic shear strain (-177). The values of change in normalised sensitivity with plastic strain increment vary very little for the different tests, between –1.2 and –3, except for tests SUD2 and LUD1. This is certainly due to the simplistic approach, which for these two tests is applied for a change in strain which is approximately an order of magnitude lower than for the other tests. The relationships between change in normalised sensitivity and increment of plastic volumetric or shear strain or increment of plastic strain are shown in Figure 3.3.10. Figure 3.3.10c shows change in normalised sensitivity plotted against increment of plastic strain. Even if the data points show some scatter, there is a visible trend, with a correlation coefficient equal to 0.6, showing that assuming direct proportionality between increment of change in sensitivity and increment of plastic strain is not unrealistic. The scatter can be attributed to the fact that the samples were retrieved from different facies. In particular the behaviour of specimens L23 and B86 is suspected to be affected by fabric, of which the effect is apparently to slow down the net rate of destructuration. This implies that if accounting for fabric, for a given increment of plastic strain the change in normalised sensitivity will be higher than that given in Table 3.3.1, and the points for these specimens, which are highlighted in Figure 3.3.10c, will become aligned with the other points. Only the point that represents specimen SH5, which was recovered from the mottled facies and showed peculiar features during the undrained shearing, is far from the best-fit line.

By analysing a wide range of tests, drained and undrained, it has been demonstrated that plastic volumetric strain and plastic shear strain have a combined effect on destructuration, therefore they cannot be used individually in a constitutive model for soft clays. A function of plastic strain has been proposed, that combines both plastic volumetric and shear strain in equal

proportions. This is the plastic strain increment defined in Equation 3.3.1. Values for the rate of change of normalised sensitivity and this plastic strain increment derived from experimental data fit the assumption of a linear relationship. Thus the choice of a damage strain where plastic volumetric and shear strain have similar importance is backed up by experimental evidence. In the description of the model to come, the damage strain will be taken equal to the plastic strain increment defined in Equation 3.3.1. Furthermore, the linearity between damage strain and change in normalised sensitivity implies that change in sensitivity can be expressed as an exponential function of the integral of this damage strain.

(ii) Limiting values of sensitivity

It is always assumed that metastable clays tend to a state on loading which is characteristic of the reconstituted clay rather than the natural clay. In existing models for structured clays this assumption is expressed in the damage function, which is such that the bounding surface of the natural clay reduces to the bounding surface of the reconstituted clay at large strain. For example the model derived by Rouainia and Muir Wood (2000) has a structure locus for the natural structured clay and a reference locus for the reconstituted clay. The structure locus collapses to be coincident with the reference locus with plastic strain. However experimental evidence shows that some metastable clays become stable before reaching the intrinsic state boundary surface (Coop *et al.*, 1995). This is attributed to fabric in the natural clay, which is not destroyed even at very large strain. Figure 3.3.11 shows data from one-dimensional compression of Bothkennar clay (specimen B86), plotted as ln$v$-lnp'. The sample was retrieved from the bedded facies, so it is expected that fabric may influence its behaviour. The data lie well outside the intrinsic normal compression line, and show an abrupt gross yield marked by a sudden increase in compressibility. However at large strains the compressibility reduces and becomes constant at the same value as that for the reconstituted clay, such that the data plot on a line parallel to the intrinsic normal compression line, but at higher values of volume. The clay has become stable before reaching the intrinsic state boundary surface. Therefore the sensitivity has asymptotically reduced to a stable value higher than unity, which means that in the sample the effects of fabric are not negligible. In this case the natural soil has a limiting value of sensitivity, greater than one. This is a reasonable hypothesis since in soft clays fabric can have a significant effect, as shown for example in Sibari clay.

Figure 3.3.12 shows graphs of sensitivity against plastic strain increment for the three reference clays, where sensitivity and plastic strain have been calculated as defined earlier in this section. In Fig. 3.3.12a, data from undrained shear tests on specimens SH13 and L23 of Bothkennar clay, and from the one-dimensional compression test on specimen B86, are shown. Specimens B86 and L23 were retrieved from the bedded facies, and specimen SH13 from the

laminated facies. Data for the test on specimen B86 show that the value of sensitivity becomes stable at strains greater than 20%, the ultimate value of sensitivity being approximately equal to 1.7. Tests on specimens SH13 and L23 have not reached high enough shear strains for it to be possible to evaluate their ultimate sensitivity, even though in the test on specimen L23 there appears to be a decrease in the rate of destructuration after 10% plastic strain. It is expected that in specimen L23, which was retrieved from the bedded facies, the effects of fabric would be significant. In Figure 3.3.12b, data from tests on specimens A0, A30, A60 and A90 performed on Pisa clay are shown. Again the tests were not taken to sufficiently high strains to determine whether there are significant effects of fabric, but oedometer tests showed that Pisa clay tends to reach a state on loading characteristic of the reconstituted clay (Fig. 2.4.4). Finally Fig. 3.3.12c shows data from tests CS1 and CS21 performed on natural Sibari clay. The behaviour of Sibari clay is different from the two other clays. Test CS1 started with a low sensitivity, very close to unity, which remained constant during shearing. Test CS23 started with a sensitivity of about 4.5, which also remained constant with plastic strain. This is typical of stable clays with structure dominated by fabric and with no bonding.

To summarise, effects of fabric can be significant even in metastable clays. A simplified definition of natural structure is to divide structure into two types; fabric and bonding, the fabric being the cause of stable behaviour, the bonding, which breaks with plastic strain, being the cause of metastable behaviour. The main effects of bonding have been reviewed in Section 3.3. The main effect of fabric is to cause metastable clays to become stable before reaching states that are typical of the reconstituted clay. In terms of modelling, this means that the sensitivity reduces to a stable value greater than unity. A destructuration law for natural clays should allow for effects of fabric to be simulated, by causing the sensitivity to reduce asymptotically to a stable value.

3.4 IMPLICATIONS FOR NUMERICAL MODELLING

The behaviour of soft natural clays is described by state, stress history and structure (see Section 2.2). Despite the great variability of their structures, soft clays follow general principles of behaviour. The main features of behaviour of soft natural clays can be divided into similarities and differences from the behaviour of reconstituted clays, and have been gathered into coherent frameworks, such as the Sensitivity framework by Cotecchia & Chandler (2000). This constitutes a basis for extending an existing model for reconstituted clays to predict the behaviour of soft natural clays.

3.4.1 Important characteristics of the behaviour of soft natural clays

The following list gives the important effects of structure on the behaviour of soft natural clays and the characteristics of destructuration that should be included in models for soft clays.

(a) Structure leads to a larger state boundary surface similar in shape to that of the state boundary surface of the reconstituted clay.
(b) The ratio of the size of the state boundary surface of the natural clay to that of the reconstituted clay is of magnitude equal to current sensitivity.
(c) Both plastic volumetric and shear strains cause destructuration.
(d) Destructuration is associated with a reduction in sensitivity, causing in undrained tests a reduction in the size of the natural state boundary surface.
(e) Destructuration is progressive, and becomes significant on reaching gross yield.
(f) The state boundary surface of the natural clay shrinks to reach a stable state boundary surface, not necessarily that of the reconstituted clay.

3.4.2 Appropriate models

The progressive aspect of degradation of structure can only be predicted by models that allow plastic deformation to occur within the state boundary surface, such as bounding surface models (Dafalias & Herrmann, 1980) or kinematic hardening models (Al Tabbaa & Wood, 1989; Stallebrass & Taylor, 1997). In such models, the cumulative plastic strains lead to progressive destructuration. Both bounding surface models and kinematic hardening models include advanced features of soil behaviour, such as non-linearity and the distinction between loading and unloading events. However only kinematic hardening models predict stress-induced anisotropy and different stress-strain responses associated with different recent stress histories, the kinematic surfaces carrying a memory of the previous stress paths. Some authors have argued that structural anisotropy should be included in models for natural clays. It was stated at the beginning of this chapter that this project is concerned with providing a simple model to simulate the general effects of destructuration in soft natural clays, and therefore structural anisotropy will not included in the model presented in the following chapter.

CHAPTER 4 A THREE-SURFACE MODEL FOR SOFT CLAYS

4.1 INTRODUCTION

The conclusions drawn from the two previous chapters are applied to the development of a new model for soft natural clays from an existing model for reconstituted clays. The chapter is divided into two main sections: firstly the base model is described and evaluated, secondly the derivation of the new model is explained.

Chapter 2 reviewed the behaviour of soft natural clays observed in laboratory tests, notably by highlighting the similarities and discrepancies between the behaviour of the natural and reconstituted soil. In Chapter 3 it was concluded that sensitivity, which decreases in parallel to destructuration to reach asymptotically an ultimate value representing the sensitivity of the equivalent stable clay, is a good parameter to use to describe current structure in soft clays. In the same chapter, it was also demonstrated that current structure or sensitivity can be assumed to change with a damage strain that can be expressed as the magnitude of the vector of plastic strain increment. In this chapter, it will be shown how a simple exponential destructuration function of this damage strain can be used to extend an existing model for reconstituted clays to predict the behaviour of soft clays.

The base model is the 3-SKH model that was initially developed by Stallebrass (1990). Variations of the 3-SKH model have been developed since it was first formulated; they include the addition of anisotropic elasticity (Jovicic, 1997), and volumetric creep (Ingram, 2000). The model can simulate advanced features of soil behaviour such as stiffness non-linearity and the effect of recent stress history, which allows it to predict successfully the behaviour of stiff reconstituted clays at small strains. However soft clays generally reach gross yield under engineering working loads, thus it is critical for design on these clays to be able to predict their behaviour at large strain. In Section 4.2.4 the ability of the 3-SKH model to predict large strain behaviour will be evaluated by comparing predictions with experimental data from tests performed on reconstituted specimens from two soft clays, Bothkennar clay and Pisa clay that have been described in Section 3.2.1. Confidence in model predictions of the behaviour of reconstituted clays will support the use of the 3-SKH model as a base model, as well as providing a source of data which can be used to help interpret predictions of the behaviour of natural clays using the new model.

4.2 THE THREE-SURFACE KINEMATIC HARDENING MODEL

The three-surface kinematic hardening (3-SKH) model was developed by Stallebrass in 1990. It was derived from the two-surface ('bubble') model formulated by Al Tabbaa (1987), and

incorporates an additional yield surface to predict the effect of recent stress history on the behaviour of reconstituted clays.

In the following a brief description of the 3-SKH model is given. This description concentrates on the aspects of the model that best characterise its capability to predict stiffness non-linearity and recent stress history. First the three surfaces are defined and the way they inter-relate is explained. Then the derivation of the hardening rule is detailed, as it will be one of the two components of the new hardening rule. The translation rules for the 3-SKH model are not described here but can be found in Stallebrass (1990). Details of the derivation of the translation rules for the new model, that have been obtained by following the same approach as used in Stallebrass (1990), will be given in Section 4.3.3.

4.2.1 Description of the model

The model was originally defined in triaxial stress space. It consists of two kinematic surfaces lying within the Modified Cam-Clay state boundary surface (Fig. 4.2.1). The intersection of the Modified Cam-Clay state boundary surface with an elastic wall forms the *bounding* surface, as it was named by Al Tabbaa & Wood (1989). The equation of the bounding surface in q'-p' plane is;

$$(p'-p_0')^2 + q'^2 / M^2 = p_0'^2 \qquad (4.2.1)$$

where p_0' equals half the length of the major axis of the bounding surface or half the preconsolidation presssure. The bounding surface is symmetrical about the p'-axis and passes through the origin; thus p_0' also defines the centre of the bounding surface.

The two kinematic surfaces are similar in shape to the bounding surface, with their size smaller by constant ratios. The history surface, which represents the limit of influence of recent stress history, has centre coordinates (p_a', q_a'). The ratio between its size and the size of the bounding surface is represented by the parameter T. The equation of the history surface is;

$$(p'-p_a')^2 + \frac{(q'-q_a')^2}{M^2} = T^2 p_0'^2 \qquad (4.2.2)$$

The yield surface defines the region in stress space within which only elastic deformations occur. This surface has centre coordinates (p_b', q_b'), and the ratio between its size and the size of the history surface is represented by the parameter S. The equation of the yield surface is;

$$(p'-p_b')^2+\frac{(q'-q_b')^2}{M^2}=T^2S^2p_0'^2 \tag{4.2.3}$$

In the original form of the model, when the stress state of the soil lies within the yield surface, the deformation of the soil is isotropic elastic and is calculated by the equations;

$$\begin{bmatrix}\delta\varepsilon_v^e\\ \delta\varepsilon_s^e\end{bmatrix}=\begin{bmatrix}\kappa/p' & 0\\ 0 & 3G_e'\end{bmatrix}\begin{bmatrix}\delta p'\\ \delta q'\end{bmatrix} \tag{4.2.4}$$

where G_e' is the elastic shear modulus.

Some changes have since been made to this expression. New versions of the model, which are now more commonly used, include anisotropic stiffness (after Graham & Houlsby, 1983) and small strain stiffness varying with state and stress (after Viggiani & Atkinson, 1995). The latter is the version that has been used here, and will be described in more detail in Section 4.2.3.

4.2.2 Hardening rule

The hardening rule was developed by Stallebrass (1990) following that formulated for the 'bubble' model by Al Tabbaa (1987). It is the same as the Modified Cam-Clay hardening rule;

$$\delta p_0'=\frac{p_0'}{\lambda-\kappa}\delta\varepsilon_v^p \tag{4.2.5}$$

where λ and κ are the compression and swelling parameters derived from a ln$v$-lnp' graph. This rule applies to all surfaces, so that the expansion or contraction of all three surfaces is directly related to changes in plastic volumetric strain. Plastic deformations follow the normality rule so the vector of plastic strain increment is always normal to all three current surfaces. Increments of plastic volumetric and shear strain can be calculated by combining the hardening rule and the normality rule, to give the equation;

$$\begin{bmatrix}\delta\varepsilon_v^p\\ \delta\varepsilon_s^p\end{bmatrix}=\frac{1}{h}\begin{bmatrix}(p'-p_b')^2 & (p'-p_b')\frac{(q'-q_b')}{M^2}\\ (p'-p_b')\frac{(q'-q_b')}{M^2} & \left(\frac{(q'-q_b')}{M^2}\right)^2\end{bmatrix}\begin{bmatrix}\delta p'\\ \delta q'\end{bmatrix} \tag{4.2.6}$$

The model defines the hardening modulus as a function $h = h_0 + H_1 + H_2$, with:

$$h_0 = \frac{(p'-p_b')}{(\lambda-\kappa)}\left[p'(p'-p_b')+q'\frac{(q'-q_b')}{M^2}\right] \qquad (4.2.7)$$

This expression is similar to the hardening rule used in the Modified Cam-Clay model, and was derived by substituting into the consistency equation for the yield surface and using the translation rule for the case when the surfaces are in contact. Following Al Tabbaa (1987) the functions H_1 and H_2 were added to h_0 by Stallebrass (1990) to solve a problem of instability at a number of points on the kinematic surfaces. The values of H_1 and H_2 were defined so that when two or more surfaces are in contact there is continuity in stiffness. Thus, following Al Tabbaa (1987) and Hashiguchi (1985), Stallebrass (1990) expressed H_1 as a function of b_1, the degree of approach of the history surface to the bounding surface, and H_2 as a function of b_2, the degree of approach of the yield surface to the history surface. The functions H_1 and H_2 are defined by the following equations;

$$H_1 = S^2\left(\frac{b_1}{b_{1\max}}\right)^{\psi}\frac{1}{\lambda-\kappa}p_0'^3 \qquad (4.2.8)$$

$$H_2 = \left(\frac{Tb_2}{b_{2\max}}\right)^{\psi}\frac{1}{\lambda-\kappa}p_0'^3 \qquad (4.2.9)$$

The quantities b_1 and b_2 are defined geometrically when the stress state is on the yield surface only; they are normalised by their maximum values, which occur when the surfaces are in the configuration shown in Fig. 4.2.2. The quantity b_1 is the scalar product of the vector β and the normal to the history surface, $\mathbf{n_h}$, at the conjugate point, divided by the size of the history surface, T. The quantity b_2 is the scalar product of the vector γ and the normal to the yield surface, $\mathbf{n_y}$, at the conjugate point, divided by the size of the yield surface, S (see Fig. 4.2.3). The exponent ψ controls the decay of stiffness inside the bounding surface.

$$b_1 = \frac{1}{Tp_0'}\left[\frac{(p'-p_b')}{S}\left[\frac{p'-p'_b}{TS}-\left[\frac{(p'-p_b')}{S}+p_a'-p_0'\right]\right]+\frac{(q'-q_b')}{SM^2}\left[\frac{q'-q_b'}{ST}-\left[\frac{(q'-q_b')}{S}+q_a'\right]\right]\right] \qquad (4.2.10)$$

$$b_2 = \frac{1}{STp_0'}\left[(p'-p_b')\left[\frac{(p'-p_b')}{S}-(p'-p_a')\right]+\frac{(q'-q_b')}{M^2}\left[\frac{(q'-q_b')}{S}-(q'-q_a')\right]\right] \quad (4.2.11)$$

$$b_{1\max} = 2p_0'(1-T) \quad (4.2.12)$$

$$b_{2\max} = 2Tp_0'(1-S) \quad (4.2.13)$$

The constitutive equations governing plastic deformations are thus;

$$\begin{bmatrix}\delta\varepsilon_v^p\\ \delta\varepsilon_s^p\end{bmatrix} = \frac{1}{h}\begin{bmatrix}(p'-p_b')^2 & (p'-p_b')\frac{(q'-q_b')}{M^2}\\ (p'-p_b')\frac{(q'-q_b')}{M^2} & \left(\frac{(q'-q_b')}{M^2}\right)^2\end{bmatrix}\begin{bmatrix}\delta p'\\ \delta q'\end{bmatrix} \quad (4.2.14)$$

where

$$h = \frac{1}{\lambda-\kappa}\left[(p'-p_b')\left[p'(p'-p_b')+q'\frac{(q'-q_b')}{M^2}\right]+S^2\left(\frac{b_1}{b_{1\max}}\right)^{\psi}p_0'^3+\left(\frac{Tb_2}{b_{2\max}}\right)^{\psi}p_0'^3\right] \quad (4.2.15)$$

4.2.3 Determination of model parameters

The three-surface kinematic hardening (3-SKH) model is defined by eight material properties:

λ gradient of the isotropic normal compression line defined in ln$v$-lnp' space

κ gradient of the elastic wall defined in ln$v$-lnp' space

N the natural logarithm of the specific volume on the isotropic normal compression line at $p \leftleftharpoons 1$kPa in ln$v$-lnp' space

M critical state friction coefficient

G_e' elastic shear modulus

T ratio of the size of the history surface to the size of the bounding surface

S ratio of the size of the yield surface to the size of the history surface

ψ exponent in the hardening function defining the rate of decay of stiffness inside the bounding surface

According to Stallebrass (1990) the majority of these properties can be obtained from simple isotropic swelling and recompression tests. Isotropic normal compression allows λ and N to be calculated while κ can be obtained from the initial part of the subsequent swelling curve where the stiffness is considered to be elastic. Values of T and S can be determined by plotting bulk modulus K' against mean effective stress p' as shown in Fig. 4.2.4. The value of S is calculated from the stress change for which the strains are elastic. The value of T corresponds to the stress change at which the two curves converge. If the soil is sheared, the stress ratio at critical state gives the value of M. The exponent in the hardening function ψ cannot be measured directly, and has to be determined by varying the value in a series of predictions of experimental data. The value used is that which gives the best fit with the experimental data. The value of the elastic shear modulus G_e' can be obtained by performing dynamic tests such as bender element or resonant column tests on the sample. When using the variation of the model that allows stiffness to vary with stress and state, the parameters needed in the equation by Viggiani & Atkinson (1995) can be derived from charts proposed by the Authors and checked against values determined experimentally in dynamic tests.

In the following, values for these material properties are calculated for the two reference clays. A summary of the values obtained is given in Table 4.2.1. These values will be used in Section 4.2.4 for the evaluation of the 3-SKH model.

(i) Compression parameters

The compression parameter λ is defined here as the gradient of the isotropic normal compression line in the ln$v$-lnp' plane. According to the critical state framework, the gradients of compression curves resulting from normal compression at any constant stress ratio have the same value. Therefore in practice λ can also be determined from data from constant stress ratio tests. In order to know the position of any point in volumetric space, a fixed point must be known in the ln$v$-lnp' plane, that enables the value of the natural logarithm of the specific volume at $p' \fallingdotseq 1$kPa, N, to be calculated. Figure 4.2.5 shows one-dimensional and isotropic compression curves from reconstituted specimens of Pisa clay plotted in the ln$v$-lnp' plane. Values of p' have been calculated for the oedometer data using a value of K_0 for normally consolidated Pisa clay that was determined by Callisto (1996). Specimen 29B was retrieved from sub-layer B3. Callisto (1996) used clay from sub-layer B3 to make reconstituted specimens, and clay from sub-layer B1 for the natural specimens, on the basis that both layers are homogeneous and have consistent properties. In fact, Pisa clay samples from layers B1 and B3 have been found to have similar index properties, thus it can be assumed that the value of λ is the same for both layers. However in most deposits, samples retrieved from different depths

generally have different index properties, leading to different values of λ. The liquid limit profile for Bothkennar clay varies with depth, thus the values of λ and N also vary with depth. There were two tests on reconstituted samples at different depths and plasticities, and given that the compression parameters of reconstituted clays are generally repeatable and closely dependent on plasticity, an interpolation can be used when no reconstituted test has been conducted. Table 4.2.1 gives the different values of λ and N for the different reconstituted specimens of Bothkennar clay that will be used in the evaluation of the 3-SKH model in Section 4.2.4.

(ii) Stiffness

The value of stiffness at very small strain, G_e', can be determined by bender element or resonant column tests. Viggiani and Atkinson (1995) demonstrated that stiffness at very small strain is dependent on stress level and overconsolidation ratio;

$$\frac{G_e'}{p_r'} = A\left(\frac{p'}{p_r'}\right)^n R_0{}^m \qquad (4.2.16)$$

where p_r' is a reference stress (1kPa), R_0 is the overconsolidation ratio and A, m and n are constants. They defined empirical relationships relating the plasticity index and the stiffness constants for stiff clays; these are shown in Figure 4.2.6. By comparing estimated values from the charts with values of shear modulus derived from bender element or resonant column tests, it is possible to find appropriate values for A, m and n.

Bothkennar clay

Figure 4.2.7 shows values of shear modulus G_e' plotted against the mean effective stress p', where G_e' was determined in bender element tests performed on reconstituted normally consolidated specimens of Bothkennar clay (Coop, 1998). The equation for the dotted line has been determined using the charts in Fig. 4.2.6, it has a gradient n=0.65 and an intercept A=900. The value of m was determined by trial and error by trying to match values calculated using Equation 4.2.16 and values determined experimentally. A value of m=0.25 was determined.

Pisa clay

Values of A, m and n for Pisa clay have been determined by Rampello *et al.* (1996) for sub-layer B3: A=560, m=0.36 and n=0.82. The clay in sub-layer B3 has an average value of plasticity index of 43%. Using the charts from Figure 4.2.6, we find similar values for A and n, but a

slightly lower value of *m, equal to* 0.25 instead of 0.36. In practice this should not lead to very different values of G'_e since the overconsolidation ratio in layers B1 and B3 is not more than 2. Calculation of the elastic shear modulus G_e' at a depth of about 9m in layer B1, where $p' \leftrightarrows 84.5$kPa and $R_0 = 1.98$, gives $G_e \leftrightarrows 27.2$MPa with $m=0.36$ and $G_e \leftrightarrows 25.3$MPa with $m=0.25$. Rampello *et al.* reported that at this depth the value of G_e' measured in low frequency torsional shear tests is about 27.5MPa, and that measured in bender element test and resonant column tests is about 35MPa. At a depth of about 18.5m in layer B3, where $p' \leftrightarrows 137$kPa and $R_0 = 1.27$, calculation using Equation 4.2.16 gives $G_e \leftrightarrows 34.5$MPa for m=0.36 and $G_e \leftrightarrows 33.6$MPa for m=0.25. Experimental values of G_e' obtained at this depth are about 30MPa by resonant column and torsional shear tests, and 43MPa by pulse transmission tests (Rampello *et al.*, 1996). Both the values of $m=0.25$ and $m=0.36$ give values of elastic stiffness that are within the range of values determined experimentally. In the subsequent analyses, the value of $m=0.36$ that was determined by Rampello *et al.* (1996) from a large number of tests will be used.

(iii) Swelling parameter, κ

Bothkennar clay

The swelling parameter κ should be determined rigorously from data from isotropic compression and swelling tests. Such data were only available for Bothkennar clay, and κ was derived by plotting the normalised value of bulk modulus, K'/p', against the normalised change in mean effective stress after a stress reversal, $\Delta p'/p_c'$, where p_c' is the preconsolidation pressure. The two curves corresponding to isotropic swelling from $p_c \leftrightarrows 100$kPa and $p_c \leftrightarrows 200$kPa are shown in Figure 4.2.8. The value of κ is equal to the inverse of K'/p' at the start of unloading. For this sample, the value of κ varies between 0.002 and 0.0035. An average value of $\kappa=0.0028$ will be used in the subsequent analyses.

Pisa clay

For Pisa clay, for which no such test was available, the value of κ has been derived from the values of the shear modulus, G_e' and Poisson's ratio, ν, using the following relationship assuming isotropic elasticity;

$$G_e' = \frac{3(1-\nu)}{2(1+\nu)} \frac{p'}{\kappa}, \qquad (4.2.17)$$

Lings *et al.* (2000) have investigated the anisotropic stiffness parameters of the stiff natural Gault clay, and found that at very small strain the vertical and horizontal Poisson's ratios are

zero or very close to zero. In Figure 4.2.9, Poisson's ratio is plotted against length of stress path for different drained probes on reconstituted Pisa clay. Callisto (1996) calculated Poisson's ratio from computed values of shear and bulk modulus, assuming the clay to be isotropic elastic. The resolution of the strain gauges used during the experiments was not small enough, but the curves show a trend with values of Poisson's ratio tending toward zero at the start of the test. Thus it can be assumed that at very small strain the value of Poisson's ratio in Pisa clay is equal to zero. It has been determined in the previous section that the elastic shear modulus G'_e calculated using Equation 4.2.16 is equal to 27.2MPa at an *in situ* stress state p≒84.5kPa, and G_e≒34.5MPa at p≒137kPa. These values are used here with Equation 4.2.17 to derive the value of κ. In this way a range of values for κ are obtained varying between 0.0046 and 0.0059. An average value of κ=0.0052 will be used in the subsequent analyses.

(iv) Strength parameter

The strength parameter needed for the 3-SKH model is the critical state friction coefficient M (Schofield & Wroth, 1968). It was determined by plotting stress ratio q/p' against shear strain ε_s for a number of drained and undrained tests, as shown in Fig. 4.2.10. The value of M for the two reference clays is assumed to be equal to that determined experimentally on reconstituted samples. Allman & Atkinson (1992) determined a value of M=1.38 for Bothkennar clay from a series of drained and undrained tests (Fig. 4.2.10 (a)). Callisto (1996) determined a value of M=0.78 for Pisa clay from two drained tests that reached failure (Fig. 4.2.10 (b)).

(v) Size of the history surface

Bothkennar clay

The size of the history surface was determined by trial and error. A series of analyses simulating a cycle of isotropic loading-unloading was carried out during which the value of T was varied while values of S and ψ were kept constant, equal to 0.1 and 2 respectively, which are typical values for reconstituted clays, and will in turn be justified later. Figure 4.2.11 shows the effect of varying T on the predicted bulk modulus during the swelling stages from p_c≒100kPa and p_c≒200kPa. Using a small value of T=0.1 leads to over-predicted values of bulk modulus, and using a large value of T=0.7 gives a better fit to the test data, the values of bulk modulus being slightly over-predicted at the beginning of swelling. However using an intermediate value of T=0.5 leads to a rapid decay of stiffness which does not reflect the behaviour of the clay. The best value to characterise the behaviour of the clay appears to be T=0.7, which will then be used in subsequent analyses.

Pisa clay

The value of T to be used to represent Pisa clay was determined using the only tests available on reconstituted samples, which were drained shearing tests from the estimated *in situ* stress with constant directions of the stress paths. Figure 4.2.12 shows the effect of simulating the full stress history, from to the end of consolidation in the oedometer (stress path ABCD), or the recompression history only (stress path BCD). The consolidation procedure followed by Callisto (1996) consisted of compressing the reconstituted specimens one-dimensionally to the preconsolidation pressure, $\sigma_c \leftarrow$200kPa in an oedometer, and swelling back to the estimated *in situ* stress, achieving an overconsolidation ratio of about 1.5. In the first case examined here, the full stress history is modelled, including the total stress relief that occurs when the specimen is taken out of the oedometer and placed in the triaxial apparatus. Then the recompression to the *in situ* stress is simulated. In the second case, only this last part is modelled. The stiffness curves shown in Figure 4.2.12 have been obtained by using a large value of T so that the effect of including the recent stress history is emphasised, that is T=0.5, and S=0.1. As a result, simulating only the recompression leads to the bulk modulus being under-predicted by a factor of up to 2 during the analysis simulating R0, and the shear modulus by a factor of up to 14 during the analysis simulating R90. Including the full stress history to be modelled has the effect of over-predicting the value of stiffness in the analysis simulating R0 by a factor of about 1.5, and gives a good fit with the test data in the analysis simulating R90. It is expected that with any size of surface, modelling only the recompression stages will always lead to the value of stiffness being significantly under-predicted, in particular for analyses simulating R90. This is due to the configuration of the surfaces at the end of recompression; this will be examined in more detail in Section 5.3.1. Here, modelling the full stress history has improved the model predictions of the behaviour of Pisa clay, and therefore in subsequent analyses the whole stress history, that is stress path ABCD, will be simulated.

Figure 4.2.13 shows the effect of varying T on the predicted value of bulk modulus during the analyses simulating tests R0 and R60. Figure 4.2.14 shows the effect of varying T on the predicted value of shear modulus during the analyses simulating tests R90 and R60. During the analyses, the values of S and ψ were again maintained constant, and equal to 0.1 and 2 respectively. The value of T=0.5 is the most appropriate for tests R60 and R90, but over-predicts values of bulk modulus by a factor of 1.5 for the simulation of test R0. However using a value of T=0.3, which gives the best fit for the experimental data obtained from test R0, would lead to values of bulk and shear modulus being under-predicted by a factor of up to 14 by the analysis simulating test R90. Thus the value of T=0.5 appears to be the best compromise to use in the analyses. Figure 4.2.15 shows predicted and experimental stress-strain curves of mean effective stress against volumetric strain obtained from the analysis simulating test R0. At large

strains, the curve obtained using a value of T=0.5 gives the best fit with the experimental data, supporting the choice of T=0.5 for the subsequent analyses.

(vi) Rate of decay of stiffness, ψ

The exponent in the hardening rule, ψ, which represents the decay of stiffness inside the bounding surface, cannot be determined directly from laboratory tests. By referring to work by Stallebrass (1990), it is possible to estimate a best value for ψ, then improve it by trial and error.

Bothkennar clay

Figure 4.2.16 shows the effect of varying ψ on predicted values of bulk modulus K' for Bothkennar clay during isotropic unloading stages following isotropic compression. The value of T=0.7 determined above and S=0.1 were constant in all the analyses. As the value of ψ influences the predicted response at large strain, it appears from the graph that a value of ψ=2 represents best the behaviour of the clay.

Pisa clay

Figures 4.2.17 and 4.2.18 show the effect of varying ψ on predicted bulk and shear modulus during analyses simulating tests R0, R60 and R90. The value of ψ=2 gives the best prediction for tests R60 and R90 at large strains, whereas ψ=3 is better for test R0. The predicted large strain behaviour is shown in Figure 4.2.19, as mean effective stress against volumetric strain for the analysis simulating test R0, and in plots of deviatoric stress against shear strain for the analyses simulating tests R60 and R90. The value of ψ=2 gives the best fit with the experimental data at large strains except for analysis simulating test R60, where it is the value of ψ=1.5. This is reflected by the predicted curve of shear modulus against shear strain shown in Figure 4.2.18b, which gives a closer fit with the test data, but higher values than experimental values. To compromise between small and large strain behaviour, the value of ψ=2 will be used in subsequent analyses.

(vii) Size of the yield surface

Bothkennar clay

The value of S was determined from a parametric study, by varying the value of the size of the yield surface TS, while maintaining T and ψ constant, using the values determined above. The experimental data used to determine S were the same data from isotropic unloading cycles used to determine the values of T and ψ. It was found that the best fit with the data occurred when

TS=0.1, or S=0.14, as shown in Figure 4.2.20 for the two swelling stages from p_c≒100kPa and p_c≒200kPa.

Pisa clay

The next series of analyses consisted of the simulation of the same three tests, but varying values of S while keeping T and ψ constant, using the values determined above. The value of S will influence the predicted response at small strains. Figure 4.2.21 shows predicted and experimental values of bulk modulus for the analyses simulating tests R0 and R60, and Figure 4.2.22 shows values of shear modulus for the analyses simulating tests R90 and R60. The analyses carried out using a value of S=0.1 give the best fit to the experimental data of tests R60 and R90. For the analysis simulating test R0, using a value of S=0.1 leads to a value of bulk modulus that is over-predicted by a factor of only 1.5. The value of S=0.1 appears to represent better the behaviour of the clay at small strain, and therefore it will be used in subsequent analyses.

4.2.4 Evaluation of the model predictions

In this section, the capability of the 3-SKH model to predict the behaviour of soft reconstituted clays is evaluated. The 3-SKH model was developed to predict the effect of recent stress history on the small strain behaviour of stiff reconstituted clays. Analyses will be carried out simulating a range of stress paths, drained or undrained, and stress histories (isotropic or K_0 consolidation, and different levels of overconsolidation) to evaluate predictions by the model of the small strain behaviour of soft clays. In addition, as was noted earlier, since loads within the engineering working range cause soft clays to reach gross yield, it is critical to be able to predict the behaviour of the these clays at large strains beyond gross yield. Therefore, in the evaluation of the 3-SKH model below, particular attention is given to the ability of the model to predict behaviour at large strains.

The 3-SKH model was initially implemented in a single element program, TERTIUS, which is described in Stallebrass (1990). The triaxial tests have been modelled as a uniform element of soil, referred to as *single element*, with the correct combination of stresses or strains being applied uniformly throughout the element. Analyses have been carried out using this program to simulate drained and undrained shear tests performed on reconstituted specimens of Bothkennar clay and Pisa clay. The values assigned to the model parameters used in the following analyses are the soil properties derived in Section 4.2.1 and summarised in Table 4.2.1. Details of the analyses are given in Table 4.2.2.

(i) Bothkennar clay

The first series of analyses modelled tests on Bothkennar clay by Allman & Atkinson (1992). The wide range of stress paths for which raw data are available make it possible to carry out a detailed evaluation.

The analyses simulated four specimens sheared under drained conditions while maintaining a constant mean effective stress p', and two specimens sheared under undrained conditions. These analyses were carried out to evaluate the change in the predicted response of the model when different consolidation histories are modelled before shearing. For that purpose, the analyses simulating drained tests were divided as follows: two analyses were carried out where the specimen is sheared from a normally consolidated state after isotropic and after K_0 compression (CIPC and CK_0PC respectively); two further analyses were carried out where the specimen is compressed anisotropically to $p' \leftrightharpoons 200$kPa then swelled back to achieve overconsolidation ratios of 2 and 4 (CK_0PC-2 and CK_0PC-4 respectively). Unlike Pisa clay, the reconstituted specimens of Bothkennar clay have only been consolidated to the same water content as the natural samples before being installed in the triaxial cell. Therefore they have not been subjected to large changes in stress outside the triaxial cell, and simulating the stress history in the triaxial cell only should be sufficient.

Figure 4.2.23 shows predicted and experimental values of shear modulus plotted against shear strain during the constant p' shear tests. The model predicts a higher value of stiffness at small strains for the specimen compressed isotropically compared to that compressed anisotropically, as observed in the test. This shows that this difference in stiffness is due to stress-induced anisotropy, which is successfully predicted by the model. Predicted data fit the experimental curves well at strains higher than 0.1%, but the values of shear modulus for strains lower than 0.1% are slightly over-predicted for the isotropically compressed specimen and under-predicted by a factor of about 3 for the anisotropically compressed specimen.

Figure 4.2.24 shows a comparison between the variation in shear modulus with shear strain when the soil is sheared from a normally consolidated state and when it is sheared from overconsolidated states for both predictions and observations. For the two analyses simulating the specimens sheared from an overconsolidated state, the predicted curves of stiffness show good agreement with the experimental data for strains higher than 0.03%, which marks the end of the predicted elastic region. The decay of stiffness with strain is also predicted correctly, confirming that the value of ψ is valid for a range of stress paths.

The curves showing the variation of deviatoric stress with shear strain computed from the analyses (Fig. 4.2.25) show that the different patterns of behaviour at large strains, in particular the strain-softening of the overconsolidated specimens CK_0PC-2 and CK_0PC-4, have been modelled correctly. This emphasises that the size of the bounding surface and its change in

size with plastic volumetric strain are computed reliably by the model. The predicted peak and final deviatoric stress are very close to the experimental data for analyses CK_0PC and CK_0PC-2, and within 15% for analysis CK_0PC-4.

Results of the analyses simulating undrained shearing tests are shown in Fig. 4.2.26 where the predicted stress paths are plotted in q'-p' space along with experimental data obtained from laboratory tests (Allman, 1992). The graph shows good agreement between predicted and experimental data. The model computes the peak deviator stress to an accuracy of about 5%. The strain-softening occurring in the overconsolidated specimen, test CK_0UC-2, was also predicted; this is particularly obvious in the plot of excess pore water pressure, u, against shear strain, ε_s (Fig. 4.2.27) where it can be seen that the excess pore pressure decreased in the specimen. The decrease in excess pore pressure predicted by the model occurs between 0.5% and 7% shear strain, whereas in the experiment it lasts from 0.5% to 2% shear strain. Plots of the shear modulus, G, against shear strain, ε_s, (Fig. 4.2.28) show that the predicted stiffnesses are close to the observed data for the overconsolidated specimen (analysis CK_0UC-2). The shear modulus for analysis CK_0UC, however, is well under-predicted between 0.05% and 1% strain. This is caused by the configuration of the kinematic surfaces in the analysis at the end of the anisotropic compression, with the history and yield surfaces being in contact and close to the bounding surface. This is characteristic of the model, and always leads to under-predicted stiffness at the start of shearing after one-dimensional compression.

(ii) Pisa clay

The second series of analyses modelled Pisa clay specimens R30 and R315. As in Section 4.2.1, the full stress history has been simulated (stress path ABCD in Figure 4.2.12), before shearing following stress paths in a constant direction. Figure 4.2.29 shows a comparison of model predictions and experimental results for the variation in bulk modulus with volumetric strain during tests on R30 and R315. The curves obtained from the analyses show a good agreement with the test data, in particular the decay of stiffness with strain is well rendered in both analyses. Predicted and experimental values of shear modulus for the same tests are shown in Figure 4.2.30. The computed values match the test data well, at very small strain for the analysis simulating R30, but only after 0.1% strain for the analysis simulating R315.

The stress-strain response at large strains is shown in Figures 4.2.31 and 4.2.32. The predicted response in a deviatoric stress against shear strain plot (Fig. 4.2.31) agrees very poorly with the test data. The predicted curves show the same trend as the experimental curves, but in both analyses for a given increase in deviatoric stress the model predicted an increase in shear strain equal to 3 times the experimental value. This is surprising in the analysis simulating R30 as the predicted stiffnesses appeared to show a good agreement with the test data however at

high strains. In Figure 4.2.32, predicted curves of mean effective stress against volumetric strain show much better agreement with the test data. Again, for a given increase of mean effective stress the model predicted a greater increase in volumetric strain than the experimental data. These differences may be due to the assumption made in the formulation of the model that the shape of the state boundary surface is elliptical. As normality is assumed, this implies that for a given stress path the amount of plastic strain is fixed by the shape of the surface. For this soil, an isotropic elliptical model may not be appropriate.

(iii) Summary

Predictions of a range of tests on reconstituted specimens of Bothkennar clay by the 3-SKH model showed good agreement with the experimental data. In particular, The model has successfully predicted the effect of stress-induced anisotropy and recent stress history on the response of the clay. Results of the analyses simulating Pisa clay specimens R30 and R315 showed that for these specimens the model could predict volumetric behaviour better than shear behaviour. Predicted curves of bulk modulus against volumetric strain agreed well with the experimental data. However predicted curves of shear modulus against shear strain were less close to the test data. The same features were found when determining parameters for Pisa clay, and should be expected to occur in the analyses of tests on the natural samples as well.

Details of the stress history for the reconstituted specimens were available for both Bothkennar and Pisa clays. For the reconstituted specimens of Pisa clay, Callisto (1996) recreated the overconsolidation history in the oedometer prior to installation of the samples in the triaxial by compressing the specimens to the preconsolidation pressure (σ_c=200kPa) and then swelling back to the *in situ* stress. In contrast, the reconstituted specimens of Bothkennar clay were only consolidated to the water content of the natural samples and therefore they have not undergone large stress changes outside the triaxial cell. As a result, it has been found that it was necessary for the Pisa clay to simulate the full stress history back to the end of consolidation in order to obtain good predictions, due to the large size of its history surface. Unlike Pisa clay, for which Callisto (1996) recreated the overconsolidation history in the oedometer, Bothkennar clay was not subjected to large changes in stress outside the triaxial cell. Therefore it was not necessary when simulating the tests on the reconstituted specimens to model the full stress history. This will be investigated in Chapter 5 when evaluating the new model against experimental data for natural specimens.

The advanced features of the 3-SKH model allow it to predict the small strain as well as the large strain behaviour of soft clays. Typically, the small strain stiffness was predicted well in analyses simulating tests on Bothkennar clay, but it was under-predicted in analyses simulating Pisa clay. The high stiffnesses shown in the experiments on Pisa clay may be due to the highly

anisotropic history of the clay before testing which might have created an anisotropic fabric in the reconstituted specimens. At large strains, the different patterns of behaviour observed in Bothkennar clay due to different stress histories prior to shearing were captured well by the model. This demonstrates that the change in size of the bounding surface is correctly predicted by the model. The limited amount of data available for Pisa clay made the determination of the parameters T, S and ψ not as precise as it should have been, and the predictions obtained non-representative of the capability of the model to predict the behaviour of this clay. However the ability of the 3-SKH model to predict the behaviour of Bothkennar clay at small and large strains over a range of stress paths gives confidence to use it as a base model for extending to the behaviour of soft natural clays.

4.3 A THREE-SURFACE MODEL FOR SOFT CLAYS

The new model is an extension of the 3-SKH model in order to predict the behaviour of soft natural clays. The basic form of the translation rules and hardening rule used in the 3-SKH model are retained, the only modification being to include the effects of structure in the size of the bounding surface. In the new model, the size of the bounding surface is related to both change in volume and change in current sensitivity. Current sensitivity represents the current degree of structure, and decreases exponentially with plastic strain, the rate of decay being governed by the parameter k, which will be defined in Section 4.3.2.

4.3.1 Description of the model

As with the 3-SKH model, the new model has been defined initially in triaxial stress space. Figure 4.3.1 shows the three surfaces that constitute the model, the history and yield surfaces lying within a natural state boundary surface. As in the model proposed by Rouainia & Muir Wood (2000), there is no explicit reference surface representing the behaviour of the reconstituted clay. Instead it is assumed that the behaviour of the natural clay is described by stress and volume in the same way as for the reconstituted clay, and by sensitivity to take account of structure.

The state boundary surface of the natural clay has the same shape as the Modified Cam-Clay state boundary surface, but it is bigger than the state boundary surface of the reconstituted clay. Unlike the state boundary surface of the reconstituted clay, it is not stable, and its size changes with both plastic volumetric and shear strain. The intersection of the natural state boundary surface with an elastic wall forms the *sensitivity* surface in the q'-p' plane. The ratio between the size of the sensitivity surface and that of the equivalent bounding surface of the reconstituted clay is measured by current sensitivity, s, and decreases with plastic strain down to

a constant value larger or equal to unity depending on the degree of any stable elements of structure, possibly arising from fabric effects. The sensitivity surface is described in the q'-p' plane by the following equation;

$$(p'-sp_0')^2+\frac{q'^2}{M^2}=(sp_0')^2 \tag{4.3.1}$$

where p_0' is the centre of the state boundary surface of the reconstituted soil and sp_0' represents the size of the natural state boundary surface. Unlike the model proposed by Rouainia & Muir Wood (2000), the two kinematic surfaces are related in size to the sensitivity surface by constant ratios. The history surface, with centre coordinates (p_a', q_a'), is defined as;

$$(p'-p_a')^2+\frac{(q'-q_a')^2}{M^2}=T^2(sp_0')^2 \tag{4.3.2}$$

The yield surface, with centre coordinates (p'_b, q'_b), is described by the following equation;

$$(p'-p'_b)^2+\frac{(q'-q'_b)^2}{M^2}=T^2S^2(sp'_0)^2 \tag{4.3.3}$$

When the stress state of the soil lies within the yield surface, the deformation of the soil is isotropic elastic, and given by the equation;

$$\begin{bmatrix}\delta\varepsilon_v^e\\ \delta\varepsilon_s^e\end{bmatrix}=\begin{bmatrix}\kappa/p' & 0\\ 0 & 3G_e'\end{bmatrix}\begin{bmatrix}\delta p'\\ \delta q'\end{bmatrix} \tag{4.3.4}$$

where G_e' is dependent on stress and state and calculated using Equation 4.2.16 following Viggiani & Atkinson (1995).

In the following the new model will be referred to as the Sensitivity three-surface kinematic hardening (S3-SKH) model.

4.3.2 Destructuration law

A simple law of destructuration is proposed, which uses sensitivity as a key parameter, and a damage strain, expressed as the accumulated plastic strain, defined in Equation 3.3.1, as the variable to which destructuration is related.

With reference to Section 3.3.2, the destructuration law should be of the form:

$$s = s_f + (s_0 - s_f) f(\varepsilon^p) \tag{4.3.5}$$

where s_0 is the value of undisturbed sensitivity, s_f is the ultimate value of sensitivity at large strains, and ε^p is the plastic strain corresponding to the accumulated plastic strain defined by Equation 3.3.1. The function f is a decreasing function of ε^p, which meets the boundary conditions;

$$f(0) = 1 \text{ and } \lim_{\varepsilon^p \to \infty} f(\varepsilon^p) = 0 \tag{4.3.6}$$

It was seen in Chapter 3 that sensitivity decreases exponentially with damage strain, thus the expression for the function f should be;

$$f(\varepsilon^p) = \exp(-j.\varepsilon^p) \tag{4.3.7}$$

The differentiated form of Equation 4.3.7 is;

$$df(\varepsilon^p) = -j \exp(-j.\varepsilon^p) d\varepsilon^p \tag{4.3.8}$$

In the constitutive equations for the model, the differentiated form (4.3.8) will be combined with the Modified Cam-Clay hardening rule (Equation 4.2.5), to govern the variation in size of the bounding surface. For consistency, j should be of the form;

$$j = \frac{k}{\lambda - \kappa} \tag{4.3.9}$$

Where k is defined as the rate of destructuration with plastic strain, and λ and κ are the compression parameters of the reconstituted clay as defined in Section 4.2.3. This leads to the following expression for the destructuration law;

$$\delta s = -\frac{k}{\lambda - \kappa}(s - s_f)\delta\varepsilon^p \tag{4.3.10}$$

This expression assumes a linear relationship between the logarithmic increment of sensitivity and the increment of plastic strain. Only two additional parameters are required to describe destructuration, the rate of destructuration, k, and the ultimate value of sensitivity, s_f. Both parameters have a physical meaning and can be derived from a single isotropic test, as will be shown in Section 4.4.2.

4.3.3 Translation rules

The translation rules control the movement of the two kinematic surfaces inside the sensitivity surface as they are dragged by the current stress state during loading. As in the 3-SKH model, for each surface, the translation rules are divided into two expressions: the first one controls the movement of a surface inside another surface, the second controls the movement of surfaces which are in contact with one or more surfaces. These translation rules ensure that when the surfaces make contact they do not intersect but meet tangentially with a common outward normal, and that they maintain contact on subsequent loading. The translation rules also allow for the expansion and contraction of the surfaces caused by plastic volumetric strain. The sensitivity surface expands or contracts according to the volumetric hardening rule used in the Modified Cam-Clay model, causing the kinematic surfaces to expand or contract, which influences the translation of the surface. The hardening rule for the Modified Cam Clay model, which was given in Equation 4.2.5, implies that the state boundary surface is stable under loading.

The sensitivity surface also contracts according to the destructuration law defined by Equation 4.3.10. In that case, the state boundary surface is no longer stable, but contracts under loading. When the sensitivity surface expands or contracts, the inner kinematic surfaces also expand or contract proportionally.

(a) Translation rules for the history surface

There are two translation rules that govern the movement of p_a' and q_a' for the history surface.

(i) Translation rule when the history surface is moving inside the sensitivity surface.

In this case the translation rule has two components. The first governs the expansion or contraction of the surfaces, the second controls the translation of the surface as it is dragged by the current stress state along a vector, β, joining the current stress state, A, and its conjugate point, A_c, on the sensitivity surface (Fig. 4.3.2).

The first component of the translation rule controls the translation of the centre of the sensitivity surface along the p'-axis caused by the change in size of the sensitivity surface;

$$\frac{\delta(sp_0')}{sp_0'}\begin{bmatrix} p_a' \\ q_a' \end{bmatrix} \tag{4.3.11}$$

The components of vector β are;

$$p_\beta' = \frac{p'-p_a'}{T} - \left(p'-sp_0'\right) \text{ and } q_\beta' = \frac{q'-q_a'}{T} - q' \tag{4.3.12a, b}$$

Therefore the translation rule for the history surface moving inside the sensitivity surface;

$$\begin{bmatrix}\delta p_a' \\ \delta q_a'\end{bmatrix} = \frac{\delta\left(sp_0'\right)}{sp_0'}\begin{bmatrix}p_a' \\ q_a'\end{bmatrix} + W_s\begin{bmatrix}\dfrac{p'-p_a'}{T} - \left(p'-sp_0'\right) \\ \dfrac{q'-q_a'}{T} - q'\end{bmatrix} \tag{4.3.13}$$

The consistency equation for the history surface is;

$$\left(p'-p_a'\right)\left(\delta p'-\delta p_a'\right) + \frac{\left(q'-q_a'\right)}{M^2}\left(\delta q'-\delta q_a'\right) = T^2\left(sp_0'\right)^2\frac{\delta\left(sp_0'\right)}{sp_0'} \tag{4.3.14}$$

Combining equations (4.3.13) and (4.3.14) gives an expression for W_s as follows;

$$W_s = \frac{\left(p'-p_a'\right)\left[\delta p' - \dfrac{\delta\left(sp_0'\right)}{sp_0'}p'\right] + \dfrac{\left(q'-q_a'\right)}{M^2}\left[\delta q' - \dfrac{\delta\left(sp_0'\right)}{sp_0'}q'\right]}{\left(p'-p_a'\right)\left[\dfrac{\left(p'-p_a'\right)}{T} - \left(p'-sp_0'\right)\right] + \dfrac{\left(q'-q_a'\right)}{M^2}\left[\dfrac{\left(q'-q_a'\right)}{T} - q'\right]} \tag{4.3.15}$$

which completes the expression describing the translation of the history surface when it is moving inside the sensitivity surface.

(ii) Translation rule when the history surface is in contact with the sensitivity surface and the loading path is such that the volumetric part of the hardening rule causes the sensitivity surface to expand.

From the geometry of the surfaces when they are in contact (see Fig. 4.3.2 (b));

$$T\left(p'-sp_0'\right) = p'-p_a' \text{ and } Tq' = q_a' \tag{4.3.16a, b}$$

Differentiating these equations gives the translation rule;

$$\begin{bmatrix}\delta p_a'\\ \delta q_a'\end{bmatrix}=(1-T)\begin{bmatrix}\delta p'\\ \delta q'\end{bmatrix}+T\begin{bmatrix}\delta(sp_0')\\ 0\end{bmatrix} \tag{4.3.17}$$

This is valid when the stress state lies on the history surface. When the stress state is inside the history surface, after unloading for example, the surface will still move to allow for the expansion or contraction of the sensitivity surface;

$$\begin{bmatrix}\delta p_a'\\ \delta q_a'\end{bmatrix}=\frac{\delta(sp_0')}{sp_0'}\begin{bmatrix}p_a'\\ q_a'\end{bmatrix} \tag{4.3.18}$$

This formulation for the translation rules leads to a small discontinuity when the stress state reaches the history surface, as Equations 4.3.17 and 4.3.18 give slightly different results. This is because the stress path, and therefore $\delta p'$ and $\delta q'$, are independent from the movement and expansion or contraction of the surfaces.

(b) Translation rules for the yield surface

The translation rules for the yield surface, which govern the movement of p_b' and q_b', are also given by two different expressions, the first when the yield surface is moving inside the history surface, the second when the yield surface is in contact with the history surface.

(i) Translation rule for the yield surface when it is moving inside the history surface.

Following the same pattern as the history surface, this translation rule is formed of two components. The first component controls the expansion or contraction of the surfaces; the second controls the translation of the surface as it is dragged by the current stress state along a vector, γ, joining the current stress state, D, and its conjugate point, D_c, on the history surface (Fig. 4.3.3). Consequently, the expression for the translation rule is of the form;

$$\begin{bmatrix}\delta p_b'\\ \delta q_b'\end{bmatrix}=\frac{\delta(sp_0')}{sp_0'}\begin{bmatrix}p_b'\\ q_b'\end{bmatrix}+Z_s\begin{bmatrix}p_\gamma'\\ q_\gamma'\end{bmatrix} \tag{4.3.19}$$

where p_γ' and q_γ' are the components of the vector γ. They are equal to;

$$p_\gamma'=\frac{(p'-p_b')}{S}-(p'-p_a') \text{ and } q_\gamma'=\frac{(q'-q_b')}{S}-(q'-q_a') \tag{4.3.20 a,b}$$

Therefore the translation rule for the yield surface moving inside the history surface is of the form;

$$\begin{bmatrix}\delta p_b'\\ \delta q_b'\end{bmatrix}=\frac{\delta(sp_0')}{sp_0'}\begin{bmatrix}p_b'\\ q_b'\end{bmatrix}+Z_s\begin{bmatrix}\dfrac{(p'-p_b')}{S}-(p'-p_a')\\ \dfrac{(q'-q_b')}{S}-(q'-q_a')\end{bmatrix} \tag{4.3.21}$$

The consistency equation for the yield surface gives;

$$(p'-p_b')(\delta p'-\delta p_b')+\frac{(q'-q_b')}{M^2}(\delta q'-\delta q_b')=T^2S^2(sp_0')^2\,\frac{\delta(sp_0')}{sp_0'} \tag{4.3.22}$$

Combining (4.3.21) and (4.3.22) gives an expression for Z_s;

$$Z_s=\frac{(p'-p_b')\left[\delta p'-\dfrac{\delta(sp_0')}{sp_0'}p'\right]+\dfrac{(q'-q_b')}{M^2}\left[\delta q'-\dfrac{\delta(sp_0')}{sp_0'}q'\right]}{(p'-p_b')\left[\dfrac{(p'-p_b')}{S}+(p'-p_a')\right]+\dfrac{(q'-q_b')}{M^2}\left[\dfrac{(q'-q_b')}{S}-(q'-q_a')\right]} \tag{4.3.23}$$

Which completes the expression describing the translation of the yield surface moving inside the history surface.

(ii) Translation rule for the yield surface when it is in contact with the history surface.

When the stress state lies on the yield surface, the geometry of the surfaces gives (see Fig. 4.3.3 (b));

$$S(p'-p_a')=p'-p_b' \quad\text{and}\quad S(q'-q_a')=q'-q_b' \tag{4.3.24}$$

Differentiating these equations leads to the translation rule;

$$\begin{bmatrix}\delta p_b'\\ \delta q_b'\end{bmatrix}=(1-S)\begin{bmatrix}\delta p'\\ \delta q'\end{bmatrix}+S\begin{bmatrix}\delta p_a'\\ \delta q_a'\end{bmatrix} \tag{4.3.25}$$

4.3.4 Hardening rule

The size of the sensitivity surface is governed by both change in volume and change in sensitivity. Thus the hardening rule is made up of two competing terms. The first term is the same as the hardening rule of the Modified Cam-Clay model derived in the ln$v$-lnp' plane and given by Equation 4.2.5; the second term is the destructuration law of the form given in Equation 4.3.10, which links change in sensitivity to change in plastic strain. It has been seen in Chapter 3 that the increment of damage strain $\delta\varepsilon^p$ is be simply expressed as the plastic strain increment given in Equation 3.3.1.

Plastic deformations follow the normality rule so that the vector of plastic strain increment is always normal to all three current surfaces. This can be expressed by the following equation when defined with respect to the yield surface;

$$\begin{bmatrix} \delta\varepsilon_v^p \\ \delta\varepsilon_s^p \end{bmatrix} = \frac{\chi}{N_b} \begin{bmatrix} p'-p_b' \\ \dfrac{q'-q_b'}{M^2} \end{bmatrix} \tag{4.3.26}$$

where $\dfrac{1}{N_b}\begin{bmatrix} p'-p_b' \\ \dfrac{q'-q_b'}{M^2} \end{bmatrix}$ is the vector representing an outward normal to the yield surface with;

$$N_b = \sqrt{(p'-p_b')^2 + \left(\frac{(q'-q_b')}{M^2}\right)^2} \tag{4.3.27}$$

Following Al Tabbaa (1987) and Stallebrass (1990), the hardening rule is first developed for the case when all the surfaces are in contact. Combining the consistency equation for the yield surface (4.3.22), the translation rule (4.3.21) for the case where all surfaces are in contact, and the normality rule (4.3.26), leads to an expression for the hardening rule similar in form to that of the 3-SKH model;

$$\begin{bmatrix} \delta\varepsilon_v^p \\ \delta\varepsilon_s^p \end{bmatrix} = \frac{1}{h_0} \begin{bmatrix} (p'-p_b')^2 & (p'-p_b')\dfrac{(q'-q_b')}{M^2} \\ (p'-p_b')\dfrac{(q'-q_b')}{M^2} & \left(\dfrac{(q'-q_b')}{M^2}\right)^2 \end{bmatrix} \begin{bmatrix} \delta p' \\ \delta q' \end{bmatrix} \tag{4.3.28}$$

But in this case the hardening modulus h_0 is defined by;

$$h_0 = \frac{p'-p_b'}{\lambda-\kappa}\left[p'(p'-p_b')+q'\frac{(q'-q_b')}{M^2}\right]\left[1-\frac{k}{p'-p_b'}\left(1-\frac{s_f}{s}\right)\sqrt{(p'-p_b')^2+\left(\frac{(q'-q_b')}{M^2}\right)^2}\right] \tag{4.3.29}$$

As first identified by Al Tabbaa (1987) and also noted by Stallebrass (1990), h_0 cannot be used on its own because of instabilities at a number of points on the kinematic surfaces. Hence, the hardening modulus is further defined as a function $h = h_0 + H_1 + H_2$. Following the approach used by Al Tabbaa (1987), Hashiguchi (1985) and Stallebrass (1990), H_1 is expressed as a function of the degree of approach, b_1, of the history surface to the bounding surface, and H_2 of the degree of approach, b_2, of the yield surface to the history surface. Therefore, as in the 3-SKH model, H_1 or H_1+H_2 become equal to zero when two or more surfaces are in contact respectively, ensuring continuity of stiffness.

The function b_1 is defined as the scalar product of the vector β and the normal to the history surface, $\mathbf{n_h}$, at the conjugate point (Fig. 4.3.4), divided by a measure of the size of the history surface, sTp_0'. The function b_1 reaches a maximum, b_{1max}, when the surfaces are in the configuration shown in Fig. 4.3.5.

$$b_1 = \frac{1}{sTp_0'}\left[\frac{(p'-p_b')}{S}\left[\frac{(p'-p_b')}{TS}-\left[\frac{(p'-p_b')}{S}+p_a'-sp_0'\right]\right]+\frac{(q'-q_b')}{SM^2}\left[\frac{(q'-q_b')}{TS}-\left[\frac{(q'-q_b')}{S}+q_a'\right]\right]\right] \tag{4.3.30}$$

$$b_{1\max} = 2sp_0'(1-T) \tag{4.3.31}$$

The function b_2 is defined as the scalar product of the vector γ and the normal to the yield surface, $\mathbf{n_y}$, at the conjugate point (Fig. 4.3.4), divided by a measure of the size of the yield surface, $sSTp_0'$. The function b_2 reaches a maximum, b_{2max}, when the surfaces are in the configuration shown in Fig. 4.3.5.

$$b_2 = \frac{1}{sSTp_0'}\left[(p'-p_b')\left[\frac{(p'-p_b')}{S}-(p'-p_a')\right]+\frac{(q'-q_b')}{M^2}\left[\frac{(q'-q_b')}{S}-(q'-q_a')\right]\right] \tag{4.3.32}$$

$$b_{2\max} = 2sTp'_0(1-S) \tag{4.3.33}$$

The components of the hardening rule H_1 and H_2 are defined in a similar way to those used by Stallebrass (1990);

$$H_1 = S^2\left(\frac{b_1}{b_{1\max}}\right)^{\psi}\frac{1}{\lambda-\kappa}(sp_0')^3 \tag{4.3.34}$$

$$H_2 = \left(\frac{Tb_2}{b_{2\max}}\right)^{\psi}\frac{1}{\lambda-\kappa}(sp_0')^3 \tag{4.3.35}$$

where λ, κ and ψ are defined as in the 3-SKH model and take the same values as those derived for the equivalent reconstituted soil. This choice will be explained in detail in Section 4.4.1.

The constitutive equations governing plastic deformations are thus;

$$\begin{bmatrix}\delta\varepsilon_v^p\\ \delta\varepsilon_s^p\end{bmatrix} = \frac{1}{h}\begin{bmatrix}(p'-p_b')^2 & (p'-p_b')\dfrac{(q'-q_b')}{M^2}\\ (p'-p_b')\dfrac{(q'-q_b')}{M^2} & \left(\dfrac{(q'-q_b')}{M^2}\right)^2\end{bmatrix}\begin{bmatrix}\delta p'\\ \delta q'\end{bmatrix} \tag{4.3.36}$$

where

$$h = \frac{1}{\lambda-\kappa}\left[(p'-p_b')\left[p'(p'-p_b')+q'\frac{(q'-q_b')}{M^2}\right]\left[1-\frac{k}{p'-p_b'}\left(1-\frac{s_f}{s}\right)\sqrt{(p'-p_b')^2+\left(\frac{(q'-q_b')}{M^2}\right)^2}\right]\right.$$

$$\left. + S^2\left(\frac{b_1}{b_{1\max}}\right)^{\psi}(sp_0')^3 + \left(\frac{Tb_2}{b_{2\max}}\right)^{\psi}(sp_0')^3\right] \tag{4.3.37}$$

It can be established by hand calculation that when the clay is not sensitive, that is s=s_f=1, this equation reduces to the equation for the hardening rule of the 3-SKH model.

4.3.5 Validation of the model

The S3-SKH model was implemented in the single element program S-TERTIUS, described later in Section 5.2.1. The S3-SKH model is described by Equations (4.3.1) to (4.3.4) and its translation rules and hardening rule are formulated in Equations (4.3.10) to (4.3.36). The program S-TERTIUS obtains solutions to these using repeated applications of an incremental

tangent stiffness approach equivalent to an Euler one-step method. The program S-TERTIUS is similar to the program TERTIUS used to perform analyses using the 3-SKH model (Stallebrass, 1990) except in the addition of the destructuration law to the hardening rule of the base model. This is a significant modification to a part of the program that is sensitive to numerical instability. The objectives of this section are firstly to demonstrate that the output of the program S-TERTIUS is consistent with the translation and hardening rules set out in Sections 4.3.3 and 4.3.4, and secondly that predicted responses by the program S-TERTIUS are numerically valid. This is achieved by firstly examining the movement of the surfaces in analyses simulating drained and undrained tests. Secondly results from analyses of an undrained compression test and a drained probing test, which are typical stress paths simulated in Chapter 5, are presented to demonstrate that the computed responses converge as the input increment of strain is decreased.

Figure 4.3.6 shows a stress path ABCD simulated using the program S-TERTIUS. The stress path ABCD consists of two drained paths where the mean effective stress is constant, AB and CD, and two drained paths where the deviatoric stress is constant, BC and DA. There is therefore a change in direction of the stress path of 90 degrees at points B, C and D. In order to check that the translation of the surfaces is correctly calculated by the program, their position is shown in the figure at various stress points along the stress path. The analyses were stress-controlled and started with the history and yield surfaces centred around the stress point at A (black circles). Along stress path AB, at B the history and yield surfaces (in blue) are aligned vertically and connected tangentially at the current stress point. After a rotation of the stress path by 90 degrees clockwise, the surfaces remain connected at the current stress point B′ on stress path BC, and on arriving at point C they are again all connected at the current stress point. However the surfaces have not had time to re-align themselves before arriving at C given the short length of the stress path BC. Another rotation of the stress path at 90 degrees clockwise brings the current stress point C′ on CD, which drags the history and yield surfaces with it. The two surfaces remain connected on arriving at point D (in red). Back at point A (in pale blue) they are still connected, and they are in a different position from the beginning of the stress path (black circles). It can be seen that, once they are in contact the two kinematic surfaces remain connected tangentially at the current stress state on loading as would be predicted by the base 3-SKH model. The history and yield surfaces translate appropriately after changes in direction of the stress path, as in the base 3-SKH model. This demonstrates that the history and yield surfaces are correctly moving with the current stress during stress-controlled analyses.

Figure 4.3.7 shows an undrained compression stress path XYZ simulated using the program S-TERTIUS. The analyses were strain-controlled, using a strain increment of 0.001%. The stress path started from an isotropic normally consolidated state, with all three surfaces connected tangentially at the current stress state (orange circles). Hand calculation for one

increment checked that the program calculated stresses correctly. The stress path follows a stable state boundary surface up to a peak deviatoric stress, then it moves inside it towards a critical state. This is consistent with the response observed in experimental tests, which adds confidence about the integrity of the model. The predicted strain-softening is caused by the destructuration law included in the hardening rule. According to the formulation of the S3-SKH model, in undrained compression destructuration should cause a reduction in the size of the state boundary surface. The positions of the surfaces at peak (in green) and during destructuration (in pink and blue) are shown in the figure. It can be seen in the figure that the three surfaces remain connected post-peak. It can also be seen that the current stress point follows the state boundary surface post-peak, so the strain-softening is due to the reduction in size of the state boundary surface with plastic strain. This is in accordance with the definition in the model that the effect of destructuration is described by changes in size of the state boundary surface.

The simulations of undrained compression tests and drained probing tests presented in Chapter 5 were obtained with a version of the program S-TERTIUS which uses single precision variables. It was found at a later stage that when using single precision variables, computed responses by the program S-TERTIUS tend towards a single curve as increments of strain are reduced, but diverge for the smallest increments of strain. This is due to the fact that single precision, which uses 7 digits only plus the exponential, is not sufficiently precise to compute changes in stress from small increments of strain. The program was later modified to use double precision variables to prove that there is convergence. Figures 4.3.8 to 4.3.11 that are described in the following demonstrate the convergence of the model predictions when using double precision variables, and show a comparison of the output curves obtained when using double and single precision variables.

Figure 4.3.8 shows results of analyses simulating undrained compression tests using the program S-TERTIUS with double precision variables. The analyses were obtained using a range of different sizes of strain increment. All stress paths started from normally consolidated states with all three surfaces connected at the current stress point. Figure 4.3.8a shows the stress paths followed during the simulations. The stress paths for all three simulations follow the state boundary surface up to a peak deviatoric stress. Post-peak, the predicted stress paths go down the critical state line. Figure 4.3.8b shows curves of deviatoric stress against shear strain. The predicted responses converge for strain increment sizes of 0.001% or less.

Figure 4.3.9 shows a comparison of computed responses using double and single precision variables for a strain increment size of 0.001%, which is the strain increment size that was used for most analyses simulating undrained compression presented in Chapter 5. Figure 4.3.9a shows the stress paths followed during the simulations. While the analysis performed using double precision variables follows the critical state line post-peak as may be expected, the analysis performed using single precision variables diverges slightly from it. This is attributed

to the inaccuracy related to the use of single precision variables. However in Figure 4.3.9b, which shows predicted curves of deviatoric stress against shear strain, the two curves are coincident. The small departure post-peak in Figure 4.3.9a is not considered to be significant and will not influence the discussion and conclusions presented in Chapter 5.

Figure 4.3.10 shows stress-strain curves obtained during simulations of a typical drained probing test using double precision variables. The direction of the stress path, shown in the figure, is at 60 degrees from the horizontal. This particular drained probing stress path was chosen as it produces the most extreme results. Both curves of mean effective stress against volumetric strain (Fig. 4.3.10a) and deviatoric stress against shear strain (Fig.4.3.10b) show that the computed responses converge for strain increment sizes of 0.0001% or less. Nevertheless the analyses simulating drained tests that are presented in Chapter 5 were performed using a strain increment size of 0.001% and single precision. Figure 4.3.11 shows that the predicted responses when using double and single precision variables with a strain increment size of 0.001% are coincident. In both graphs shown in Figure 4.3.10 the difference between the curves computed using strain increments of 0.001% and 0.0001% is not significant. It will not affect the predictions presented in Section 5.3 and therefore the evaluation of the model.

4.4 DETERMINATION OF PARAMETERS FOR THE S3-SKH MODEL

This section focuses on the derivation of the soil properties used in the S3-SKH model. The first part evaluates whether the values of parameters determined for the 3-SKH model and used in analyses of reconstituted clay can remain the same and be used in analyses of natural clay. The second part details the determination of the values of parameters that are used only in the S3-SKH model by describing a methodology applicable to data from standard laboratory tests.

4.4.1 Applicability of the parameters used in the 3-SKH model to natural clays

(i) Elastic stiffness

There is evidence that for stiff clays the stiffness relationship proposed by Viggiani & Atkinson (1995) is valid for both reconstituted and natural samples, using the same exponents. Figure 4.4.1 shows normalised stiffness data for Pappadai clay plotted against overconsolidation ratio for reconstituted specimens, or yield stress ratio, defined as the ratio of the vertical effective stress at gross yield to the current vertical effective stress, for natural specimens. By normalising by stress to the power n, where n is the exponent used in Equation 4.2.16, Cotecchia (1996) showed that there is no difference between the small strain stiffness of natural and reconstituted clays if the difference in stress and state is accounted for. Similar comparisons of stiffness have

also been made by Rampello & Silvestri (1993) for Vallericca clay and Coop *et al.* (1995) for Boom clay, both of which are stiff clays (see Section 2.2.5).

Figure 4.4.2 shows normalised stiffness data, G'/p'^{n}, for natural and reconstituted specimens of Bothkennar clay plotted against overconsolidation ratio, R_0. The value of the exponent n is equal to the value 0.65, which has been determined in Section 4.2.3. The graph also shows the values obtained using Equation 4.2.16 from Viggiani & Atkinson (1995), which represent the elastic stiffness G_e'. Bender element tests were performed at City University on normally consolidated reconstituted specimens. The value calculated for R_0=1 using Equation 4.2.16 matches these experimental values. For the tangent stiffnesses determined from local strain measurements at 0.01% strain, all the data plot very close to each other when differences in stress and state are accounted for, even though the experimental data for natural and reconstituted samples were obtained from different sets of tests. It can be reasonably assumed that for soft clays as for stiff clays, the equation proposed by Viggiani & Atkinson (1995) is valid for natural and reconstituted samples, using the same exponents.

(ii) Swelling parameter κ

It has been demonstrated in the previous section that the elastic shear moduli of natural and reconstituted samples are typically the same. This implies that the value of the elastic swelling parameter κ can also be assumed to be the same. In the subsequent analyses, the values of κ derived for the reconstituted clay will be used in analyses simulating the natural clay.

(iii) Size of the kinematic surfaces, and the parameter ψ

Ingram (2000) has investigated the effect of increasing the size of the bounding surface on predictions of the behaviour of stiff natural Boom clay using the 3-SKH model. The predictions were compared to experimental data from a series of tests carried out by Coop *et al.* (1995) on both natural and reconstituted specimens. The normal compression lines of the natural and reconstituted clay identified by Coop *et al.* from high pressure oedometer tests plot nearly parallel to each other. This defined the sensitivity of Boom clay, which is equal to 1.55. Ingram (2000) carried out a series of analyses modelling laboratory tests on natural and reconstituted specimens using parameters calculated using data from reconstituted specimens in both cases. The natural clay was modelled in two ways, firstly by assuming that the preconsolidation pressure is on the intrinsic normal compression line, so that the compression history is the same as for reconstituted tests, and secondly by assuming that the state boundary surface is consistent with a preconsolidation pressure on the natural normal compression line. Ingram (2000) found that the predictions using the natural state boundary surface follow anisotropic paths which are

closer to the laboratory data than the predictions made using the intrinsic state boundary surface (see Fig. 4.4.3). The fact that the 3-SKH model can produce anisotropic stress paths similar to those observed in the laboratory tests indicates that the anisotropy of the stress paths of the Boom clay is due to stress-induced anisotropy resulting from the recent stress history, which are included in the model. The stiffness data also showed that the model prediction was improved if the appropriate size of the bounding surface was used. This means that not only the larger size of the bounding surface has a significant effect on predictions, but also the larger size of the two kinematic surfaces is important as they govern the stress-induced anisotropy arising from recent stress history. This confirms the reasonableness of the assumption that was made in the definition of the surfaces, that their size is related to the size of the structure surface. Ingram (2000) found that using the same values of ratios T and S still gives good quality predictions. In the analyses used to evaluate the model in Chapter 5 the values of T and S used to model the natural clay will be the same as those used to model the reconstituted clay and determined in Section 4.2.3.

The exponent ψ, which controls the decay of stiffness, is assumed to be independent of destructuration. The effect of ψ can be detected by modelling the behaviour of reconstituted clay with no recent stress history. It is however not possible to measure ψ independently in natural clays, as destructuration will also influence the decay of stiffness. It will be assumed in subsequent analyses that the value of ψ is the same for reconstituted and natural clay.

4.4.2 Determination of the parameters representing structure

In the Sensitivity 3-SKH model the size of the sensitivity surface is related to both change in volume and change in sensitivity. Current sensitivity is expressed as the parameter s, and its reduction with plastic strain is governed by the destructuration law described by Equation 4.3.10. The destructuration law is expressed in such a way that only three additional parameters are needed to be able to evaluate the change in current sensitivity during loading; the "initial" sensitivity, s_0, which defines the starting value from which sensitivity is reducing, the rate of destructuration, k, which controls how much sensitivity reduces when a change in plastic strain occurs, and the "ultimate", stable or fabric-related sensitivity, s_f, which is the asymptotic value at which current sensitivity stabilises. The destructuration law has been designed so that the parameter, k, can be derived directly from a simple isotropic compression test.

(i) Initial sensitivity

The initial sensitivity determines the initial size of the structure surface. In boundary value problems, this should represent the degree of structure developed during and after

sedimentation, and should be derived from an interpretation of the geological history. This is obviously difficult, and may require a number of assumptions to be made. The methodology for determining s_0 proposed here is valid for modelling laboratory triaxial tests when the recent stress history is known. In this case, the value of initial stress sensitivity can be determined by back-analysing from a state during the test, for which the sensitivity is known. The value of initial sensitivity determined in this way will be less than the undisturbed sensitivity in the ground, due to disturbance caused by sampling (see section 1.5). There are two ways of determining sensitivity from laboratory specimens: in terms of strength (Terzaghi, 1944), when undrained compression test data are available, or in terms of stress (Cotecchia and Chandler, 2000), when isotropic or one-dimensional compression test data are available. These two methods are detailed in the folllowing, and summarised in the flow chart shown in Table 4.4.1.

The first method, which defines sensitivity as the ratio of the undrained shear strengths of the natural and the reconstituted clay at the same water content, implies that it is necessary to determine the value of the undrained shear strength of the natural clay. Undrained shear strength is not a fundamental soil property as different methods of measuring it such as vane shear test, BS fall cone test or triaxial compression test, would give different results. In the laboratory, the tests that give most consistent values of the undrained shear strength are the BS fall cone test and the triaxial test. The vane shear test, which is sometimes used, is less reliable as its results are very sensitive to the rate of shearing. The undrained shear strength of the reconstituted soil has to be determined using the same type of test for consistency. Leroueil *et al.* (1983) determined a correlation between intrinsic undrained shear strength and liquidity index for a wide range of clays;

$$S_u^* = \frac{1}{(LI - 0.21)^2} \tag{4.4.1}$$

where S_u^* is the intrinsic undrained shear strength and LI is the liquidity index determined from the fall cone test. Equation (4.4.1) is illustrated in Fig. 4.4.4. This equation can be used to calculate S_u^* when there are no data available from a test on a reconstituted specimen which is equivalent to that performed on the natural specimen.

The second method that can be used to determine sensitivity uses isotropic or one-dimensional compression test data. It uses the definition of the stress sensitivity in the Sensitivity framework (see Figure 2.5.11). Gross yield usually marks the onset of significant destructuration, therefore it can be assumed that the value of sensitivity at yield gives a reasonable value for s_0 at the start of compression, where s_0 is defined using data from isotropic compression tests as;

$$s_0 = {p'_{iy}}\Big/{p^*_{ie}} \tag{4.4.2}$$

where p'_{iy} is the gross yield stress in isotropic compression, and p^*_{ie} is the equivalent pressure at the intersection of the elastic wall and the intrinsic isotropic normal compression line. The value of p^*_{ie} can be calculated from the equation;

$$p^*_{ie} = \exp\left(\frac{N - \ln(v) - \kappa \ln(p')}{\lambda - \kappa}\right) \tag{4.4.3}$$

where N, λ and κ are the compression and swelling parameters defined for the reconstituted clay as in Section 4.2.3 and v is the current specific volume. When no data are available from volumetric compression tests on reconstituted specimens, the values of N and λ can be derived from the liquid limit for the natural specimen, by using a relationship similar to that proposed by Coop & Cotecchia (1995), which is described in Section 1.4.3.

According to the Sensitivity framework, the values of stress sensitivity should be the same as those of strength sensitivity. Fig. 4.4.5 compares the variation in sensitivity with depth, computed from data from natural samples of Bothkennar clay using three methods. All the methods show the fluctuations corresponding to the different facies of the clay in the ground, which is evidence that even when disturbed, the clay retains the characteristics of its facies. From the graph, it appears that values of sensitivity computed from laboratory BS fall cone data and using compression data were obtained from samples that were less disturbed, and are in very good agreement. It is also possible that the BS fall cone test and volumetric compression tests cause less destructuration before failure. The values of sensitivity obtained from undrained triaxial compression tests on natural specimens are lower. This would be expected because generally the specimens would have been compressed before shearing, therefore the sensitivity would have already reduced before the start of the undrained test. It could also be that there is inaccuracy in the relationship used to estimate the undrained shear strength of the reconstituted clay from the liquidity index (Leroueil *et al.*, 1983).

(ii) Rate of change of sensitivity with plastic strain

This section explains the method used to determine k directly from a simple isotropic compression test.

In the destructuration law given by Equation 4.3.10, there is a linear relationship between change in normalised sensitivity and in the damage strain, for which the gradient is directly proportional to k.

Firstly the magnitude of the increment in damage strain needs to be determined. During isotropic compression starting from an isotropic stress state, there is no shear deformation and hence computing the damage strain is straightforward. For each increment of stress, the increment of elastic volumetric strain can be neglected so that the increment of plastic volumetric strain can be considered equal to the increment of total volumetric strain, which can be calculated from the equation;

$$\delta\varepsilon^{p} = \delta\varepsilon_{v}^{p} = -\delta v / v \tag{4.4.4}$$

where v is the current specific volume and δv is the change of specific volume calculated from the isotropic compression curve. Strain is calculated with respect to the current volume, to be consistent with the model.

Secondly it is necessary to compute the increment of change in sensitivity, $\delta s/(s - s_f)$, for each increment of stress for normally consolidated states. The current sensitivity, s, is calculated using an expression similar in concept to that of the sensitivity framework (Cotecchia and Chandler, 2000);

$$s = p' / p^{*}_{ie} \tag{4.4.5}$$

where p' is the current mean effective stress for normally consolidated states and p^{*}_{ie} is the equivalent pressure calculated using Equation 4.4.3. By using invariant variables and comparing pressures on isotropic compression curves, this definition of current sensitivity ensures that the quantity s represents the ratio of the size of the sensitivity surface to the size of the equivalent surface for a sensitivity equal to unity, that is it relates correctly to the S3-SKH model.

The change in sensitivity and the magnitude of increment in damage strain are calculated for each increment of stress on the normal compression line. Each point is then plotted on a graph of $\delta s/(s - s_f)$ against $\delta\varepsilon^{p}$ and a regression line is fitted, of which the gradient is $k/(\lambda - \kappa)$. The value of k can then be directly calculated.

In practice, this approach can lead to results which are difficult to interpret as the quantities analysed are very small and the smallest inaccuracy leads to significant scatter. Another approach is to fit a straight line through the initial part of the normal compression curve of the natural clay, of equation;

$$v = N_n - \lambda_n \ln(p') \tag{4.4.6}$$

where N_n and λ_n are compression parameters determined in the ln$v$-lnp' plane for the natural clay. It has been demonstrated in Section 4.4.1 that the same swelling parameter κ can be used for both natural and reconstituted clays, therefore differentiation of Equation 4.4.6 gives a relationship for the natural clay similar to the hardening rule for the Modified Cam-Clay model;

$$\delta p'_{iy} = \frac{p'_{iy}}{\lambda_n - \kappa} \delta \varepsilon_v^p \qquad (4.4.7)$$

where p_{iy} is the current stress on the isotropic normal compression curve of the natural clay (Fig. 4.4.6). If in the clay the effect of fabric is significant, the clay will tend towards a stable state different from the intrinsic state and represented by the parameter s_f. Differentiation of the equation for the isotropic compression line of the equivalent stable clay gives;

$$\delta p^*_{if} = \frac{p^*_{if}}{\lambda - \kappa} \delta \varepsilon_v^p \qquad (4.4.8)$$

where p^*_{if} is the equivalent pressure on the isotropic compression line of the equivalent stable clay.

In isotropic compression the increment of plastic strain is equal to the increment of plastic volumetric strain if the soil is isotropic, so the destructuration law expressed by Equation 4.3.10 can be rearranged as;

$$\delta s = -\frac{k}{\lambda - \kappa}\left(s - s_f\right)\delta \varepsilon_v^p \qquad (4.4.9)$$

with $s - s_f = {p'_{iy}}/{p^*_{if}}$, combining equations (4.4.6), (4.4.7) and (4.4.8) leads to an expression for the rate of destructuration;

$$k = \frac{\lambda_n - \lambda}{\lambda_n - \kappa} \qquad (4.4.10)$$

(iii) Ultimate sensitivity

When effects of fabric are not negligible, the state of the clay becomes stable before reaching the intrinsic state boundary surface. The effects of fabric are included in the destructuration law

(Equation 4.3.10) so that the value of s does not reduce to unity at very large strain, but to a value s_f larger than unity. The value of s_f can be derived from a volumetric compression test performed to very large strains, as shown in Figure 3.3.11. In stable clays like Sibari clay, the values of initial and ultimate sensitivity are the same.

4.5 SUMMARY

This chapter has evaluated the ability of an existing model for reconstituted and stable stiff clays, the 3-SKH model, to predict the behaviour of two reference soft reconstituted clays, in order to use it as a base model which is subsequently extended to predict the behaviour of soft natural clays. Then this new model has been proposed, the sensitivity three-surface kinematic hardening (S3-SKH) model, which simulates effects of structure on the behaviour of soft natural clays.

The 3-SKH model was developed to predict the effect of recent stress history on the small strain stiffness of reconstituted and stable stiff clays. Its formulation as a kinematic hardening model allows it to predict successfully stiffness non-linearity and stress-induced anisotropy arising from the recent stress history. It has been proven in Section 4.2.4 that it also gives a good prediction for the behaviour of soft clays, in particular at large strains. The two reference clays used in this dissertation have a large size of history surface, which stresses the importance of having a model able to simulate the effect of recent history for such clays. A simple exponential destructuration law has been used to extend the 3-SKH model to predict the behaviour of soft natural clays.

The key features of the new S3-SKH model are:

- The effect of structure is simulated by enlarging the size of the surfaces by a factor equal to the value of the current sensitivity of the clay.
- Destructuration is modelled as a reduction in sensitivity with plastic strain. Sensitivity is assumed to decrease exponentially with a damage strain equal to the magnitude of the accumulated plastic strain.
- Unlike the classic critical state models, the state boundary surface is not stable but its size decreases with plastic strain.
- In the model, all the effects of structure on the behaviour of soft natural clays are accounted for by the size of the state boundary surface and changes in this size.
- The S3-SKH model requires only three additional parameters to represent structure, that reduce to two in some clays, where the effects of fabric are negligible so that the ultimate value of sensitivity is unity.

- These parameters are soil properties and can be derived rigorously from a single isotropic compression test.
- The values of the other parameters remain the same as those used in the 3-SKH model which are derived from data from tests on reconstituted soil. This has been proven to be a reasonable assumption, in particular, for the elastic stiffness parameters, A, m and n, the swelling parameter, κ, and the sizes of the inner surfaces, T and S.

The next chapter consists of an evaluation of the S3-SKH model against experimental data obtained from tests performed on natural specimens of Bothkennar and Pisa clays.

CHAPTER 5 EVALUATION OF MODEL PREDICTIONS

5.1 INTRODUCTION

In this chapter, the capability of the S3-SKH model to predict the behaviour of soft natural clays is examined. This will be achieved in two stages;

In Section 5.2, a numerical study will assess the ability of the model to simulate effects of fabric and bonding by presenting predicted data for volumetric response during isotropic compression and the response during undrained triaxial compression. Single precision was used for the analyses, therefore it is expected that in analyses simulating undrained shearing post-peak the predicted stress path deviates slightly from the critical state line (see Section 4.3.5). The effect of varying the stress history of the soil before shearing on the predicted undrained shear strength and the subsequent reduction in strength will be investigated. Finally, the correspondence between the sensitivity surface and onset of significant destructuration will be examined by performing analyses simulating drained probing tests. The analyses were performed using a strain increment of 0.001%, but the negligible effect of size of strain increment shown in Section 4.3.5 would not have influenced the computed results.

In Sections 5.3 model predictions will be compared to experimental data obtained from laboratory element tests on the two reference clays, Bothkennar and Pisa clay, which both have a metastable structure. The ability of the model to predict the peak natural strength will be examined. An assessment of the predicted level of destructuration will be given both in compression and shearing, drained and undrained, accounting for the fact that when strain-softening occurs during a triaxial test it is very possible that stresses and strains localise in the sample. Finally the advantage of including a parameter for a stable element of structure arising from fabric will be shown in Section 5.3.6 by comparing predictions with experimental data from samples of Bothkennar clay, the behaviour of which appears to be influenced by fabric.

5.2 MODELLING EFFECTS OF STRUCTURE IN SOFT NATURAL CLAYS USING THE S3-SKH MODEL

This section has three main objectives;

- To check that the predicted response is consistent with the formulation of the model, in particular that the predicted volumetric response can be described by the sensitivity framework.
- To examine the effect of varying the recent stress history on the predicted undrained shear strength and subsequent destructuration.

- To verify that despite the assumptions made in the formulation of the damage strain and the destructuration law, the main patterns of behaviour observed in soft natural clays are reproduced by the model.

5.2.1 Programme of analyses

In order to achieve the objectives cited above, five series of analyses have been carried out;

(i) A series of isotropic compression tests, in which plastic volumetric strains are dominant, was simulated for reconstituted and natural samples. The analysis CIr simulates reconstituted soil, and analyses CI1, CI2 and CI3 simulate natural soil. The analyses started from an isotropic state and slightly overconsolidated. Both natural and reconstituted samples started with the stress state on the same elastic wall, at points B and A respectively in Figure 5.2.1a, so that the difference in structure is represented by an offset in stress. The stable structure parameter s_f was varied for the analysis of natural soil so that the effect of fabric on the predicted volumetric response was examined and its consistency with the sensitivity framework was verified. In the first case, CI1, the effects of fabric dominate the behaviour such that s_f=s_0=5 and the response is that of a clay with a stable structure. If there is no effect of fabric, CI3, s_f=1, and the natural clay reaches a state on loading typical of that of the reconstituted clay. Finally, if both the effects of fabric and bonding are of importance, CI2, the value of s_f will be between 1 and 5; for the analyses presented here s_f=2.

(ii) The predicted response during undrained shearing, in which plastic shear strains are dominant, was studied by performing a series of analyses simulating a reconstituted sample, CUr, and natural samples, CU1, CU2 and CU3. At the start of the analyses, an isotropic normally consolidated state was assumed with the simulations of natural and reconstituted samples starting on the same elastic wall, at points B and A respectively in Figure 5.2.1b. As above, the structure parameter s_0 was constant and equal to 5 but s_f was varied to examine the effect of fabric on the predicted response. Analysis CU1 was carried out using a value of s_f=5, analysis CU2 used s_f=2 and analysis CU3 used s_f=1. The analyses had to be carried out to reach large strains up to 50% so that the computed behaviour near failure could be observed for analyses CU1, CU2 and CU3. Triaxial tests are generally terminated at smaller strains but the true strains are much larger in the shear planes in samples where localisation has occurred.

(iii) A third series of analyses was carried out to investigate the effect of overconsolidation on the predicted behaviour of natural samples during undrained compression. Most soft natural clays are normally consolidated or lightly overconsolidated, but in certain cases

thixotropic hardening can cause the clay to reach levels of apparent overconsolidation up to 4, for example St-Alban clay in Figure 2.3.15. For these analyses, all modelling natural samples, the initial stress states were again on the same elastic wall but at different levels of overconsolidation. Analysis CU3 started from an isotropic normally consolidated state (point B1 in Figure 5.2.1c); analysis CU32 started from an overconsolidation ratio of 1.5 (point B2 in Figure 5.2.1c); analysis CU33 from an overconsolidation ratio of 2.5 (point B3) and analysis CU34 from an overconsolidation ratio of 5 (point B4).

(iv) Another series of analyses simulated natural samples subjected to different stress histories before undrained shearing, in order to examine the effect on the predicted undrained shear strength and subsequent reduction in strength. A small size of the history surface was used in this parametric study so that the effects of recent stress history would not overshadow the effects of destructuration on the predicted response. All samples started from the same isotropic state p'=15kPa. Analysis CU41 modelled isotropic compression to a stress greater than the gross yield stress p'=200kPa before shearing; analysis CU42 anisotropic compression to reach a stress beyond gross yield p'=150kPa. Analyses CU43 and CU44 also modelled anisotropic compression to p'=150kPa, but this was followed by swelling back to p'=120kPa and p'=55kPa respectively.

(v) Finally, a series of drained probes was simulated to investigate the correspondence between the sensitivity surface and the onset of significant destructuration. The analyses modelled anisotropic compression to a stress before gross yield, p'=105kPa, followed by swelling back to p'=100kPa before drained shearing following constant directions of stress paths (Figure 5.2.2). Analyses CD45, CD90 and CD-45 were sheared towards failure, while CD0 followed an isotropic stress path.

The analyses were carried out using the S3-SKH model implemented in the single element computer program S-TERTIUS. As with the TERTIUS program (Stallebrass, 1990), the triaxial test has been modelled as a uniform element of soil, referred to as a single element, with the correct combination of stresses or strains being applied uniformly throughout the element (see Figure 5.2.3). This can lead to a predicted response that is different from that observed in the experiment, as non-uniform stress distributions and strain localisation might have occurred in the sample during the test. As was explained in Section 1.3.3, when localisation occurs the overall strains are much smaller than the real strains occurring in the shear planes in the sample. This implies that the model should then predict higher strains during the analyses than those observed during the tests.

The parameters used in the analyses are given in Table 5.2.1. They are typical parameters representative of soft clays. The values of T and S were chosen to be small, unlike the values determined for Bothkennar and Pisa clay, so that the aspects of behaviour observed are influenced mostly by effects of destructuration, and less by recent stress history. A summary of the analyses is given in Tables 5.2.2 to 5.2.6.

5.2.2 Simulation of effects of fabric and bonding

This section aims to assess the capability of the model to simulate effects of fabric and bonding. The model is validated by showing the consistency between the output data and the constitutive equations and input parameters. The agreement between the model prediction and general features of the observed behaviour of these clays reported in the literature and reviewed in Chapter 2 is also examined.

(i) Pre-failure deformation

Model predictions of small strain stiffness are shown in Figure 5.2.4 with results of analyses CUr simulating a reconstituted sample, CU1 simulating a natural sample with a stable structure, and CU3 simulating a natural sample with a metastable structure. Very small increments of strain were used in the analyses so that the elastic stiffness G_e' could be computed from the output data. This value corresponds to the plateau value of G in Figure 5.2.4. Since the natural and reconstituted samples were normally consolidated at the start of shearing, the value of the elastic stiffness depends on the value of mean effective stress only. With a value of stiffness parameter n=0.65, the offset in stress due to structure illustrated in Figure 5.2.1b causes the value of elastic stiffness of the natural samples to be greater than that of the reconstituted sample by a factor of $(125/25)^{0.65}$, which is equal to 2.85. The values of stiffness computed from the plot are related by a ratio of 2.85, confirming that the output data are in agreement with the input data. This difference in the values of elastic shear modulus in the natural and reconstituted samples is due to the combined effects of fabric and bonding, and relates to the behaviour described by Shibuya et al. (2000), who quantified structure in terms of stiffness. The predicted stiffness curves for natural samples CU1 and CU3 are the same at small strains up to 3% because both samples remain in a normally consolidated state during the undrained compression and, as will be demonstrated later, follow the same stress path on the state boundary surface up to a peak.

(ii) Stress-dilatancy

The shape of the three surfaces in the S3-SKH model is elliptical and of aspect ratio equal to the friction coefficient M, like that of the "yield" surface in the Modified Cam Clay model. The normality rule causes the flow rule for such models to be expressed as in Equation 1.4.11. Figure 5.2.5 shows the stress-dilatancy relationships computed for run CUr on a reconstituted sample, and runs CU1, CU2 and CU3 on natural samples. The natural and reconstituted samples were sheared undrained from a normally consolidated state, and, as will be demonstrated below, remained on the state boundary surface after shearing. As expected, all curves plot very close to the curve representing the flow rule for the Modified Cam Clay model, confirming that the S3-SKH model prediction is correct.

(iii) Effect of fabric on the predicted volumetric response

The isotropic compression curve for analysis CIr, the reconstituted clay, is shown in Figure 5.2.6, plotted in normalised volumetric space lnv_n-lnp′. As expected, after reaching gross yield the curve follows the isotropic intrinsic compression curve as defined in Section 1.7. Contours of sensitivity have also been sketched in Figure 5.2.6, where the sensitivity s has been calculated following Equation 4.4.2. After gross yield, the compression curve for analysis CI1, for which s_f is equal to 5, follows a line parallel to the isotropic intrinsic compression curve, and coincident with the line representing the contour of sensitivity 5. The predicted stable response is consistent with the formulation of the model (see Equation 4.3.10), and is typical of the behaviour of clay with a stable structure, of sensitivity equal to 5. Analysis CI3 shows a result typical of metastable clays, as after gross yield the compression curve tends to states on the isotropic intrinsic compression line. The predicted response is that of clays where the effects of bonding dominate the behaviour. The degradation of structure that occurs in a natural sample is successfully modelled with the value of current sensitivity s decreasing from 5 to 1 as the compression curve crosses contours of decreasing sensitivity. The effects of fabric and bonding have been combined in analysis CI2, with the ultimate sensitivity equal to 2. Even though the value of the parameter k, which controls the rate of destructuration, was the same in all analyses representing natural samples, the effect of modelling fabric using a limiting value of sensitivity greater than 1 has reduced the computed rate of destructuration. This is because the destructuration law formulated in Equation 4.3.10 and used in the model is such that the increment of change of sensitivity, δs, depends on the current value of $(s-s_f)$ as well as on the damage strain increment, δe^p. This implies that for the same increment of damage strain and same value of current sensitivity, if the stable element of structure resulting from fabric is higher, the increment of change in sensitivity is lower. Destructuration stops when the value of s

reaches the value of s_f. This is shown in Figure 5.2.6, where the compression curve for analysis CI2 tends to a stable state on the line representing the contour of sensitivity equal to 2.

(iv) Effect of fabric on the predicted response during undrained compression

The stress-strain curves obtained from analyses CUr, on the reconstituted clay, and CU1, CU2 and CU3, on the natural clay, are shown on a plot of deviatoric stress against shear strain in Figure 5.2.7. Samples CUr and CU1 show the same patterns of behaviour, strain-hardening to a critical state. In samples CU2 and CU3, strain-softening occurs. On reaching a strain of 50%, which is likely to be reached if localisation occurs, the data from analyses CU2 and CU3 are near stabilisation, and the computed current sensitivities are close to 2 and 1 respectively.

Figure 5.2.8 shows the evolution of the size of the state boundary surface during undrained shearing, by normalising the stress paths with respect to p_{ie}^*, the equivalent pressure at the intersection of an elastic wall and the isotropic intrinsic normal compression line. The normalised stress path obtained from analysis CUr follows the wet side of the state boundary surface up to the critical state line. The stress paths predicted in analyses CU1 to CU3 are well outside the intrinsic state boundary surface. The stress path from analysis CU1 follows the wet side of the natural state boundary surface, which is larger than that of the reconstituted clay by a factor of 5, up to a natural critical state point. However analyses CU2 and CU3 move towards a critical state line inside the apparent natural state boundary surface after reaching an apex just inside the state boundary surface for a stable sensitivity equal to 5. The slight departure of the stress paths from the critical state line post-peak is due to the use of single precision variables in the computations as explained in Section 4.3.5.

Figure 5.2.9 shows the stress paths for all tests, where the stresses have further been normalised for current structure, represented by s. The stress paths for all tests all plot on a single state boundary surface. Thus for normally consolidated soils the model predicts that after reaching the peak deviatoric stress, the stress path remains on the state boundary surface while it is shrinking towards a stable size (that is the size of the intrinsic state boundary surface when the effects of bonding are dominant). The equivalence between strength and stress sensitivity assumed in Section 3.3.1, and used in the formulation of the constitutive equations, means that the degradation of structure is simulated by a reduction in size of the state boundary surface. Consequently, in common with models that do not simulate destructuration, the behaviour of natural samples predicted by the S3-SKH model depends on stress and state only, where the state is determined with respect to the size of the state boundary surface. It is therefore critical to use the correct values of parameters that control destructuration, that is s_0, s_f and k.

5.2.3 Prediction of undrained shear strength and subsequent reduction in strength with plastic strain

A first series of analyses was carried out to examine how the combined effects of destructuration and overconsolidation influence the predicted behaviour during undrained compression. As noted in Section 5.2.1, the series consisted of four analyses modelling shearing from isotropic states at different levels of overconsolidation. The effect of fabric is not investigated here, therefore all samples have a value of s_f=1. Figure 5.2.10 shows the stress paths followed by the different samples in the q′-p′ plane. The analysis representing normally consolidated loading, CU3, is the same as in the previous section. Its stress path follows the state boundary surface for a stable clay of sensitivity equal to 5 up to a peak, before moving down towards a critical state. Again the deviation from the critical state line is due to the use of single precision variables in the analyses. Analysis CU33, which modelled shearing from an overconsolidation ratio of 2.5, shows an initial response that is typical of overconsolidated stable clays. The stress path heads towards a critical state at the intersection of the critical state line and the state boundary surface of a stable clay of sensitivity equal to 5, but, as it nears the critical state stress ratio changes direction and moves towards a critical state inside the natural stable state boundary surface. This is clearer in analysis CU34, where the computed stress path initially moves up the critical state line, but as the metastable state boundary surface starts decreasing significantly in size the stress path is forced to move down with it. This creates the loop observed in analysis CU34 in Figure 5.2.10. Curves of shear modulus against shear strain are shown for the four analyses in Figure 5.2.11. The values of elastic stiffness calculated using Equation 4.2.16 (Viggiani & Atkinson, 1995) are 23MPa, 19MPa, 16MPa and 12MPa for analyses CU3, CU32, CU33 and CU34 respectively. These values agree with the pattern of curves shown in Figure 5.2.11.

The large strain behaviour is shown as a plot of deviatoric stress against shear strain in Figure 5.2.12. As expected, the curve for analysis CU3 reaches a peak strength 50% higher than that reached by the curves for analyses CU33 and CU34. The curve for analysis CU32, simulating undrained shearing from a lightly overconsolidated state, reaches a lower peak strength, which is reflected by the corresponding stiffness curve in Figure 4.2.11. In analysis CU32, destructuration occurs at a higher apparent rate than for the other analyses, indicating that the effects of structure may be more apparent for more heavily overconsolidated samples than for lightly overconsolidated. This results from the greater stiffness of the more heavily overconsolidated samples that prevents a too rapid destructuration and allows then to develop a more pronounced peak strength.

The effect of modelling different stress histories on the predicted undrained shear strength and destructuration was investigated, as described in Section 5.2.1. The compression

curves corresponding to the different stress histories are shown in the lnv-lnp′ plane in Figure 5.2.13. In analysis CU41, modelling isotropic compression to p′=200kPa leads to virtually no destructuration being computed during the compression stage. In analyses CU42, CU43 and CU44, which modelled anisotropic compression to p′=150kPa, a large amount of destructuration is computed. It is thus expected that not much destructuration will be predicted during the subsequent undrained compression.

Figure 5.2.14 shows the stress paths followed by the four analyses. CU41 does not show any strain-softening before the end of the analysis, which finished at 20% strain, and its stress path moves towards the critical state line. Destructuration is nevertheless occurring as the stress path is moving inside the initial state boundary surface. CU42 has a much less stiff response at the start of shearing, and the predicted stress path does not reach a peak but immediately moves down to a critical state as strain-softening is predicted. In practice samples are generally left to rest between the compression and shearing stages. Typically some creep occurs and the behaviour of a sample with a compression history similar to that modelled by analysis CU42 would show a stiff initial behaviour, with a marked peak, before heading downwards as the structure degrades. The S3-SKH model cannot reproduce this behaviour as a model for creep is not included. Analyses CU43 and CU44, in which swelling was modelled before shearing, gave an initial response that is stiffer than that of analysis CU42, as expected. Both analyses predict a brittle behaviour, with a marked kink at peak strength before strain-softening. This is more typical of samples that are sheared from their in situ stress state (see specimen SCU1 in Figure 3.2.11).

The small strain behaviour computed is shown on a plot of shear modulus against shear strain in Figure 5.2.15. Analysis CU42 reached normally consolidated states prior to shearing, thus its stiffness is very low at the beginning of the shearing stage, as is shown in Figure 5.2.12. The elastic stiffness calculated using Equation 4.2.16 are 32MPa, 27MPa and 19MPa for analyses CU41, CU43 and CU44 respectively. These values also agree with the graph shown in Figure 5.2.15.

5.2.4 Sensitivity surface and onset of significant destructuration

A series of drained probes has been simulated, in order to define the surface marking the onset of significant destructuration following Callisto (1996) and Smith (1992). The stress paths have been normalised with respect to the equivalent pressure at the intersection of an elastic wall and the isotropic intrinsic compression line, p_{ie}^*. Figure 5.2.16 shows the normalised stress paths together with the intrinsic state boundary surface and the natural state boundary surface at the start of the probes if the initial sensitivity s_0 is equal to 5. At the start of the simulation of drained probes, the value of sensitivity was equal to 4.47. The output data from the analyses

show that at the apex of the change in direction of the stress paths, s=4.3 for CD0, s=4.44 for CD45, s=4 for CD90 and s=4.24 for CD-45. However this reversal in direction in the stress paths defines an outer surface almost coincident with the state boundary surface for a sensitivity of 3.8. Therefore this outer surface does not identify the sensitivity surface at the beginning of the tests. After reversing in direction, the stress path from analysis CD0 moves towards the isotropic intrinsic compression point. The stress paths from analyses CD45 and CD90 move towards the intrinsic critical state point in compression, and analysis CD-45 towards the intrinsic critical state point in extension.

By normalising by the current sensitivity (computed s) the normalised stress paths become typical of stress paths for reconstituted samples (see Figure 5.2.17). The various stress paths move towards the normalised isotropic compression point (analysis CD0) and the critical state points in compression (analyses CD45 and CD90) and in extension (analysis CD-45) on the surface, and define a stable state boundary surface. This emphasises that the effect of structure is purely due to change in sensitivity, which is directly associated with the size of the state boundary surface.

Contours of strain energy per unit volume are shown on the stress paths normalised by p_{ie}^* which are plotted in Figure 5.2.18. The outer surface defined by the points of stress path reversal coincides with the contour of strain energy W=1kJ/m^3. This value, which was obtained using values of parameters representative of soft clays, is in agreement with the behaviour reported for several soft natural clays, for example Pisa clay (Callisto, 1996), or St-Alban clay (Tavenas et al., 1979).

5.2.5 Summary

This section has shown that predictions by the S3-SKH model are consistent with the formulation of the model. Among the predictions presented, some interesting features of behaviour were noted, such as the loop predicted in a stress path obtained for an analysis simulating undrained shearing from an overconsolidated state. This section also demonstrated that the S3-SKH model predicts features of behaviour corresponding to an accepted response for this kind of clays. For example the model predicts an increase in compressibility at gross yield during volumetric compression, a reduction in strength post-peak during undrained shearing, and the coincidence between the gross yield curve and a contour of strain energy. In the following section, a detailed comparison with Bothkennar and Pisa clays will be presented. Two key issues will be addressed; firstly how to perform the analyses, and secondly how close the predictions are to the experimental results despite the assumptions made when performing these analyses, in particular concerning the determination of initial stress state and sensitivity.

5.3 MODELLING LABORATORY ELEMENT TESTS ON SOFT NATURAL CLAYS WITH A METASTABLE STRUCTURE

This section evaluates the model against test data from the literature for samples from two soft clays with a metastable structure, Bothkennar and Pisa clays. The major problem encountered when modelling soft natural clays with a metastable structure, is the difficulty in determining a starting point for the analyses. This problem is linked to the uncertainty in determining the stress history that should be simulated and which value of initial sensitivity to associate with it. In the following, Sections 5.3.1 and 5.3.2 examine in more detail the implications of these uncertainties on the model predictions.

5.3.1 Simulation of stress history

When using the S3-SKH model, simulation of the recent stress history can change predictions dramatically, thus it is critical to model it correctly. This can be done reliably for reconstituted samples, for which the full stress history is known, but for natural samples retrieved from the ground there is a lot of uncertainty about how to model all the processes that the soil has undergone prior to testing. In particular, as seen in Section 1.3.2, soft natural clay samples are often disturbed during sampling, transport, storage, preparation and installation in the apparatus. The main effects of this disturbance are a reduction in the mean effective stress and in the preconsolidation pressure. By simulating these effects in a simplified way, the conditions at the start of testing may be closer to what really happened, and the prediction be significantly improved. Ladd & Lambe (1963) suggested that during sampling the sample experiences a total stress relief while following an undrained stress path to the isotropic axis. Then the subsequent disturbance due to other processes is more or less equivalent to isotropic unloading resulting from dissipation of excess pore pressure in the sample. The whole process corresponds to a total stress path going from the start point, in the ground, to the end point, at the end of sampling and preparation. In order to verify to what extent the simulation of sampling and disturbance can be simplified, a comparative study has been carried out, with one analysis simulating effective stress paths corresponding to undrained unloading and isotropic swelling and the other analysis simulating drained unloading direct to the reduced mean effective stress (see Figure 5.3.1). The advantage of this last analysis is that it is better defined as now both start and end points are known. The parameters and initial conditions for these two analyses are given in Table 5.3.1. Figure 5.3.2 shows the configuration of the surfaces at the end of sampling and preparation. While the sensitivity and history surfaces are in the same location, there is a slight difference in the position of the yield surface at the end of the two simulations. This difference will not affect results for the subsequent analyses, in particular since in the tests simulated the shearing stages

were always preceded by a recompression stage. Therefore in subsequent analyses, the simplified drained stress path will be used to simulate sampling and preparation of the sample.

As noted above, after being placed in the apparatus, the natural specimens are usually recompressed to their in situ stress state. In general the amount of volumetric strain occurring during recompression is small (Hight et al., 1992b). Researchers involved in testing soft natural clays usually devise the stress path followed during recompression with the aim of minimising the amount of disturbance created by the process.

Bothkennar clay specimens tested by Allman (1992) and by Smith (1992) were subjected to different reconsolidation histories prior to shearing. When the specimens were installed in the apparatus, they were typically under an initial isotropic effective stress, which was usually reduced to a value around 20kPa as a result of the disturbance caused by the processes associated with sampling and preparation. Smith accounted for the overconsolidation history by simulating a compression stage to the preconsolidation pressure, followed by a swelling stage to the in situ stress (stress path ABCD in Figure 5.3.3). Allman followed a less destructive method of reconsolidating, by compressing the specimen isotropically to its in situ horizontal effective stress, then increasing the vertical effective stress only to its in situ value (stress path AED in Figure 5.3.3).

Pisa clay specimens tested by Callisto (1996) were recompressed following stress path AED in Figure 5.3.3. Callisto assumed that only a small amount of disturbance occurred in the samples, so that after sampling they were in an isotropic stress state equal to the measured suction pressure p'=55kPa. The specimens were compressed isotropically to reach the value of horizontal effective stress in situ σ_h'=75.5kPa, after which the vertical stress only was increased to reach the value of vertical effective stress in situ σ_v'=113.5kPa.

In practice, determination of the in situ stress state is difficult. Because soft natural clays are disturbed easily, the void ratio in situ also cannot be measured reliably. In this dissertation, it has been assumed that the values of void ratio in situ and at the end of recompression are about the same. This simplification, which avoids repeated analyses to try to fit the exact void ratio at the beginning of the tests, leads to predicted values of void ratio at the end of recompression which are slightly different from those in the experiments. The real implication is that when normalising for volume, predicted and experimental stress paths will not start from the same place. What is really important is to be at a correct state at the start of shearing. Since all the specimens simulated here are significantly to the wet side of critical, a slight difference in void ratio should not have a substantial effect on the predictions.

A comparative study was carried out to examine the effect on the predicted response of simulating the full stress history, that is the stress paths imposed during sampling and preparation as well as the recompression history, on the predicted response. Figure 5.3.4a shows stress paths for Bothkennar clay specimen SCU1 predicted by simulating the full stress history.

Figure 5.3.4b shows stress paths for the specimen predicted by simulating the recompression history only. It is clear from these graphs that including the sampling and preparation history in the computation significantly improves the predictions. This is due to the large value of T that fixes the size of the history surface, implying that the recent stress history greatly influences the response of the soil. Figure 5.3.5 shows the configuration of the surfaces during recompression when only recompression has been modelled (stress path BCDE). At the end of the process, the stress point is close to the sensitivity surface, thus the predicted value of stiffness at the start of shearing will be low, and the predicted value of undrained shear strength will be limited. Figure 5.3.6 shows the configuration of the surfaces when the full stress history has been simulated. The size of the history surface is large due to the large size of the sensitivity surface and to the high value of T. As a result, the kinematic surfaces have remained in the same position, thus the stress point is still quite centred at the start of shearing. The large size of the sensitivity surface also allows a high stiffness and undrained shear strength to be predicted. Figure 5.3.7 shows a comparison of the predicted stress paths for Pisa clay specimen AUC when the full stress history has been simulated and when only the recompression history has been simulated. As for Bothkennar clay, modelling the full stress history significantly improves the prediction. Therefore for all the analyses presented in the following sections, the full stress history was recreated.

5.3.2 Uncertainty in determining initial sensitivity

If the full stress history needs to be modelled, as concluded in the previous section, it is necessary to determine the sensitivity in the ground. As was noted in Section 4.4.2, there is no reliable way of measuring sensitivity in the ground because soft clays are easily disturbed. Table 4.4.1 describes methods used to determine values of sensitivity from undrained compression or volumetric compression test data. Assuming that little destructuration occurs before gross yield during these tests, values calculated using the flow chart in Table 4.4.1 give a good estimate of the value of sensitivity at the start of the test but not the sensitivity in situ. The value of sensitivity in the ground could be determined by back-analysing from a state where the sensitivity is known, but this procedure would assume that the destructuration predicted by the model is correct. For the two clays examined in this dissertation, Bothkennar clay and Pisa clay, methods have been adopted which depend on the data available for each soil. The following section explains these methods. In both cases, the sensitivities have been derived from laboratory test data, but as was seen in Figure 5.3.6 the effect of sampling and recompression on the sensitivity surface and hence on the value of sensitivity is predicted to be very small.

5.3.3 Determination of soil parameters

The parameters used in the analyses were the parameters used in the 3-SKH model that were determined in Section 4.2.3 for the reconstituted clay, plus the three structure parameters. For Pisa clay, the two samples used for the tests have been found by Callisto (1992) to have similar properties. For Bothkennar clay, due to the great variability of soil properties with depth, different sets of parameters have been used in the various tests, all derived in a consistent way. As was noted above the values of initial sensitivity are still uncertain. The analyses that will be presented next give an evaluation of the predictions that can be obtained by using structure parameters derived in a rigorous way. The soil parameters for Bothkennar clay and Pisa clay are summarised in Tables 5.3.2 and 5.3.3.

(i) Bothkennar clay

Samples of Bothkennar clay were retrieved from a wide range of depths and different facies. Figure 4.4.5 in Section 4.4.2 shows the variation in sensitivity with depth, and encompasses values of sensitivity that have been calculated following the different methods described in Table 4.4.1. For depths below 6m, the values of sensitivity computed by Hight et al. (1992) and based on fall cone results define the upper limit to the range of values. The values of sensitivity computed from the Sensitivity framework using compression data (Cotecchia & Chandler, 2000) generally define the lower limit, except for depths below 13m, where this is defined by values of sensitivity derived from triaxial shearing results. Therefore for each depth there is a corresponding range of values of sensitivity. Given that a small difference in the value of initial sensitivity can lead to a great difference in the response by the S3-SKH model, in the following predictions using both the upper and lower bound values of sensitivity will be presented. Table 5.3.4 gives a summary of the values used in the analyses.

Since there were not enough data available to determine the parameter k, which controls the rate of destructuration with plastic strain, for each facies, it is assumed to be the same for all the samples. It is reported in the literature (Hight et al., 1992) that each facies type has a distinctive macro-fabric and micro-fabric which appear to influence the response to sampling. Therefore it is expected that there will be some inconsistencies between experimental and predicted data for different facies.

(ii) Pisa clay

The samples of Pisa clay were retrieved from the sub-layers B1 and B3 of the Upper Clay layer of the subsoil of the Tower of Pisa. Both sub-layers B1 and B3 are considered to be

homogeneous. It is therefore expected that for each layer a single value of initial sensitivity will be needed to model all laboratory tests. The value of initial sensitivity can be determined in terms of stress sensitivity from available isotropic compression test data on natural specimens. Figure 5.3.8 shows the isotropic compression curves obtained from specimens from samples 19B and 29A from sub-layers B1 and B3 respectively. For each sample the value of s_0 can be computed following the method detailed in Section 4.4.2. The values obtained are s_0=3.5 for sample 19B and s_0=2.8 for sample 29A.

5.3.4 Programme of analyses

A wide range of test data was available for Bothkennar clay, but a more restricted selection had to be used for Pisa clay. The most critical aspect of a model for soft natural clays is its ability to predict undrained shear strength and the subsequent reduction in strength with plastic strain. For Bothkennar clay, a selection of undrained triaxial compression tests was chosen to be modelled, for which different stress histories had been applied prior to shearing. For Pisa clay, only one undrained compression and one undrained extension test were simulated as they were the only tests available. A series of isotropically consolidated drained tests was also modelled to investigate the effect of compressing beyond gross yield before shearing on the predicted response. Finally a series of drained probes was available for both clays. These data were used to examine whether the onset of significant destructuration, which is visible by normalising for volume, is correctly predicted. The analyses simulating specimens of both Bothkennar and Pisa clays, which are summarised in Tables 5.3.5 and 5.3.6, are detailed below.

(i) Bothkennar clay

Experimental data for the different tests were available from the literature (Allman, 1992, and Smith, 1992). All samples were high quality samples, retrieved by using either the Laval method (tests beginning with L) or the Sherbrooke method (tests beginning with S). Specimens SCU1, SH13 and L23 were recompressed to the in situ stress before shearing undrained. As noted in Section 5.3.1, Smith and Allman followed different methods of recompression. Smith recompressed specimen SCU1, which was retrieved from the bedded facies, following the stress path ABCD shown in Figure 5.3.3 in order to simulate the lightly overconsolidated stress history. Allman recompressed specimens SH13 and L23, retrieved from the laminated and bedded facies respectively, following the stress path AED in Figure 5.3.3, in order to create as little disturbance as possible. Specimens SUD2, from the bedded facies, and LUD1, from the mottled facies, were compressed isotropically and anisotropically respectively to stresses greater than the gross yield stresses, before shearing undrained (see Figure 5.3.9). Finally specimens

LCD0, LCD55, LCD70 and LCD315, which were retrieved from the mottled facies, were recompressed to the in situ stress by Smith along the ABCD stress path in Figure 5.3.3. They were then subjected to drained stress paths radiating from the in situ stress point, forming angles of 0, 55, 70 and 315 degrees to the horizontal (see Figure 5.3.10).

(ii) Pisa clay

Experimental data for the different tests were available from the literature (Callisto, 1996; Rampello et al., 1996). The specimens tested by Callisto were retrieved from samples 19B in sub-layer B1. As noted above, Callisto recompressed Pisa clay specimens to the in situ stress following the stress path AED in Figure 5.3.3. Specimens AUC and AUE were then sheared undrained, in compression and extension respectively. Specimens A0, A30, A60 and A90 were subjected to drained stress paths radiating from the in situ stress point, forming angles of 0, 30, 60 and 90 degrees to the horizontal (see Figure 5.3.11). The series of drained tests on specimens CID1, CID2 and CID3, which were retrieved from sample 29A in sub-layer B3, were isotropically compressed to stresses equal to 98kPa, 196kPa, and 294kPa, before being sheared. The stress paths are shown in Figure 5.3.12. There was no information available about the in situ state of the specimens tested, therefore the analyses were started from the same isotropic state p'=20kPa, with the history and yield surfaces as near to as possible centred on the stress point. Since the specimens were isotropically compressed before shearing, the recent stress history before shearing could be modelled, so that the configuration of the surfaces at the end of compression and before shearing was correct.

5.3.5 Modelling destructuration

(i) Bothkennar clay

Consolidated undrained tests

In Figure 5.3.13, predicted stress paths for the test using specimen SCU1 are plotted in the q'-p' plane. Two sets of predictions are presented using initial values of sensitivity of 5 and 9, together with the experimental data. When the full stress history is simulated, the model predicts the high stiffness at the beginning of the undrained shearing stage. The predicted stress paths reach a peak strength, then the strength decreases as the specimen is strain-softening due to destructuration. The stress path predicted with $s_0 = 9$ reaches a peak strength well above the critical state line because the state of the soil at the start of shearing is on the dry side of critical. Both predicted stress paths show a brittle behaviour similar to that in the experiment. Within the

range of sensitivities examined, the undrained shear strength could be predicted with an accuracy of ±20%, the two predicted curves plotting above and below the experimental curve. However too large a value of s_0 leads to predicted behaviour typical of highly overconsolidated rather than lightly overconsolidated clays. Predicted and experimental stress-strain responses are shown in Figure 5.3.14. The model did not reproduce the rapid decrease in strength observed at relatively small strains, but for strains greater than 3%, the predicted and experimental rates of reduction in strength with strain are quite similar for both predicted sets of data. There is no information indicating whether specimen SCU1 developed shear planes, and therefore no conclusion can be drawn about the sharp post-peak decrease in strength observed during the experiment.

Figures 5.3.15 and 5.3.16 show the experimental and predicted stress paths for tests L23 and SH13 plotted in the q′-p′ plane. As above, the predicted data give the upper and lower bound stress paths obtained using the maximum and minimum values of initial sensitivity described in Figure 4.4.5. In specimen L23, the upper bound sensitivity (s_0=13.5) leads to a prediction of the undrained shear strength of the specimen that matches the measured value. For specimen SH13, it is the computation using the lower bound sensitivity (s_0=10) that gives an undrained shear strength which is very close to the experimental value. Because of the use of single precision variables in the analyses, for both tests the predicted stress paths are to the left of the critical state line post-peak. Plots of the shear modulus against shear strain are shown in Figures 5.3.17 and 5.3.18 and confirm that the two highlighted values of sensitivity give the best-fit with the experimental data.

Figures 5.3.19 and 5.3.20 show graphs of deviatoric stress against shear strain. The predicted data reach peak strength at the same strain as in the experiment. During the analyses the specimens were sheared to reach the same strain as in the test. For the same amount of strain, the final deviatoric stress computed for specimen L23 is under-predicted by 30%, and by 14% for specimen SH13. For both tests the reduction in sensitivity predicted by the model during destructuration is therefore greater than that observed in the experiment. This direct comparison may not be valid because of the possibility of stress non-uniformity associated with strain-softening. However qualitatively test data seem to approach a quasi-stable state at 20% strain while predicted data still show a large reduction in shear strength. The over-prediction of destructuration cannot be explained by strain localisation, as strain localisation would cause the opposite effect, which is to slow down the apparent net rate of destructuration. For specimen L23, which was retrieved from the bedded facies, it is possible that there may be effects of fabric slowing the process of destructuration and allowing the specimen to reach a stable state before the intrinsic state. It has been shown in Section 5.2.2 that including fabric in the computations has the effect of reducing the net rate of destructuration. The advantage of including fabric effects in the analyses simulating specimen L23 will be investigated in the next

section. For specimen SH13, which was retrieved from the laminated facies, the influence of fabric is less significant. Clayton et al. (1992) observed that specimens from the laminated facies of Bothkennar clay underwent more destructuration during sampling and reconsolidation, particularly in the case of the Sherbrooke specimens. It is therefore possible that specimen SH13 had undergone more destructuration prior to shearing than was predicted, so that during the test it was at a state closer to a stable state than was computed by the model. It must be noted that in all cases, the predicted and experimental forms of the stress path are similar, which implies that the shear/volumetric coupling at the start of the test is predicted correctly. Thus the behaviour of these specimens of Bothkenar clay is not affected by strong anisotropy.

Consolidated drained tests

Smith (1992) performed a series of drained probes on intact specimens from the mottled facies of Bothkennar clay. The specimens were reconsolidated to in situ stresses by accounting for the overconsolidation history, as described in Section 5.3.4. The full stress history was simulated in the analyses. The different stress paths followed in the test, which radiated out from the in situ stress state, are shown in the q′-p′ plane in Figure 5.3.10. The stress paths cross lines of constant stress ratio, hence the compression curves obtained in the laboratory also cross lines corresponding to constant stress ratio lines in volumetric space. Predicted and experimental compression curves are plotted in the lnv-lnp′ plane in Figure 5.3.21. The predicted curves at a greater angle to the horizontal, that is crossing more lines of constant stress ratio, have a higher compression index, as is observed in the experiment. This phenomenon occurs simultaneously with destructuration, which would cause the same pattern of curves to occur, therefore it is difficult to distinguish the effect of destructuration in the volumetric plane.

The destructuration effect can be seen by normalising with respect to the equivalent pressure at the intersection of an elastic wall and the isotropic intrinsic compression line. Figure 5.3.22 shows the normalised stress paths obtained in the laboratory. All the tests show a reversal in normalised stress path direction. The points where they reverse define an outer surface that represents the onset of significant destructuration. The starting point of the normalised predicted stress paths coincides with that of the experimental stress paths. This implies that in the simulations the samples started from the same state as in the tests, thus the change in size of the bounding surface during sampling, preparation and recompression was predicted correctly. The process of destructuration was successfully predicted as the predicted normalised stress paths also define a limit state surface at the points where they reverse in direction. The predicted surface is coincident with the experimental surface except in the area of negative deviatoric stress. This may be due to the soil having different strengths in compression and extension,

which is not simulated by the model. The specimens were sheared to reach the same stress point in the analyses as in the experiment.

Figures 5.3.23 to 5.3.26 show comparisons of the predicted and experimental stress-strain curves for each drained probe. The predicted data show good agreement with the experimental data for tests LCD0 and LCD70, but in tests LCD55 and LCD315, the volumetric strains were under-predicted by 25% and 40% respectively, and shear strains by 40% and 30%. In fact it was also found in simulations of reconstituted Pisa clay specimens in Section 4.2.4, that for specimens sheared along stress paths when there is only a gradual change in stress ratio, the agreement with the test data was poor. However, the predicted surface defining the onset of significant destructuration in natural Bothkennar clay matched that determined from the test data for positive deviatoric stresses. This demonstrates two points; firstly that the change in size of the sensitivity surface is correctly predicted; and secondly that the assumption that plastic volumetric and shear strains are the same importance in the destructuration law is reasonable. For Bothkennar clay, the predictions of destructuration during drained tests are better than for undrained tests. It is possible that localisation plays a role in the undrained behaviour of soft natural clays but, as was noted before, the effect of shear planes would be the opposite of that observed here.

Undrained behaviour following consolidation to large strains

In the tests on specimens SUD2, from the bedded facies, and LUD1, from the mottled facies, which were performed by Smith (1992), the specimens were consolidated to stresses greater than the gross yield stress prior to shearing. Specimen SUD2 and specimen LUD1 were compressed isotropically and one-dimensionally respectively (see Figure 5.3.9). The predicted and experimental compression curves for the two tests are shown in Figure 5.3.27. From these curves it can be concluded that the initial sensitivity of 3.6, which was derived from test data for specimen SUD2 using the sensitivity framework, is slightly too low to use in the computations. In contrast, the initial sensitivity of 6, which was derived from test data for specimen LUD1, gives a good fit with the test data. This means either that the amount of destructuration that has occurred during sampling and preparation in specimen SUD2 is greater than that in specimen LUD1, or that isotropic compression causes more destructuration than one-dimensional compression, as was suggested by Cotecchia & Chandler (2000). Since the first hypothesis disagrees with observations by Hight et al. (1992b) that samples from the mottled and laminated facies are more likely to be destructured during sampling than samples from the bedded facies, the suggestion proposed by Cotecchia & Chandler might be the correct explanation. Thus the value of initial sensitivity for SUD2 computed from the isotropic compression test data is lower than the sensitivity in the ground. However, assuming the amount of destructuration predicted

by the model is correct, the value of initial sensitivity for LUD1 computed from one-dimensional compression test data gives a good estimation of the sensitivity in the ground. The good agreement between the predicted and experimental compression curves for LUD1 ensures that at the beginning of shearing, where the clay is in a normally consolidated state, the value of sensitivity is correct.

Figure 5.3.28 shows the predicted and experimental stress paths for test SUD2. The predicted stress path corresponding to s_0=3.6 reaches a peak strength with an accuracy of 11%, and the amount of destructuration is predicted with an accuracy of 4%. Using an initial sensitivity of 9 gives a better prediction of the undrained shear strength, but the value of 9 does not fit with the compression curve of SUD2. It is suspected that fabric may influence the behaviour of specimen SUD2, which was retrieved from the bedded facies, and may have caused the net rate of destructuration to be lower.

Figure 5.3.29 shows predicted and experimental stress paths for specimen LUD1. The predicted stress path for s_0=6 has an initial stiffness lower than in the experiment. This pattern of prediction was also found when simulating one-dimensionally compressed undrained compression tests on reconstituted specimens of Bothkennar clay in Section 4.2.4. The stress state at the beginning of shearing is close to the sensitivity surface, thus the predicted stiffness, which depends on the distance to this surface, is low. During the laboratory test, Smith (1992) let the specimen rest at the end of the anisotropic compression, therefore creep must have occurred, which is not simulated by the model. The effect of creep does not seem to be as significant in specimen SUD2, which is in an isotropic state, as in specimen LUD1. Specimen LUD1 reaches its peak strength at a higher stress ratio than in the experiment. After peak, the predicted stress path is supposed to move down the critical state line as destructuration occurs. The stress paths in Figure 5.3.29 are to the left of the critical state line, due to the accumulated errors computed by the program S-TERTIUS when using single precision variables. Quantitatively, the predicted reduction in strength due to destructuration at the end of shearing is 25% greater than in the experiment, as shown in Figure 5.3.30. Qualitatively a larger decrease in strength than in the experiment is predicted post-peak.

Normalised behaviour during undrained compression tests

Figures 5.3.31 to 5.3.35 show the stress paths for specimens SH13, L23, SCU1, SUD2 and LUD1 normalised for composition by M, and for volume by the equivalent pressure at the intersection of an elastic wall and the isotropic intrinsic compression line. The predicted normalised stress paths start at a state different from that in the experiment. For specimens SH13, L23 and SCU1, as was explained earlier, this is due to the approximation made about the specific volume in situ when simulating the full stress history, which leads to small differences

in the predicted and experimental value of specific volume at the start of shearing. For specimens SUD2 and LUD1, this is also because the volumetric strain that was predicted during the compression stage was different from that occurring during the test. In these figures the effect of volume is misleading. For example, the analyses which gave a best fit with the test data on the q′-p′ plots in Figures 5.3.15 and 5.3.16 appear to predict too high a strength in the normalised plots in Figures 5.3.31 and 5.3.32. This demonstrates that this normalisation, which is very sensitive to values of specific volume, is not representative of the behaviour of the clay. It is rather the value of sensitivity that characterises the predicted response of the clay.

In Figure 5.3.36, a selection of stress paths has been further normalised by initial sensitivity, S_t. For the analyses simulating tests SCU1, L23 and SH13, the values of initial sensitivity used to normalise are the estimated values of sensitivity in the ground. For analyses simulating tests SUD2 and LUD1, it is the value at the end of the compression stage, where the sensitivity is known. The stress paths shown in Figure 5.3.36 correspond to the best-fits obtained in the analyses simulating tests SH13, L23, SUD2 and LUD1. Both the predicted and experimental data fall within a single normalised state boundary surface. This demonstrates that initial sensitivity describes the size of the initial natural state boundary surface, irrespective of whether it is calculated using volumetric or undrained shearing test data. Again the state at the start of shearing predicted by the model is different from that during the experiments, but the same patterns of behaviour can be observed for both sets of data.

When the value of initial sensitivity had been determined reliably, the S3-SKH model could simulate well the drained behaviour of natural Bothkennar clay specimens. These drained tests involved both plastic volumetric and shear strains, sometimes in equal quantities, thus the choice of damage strain for the destructuration law seems reasonable. The undrained behaviour of the natural specimens was predicted with less success. The range of values of sensitivity selected for the analyses proved to be sufficient to predict the undrained shear strength with an accuracy of between 10 and 20%. However the amount of destructuration predicted by the model is always greater than that observed in the experiments. Since the drained probes could be predicted well, the systematic over-prediction in the undrained analyses cannot be attributed to the relative influence of plastic volumetric and shear strains in the damage strain. A straightforward comparison of predicted and test data may not be valid post-peak due to the possibility of localisation. However predictions could be improved qualitatively by revising the determination of the parameter k. It has been assumed for these analyses that the parameter k, which controls the rate of destructuration, is the same for all samples. This assumption may be too simplistic, and destructuration may occur at a lower rate in some samples from different facies. It has been seen in Section 5.2 that to use a value of ultimate sensitivity greater than unity in the analyses leads to an apparent net rate of destructuration that is slower than when no effect of fabric is simulated. Since the bedded facies, and possibly the laminated facies, show

some fabric in their macrostructure, it is thought that this fabric has a significant effect on the destructuration, causing the sample to become stable before reaching the intrinsic state. This will be investigated in the next section.

(ii) Pisa clay

Isotropic tests

The isotropic compression tests on specimens from samples 19B and 29A were performed directly on the undisturbed specimens. The specimens were compressed to stresses beyond gross yield, then they were swelled back and finally recompressed to higher stresses beyond a new gross yield point, as shown in Figure 5.3.37, where the predicted data are plotted with the experimental data. The predicted compression curves for both specimens agree with the experimental data up to the point of stress reversal, after which the hysteresis loop and the lower part of the curve are predicted less successfully. However the lower part of the experimental curve for sample 19B is suspected to be incorrect. In general the net rate of destructuration is at its maximum at gross yield, causing the slope of the compression curve to be also at a maximum at gross yield, then this slope decreases asymptotically to reach the same value as the compression curve of the reconstituted clay. Since there is a good agreement between the predicted and experimental curves around gross yield, the values of sensitivity used in this analysis will also be used for the following analyses.

Consolidated drained tests

Figure 5.3.38 shows a comparison of the predicted and experimental compression curves obtained for these tests, plotted in the lnv-lnp′ plane. The isotropic normal compression line for the reconstituted soil is also shown on the graphs. Generally, the model tends to over-predict the amount of plastic volumetric strain occurring during the drained shearing probes.

Figure 5.3.39 shows the predicted and experimental stress paths, where the stresses have been normalised with respect to the equivalent pressure at the intersection of an elastic wall and the isotropic intrinsic compression line. The predicted stress paths show the same patterns of behaviour as the experimental stress paths, with points of reversal in direction describing an outer surface. The limit surfaces defined by the predicted data and the test data are however not very close. The fact that the model can predict correctly isotropic compression from an isotropic state (test 19B described above) shows that both the initial sensitivity s_0 and the rate of destructuration k are reliable parameters for sample 19B. Also test A0, during which only a small amount of plastic shear strain occurred, has the closest agreement between the

predicted and test data. In the analyses simulating tests A30 and A60, gross yield occurs at stresses lower than in the experiment, leading to significant destructuration to be predicted. This may be due to structural anisotropy in the natural samples (less destructuration in the K_0 direction).

Figure 5.3.40 shows the stress-strain curves for tests A0, A30 and A60 in the p'-ε_v plane. As noted above, the model predicted gross yield to occur at lower stresses than in the experiment, unlike the drained probes on Bothkennar clay where gross yield was predicted to occur at higher stress than in the test. In the analyses simulating tests A30 and A60, the volumetric strain is over-estimated by more than 20% and 50% respectively, whereas in Bothkennar clay it was under-estimated by as much as 40%.

Figure 5.3.41 shows the stress-strain curves for analyses A60 and A90 in the q'-ε_s plane. In analysis A60, the strength was under-predicted by 20%. Since the analysis simulating the drained probe on reconstituted specimen R30 gave similar results to the analysis simulating A30, in particular with the volumetric strain being over-predicted by 25% (see Section 4.2.4), a better agreement between analysis A30 and the test data could not be expected. However, generally the patterns of stress-strain response during the drained probes have been predicted correctly, except for specimen A90 where some strain-softening had occurred during the experiment, which was not modelled during the analysis. The stress path for specimen A90 has a peculiar shape, which may be an indication that localisation occurred in the specimen during the experiment, causing the strain-softening.

Consolidated undrained tests

Figure 5.3.42 shows a comparison of the predicted and experimental stress paths for both tests. In compression, the predicted stress path reaches a peak strength on the critical state line then follows it down to a critical state. The peak stress ratio that is higher than the critical state stress ratio and the loop observed in the test were not predicted by the model, leading to the undrained shear strength being under-predicted by 20%. A similar loop was observed by Burland (1990) for Norwegian clays. He suggested that up to peak strength soft clays are composed of packets of particles linked together by bonds and behave similarly to granular materials, hence the dilatant behaviour, whereas after peak the packets break down and the behaviour becomes contractant. In extension, where the analysis was performed using the same friction coefficient M as in the compression test, the predicted and experimental data agree rather well. It is thought that instability due to necking of the specimen caused the decrease in stress ratio post-peak. The predicted stress path has only been taken to the same strain as the experimental data, and would continue to the M=0.85 envelope. The fact that the natural sample fails at a lower stress ratio is a confirmation that, as is generally the case, M in extension is lower than M in compression.

Figure 5.3.43 shows the curves of deviatoric stress q′ against shear strain for both tests. In compression, the predicted rate of reduction in strength is consistent with the experimental data for strains greater than 5%, that is after the initial abrupt reduction in strength. In extension, no destructuration is visible in either the test data or the predicted data and the predictions fit with the test data quite well. The strain-hardening predicted by the model at these states occurs because failure will be at a higher strain than in compression so that the analyses have not yet reached the peak strength and the onset of strain-softening with destructuration.

Predicted and experimental excess pore water pressures are plotted against shear strain in Figure 5.3.44. The predicted data show a steady increase in pore pressure in compression, while the experimental data are quite irregular. The slight decrease in pore pressure observed during the experiment at about 1-2% shear strain, which implies a dilatant response, coincides with the loop observed in the stress path. Figure 5.3.45 shows values of the shear modulus, computed from the predicted and experimental data for tests AUC and AUE, plotted against shear strain. The predicted curves are in reasonable agreement with the experimental curves for strains greater than 0.025%. This shows that the size of the sensitivity surface, which indirectly determines the values of stiffness, was correctly predicted during the analyses.

Drained tests following isotropic consolidation

In tests CID2 and CID3 the specimens were compressed to stresses beyond gross yield, so that they were normally consolidated at the start of shearing. In test CID1, at the start of shearing the specimen has an apparent overconsolidation ratio of about 2 and the sample has not yet reached gross yield. Figure 5.3.46 shows a comparison of the predicted and experimental stress-strain curves for all three tests in the q'-ε_s plane. The predicted values of strength are under-estimated by 20%, but show similar patterns of behaviour to those observed in the test data, with lower strengths at smaller confining stresses (test CID1) and higher strengths at large confining stresses (test CID3). Figure 5.3.47 shows values of stress ratio q'/p' plotted against shear strain. While the experimental data show that a critical state was reached in test CID1 at a stress ratio of 0.85, the predicted data are only getting near the critical state, reaching a value of stress ratio of 0.72 at a strain of 20%. Generally the predicted response reaches a given stress ratio at a higher strain than the experimental data.

A comparison of the predicted and experimental volumetric responses is given in Figure 5.3.48. The S3-SKH model predicts the right pattern of behaviour, with less volumetric strain during test CID1 and approximately the same magnitude of volumetric strain during tests CID2 and CID3. In Figure 5.3.49, the predicted and experimental stress paths have been normalised with respect to the equivalent pressure on the isotropic intrinsic compression line. The predicted and experimental stress paths start from different states because the model predicted different

volumetric strains during the isotropic compression to those measured in the experiments. There is however good agreement between the two sets of data, with the stress paths reversing in direction to move towards the intrinsic critical state point. This behaviour can only be simulated by modelling destructuration.

5.3.6 Modelling the effects of fabric

The effects of bonding and fabric are combined in most clays. In such clays, destructuration still occurs, but the clay becomes stable before reaching the intrinsic state. It has been seen in the previous section that in the samples of Bothkennar clay that have been retrieved from the bedded facies, the net rate of destructuration seems to be lower. The macro-fabric formed by the bedded stratigraphy is thought to provide an ultimate stable state different from the intrinsic critical state.

Figure 5.3.50a shows the one-dimensional compression curve obtained by Allman (1992) from tests on specimen B86, which was recovered from the bedded facies. The compression curve of the intact clay does not reach the intrinsic compression curve but converges asymptotically to a line parallel to it. The ultimate value of sensitivity, calculated using the Sensitivity framework, was found to be equal to 1.5. Figure 5.3.50b shows the predicted data for a one-dimensional compression test simulating the test on specimen B86. The effects of including fabric are examined by showing results of analyses using an ultimate value of sensitivity equal to 1 (no effect of fabric) and equal to 1.5 (allowing for fabric). Unlike the analyses of the undrained tests, the amount of destructuration predicted by the model is lower than that in the experiment, so that the predicted compression curves only reach a stable state at stresses greater than 5,000kPa. The same pattern of behaviour was observed in the parametric study results in Section 5.2, where very large strains had to be simulated to reach stable states. The pattern of behaviour observed in test B86, where the clay becomes stable before reaching the intrinsic state, can only be reproduced when simulating fabric as well as bonding.

Specimen L23 was also retrieved from the bedded facies therefore it is thought that its response on loading is also influenced by fabric. In particular, the net rate of destructuration seems to be slower than in specimens from other facies. In Figure 5.3.51, stress paths for the undrained compression stage are shown for the test data and for the predicted data from two analyses, one accounting for fabric and the other not. As in Section 5.2, the simulation of the effect of fabric during the analysis appears to have reduced the net rate of destructuration so that the strength at the end of shearing is the same as in the experiment. Figure 5.3.52 shows the stress-strain curves obtained from the test and the two analyses. The curve resulting from the analysis with fabric shows a better agreement with the test data, with the peak strength over-predicted by only 6% and the rate of destructuration being lower. The stress ratio is over-

predicted by 10% in both analyses, again due to accumulated inaccuracies during the analysis using S-TERTIUS with single precision variables. However the specimen seems to reach a stable state at a similar strain to that observed in the experiment only in the case when fabric is simulated (see Figure 5.3.53). The change in pore water pressure is plotted against shear strain in Figure 5.3.54. Again the analysis including fabric gave a better prediction of the increase in excess pore pressure than the analysis where fabric was not simulated. If direct comparisons may not be valid in the strain-softening region, the qualitative predicted response has been improved with the specimen reaching quasi-stability at 20% strain.

5.3.7 Summary

The simple expression for the destructuration law proves sufficient to improve predictions of the behaviour of the two metastable clays, Bothkennar clay and Pisa clay. Generally the predicted response in isotropic compression is very satisfactory, which is to be expected since the structure parameters have been derived from such tests. For other tests, drained or undrained, the predicted response is qualitatively similar to that observed in the experiments. The S3-SKH model can predict the increase of compressibility occurring in compression, and the decrease in strength occurring in undrained shearing. Quantitatively, the analyses gave results within 20% of the experimental data. During compression, the model can predict reliably the amount of destructuration, but only reaches stable states at very large strains. During shearing, drained or undrained, the amount of destructuration up to peak has generally been well predicted for Bothkennar clay and over-predicted for Pisa clay. After peak, the model tends to over-predict the amount of destructuration, in particular for undrained shear tests.

It is interesting to note that simulation of drained probes radiating from the in situ stress gave different results for Pisa and Bothkennar clays. The amount of volumetric strain and the strength were under-predicted for Bothkennar clay and over-predicted for Pisa clay. However the predicted limit surface defined by the points of stress path reversal in normalised stress space was a good fit with the test data for Bothkennar clay, but was well inside the experimental curve for Pisa clay, in particular at stresses around the direction of the stress paths for tests A30 and A60. The same poor agreement between predicted and test data was observed in the analyses simulating reconstituted Pisa clay in Section 4.2.4. This may be due to significant structural anisotropy in Pisa clay caused by the strongly anisotropic stress history, both in the natural and reconstituted clay. However these are second order features. The main feature of behaviour is the destructuration in Pisa clay, which can only be predicted by a model including structure and degradation of structure.

5.4 DISCUSSION OF THE NUMERICAL RESULTS

The simple destructuration law used in the S3-SKH model is sufficient to improve significantly predictions of the behaviour of soft natural clays. Section 5.2 has validated the S3-SKH model by showing that it can predict features of behaviour corresponding to an accepted response for soft natural clays. The law requires only three additional structure parameters to cover a wide range of behaviours. The performance of the three structure parameters has been evaluated against data from tests on natural Bothkennar and Pisa clays in the previous section. The following conclusions have been drawn:

- The value of initial sensitivity is critical to predict undrained shear strength, and the onset of significant destructuration, correctly. For modelling laboratory single element tests the initial sensitivity s_0 can be computed from isotropic compression or K_0-compression test data, using a rigorous definition similar to that in the Sensitivity framework. It has been shown that for metastable clays such as Bothkennar and Pisa clays, it is necessary to simulate the full stress history, that is sampling and preparation of the sample. This implies that the initial sensitivity to be used in the analyses is the sensitivity in the ground, but for metastable clays, which are subject to disturbance prior to testing, there is always an uncertainty about these values. Analyses simulating undrained tests SCU1, L23 and SH13 on Bothkennar clay were performed for a range of values of initial sensitivity representing the sensitivity in the ground, that were computed using different methods since there were no data available to derive these values by using the Sensitivity framework. For analyses L23 and SH13, the limit values s_0=13.5 and s_0=10 gave very good predictions of the undrained shear strength. For analysis SCU1, the two limit values of sensitivity enclosed the experimental value of undrained shear strength. Values of initial sensitivity could be computed by using the Sensitivity framework for specimens LCD, SUD2 and LUD1 of Bothkennar clay and for all specimens of Pisa clay. The results of analyses simulating the drained probes LCD gave a very good agreement between predicted and experimental normalised gross yield curves, which define the onset of significant destructuration. The results of analyses simulating tests SUD2 and LUD1 showed that the value of initial sensitivity calculated for analysis LUD1 gave a good fit with test data from the compression stage, but that the value used for analysis SUD2 was too small. However the values of undrained shear strength could still be predicted within a range of 4% of the experimental value for analysis LUD1, and within 11% for analysis SUD2. The results of analyses simulating test AUC on Pisa clay led to the undrained shear strength being under-predicted by 20%. The results of analyses simulating tests A0, A30, A60 and A90 gave a rather good fit with test data from tests A0 and A90, but in analyses A30 and A60 the gross yield was

predicted to occur at a much lower stress than in the experiment, leading to the predicted normalised gross yield curve being well inside the experimental curve. This indicates that either the value of initial sensitivity used in the analyses was too small, or the behaviour of Pisa clay is strongly influenced by structural anisotropy. To summarise, to use a value of initial sensitivity rigorously calculated by using the Sensitivity framework leads to predictions of the undrained shear strength within 10% of the experimental data for Bothkennar clay, and within 20% for Pisa clay. Predictions of the onset of significant destructuration were close for Bothkennar clay, but under-predicted for Pisa clay. Thus the initial sensitivity derived by using the Sensitivity framework can be considered as a reliable parameter to use in analyses simulating soft clays.

- The destructuration law assumes direct proportionality between change in sensitivity and change in damage strain, where the damage strain is equal to the magnitude of the vector of plastic strain increment. The rate of destructuration k can be computed rigorously from isotropic compression test data. The results of analyses of isotropic or K_0-compression tests are therefore generally in good agreement with the experimental data. Analyses simulating tests on Bothkennar and Pisa clays, that involve a significant amount of plastic shear strain, such as undrained tests or drained tests going towards failure, were performed. The analyses simulating undrained tests L23 and LUD1 over-predicted the destructuration by 25-30%, and the analysis simulating test SH13 by 14%, but no straightforward conclusion can be made since localisation is likely to have occurred in the specimens during strain-softening. The analyses simulating drained probes LCD55 and LCD70 tended to under-predict destructuration, in particular in analysis LCD55 the volumetric and shear strains were under-predicted by about 30%. The analysis simulating test AUC on Pisa clay showed that the predicted net rate of destructuration was the same as in the experiment at strains higher than 5%. The analyses simulating drained probes A30 and A60 predicted too much destructuration, but this is due to the gross yield being predicted to be at lower stresses than in the experiment. To summarise, the model tends to over-predict destructuration by about 30% in undrained and drained tests going to failure. A quantitative comparison may not be possible, but qualitatively the amount of destructuration is well over-predicted. However the good prediction of the anisotropic compression of LUD1 and of drained probe LCD70 showed that a destructuration law that assumes equal importance of volumetric and shear strain is reasonable. The advantage of using the simple law described here is that the rate of destructuration can be calculated rigorously from isotropic compression test data, thus discarding all risks of uncertainties associated with localisation.
- The S3-SKH model has been shown to differentiate between the behaviour of stable and metastable clays by including a fabric factor in the analyses, the ultimate sensitivity s_f. For clays where only the effects of fabric are present, predictions by the model are equivalent to

predictions by the base 3-SKH model with the appropriate state boundary surface for the natural soil. This is consistent with the results obtained by Ingram (2000) for the stable stiff natural Oxford and Boom clays. For clays where the effects of fabric and bonding are combined, such as the bedded facies of Bothkennar clay, the use of the ultimate sensitivity parameter allows the model to predict that the destructuration slows down as the specimen becomes stable before reaching the intrinsic state. In particular it was demonstrated that the prediction of the behaviour of specimen L23, which was retrieved from the bedded facies, is significantly improved by accounting for effects of fabric. Results of the analysis simulating test L23, which included fabric, still predicted a value of undrained shear strength within 6% of the experimental value, and the destructuration was slower. Thus ultimate sensitivity is an important parameter to include in analyses simulating soils with a significant effect of structure relating to fabric.

- The significant over-prediction of destructuration in Pisa clay by the S3-SKH model is thought to be related to structural anisotropy. In particular, the normalised gross yield curve obtained in the laboratory for the drained probes is anisotropic whereas the predicted normalised stress paths define a curve which is isotropic. Also, for drained probes in directions close to the K_0 direction (tests A30 and A60) gross yield was predicted to occur at stresses lower than in the experiment, leading to destructuration being significantly over-predicted. The model proposed by Gajo & Muir Wood (2001), which includes both structural anisotropy and degradation of structure, does not seem to improve significantly predictions of the behaviour of Bothkennar clay (see Section 2.6.3). However, since structural anisotropy appears to affect the behaviour of Pisa clay more, this model may improve predictions for clays like Pisa.

CHAPTER 6 SUMMARY AND CONCLUSIONS

The behaviour of soft natural clays is described by state, stress history and structure. Natural structure is generally unstable in soft clays and breaks down under loading, which makes it difficult to predict the stability of geotechnical structures built on these clays and the settlement of the foundation soil. The key aim of this work was to improve predictions of the behaviour of soft natural clays by; firstly determining whether a single parameter can be used to describe structure and degradation of structure; secondly establishing what controls degradation of structure and hence deriving an expression characterised by this parameter to describe this process; and thirdly evaluating whether a model including structure and degradation of structure described in this way is sufficient to predict all aspects of the behaviour of soft natural clays.

The methodology adopted was to use existing work on structured soils. In particular, the Sensitivity framework (Cotecchia & Chandler, 2000), which proposes sensitivity as the parameter that should be used to represent structure in both volumetric and stress space, was applied to the behaviour of three soft natural clays, Sibari, Bothkennar and Pisa clay. Experimental data for these clays were available from the literature. The three clays have different types of structure and display a range of behaviour typical of clays that have a low to medium sensitivity. Having decided that sensitivity is an appropriate parameter to describe effects of structure in these clays, an expression to describe the degradation of structure was derived from observations of experimental results for the two metastable clays, Bothkennar and Pisa clays. The law was used to extend an existing model, the 3-SKH model, which was initially developed by Stallebrass (1990) for reconstituted and stable stiff clays. The new model was developed following basic concepts that were originally proposed by Gens & Nova (1993) to model structured soils, and were later applied to the development of a number of constitutive models for these soils (Gajo & Muir Wood, 2001; Kavvadas & Amorosi, 2000; Rouainia & Muir Wood, 2000; Tamagnini & d'Elia, 1999). Model predictions were then compared to experimental results obtained from a range of tests that were performed on natural Bothkennar clay (Allman, 1992; Smith, 1992) and Pisa clay (Callisto, 1996; Rampello *et al.*, 1996).

6.1 SENSITIVITY: A PARAMETER TO REPRESENT STRUCTURE

The degree of structure is usually quantified by sensitivity, the ratio of the undrained shear strength of the natural clay to that of the reconstituted clay (Terzaghi, 1944). By linking sensitivity to the volumetric response of the clays, Cotecchia & Chandler (2000) established a framework for natural clays that defines the effect of natural structure in terms of sensitivity. Cotecchia & Chandler demonstrated that up to gross yield values of sensitivity could be calculated in terms of undrained shear strength as defined above, or in terms of gross yield

stress by using the Sensitivity framework. It was shown in Chapter 3, using experimental data from the two metastable soft clays, Bothkennar and Pisa clays, that sensitivity changes in parallel with destructuration. Destructuration is associated with a reduction in strength sensitivity during undrained shearing and in stress sensitivity during volumetric compression, causing, in undrained tests, a reduction in the size of the state boundary surface. By demonstrating that the change in normalised sensitivity calculated from volumetric compression and undrained shearing tests can be expressed as a single function of plastic strain, it was shown that the equivalence between strength and stress sensitivity suggested by Cotecchia & Chandler can be extended to the behaviour post-gross yield. The single parameter sensitivity, which represents the ratio of the size of the state boundary surface of the natural clay to that of the reconstituted clay, can be used to describe the behaviour of soft natural clays both pre- and post-gross yield.

6.2 THE SENSITIVITY THREE-SURFACE KINEMATIC HARDENING (S3-SKH) MODEL

An expression for the degradation of structure has been proposed, derived rigorously from experimental data for tests on Bothkennar and Pisa clays. It was first shown in Chapter 3 that the reduction in sensitivity associated with destructuration is a function of both plastic volumetric and shear strain. A comparative study of the relative influence of plastic volumetric and shear strains on the destructuration has led to the formulation of an expression for the damage strain in which both volumetric and shear strain are of equal importance. The damage strain is simply equal to the magnitude of the vector of the plastic strain increment. It was also demonstrated in Chapter 3 that there is a good correlation between the increment of change in normalised sensitivity and the accumulated plastic strain. By assuming direct proportionality between the two quantities, a destructuration law was derived so that change in sensitivity could be described by an exponential function of the damage strain. A parameter representing a stable element of structure arising from fabric, called ultimate sensitivity, was included in the destructuration law to allow the natural clay to reach a state on loading which is not necessarily the intrinsic state. The destructuration law only requires three parameters; initial sensitivity s_0, which represents the degree of structure in the natural clay; ultimate sensitivity s_f, which represents the degree of structure that is stable due to fabric; and the parameter k, which controls the rate of destructuration with plastic strain. All three parameters can be derived using data from a single isotropic compression test.

The destructuration law was used to extend an existing model, the 3-SKH model (Stallebrass, 1990), which was developed for reconstituted and stable stiff clays. The 3-SKH model includes advanced features of behaviour such as stiffness non-linearity and stress-induced anisotropy arising from the recent stress history. The 3-SKH model was first evaluated

against experimental data from tests on reconstituted Bothkennar and Pisa clay samples. In general the 3-SKH model could predict successfully the behaviour of Bothkennar clay both at small strains up to 1% and at large strains, but less successfully that of Pisa clay. It is thought that significant effects of structural anisotropy may influence the response of this clay under loading, leading to under-prediction of strength and stiffness. The same patterns of prediction were expected to be found in the analyses of tests on the natural clay samples.

The new S3-SKH model has two key features. Firstly, in the model, all effects of structure on the behaviour of soft natural clays are accounted for by the size of the state boundary surface and changes in this size. Secondly, the S3-SKH model uses only three new parameters, which are part of the destructuration law. The other parameters remain the same as those used in the 3-SKH model, and the values of these parameters are the same as those derived using data from reconstituted tests.

6.3 EVALUATION OF THE S3-SKH MODEL

Chapter 5 has highlighted problems associated with modelling soft natural clays. The main difficulty consists in determining the stress state from which to start the analyses, and the value of initial sensitivity. It was found that for the two clays examined, that is Bothkennar and Pisa clays, the full stress history had to be modelled, implying that the analyses should start from the in situ state. However this cannot be determined easily since soft clays are very likely to have been disturbed during sampling and the preparation of the sample for laboratory tests. Sensitivity in the ground is also very likely to have reduced during sampling and preparation of the sample. These two uncertainties influenced the results obtained in the analyses.

In Section 2.6.4 it was stated that the assessment of the model would be in two parts. Firstly, the model should be able to reproduce qualitatively the patterns of behaviour described in the literature for soft natural clays, such as strain-softening in undrained compression tests and increase in compressibility in volumetric compression tests. This has been achieved reasonably well for both Bothkennar and Pisa clays. Secondly, given that the parameters describing destructuration are derived from isotropic compression tests, the model should be able to predict with a reasonable accuracy the undrained shear strength of the soil. As is detailed below, the match between predicted and experimental values of undrained shear strength was satisfactory. Post-peak, where the single precision of the programme is not enough, the comparison between predicted and experimental data post-peak strength could not be made directly due to possible localisation associated with strain-softening. For drained probing tests, use of a strain increment of 0.001% did not seem to affect numerical simulations which compare qualitatively well with the experimental results.

A range of stress paths was simulated by the model. Analyses simulated volumetric compression, and drained and undrained shearing tests, after different stress histories, which were performed on Bothkennar clay (Allman, 1992; Smith, 1992) and Pisa clay (Callisto, 1996; Rampello et al., 1996).

(i) Undrained shear strength

The value of initial sensitivity used in analyses generally determines the predicted value of undrained shear strength. The best predictions of undrained shear strength were obtained in the analyses simulating tests L23 and SH13 on Bothkennar clay. These analyses were performed using two limiting values of initial sensitivity for each test, which delimited the range of in situ values that were calculated by using different methods. Other analyses were performed where the value of initial sensitivity had been computed in a more rigorous way by using a definition from the Sensitivity framework. The analyses simulating tests on Bothkennar clay resulted in values of undrained strength that were under-predicted by 11% for analysis SUD2, and over-predicted by 4% for analysis LUD1. The analysis simulating test AUC on Pisa clay, which also used a value of initial sensitivity computed from the Sensitivity framework, under-predicted the value of undrained shear strength by 20%, mostly due to the peculiar shape of the effective stress path. The stiffnesses at the start of the analyses matched well the experimental results, leading to peaks being predicted at the correct strain. These results are comparable to those by Rouainia & Muir Wood (2000), with a slightly better prediction of stiffness with the S3-SKH model. It can be concluded that deriving the value of initial sensitivity from volumetric compression data by using the Sensitivity framework leads to a reasonable prediction of undrained shear strength. This forms a reliable method which provides a consistent way of determining initial sensitivity, which is a key parameter in the model. Thus the model is able to predict the value of undrained shear strength as well as other similar models, but with the advantage of using a value of initial sensitivity computed from data from volumetric compression only.

(ii) Destructuration

Parameter k, which controls the rate of destructuration with plastic strain, is derived from volumetric compression data. Analyses simulating volumetric compression, such as the compression stage in analysis LUD1, are usually in good agreement with the test data. The destructuration law was assessed by comparing predictions of tests involving mostly shear strains, such as undrained tests, with test data, even though in these tests a direct comparison between predicted and experimental data post-peak strength is rather complicated. The results of

analyses simulating tests SCU1, SUD2 and LUD1 on Bothkennar clay, which were loaded following different stress histories prior to shearing, showed qualitatively good agreement with the response observed in the experiments. This demonstrates that the change in size of the sensitivity surface was correctly predicted by the model. Quantitatively destructuration occurring post-peak was over-predicted in the analyses simulating undrained tests on Bothkennar clay, by 25-30% in analyses L23 and LUD1 and by 14% in analysis SH13. These results are similar to other models such as that by Rouainia & Muir Wood (2000). In the analysis simulating test AUC on Pisa clay, the net rate of destructuration agreed with the test data at strains higher than 5%. However in all predictions involving strain-softening it should be remembered that post-peak stresses and strains may be non-uniform and therefore that such a direct comparison may not be valid. The over-prediction of destructuration cannot be explained by strain localisation only as this would result in the opposite effect, that is a lower apparent rate of destructuration. The assumption that the parameter k, which controls the rate of destructuration, is the same for all facies of Bothkennar clay may then not be correct and led to the amount of destructuration being over-predicted. Good prediction of drained probes LCD0 and LCD70 on Bothkennar clay, which involved both volumetric and shear strain and where occurrence of localisation is unlikely, verified that a destructuration law where both quantities are of the same importance is valid.

(iii) Effect of fabric

It was demonstrated that including an ultimate sensitivity to represent a stable element of structure in samples that were thought to have a significant fabric, such as samples retrieved from the bedded facies in Bothkennar clay, causes the apparent net rate of destructuration to reduce. This improved significantly the prediction of destructuration in specimen L23 from Bothkennar clay, which then reached a quasi-stable state which it did not when fabric was not accounted for. Ultimate sensitivity is then a key parameter, of the same importance as initial sensitivity and rate of destructuration, in soils where the effect of fabric is significant.

(iv) Structural anisotropy

Structural anisotropy, which is not included in the model, is thought to have a significant effect on the behaviour of Pisa clay. This is mostly visible in results of the analyses simulating drained probes A30 and A60, where gross yield is predicted to occur at lower stresses than in the experiments, and in the initial part of the effective stress path for the analysis of AUC. For such a soil, including structural anisotropy in the model will certainly help improving predictions.

6.4 LIMITATIONS OF THE CURRENT RESEARCH AND PROPOSALS FOR FURTHER WORK

The S3-SKH model contributes to advances in numerical modelling of soft natural soils in two main ways: firstly it uses a simple destructuration law in which plastic volumetric and shear strains are of same importance, and secondly, as a consequence, it uses parameters derived from isotropic compression tests only. This has the advantage of avoiding problems associated with localisation in the determination of the parameters. Results of analyses on two soft clays of low to medium sensitivity have proven that the simple law of destructuration used in the model is sufficient to simulate the degradation of structure in both drained and undrained tests. Predictions by the S3-SKH model are similar to predictions by other numerical models that have been presented in the literature, despite the simple formulation of the destructuration law and to the uncertainty associated with the determination of initial sensitivity. In particular, the S3-SKH model manages to predict the undrained shear strength and stiffness of soft natural clays with an accuracy of between 3% and 20%. As was stressed above, there is a lot of uncertainty associated with analyses simulating tests on soft natural clay samples, in particular in the determination of a starting point for the analyses. A number of assumptions had to be made, and their accumulated effect may limit the extent to which predictions can be compared directly to experimental data. An important assumption was that the effect of localisation is small in soft natural clays and does not affect experimental results post-peak during undrained tests. If this assumption is not correct, then comparisons of predicted and experimental data post-peak will be more complicated.

The model was evaluated against test data from two clays only, which are thought to display a range of behaviour typical of soft natural clays that have a low to medium sensitivity and a metastable structure. The limited amount of data available for these two clays made it difficult to estimate parameters such as initial and ultimate sensitivity with great confidence, which may add a degree of uncertainty to the predictions.

The general issues which will have to be developed to take the model further are;

- Firstly the problems associated with the program S-TERTIUS would need to be solved. This would require converting the program to use double precision, and to examine the influence of the size of the strain increment further in single element analyses.
- Then the S3-SKH model would need to be evaluated against a larger number of soft clays of low to medium sensitivity. Performing the appropriate tests in the triaxial cell to derive the parameters for the base model and the three additional structure parameters would increase confidence in the capability of the model to predict the behaviour of these clays.

- The importance of each parameter used in the destructuration law should be investigated by performing a parametric study. This would determine the sensitivity of the model to these parameters and would lead to an optimisation in selecting these parameters.
- In view of implementing the model in finite element code, it would then be necessary to investigate how soil structure degrades in general stress space, such as the influence of the intermediate stress, the effect of the rotation of the principal stress axes, and in particular the relative influence of plastic volumetric and shear strain on the destructuration. This is critical not only for the S3-SKH model but also for all other numerical models simulating structure and its degradation. This will require tests to be carried out in simple shear apparatus, true triaxial cell or in hollow cylinder apparatus. Experimental results from these tests would help determining whether features of behaviour found in general stress space can be generated by simply extrapolating the model from axisymmetric to general space. If the extrapolation was not enough to simulate effects of structure in general stress space, the shape of the failure surface, which is at the moment circular in deviatoric space, would need to be re-thought.
- The extension of the model into general stress space would require reconsidering two issues. Firstly, it was postulated in the formulation of the current model that there is a correspondence between volumetric and deviatoric characterisation. This postulate was assessed for triaxial test data by Cotecchia & Chandler (2000). They showed that in triaxial space sensitivity can be measured in terms of strength by using undrained shear strength data and also in terms of gross yield stress by using volumetric compression data. They then showed that sensitivity is a measure of the ratio of the size of the state boundary surface of the natural soil to that of the corresponding reconstituted soil. However there is no evidence of this link yet in a general stress space, and this needs investigating. Secondly, it was also postulated that the sensitivity of the soil can reach an ultimate value, the "ultimate sensitivity", which is not necessary equal to unity. This postulate was based on results from triaxial tests and is thought to be related to stable elements of structure arising from fabric (Coop & Cotecchia, 1995; Cotecchia & Chandler, 1998). Fearon and Coop (2000) have shown that in some structurally complex clays the structure is not completely broken even by remoulding the soil. They showed that if the soils were further worked by mincing, then the strength was further reduced. For such clays it is thought that no strain path could achieve a level of destructuration so that sensitivity decreases down to unity, and therefore that there is an ultimate value of sensitivity different to unity. However for some other clays there might be some strain paths in general stress space that can be imposed, possibly cyclically, which do have the effect of removing all sensitivity. This has not been proven yet and will require a programme of experiments to be designed to investigate the strength of

the natural clay subjected to general stress paths as compared to the strength of the corresponding reconstituted clay.

- If the S3-SKH model was found to be appropriate for all types of loading, the next step would be to evaluate the advantages of using the S3-SKH model in finite element analyses of real field events. The results from the above can be implemented in the finite element code CRISP in the way described by Stallebrass & Taylor (1997). However the difficulty in determining an appropriate starting point for the analyses will be accentuated. The recent stress history will have to be estimated from knowledge of the geological history. Ingram (2000) established a method that could be used to simulate the formation of natural structure when modelling boundary value problems, but suggested that more work should be devoted to understanding the geological history. A first step to investigate this would be to simulate the formation and degradation of structure in model tests and comparing predictions obtained in finite element analyses against the experimental results.
- Obviously, more complexity can be added to the model, such as structural anisotropy or creep and ageing, so that predictions can be improved. It is thought that the behaviour of Pisa clay for example is influenced by structural anisotropy. The combination of a model similar to that proposed by Gajo & Muir Wood (2001), which includes both structural anisotropy and degradation of structure, with the S3-SKH model, could lead to much better prediction of the behaviour of such clays.

6.5 CONCLUSION

A model such as the S3-SKH model, which uses sensitivity as a single parameter to represent structure and a single expression to describe the degradation of structure characterised by sensitivity, is sufficient to predict the effects of destructuration in soft natural clays. The approach proposed in this dissertation achieves a reasonable balance between complexity of input to the model and benefit in the improvements to the results of the analyses. In order that such a model can be used with confidence, efforts should be made to find reliable methods of determining the *in situ* stress states and sensitivities for these soils.

REFERENCES

Allman M.A. (1992) *Bothkennar laboratory testing*. Internal report GE/92/09, City University

Allman M. A. & Atkinson J. H. (1992). Mechanical properties of reconstituted Bothkennar clay. *Géotechnique* **42**, No. 2, 289-302

Al-Tabbaa A. (1987). *Permeability and stress-strain response of speswhite kaolin*. PhD Thesis, University of Cambridge

Al-Tabbaa A. & Wood D.M. (1989). An experimental based 'bubble' model for clay. *Proc. Third Int. Conf. On Numerical Methods in Geomechanics*, 91-99

Atkinson J.H. (2000). Non-linear stiffness in routine design. *Géotechnique* **50**, No. 5, 487-508

Atkinson J. H. & Richardson D. (1987). The effect of local drainage in shear zones on the undrained strength of overconsolidated clay. *Géotechnique* **37**, No. 3, 393-403

Best C. (1994). *Investigation of the influence of structure on the mechanics of soils*. Part *III Project Report; Dept. of Civil Engineering, City University, London*

Bjerrum L. (1967). Seventh Rankine Lecture: Engineering geology of normally consolidated marine clays as related to settlements of buildings. *Géotechnique* **17**, No. 2, 81-118

Burland J. B. (1990). On the compressibility and shear strength of natural clays. *Géotechnique* **40**, No. 3, 329-378

Butterfield R. (1979). A natural compression law for soils (an advance on e-lnp'). *Géotechnique* **29**, No. 4, 469-480

Callisto L. (1996). *Studio sperimentale su un'argilla naturale: il comportamento meccanico dell'argilla di Pisa*. Tesi per il conseguimento del titulo di Dottorato di Ricerca, Universita La Sapienza, Roma

Chazallon C. & Hicher P. Y. (1995). An elastoplastic model with damage for bonded geomaterials. *Numerical models in Geomechanics, NUMOG V*, Pande & Pietruszczak (eds), Balkema, Rotterdam, 21-26

Clayton C.R.I., Hight D.W. & Hopper R.J. (1992). Progressive destructuring of Bothkennar clay: implications for sampling and reconsolidation procedures. *Géotechnique* **42**, No. 2, 219-239

Coop M.R. (1998). Private communication

Coop M.R., Atkinson J.H. & Taylor R.N. (1995). Strength and stiffness of structured and unstructured soils. *Proc. 11th ECSMFE,* Copenhagen **1**, 55-62

Coop M.R. & Cotecchia F. (1995). The compression of sediments at the archeological site of Sibari. *Proc. 11th ECSMFE*, Copenhagen **8**, 19-26

Cotecchia F. (1996). *The effects of structure on the properties of an Italian pleistocene clay*. PhD Thesis, University of London

Cotecchia F. & Chandler R.J. (1997). The influence of structure on the pre-failure behaviour of a natural clay. *Géotechnique* **47**, No.3, 523-544

Cotecchia F. & Chandler R.J. (1998). One-dimensional compression of a natural clay: Structural changes and mechanical effects. *The Geotechnics of Hard Soils-Soft Rocks,* Evangelista & Picarelli (eds), Balkema, Rotterdam, 103-113

Cotecchia F. & Chandler R. J. (2000). A general framework for the mechanical behaviour of clays. *Géotechnique* **50**, No. 4, 431-447

Dafalias, Y.F. & Herrman, L.R. (1980). A Bounding Surface Plasticity Model. *Proc. Int. Symp. Soils Under Cyclic Trans. Load.*, Swansea, A.A.Balkema Publ., Rotterdam, 335-345

Delage P. and Lefebvre G. (1984). Study of the structure of a Champlain clay and its evolution during consolidation. *Canadian Geotechnical Journal* **21**, 21-35

Fearon R.E. & Coop M.R. (2000). Reconstitution: what makes an appropriate reference material? *Géotechnique* **50**, No. 4, 471-477

Gajo A. & Muir Wood D. (2001). A new approach to anisotropic, bounding surface plasticity: general formulation and simulations of natural and reconstituted clay behaviour. *Int. J. Numer. Anal. Meth. Geomech.* **25**, 207-241

Gens A. & Nova R. (1993). Conceptual bases for a constitutive model for bonded soil and weak rocks. *Proc. Int. Conf. on Hard soils Soft rocks*, Athens

Graham J. & Houlsby G. T. (1983). Anisotropic elasticity of a natural clay. *Géotechnique* **33**, No. 2, 165-180

Graham J. & Li E. C. C. (1985). Comparison of natural and remoulded plastic clay. *Journal of Geotechnical Engineering*, ASCE, **111**, No. 7

Hashigushi K. (1985). Two- and three-surface models of plasticity. *Proc. 5th Int. Conf. Numerical Methods Geomechanics*, Nagoya, 125-134

Hight D.W., Bond A.J. & Legge J.D. (1992). Characterisation of the Bothkennar clay: an overview. *Géotechnique* **42**, No. 2, 199-217

Hight D.W., Böese R., Butcher A.P., Clayton C.R.I. & Smith P.R.l (1992b). Disturbance of the Bothkennar clay prior to laboratory testing. *Géotechnique* **42**, No. 2, 303-347

Houston W. N. & Mitchell J. K. (1969). Property interrelationships in sensitive clays. *Journal of the soil mechanics and foundations division. Proc. ASCE* **95**, No. SM4, 1037-1061

Ingram P.J. (2000). *The application of numerical models to natural stiff clays*. PhD Thesis, City University, London

Jardine R. J. (1985*). Investigation of pile-behaviour with special reference to the foundations of off-shore structures*. PhD Thesis, University of London

Jovicic V. (1997). *The measurement and interpretation of small starin stiffness of soils*. PhD Thesis, City University, London

Kavvadas M. & Amorosi A. (2000). A constitutive model for structured soils. *Géotechnique* **50**, No. 3, 263-273

Kavvadas M. J. & Anagnostopoulos A. G. (1998). A framework for the mechanical behaviour of structured soils. *The geotechnics of Hard Soils-Soft Rocks*, Evangelista & Picarelli (eds), Balkema, Rotterdam, 591-601

Ladd C. C. & Lambe T.W. (1963). The strength of "undisturbed" clay determined from undrained tests. *Laboratory shear testing of soils*, A.S.T.M. Special Technical Publication No. 361

Lagioia R. and Nova R. (1995). An experimental and theoretical study of the behaviour of a calcarenite in triaxial compression. *Géotechnique* **45**, No. 4, 633-648

Lambe T. W. and Whitman R. V. (1969). Soil Mechanics. John Wiley & Sons Inc., New York

Leroueil S. & Vaughan P. R. (1990). The important and congruent effects of structure in natural soils and weak rocks. *Géotechnique* **40**, No. 3, 467-488

Leroueil S., Tavenas M., Brucy F., La Rochelle P. L. and Roy M. (1979) Behaviour of destructured clay. Journal of the Geotechnical Engineering Division, ASCE, 105, N. GT6, pp. 759-778

Leroueil S., Tavenas F. & Le Bihan JP. (1983). Propriétés caractéristiques des argiles de l'est du Canada. Can. Geotech. J. **20**, 681-705

Leroueil,S. Magnan, J.P. & Tavenas, F. (1990). *Embankments on soft clays*. Ellis Horwood series in Civil Engineering

Lings M.L., Pennington D.S. & Nash D.F.T. (2000). Anisotropic stiffness and their measurement in stiff natural clay. *Géotechnique* **50**, No. 2, 109-125

Liu M.D. & Carter J.P. (2000). Modelling the destructuring of soils during virgin compression. *Géotechnique* **50**, No. 4, 479-483

Mitchell R. J. (1970). On the yielding and mechanical strength of Leda clay. *Canadian Geotechnical Journal* 7, 297-312

Mitchell J. K. (1982). *Fundamentals of soil behaviour*. John Wiley & Sons, Inc.

Nagaraj T. S., Pandian N. S. and Narasimha Raju P. S. R. (1998). Compressibility behaviour of soft cemented soils. *Géotechnique* **48**, No. 2, 281-288

Oka F., Leroueil S & Tavenas F. (1989). A constitutive model for natural soft clay with strain softening. *Soils and foundations* **29**, No. 3, 54-66

Parry R. H. G. (1960). Triaxial compression and extension tests on remoulded saturated clay. *Géotechnique* **42**, 166-180

Paul M.A., Peacock J.D. & Wood B.F. (1992). The engineering geology of the Carse clay at the National Soft Clay Research Site, Bothkennar. *Géotechnique* **42**, No. 2, 183-198

Ramanatha Iyer, T.S. (1975). The behaviour of Drammen plastic clay under low effecctive stresses. *Canadian. Geotech. J.* **12**, 70-83

Rampello S. & Callisto L. (1998). A study on the subsoil of the Tower of Pisa based on results from standard and high-quality samples. *Canadian Geotech. J.* **35**, No. 6, 1074-1092

Rampello, S., Callisto, L. & Viggiani, G.M.B. (1996). *The leaning Tower of Pisa. Soil parameters for the numerical modelling of the tower resulting from the most recent investigations*. Studi e Ricerche 3/96, The University of Rome "La Sapienza".

Rampello S. & Silvestri F. (1993). The stress-strain behaviour of natural and reconstituted samples of two overconsolidated clays. *Geotechnical Engineering of Hard Soils Soft Rocks*, Anagnostopoulos et al. (eds), Balkema, Rotterdam, 769-778

Roscoe K. H. & Burland J. B. (1968). *On the generalised stress-strain behaviour of wet clay.* Engineering Plasticity (J. Heymann and F. A. Leckie, eds), Cambridge University Press, Cambridge, 535-609

Rouainia M. & Muir Wood D. (2000). A kinematic hardening constitutive model for natural clays with loss of structure. *Géotechnique* **50**, No. 2, 153-164

Schmertmann J.H. (1969). Swell sensitivity. *Géotechnique* **19**, No. 4, 530-533

Schofield A. N. & Wroth C. P. (1968). *Critical State Soil Mechanics*. McGraw-Hill Book Co., London

Shibuya S., Mitachi T. & Hwang S.C. (2000). Case studies of in situ structure of natural sedimentary clays. *Soils and foundations* **40**, No. 3, 87-100

Skempton A. W. (1970). The consolidation of clays by gravitational compaction. *Q. J. Geological Soc.* **125**, 373-411

Skempton A. W. & Northey R. D. (1952). The sensitivity of clays. *Géotechnique* **3**, 30-53

Smith P. R. (1992). *The behaviour of natural high compressibility clays with special reference to consolidation of soft ground.* PhD Thesis, London University

Smith P. R., Jardine R. J. & Hight D. W. (1992). On the yielding of Bothkennar clay. *Géotechnique* **40**, No. 2, 257-274

Stallebrass S. E. (1990). *Modelling the effect of recent stress history on the behaviour of overconsolidated soils.* PhD Thesis, City University, London

Stallebrass S.E. & Taylor R.N. (1997). Prediction of ground movements in overconsolidated clay. *Géotechnique* **47**, No. 2, 235-253

Tamagnini C. & D'Elia M. (1999). A simple bounding surface for bonded clays. *Pre-failure Deformation Characteristics of Geomaterials*, Jamiolkowski, Lancellotta & Lo Presti (eds), Balkema, Rotterdam, 565-572

Tavenas F. and Leroueil S. (1977). Effects of stresses and time on yielding of clays. *Proc. 9th Int. Conf. Soil Mech. Fdn Engng, Tokyo* **1**, 319-326

Tavenas F., Des-Rosiers J. P., Leroueil S., La Rochelle P. & Roy M. (1979). The use of strain energy as a yield and creep criterion for lightly overconsolidated clays. *Géotechnique* **29**, No. 3, 285-303

Tavenas F. & Leroueil S. (1985). Discussion. *Proc. 11th Int. Conf. Soil Mech. Fdn Engng, San Francisco* **5**, 2693-2694

Terzaghi K. (1936). Stability of slopes of natural clays. *Proc. First Int. Conf. Soil Mech.* **1**, 161

Terzaghi, K. (1941). Undisturbed clay samples and undisturbed clays. *J. Boston Soc. Civ. Engng*, **28**, 211-231

Terzaghi K. (1944). Ends and means in Soil Mechanics. *Engineering journal*, Canada, **27**, 608

Viggiani G. & Atkinson J. H. (1995). Stiffness of fine-grained soil at very small strains. *Géotechnique* **45**, No. 2, 249-265

Soil properties and tests on block samples

Block sample no.	Depth meters	Natural m.c.	W_L %	W_p %	Vane kg/cm²	σ_v' *In situ* kg/cm²	P_a kg/cm²	% clay	s c. g/L	S_t
94–25	19.0	48%	32	22	1.7	1.8	4.5	60	0.1	500+
94–21	16.1	45%	31	22	1.6	1.5	4.5	60	0.4	500+
94–18	13.7	55%	47	22	1.3	1.3	4.5	71	2.1	100+

Specimen number	Type of test	Initial effec. cell pressure σ_c' kg/cm²	Description of failure (Shear angle measured from horiz.)	ϵ_f %	Post failure stress–strain
94–25–14	CID*	0.05	Vert split, 77° plane, dilation	1.2	Large drop of q
94–25–16	CID	0.5	Shear at 52°, v pos, $\frac{\delta v}{\delta \varepsilon}$ negative	1.5	Small drop of q
94–25–9	CID	1.0	Shear at 50°, vol comp at failure	1.6	Nearly constant q
94–25–19	CID	1.5	Bulging	8.0	Small linear increase of q with strain
94–25–12	CID	2.0	Bulging	9.0	
94–25–18	CID	2.5	Bulging	10.0	
94–25–20	CID	3.0	Bulging	10.0	
94–25–21	CID	3.5	Bulging	10.0	
94–25–13	CIU†	0.05	Shear 67°, pore water suction	1.0	Drop to $q_f/2$
94–25–14	CIU	0.5	Shear 67°, δu positive, $\delta u/\delta \epsilon$ neg.	1.5	20% drop of q
94–25–11	CIU	1.0	Shear 62°, δu positive, $\delta u/\delta \epsilon \approx 0$	1.3	20% drop of q
94–25–10	CIU	2.0	Shear 65°	1.2	Gradually decreasing value of q Less drop in q with increase in σ_c'
94–25–7	CIU	3.0	Shear 62°	1.5	
94–25–17	CIU	3.5	Shear 54°	1.6	
94–18–2	CIU	4.0	Not noted	1.3	
94–18–3	CIU	6.0	Not noted	1.8	
94–18–6	CIU	8.0	Not noted	1.9	
94–21–19	CIU	6.0	Bulging	2.0	
94–21–22	CIU	8.0	Shear 60°	1.8	

*CID = consol. isotropically, drained shear.
†CIU = consol. isotropically, undrained shear.

Table 1.3.1 Description of failure and post-failure behaviour during consolidated drained and undrained tests on Leda clay (after Mitchell, 1970)

	Bothkennar	Pisa	Sibari
age deposition	5000-3000 BP	7000 BP	10,000 BP
rate of deposition	8mm/year	2.5mm/year	10mm/year
conditions of deposition	tidal transport in shallow offshore environment	shallow brackish-water lagoon	transitional; alluvial continental and intertidal
salinity	marine	marine	marine
clay minerals	illite	illite/vermiculite	illite/chlorite
organic content	3-8%	10%	less than 1% 13% in peat strata
fabric	sedimentary structure in bedded facies silt laminae in laminated facies	N/A	interbedding of sand and silt within silty clay
bonding	locally in bedded facies	N/A	N/A
plastic limit	25%	25%	23%
liquid limit	65-80%	80%	42-52%
plasticity index	25-55%	40-50%	19-29%
OCR	1.4-1.6	1.2-2	1
sensitivity	5- 15 (BS fall cone)	5 (vane shear)	2.5-3.5 (triaxial)

Table 3.2.1 Geological history and lithology of the three reference clays

Sample	Nature	Initial state		
		p_i' (kPa)	p_{ie}^* (kPa)	S_t
CS1r	Reconstituted	616.1	852.6	1
CS23		544.7	838.7	1
CS25		548.3	835	1
CS10	Natural	359.6	238.4	2.3
CS20		548.5	446.5	2
CS21		527.6	281.8	3.2

Table 3.2.2 Shear tests on Sibari clay samples and normalising parameters (data from Coop & Cotecchia, 1995)

Sample	Nature	Initial state			Loading
		p_i' (kPa)	p_{ie}^* (kPa)	S_t	
B51	Reconstituted	100.2	123.6	1	Compression
B71		99.7	252.9	1	
B72		149.7	223.6	1	
SCU1	Natural	36	15.1	5.5	Compression
SH13		46.3	12.3	6	
L23		60.4	10.8	9	
SUD2		118.5	52.2	2.56	
LUD1		104.7	40.1	3.5	

Table 3.2.3 Undrained shear tests on Bothkennar clay samples and normalising parameters (data from Allman, 1992; Smith, 1992)

Sample	Nature	Initial state			Loading	Drainage
		p_i' (kPa)	p_{ie}^*	S_t		
R0	Reconstituted	87.8	218.7	1	Compression probes	Drained
R30		88	213.1	1		
R60		87.7	192.5	1		
R90		88.6	211.7	1		
A0	Natural	88.3	60.2	3.5	Compression probes	Drained
A30		88.1	56.3	3.5		
A60		88.7	62.2	3.5		
A90		88.3	58.1	3.5		

Table 3.2.4 Drained probes on Pisa clay samples and normalising parameters (data from Callisto, 1996)

		strain			sensitivity		rate of change of sensitivity with plastic strain	rate of change in normalised sensitivity with plastic strain	rate of change of normalised sensitivity with plastic volumetric strain	rate of change of normalised sensitivity with plastic shear strain
		$\Delta\varepsilon_v^p$	$\Delta\varepsilon_s^p$	$\Delta\varepsilon^p$	Δs	$\Delta s/s_0$				
		%	%	%		%				
Pisa	A0 isotropic	3.77	0.53	3.8	-0.092	-3	-2.4	-0.8	-0.8	-5.7
	19B isotropic	32	0	32	-1.5	-57	-4.7	-1.8	-1.8	infinite
	A30 drained probe	6.7	4.97	8.34	-0.43	-12	-5.1	-1.44	-1.8	-2.4
	A90 drained probe	0.385	11.9	11.9	-0.7	-21	-5.9	-1.73	-54.5	-1.8
	AUC undrained	1.01	26.66	26.7	-2.28	-51	-8.5	-1.9	-50.5	-1.9
Bothkennar	SUD2 isotropic	0.49	0	0.49	-0.37	-14.5	-75.5	-29.6	-29.6	infinite
	LUD1 K_0-comp.	2.18	1.48	2.635	-1.74	-35	-66	-13.3	-16	-23.6
	SH13 undrained	0.24	13.67	13.7	-1.25	-22	-9.1	-1.6	-91.7	-1.6
	L23 undrained	0.36	16.6	16.6	-2.5	-28	-15	-1.7	-77.8	-1.7
	SH5 undrained	0.43	17.54	17.54	-1.52	-20.45	-8.7	-1.2	-47.6	-1.2
	LCD0	9	-0.1	9	-0.94	-17.7	-10.4	-1.97	-1.97	177
	LCD55	7.1	7	9.97	-1.18	-25.9	-11.83	-2.6	-3.65	-3.7
	LCD70	11.8	17.14	20.8	-2.41	-62.35	-11.6	-3	-5.3	-3.64
	B86 Ko-comp.	18.96	13	23	-2.24	-59.5	-9.74	-2.6	-3.1	-4.6

Table 3.3.1 Rate of change of sensitivity with increment of plastic volumetric strain, plastic shear strain, increment of plastic strain (Pisa clay: data from Callisto, 1996; Rampello *et al.*, 1996; Bothkennar clay: data from Allman, 1992; Smith, 1992)

Soil	Sample/depth (m)	W_L (%)	λ	N	κ	M	ν	A	m	n	T	S	ψ
Bothkennar clay	3.5-6.5m	67	0.082	1.1	0.0028	1.38	0.3	900	0.25	0.65	0.7	0.14	2
Pisa clay	29B/18.13-18.33m	74.2	0.14	1.575	0.0052	0.78	0.3	560	0.36	0.82	0.5	0.1	2

Table 4.2.1 Summary of parameters used for evaluation of 3-SKH model prediction of triaxial tests on reconstituted samples of the reference clays

	Analyses	Initial state		End of recompression		Shearing stage	
		p′ (kPa)	p_0' (kPa)	p′ (kPa)	R_0	Loading	Drainage
Bothkennar clay	CIPC	6.5	12.22	200	1	Compression	Drained (constant p′)
	CK_0PC	4.2	17.46	200	1		
	CK_0PC-2	20	25.34	100	2		
	CK_0PC-4	30.83	34.15	50	4		
	CK_0UC	9.3	13.9	100	1		Undrained
	CK_0UC-2	15.3	24.35	100	2		
Pisa clay	R30	88.2	112.9	88.2	2.5	Compression probes	Drained (30°)
	R315	88.2	114	88.2	2.5		Drained (315°)

CI consolidated isotropically
CK_0 consolidated anisotropically

Table 4.2.2 Summary of analyses used for evaluation of the 3-SKH model, modelling triaxial tests on reconstituted samples of the reference clays

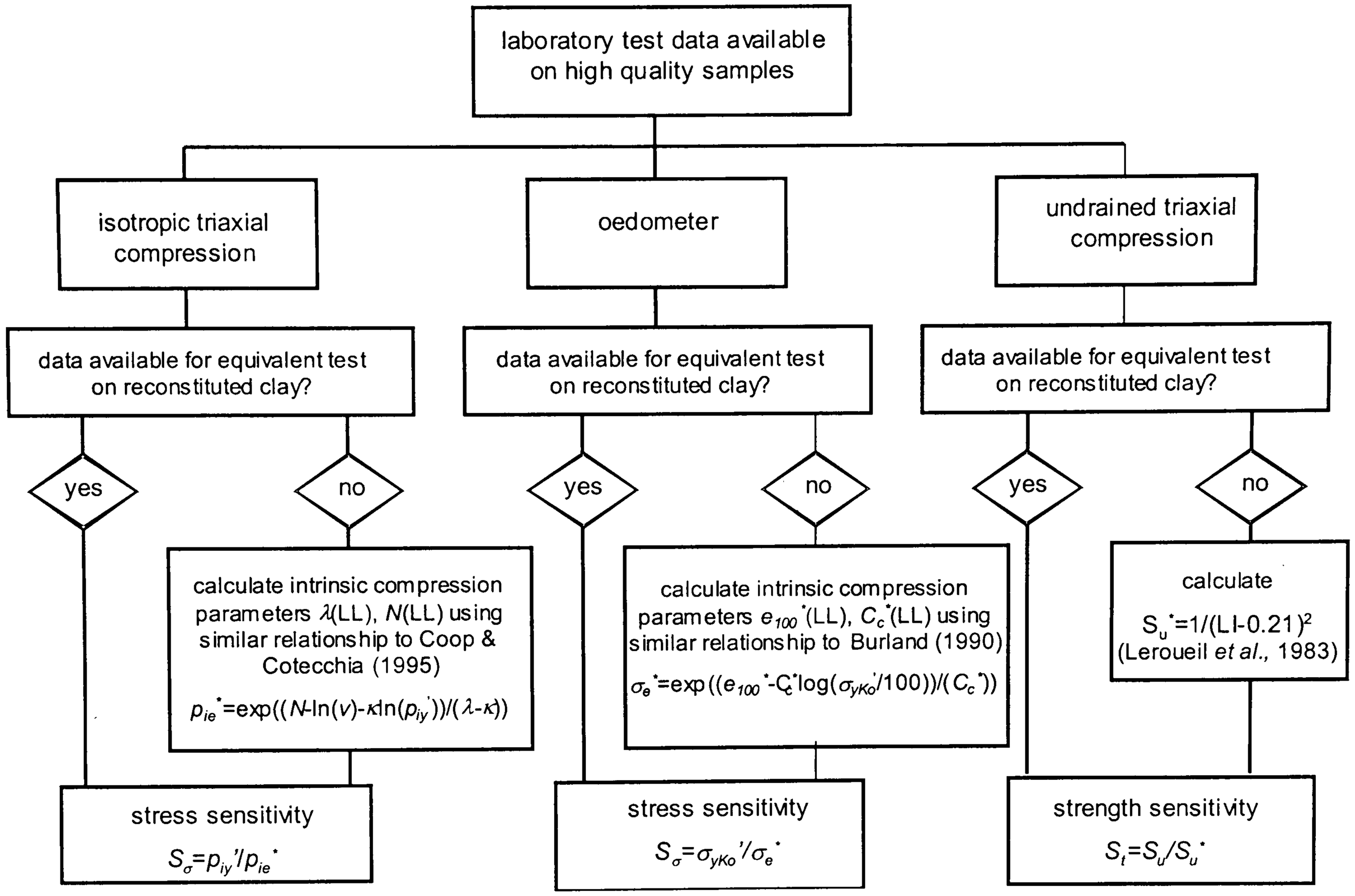

Table 4.4.1 Flow chart demonstrating how to calculate the initial sensitivity s_0 from existing test data

Analysis	M	λ	κ	ν	T	S	ψ	A	m	n	s_0	s_f	k
CIr	1	0.1	0.005	0.3	0.2	0.05	2	1000	0.25	0.65	1	1	0
CI1	1	0.1	0.005	0.3	0.2	0.05	2	1000	0.25	0.65	5	5	0.5
CI2												2	
CI3												1	
CUr	1	0.1	0.005	0.3	0.2	0.05	2	1000	0.25	0.65	1	1	0
CU1	1	0.1	0.005	0.3	0.2	0.05	2	1000	0.25	0.65	5	5	0.5
CU2												2	
CU3												1	
CU32	1	0.1	0.005	0.3	0.2	0.05	2	1000	0.25	0.65	5	1	0.5
CU33												1	
CU34												1	
CU41	1	0.1	0.005	0.3	0.2	0.05	2	1000	0.25	0.65	5	1	0.5
CU42												1	
CU43												1	
CU44												1	
CD0	1	0.1	0.005	0.3	0.2	0.05	2	1000	0.25	0.65	5	1	0.5
CD45												1	
CD90												1	
CD-45												1	

Table 5.2.1 Summary of parameters used in the parametric study

Analysis	Soil	Initial state (in situ)			Loading	Drainage
		p_i' (kPa)	p_0' (kPa)	v_i		
CIr	reconstituted	15	12.86	2.406	Isotropic compression	Drained
CI1	natural	75	12.86	2.387		
CI2		75	12.86	2.387		
CI3		75	12.86	2.387		

Table 5.2.2 Summary of analyses simulating isotropic compression on reconstituted and natural soil

Analysis	Soil	Initial state (in situ)			Loading	Drainage
		p_i' (kPa)	p_0' (kPa)	v_i		
CUr	reconstituted	25	12.5	2.406	Compression	Undrained
CU1	natural	125	12.5	2.387		
CU2		125	12.5	2.387		
CU3		125	12.5	2.387		

Table 5.2.3 Summary of analyses simulating undrained compression tests on reconstituted and natural soil from a normally consolidated state

Analysis	Soil	Initial state (in situ)			Loading	Drainage
		p_i' (kPa)	p_0' (kPa)	R_0		
CU3	natural	125	12.5	1	Compression	Undrained
CU32		75	12.5	1.7		
CU33		50	12.5	2.5		
CU34		25	12.5	5		

Table 5.2.4 Summary of analyses simulating undrained compression tests on natural soil from different overconsolidation levels

Analysis	Soil	Initial state (in situ)			End of recompression		Recompression stage	Shearing stage	
		p_i' (kPa)	p_0' (kPa)	v_i	p_c' (kPa)	R_0		Loading	Drainage
CU41	natural	25	12.5	2.406	200	1.14	Isotropic compression	Compression	Undrained
CU42		25	12.5	2.406	150	1	One-dimensional compression		
CU43		25	12.5	2.406	120	2	One-dimensional compression and swelling		
CU44		25	12.5	2.406	60	3.46	One-dimensional compression and swelling		

Table 5.2.5 Summary of analyses simulating undrained compression tests on natural soil after different stress histories

Analysis	Soil	Initial state (in situ)			End of recompression		Recompression stage	Shearing stage	
		p_i' (kPa)	p_0' (kPa)	v_i	p_c' (kPa)	R_0		Loading	Drainage
CD0	natural	75	12.86	2.387	93.3	1.5	One-dimensional compression and swelling	Compression probes	Drained (0 degree)
CD45		75	12.86	2.387	93.3	1.5	One-dimensional compression and swelling		Drained (45 degree)
CD90		75	12.86	2.387	93.3	1.5	One-dimensional compression and swelling		Drained (90 degree)
CD-45		75	12.86	2.387	93.3	1.5	One-dimensional compression and swelling		Drained (-45 degree)

Table 5.2.6 Summary of analyses simulating drained probes on natural soil

PARAMETERS											INITIAL STATE *in situ*				END OF SAMPLING	
M	λ	N	κ	ν	T	S	ψ	A	m	n	p' (kPa)	q' (kPa)	p_0' (kPa)	r	p' (kPa)	q' (kPa)
1.6	0.11	1.316	0.0028	0.3	0.7	0.14	2	900	0.25	0.65	35.7	20	7.55	5	25	0

Table 5.3.1 Parameters used for simulation of sampling and preparation history, and stress states before and after sampling and preparation

Sample	Depth (m)	facies	M	λ	N	κ	ν	T	S	ψ	A	m	n
LCD0	5.2-5.5	mottled	1.6	0.108	1.358	0.0028	0.3	0.7	0.14	2	900	0.25	0.65
LCD55													
LCD70													
LCD315													
L23	12.5-12.7	bedded	1.6	0.087	1.143	0.0028	0.3	0.7	0.14	2	900	0.25	0.65
SH13	8.6-9.0	laminated	1.6	0.097	1.21	0.0028	0.3	0.7	0.14	2	900	0.25	0.65
SCU1	6	bedded	1.6	0.11	1.316	0.0028	0.3	0.7	0.14	2	900	0.25	0.65
SUD2	6	bedded	1.6	0.11	1.316	0.0028	0.3	0.7	0.14	2	900	0.25	0.65
LUD1	5.4	mottled	1.6	0.0936	1.189	0.0028	0.3	0.7	0.14	2	900	0.25	0.65
B86	17.3-17.5	bedded	1.6	0.082	1.1	0.0028	0.3	0.7	0.14	2	900	0.25	0.65

Table 5.3.2 Summary of parameters used for evaluation of S3-SKH model prediction of triaxial tests on natural Bothkennar clay samples

Sample	Test	Depth (m)	sub-layer	λ	N	κ	M	ν	T	S	ψ	A	m	n
19B	LCD0	12.81-13.01	B1	0.14	1.575	0.0052	0.85	0.3	0.5	0.1	2	560	0.36	0.82
	LCD30													
	LCD60													
	LCD90													
	AUC													
	AUE													
29A	CID1	17.93-18.1	B3	0.14	1.575	0.0052	0.85	0.3	0.5	0.1	2	560	0.36	0.82
	CID2													
	CID3													

Table 5.3.3 Summary of parameters used for evaluation of S3-SKH model prediction of triaxial tests on natural Pisa clay samples

Soil	Sample	s_0		s_f	k	Comments
		lower bound	upper bound			
Bothkennar clay	L23	8	13.5	1	0.45	Section 5.3.5
				6		Section 5.3.6
	SH13	10	14.5	1		
	SCU1	5	9	1		
	SUD2	3.6	9	1		
	LUD1	6	7.5	1		
	LCD	4.5		1		
	B86	5		1.5		
Pisa clay	19B	3.5		1	0.23	
	29A	2.8		1		

Table 5.3.4 Values of initial sensitivity used for evaluation of the S3-SKH model prediction of triaxial tests on natural samples of Bothkennar and Pisa clays

Test	Initial state (in situ)		Recompression stage	Shearing stage		Comments
	p'_i (kPa)	p'_0 (kPa)		Loading	Drainage	
LCD0	34	7.9	A-E-D	Compression probes	Drained (0 degree)	Consolidated drained
LCD55					Drained (55 degrees)	
LCD70					Drained (70 degrees)	
LCD315					Drained (315 degrees)	
L23	60.4	5.336	A-E-D	Compression	Undrained	Consolidated undrained
SH13	46.27	5.89	A-E-D	Compression	Undrained	
SCU1	35.7	7.55	A-B-C-D	Compression	Undrained	
SUD2	35.7	6.586	A-B-F	Compression	Undrained	Recompressed beyond yield
LUD1	34	4.47	A-B-E	Compression	Undrained	
B86	40	17.86	none	Compression constant stress ratio	Drained	

Table 5.3.5 Summary of analyses used for the evaluation of the S3-SKH model predictions of triaxial tests on natural Bothkennar clay samples

Sample	Test	Initial state		Recompression stage	Shearing stage		Comments
		p'_i (kPa)	p'_0 (kPa)		Loading	Drainage	
19B	A0	88.2	29.14	A-E-D	Compression probes	Drained (0 degree)	
	A30					Drained (30 degrees)	
	A60					Drained (60 degrees)	
	A90					Drained (90 degrees)	
	AUC			A-E-D	Compression	Undrained	
	AUE			A-E-D	Extension	Undrained	
29A	CID1	43.3	43.13		Compression	Drained constant p'	isotropically compressed to 98kPa before shearing
	CID2						isotropically compressed to196kPa before shearing
	CID3						isotropically compressed to 294kPa before shearing

Table 5.3.6 Summary of analyses used for the evaluation of the S3-SKH model predictions of triaxial tests on natural Pisa clay samples

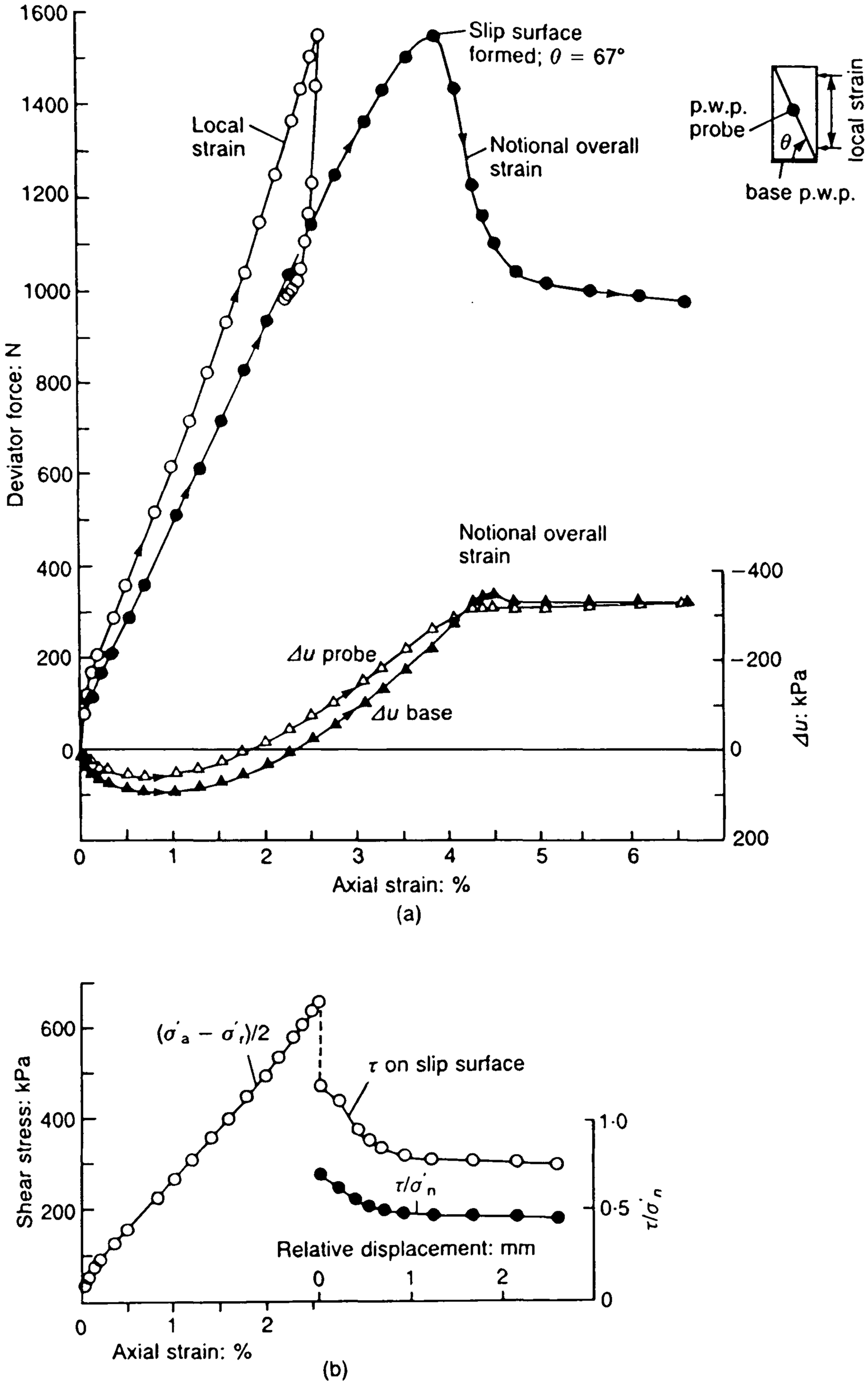

Figure 1.3.1 Post-rupture behaviour of Todi clay in unconsolidated undrained trixial test (after Burland, 1990)

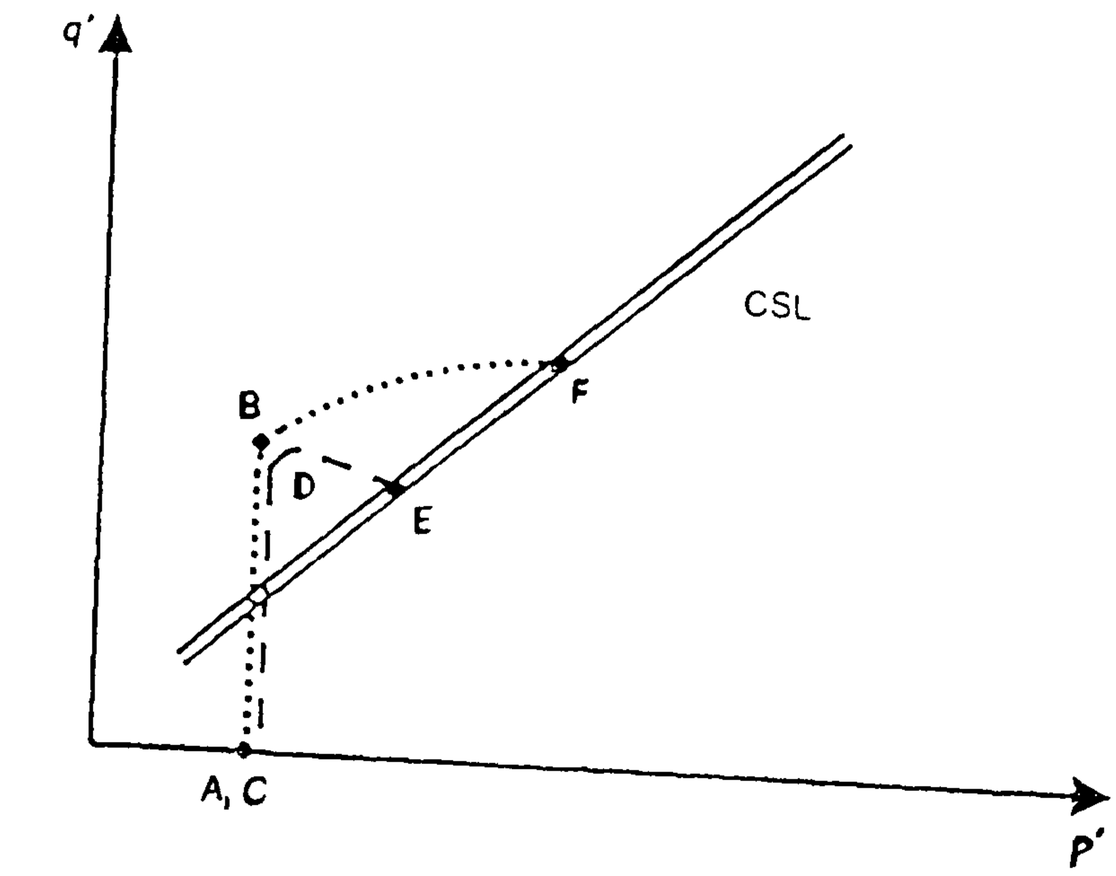

(a)

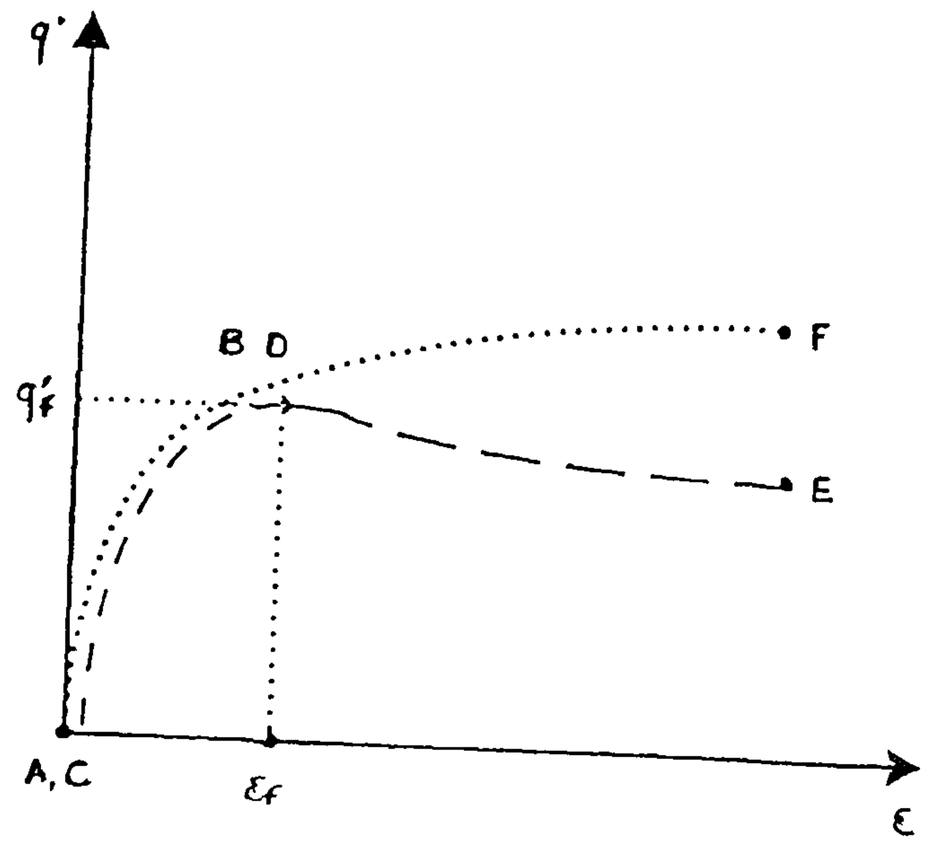

(b)

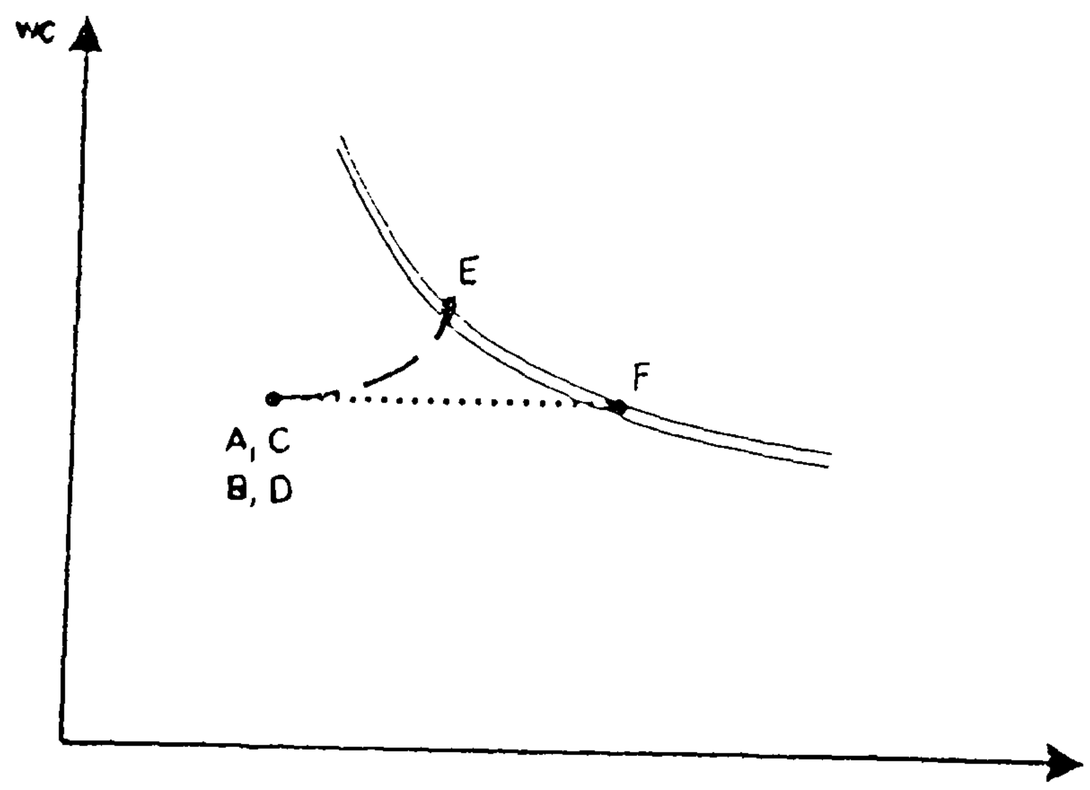

(c)

Figure 1.3.2 Behaviour of a sample with a dilating shear band (after Atkinson & Richardson, 1987)

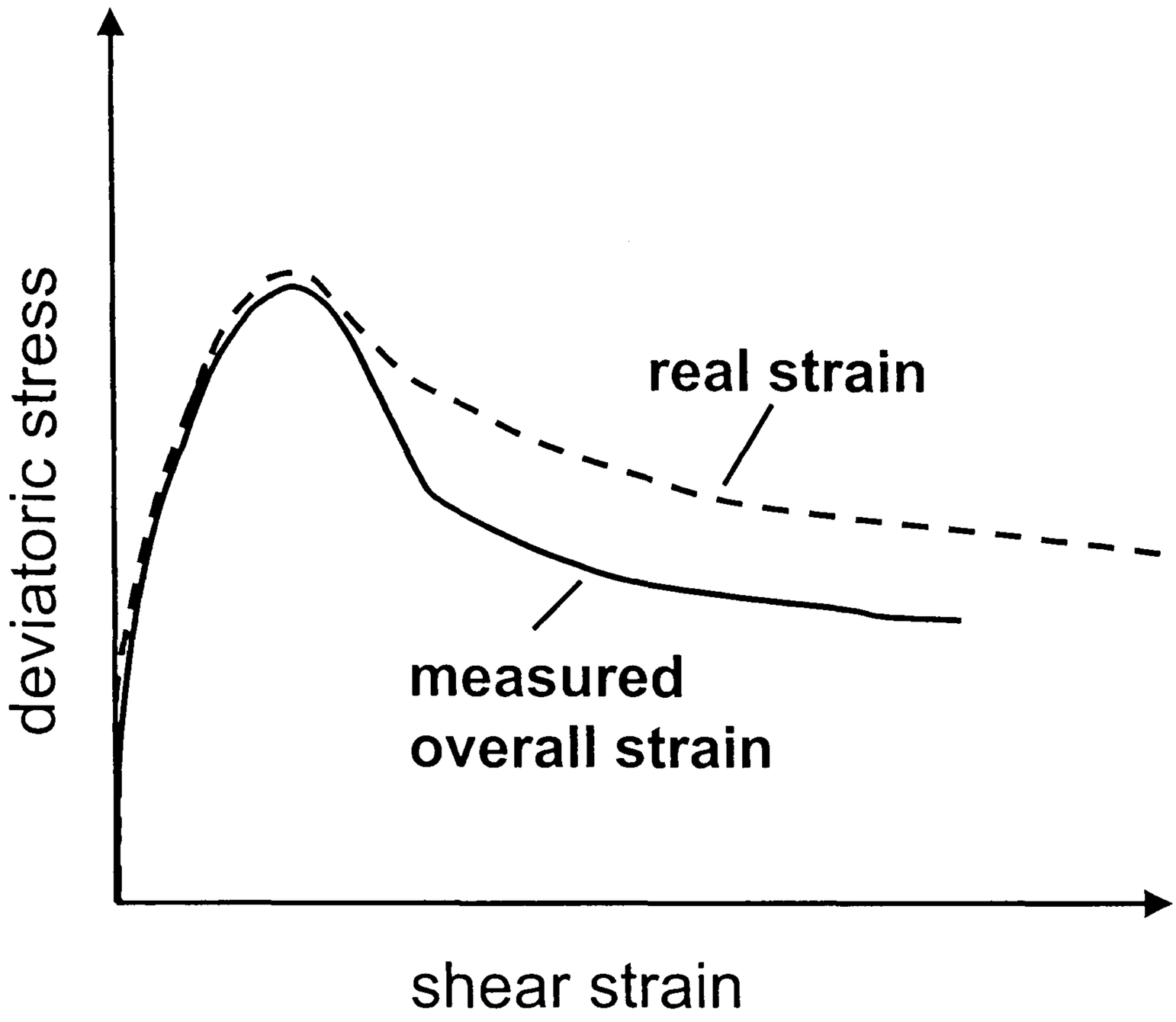

Figure 1.3.3 Effects of shear planes on the measurement of axial strains

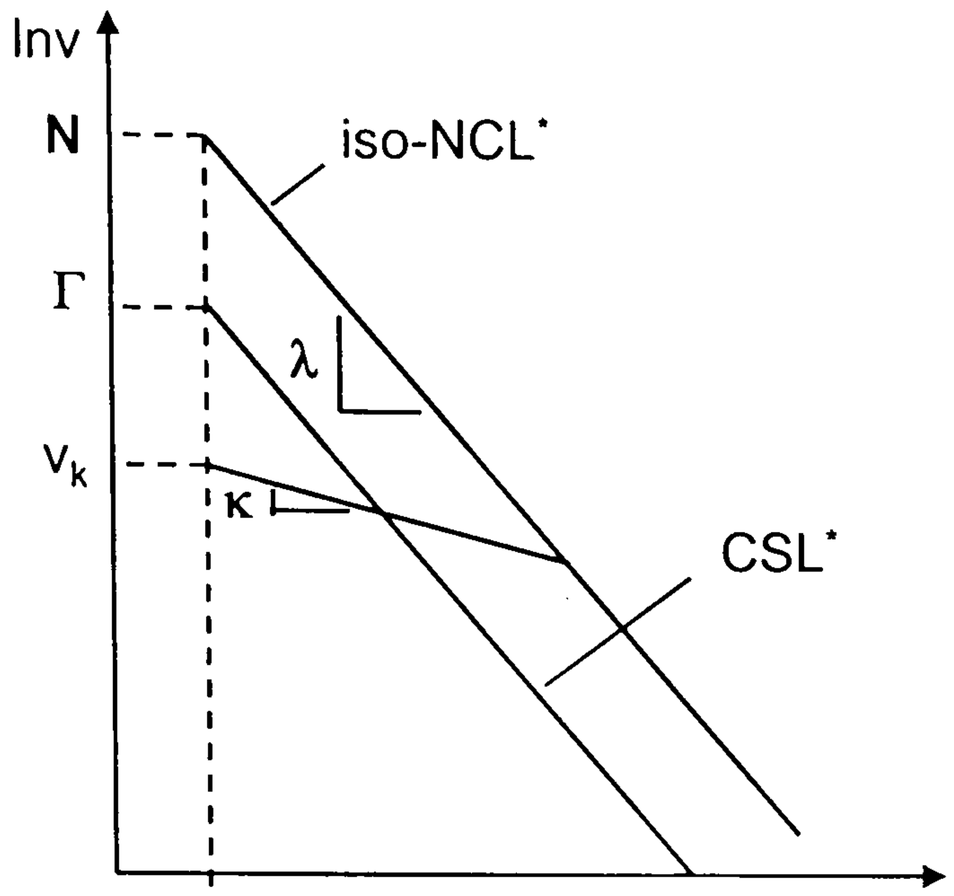

Figure 1.4.1 Critical state framework: intrinsic critical state line, isotropic normal compression line and swelling line.

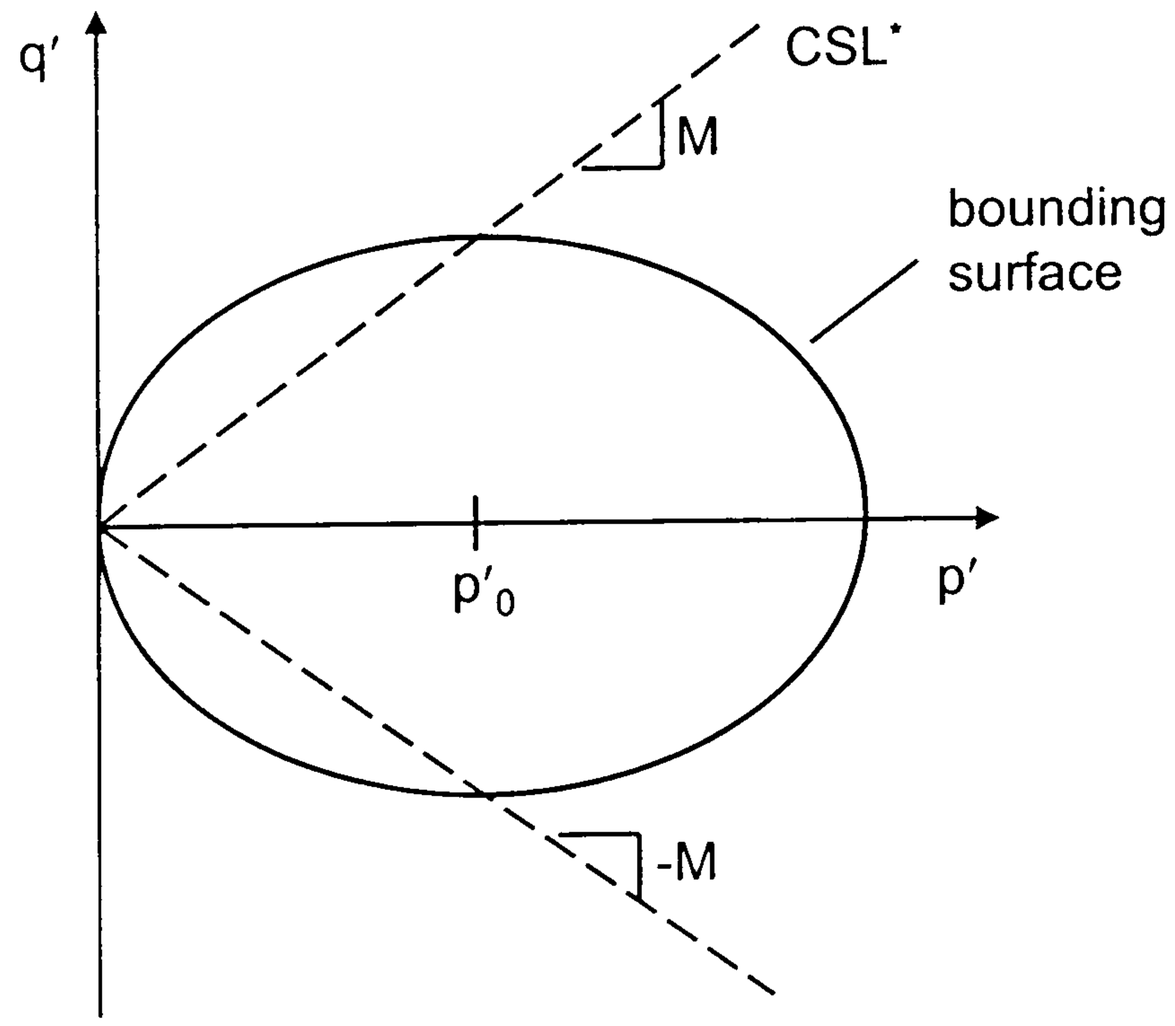

Figure 1.4.2 Intersection of the state boundary surface with an elastic wall

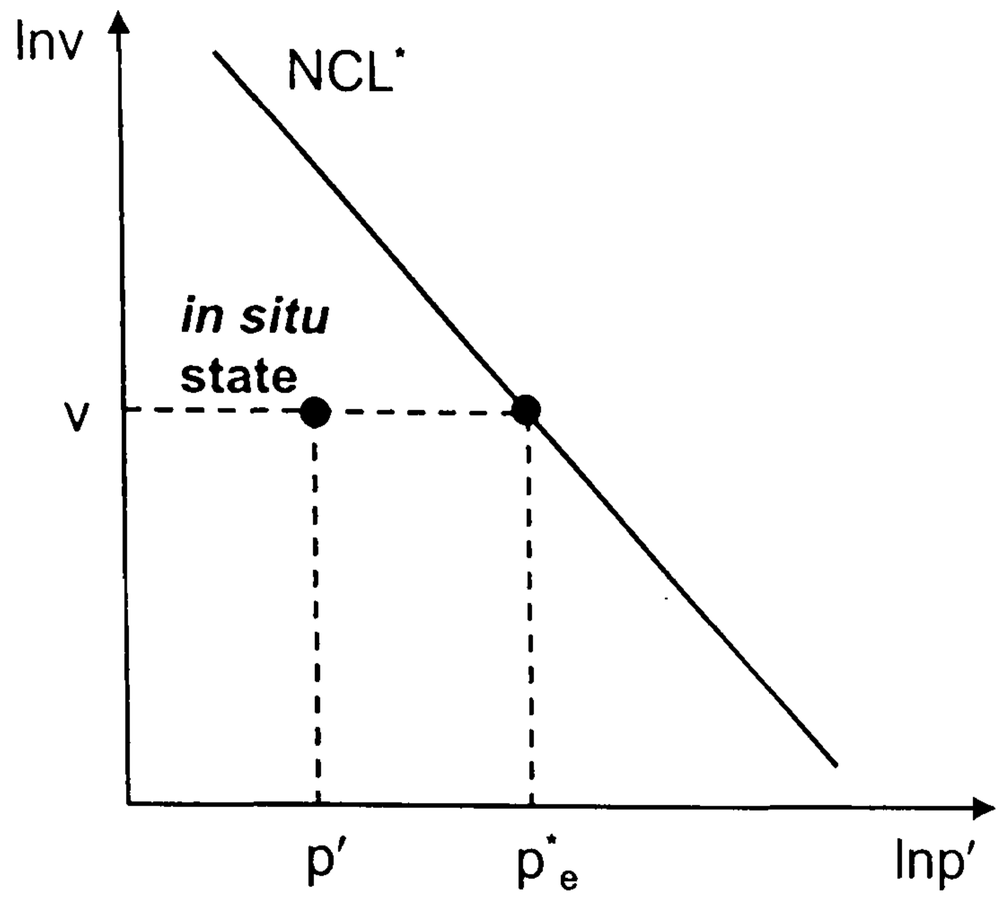

Figure 1.4.3 Equivalent pressure on the intrinsic normal compression line

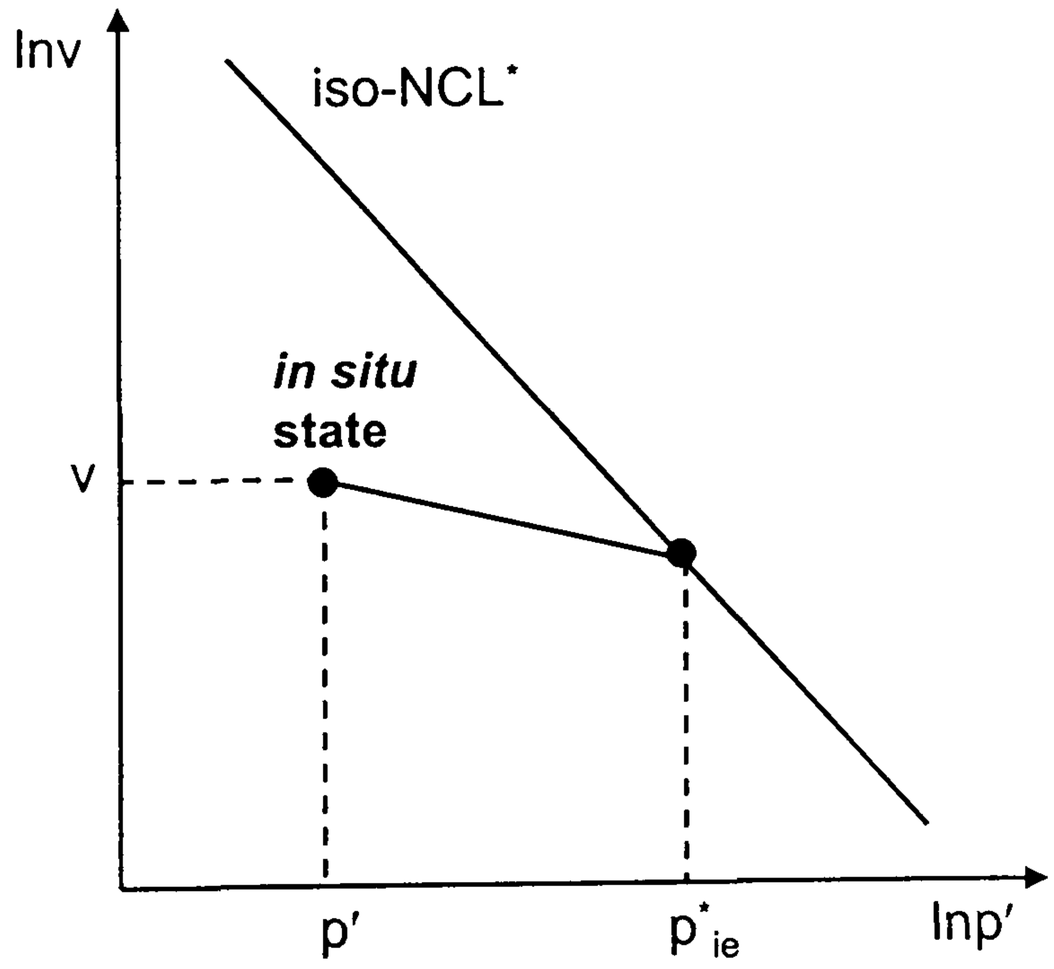

Figure 1.4.4 Equivalent pressure on the isotropic intrinsic normal compression line

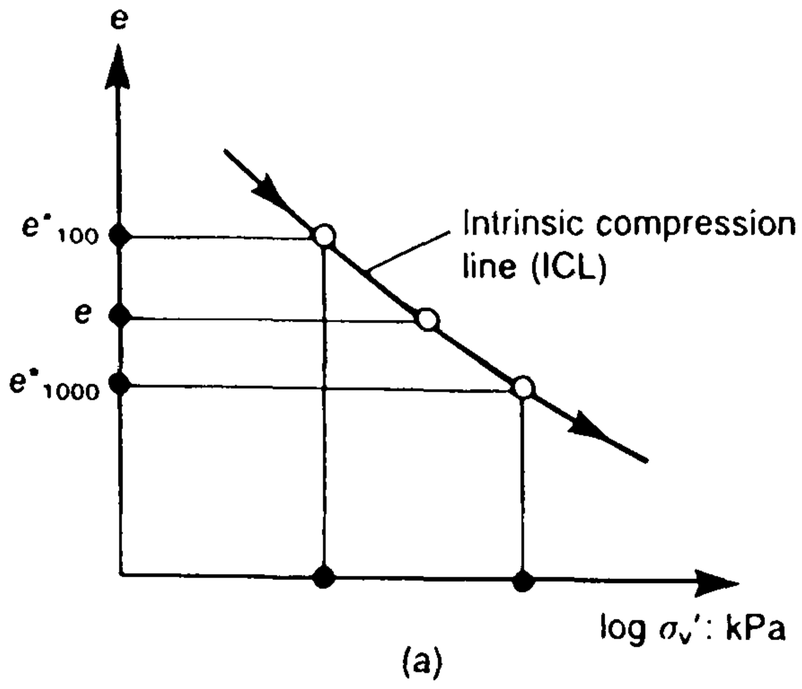

Figure 1.4.5 The use of void index I_v to normalise with respect to composition (after Burland, 1990)

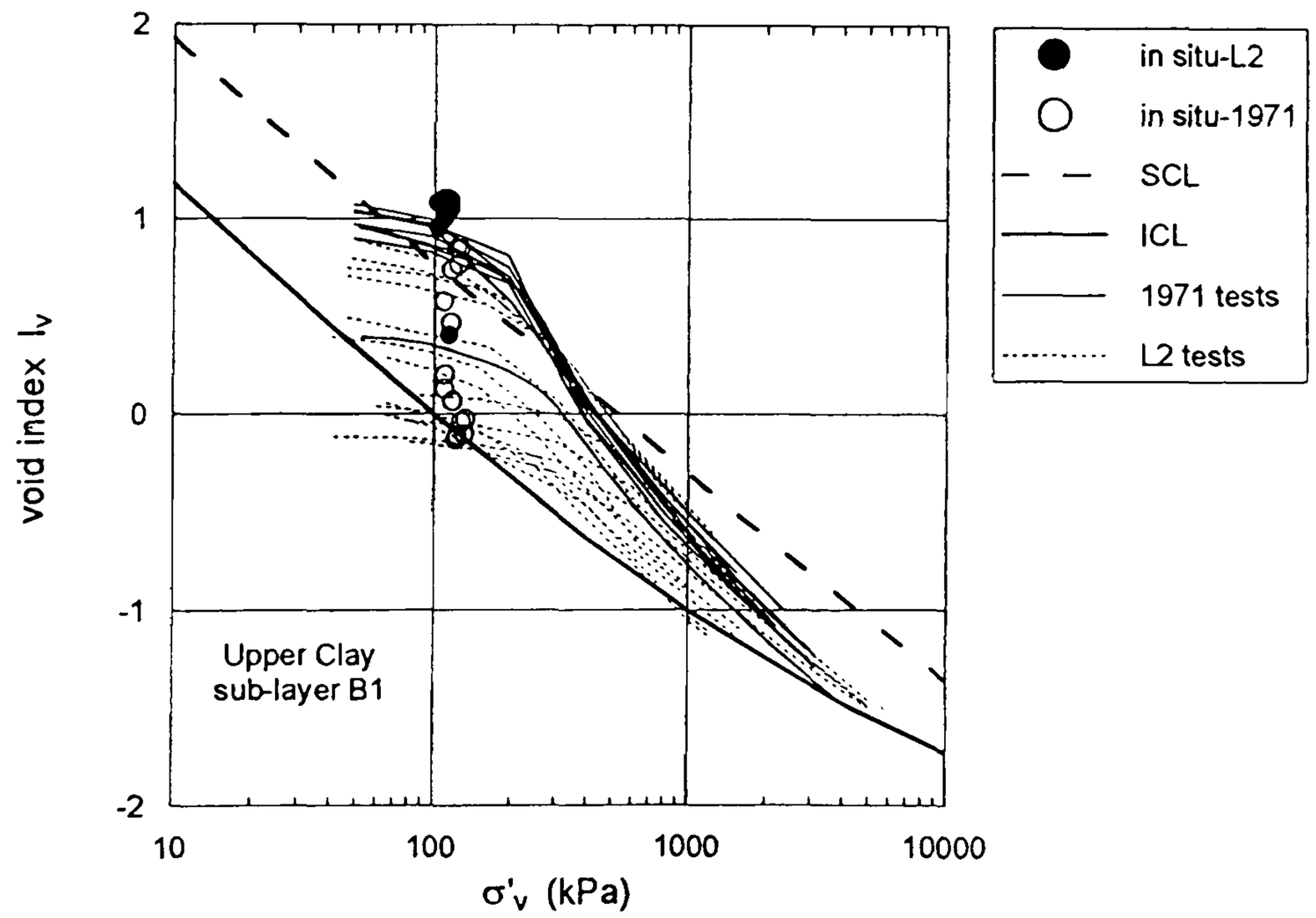

Figure 1.4.6 Normalised one-dimensional compression curves for Pisa clay (after Rampello *et al.*, 1996)

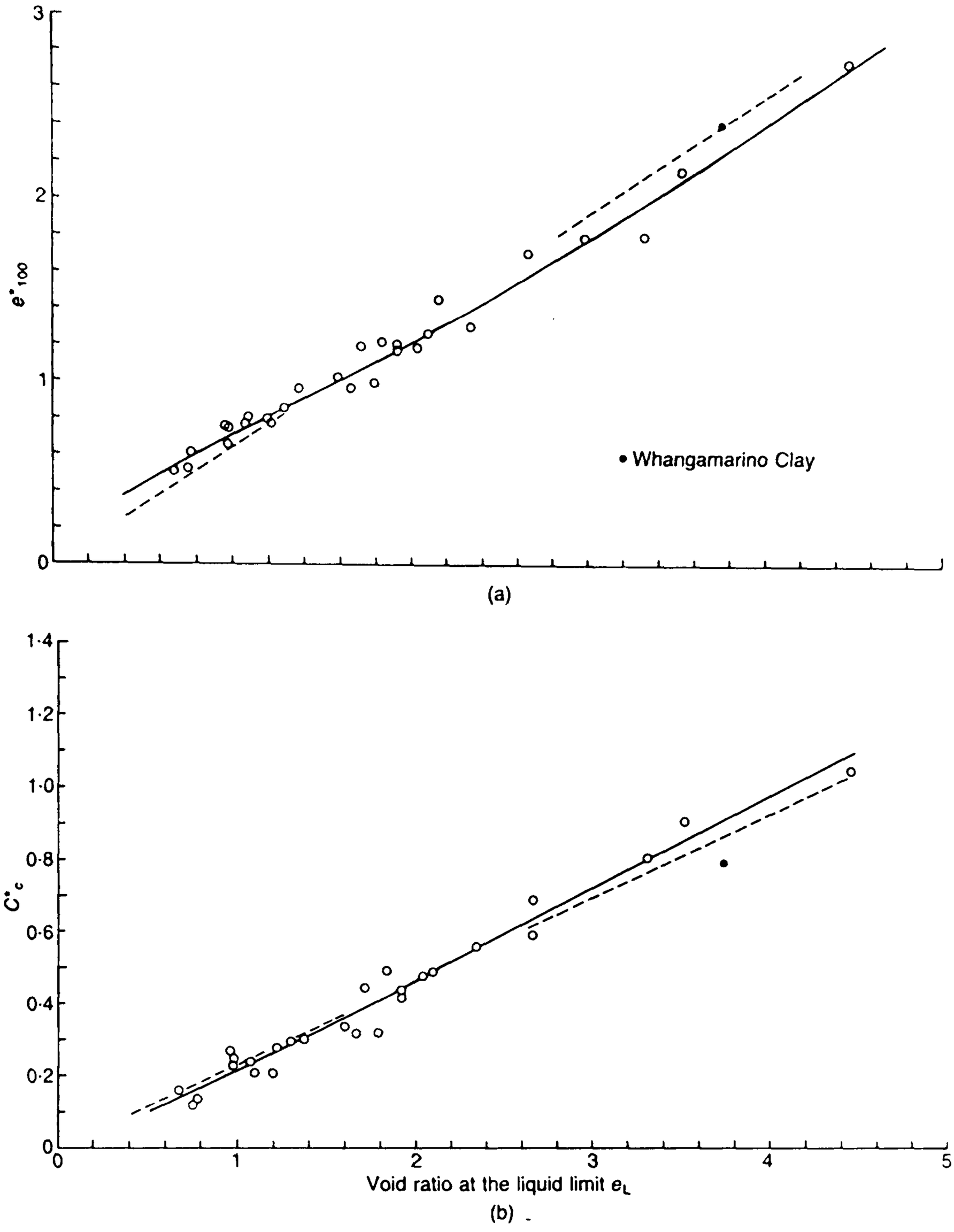

Figure 1.4.7 Relationships between e_L and constants of compressibility e^*_{100} and C^*_c (after Burland, 1990).

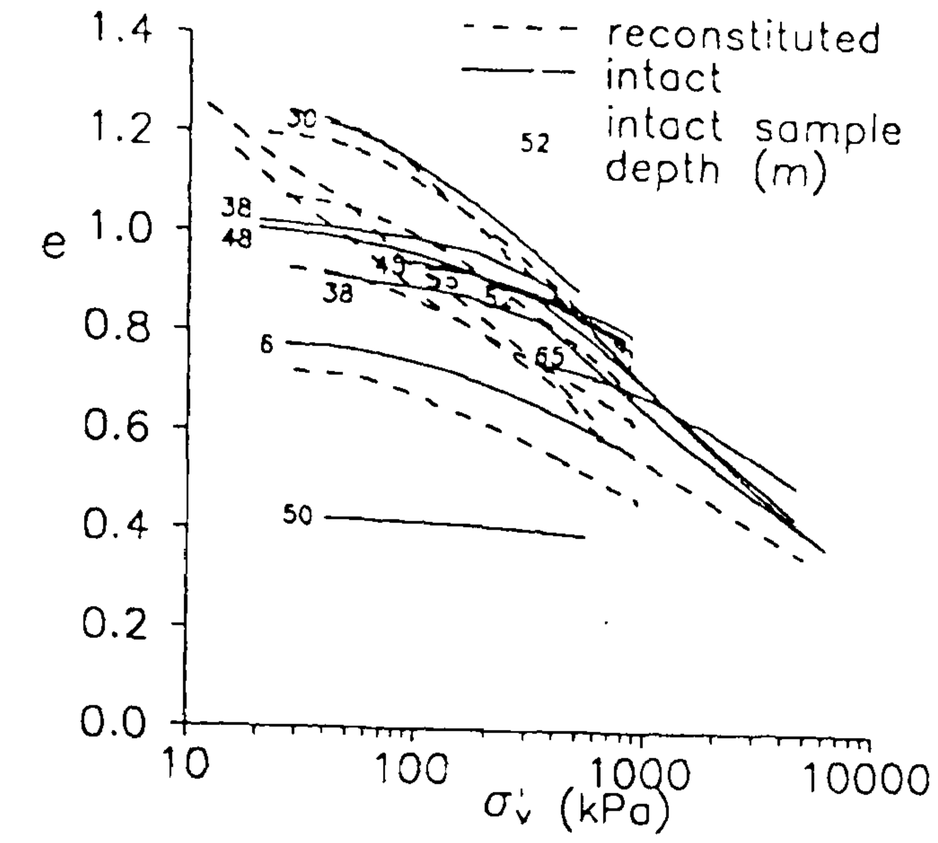

(a)

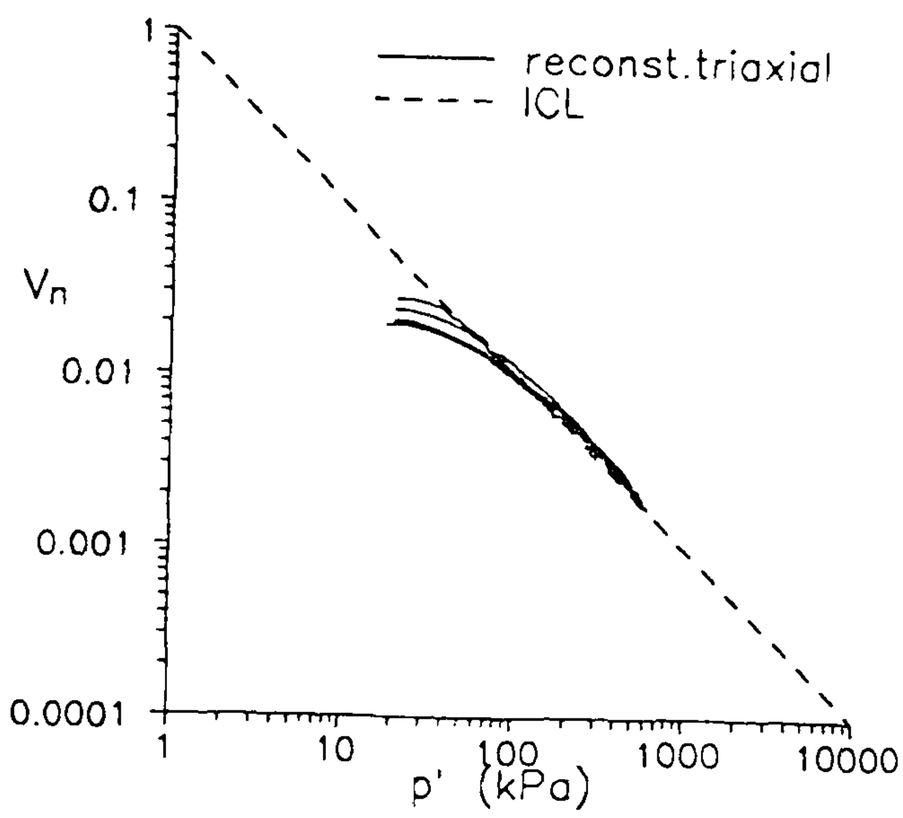

(b)

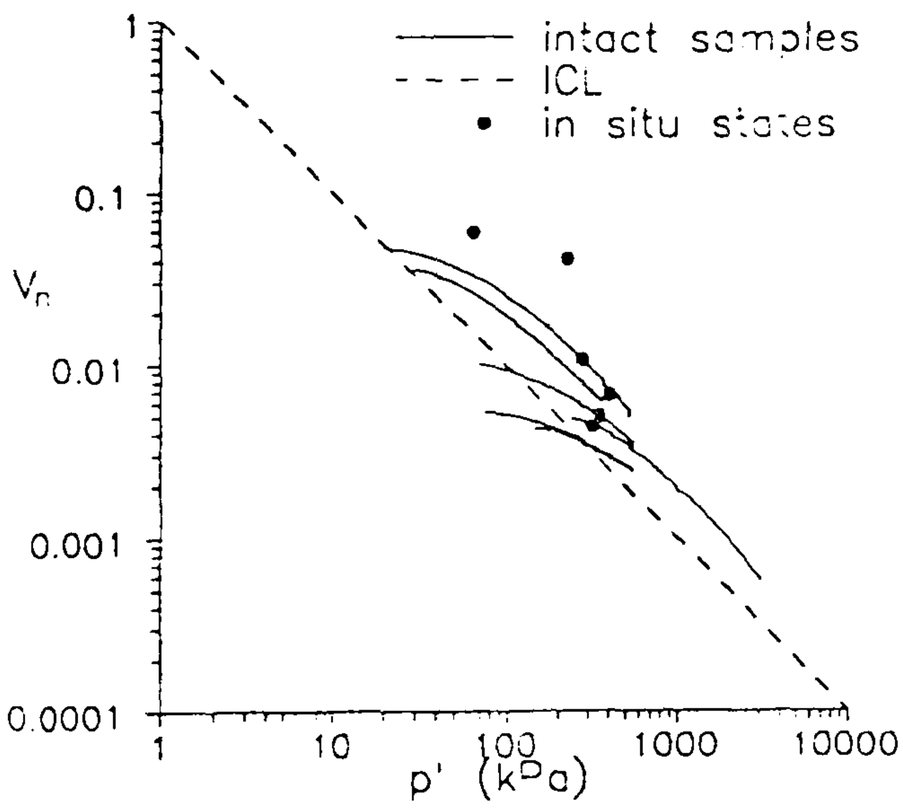

(c)

Figure 1.4.8 One-dimensional compression data from oedometer and triaxial tests on Sibari clay (a) in e-lnσ_v' plane (b) normalisation of the reconstituted test data with respect to v_n (c) normalisation of the intact test data with respect to v_n (after Coop & Cotecchia, 1995)

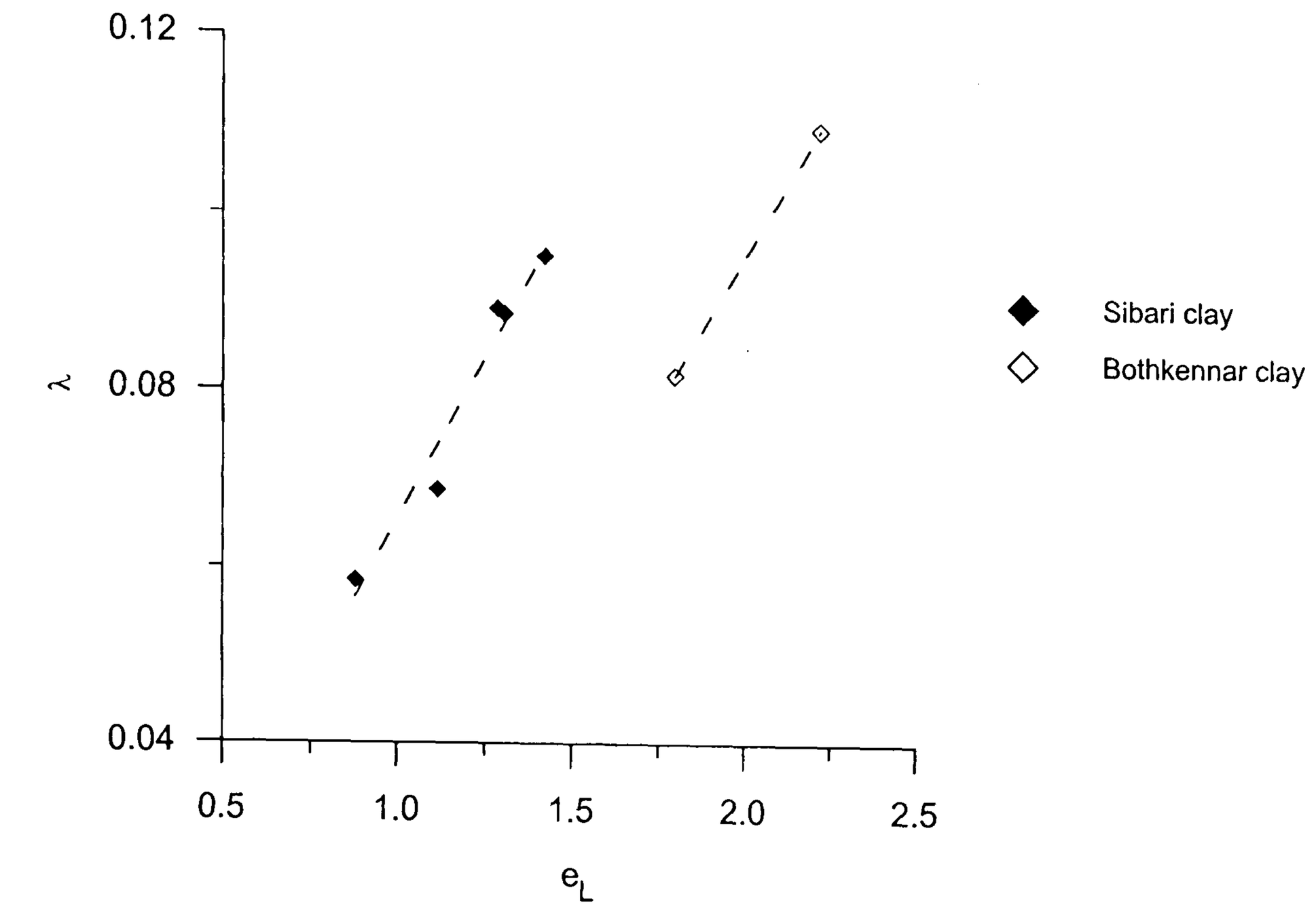

(a)

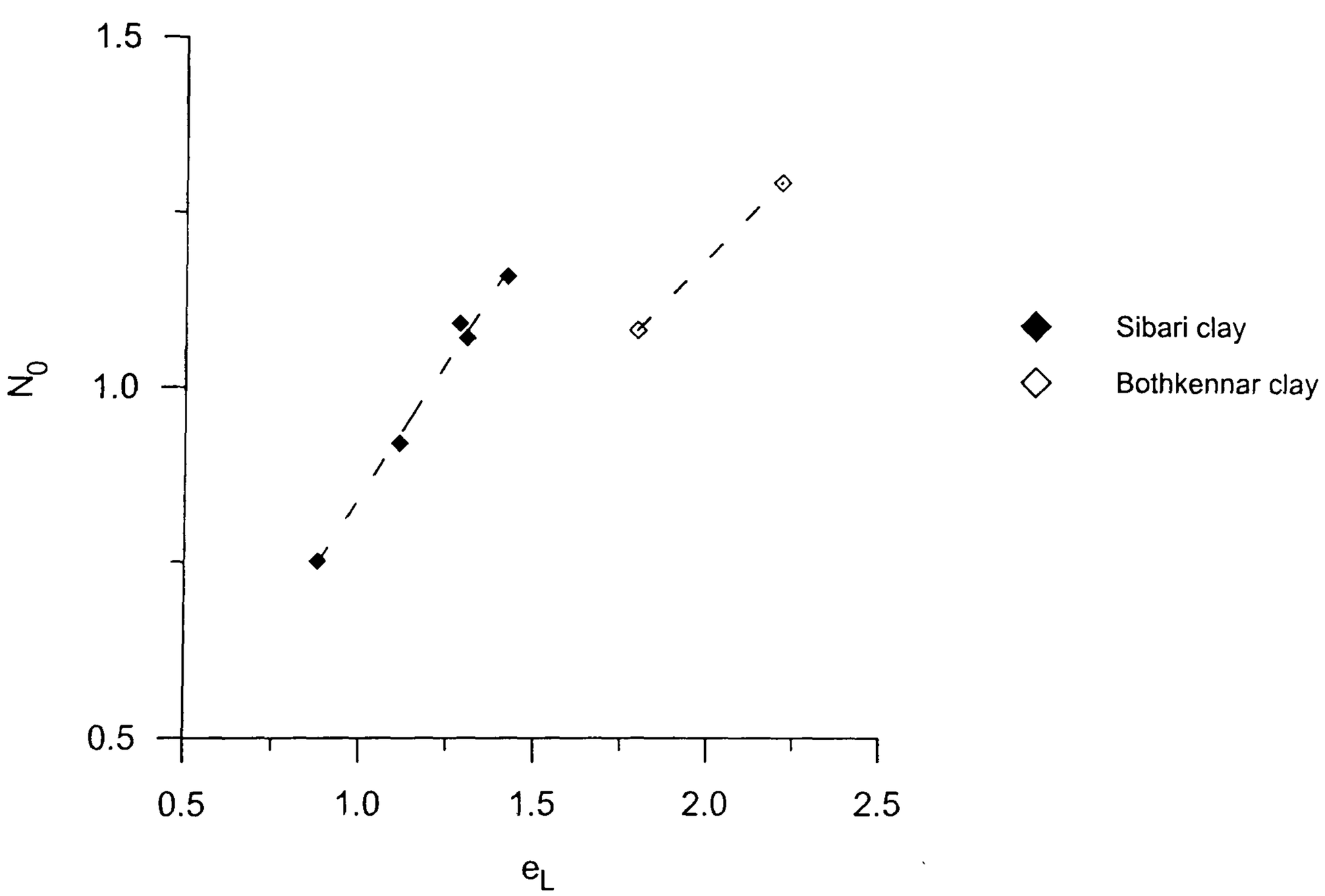

(b)

Figure 1.4.9 Relationship between void ratio at liquid limit e_L and compression parameters (a) λ (b) N_0, for Sibari and Bothkennar clay (data from Allman, 1992; Coop & Cotecchia, 1995; Smith, 1992)

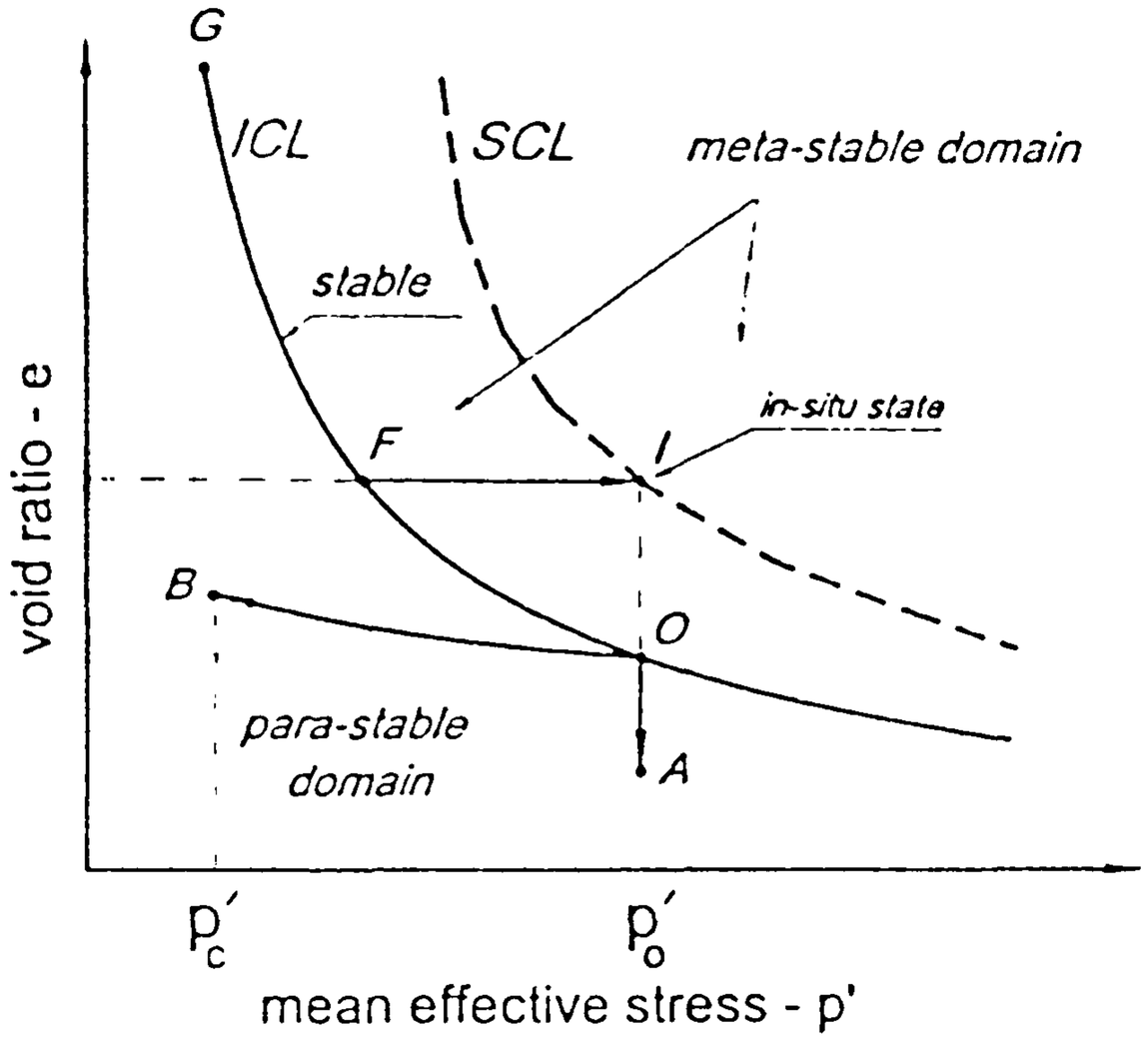

Figure 2.2.1 Mechanisms causing the development of structure in soils: (GFO)=intrinsic compression, (OA)=ageing, (OB)=overconsolidation, (FI)=concurrent structure development (after Kavvadas & Anagnostopoulos, 1998)

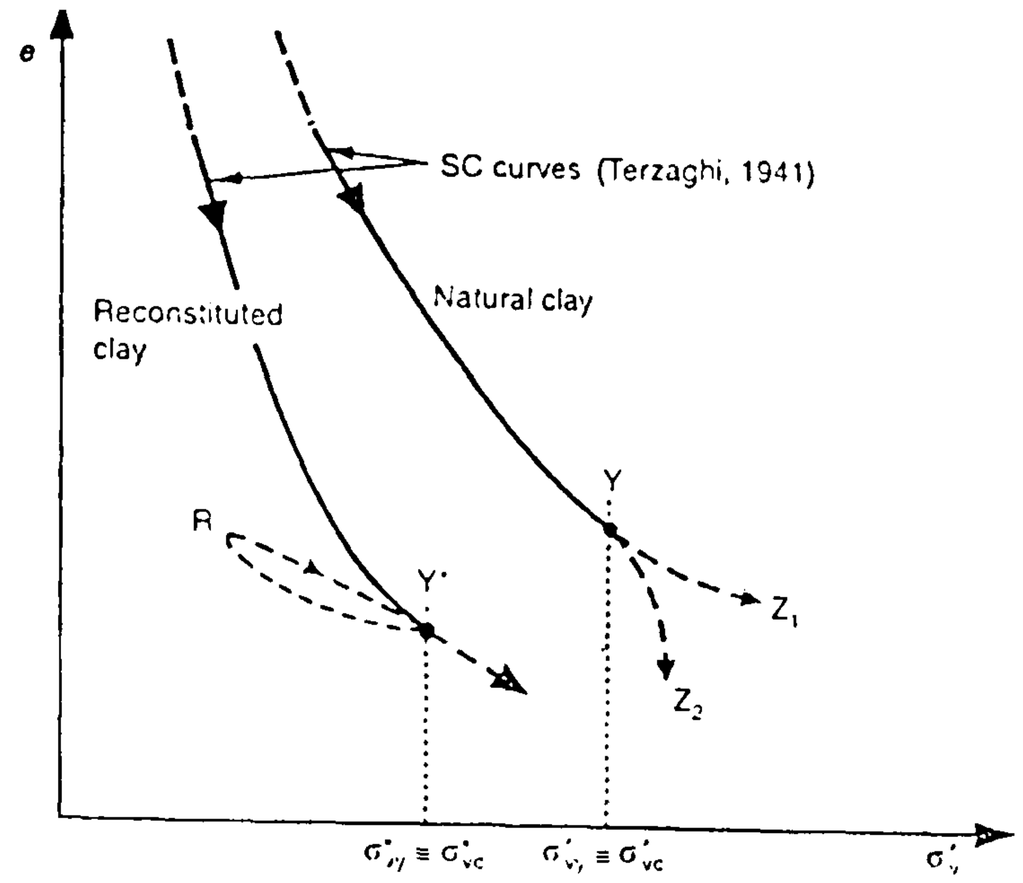

(a)

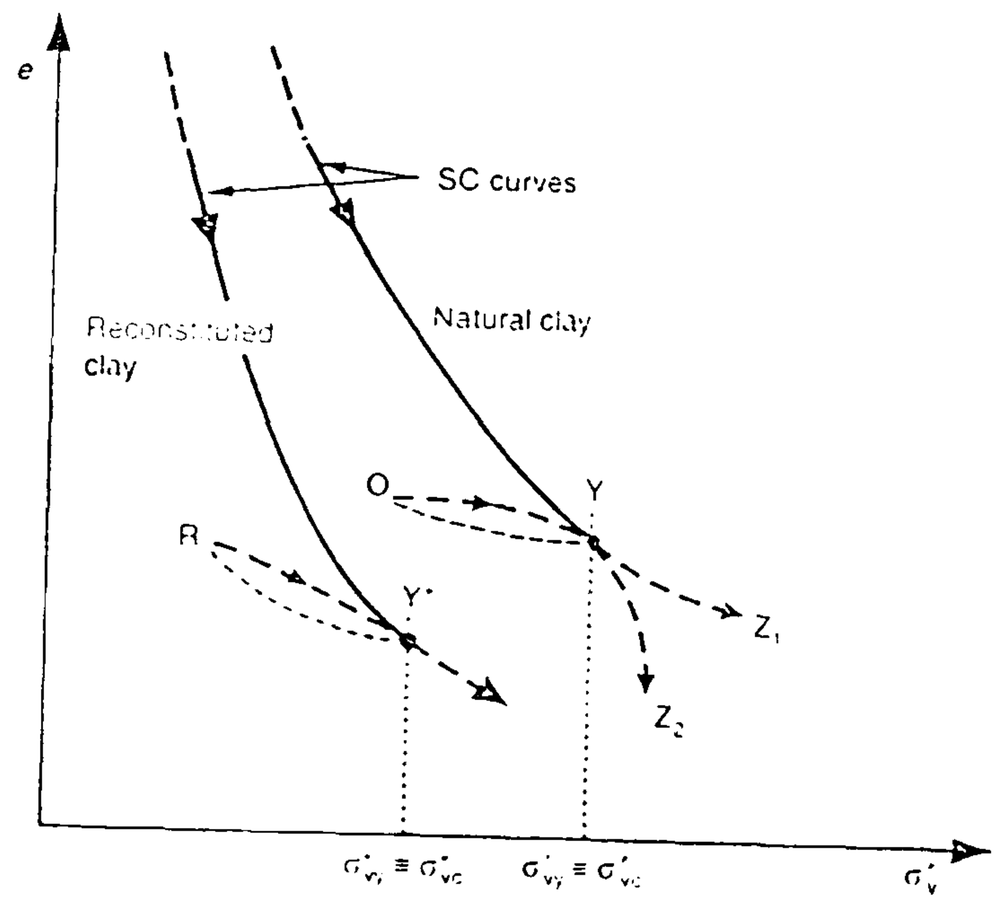

(b)

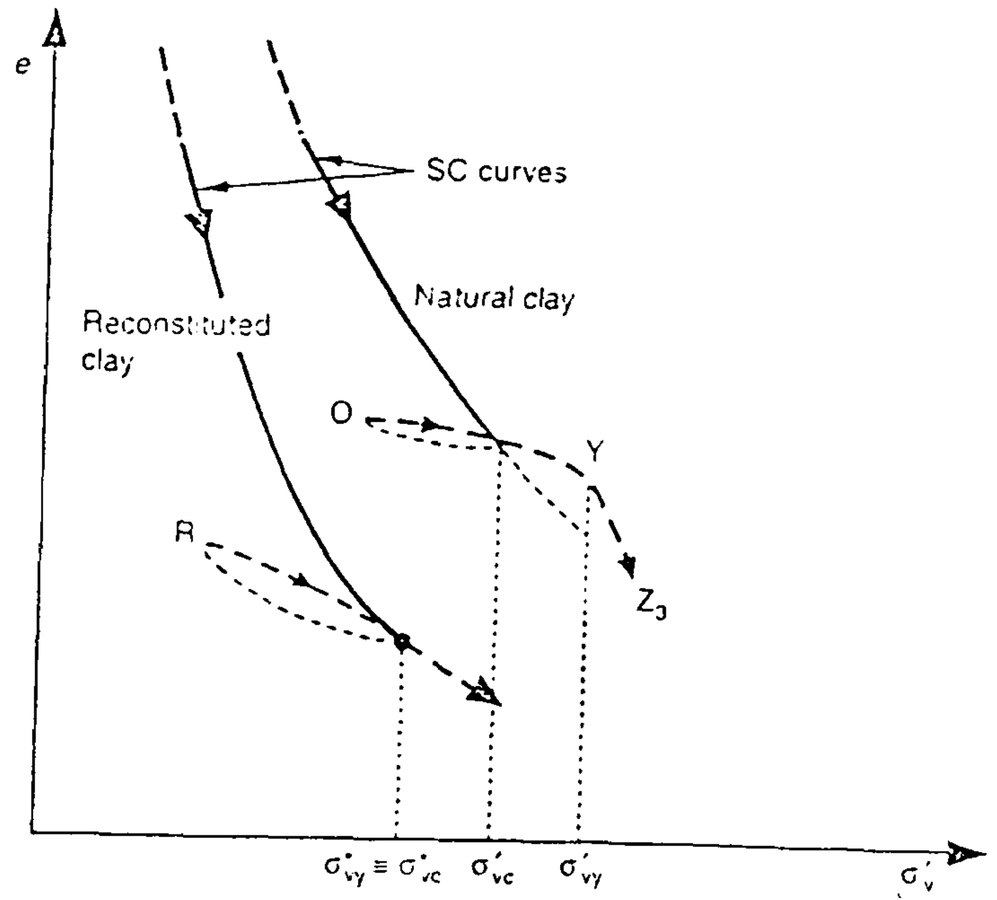

(c)

Figure 2.2.2 Response of clays to one-dimensional compression. The natural clay is (a) normally consolidated with a sedimentation structure (b) simply over-consolidated (c) overconsolidated with a post-sedimentation structure at gross yield (after Cotecchia & Chandler, 2000)

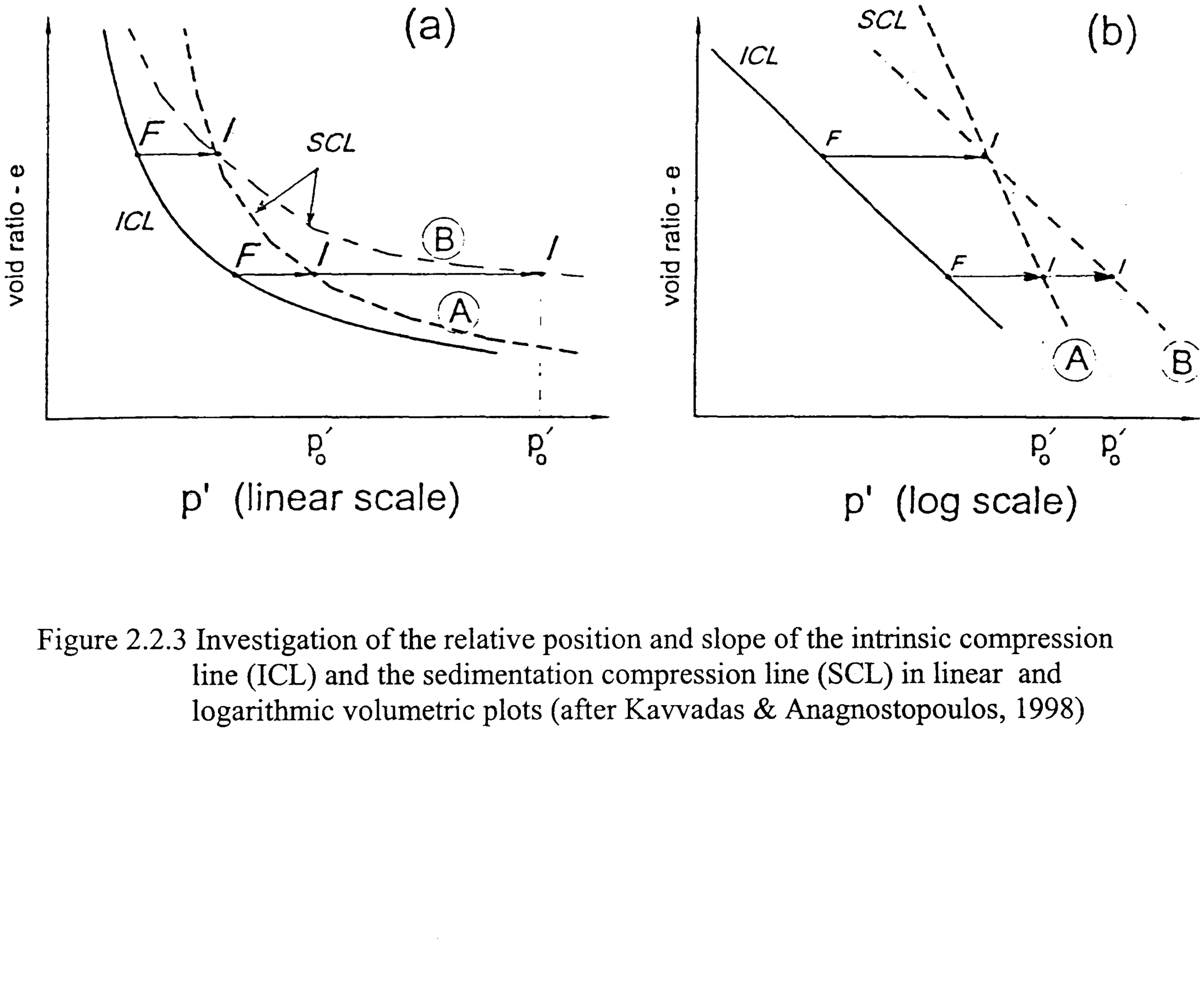

Figure 2.2.3 Investigation of the relative position and slope of the intrinsic compression line (ICL) and the sedimentation compression line (SCL) in linear and logarithmic volumetric plots (after Kavvadas & Anagnostopoulos, 1998)

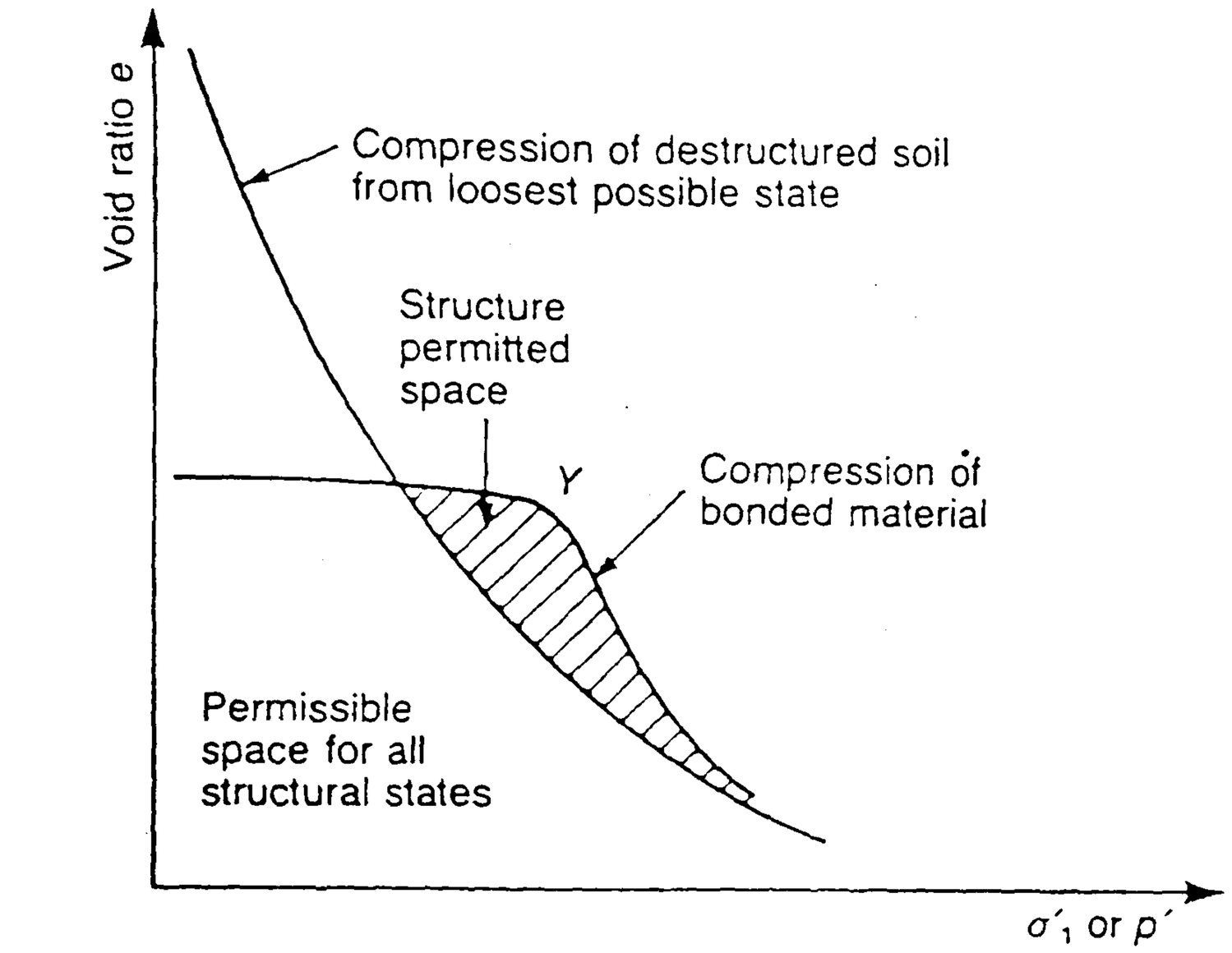

Figure 2.3.1 Comparison of "structured" and "destructured" compression in the oedometer test (after Leroueil & Vaughan, 1990)

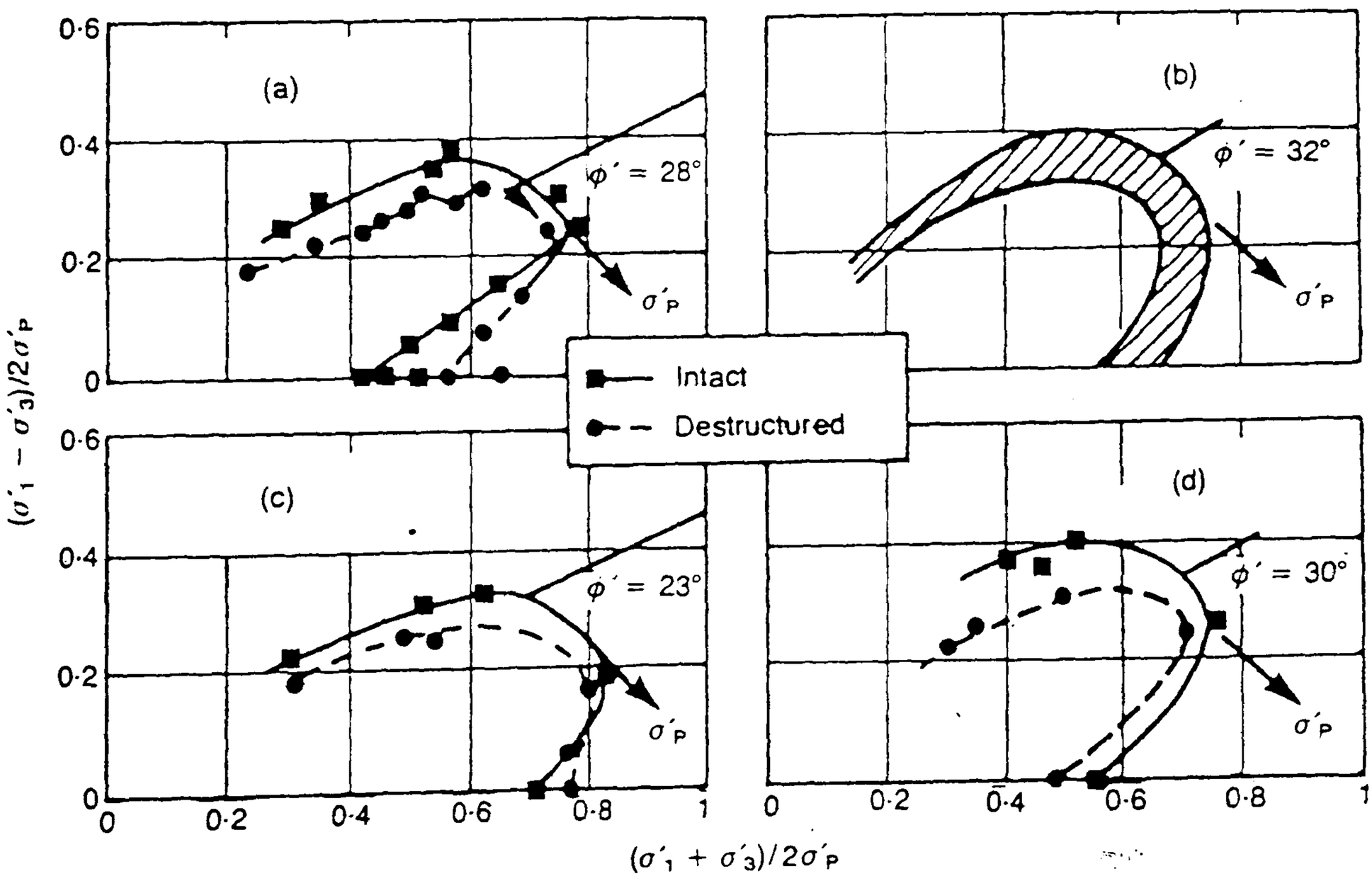

Figure 2.3.2 Limit state curves of intact and "destructured" natural clays (after Tavenas & Leroueil, 1985)

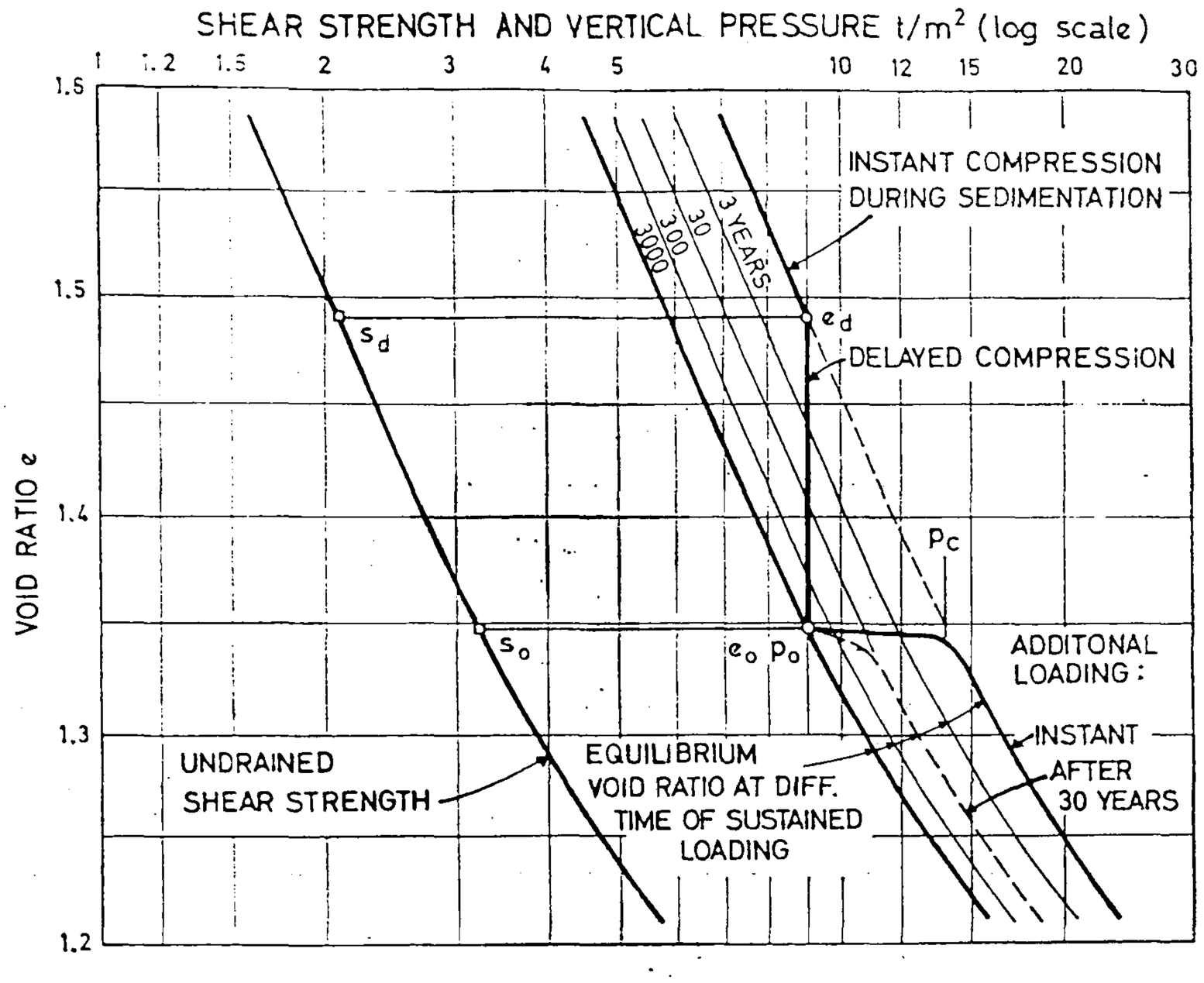

(a)

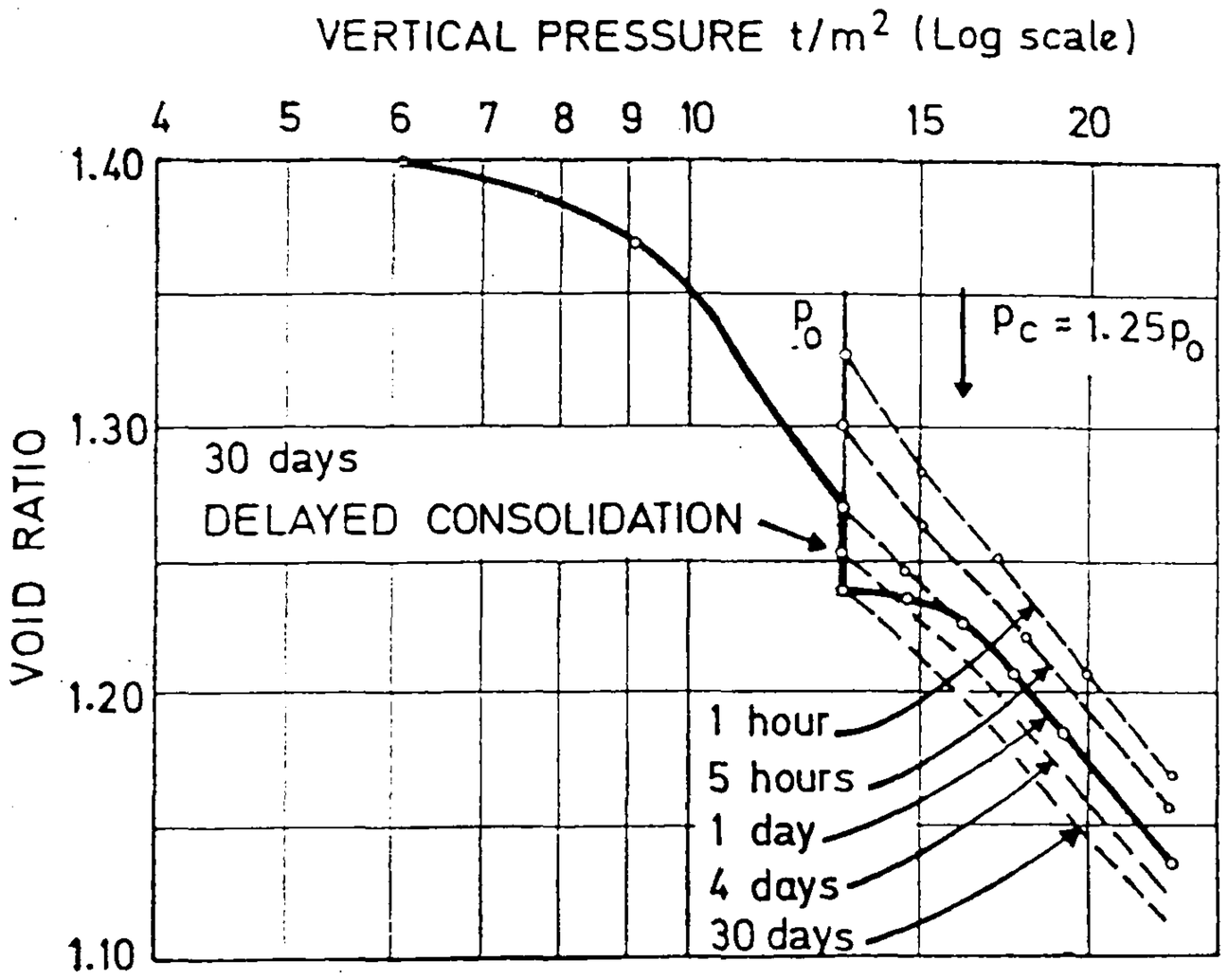

(b)

Figure 2.3.3 Compressibility and strength of a clay exhibiting delayed consolidation (a) schematic diagram (b) data from tests on plastic Drammen clay (after Bjerrum, 1967)

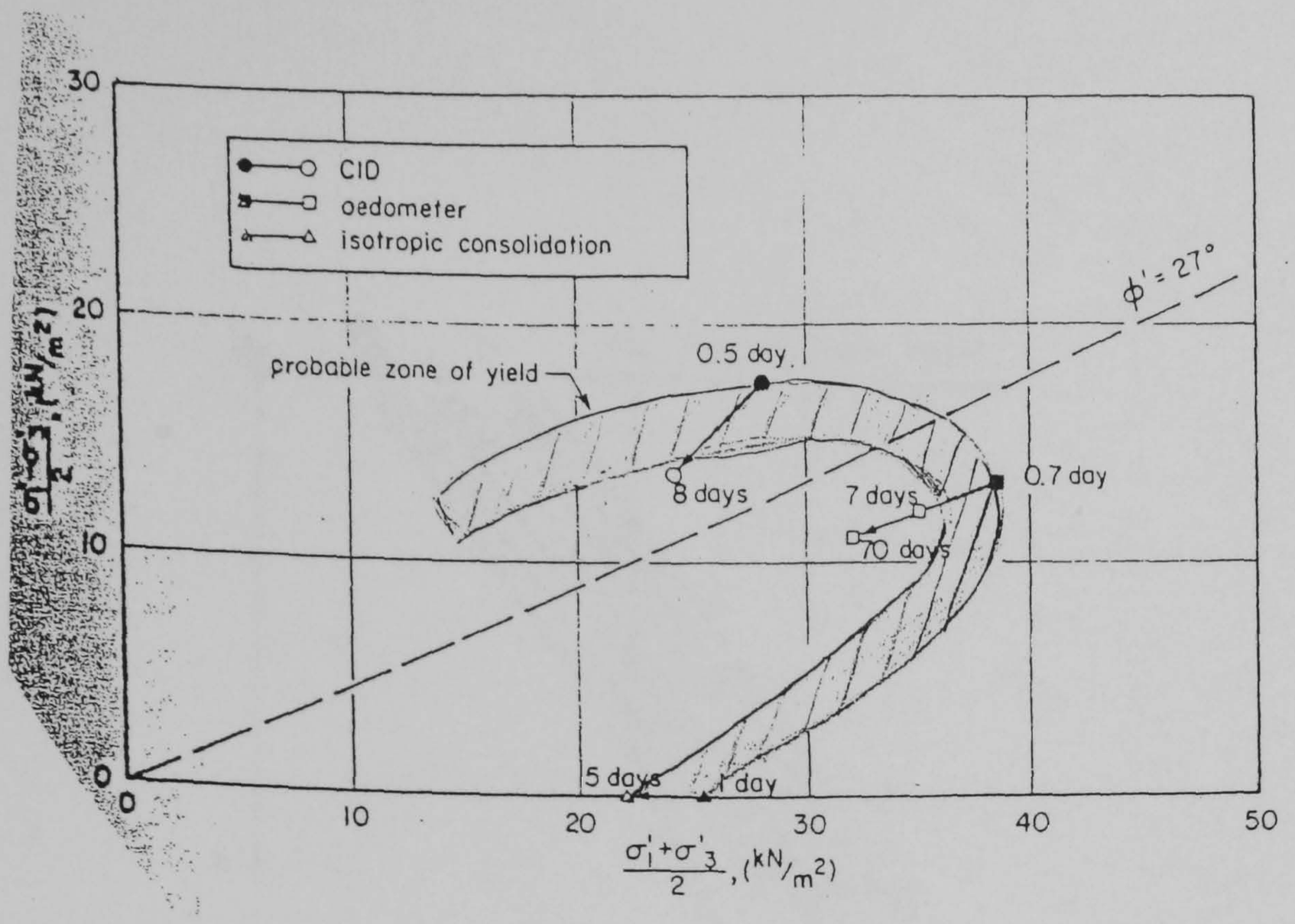

(a)

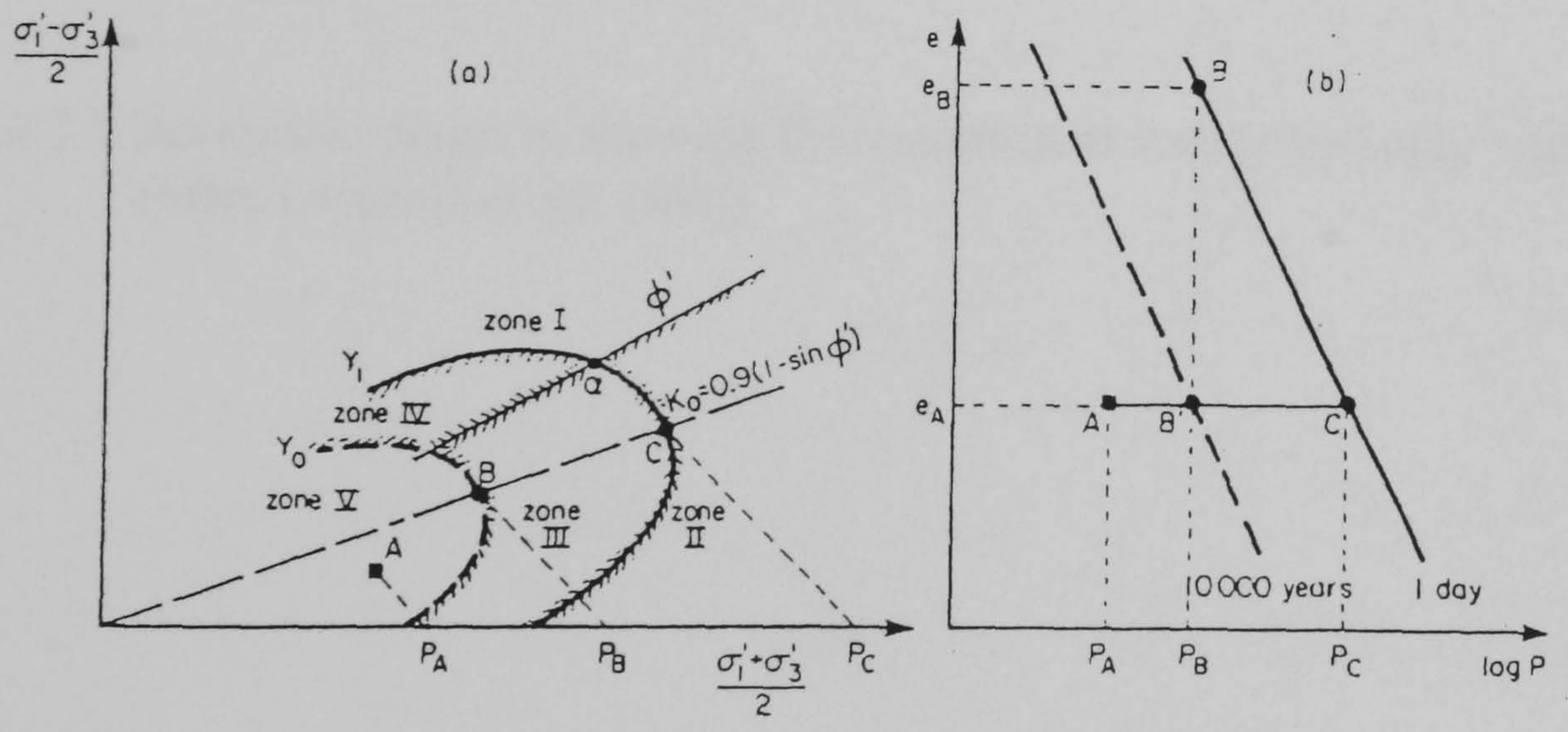

(b)

Figure 2.3.4 Effect of ageing on the gross yield curve (a) data from tests on St-Alban clay 3m (b) proposed model (after Tavenas & Leroueil, 1977)

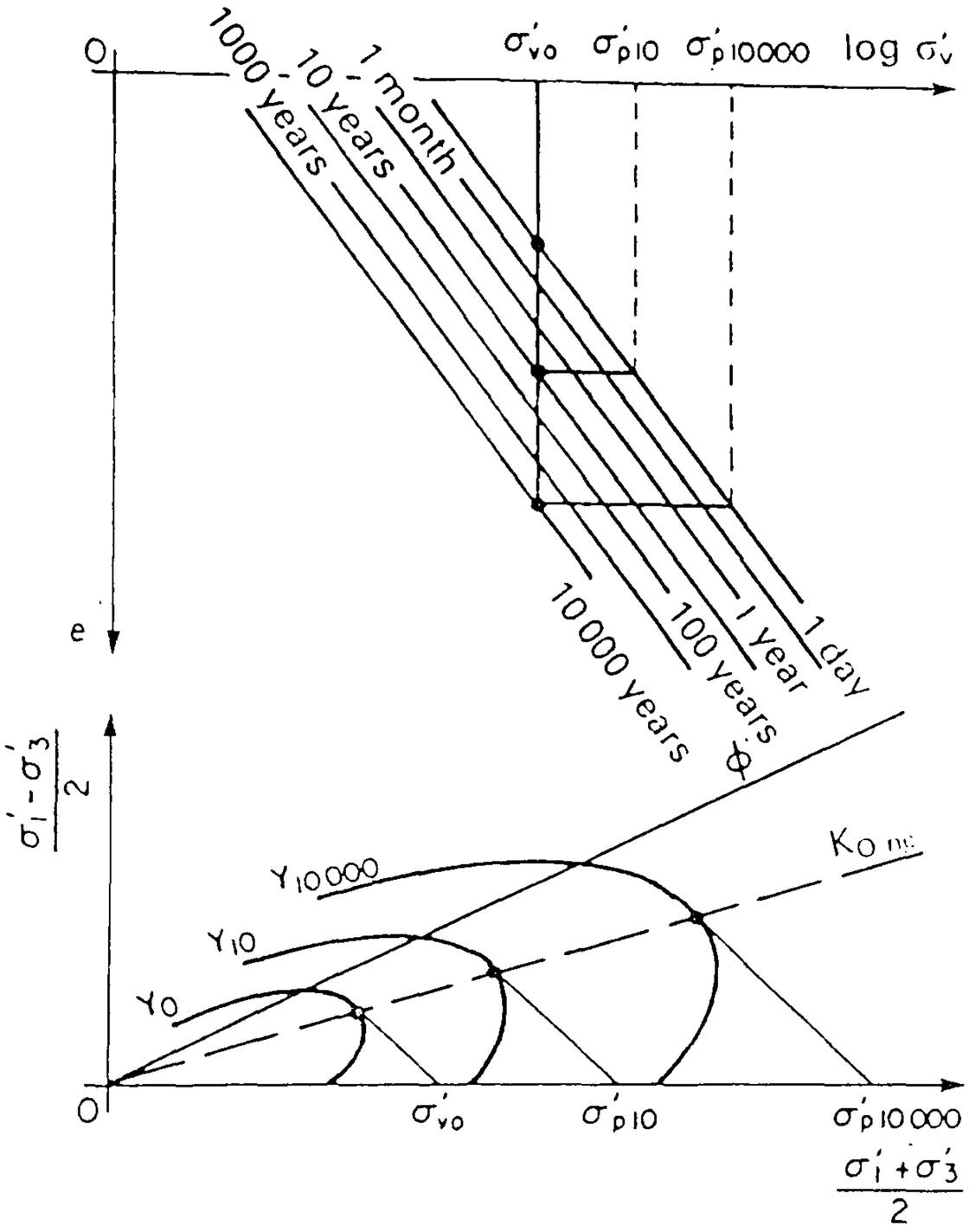

Figure 2.3.5 Schematic diagram showing the variation in strength of clay with ageing (after Leroueil *et al.*, 1990)

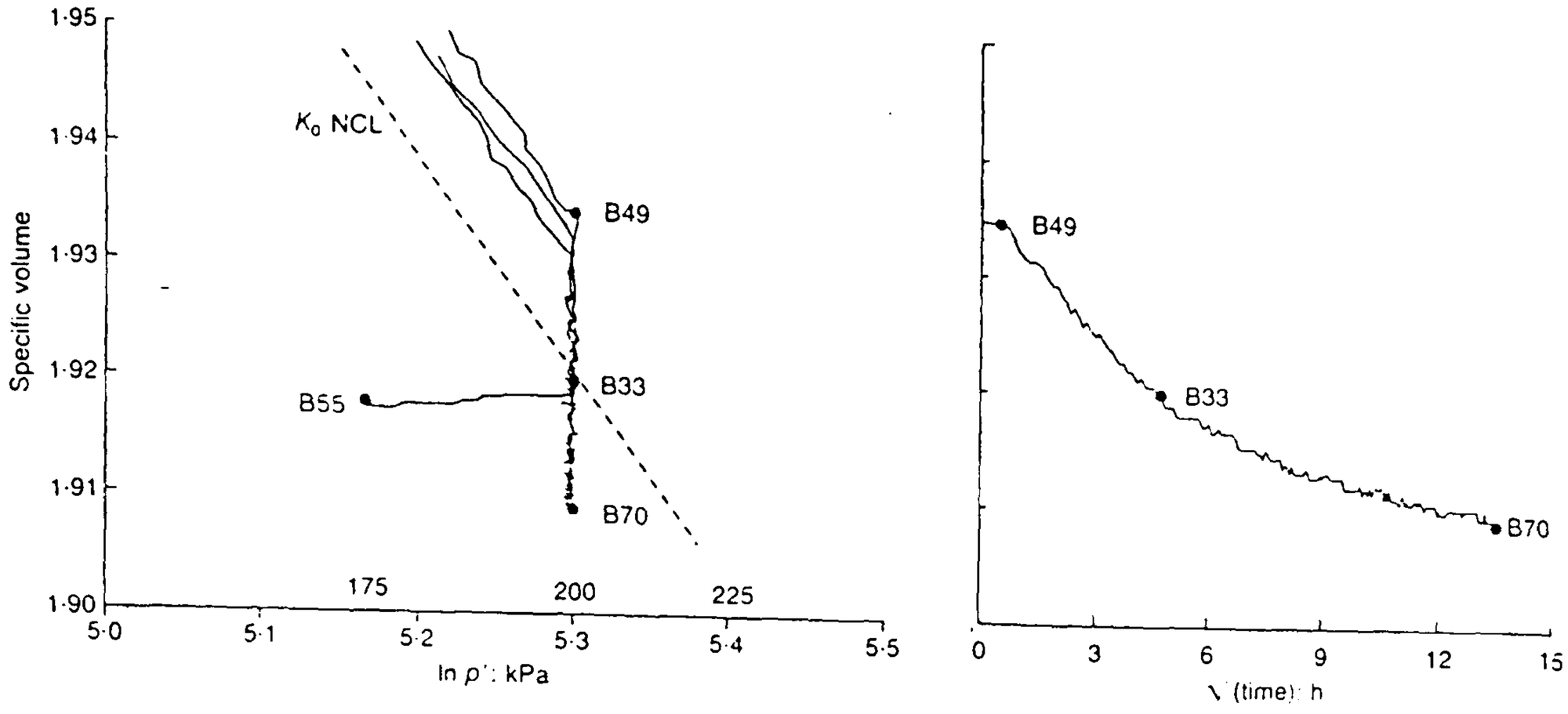

(a)

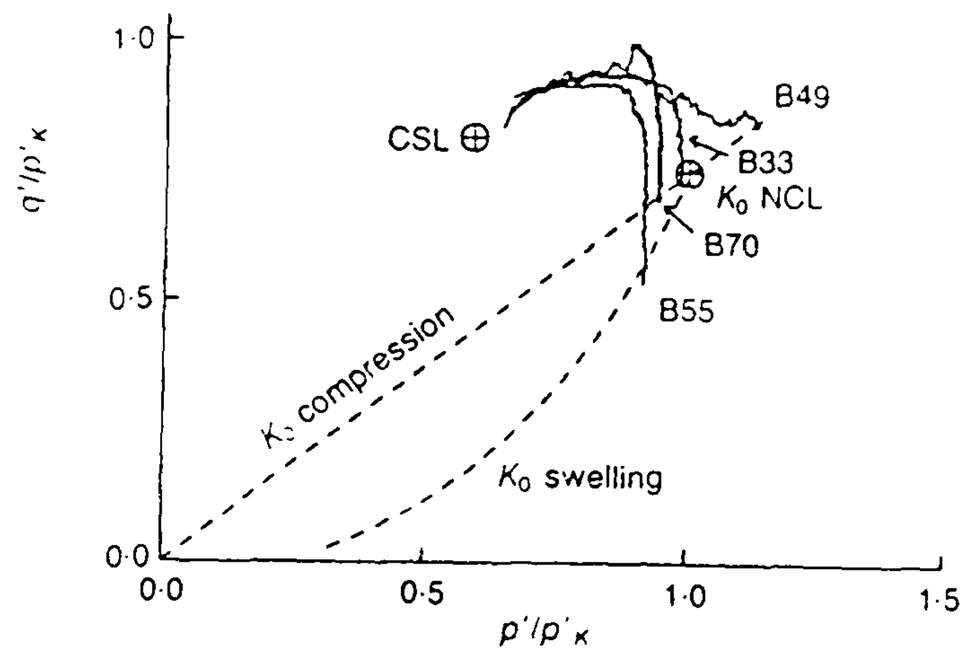

(b)

Figure 2.3.6 Influence of ageing in reconstituted Bothkennar clay on (a) initial states of one-dimensionally compressed samples (b) normalised stress paths for drained compression tests (after Allman & Atkinson, 1992)

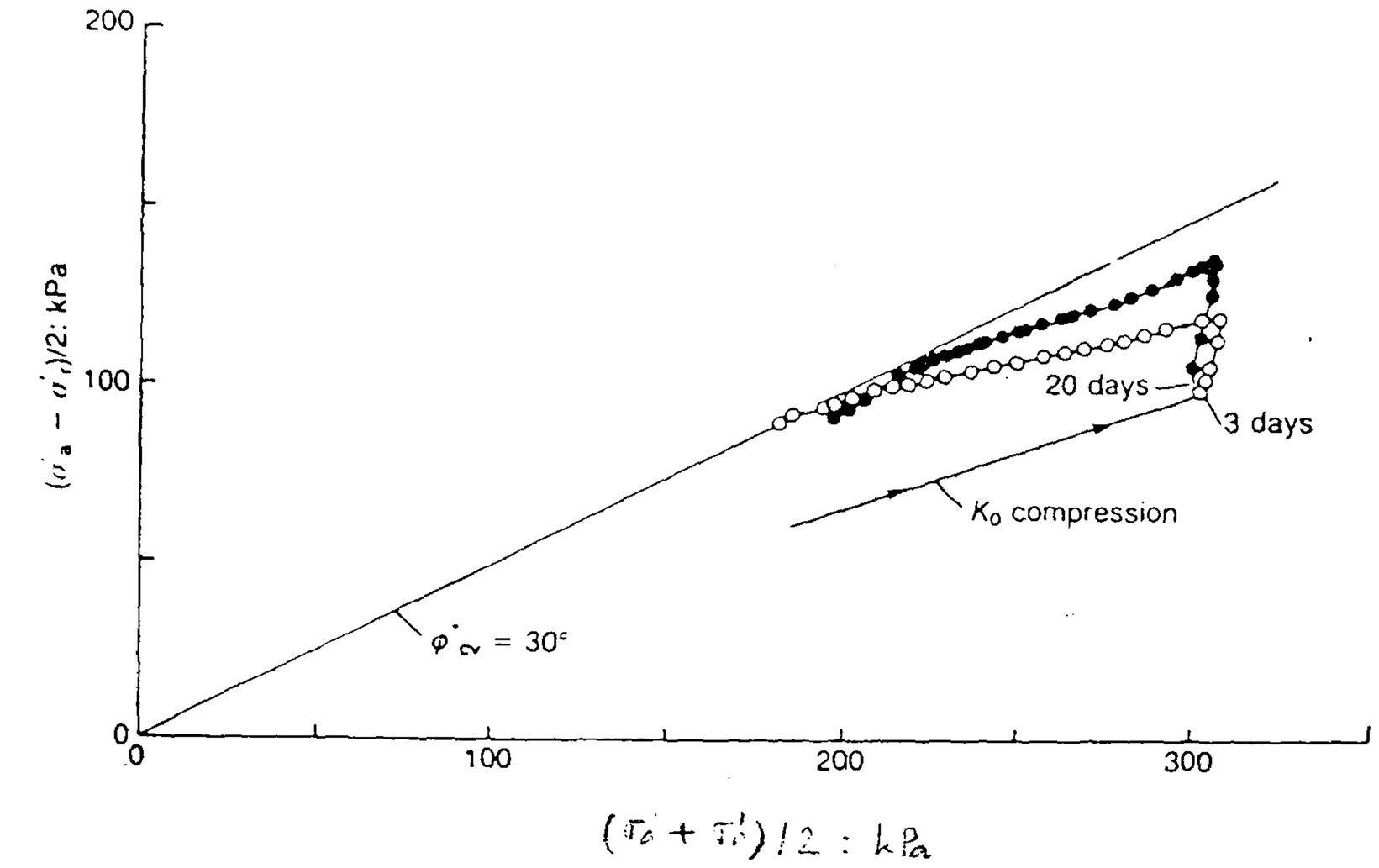

Figure 2.3.7 Influence of ageing on undrained effective stress paths for triaxial compression tests on reconstituted Magnus clay samples (after Burland, 1990; data from Jardine, 1985)

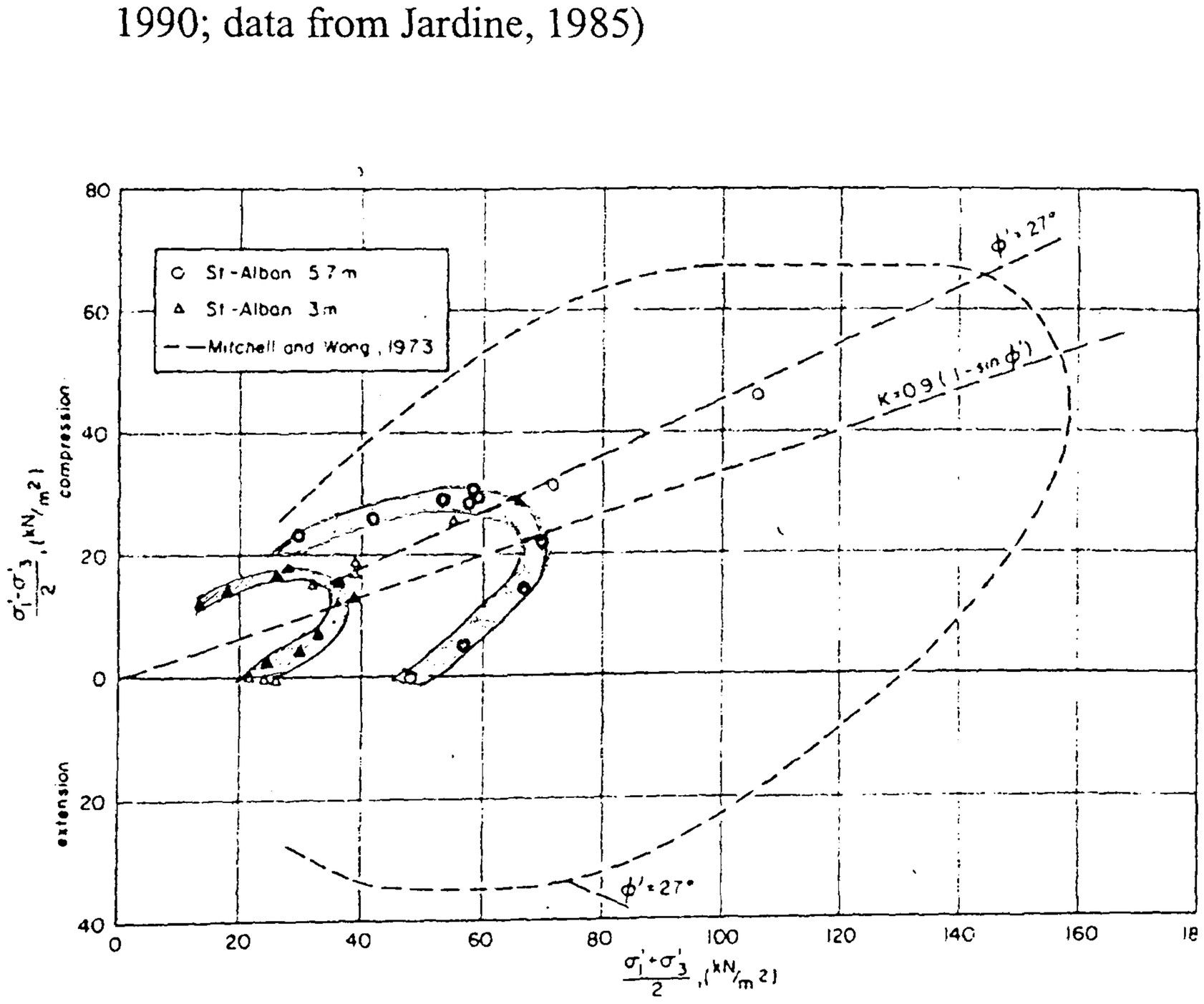

Figure 2.3.8 Gross yield curves for St-Alban clay, 3m and 5.7m, and Ottawa clay (after Tavenas & Leroueil, 1977)

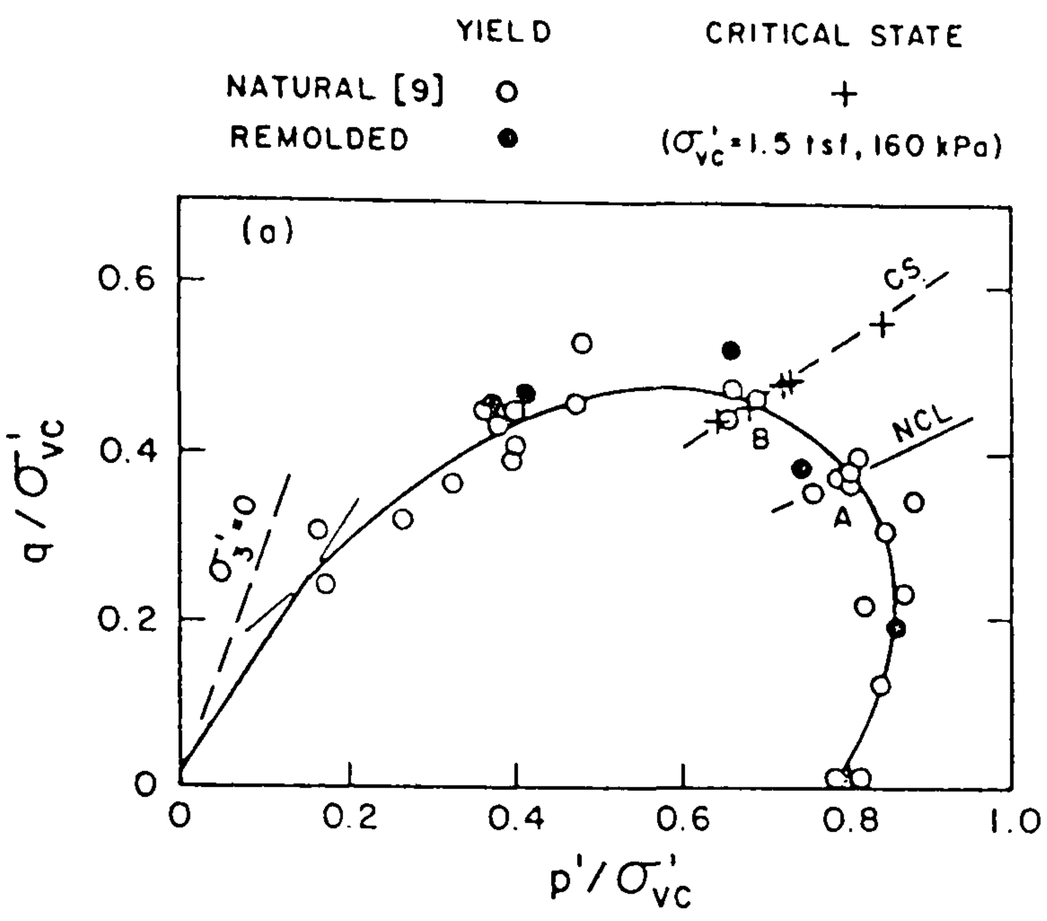

Figure 2.3.9 Normalised gross yield curve for natural and reconstituted Winnipeg clay (after Graham & Li, 1985)

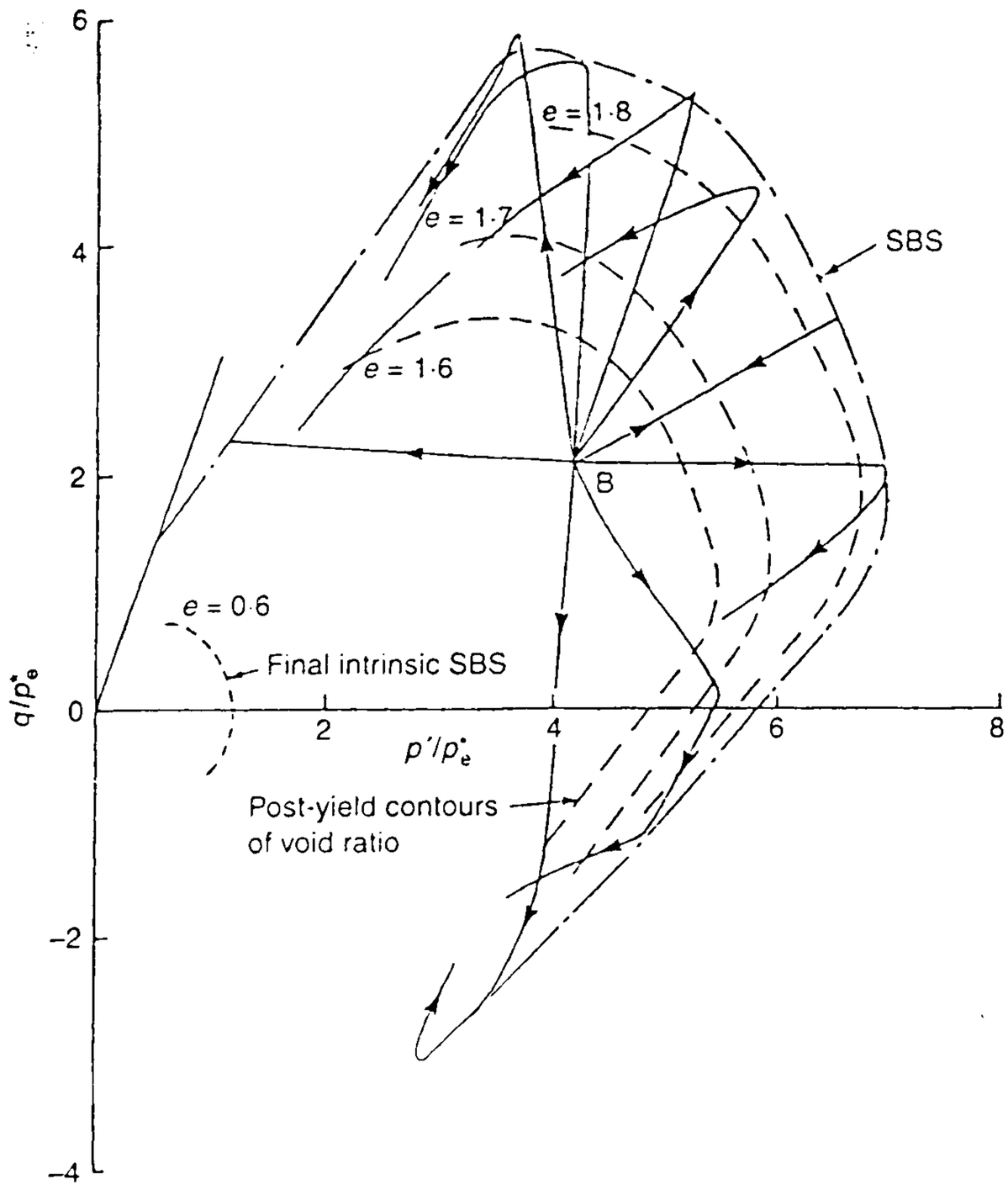

Figure 2.3.10 Normalised gross yield curves for natural Bothkennar clay (after Cotecchia & Chandler, 2000; data from Smith, 1992)

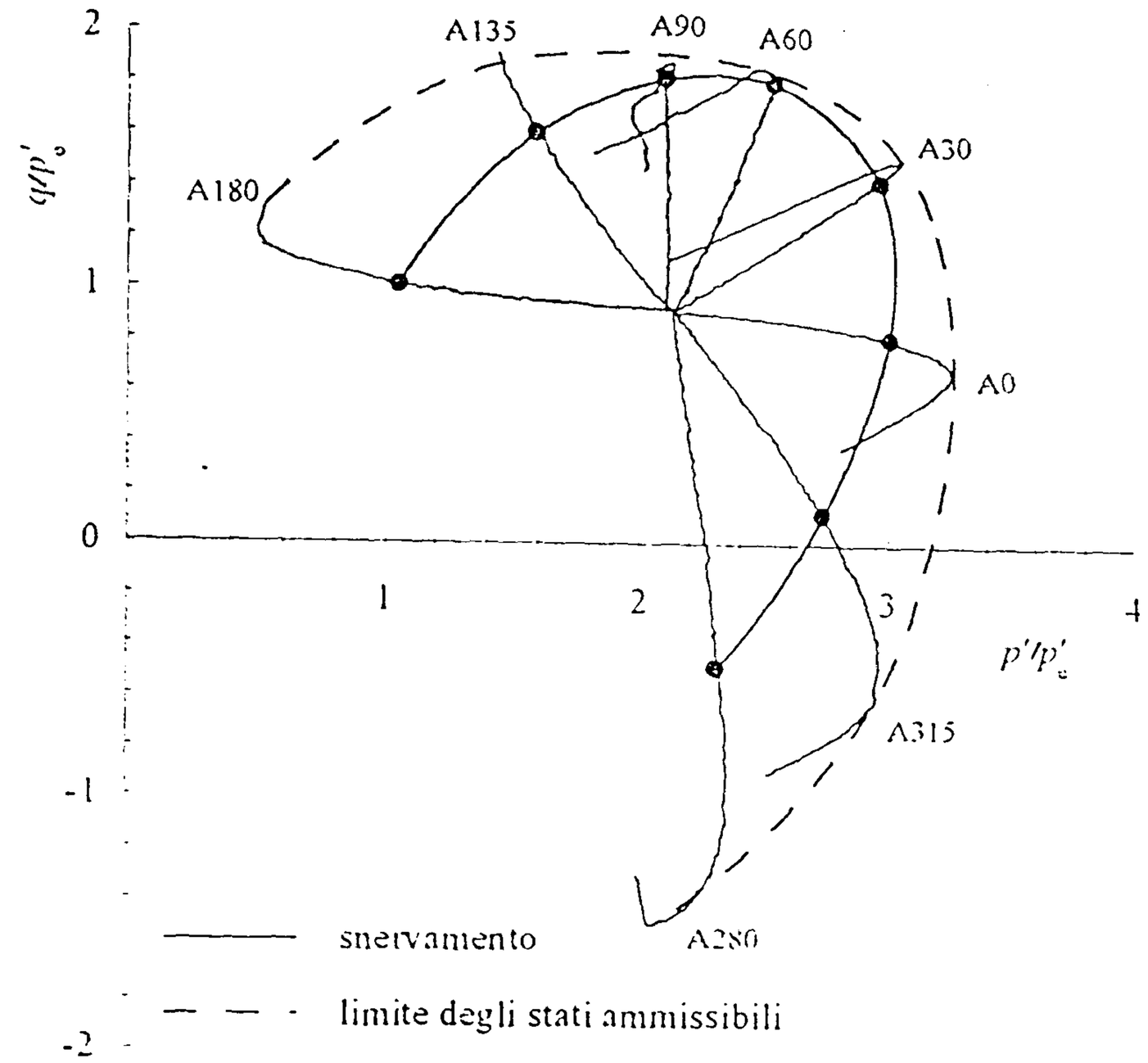

Figure 2.3.11 Normalised gross yield curve for natural Pisa clay (after Callisto, 1996)

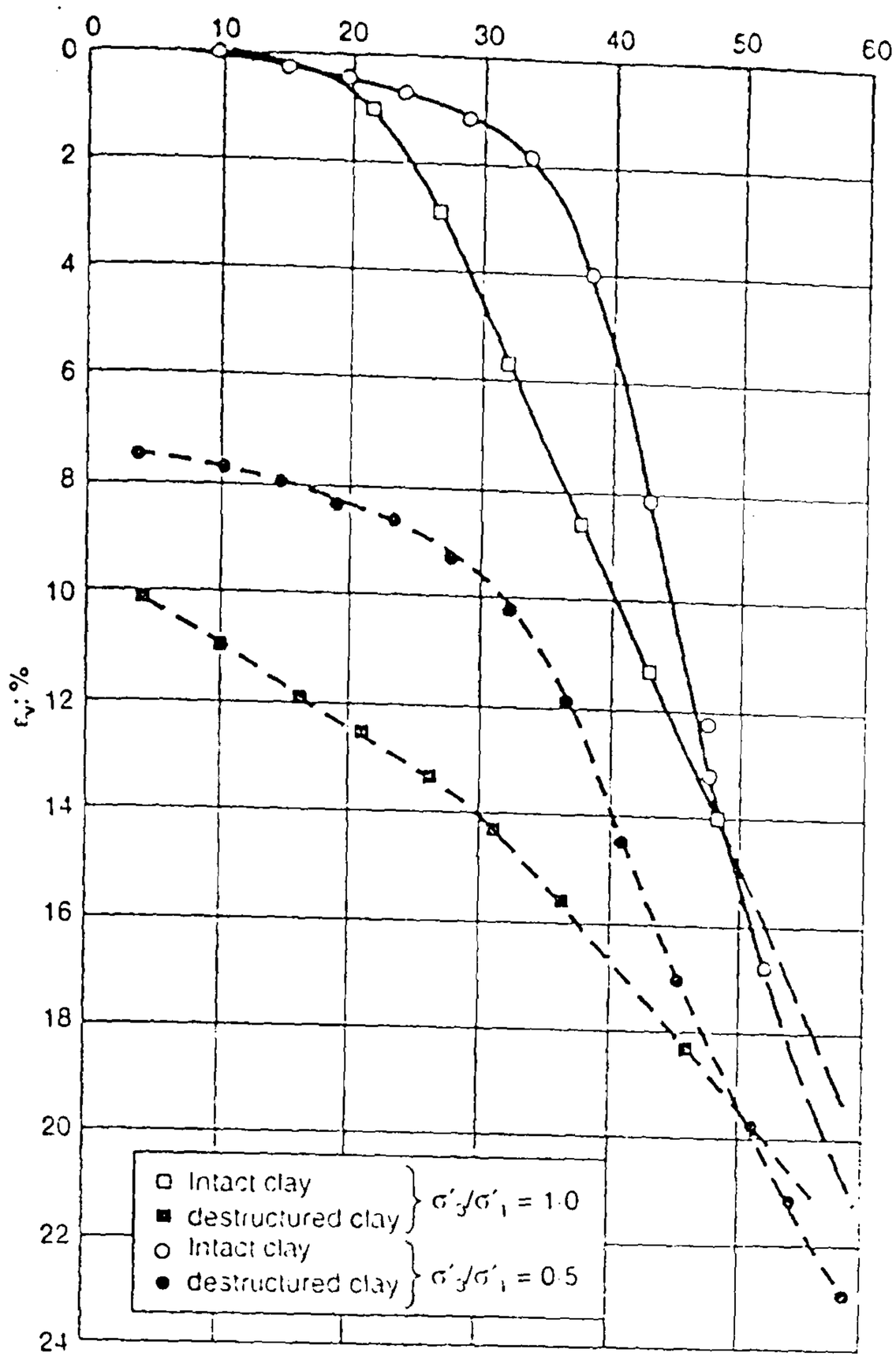

Figure 2.3.12 Compression curves for natural and reconstituted St-Alban clay samples (after Leroueil *et al.*, 1979)

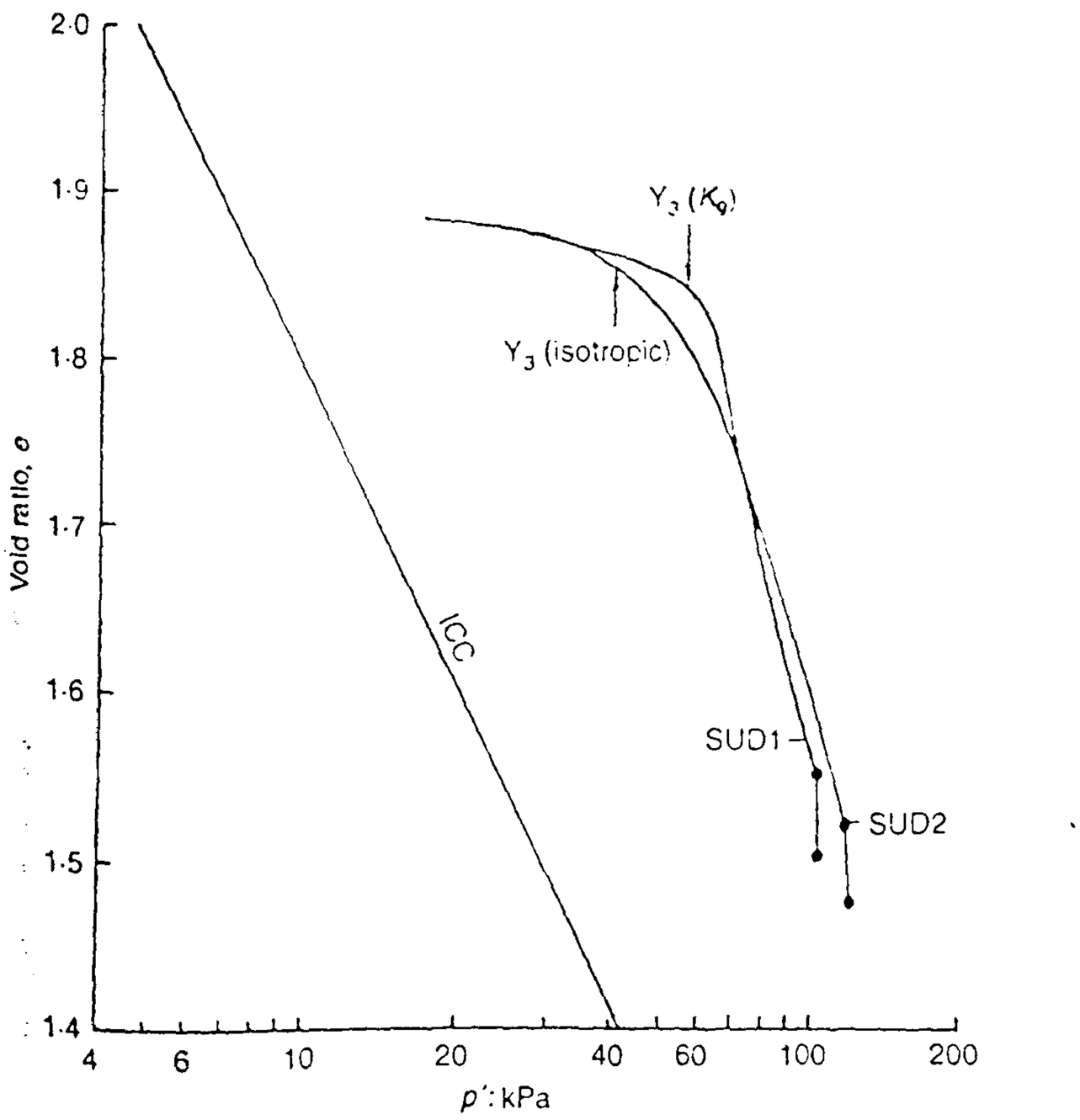

Figure 2.3.13 Compression curves for natural and reconstituted Bothkennar clay samples (after Smith, 1992)

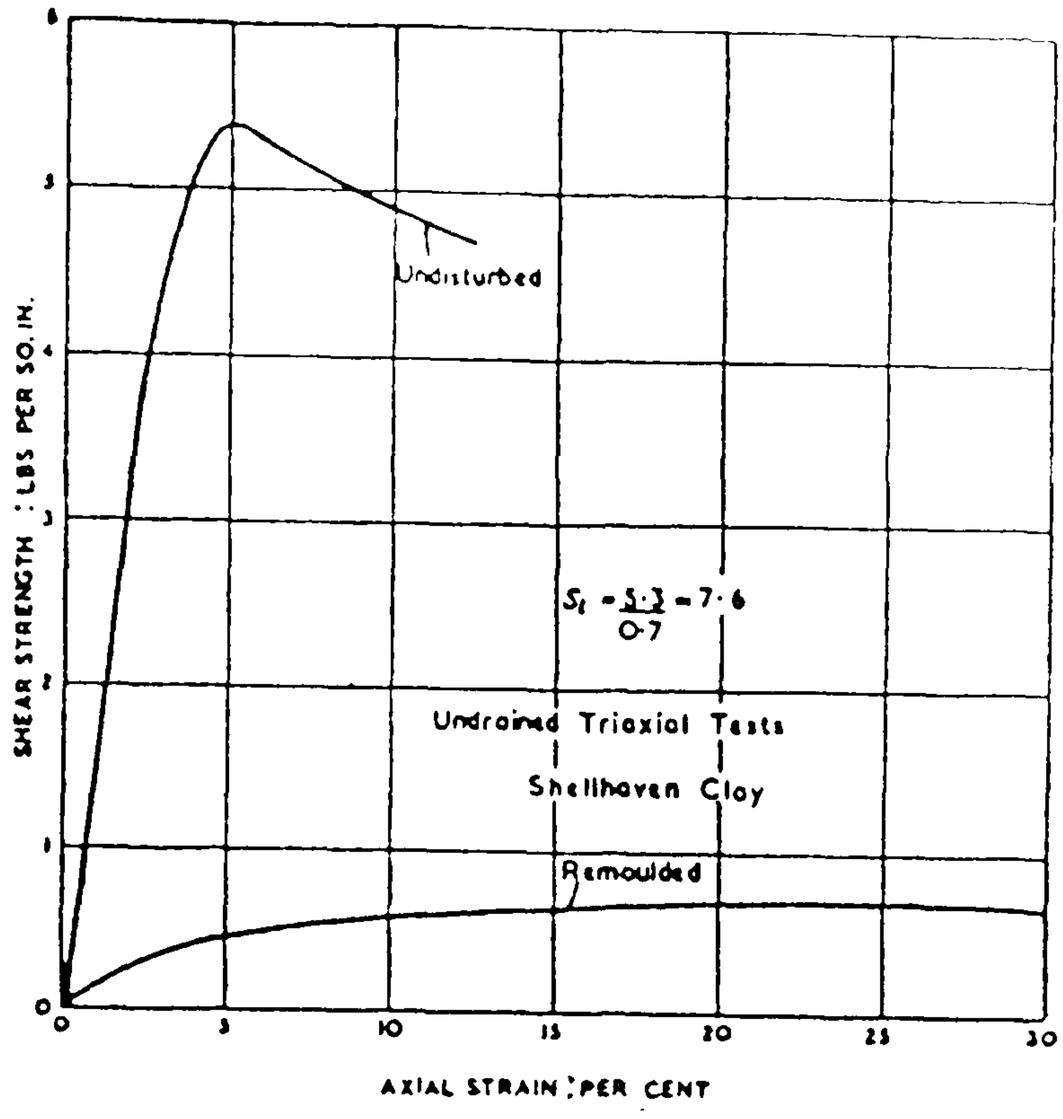

Figure 2.3.14 Stress-strain curves in undrained compression tests on "undisturbed" and remoulded samples of a typical sensitive clay, Shellhaven clay (after Skempton & Northey, 1952)

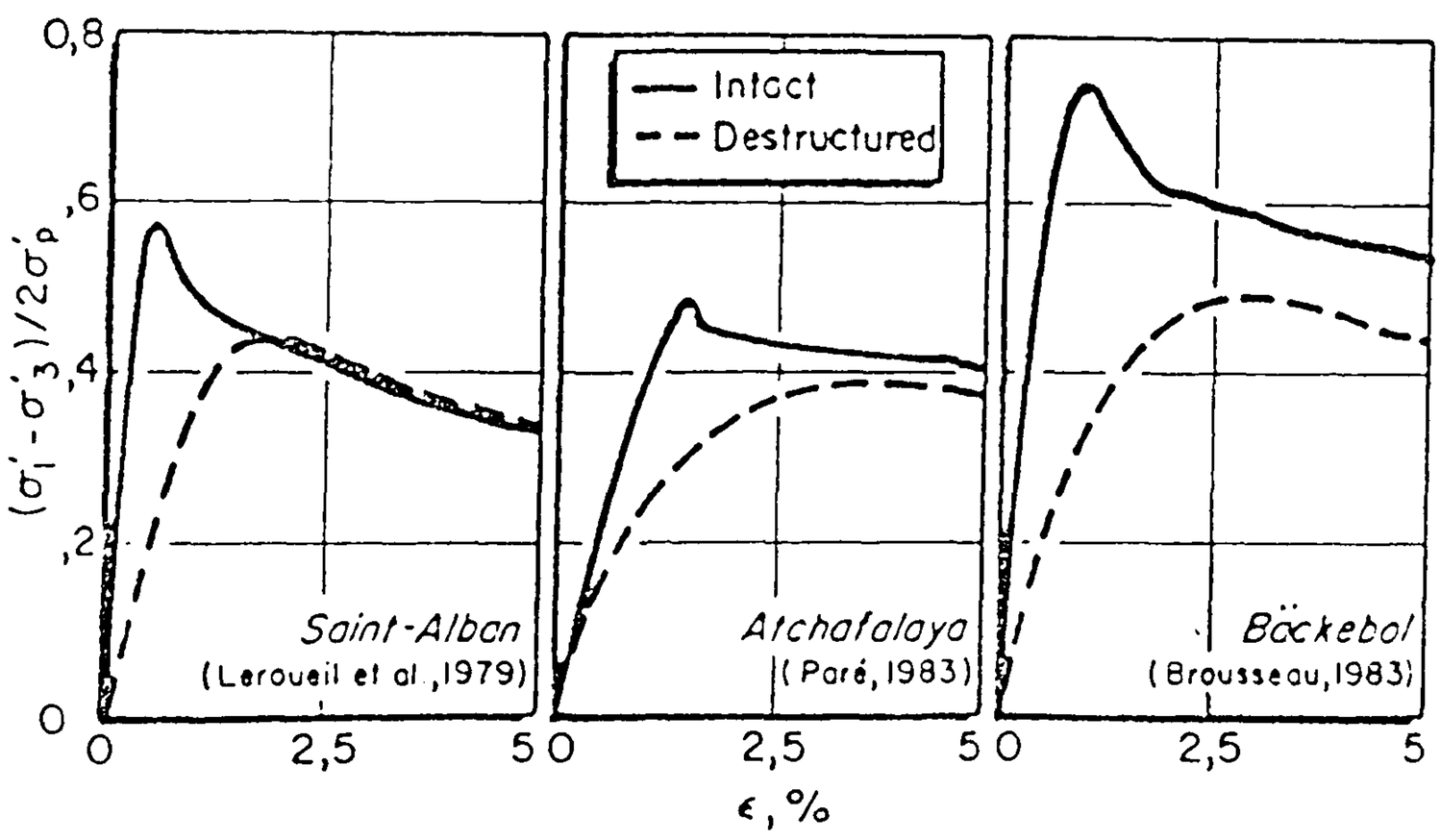

Figure 2.3.15 Stress-strain curves in undrained compression tests on intact and "destructured" soft clays (after Tavenas & Leroueil, 1985)

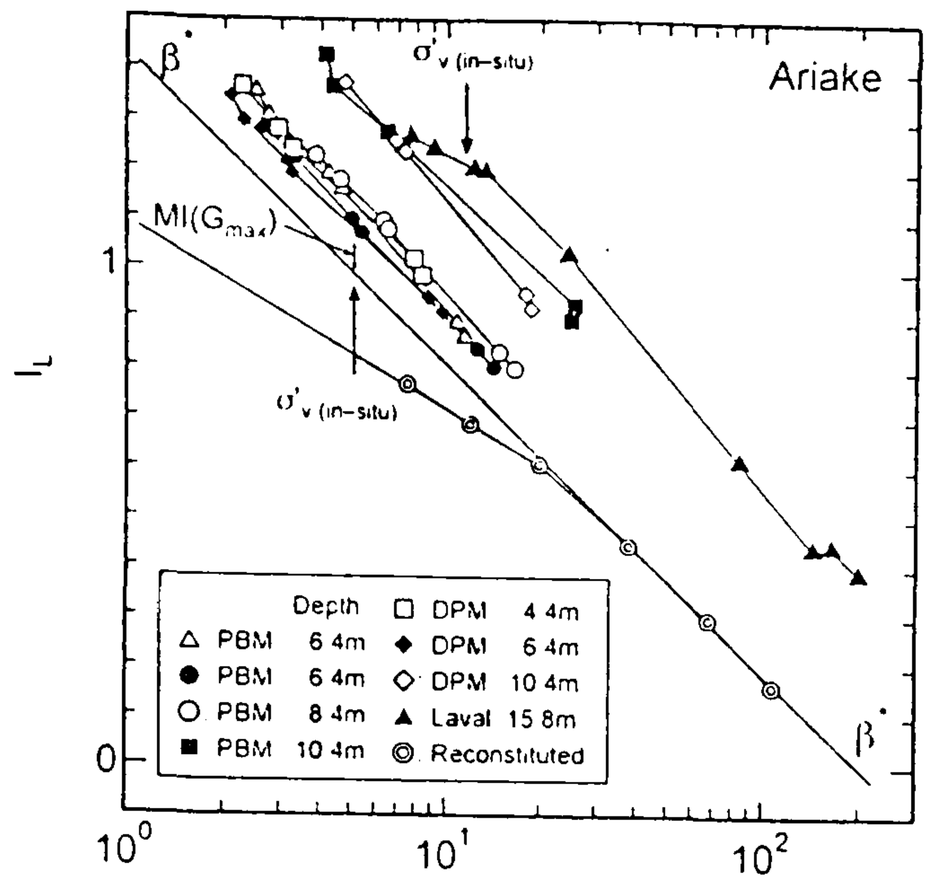

(a)

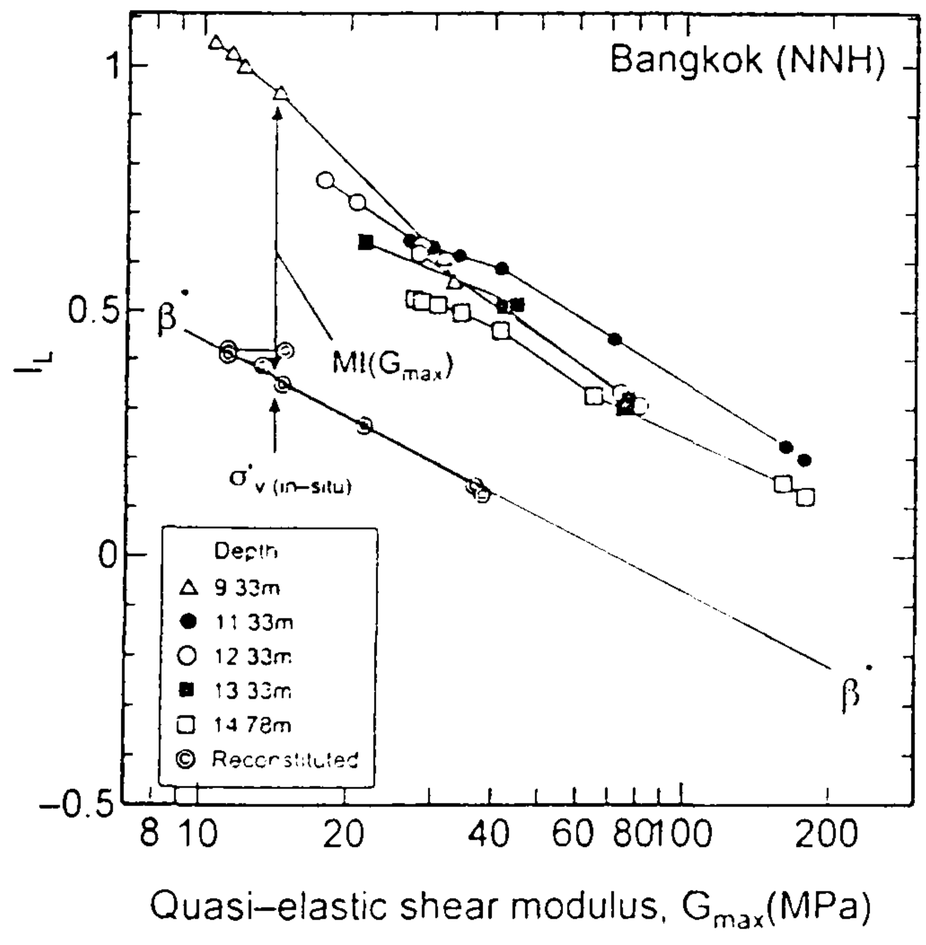

(b)

Figure 2.3.16 Relationship between liquidity index (I_L) and elastic shear modulus, G_{max} during one-dimensional compression test in (a) Ariake clay (b) Bangkok clay (after Shibuya *et al.*, 2000)

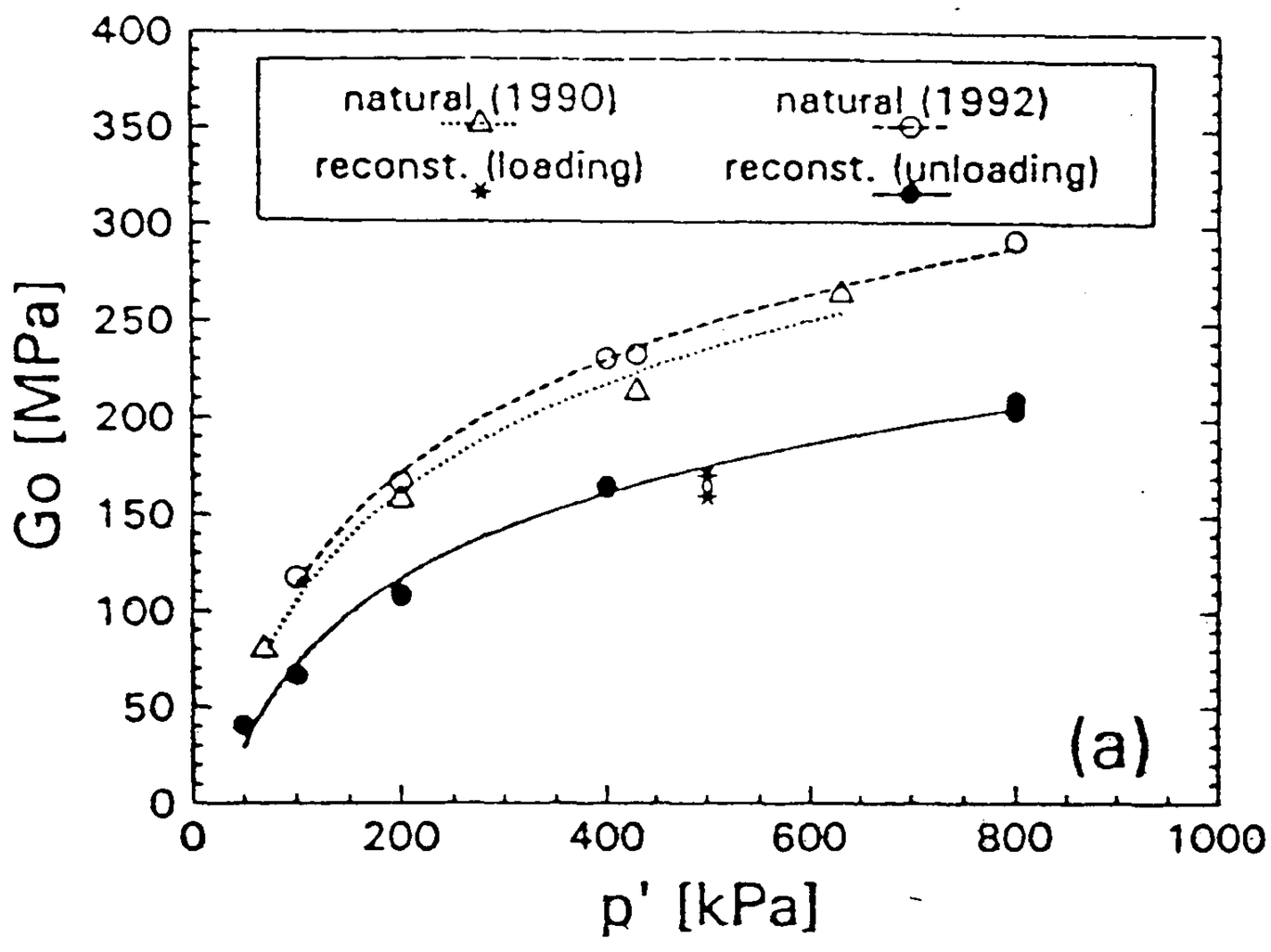

(a)

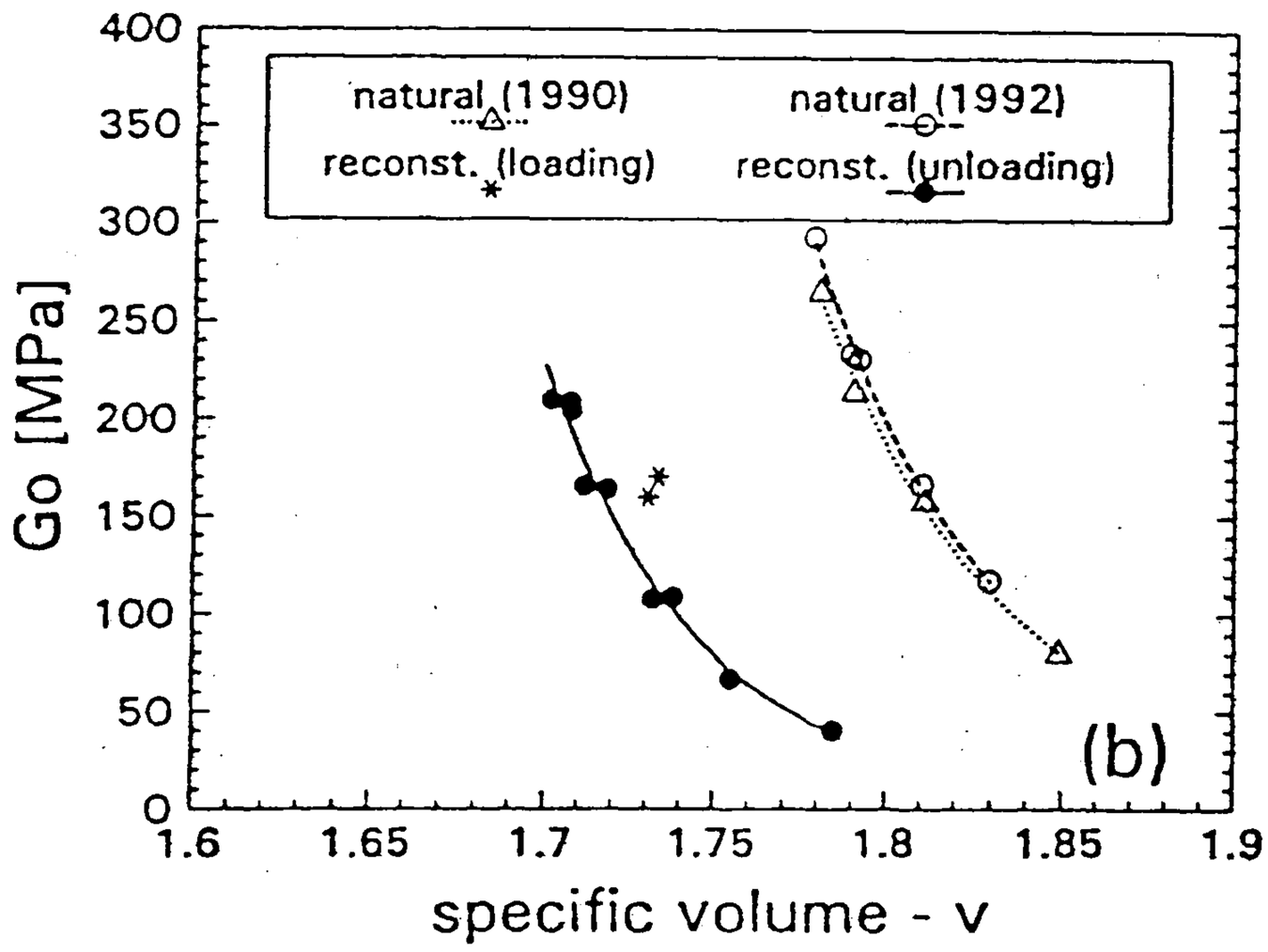

(b)

Figure 2.3.17 Vallericca clay: relationship between elastic shear modulus (G_0) and (a) mean effective stress (b) specific volume (after Rampello & Silvestri, 1993)

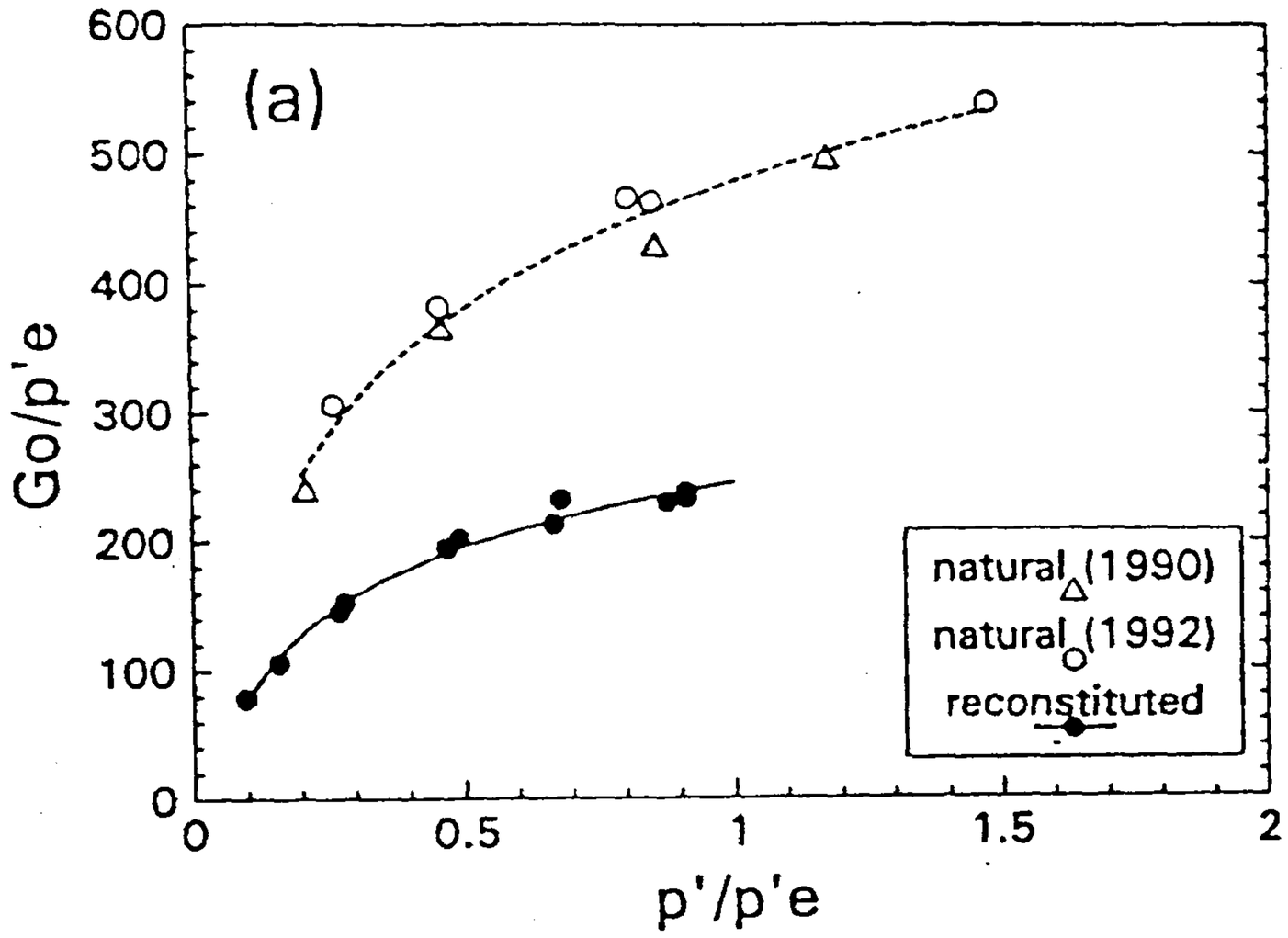

(a)

(b)

Figure 2.3.18 Vallericca clay: elastic shear modulus (G_0) normalised by the (a) intrinsic (b) appropriate equivalent pressure (after Rampello & Silvestri, 1993)

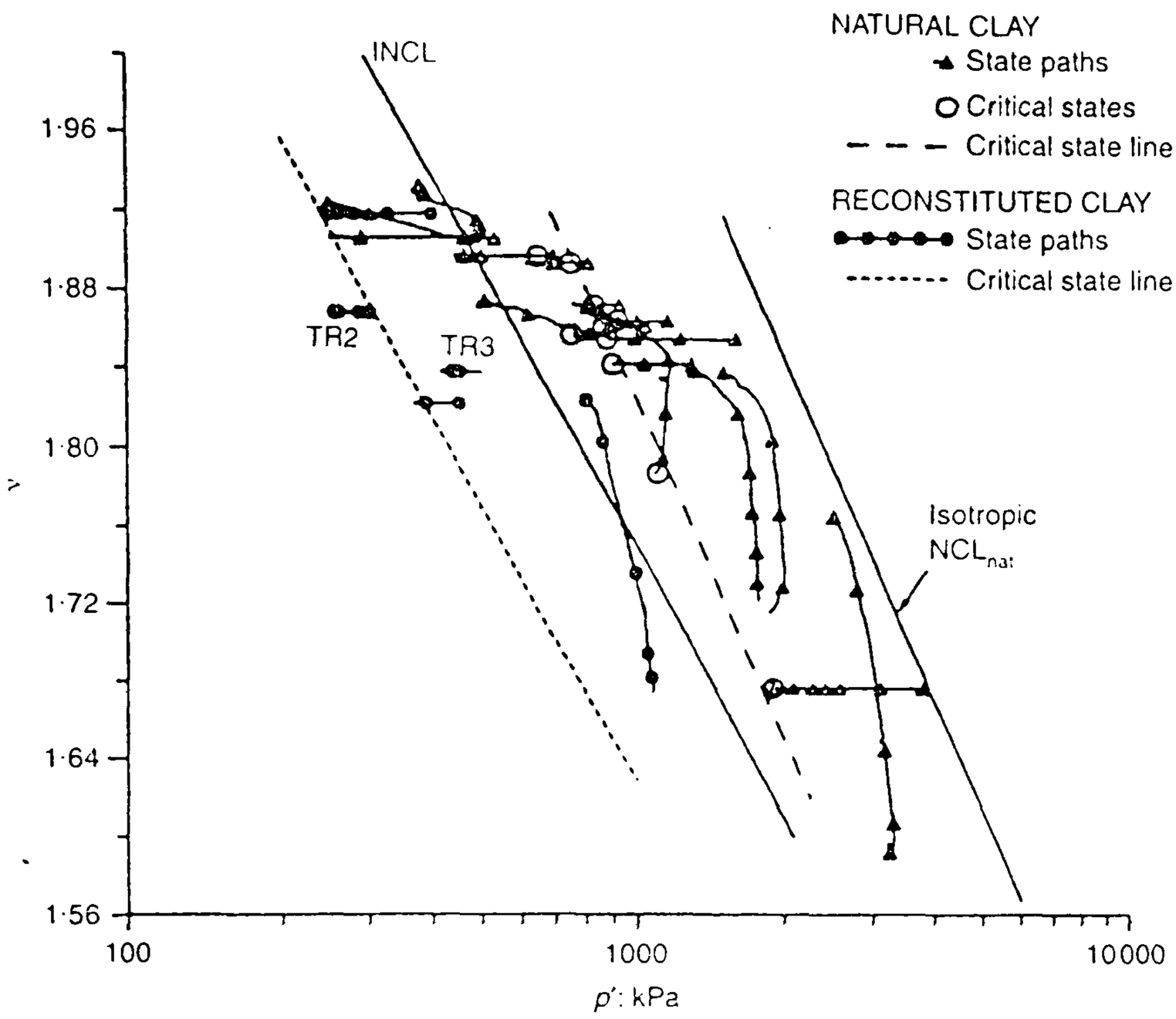

Figure 2.3.19 *v-p'* paths and critical states of natural and reconstituted Pappadai clay samples (after Cotecchia & Chandler, 1997)

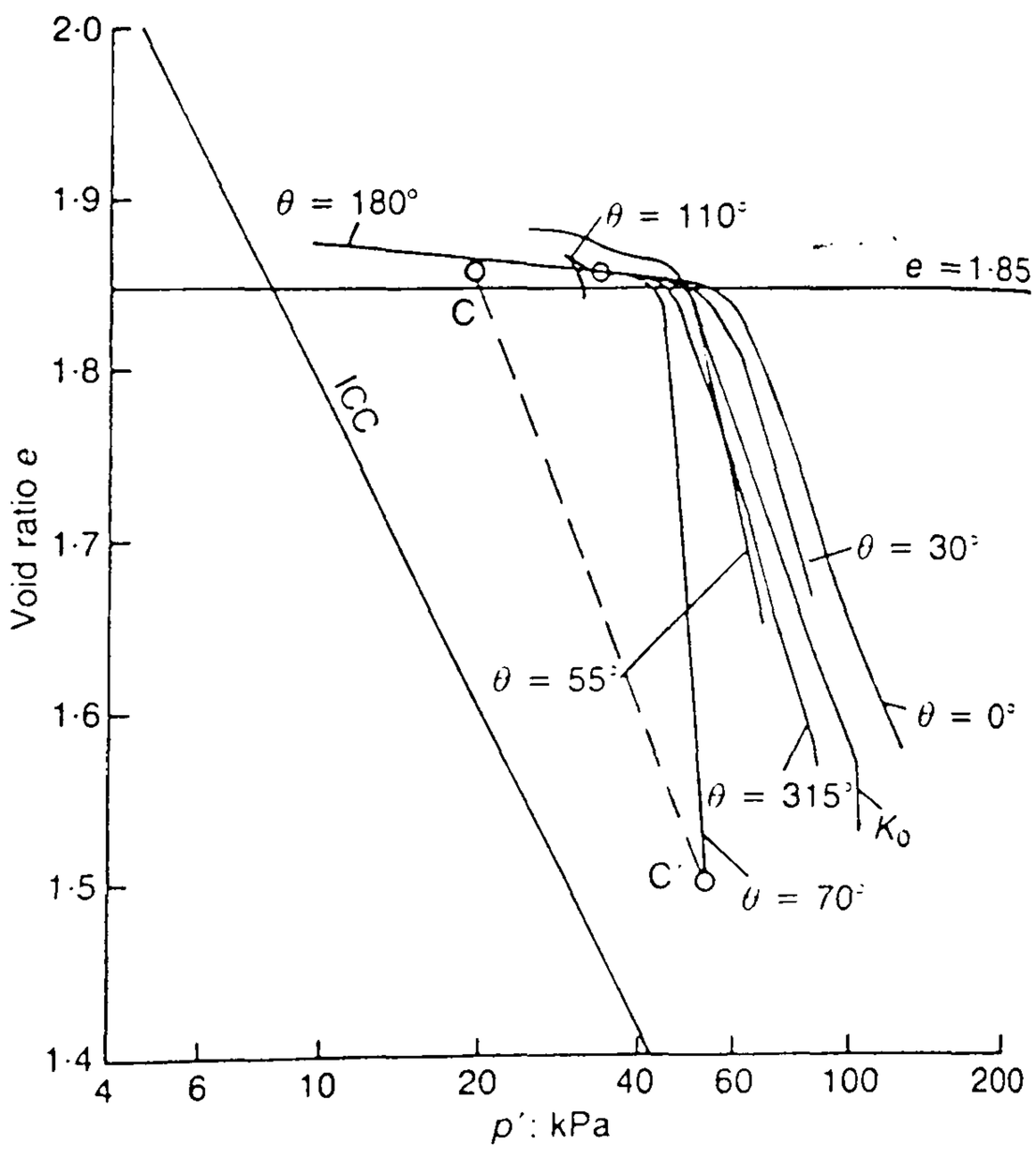

Figure 2.3.20 *v-p'* paths and critical states of natural Bothkennar clay samples during drained probes (after Smith *et al.*, 1992)

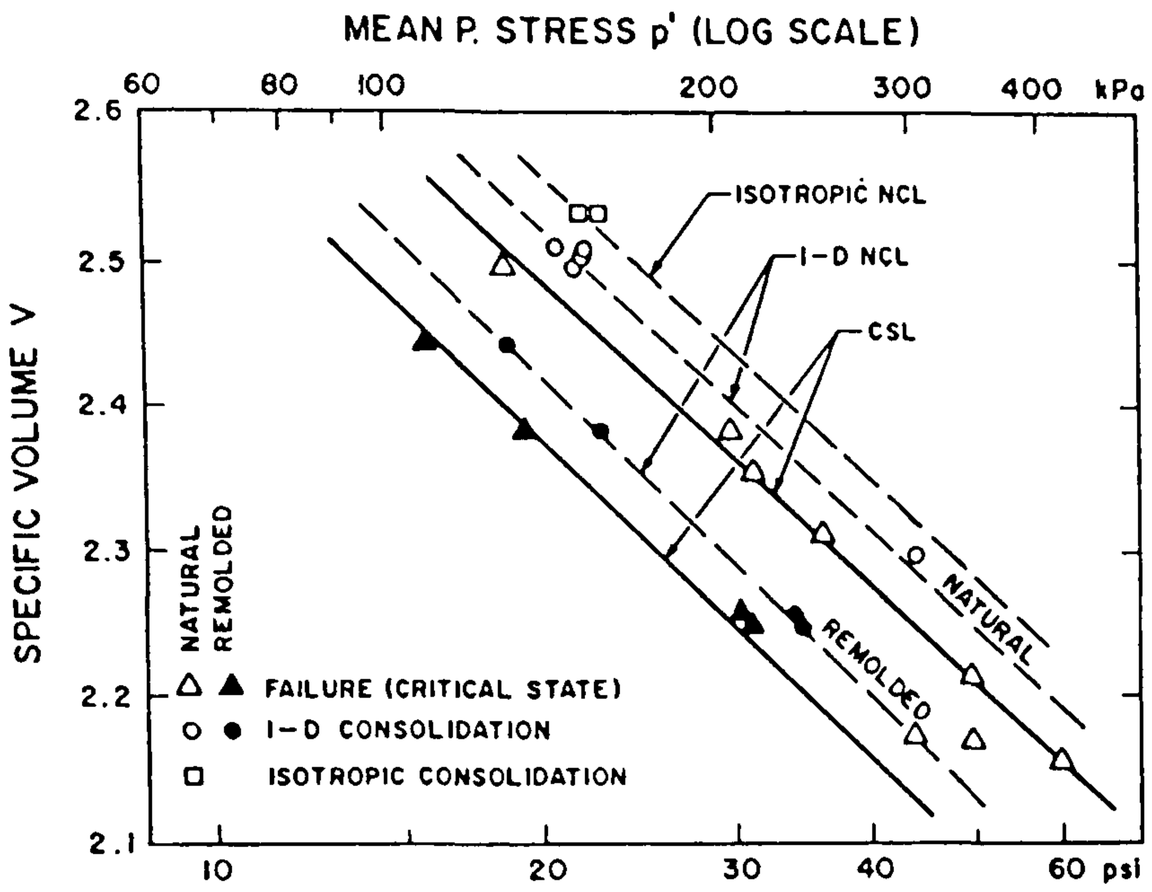

Figure 2.3.21 Consolidation and critical states of natural and reconstituted Winnipeg clay (Graham & Li, 1985)

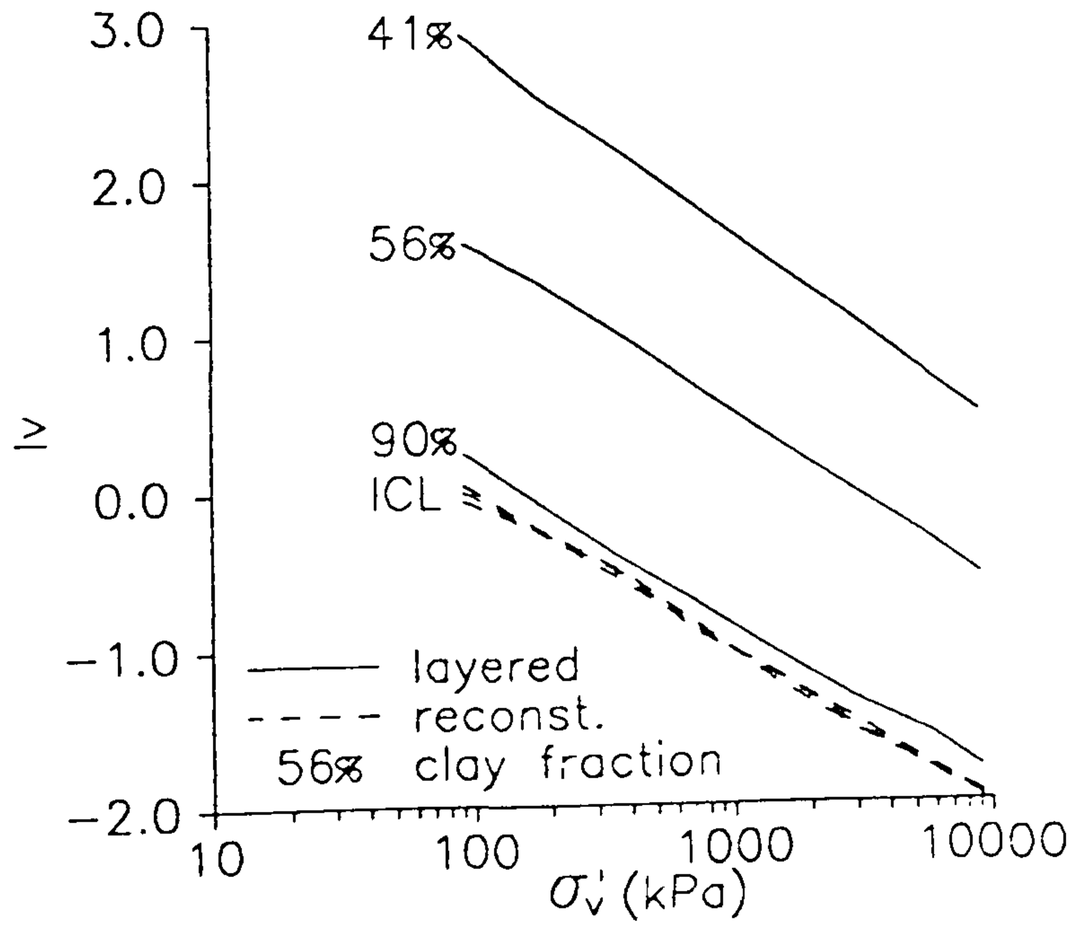

Figure 2.3.22 Normalised compression data for layered samples (after Coop & Cotecchia, 1995; data from Best, 1994)

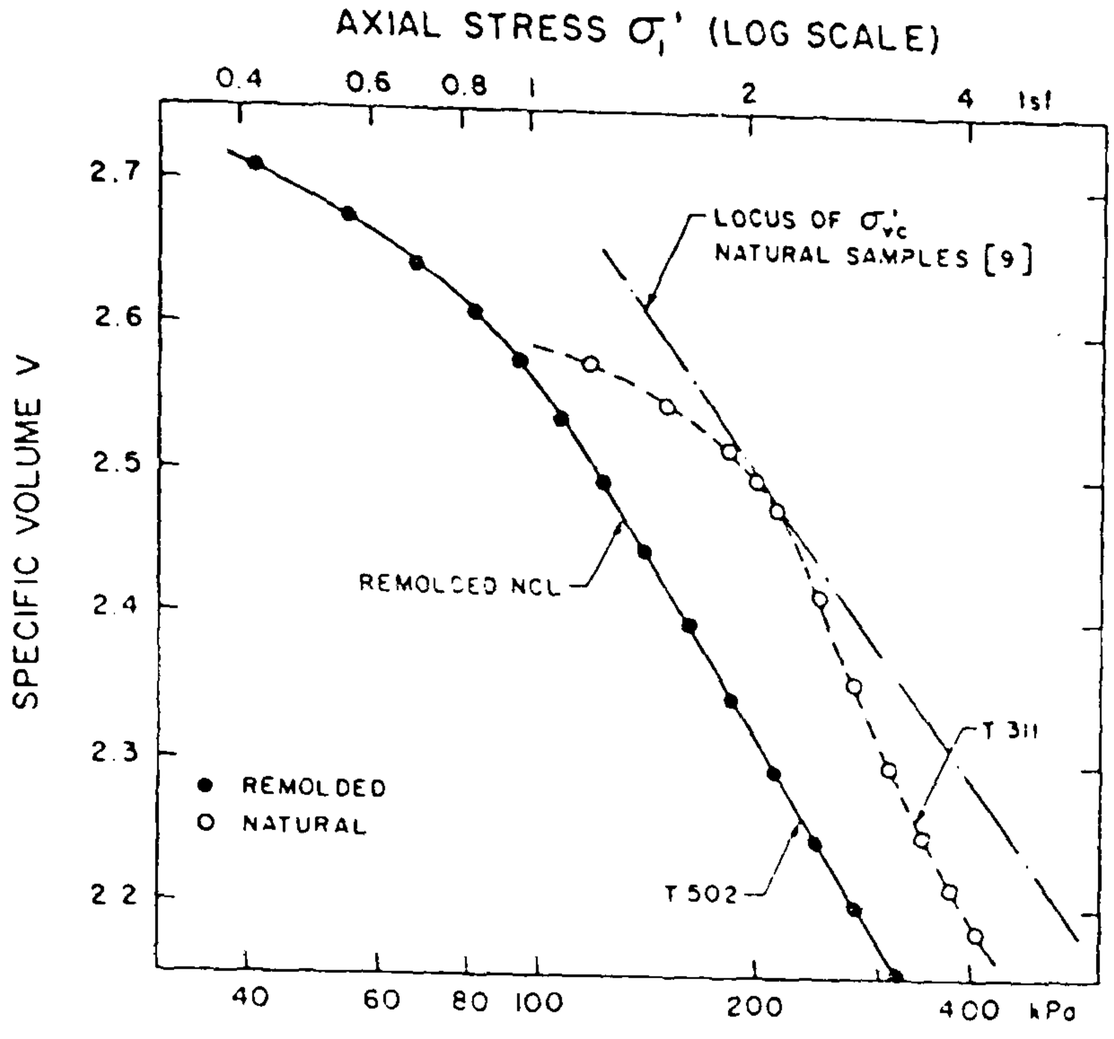

Figure 2.4.1 One-dimensional compression data for natural and reconstituted Winnipeg clay samples (after Graham & Li, 1985)

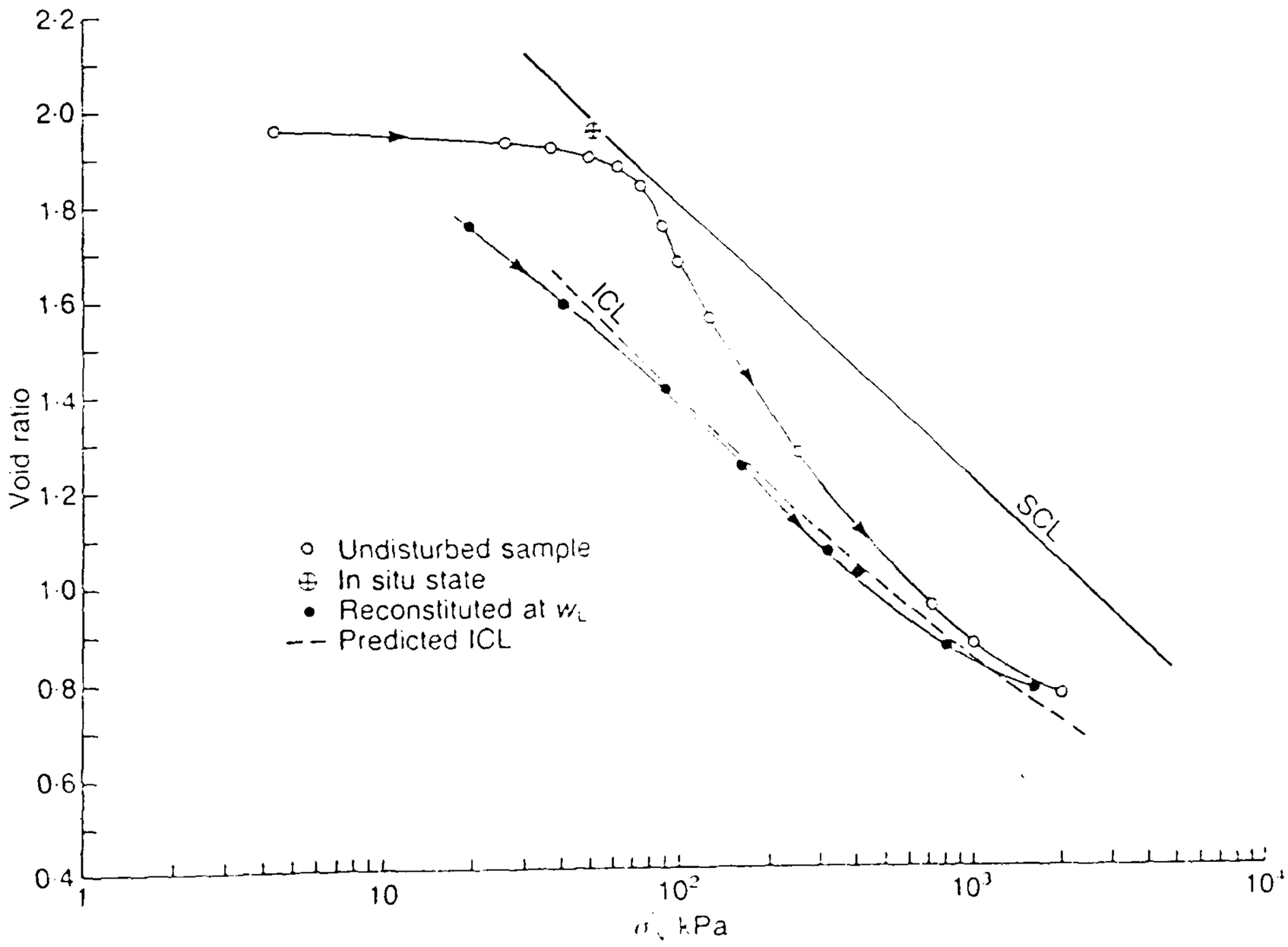

Figure 2.4.2 One-dimensional compression test data for natural and reconstituted Bothkennar clay samples 6.5m (after Burland, 1990)

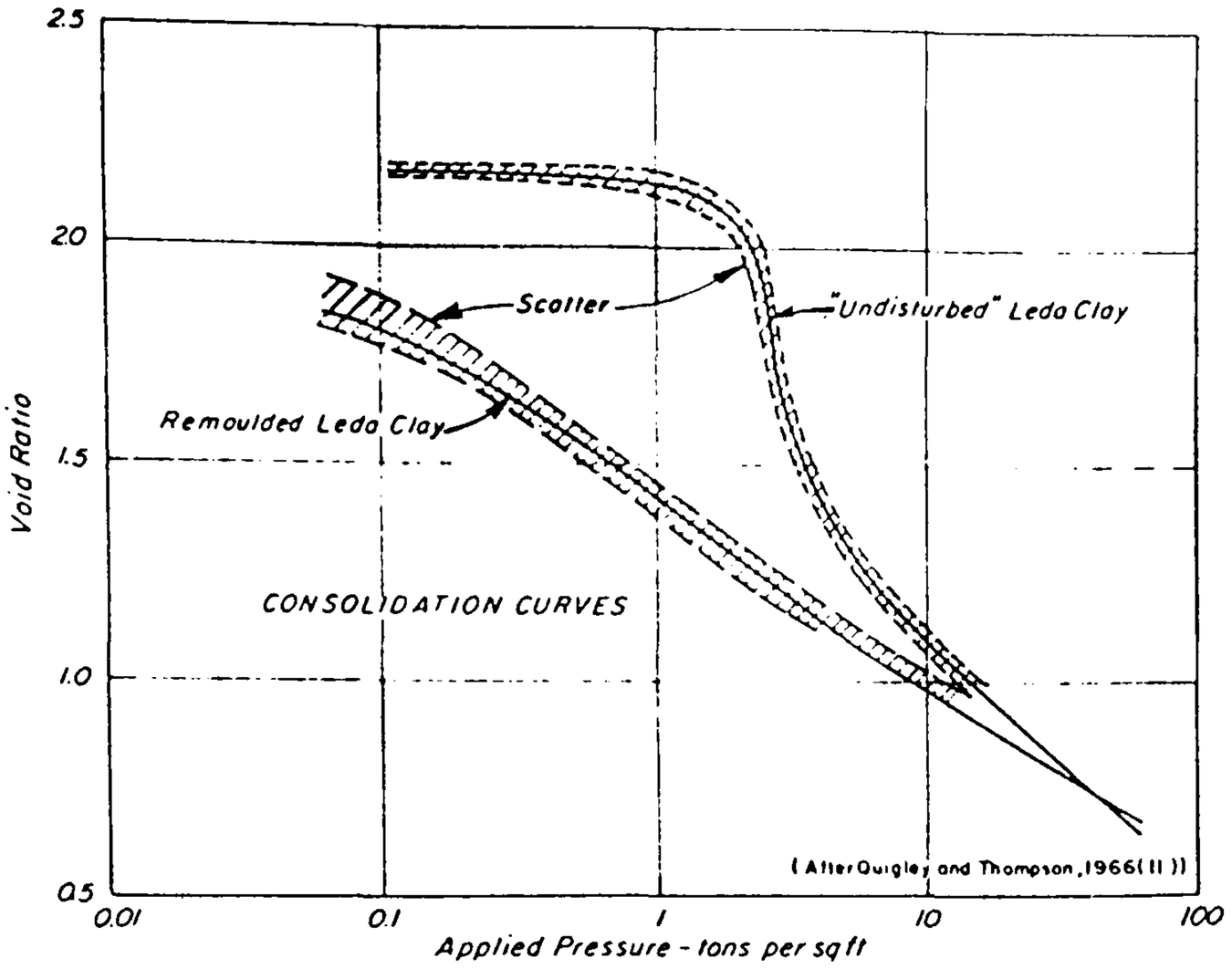

Figure 2.4.3 One-dimensional compression data for natural and reconstituted Leda clay samples (after Houston & Mitchell, 1969)

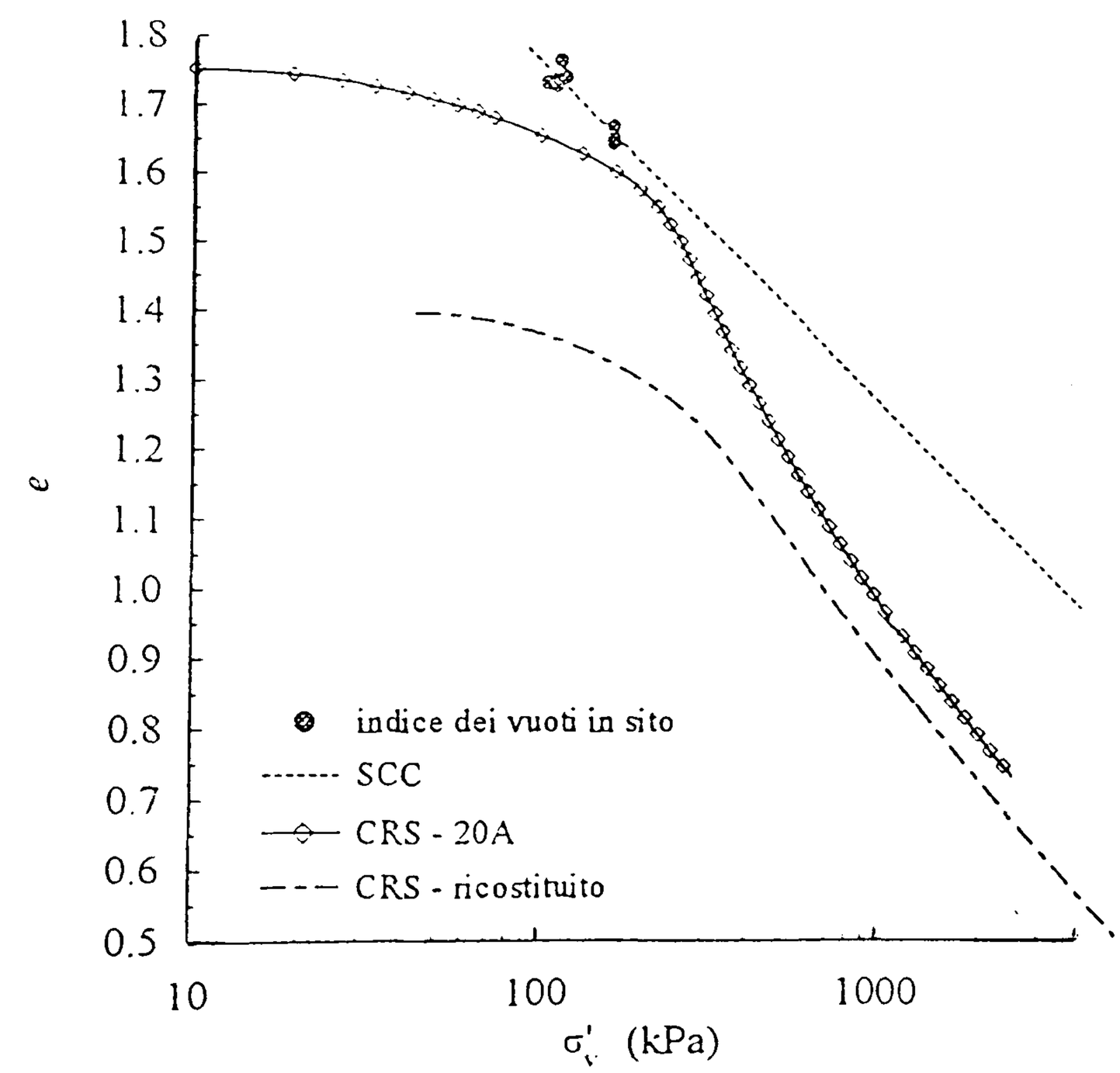

Figure 2.4.4 One-dimensional compression test data for natural and reconstituted Pisa clay samples (after Callisto, 1996)

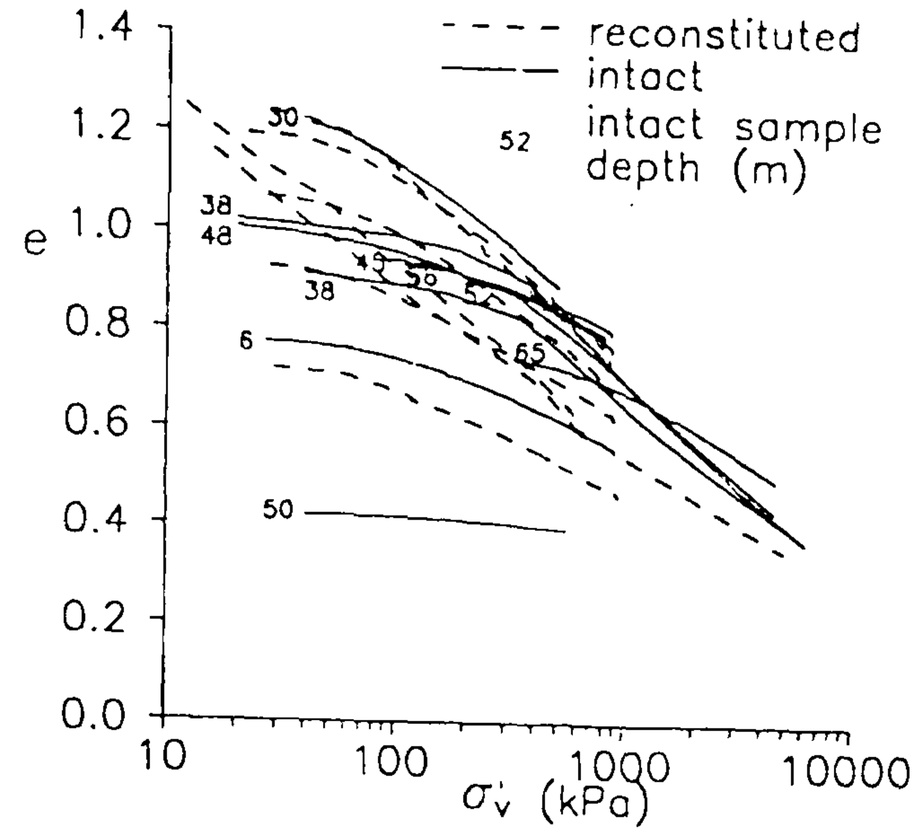

(a)

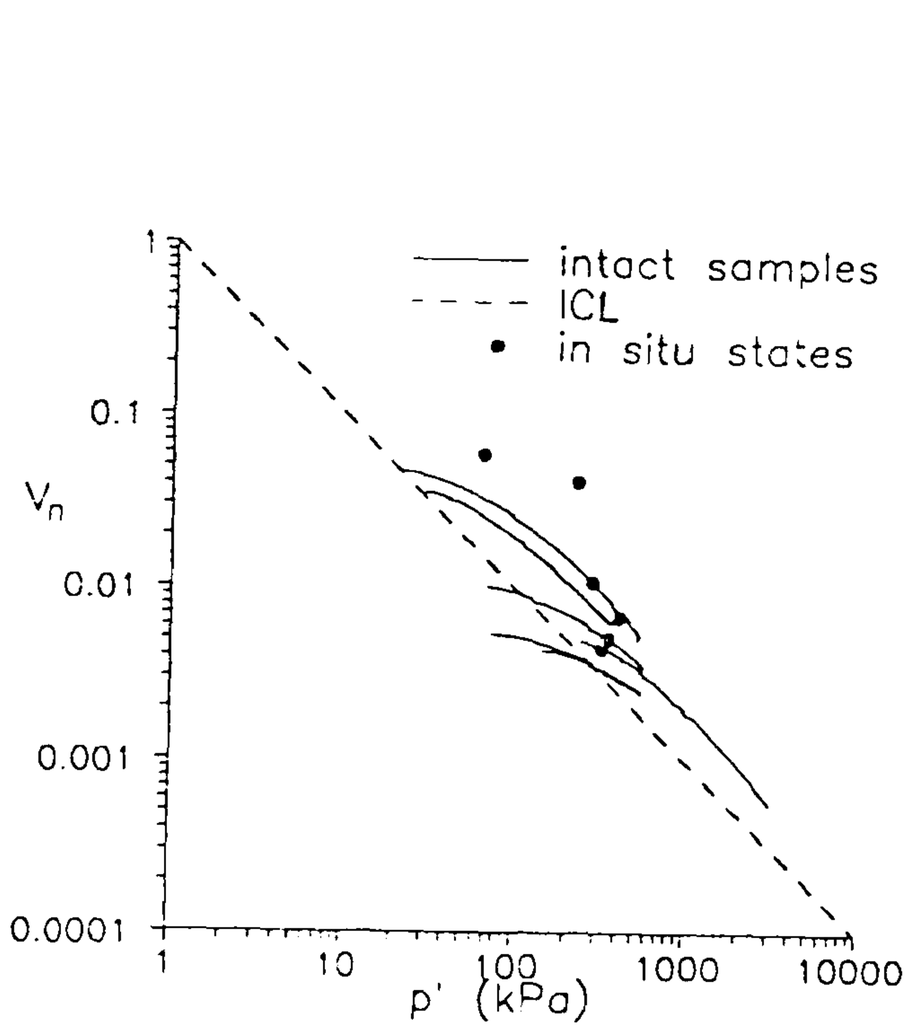

(b)

Figure 2.4.5 One-dimensional compression data from oedometer and triaxial tests on natural and reconstituted samples of Sibari clay. The data are plotted in (a) the e-log σ_v' plane (b) the normalised ln v_n-ln p' plane (after Coop & Cotecchia, 1995)

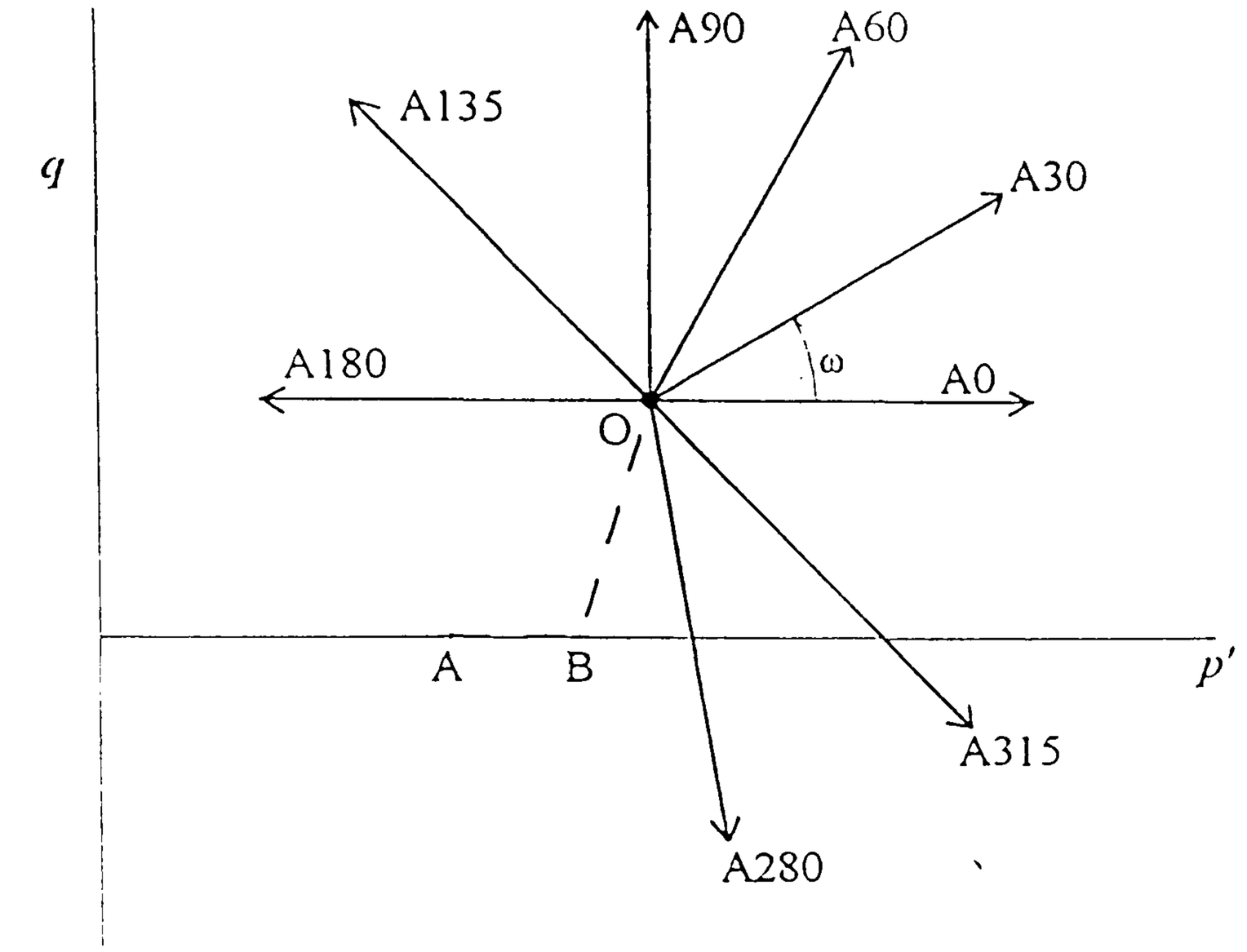

(a)

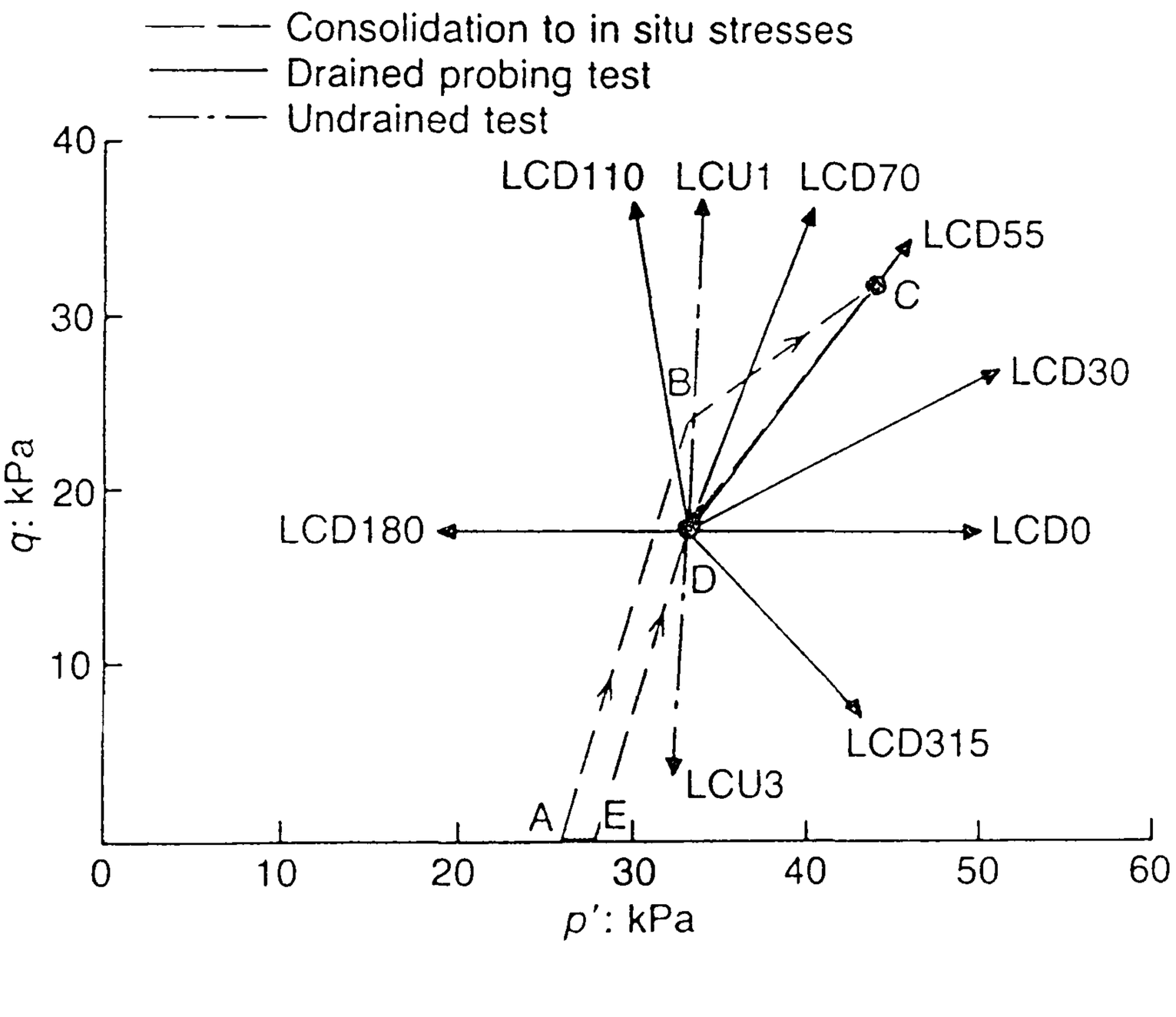

(b)

Figure 2.4.6 Stress paths during drained probes performed on (a) Pisa clay (after Callisto, 1996) (b) Bothkennar clay (after Smith *et al.*, 1992)

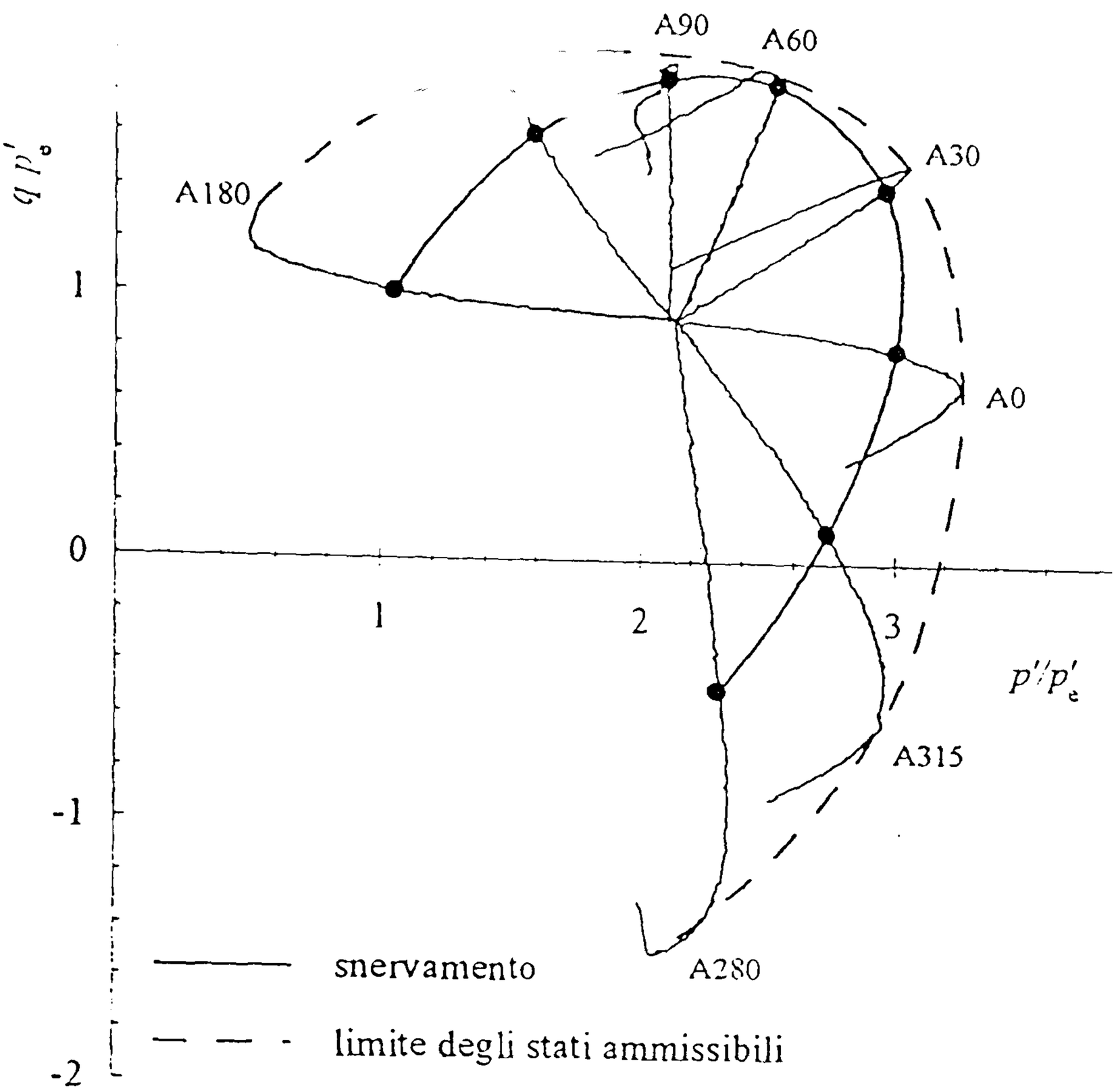

(a)

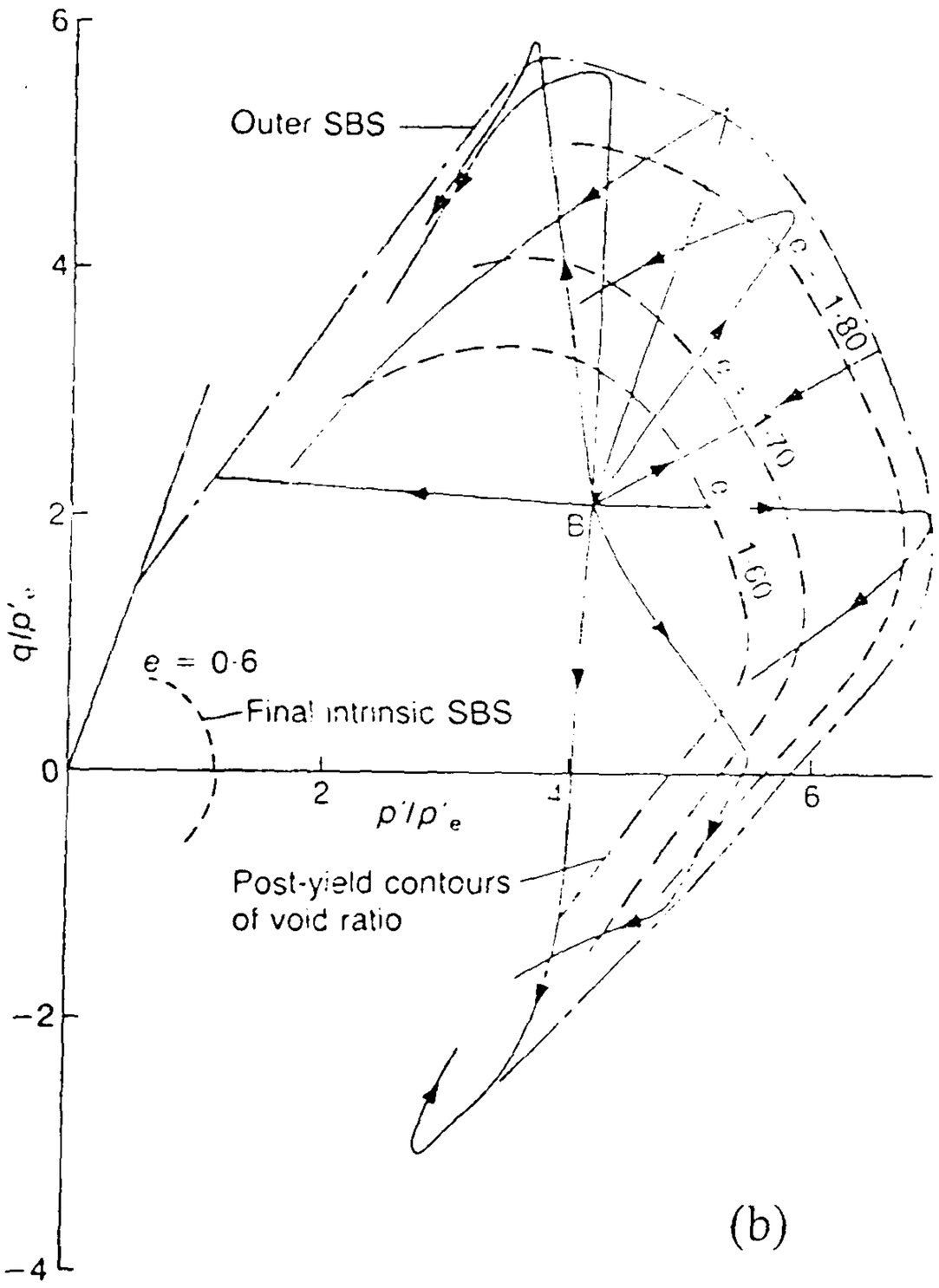

(b)

Figure 2.4.7 Normalised stress paths during drained probes performed on (a) Pisa clay (after Callisto, 1996) (b) Bothkennar clay (after Smith *et al.*, 1992)

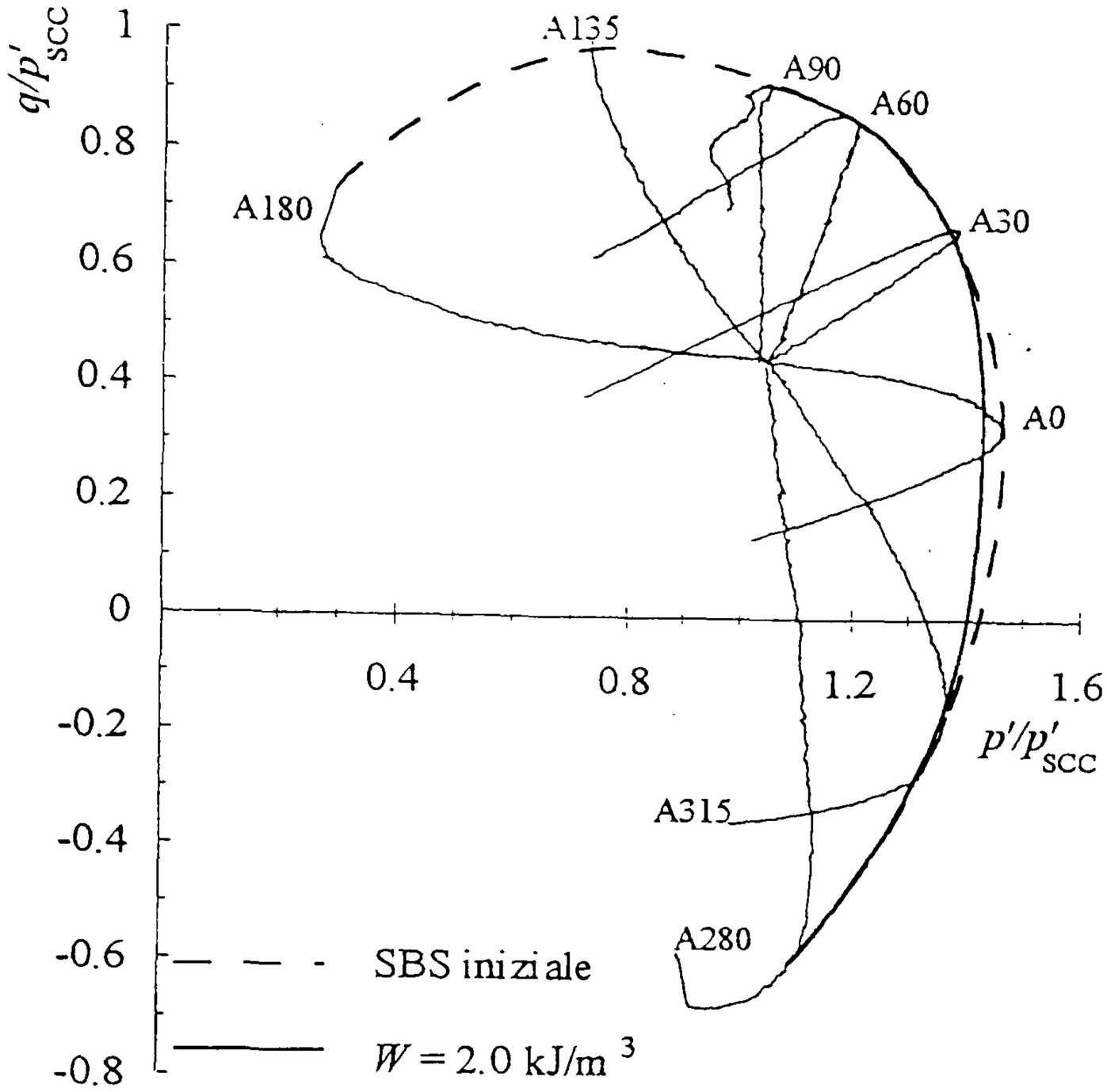

Figure 2.4.8 Contour of strain energy and normalised gross yield curve of Pisa clay (after Callisto, 1996)

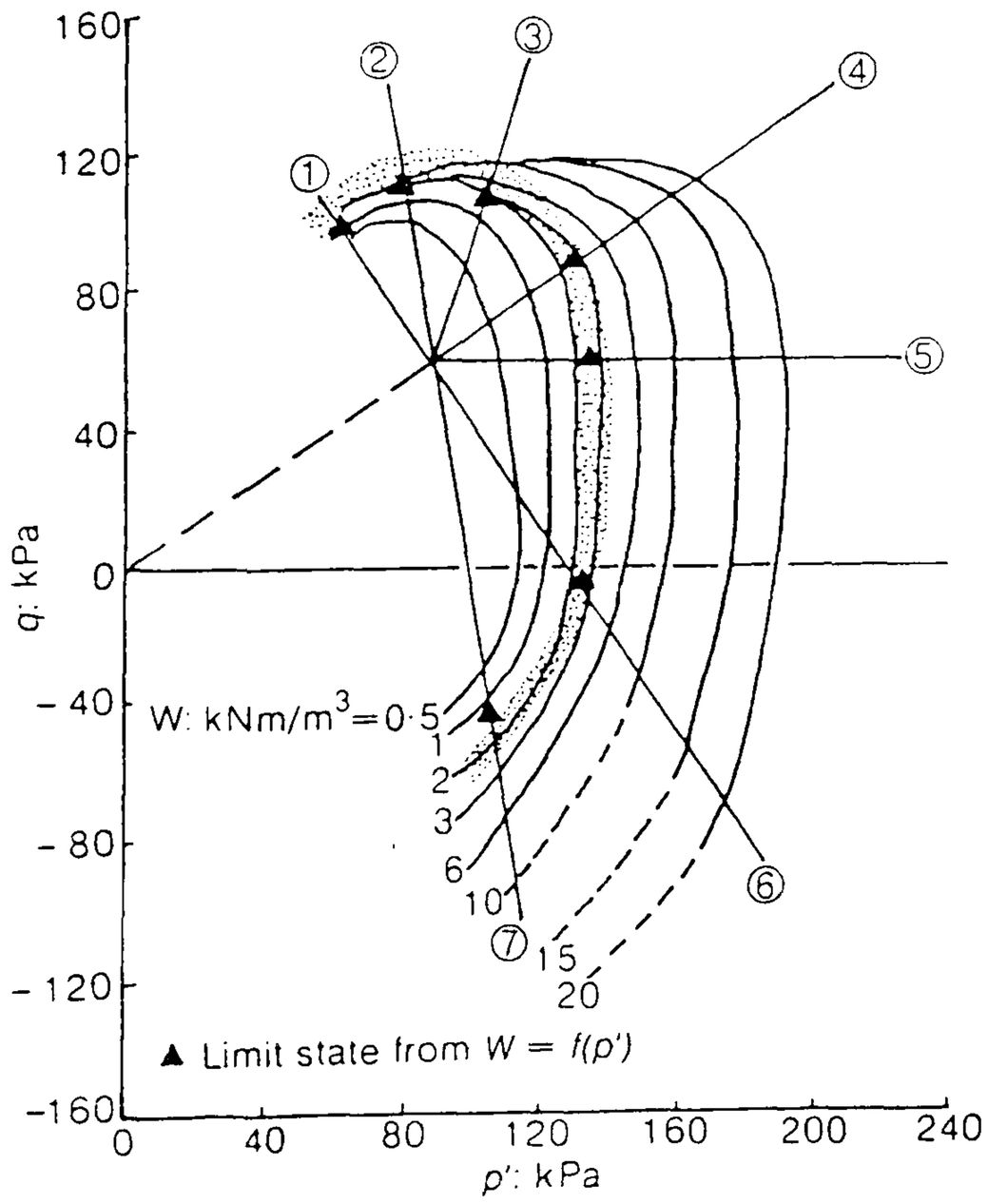

Figure 2.4.9 Contours of strain energy and gross yield curve of Saint-Louis clay (after Tavenas *et al.*, 1979)

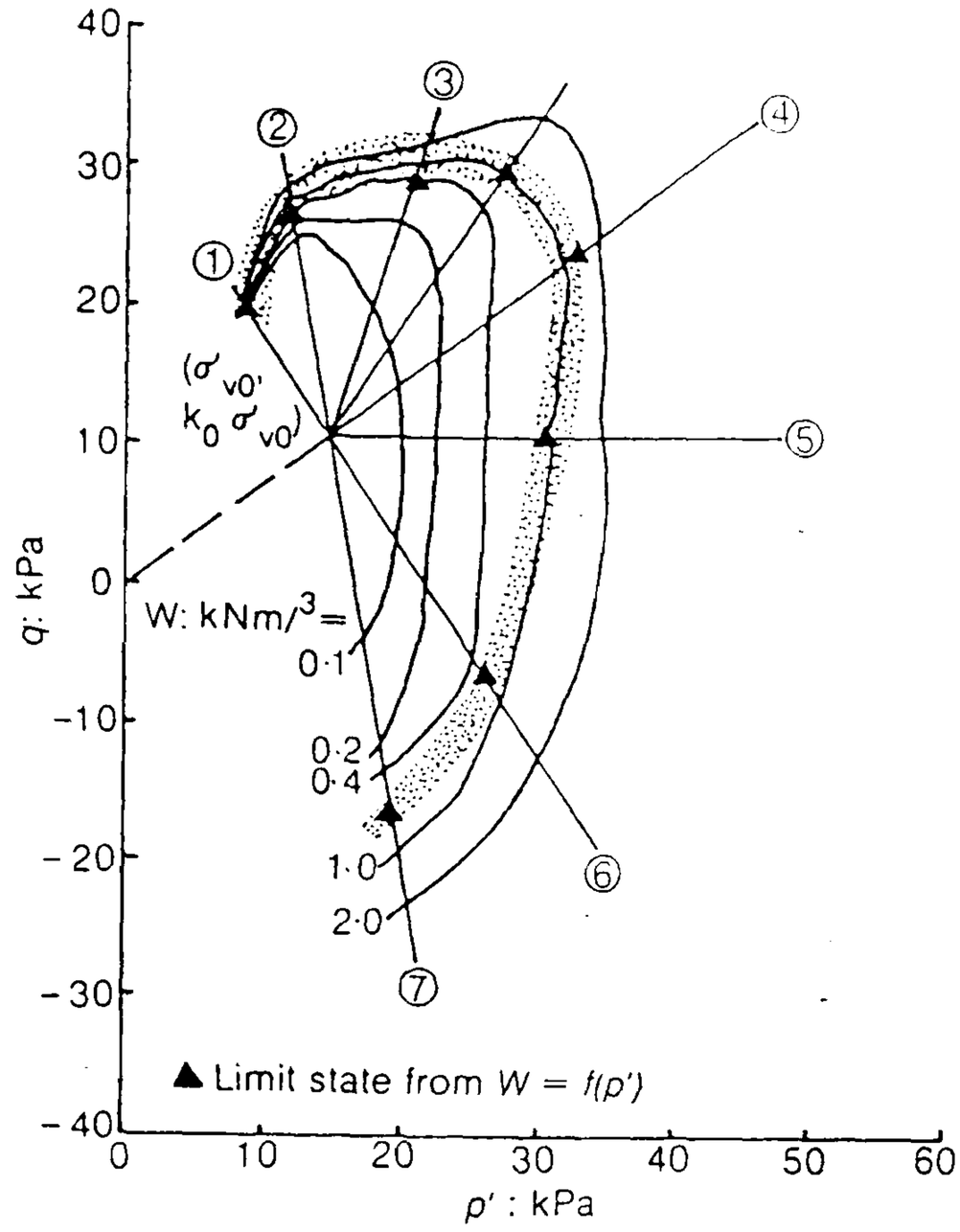

(a)

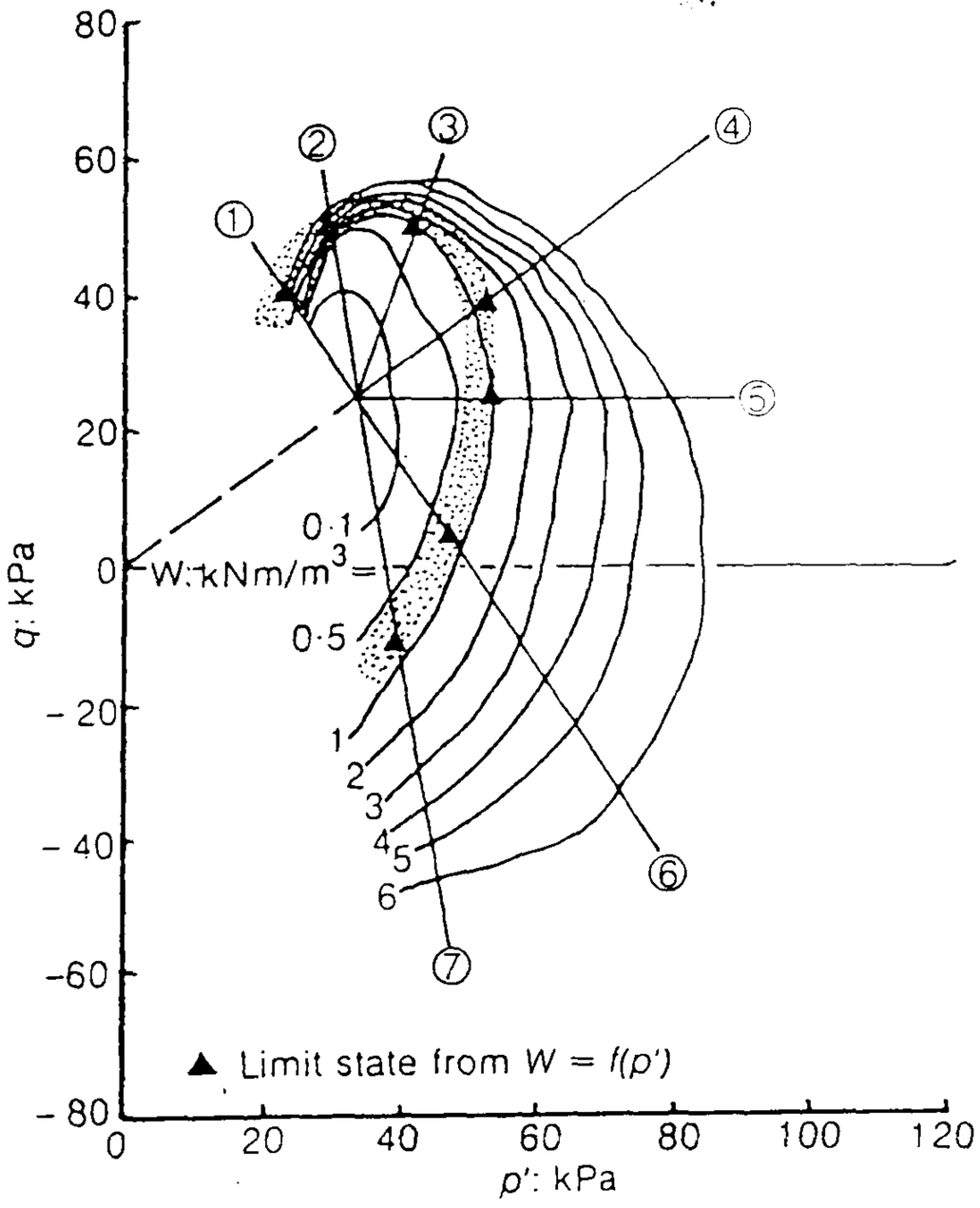

(b)

Figure 2.4.10 Contours of strain energy and gross yield curve of Saint-Alban clay at (a) 3.0m depth (b) 5.7m depth (after Tavenas *et al.*, 1979)

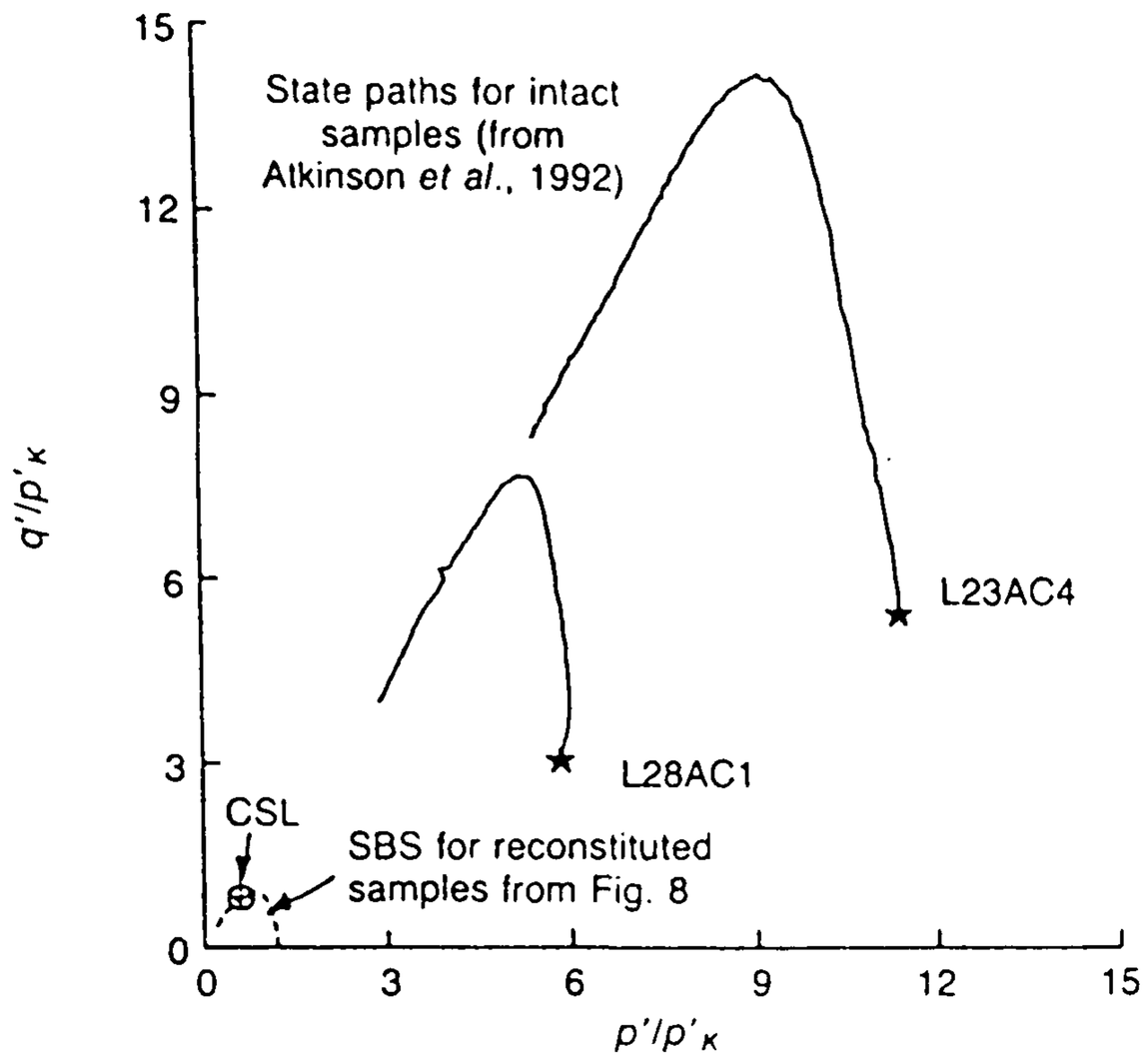

Figure 2.4.11 Normalised stress paths during undrained compression tests on natural Bothkennar clay samples (after Allman & Atkinson, 1992)

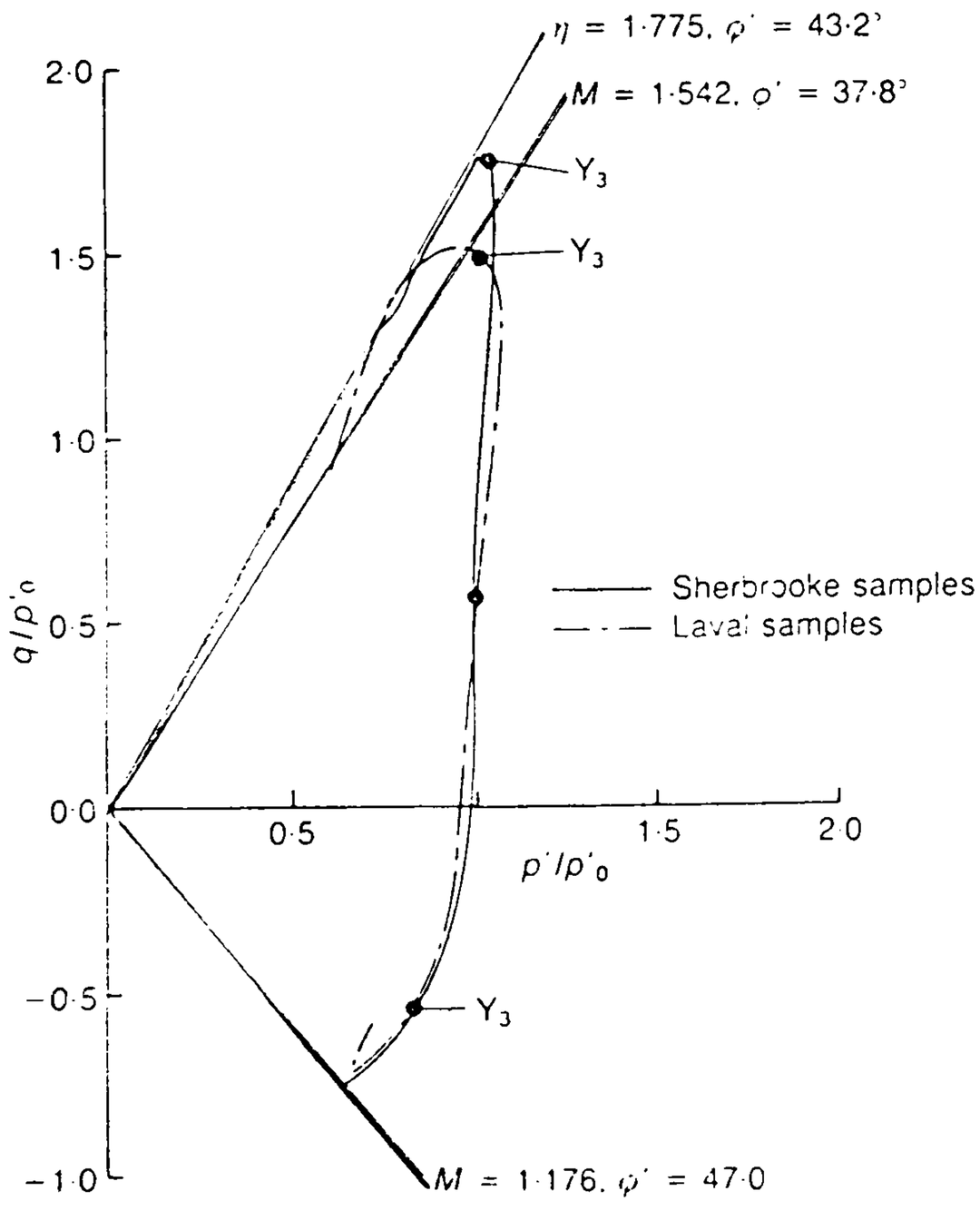

Figure 2.4.12 Normalised stress paths during undrained compression and extension tests on Bothkennar clay samples (after Smith *et al.*, 1992)

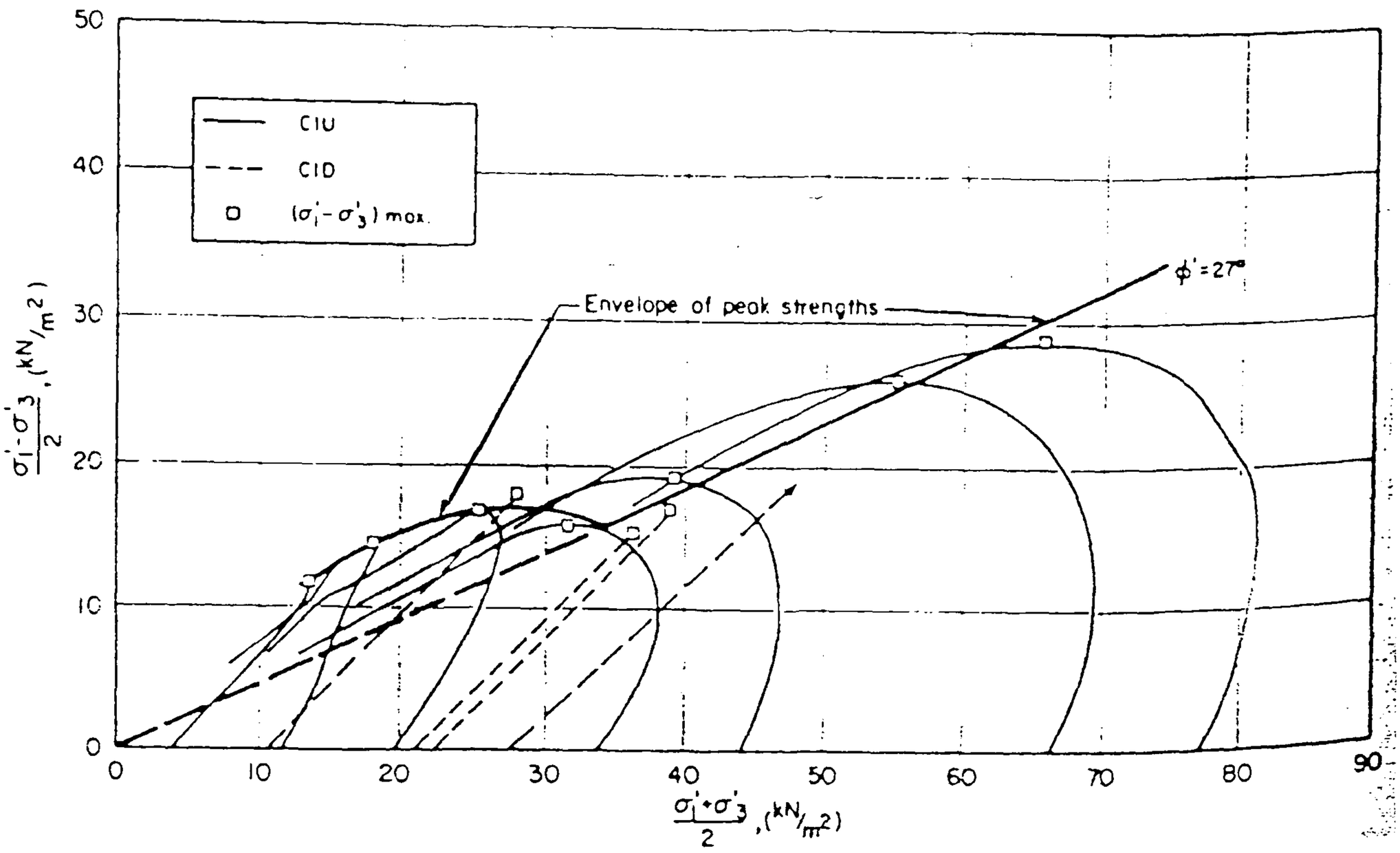

Figure 2.4.13 Stress paths during undrained compression tests on natural Saint-Alban clay samples (after Tavenas & Leroueil, 1977)

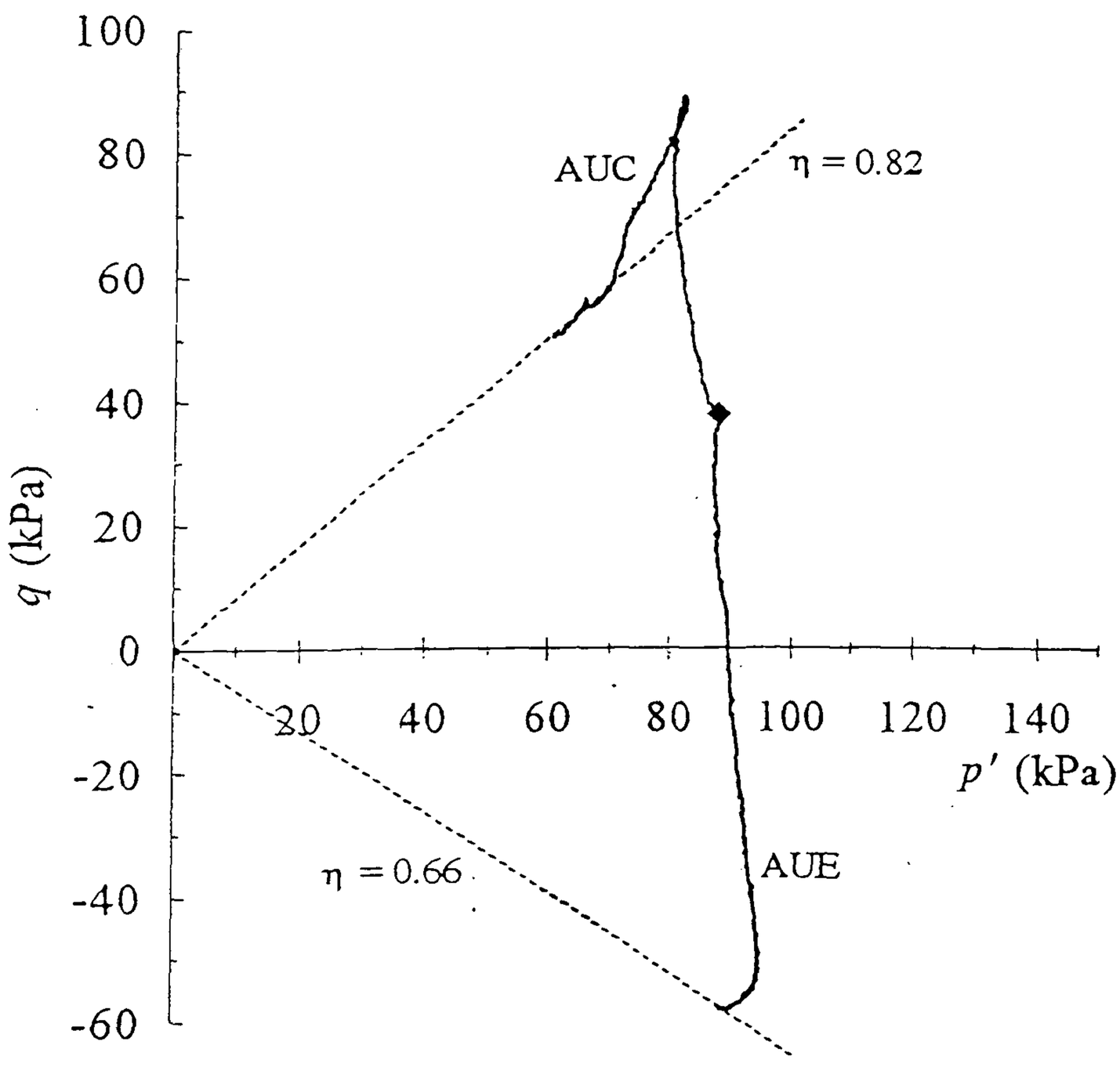

Figure 2.4.14 Stress paths during undrained compression and extension tests on natural Pisa clay samples (after Callisto, 1996)

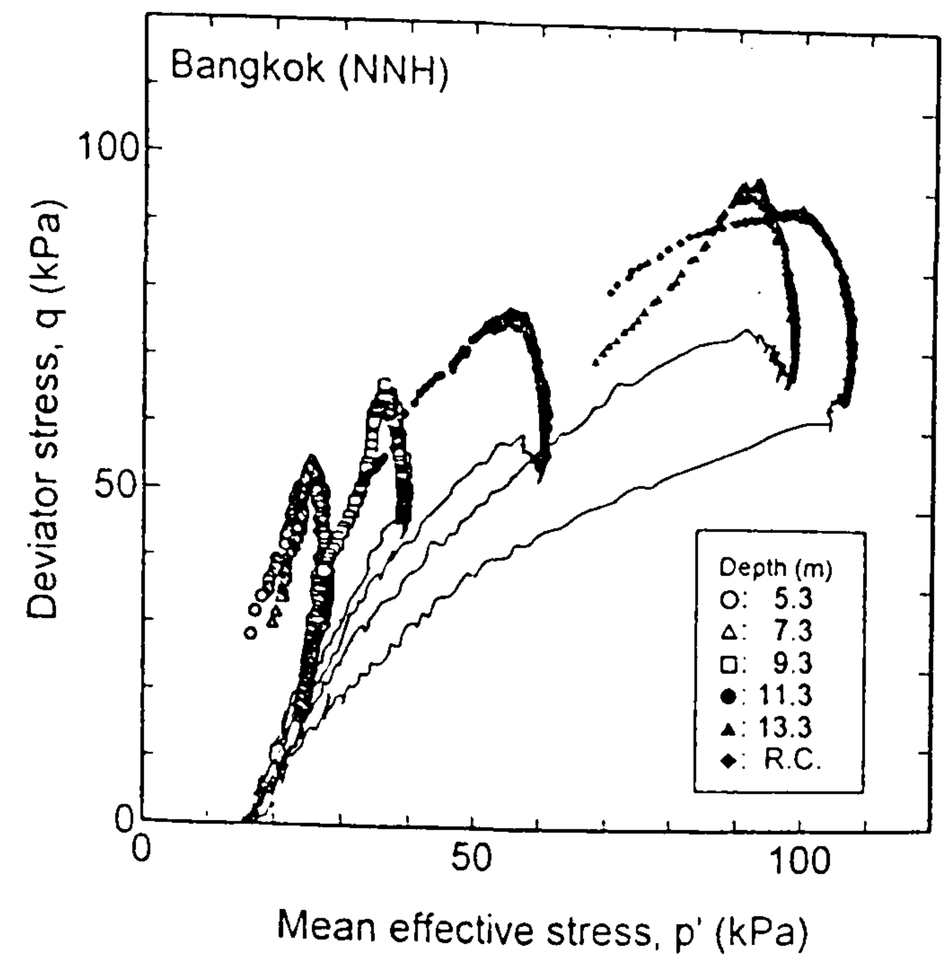

Figure 2.4.15 Stress paths during undrained compression tests on one-dimensionally compressed natural Bangkok clay samples (after Shibuya *et al.*, 2000)

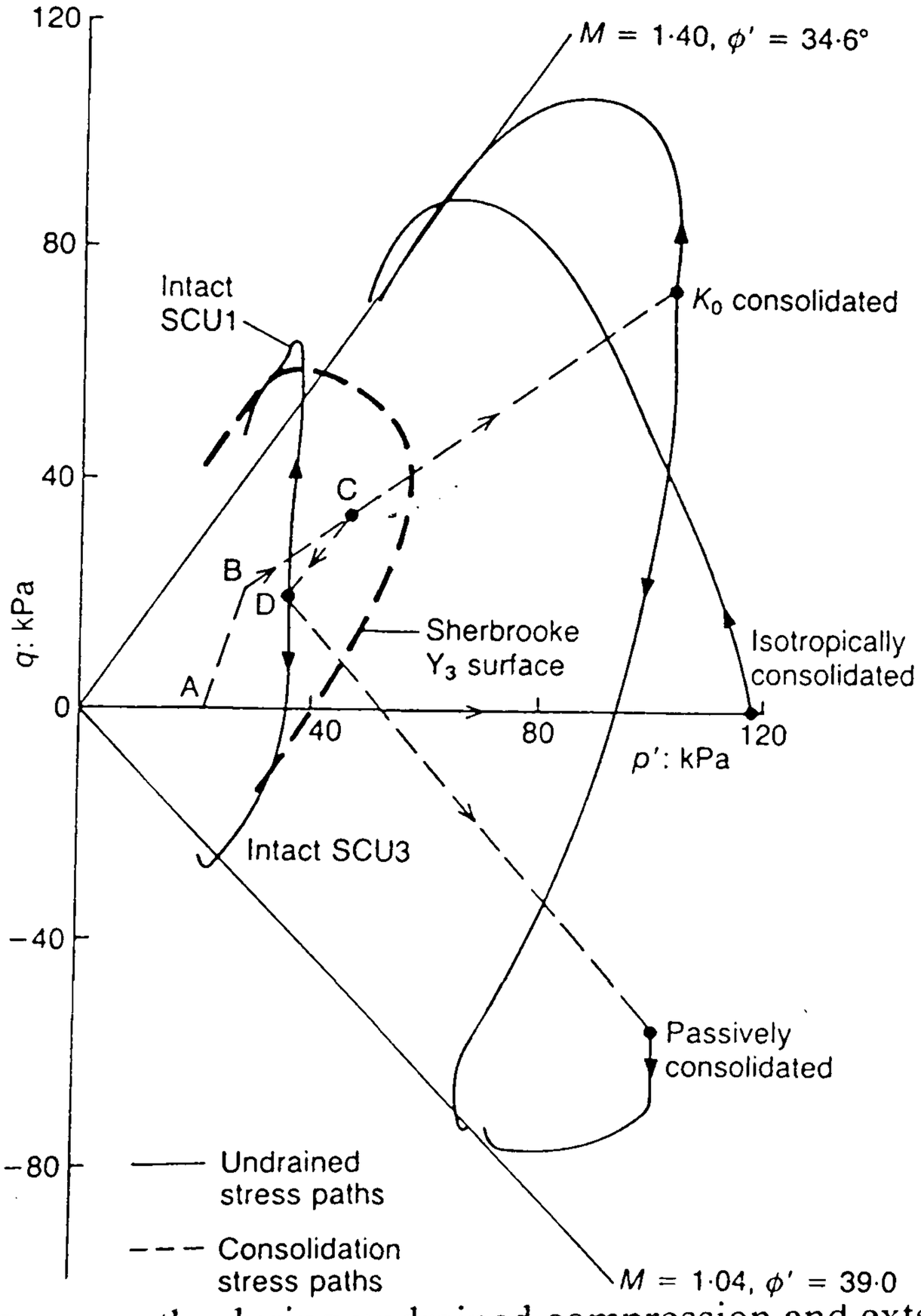

Figure 2.4.16 Stress paths during undrained compression and extension tests on isotropically and anisotropically compressed natural Bothkennar clay samples (after Smith *et al.*, 1992)

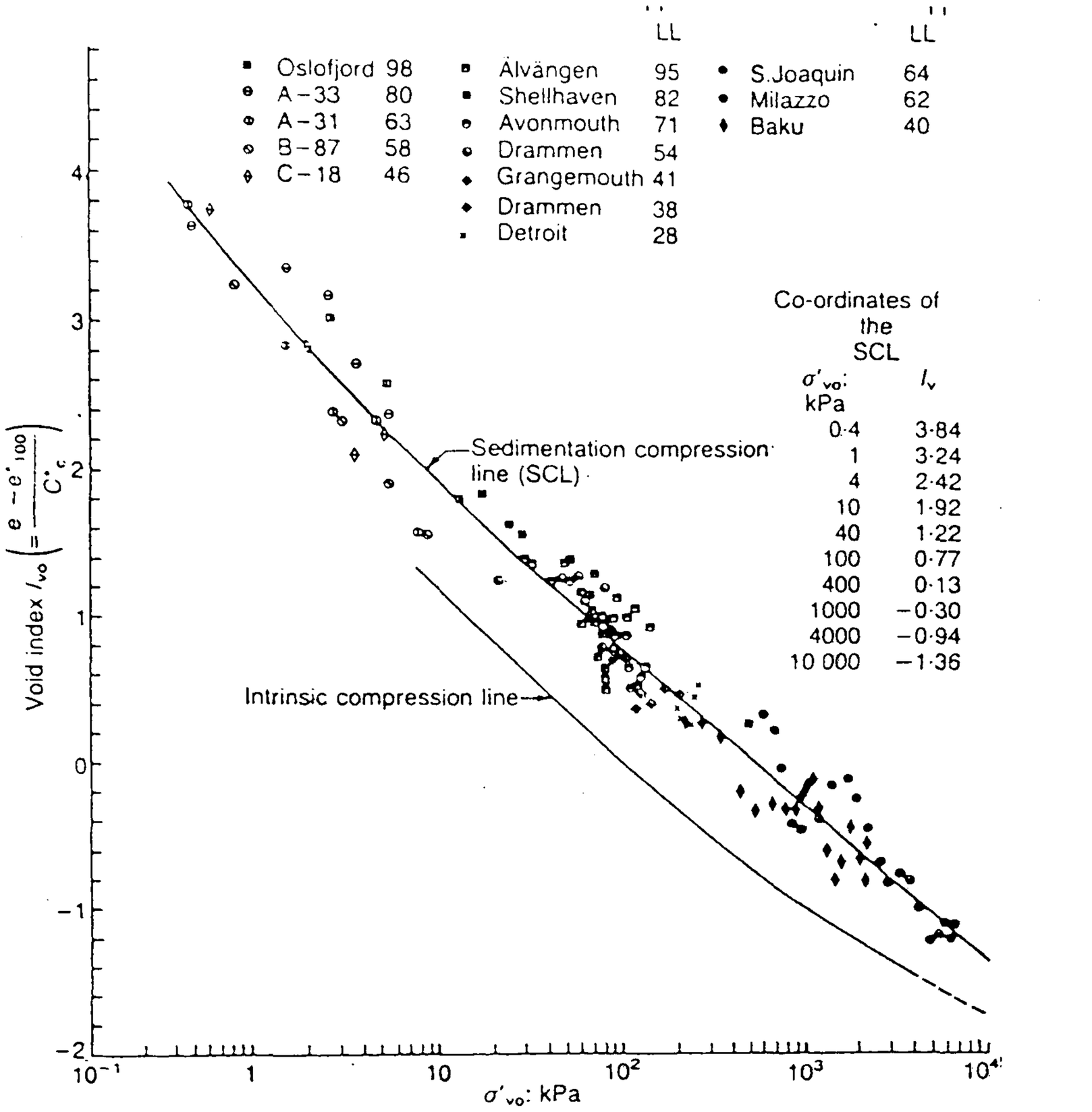

Figure 2.5.1 Relationship between void index and *in situ* vertical effective stress for a range of normally consolidated clays of medium sensitivity (after Burland, 1990)

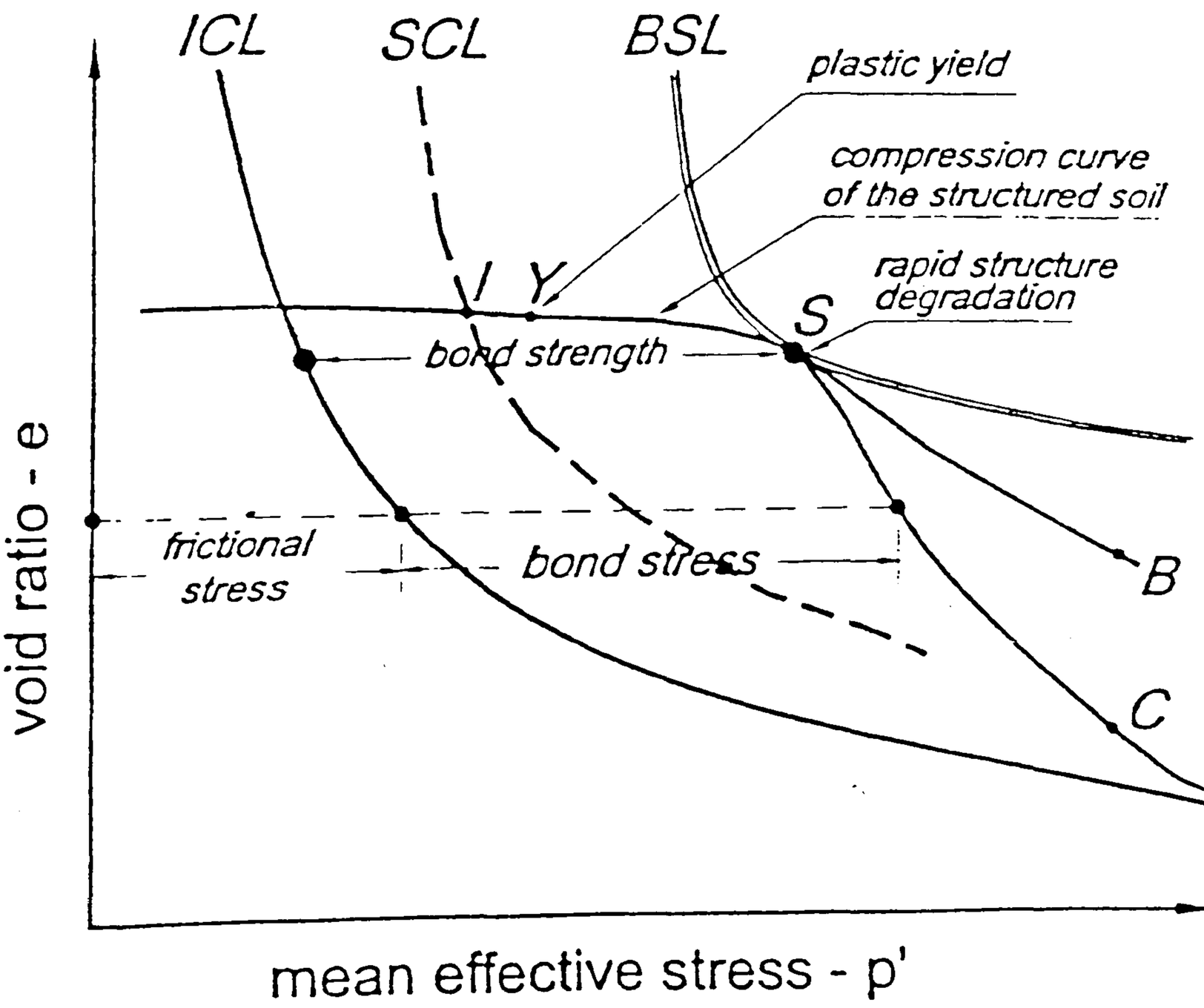

Figure 2.5.2 Schematic diagram showing the compression curve of a structured soil (after Kavvadas & Anagnostopoulos, 1998)

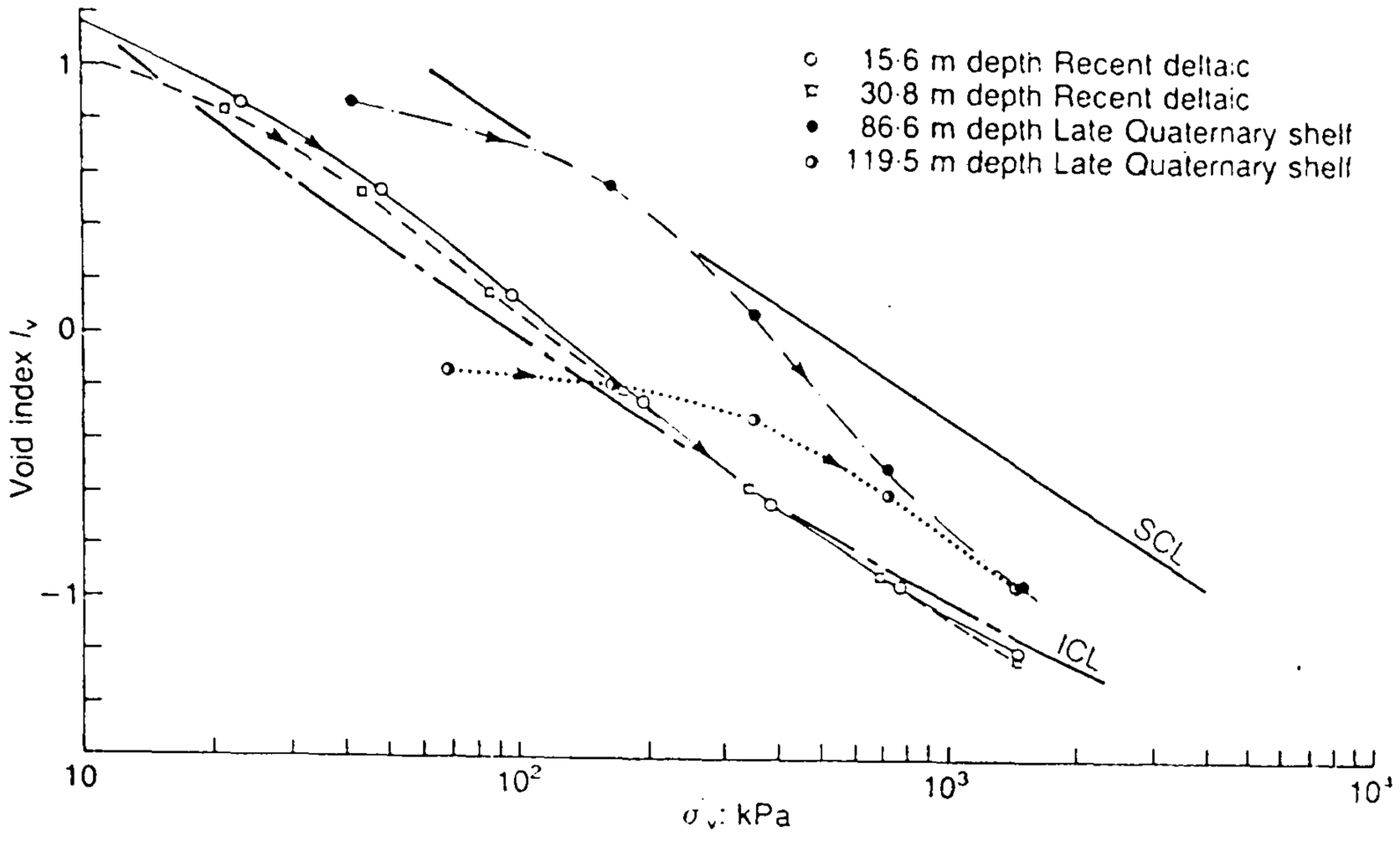

Figure 2.5.3 One-dimensional compression data from oedometer tests on Mississippi Delta clay (after Burland, 1990)

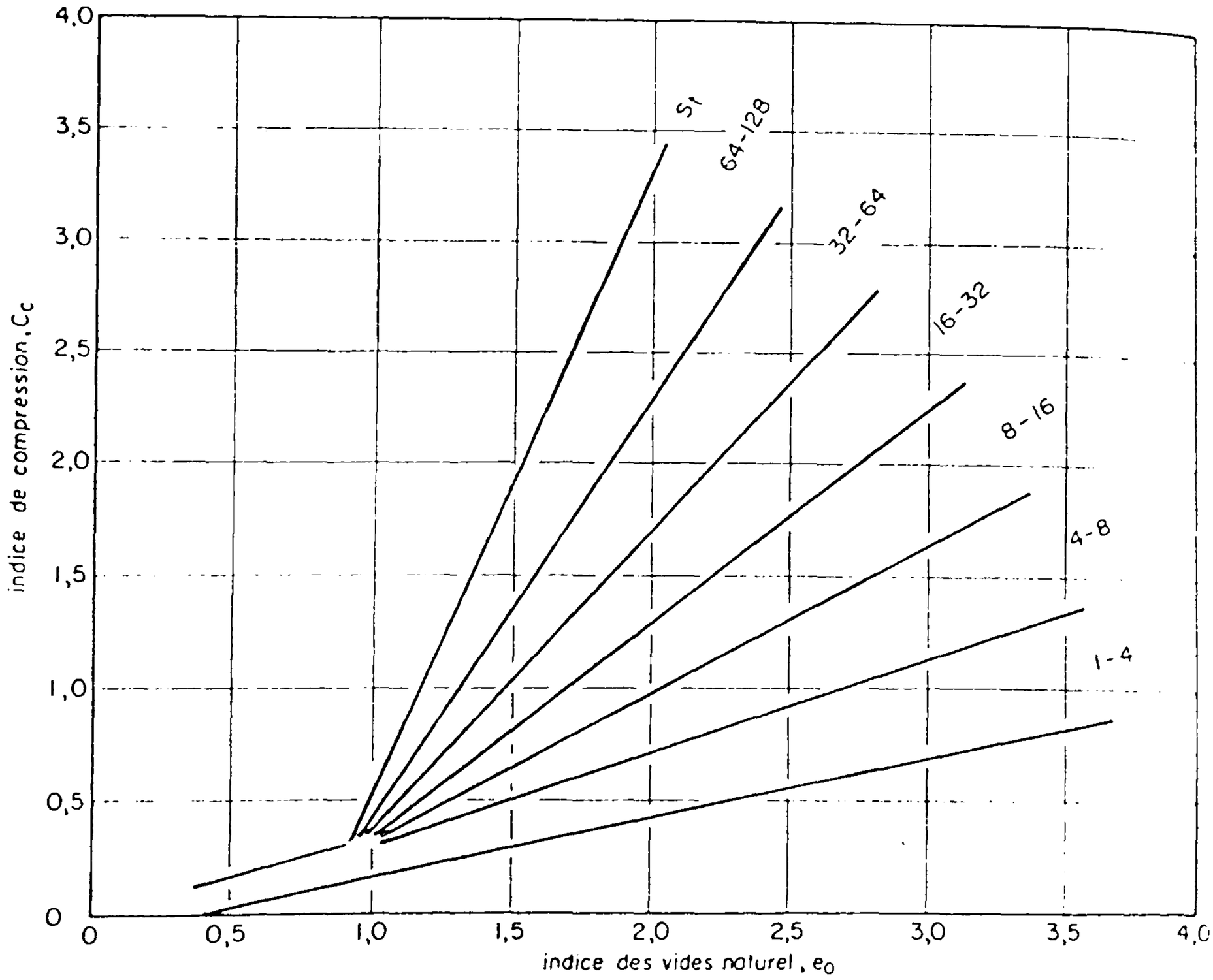

Figure 2.5.4 Relationship between compressibility index (C_c), initial void ratio (e_0) and sensitivity (S_t) (after Leroueil *et al.*, 1983)

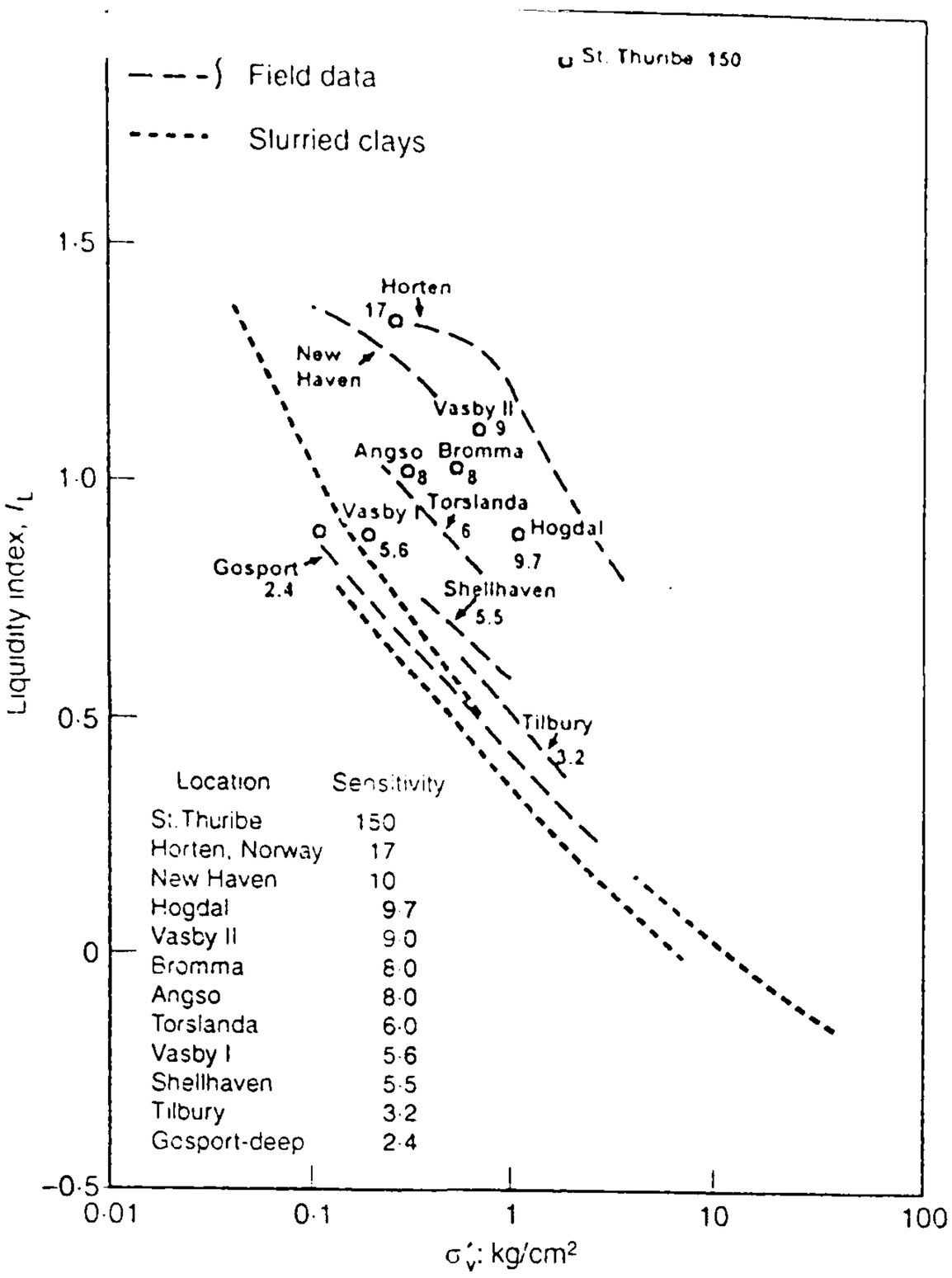

Figure 2.5.5 *In situ* states of normally consolidated natural clays and normal compression lines of reconstituted clays (after Cotecchia & Chandler, 2000; data from Skempton & Northey, 1952)

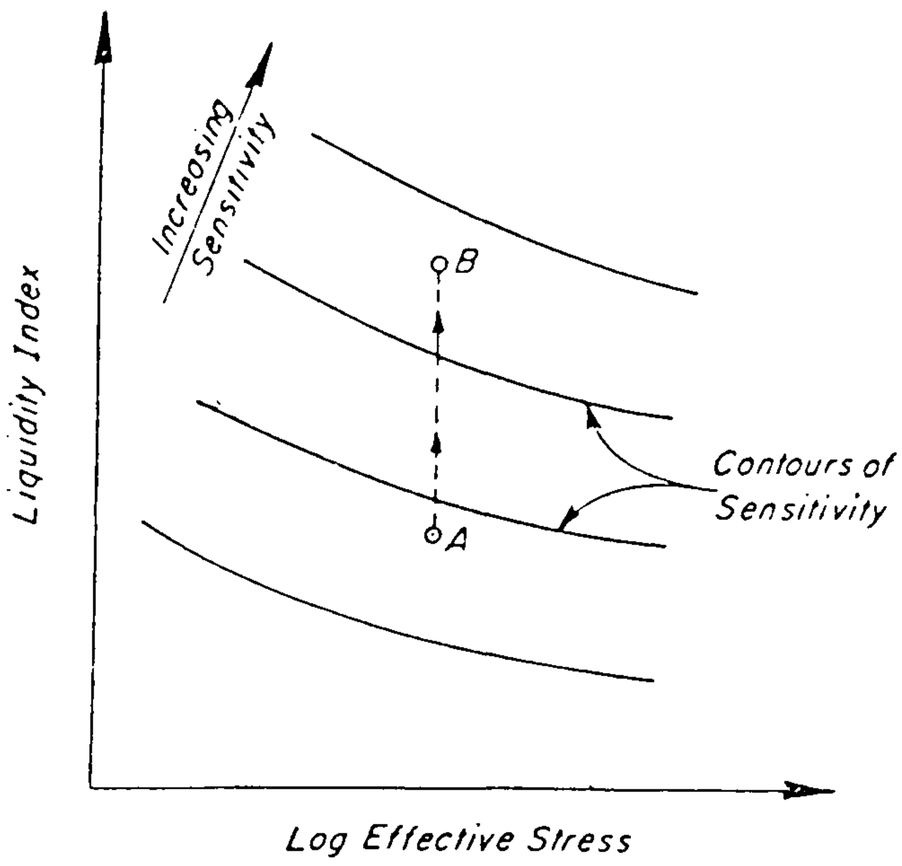

Figure 2.5.6 Relationship between liquidity index, effective stress and sensitivity (after Houston & Mitchell, 1969)

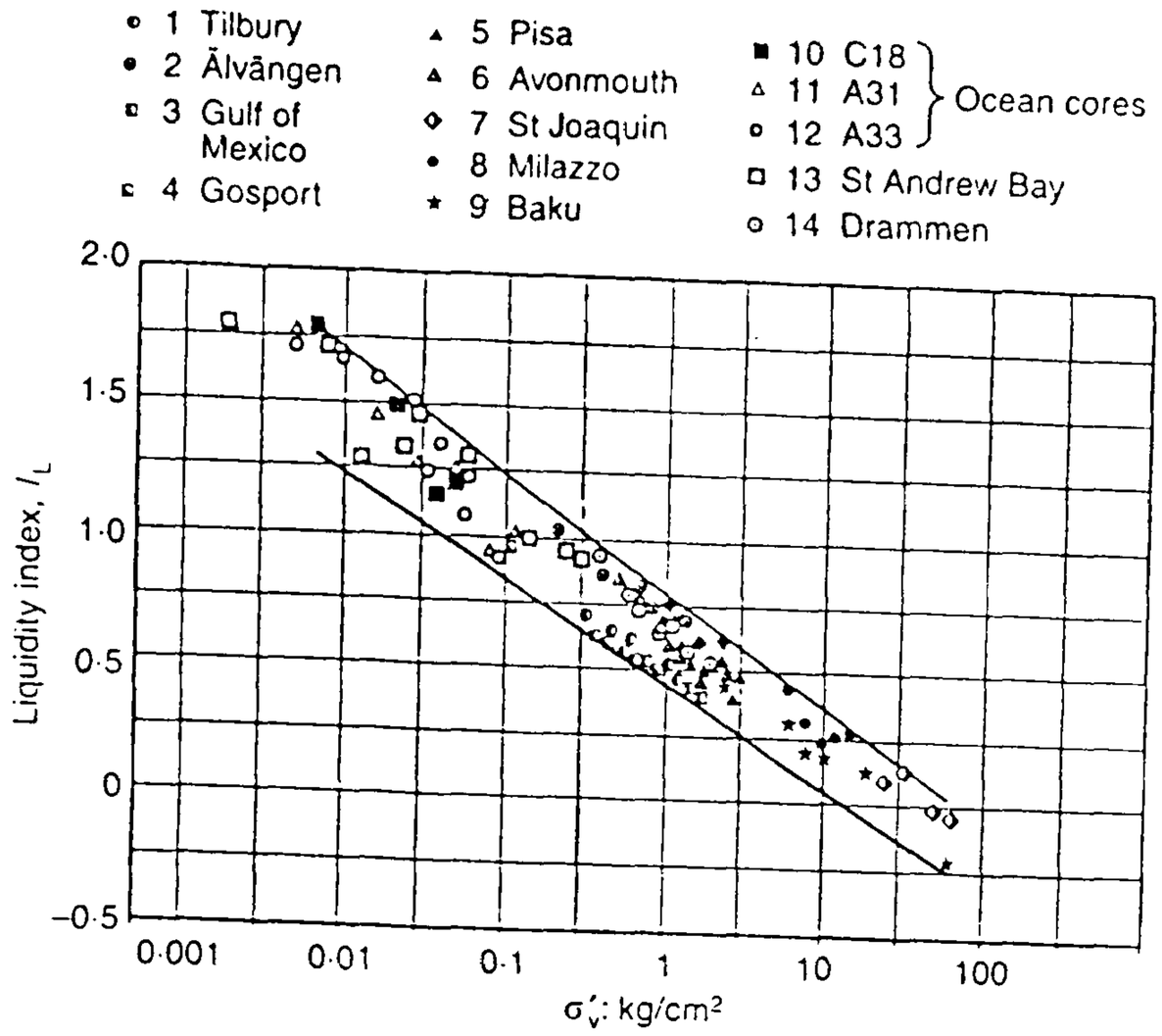

(a)

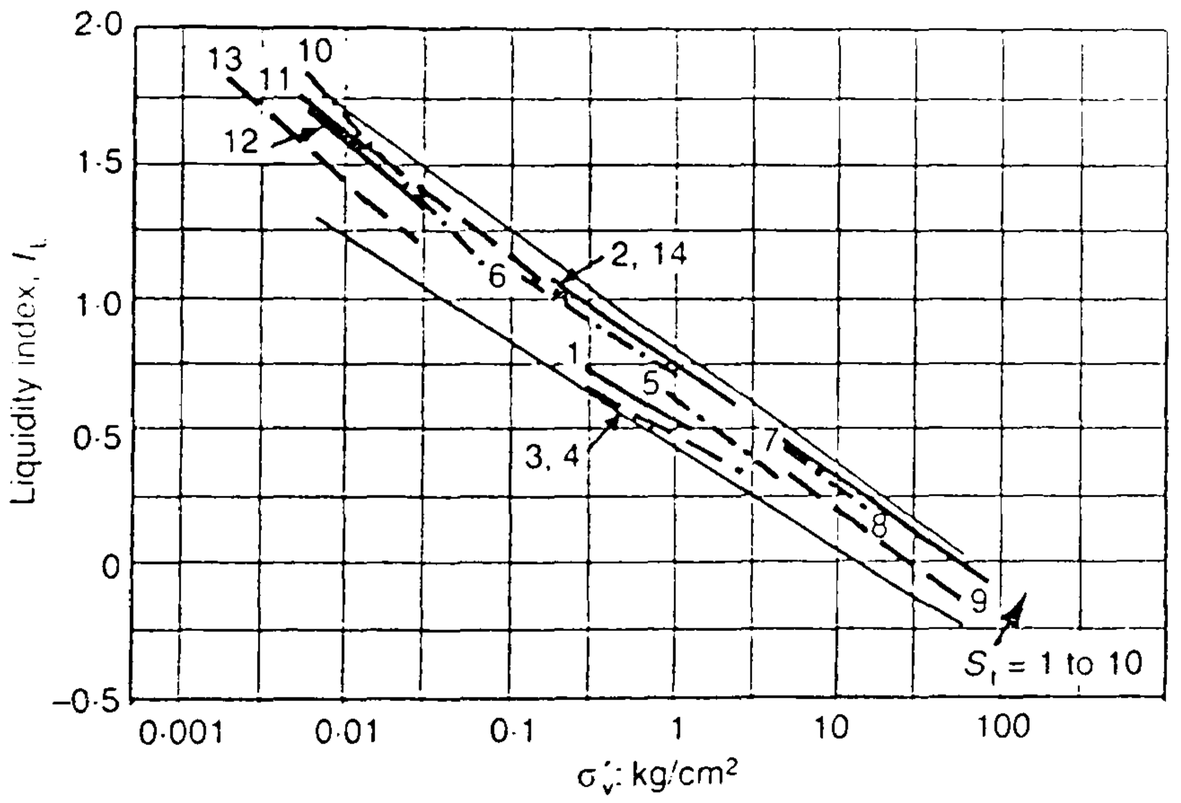

(b)

Figure 2.5.7 (a) *In situ* states of normally consolidated clays (data from Skempton, 1970) and (b) the corresponding sedimentation compression curves (after Cotecchia & Chandler, 2000)

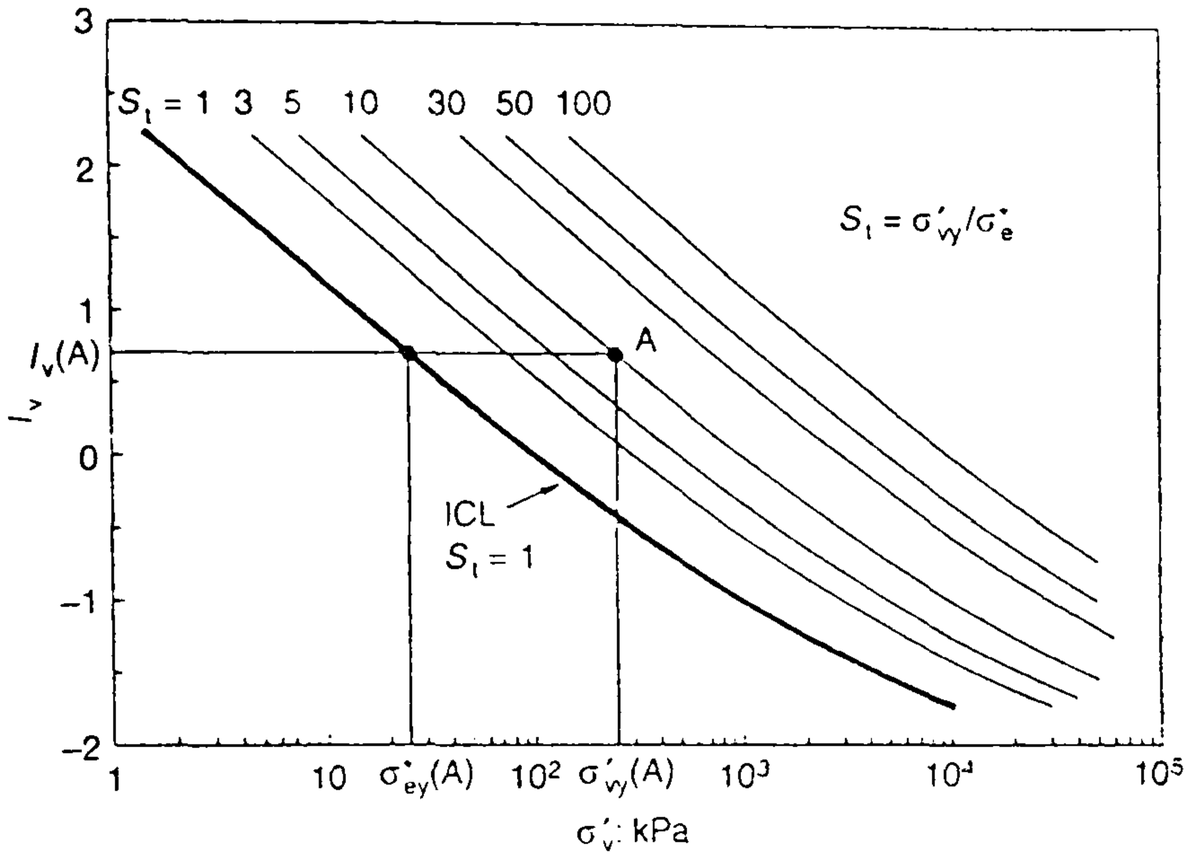

Figure 2.5.8 Sedimentation compression curves in the idealised Sensitivity framework (after Cotecchia & Chandler, 2000)

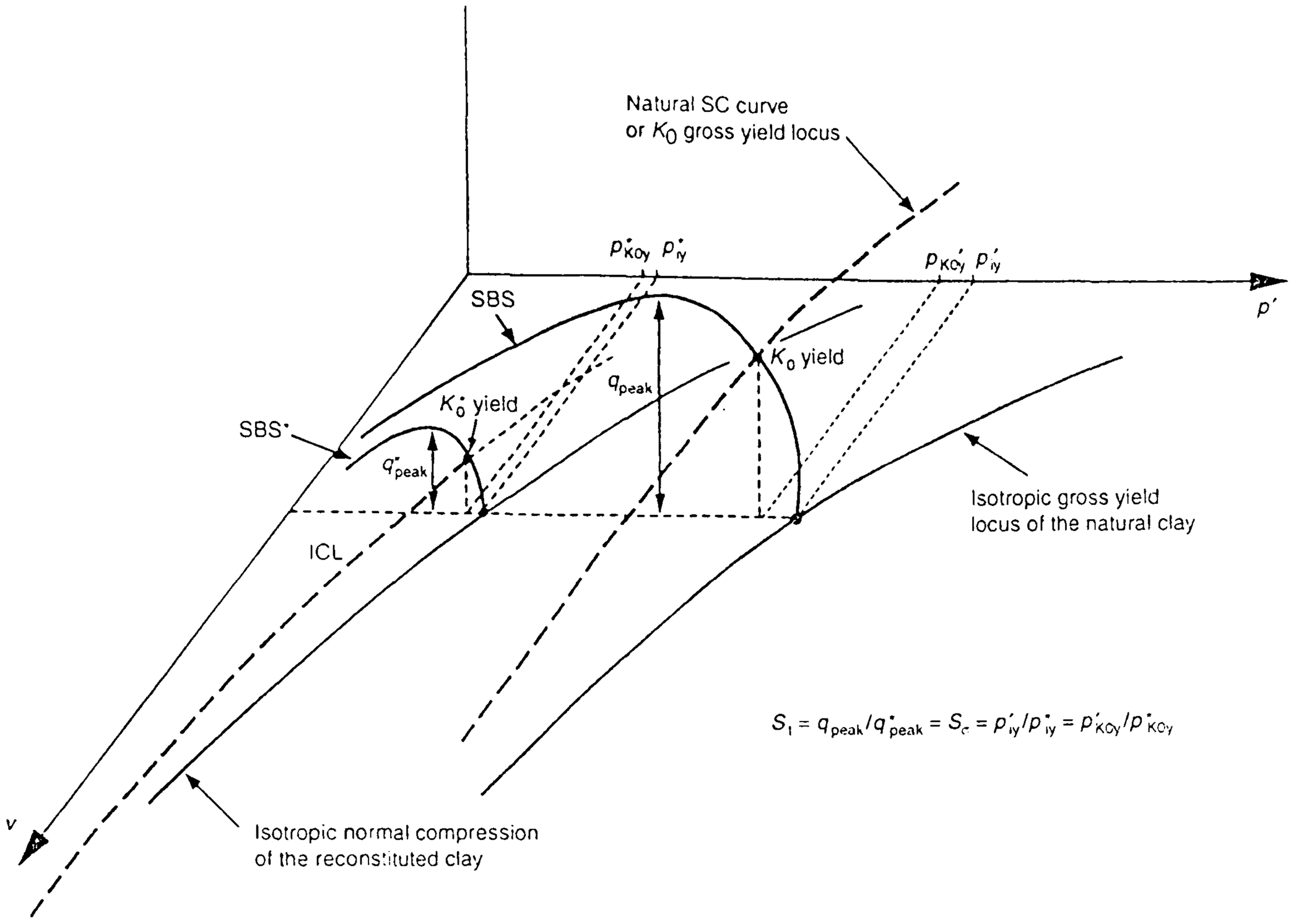

Figure 2.5.9 Idealised behaviour of a natural clay and of the same clay when reconstituted (after Cotecchia & Chandler, 2000)

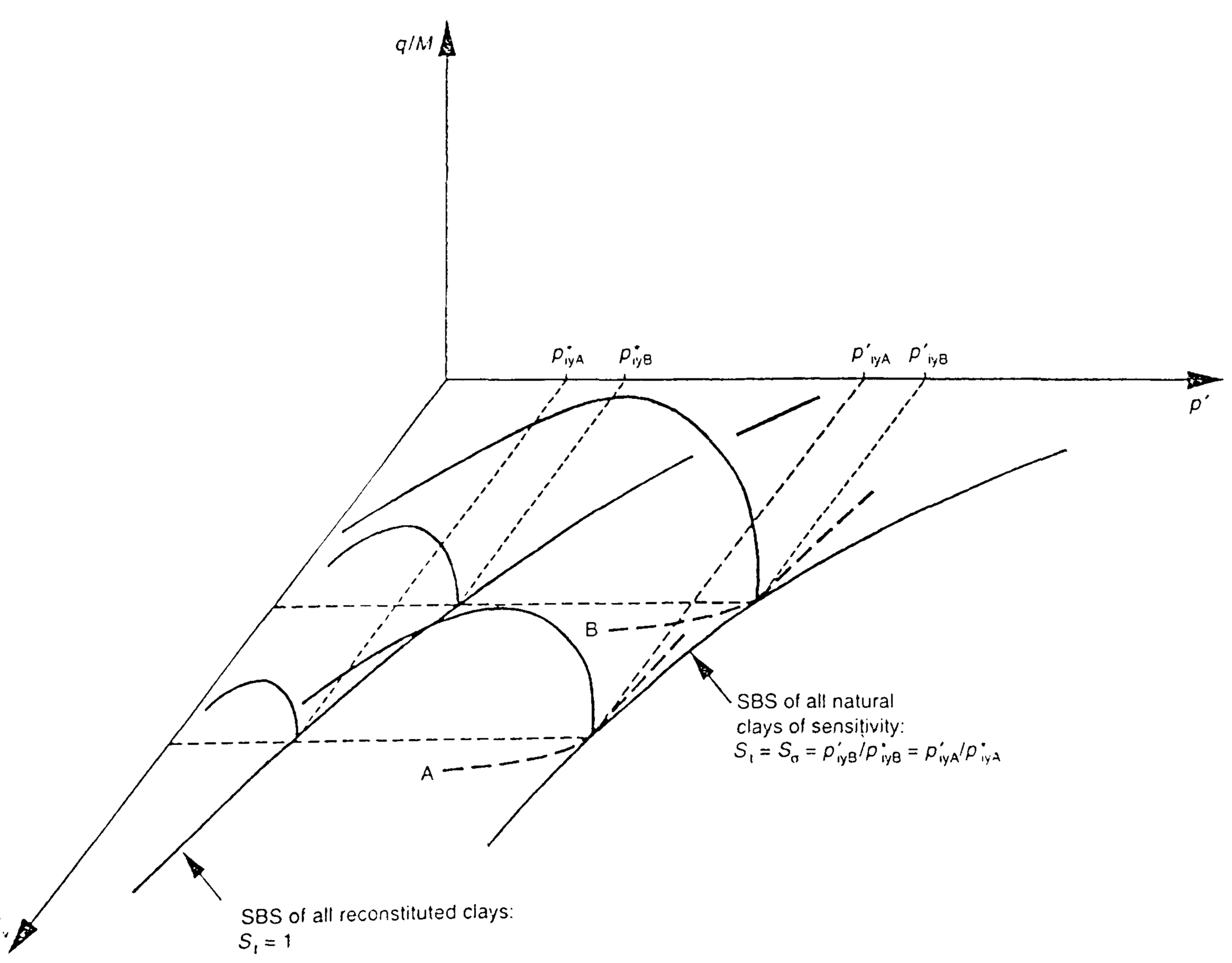

Figure 2.5.10 Idealised normalised behaviour of different natural clays of given sensitivity and of reconstituted clays (after Cotecchia & Chandler, 2000)

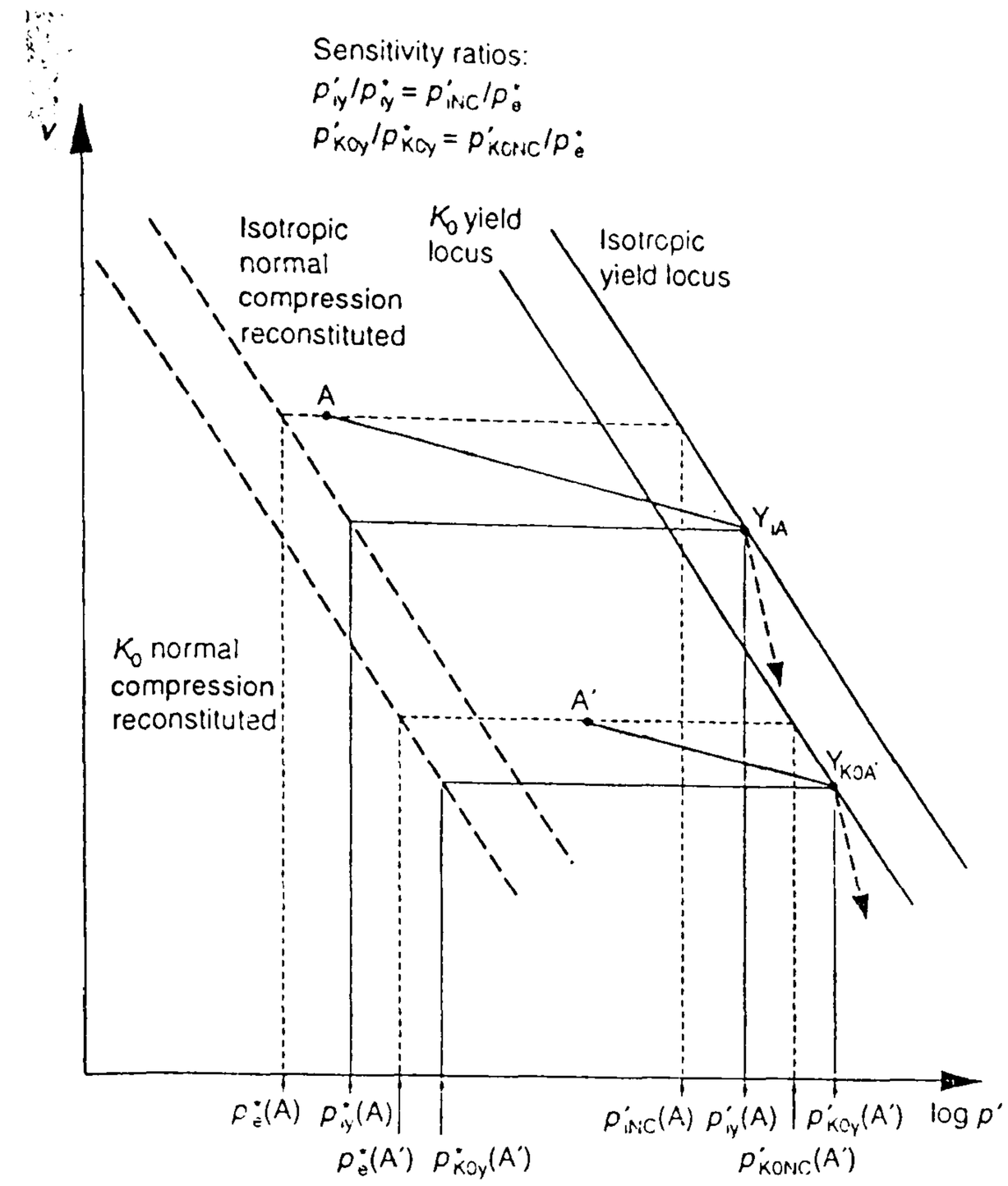

Figure 2.5.11 Normalising factors for volume and structure (after Cotecchia & Chandler, 2000)

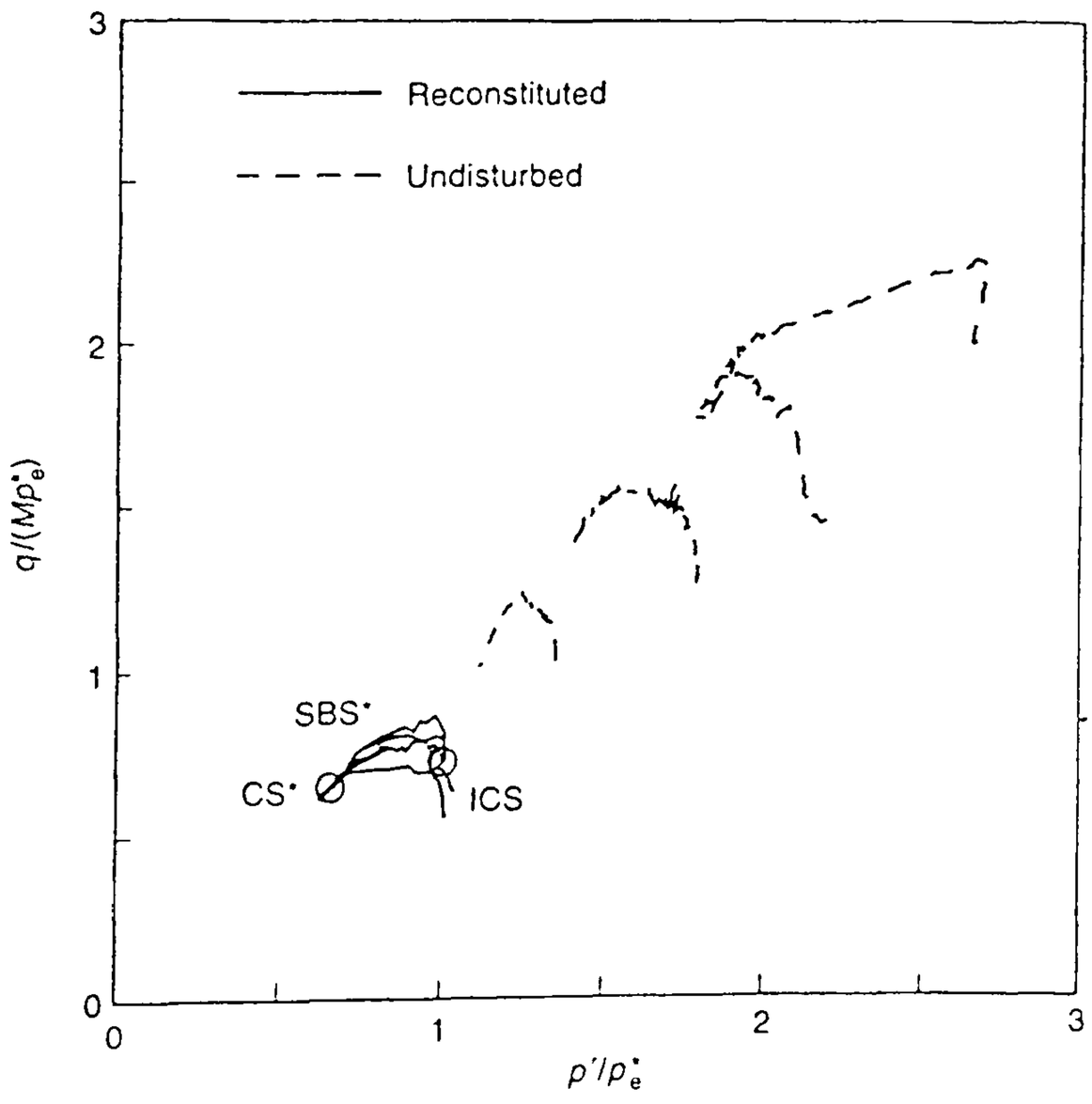

Figure 2.5.12 Shear tests on Sibari clay samples normalised for volume and composition (after Coop & Cotecchia, 1995)

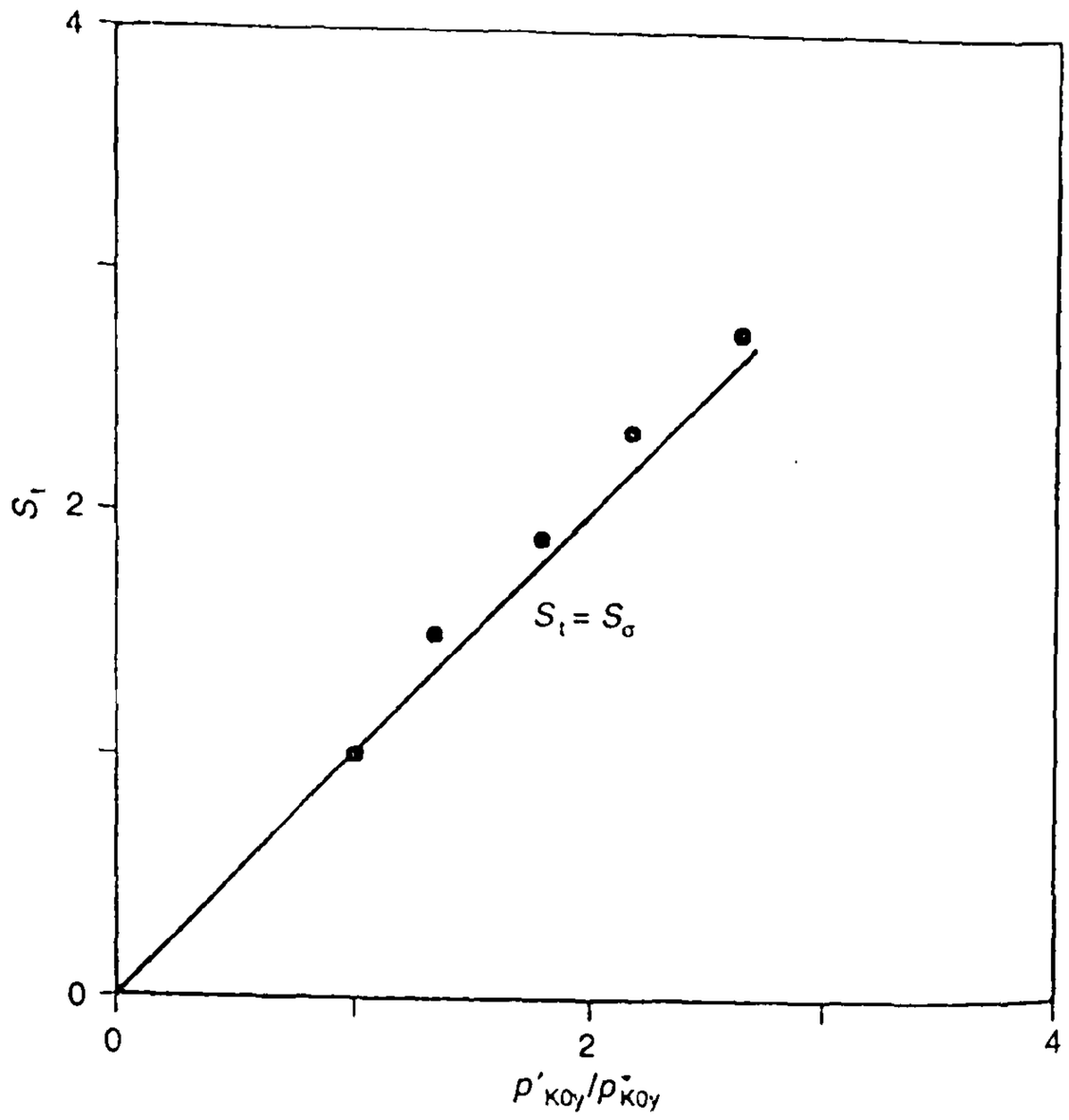

Figure 2.5.13 Strength sensitivities of the Sibari clay plotted against stress sensitivity (after Cotecchia & Chandler, 2000)

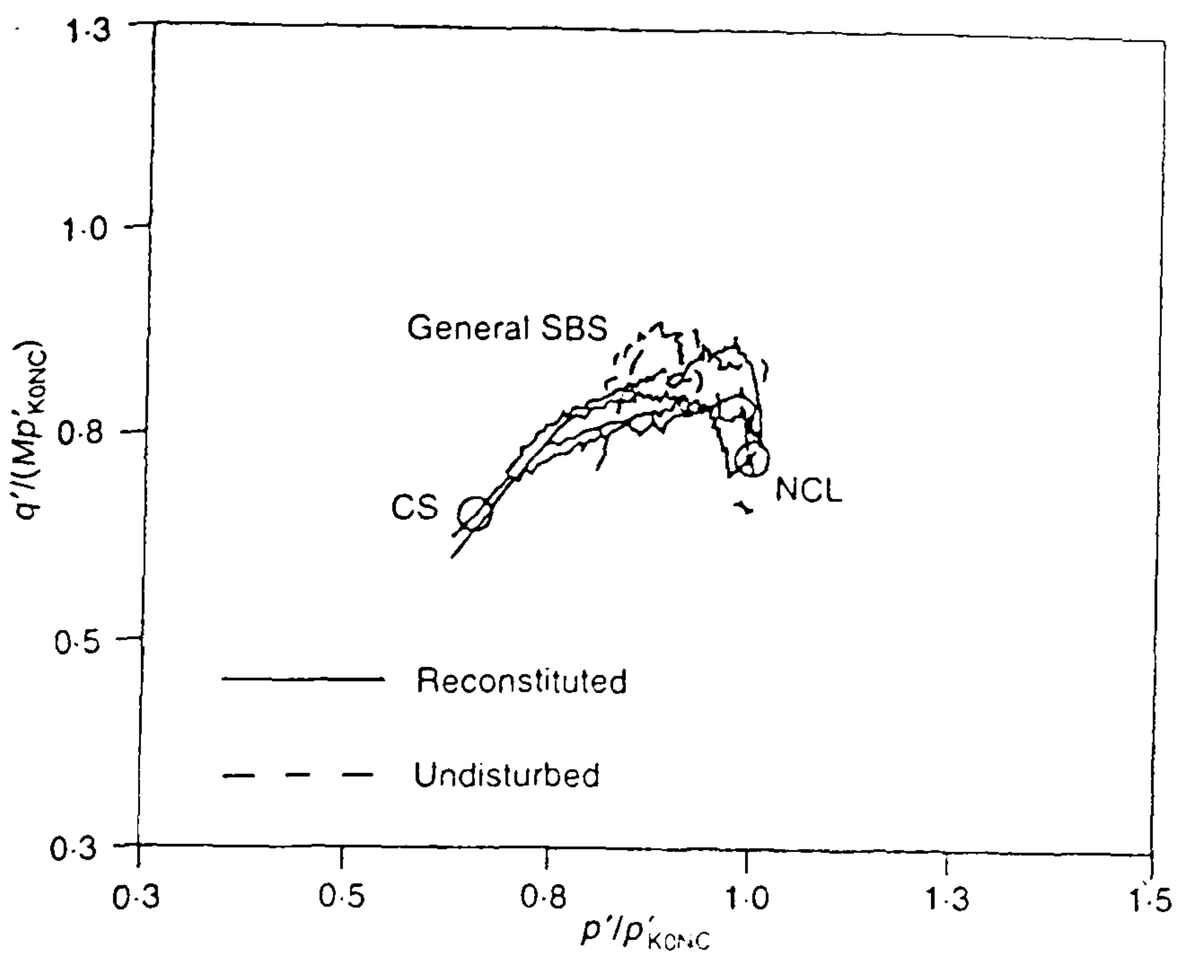

Figure 2.5.14 Shear test data for natural and reconstituted Sibari clay samples normalised for volume, composition and structure (after Cotecchia & Chandler, 2000)

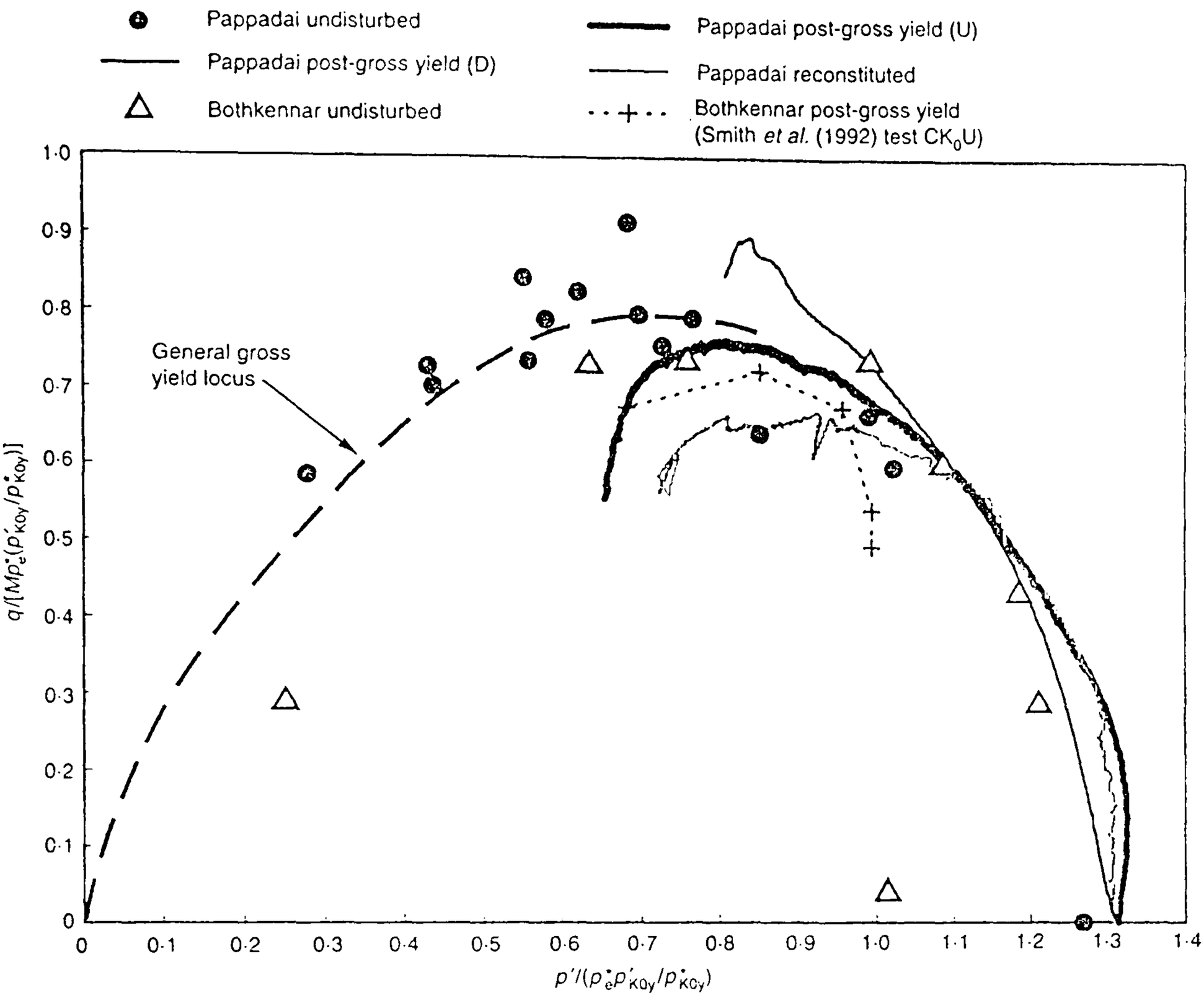

Figure 2.5.15 Behaviour of Pappadai and Bothkennar clay normalised for volume, composition and structure (after Cotecchia & Chandler, 2000)

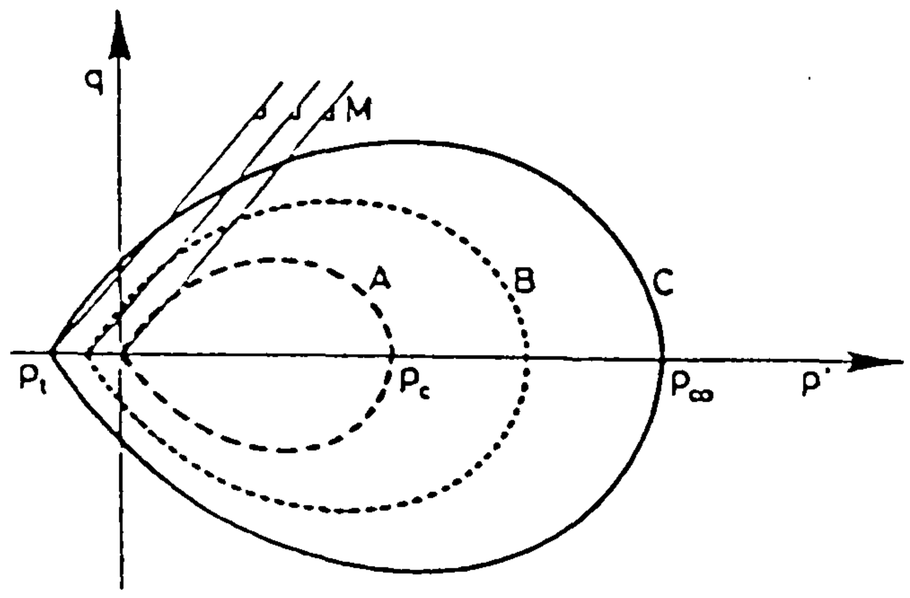

Figure 2.6.1 Successive yield surfaces for increasing degrees of bonding. Surface A corresponds to unbonded material. (after Gens & Nova, 1993)

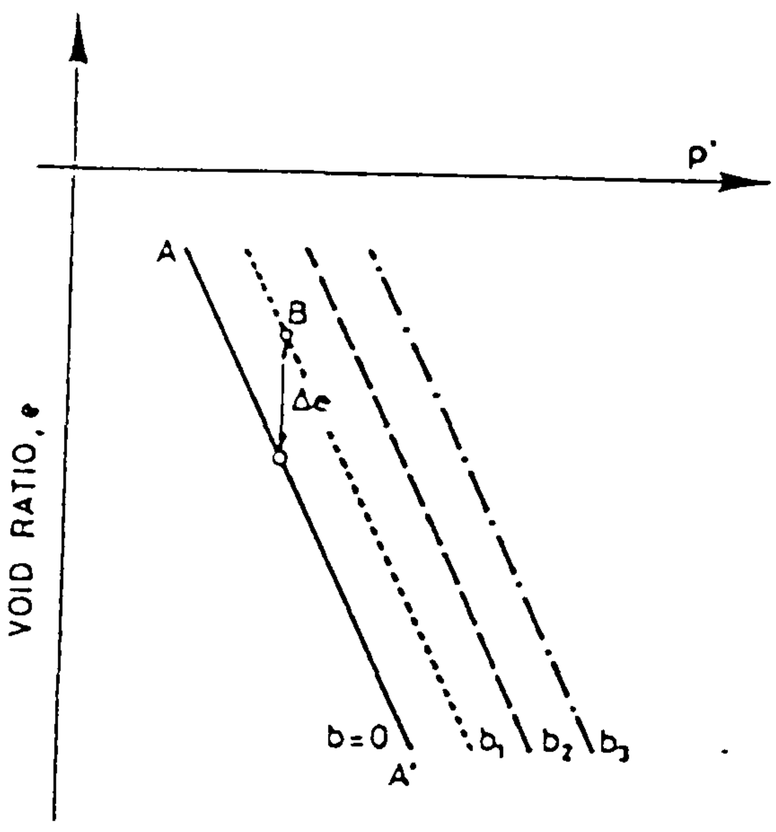

Figure 2.6.2 Isotropic normal compression curves for materials with various degrees of bonding (after Gens & Nova, 1993)

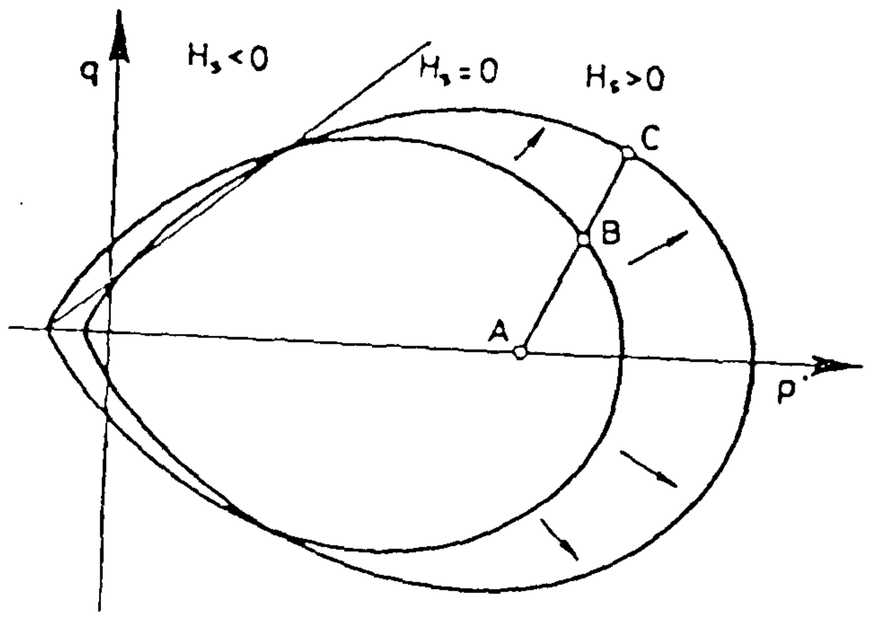

(a)

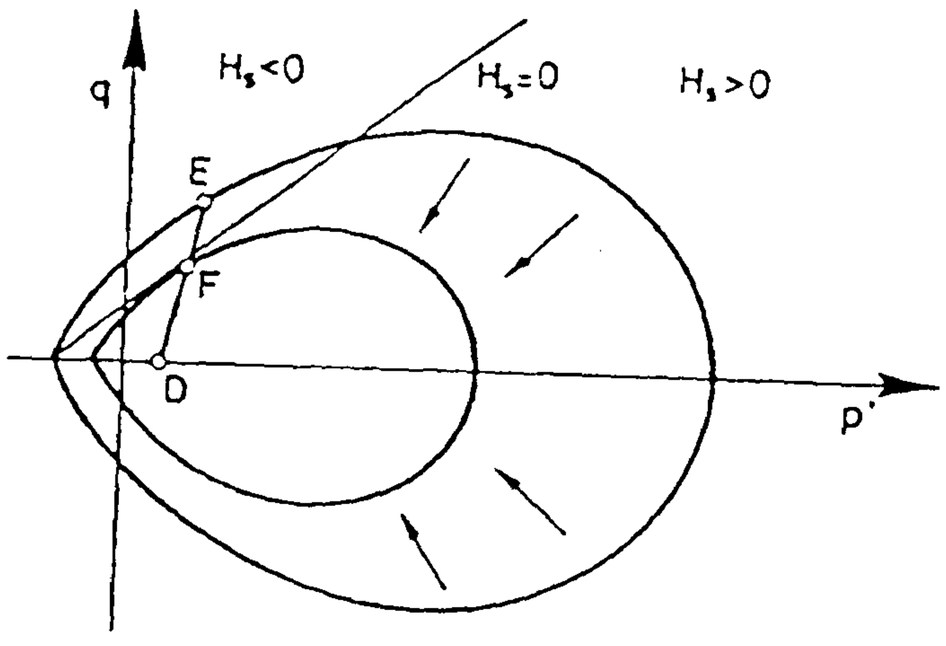

(b)

Figure 2.6.3 Evolution of the yield surface when (a) strain-hardening dominates the behaviour of the bonded material (b) destructuration dominates the behaviour (after Gens & Nova, 1993)

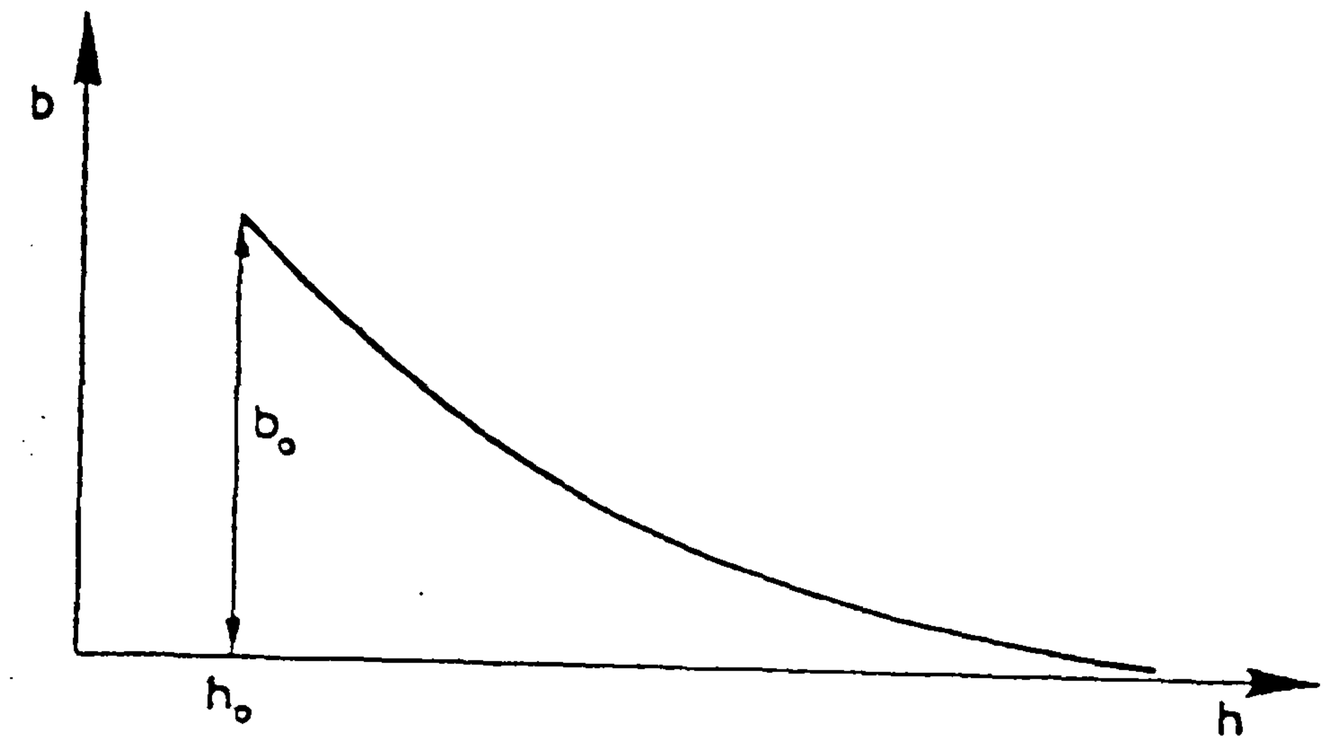

Figure 2.6.4 Reduction of bonding, *b*, with increasing damage, *h* (after Gens & Nova, 1993)

Figure 2.6.5 Computed isotropic compression curves for materials with different amounts of bonding (after Gens & Nova, 1993)

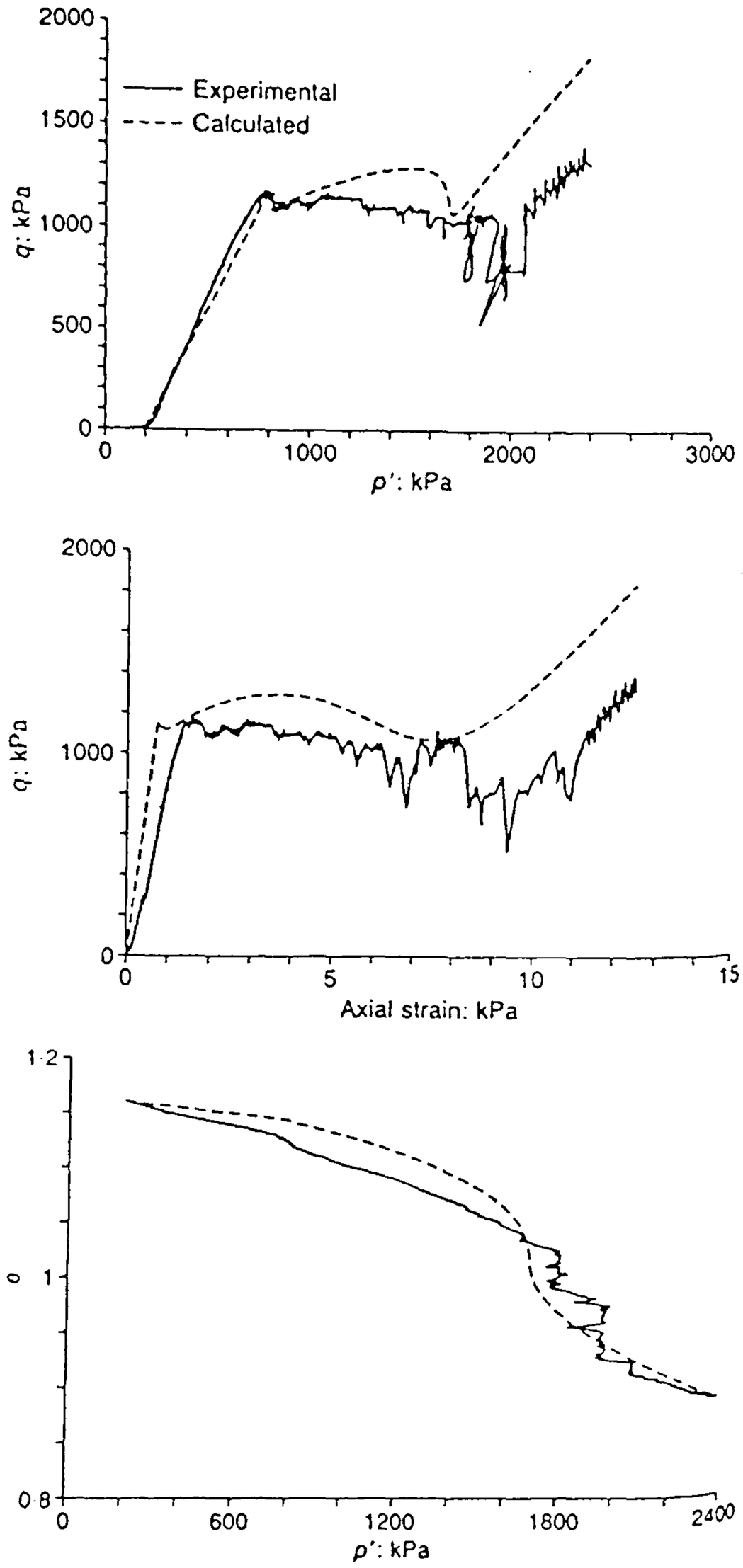

Figure 2.6.6 Comparison of computed and experimental curves for one-dimensional compression test on a calcarenite sample (after Lagioia & Nova, 1995)

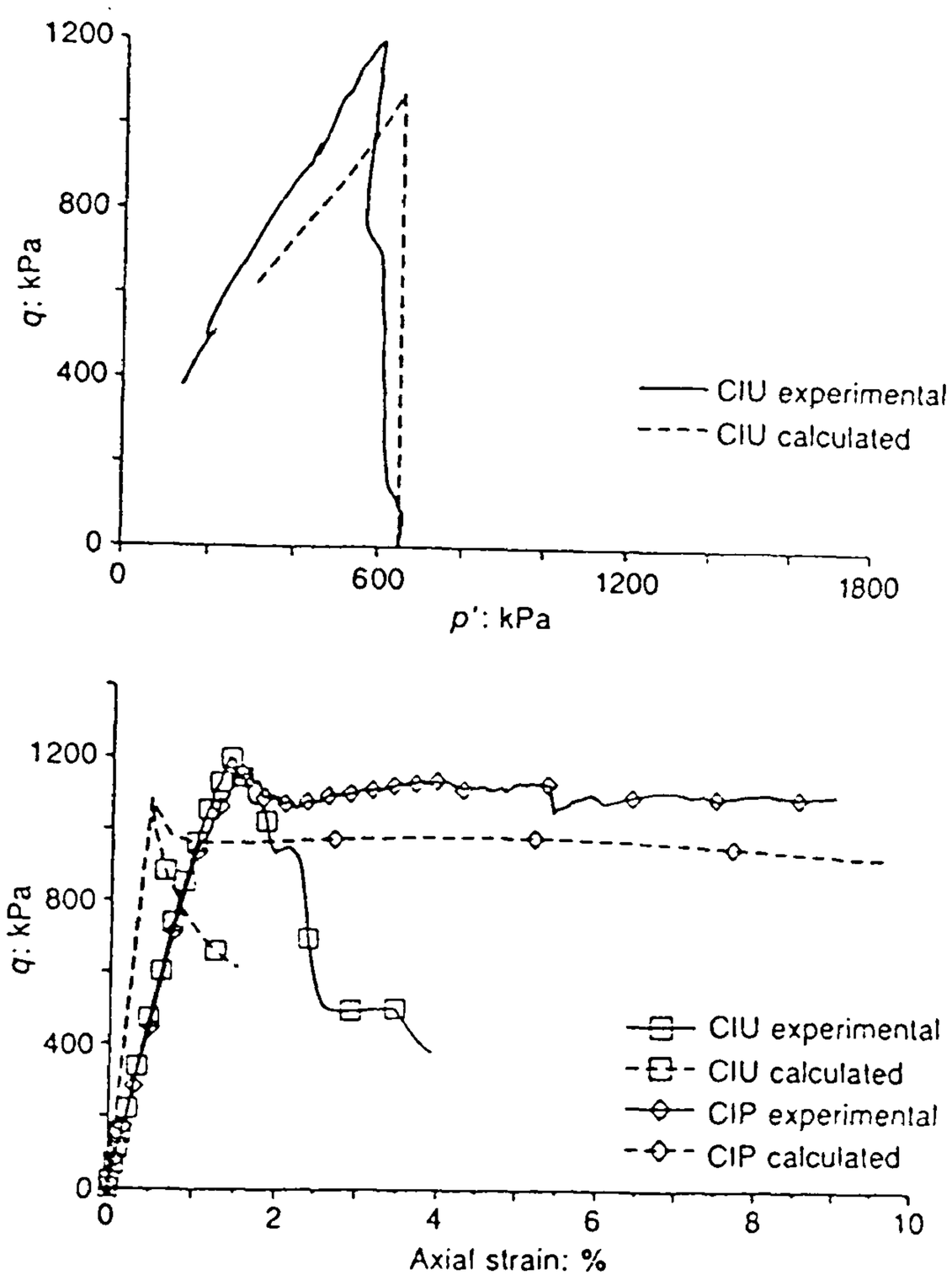

Figure 2.6.7 Comparison of computed and experimental curves for undrained compression and constant p' tests on a calcarenite sample (after Lagioia & Nova, 1995)

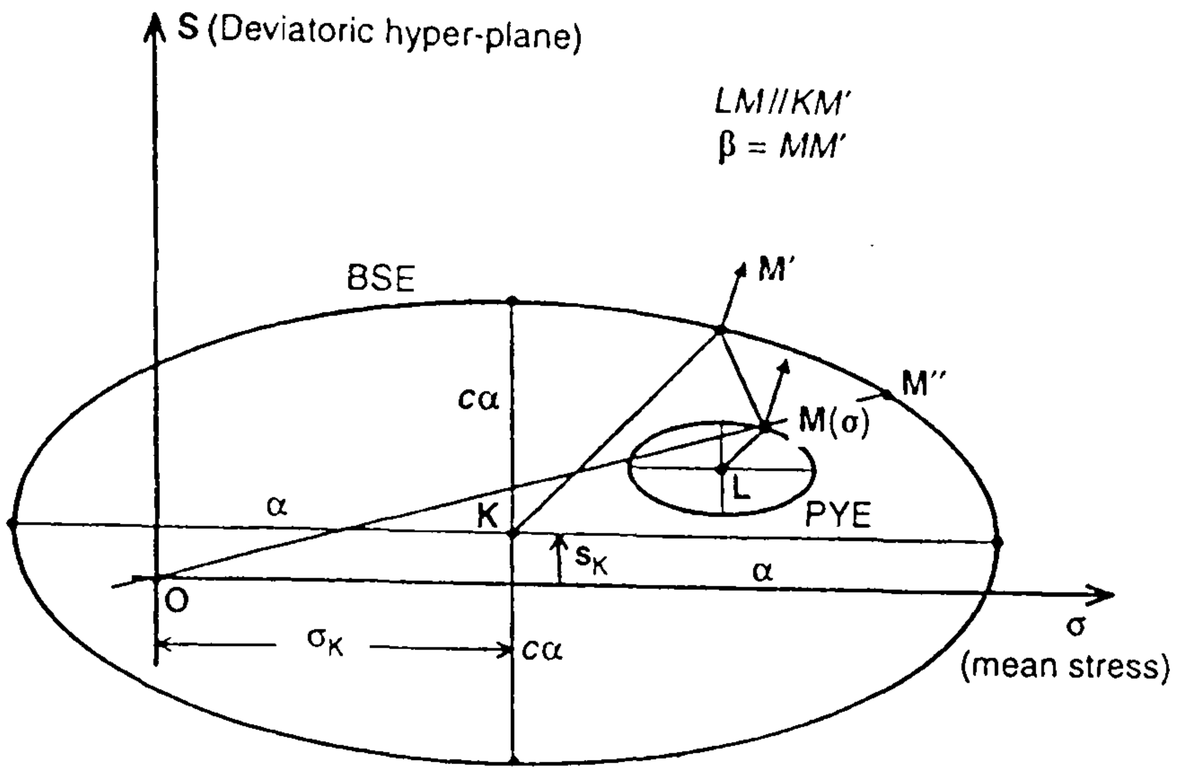

Figure 2.6.8 Characteristic surfaces for the Model for Structured Soils (after Kavvadas & Amorosi, 2000)

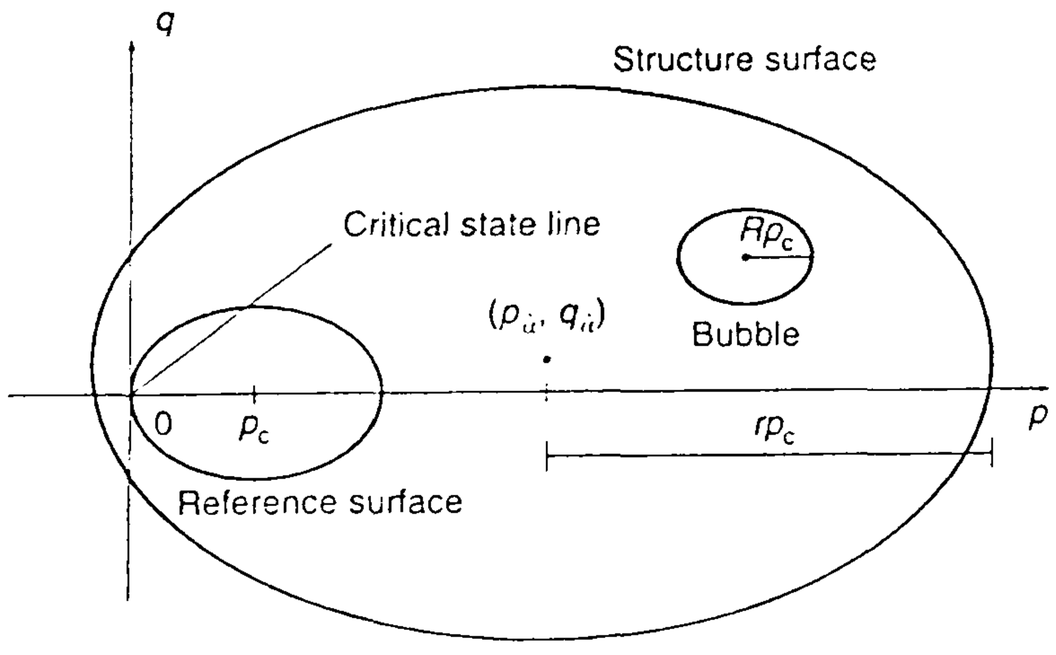

Figure 2.6.9 Characteristic surfaces for the Model for destructuration of clays (after Rouainia & Muir Wood, 2000)

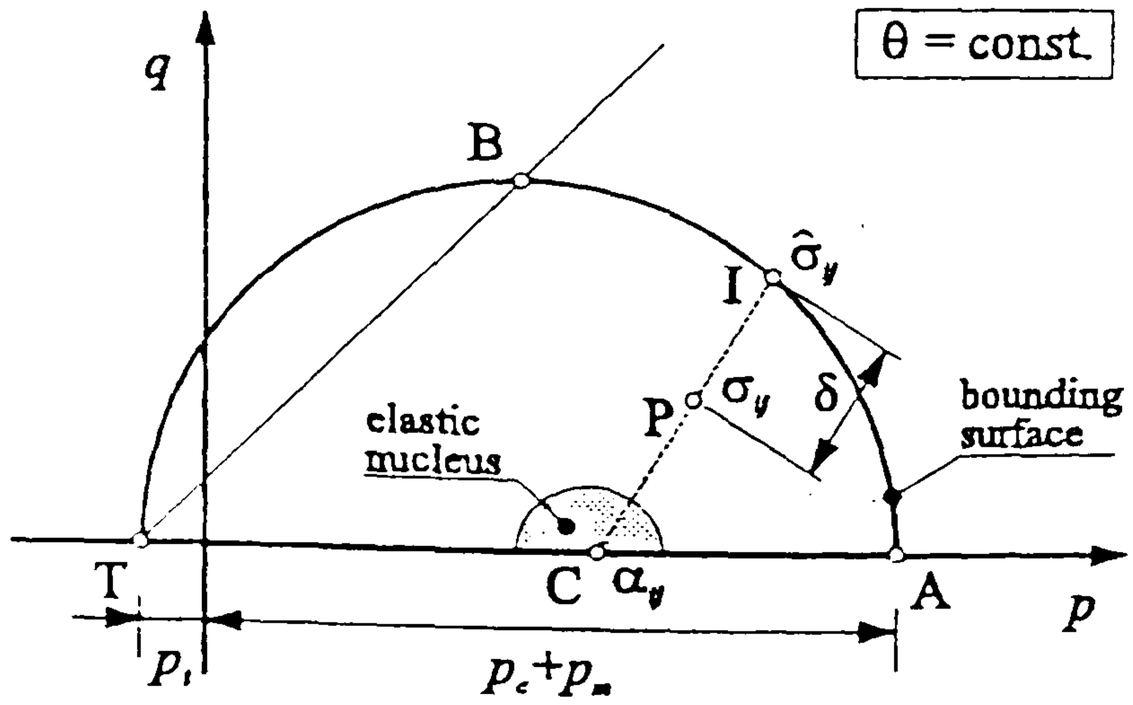

Figure 2.6.10 Characteristic surfaces for the bounding plasticity model for structured clays (after Tamagnini & d'Elia, 1999)

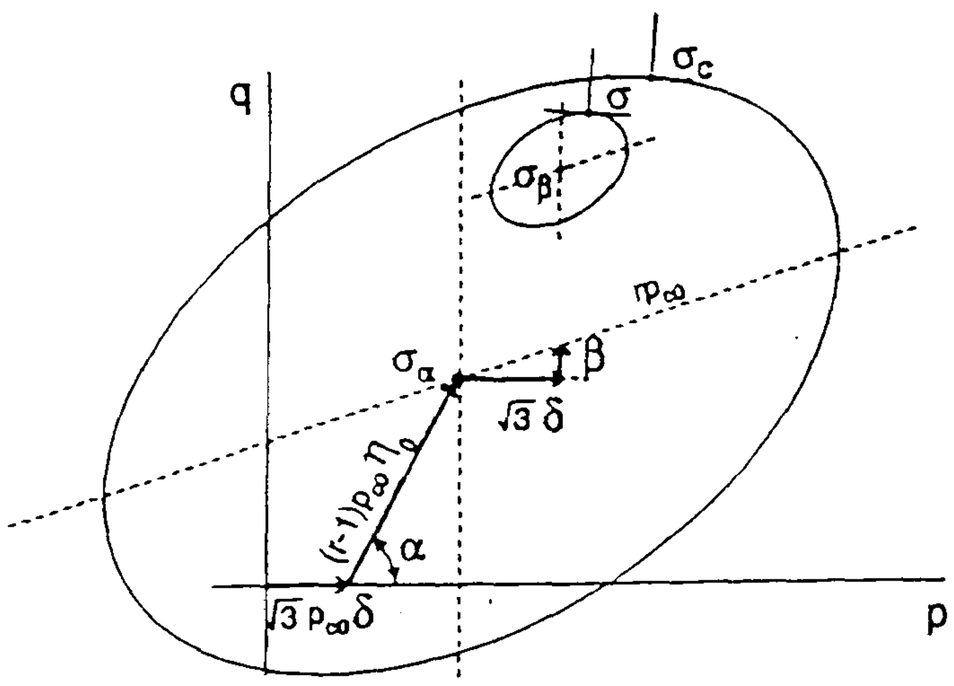

Figure 2.6.11 Characteristic surfaces for the anisotropic model with destructuration of clays (after Gajo & Muir Wood, 2001)

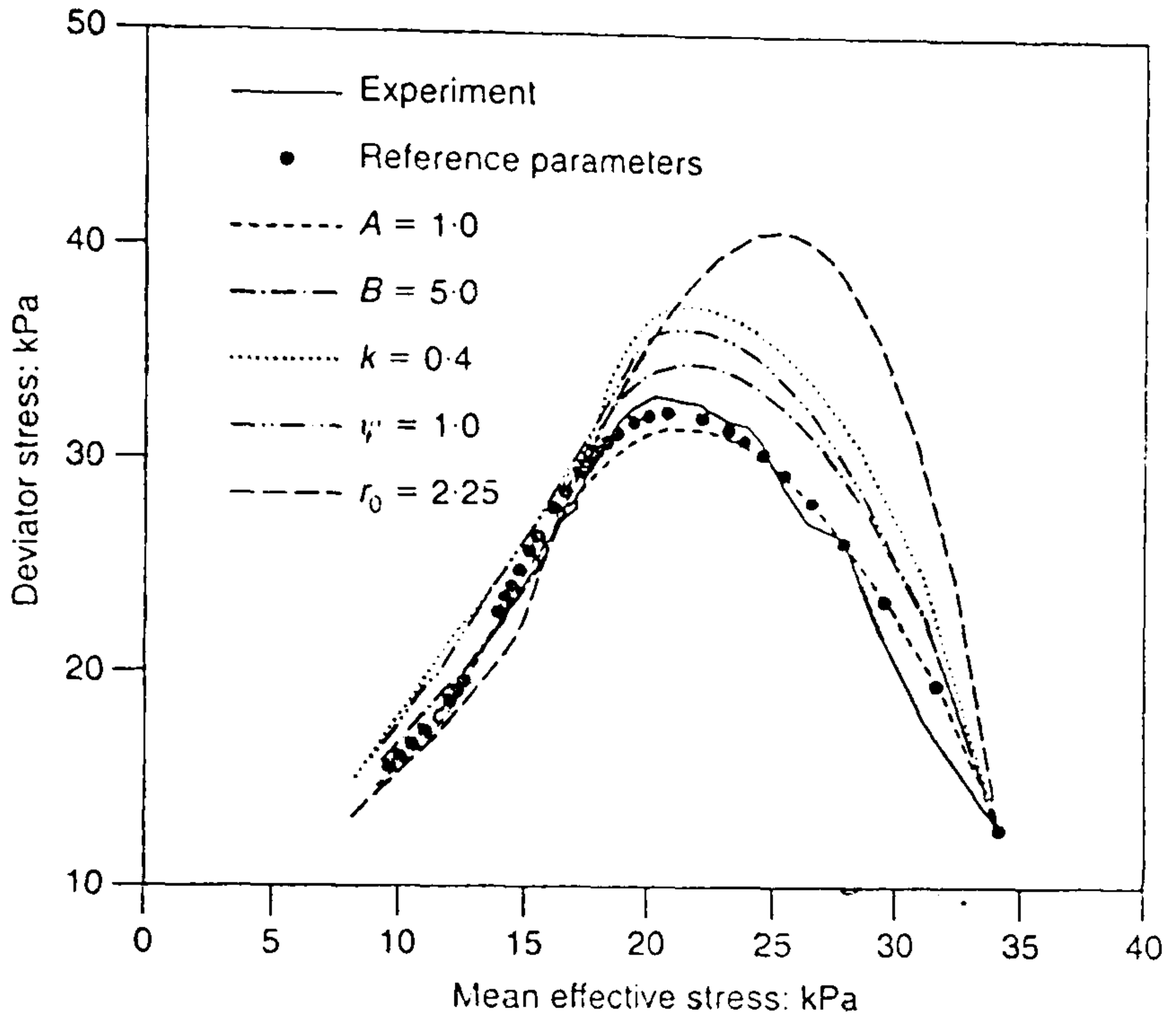

Figure 2.6.12 Effect of varying parameters on predicted stress path during undrained triaxial compression tests on Norrköping clay (after Rouainia & Muir Wood, 2000)

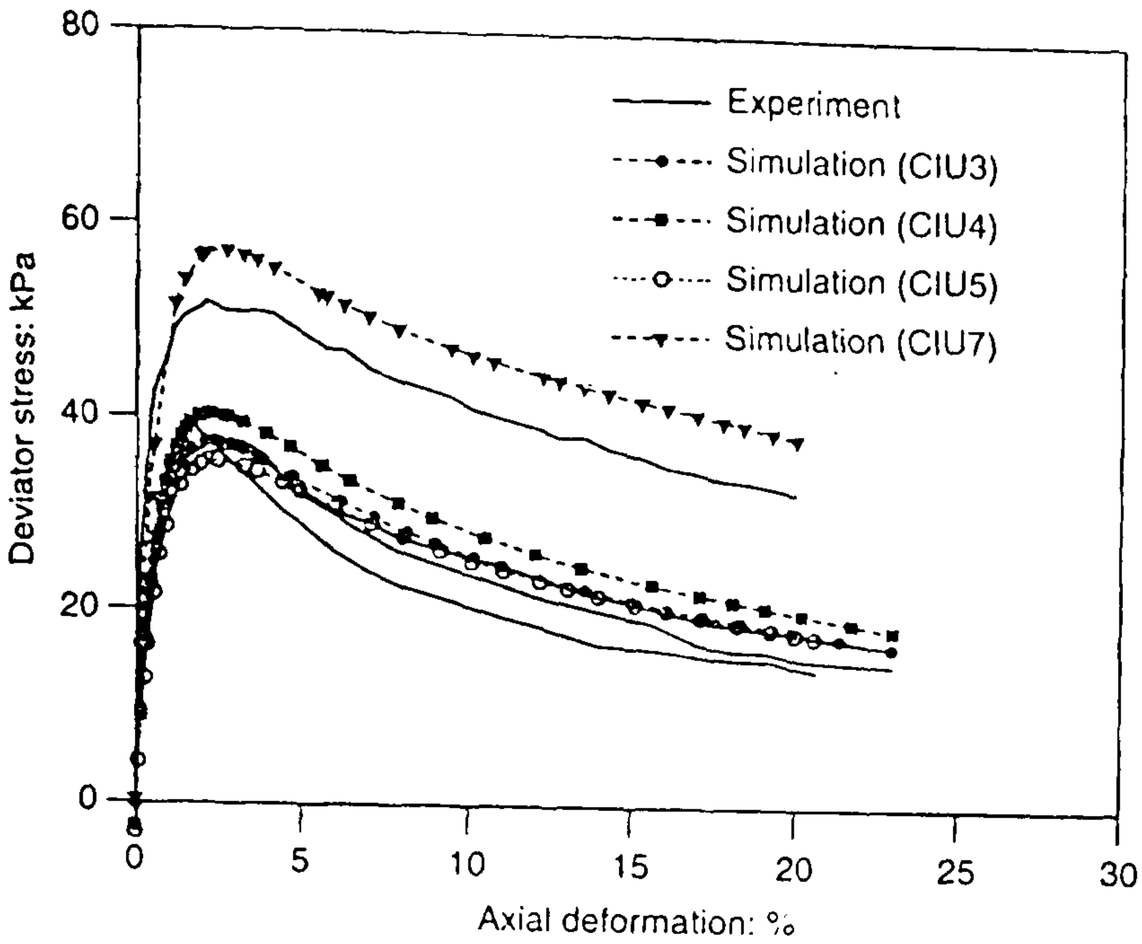

(a)

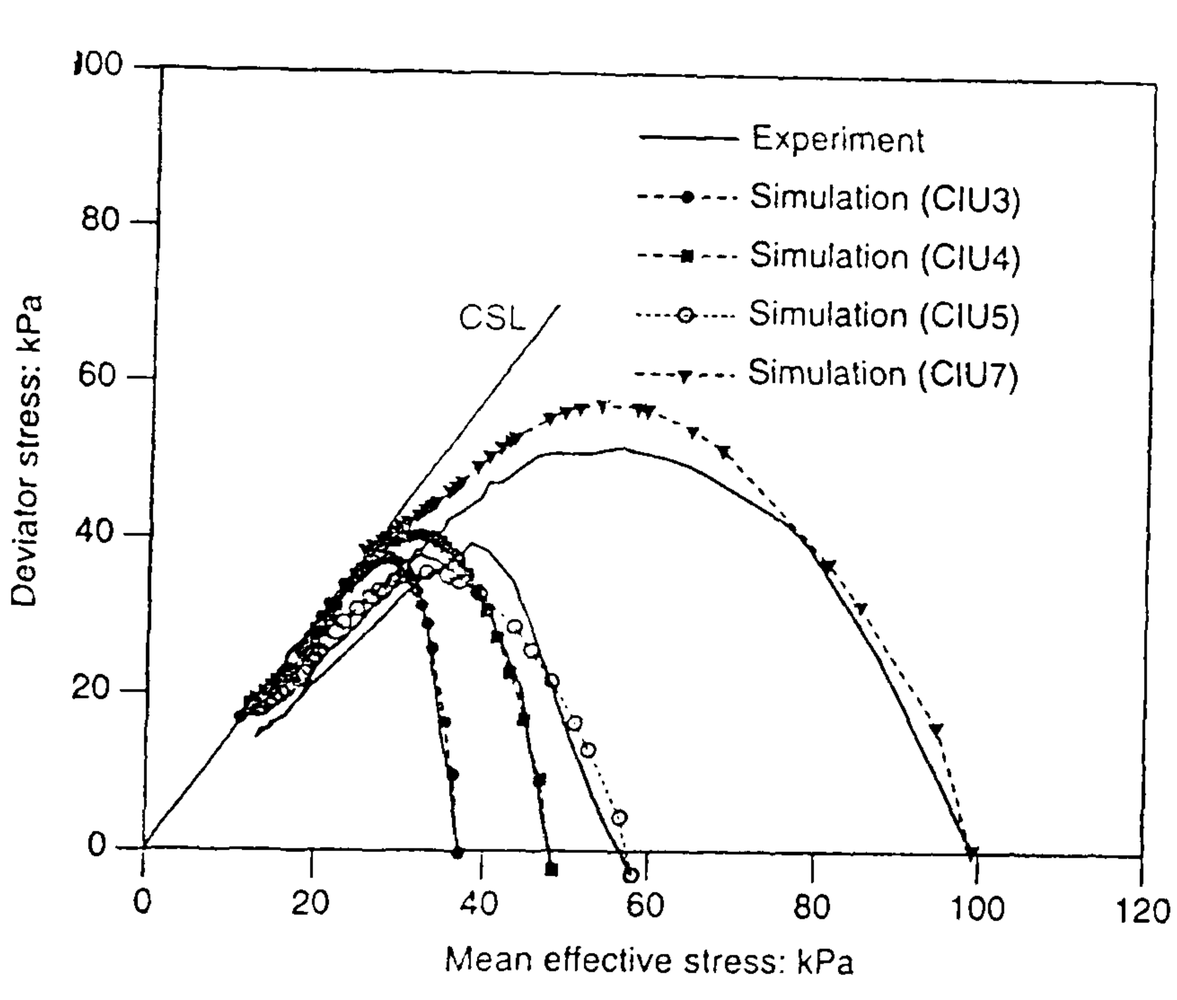

(b)

Figure 2.6.13 Comparison of computed and experimental data for undrained triaxial compression tests on isotropically consolidated clay (a) stress-strain response (b) effective stress paths (after Rouainia & Muir Wood, 2000)

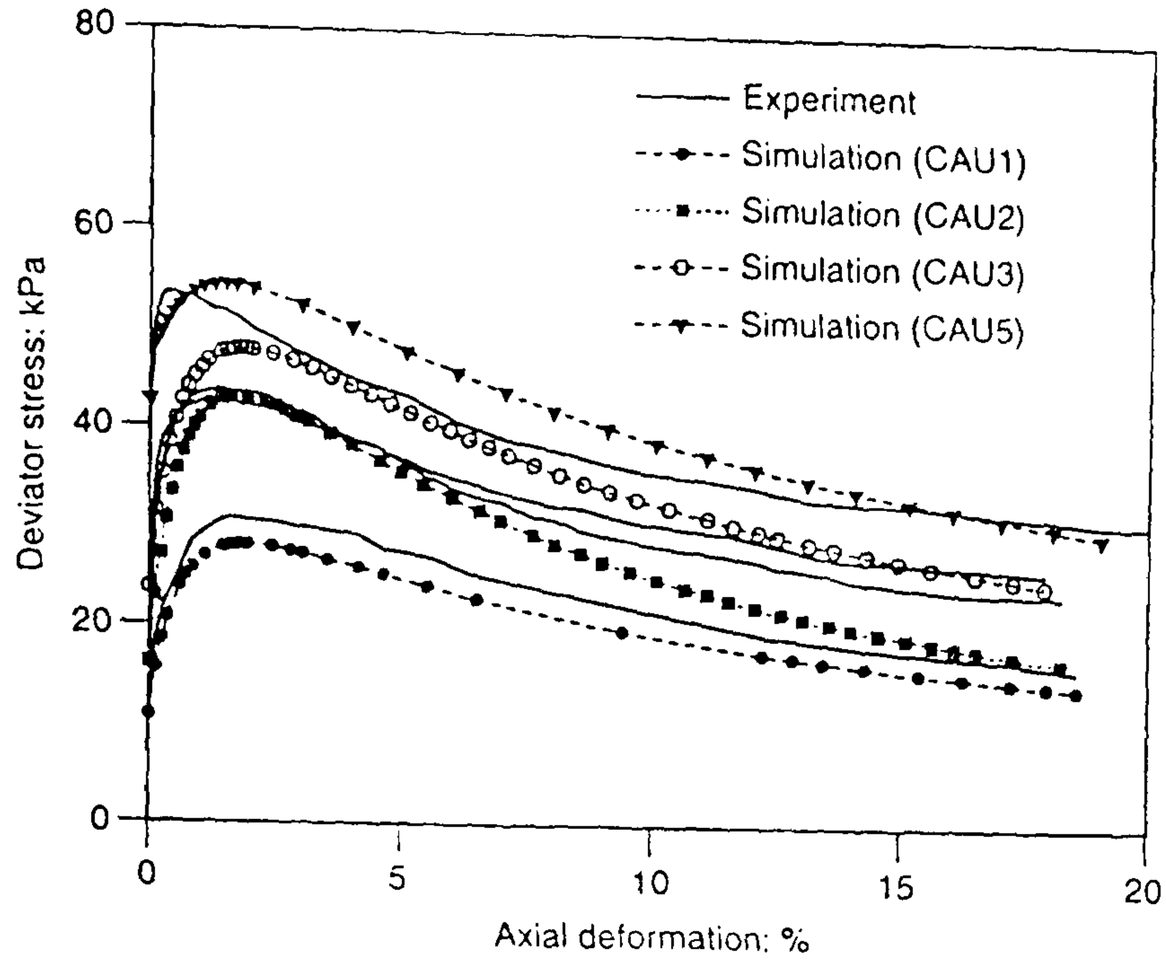

(a)

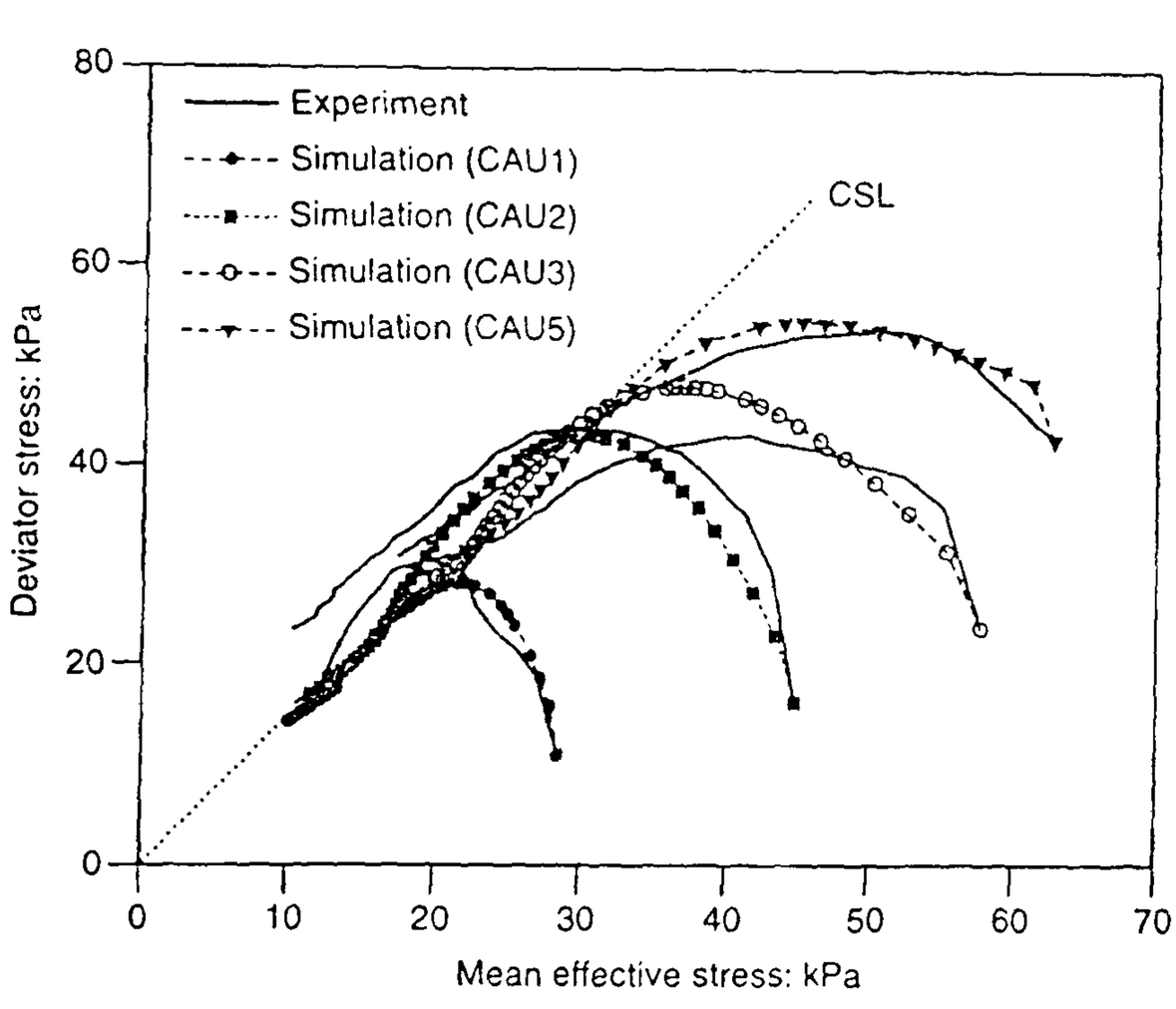

(b)

Figure 2.6.14 Comparison of computed and experimental data for undrained triaxial compression tests on anisotropically consolidated clay (a) stress-strain response (b) effective stress paths (after Rouainia & Muir Wood, 2000)

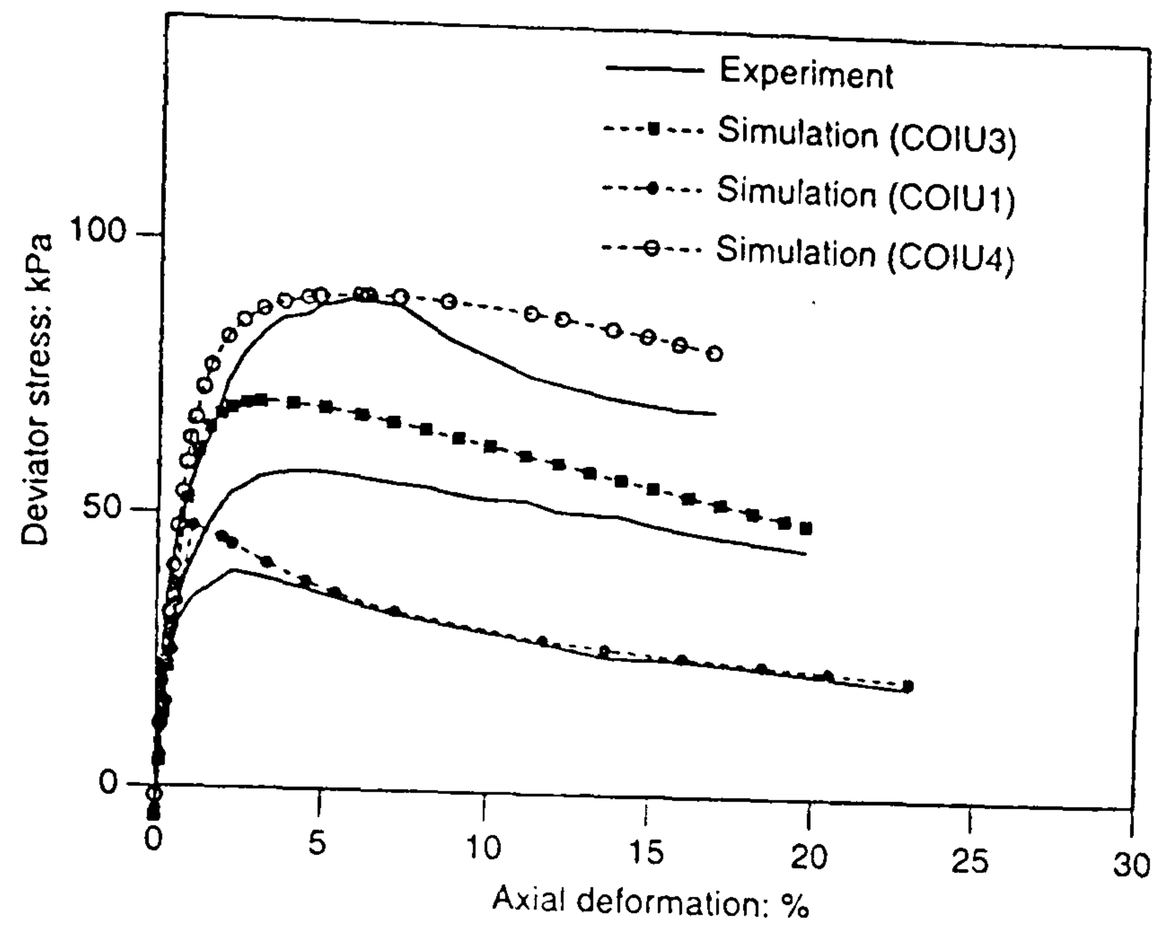

(a)

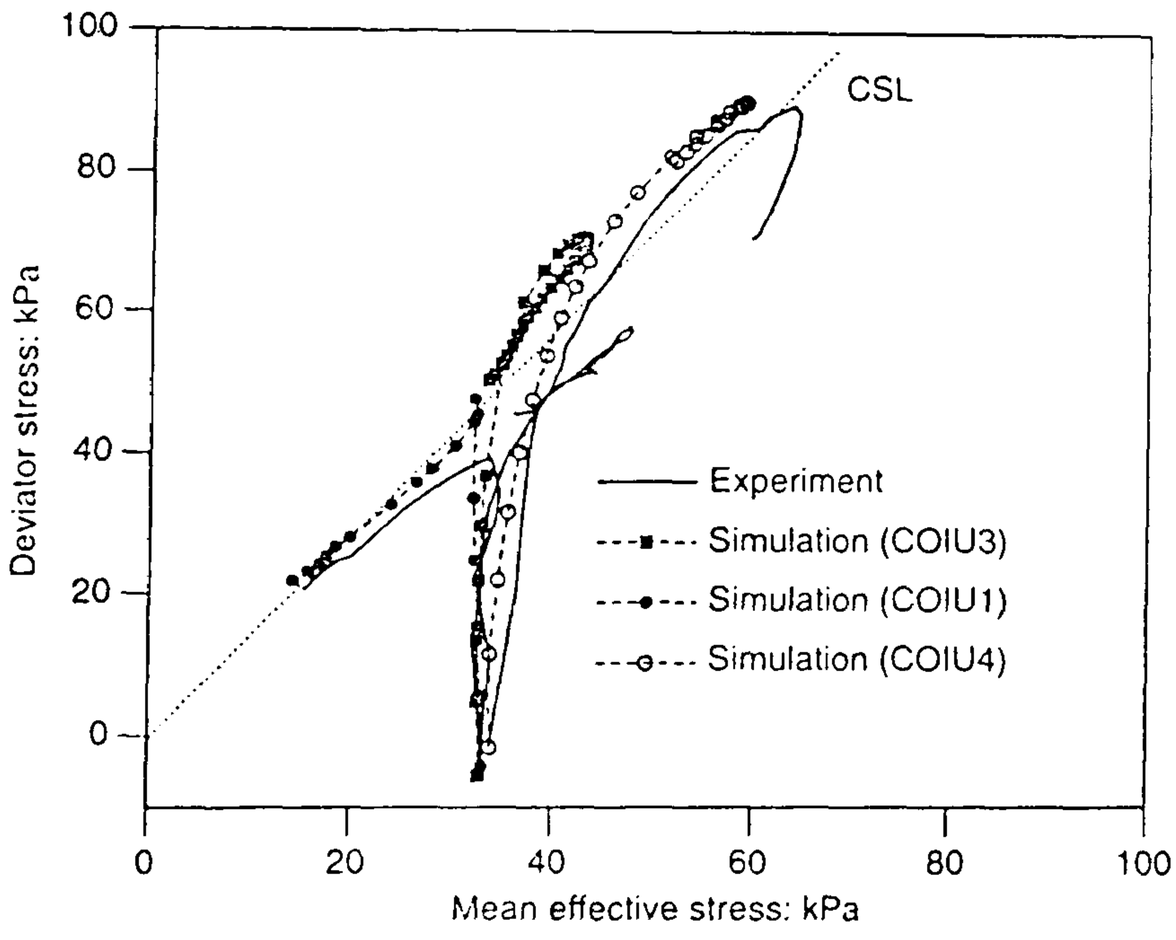

(b)

Figure 2.6.15 Comparison of computed and experimental data for undrained triaxial compression tests on isotropically overconsolidated clay (a) stress-strain response (b) effective stress paths (after Rouainia & Muir Wood, 2000)

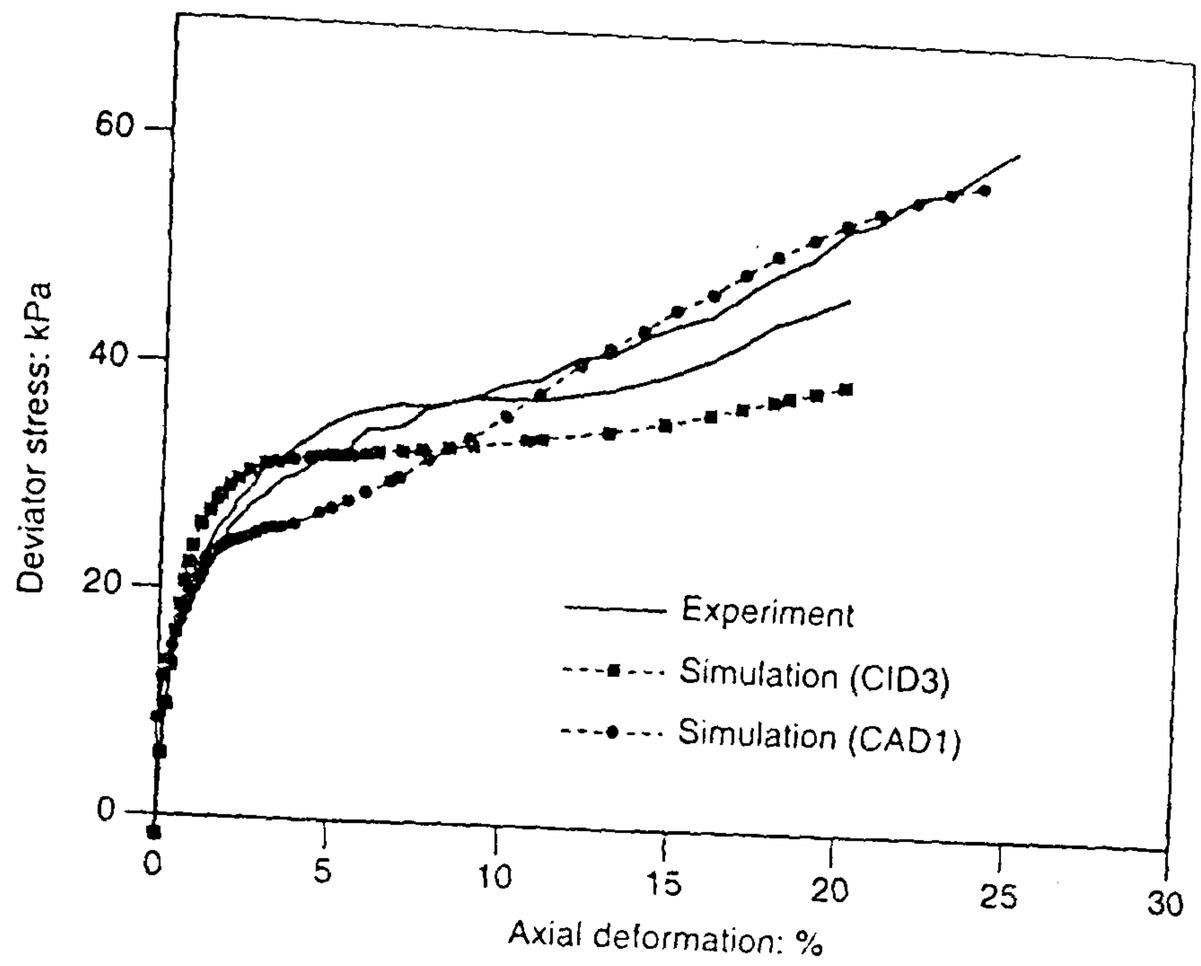

(a)

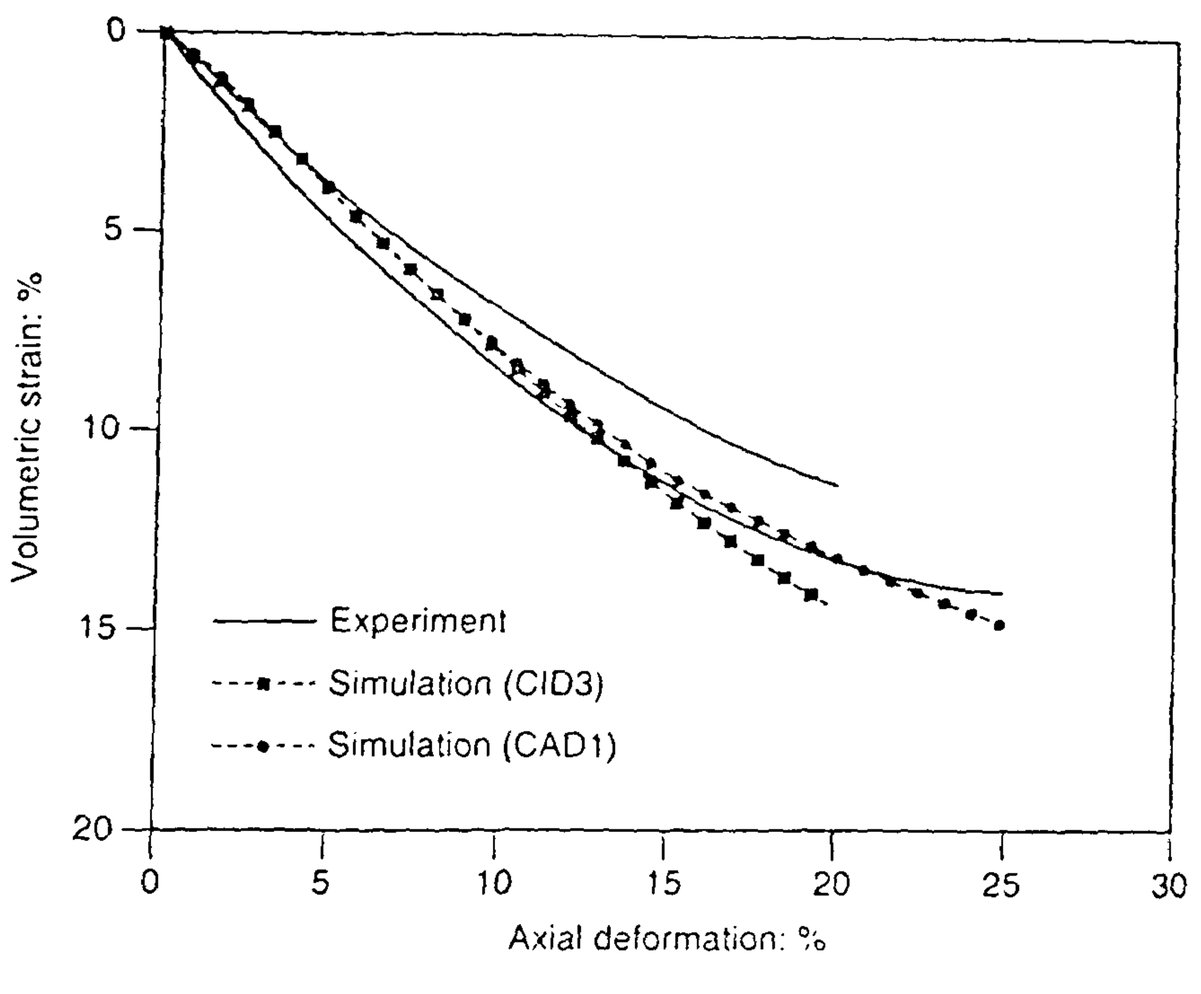

(b)

Figure 2.6.16 Comparison of computed and experimental data for drained triaxial compression tests on isotropically and anisotropically consolidated clay (a) stress-strain response (b) volumetric strain (after Rouainia & Muir Wood, 2000)

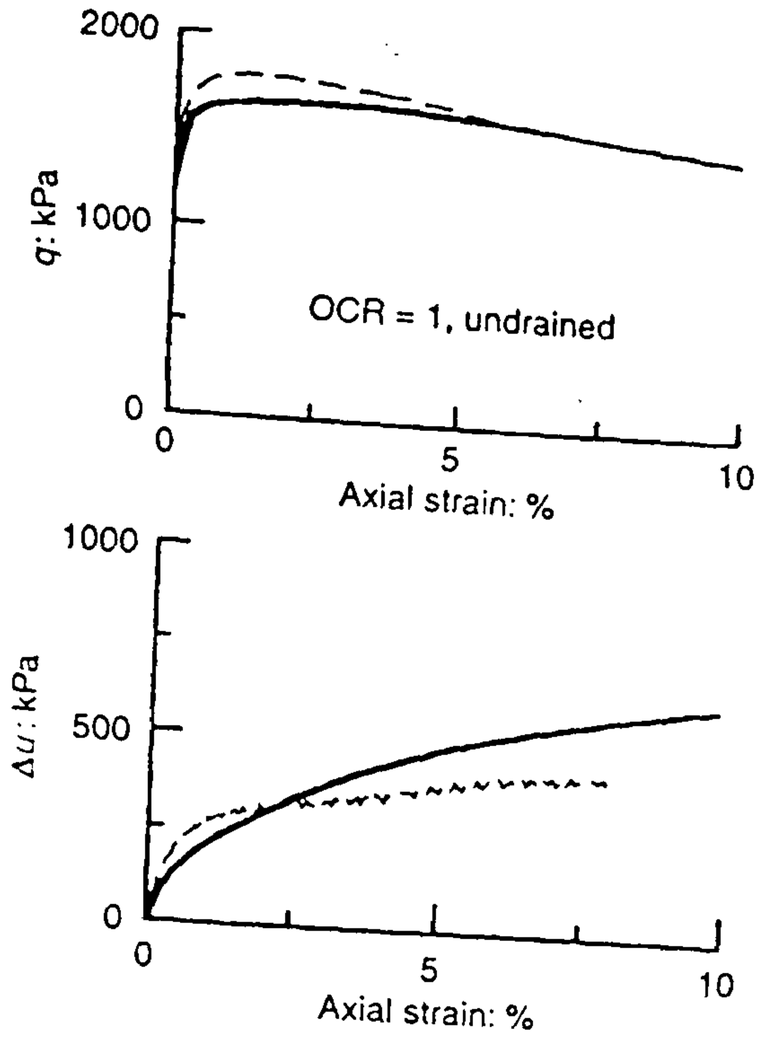

(a)

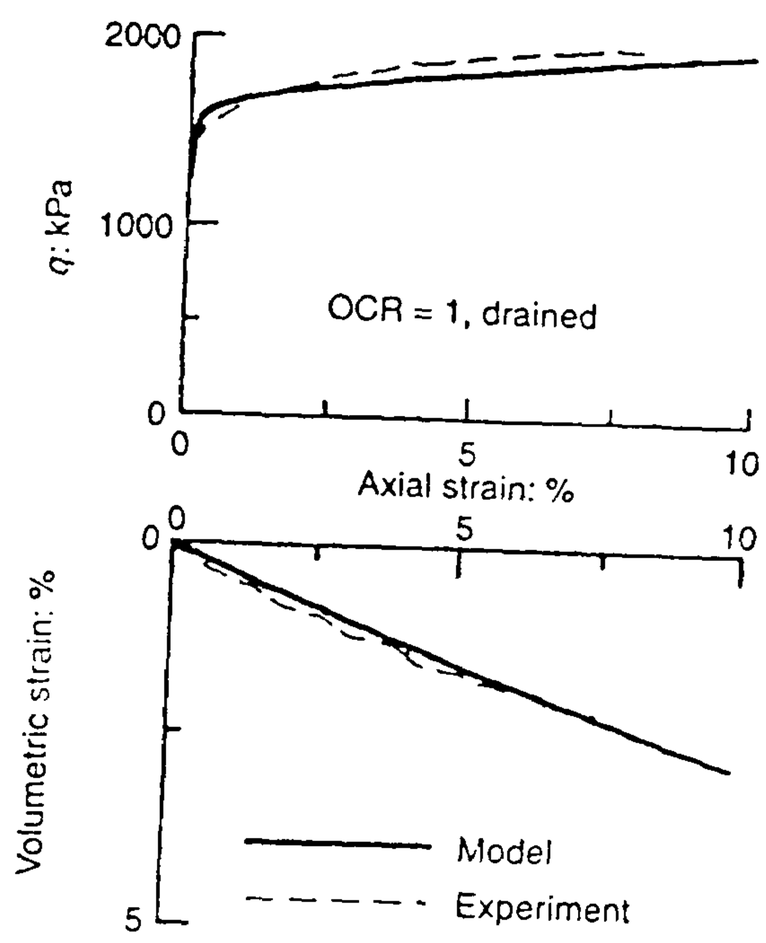

(b)

Figure 2.6.17 Comparison of computed and experimental data for triaxial compression tests on anisotropically consolidated Vallericca clay (a) undrained test (b) drained test (after Kavvadas & Amorosi, 2000)

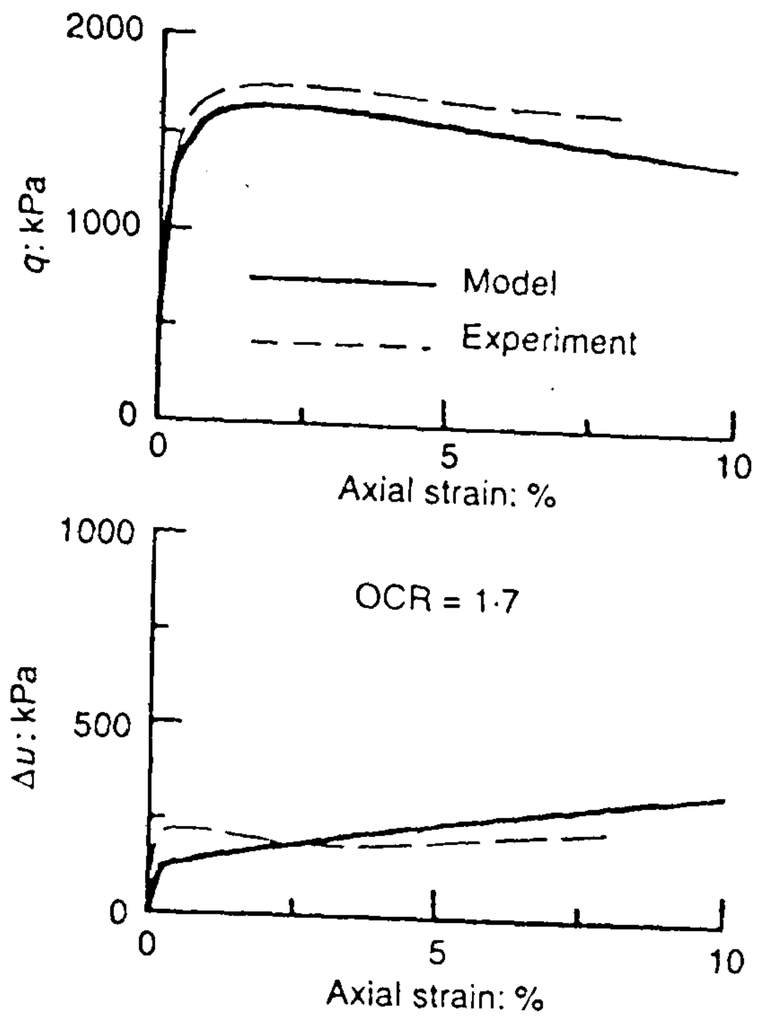

(a)

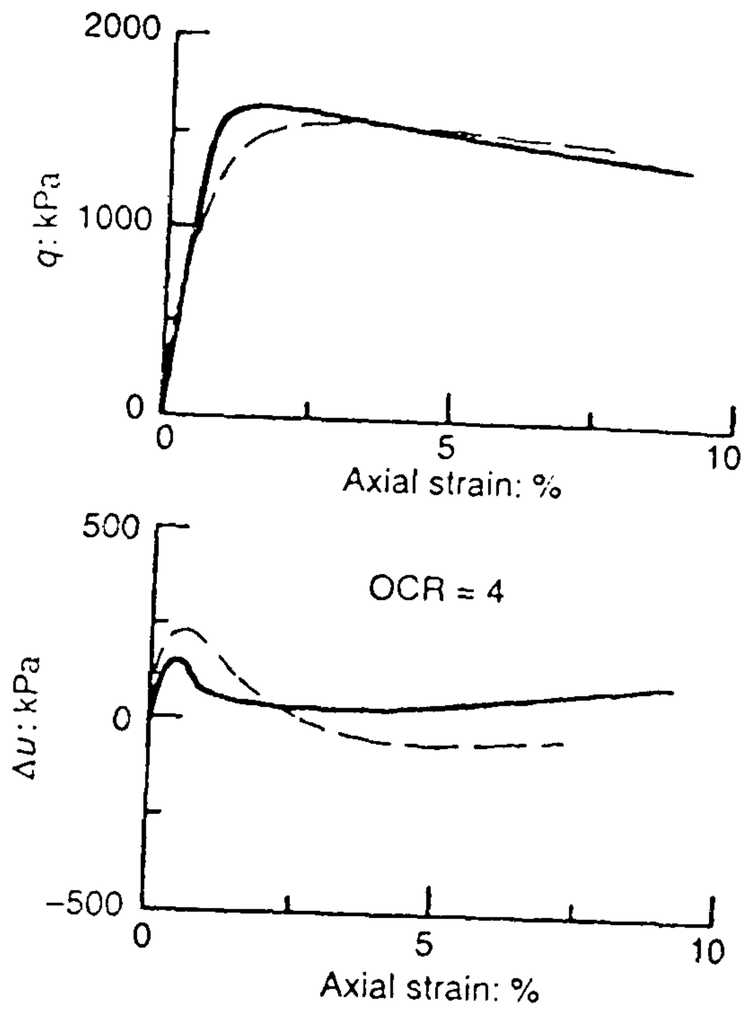

(b)

Figure 2.6.18 Comparison of computed and experimental data for triaxial compression tests on anisotropically overconsolidated Vallericca clay (a) OCR=1.7 (b) OCR=4 (after Kavvadas & Amorosi, 2000)

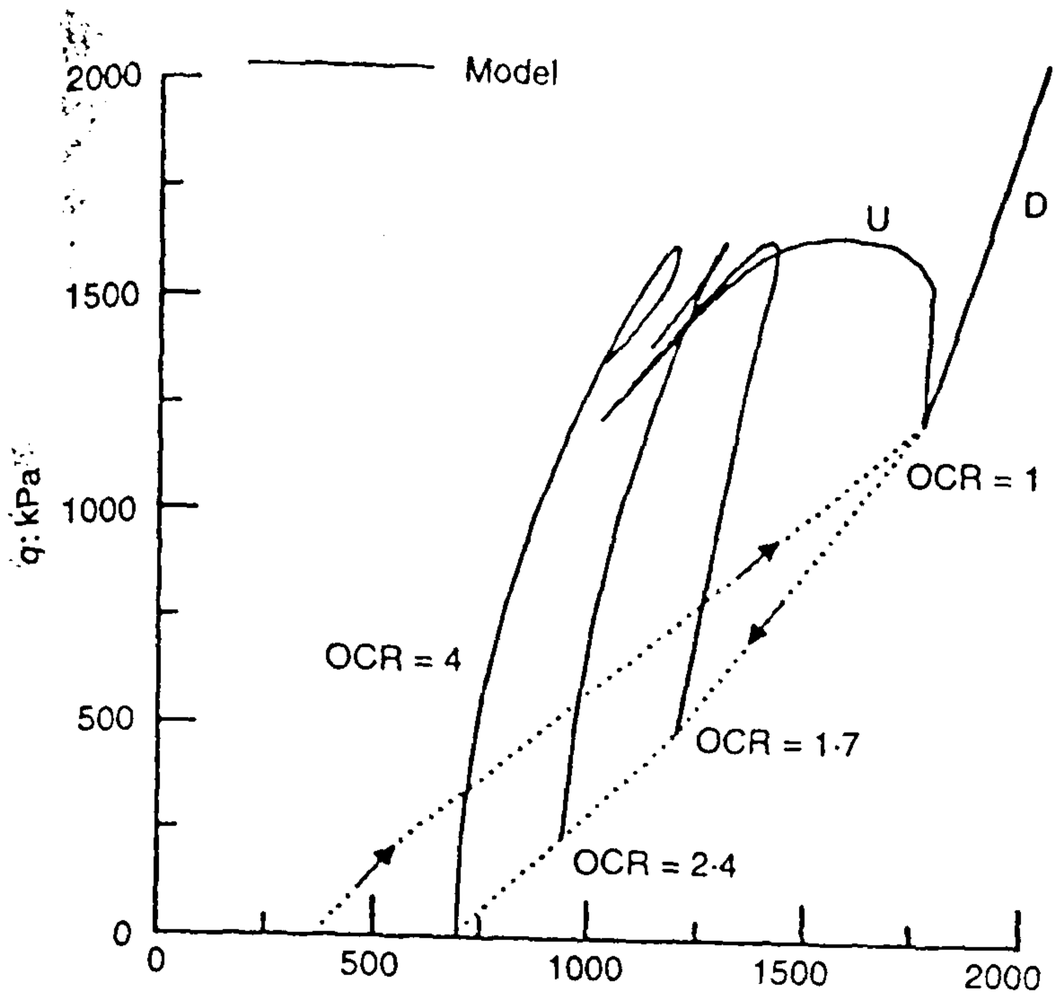

(a)

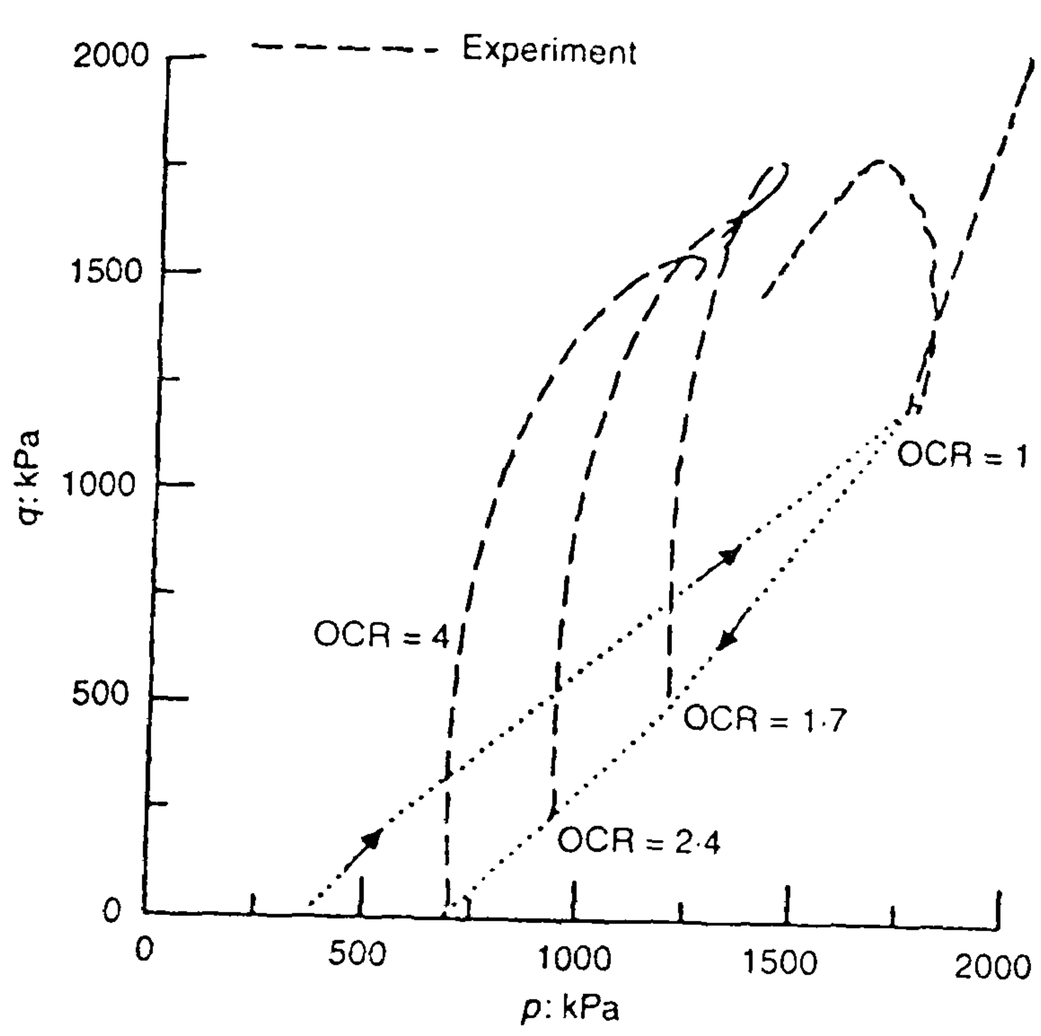

(b)

Figure 2.6.19 Comparison of computed and experimental stress paths for drained (D) and undrained (U) triaxial compression tests on anisotropically consolidated and overconsolidated Vallericca clay (a) prediction (b) experiment (after Kavvadas & Amorosi, 2000)

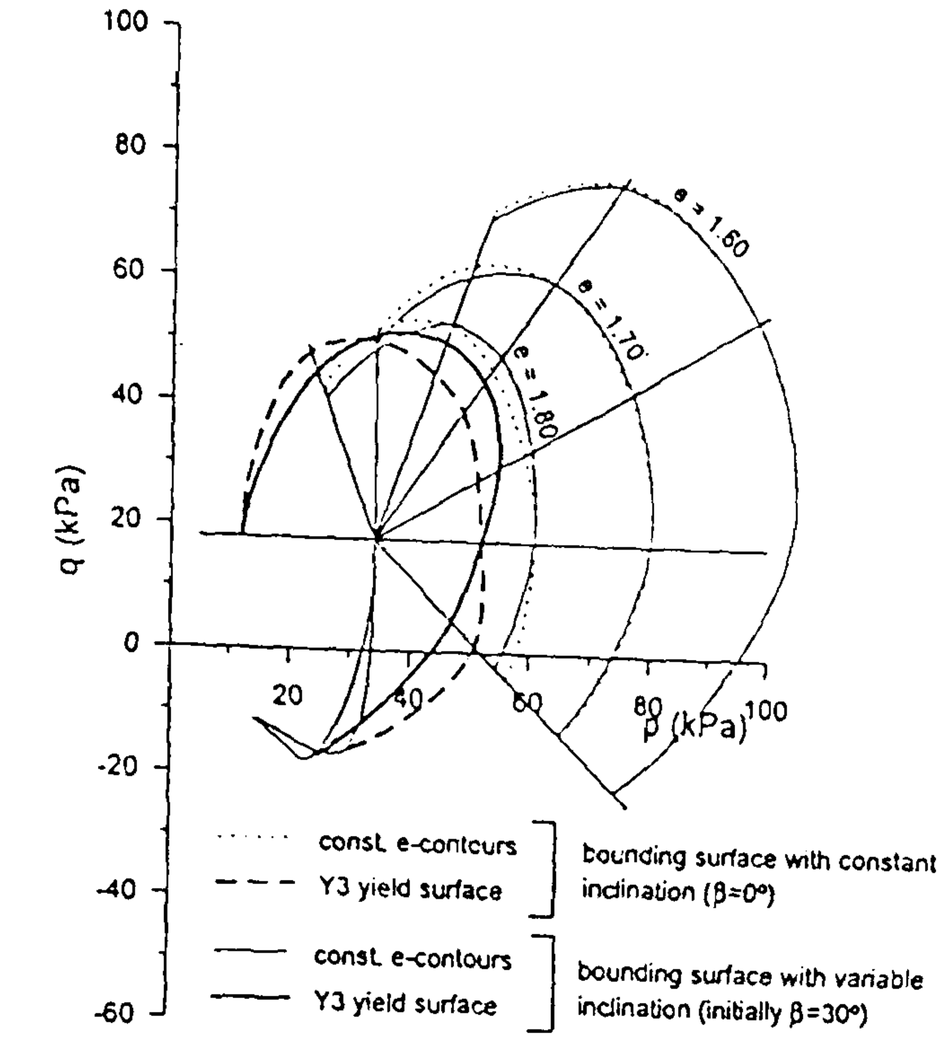

(a)

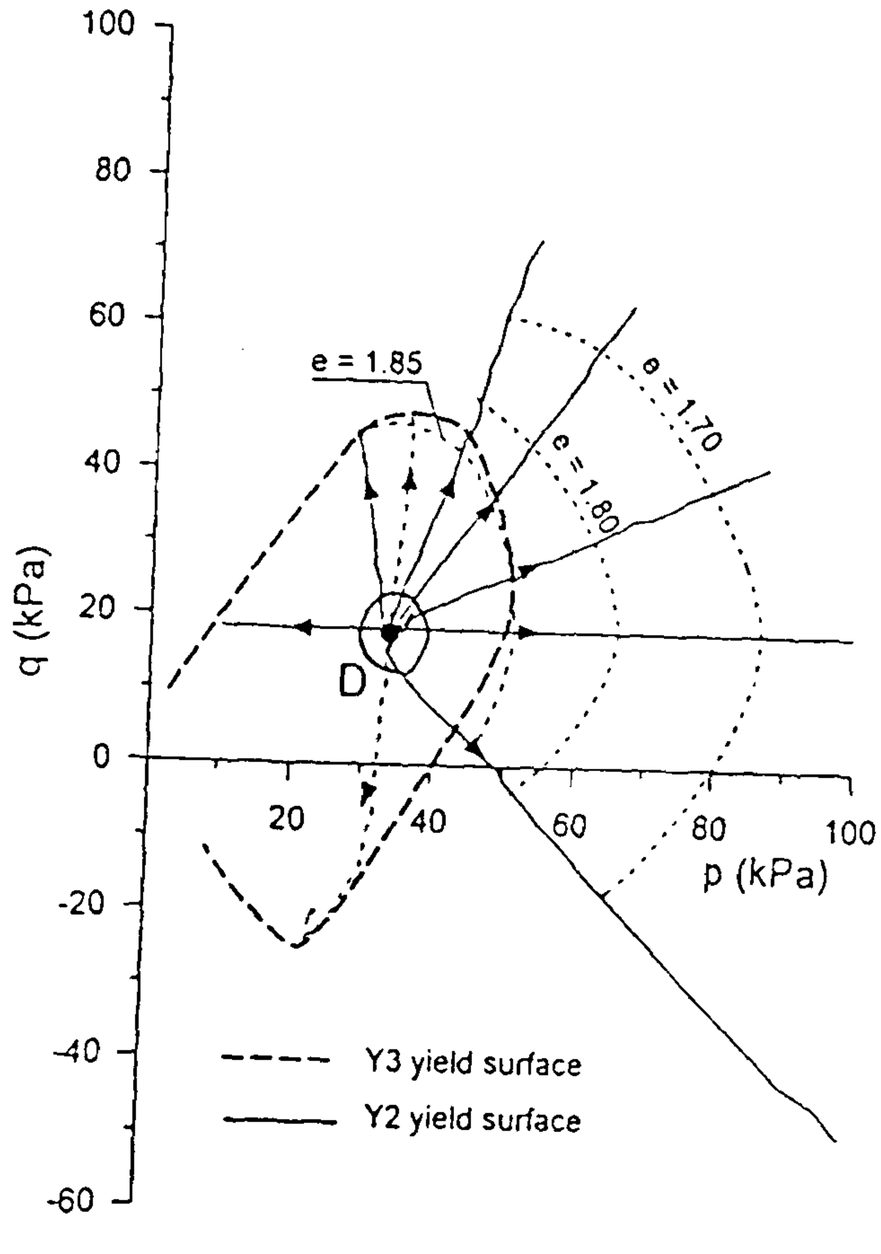

(b)

Figure 2.6.20 Comparison between (a) predicted yielding characteristics of natural Bothkennar clay in drained probes obtained with rotating surfaces and with surfaces having a constant inclination of 0° in q-p plot
(b) experimental results by Smith *et al.* (2000)
(after Gajo & Muir Wood, 2001)

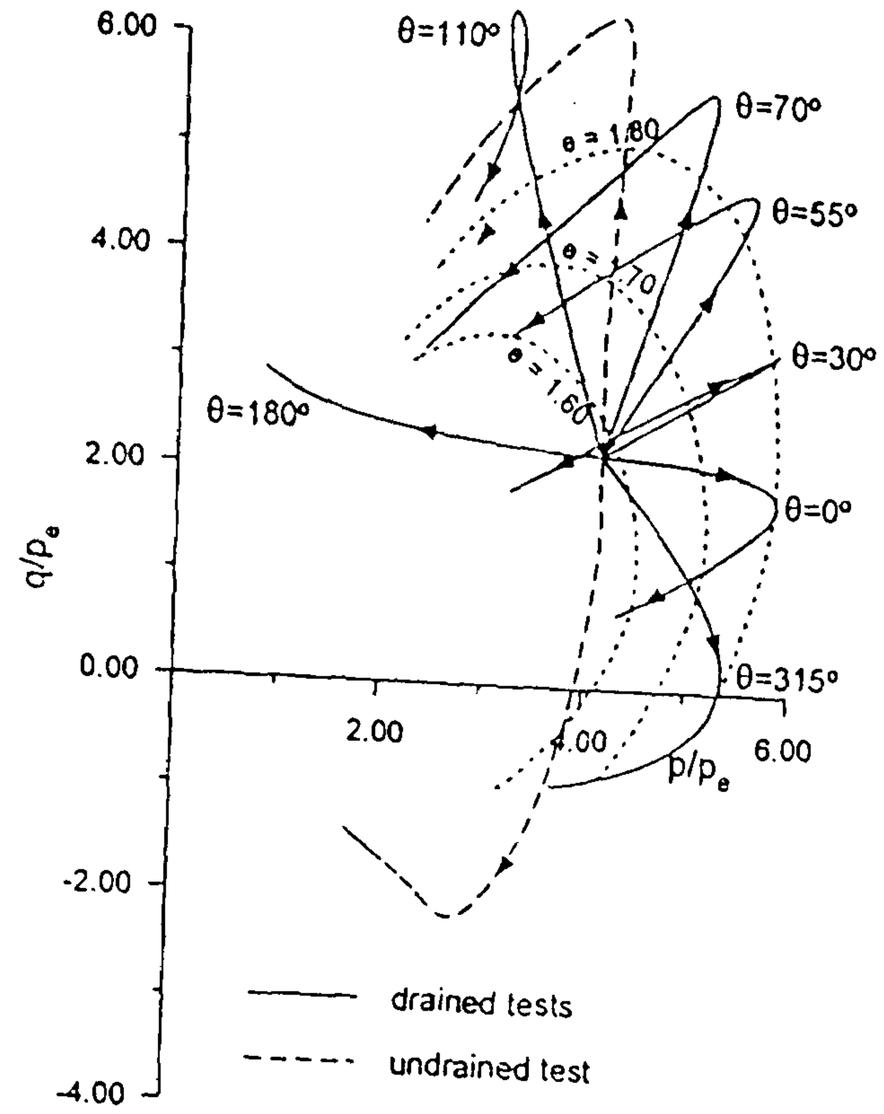

(a)

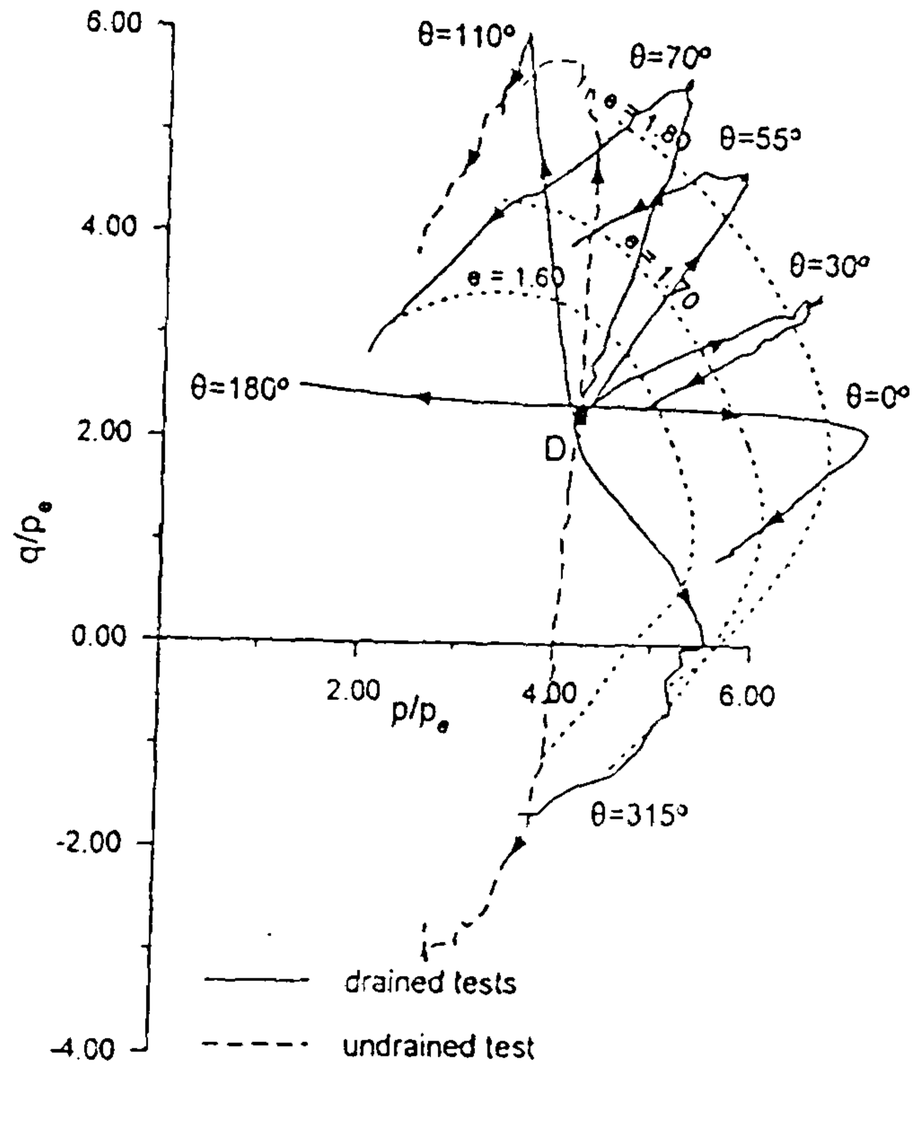

(b)

Figure 2.6.21 Comparison between (a) predicted normalised large strain behaviour of natural Bothkennar clay in drained probes and (b) experimental results by Smith *et al.* (1992) (after Gajo & Muir Wood, 2001)

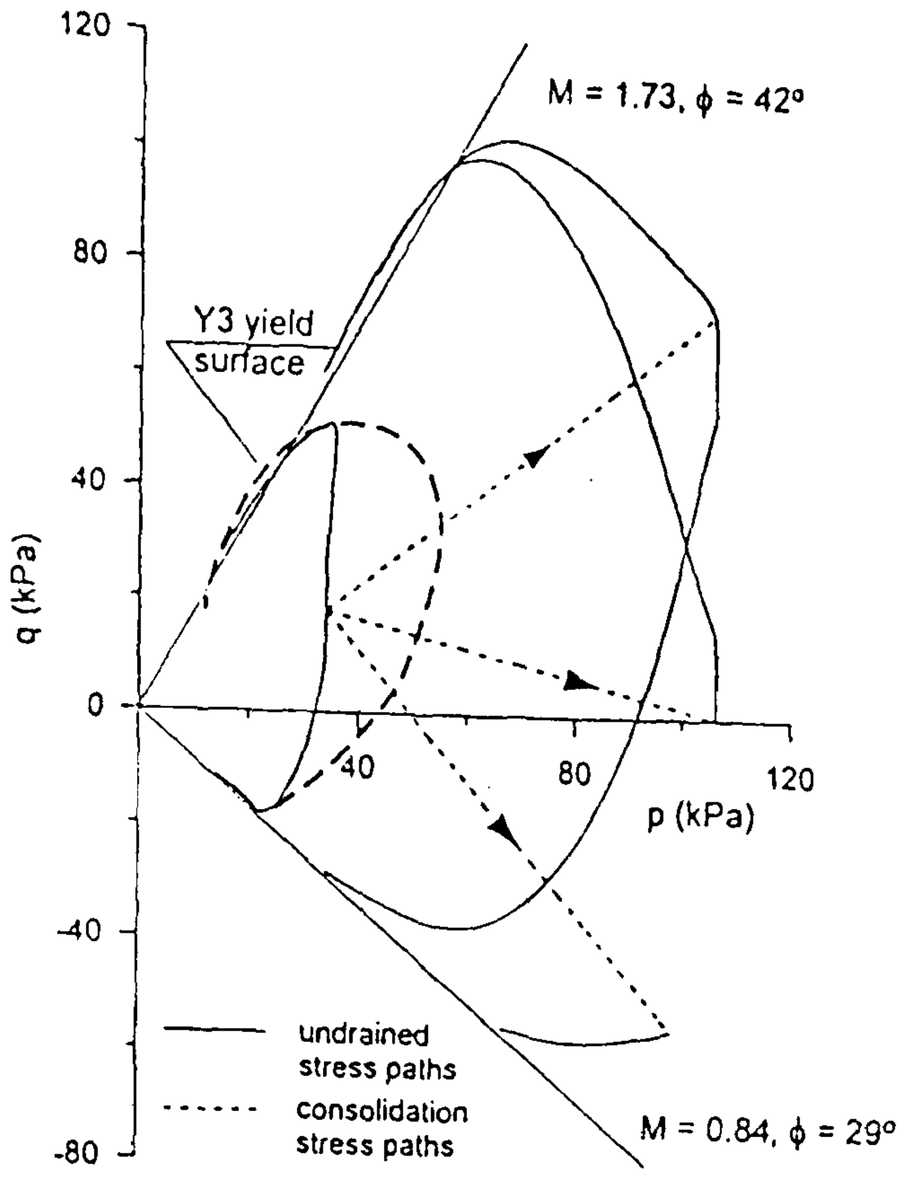

(a)

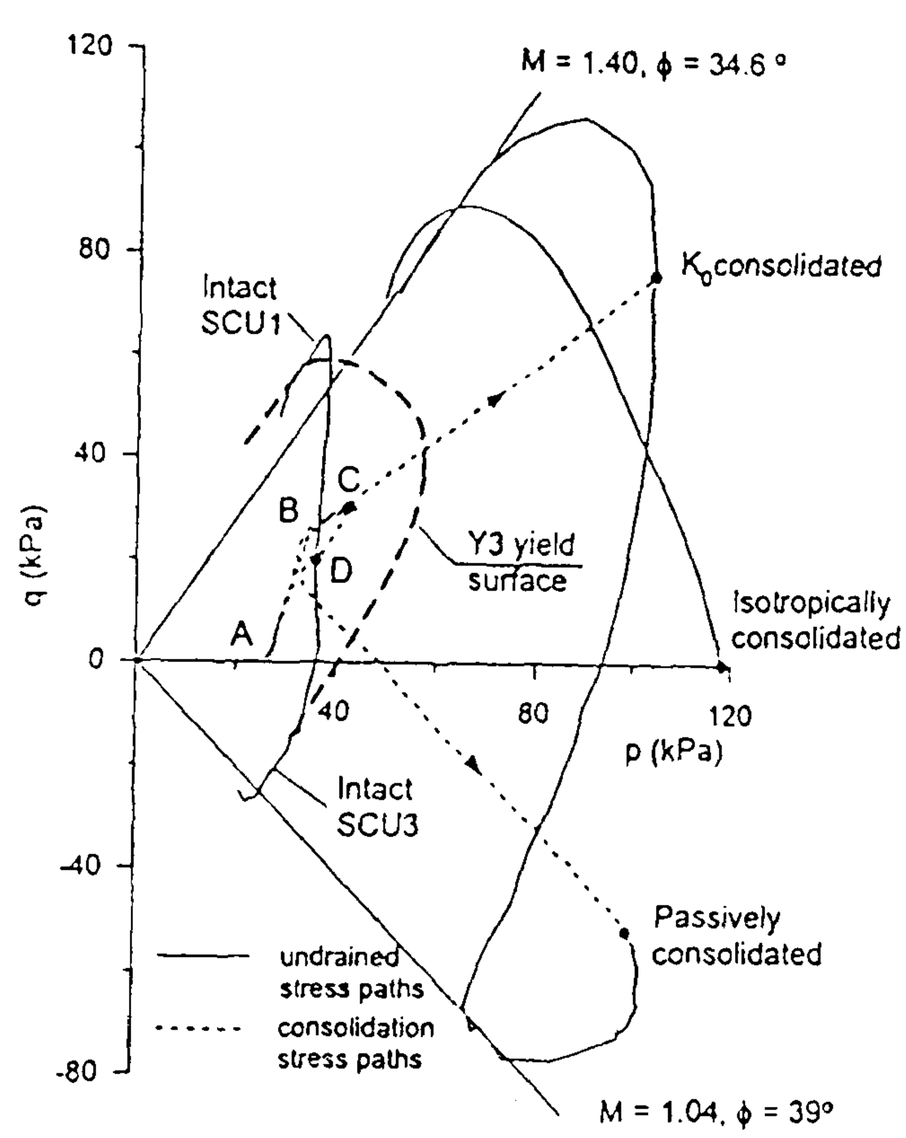

(b)

Figure 2.6.22 Comparison between (a) predicted and (b) measured undrained effective stress paths followed by natural Bothkennar clay samples and by Bothkennar clay samples compressed beyond gross yield in triaxial tests (after Gajo & Muir Wood, 2001; test data from Smith *et al.*, 1992)

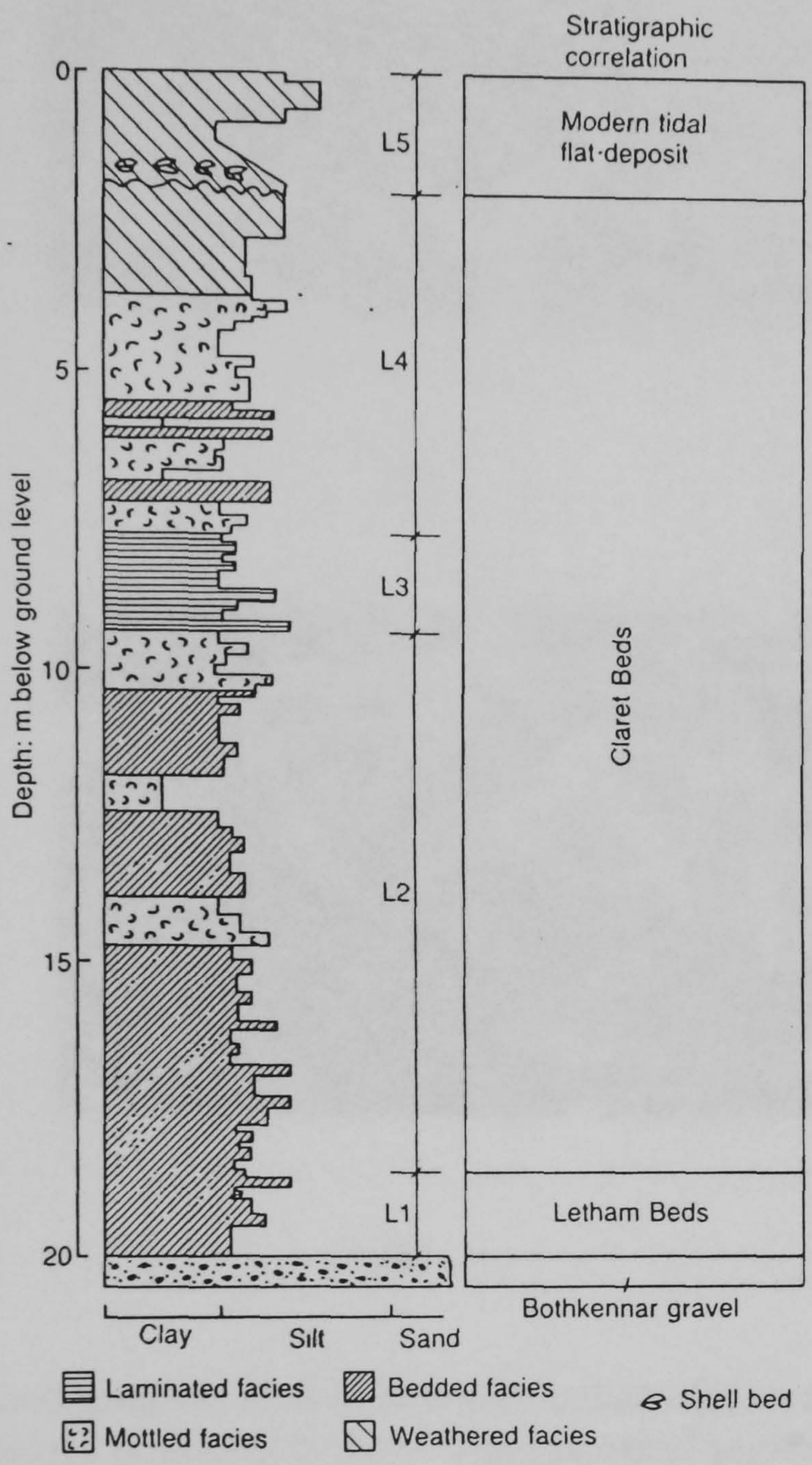

Figure 3.2.1 Facies sequence at Bothkennar (after Paul *et al.*, 1992)

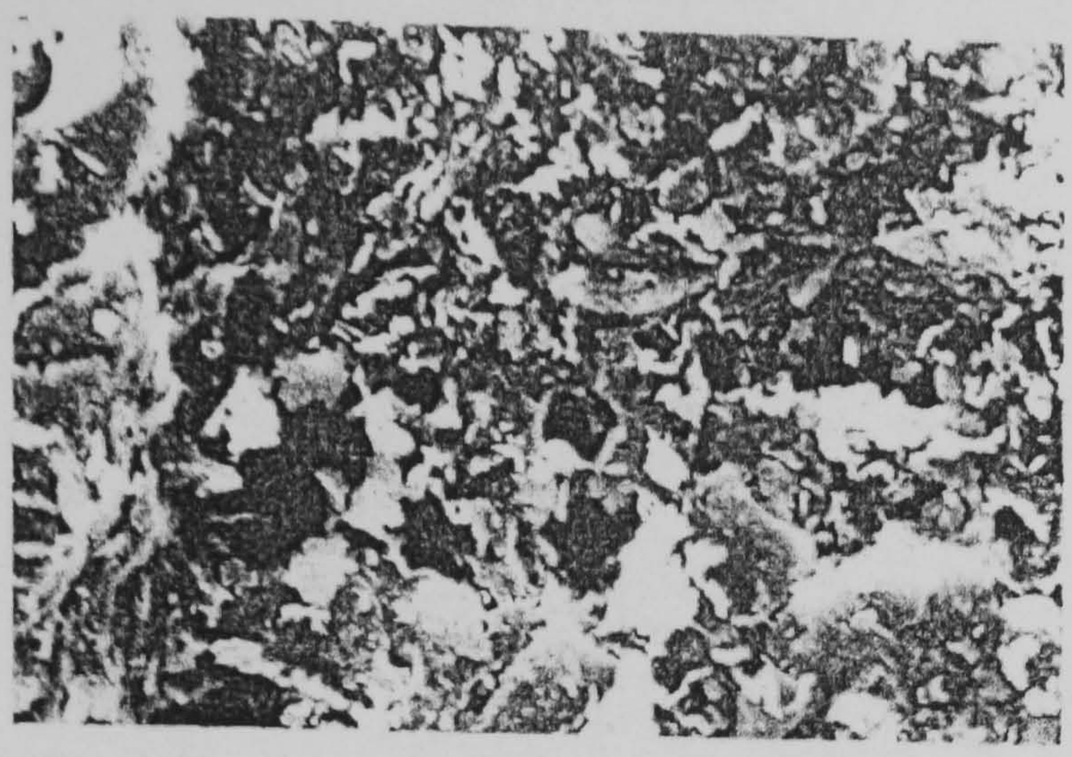

(a)

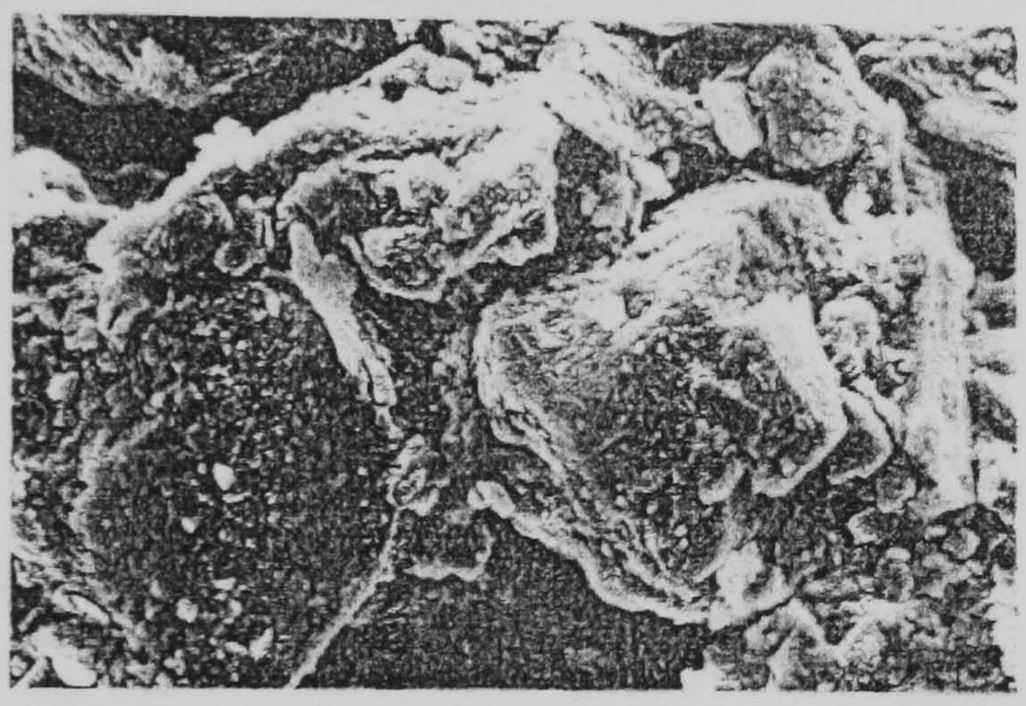

(b)

Figure 3.2.2 S.E.M. photograph of Bothkennar clay bedded facies showing (a) clay mineral fabric typical of bedded facies (vertical section) (b) silt-sized quartz grains being evidence of point cementation (after Paul *et al.*, 1992)

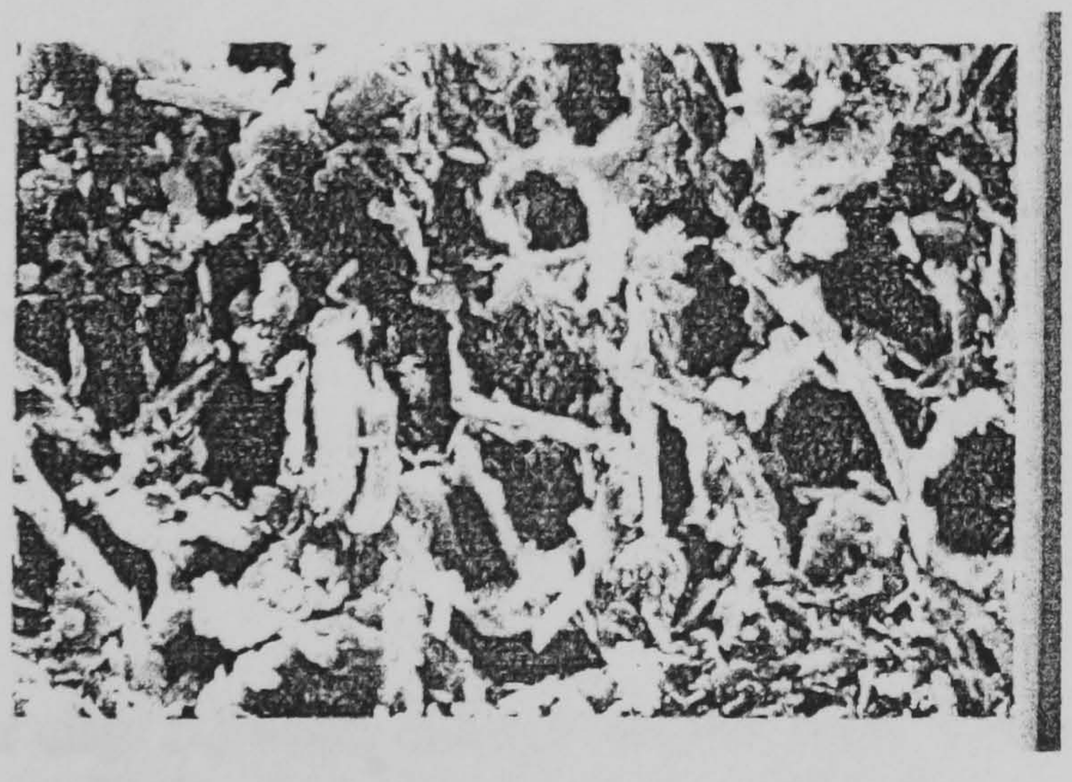

Figure 3.2.3 S.E.M. photograph showing Bothkennar clay fabric typical of the mottled facies (after Paul *et al.*, 1992)

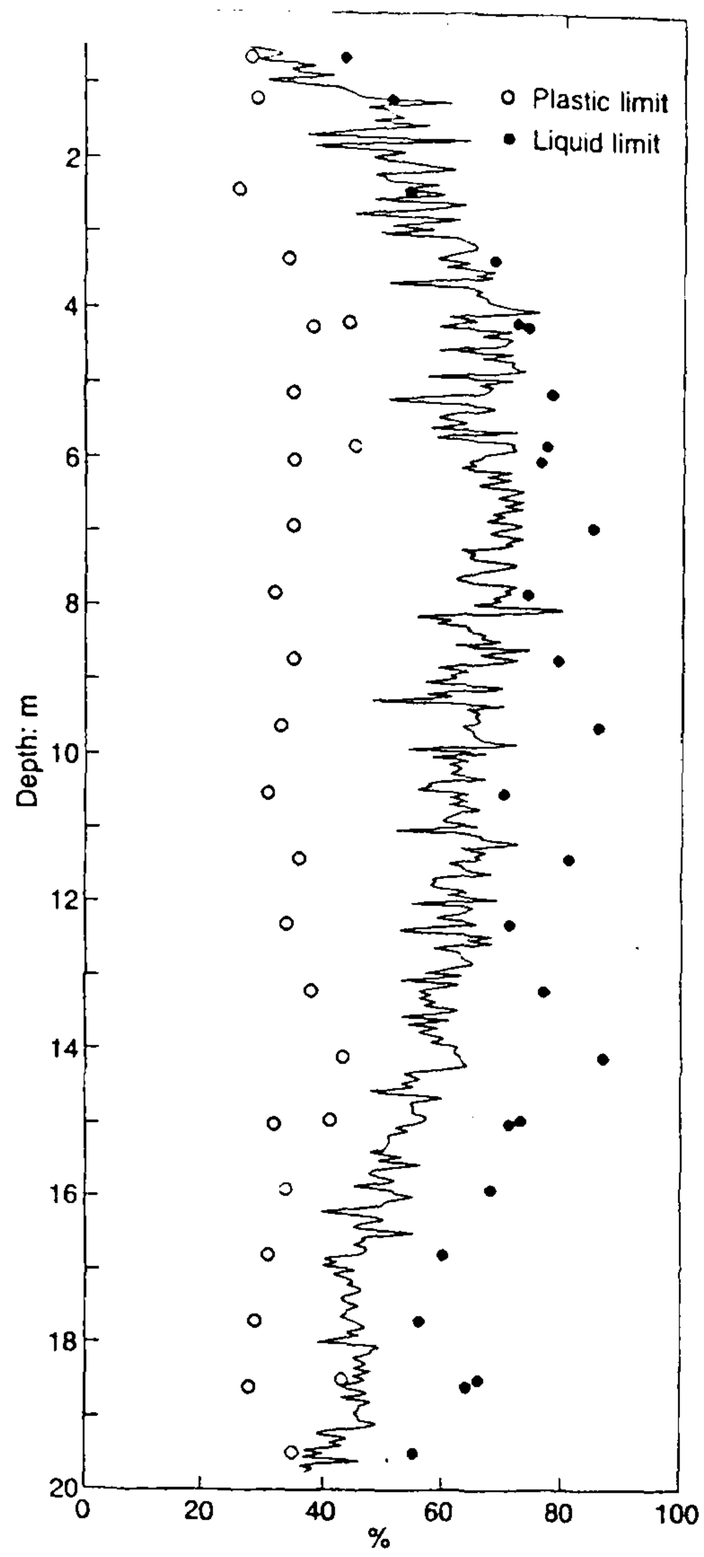

(a)

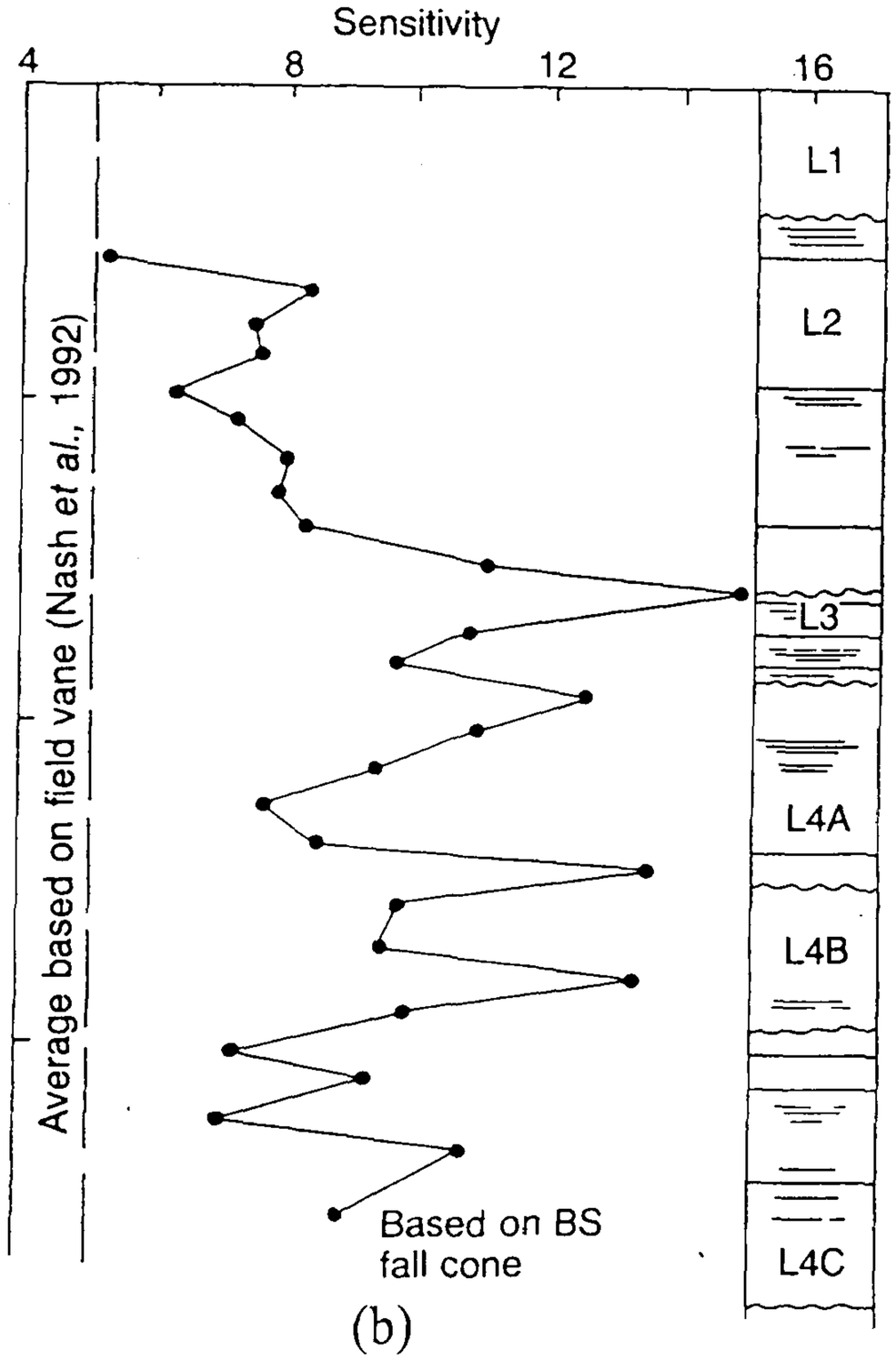

(b)

Figure 3.2.4 Bothkennar clay: (a) water content and Atterberg limits (after Paul *et al.*, 1992) (b) sensitivity determined based on BS fall cone tests (after Hight *et al.*, 1992)

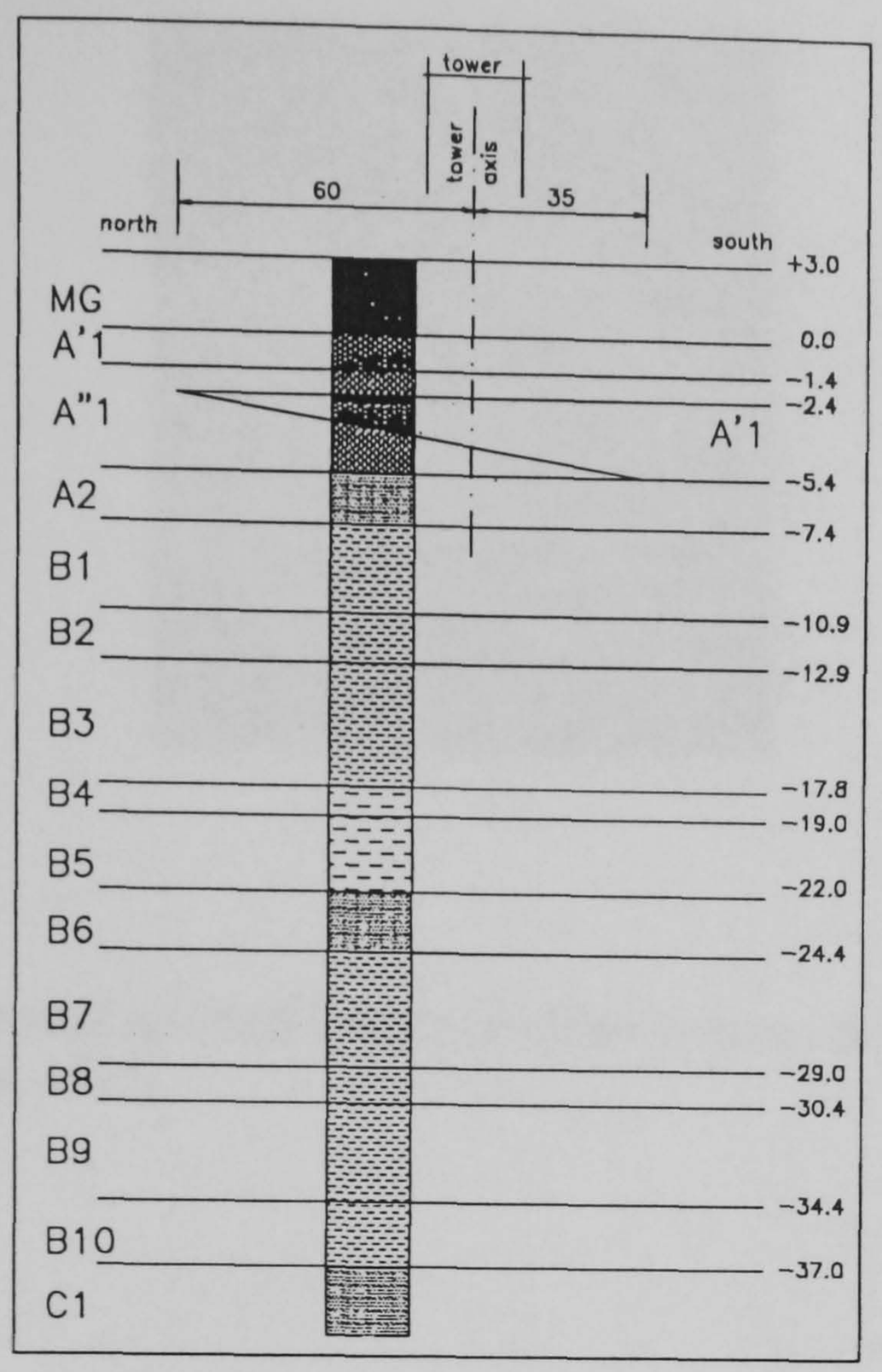

Figure 3.2.5 Simplified schematic of the subsoil of the Tower of Pisa (after Rampello & Callisto, 1998)

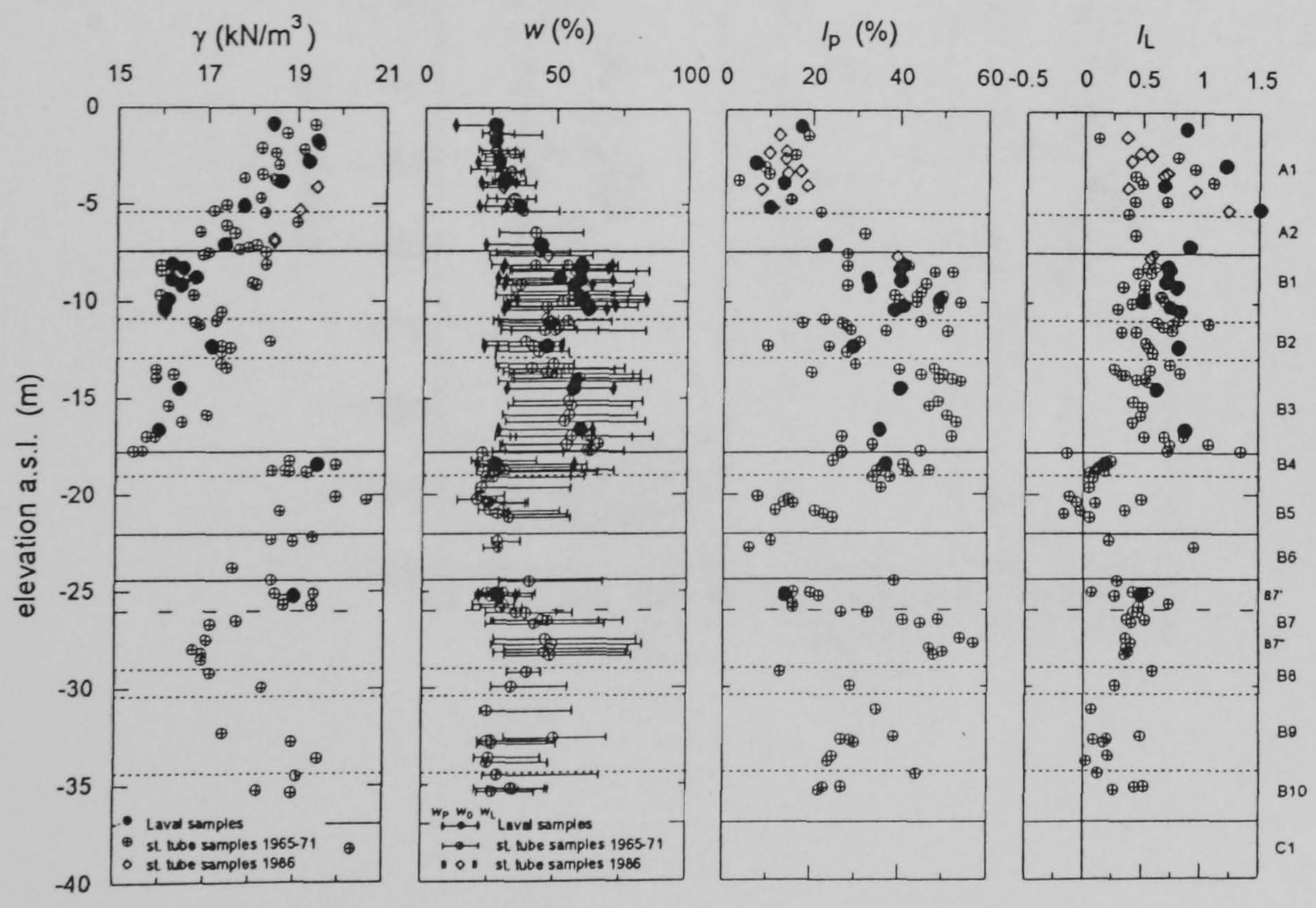

Figure 3.2.6 Pisa clay: profiles of physical and index properties (after Rampello & Callisto, 1998)

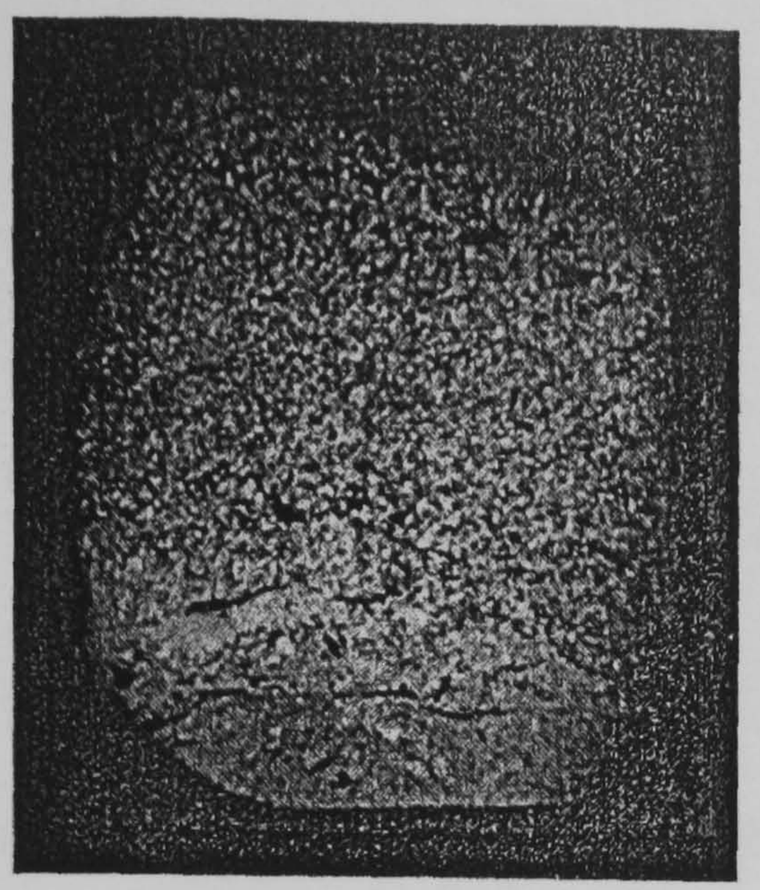

Figure 3.2.7 Thin section of an intact sample of Sibari clay (6.5m depth) (after Coop & Cotecchia, 1995)

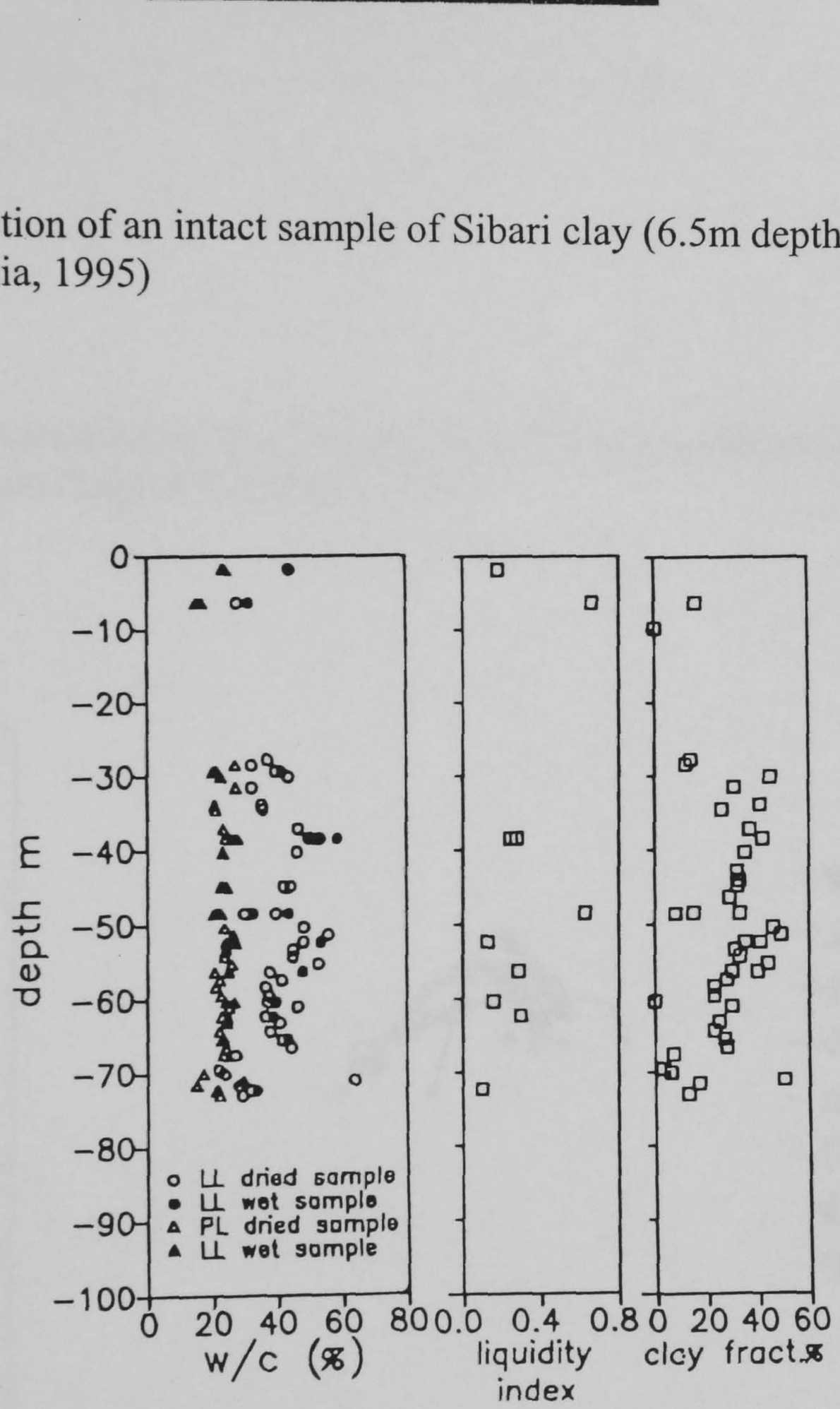

Figure 3.2.8 Sibari clay: profiles of physical and index properties (after Coop & Cotecchia, 1995)

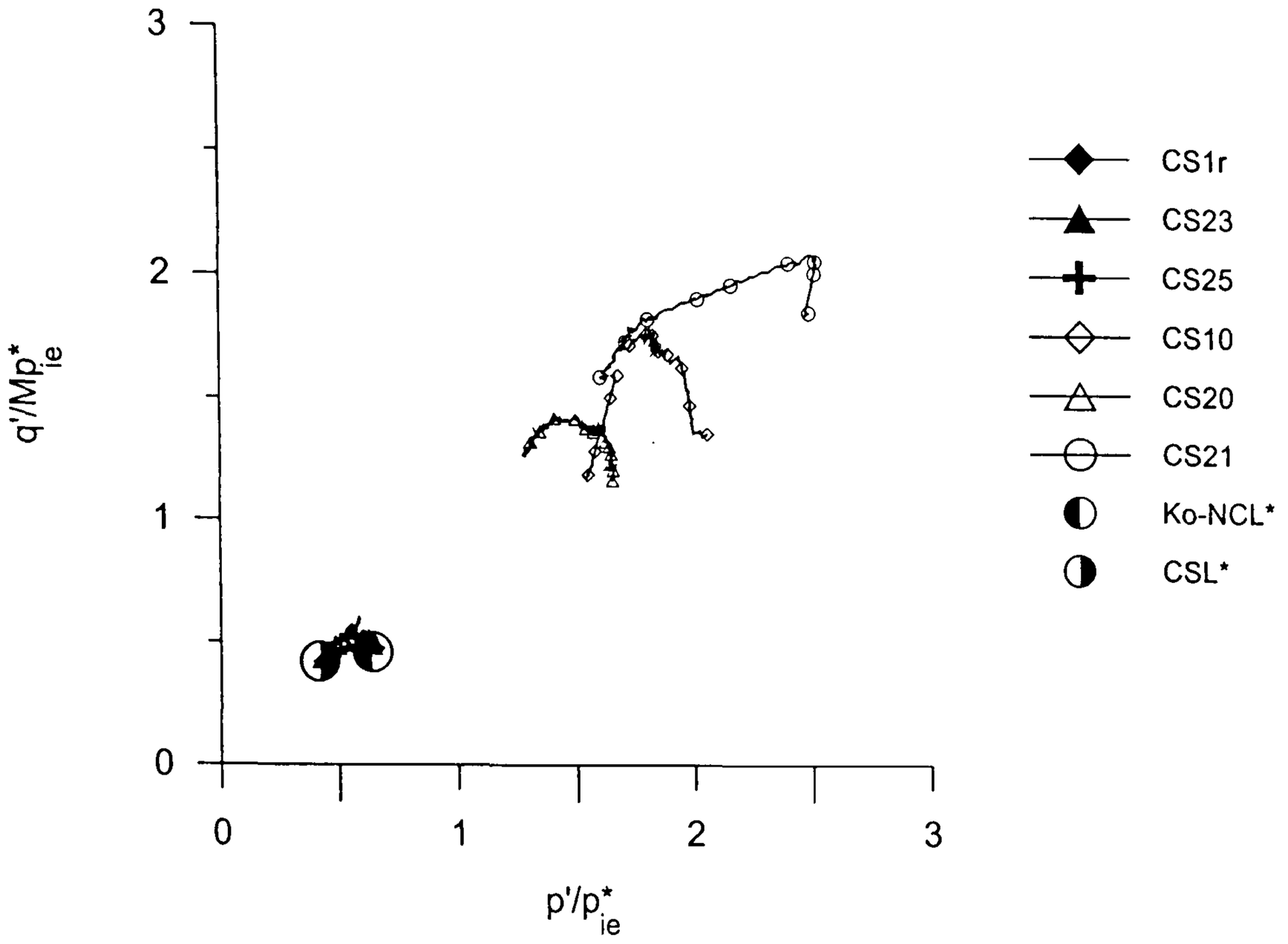

Figure 3.2.9 Shear tests on Sibari clay samples normalised for volume and composition (data from Coop & Cotecchia, 1995)

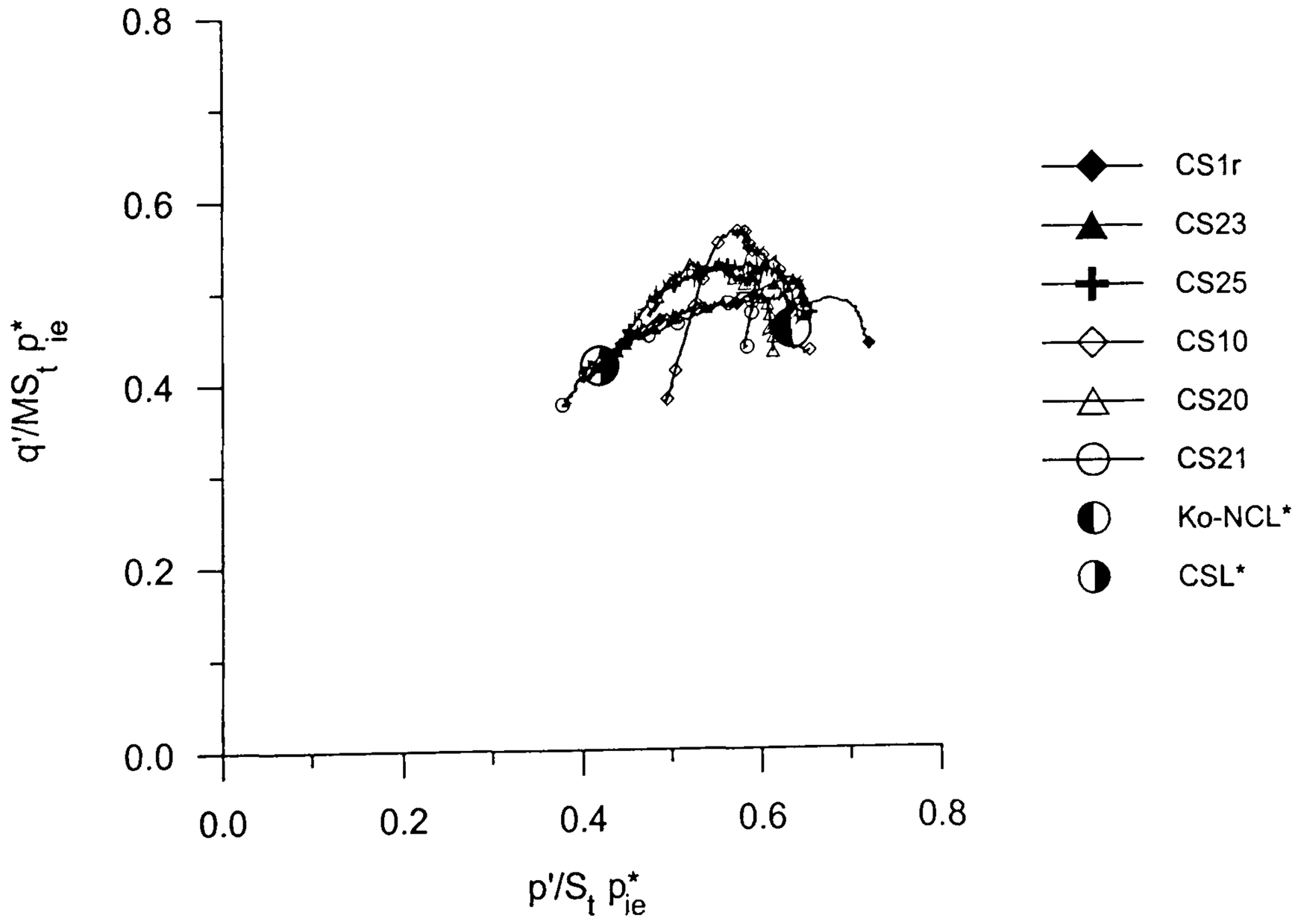

Figure 3.2.10 Shear tests on Sibari clay samples normalised for volume, composition and structure (data from Coop & Cotecchia, 1995)

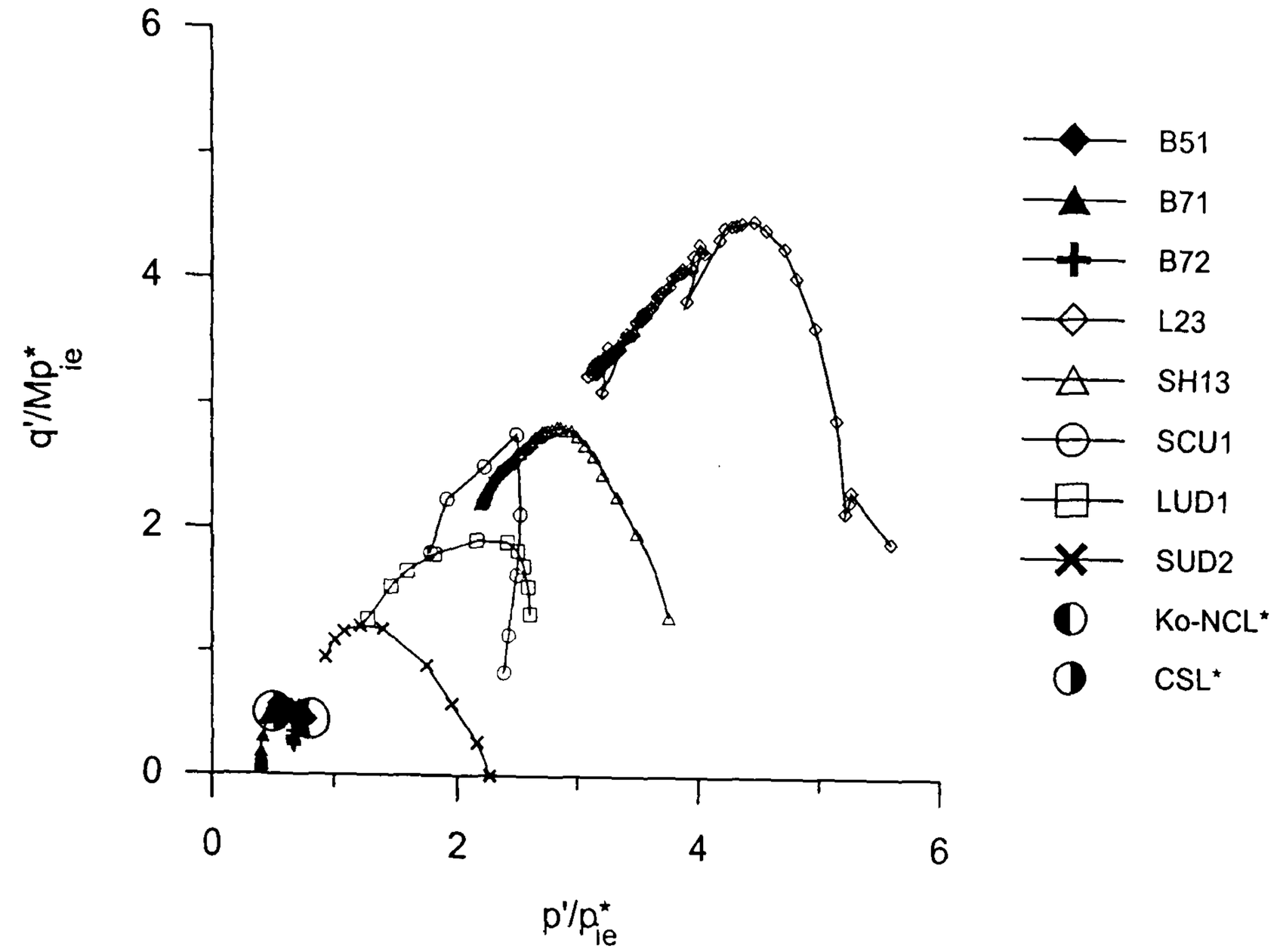

Figure 3.2.11 Undrained shear tests on Bothkennar clay samples normalised for volume and composition (data from Allman, 1992; Smith, 1992)

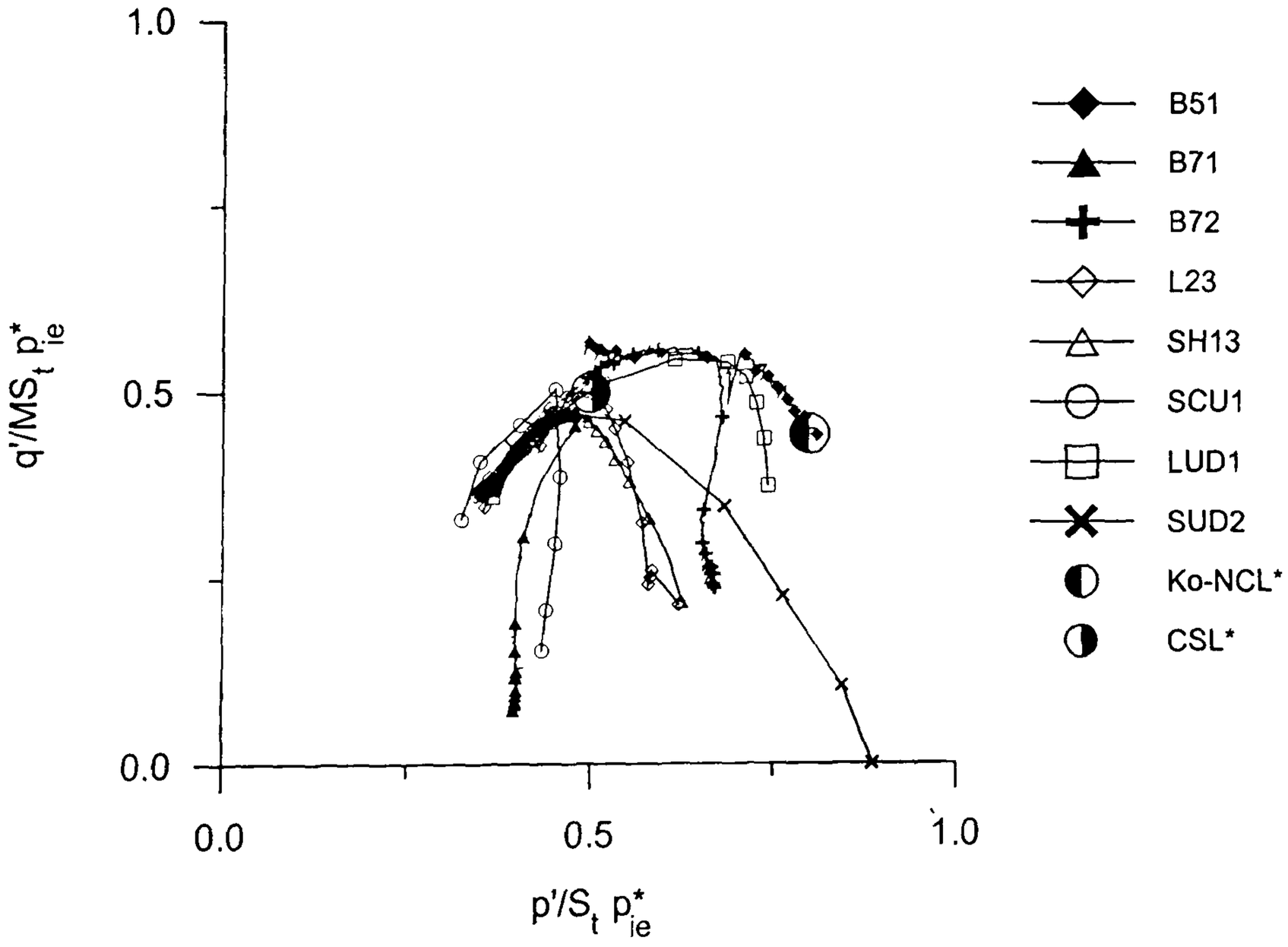

Figure 3.2.12 Undrained shear tests on Bothkennar clay samples normalised for volume, composition and structure (data from Allman, 1992; Smith, 1992)

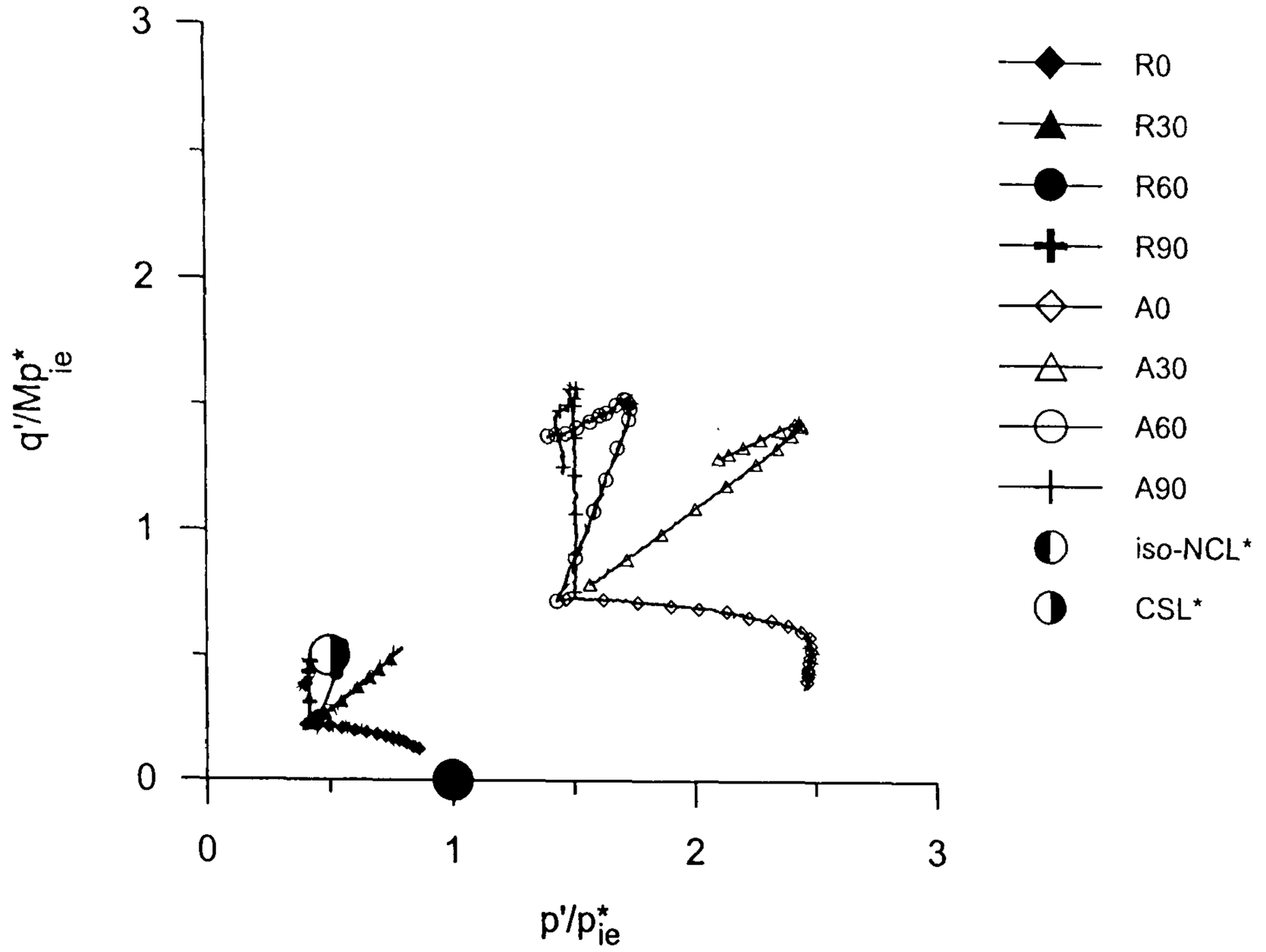

Figure 3.2.13 Drained probes on Pisa clay samples normalised for volume and composition (data from Callisto, 1996)

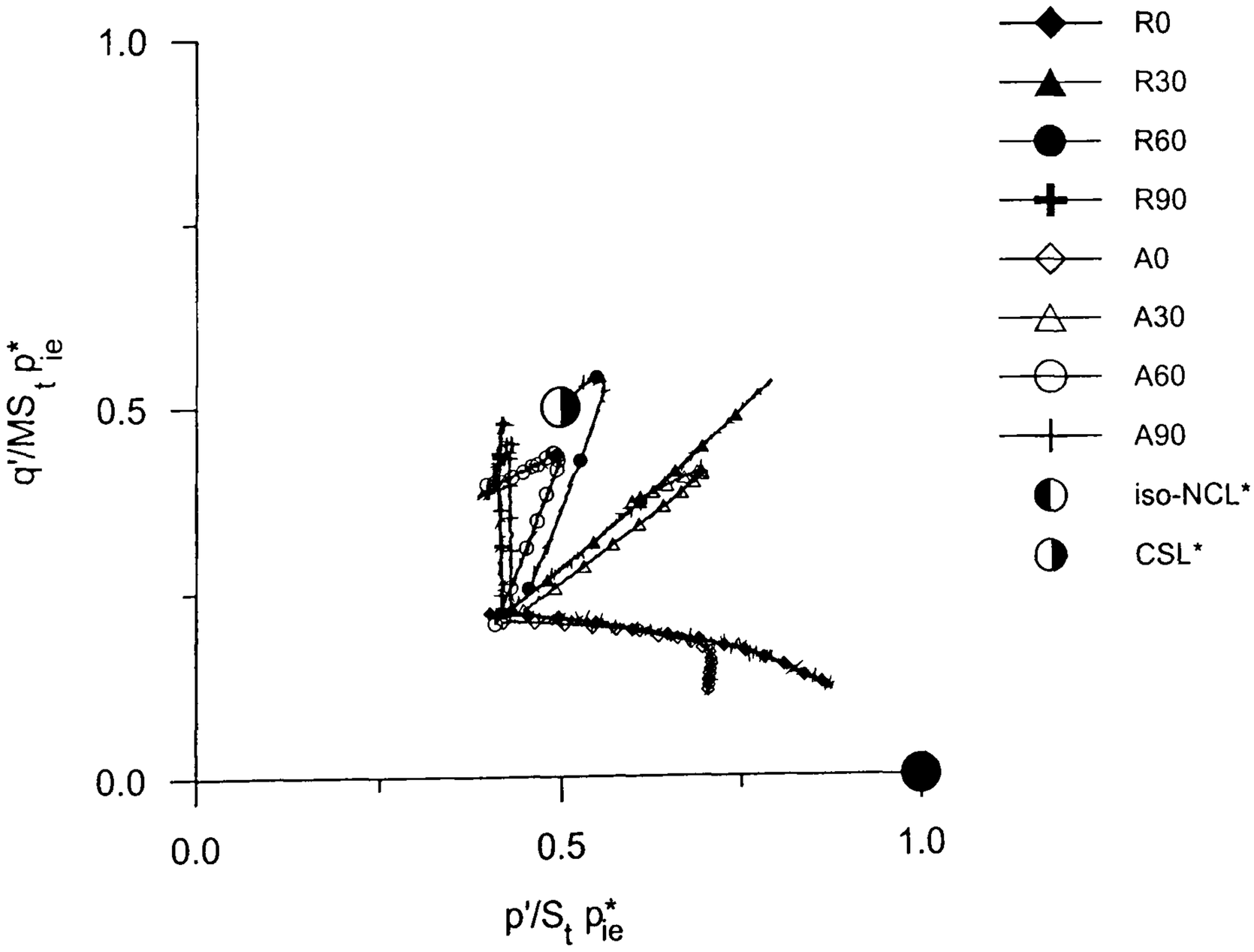

Figure 3.2.14 Drained probes on Pisa clay samples normalised for volume, composition and structure (data from Callisto, 1996)

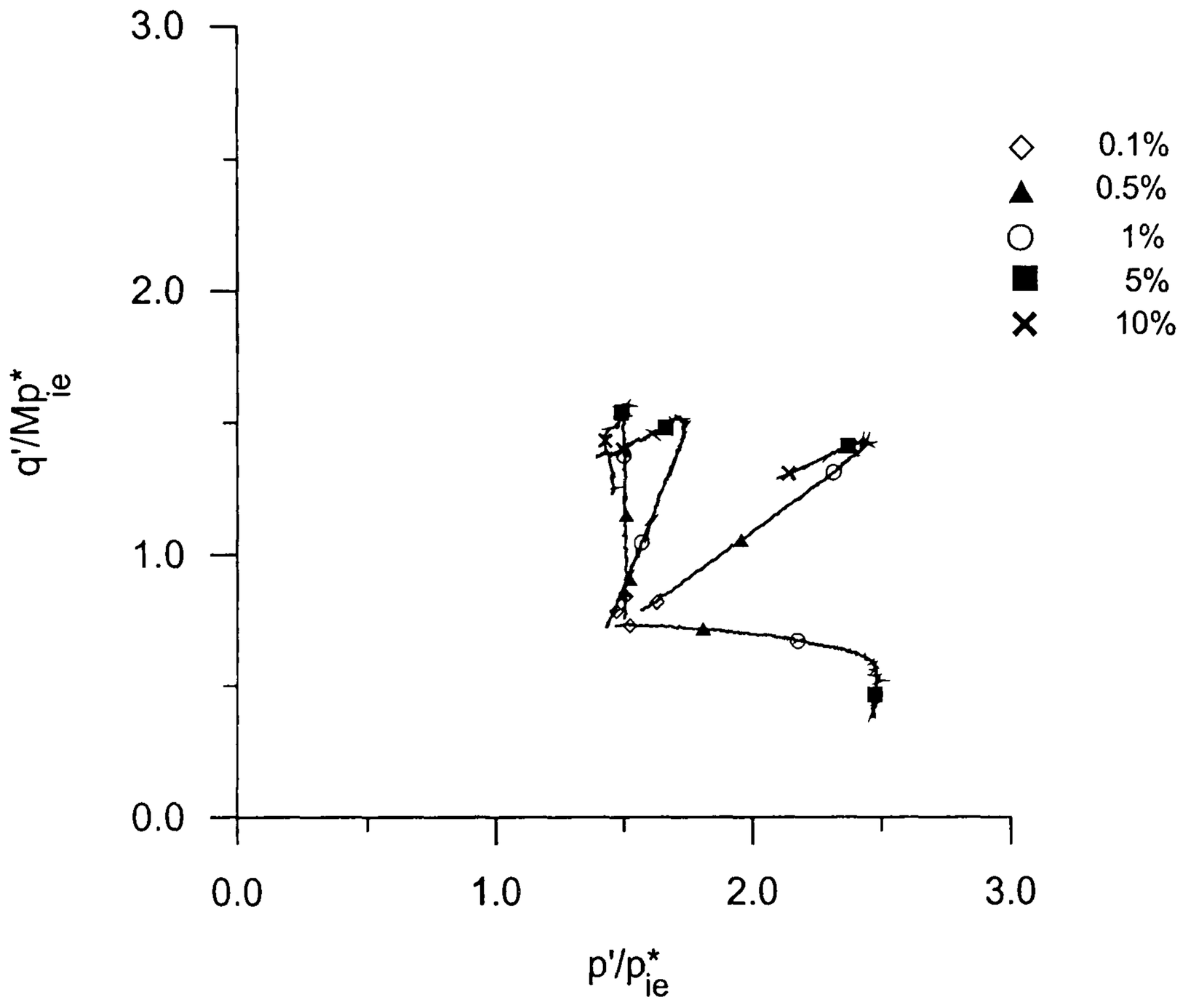

Figure 3.2.15 Contours of magnitude of vectors of plastic strain increment during drained probes on natural Pisa clay samples (data from Callisto, 1996)

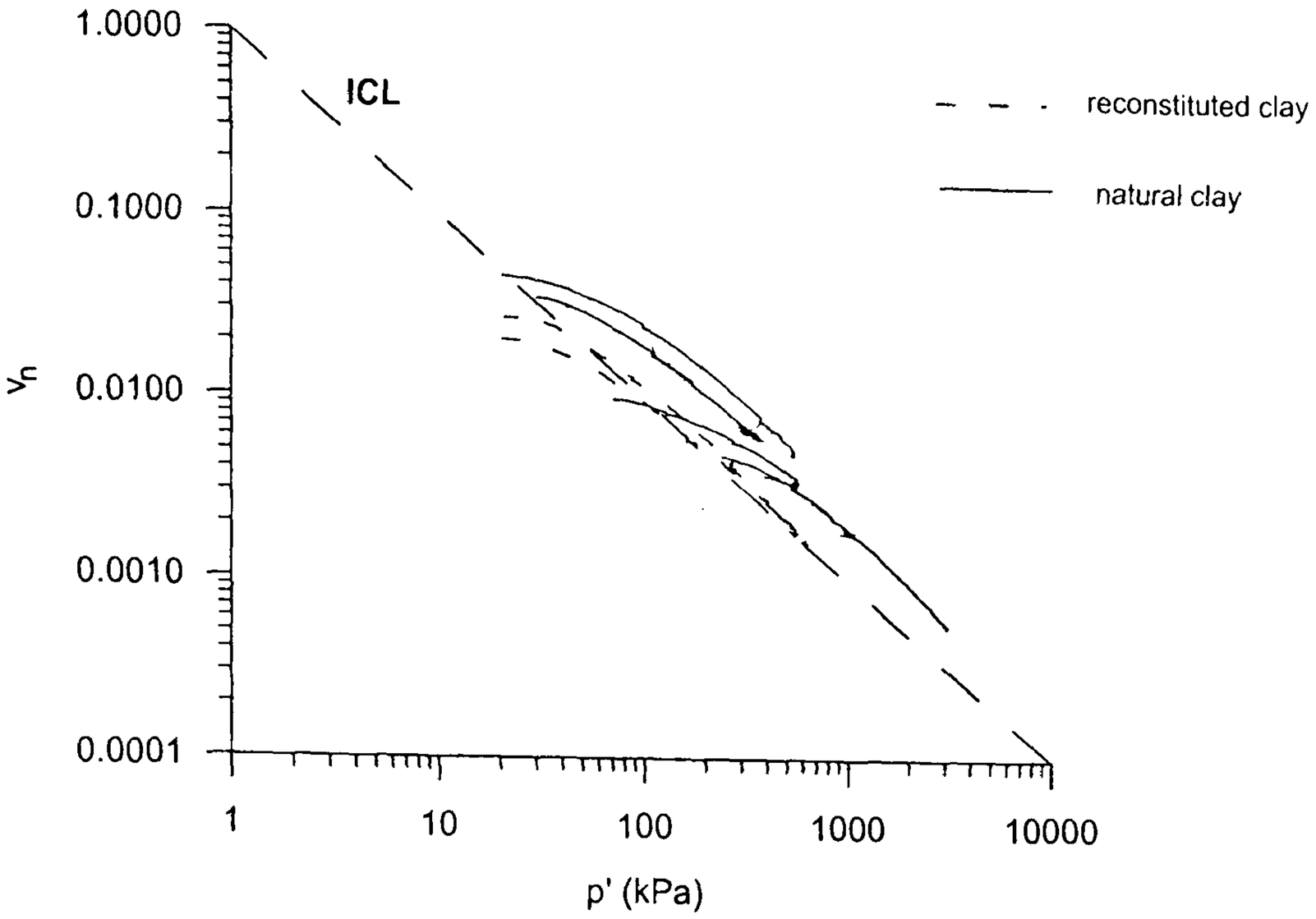

Figure 3.3.1 One-dimensional compression tests on Sibari clay samples normalised by composition (data from Coop & Cotecchia, 1995)

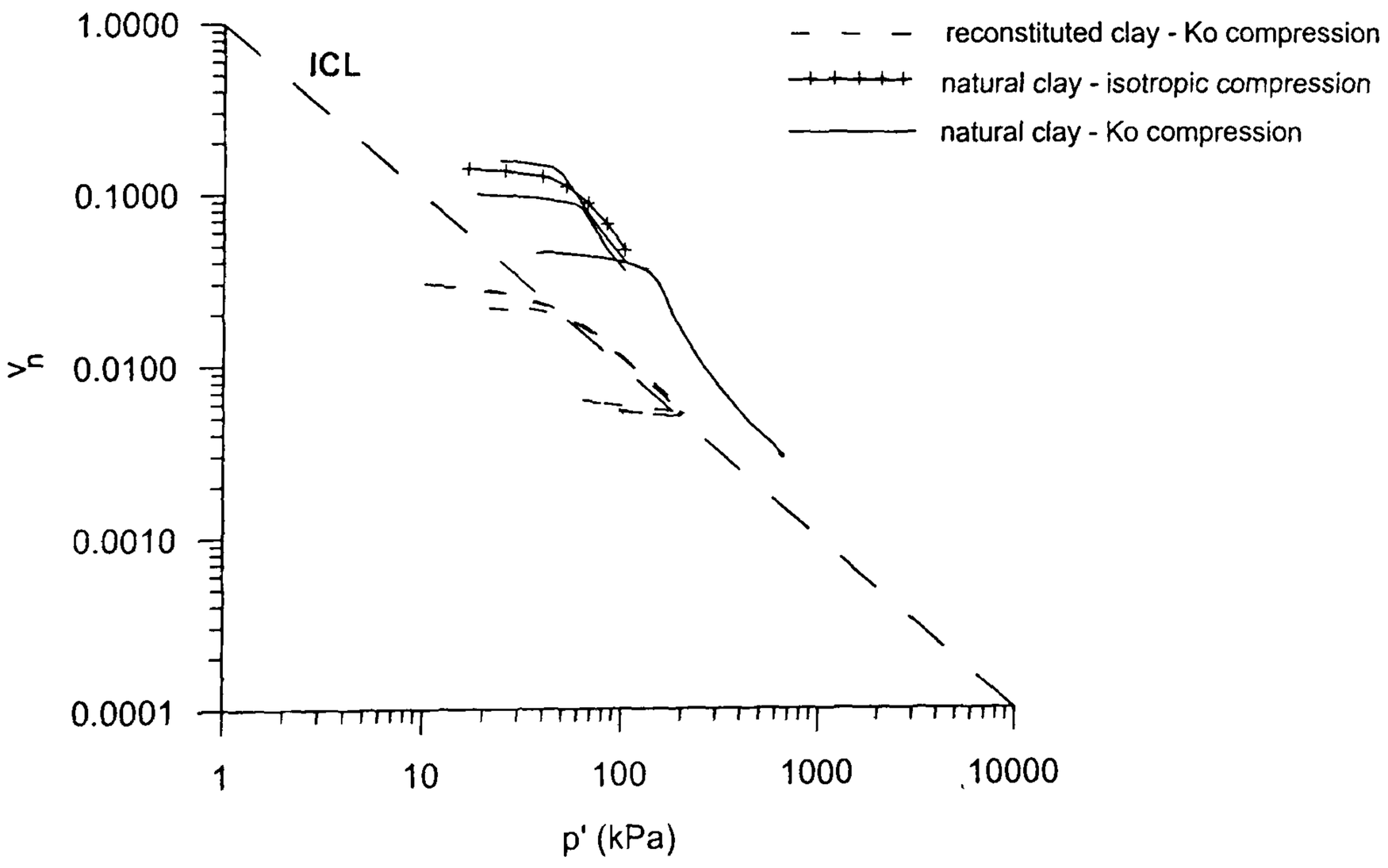

Figure 3.3.2 Isotropic and one-dimensional compression tests on Bothkennar clay samples normalised by composition (data from Allman, 1992; Smith, 1992)

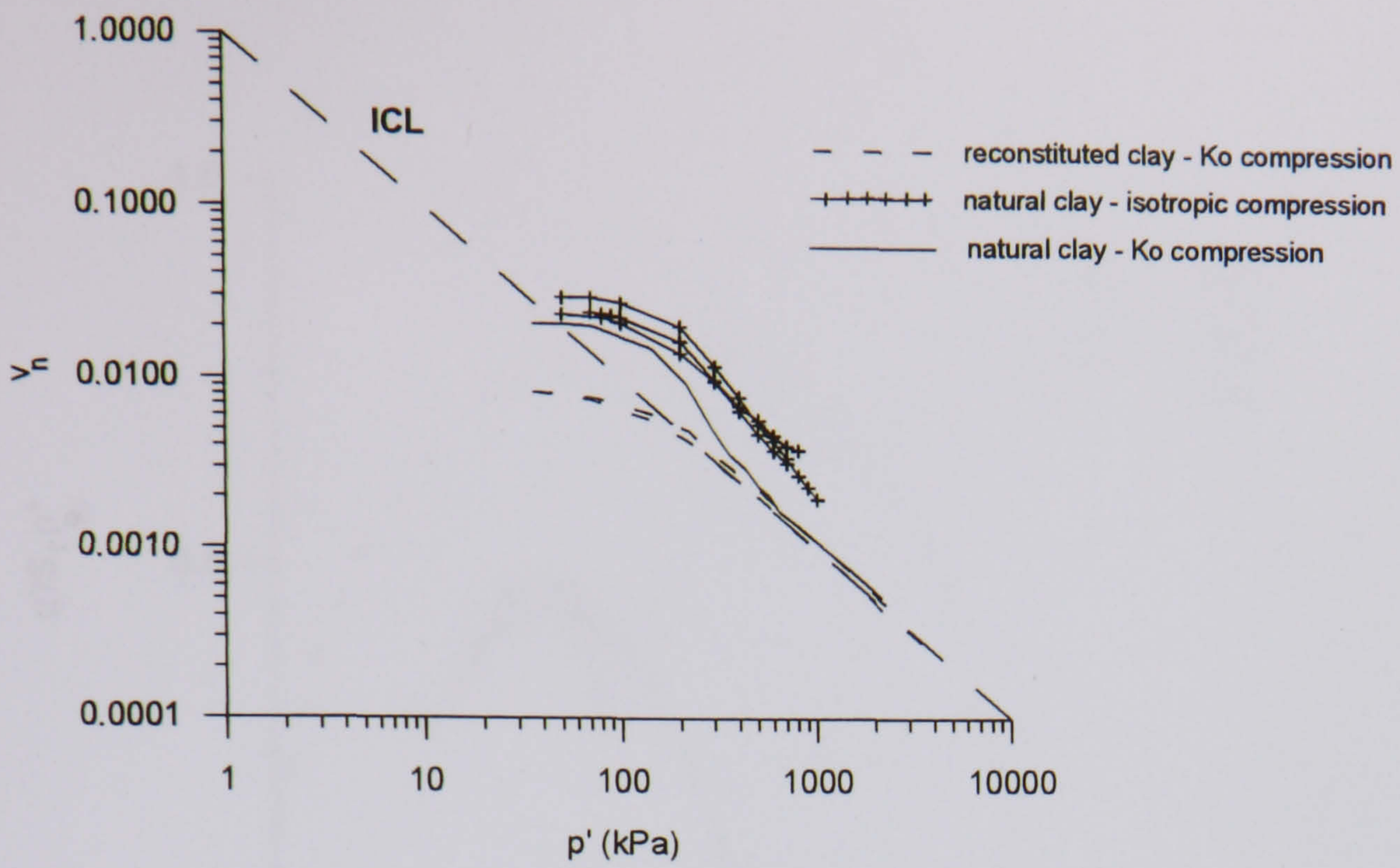

Figure 3.3.3 Isotropic and one-dimensional compression tests on Pisa clay samples normalised for composition (data from Callisto, 1996)

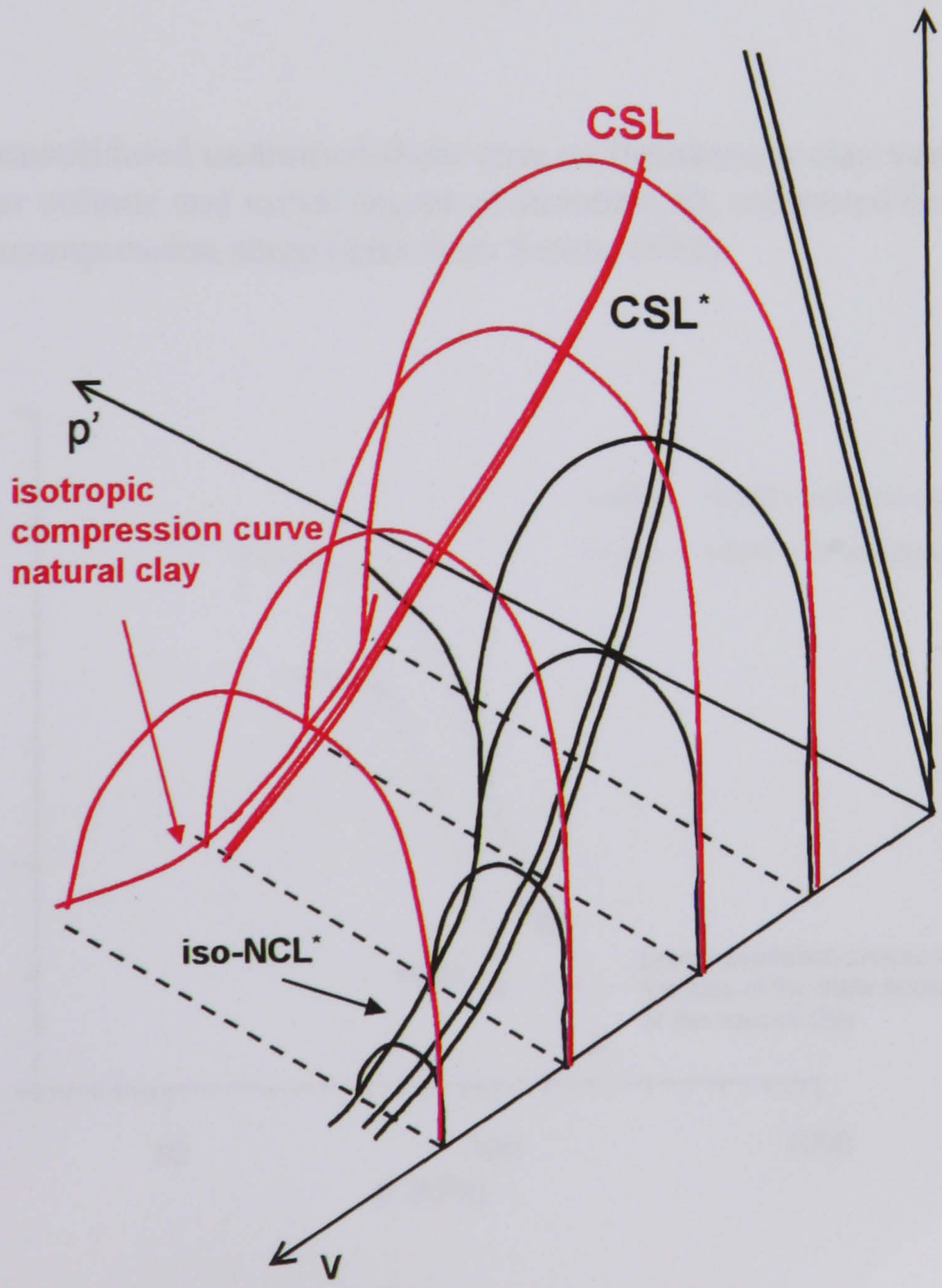

Figure 3.3.4 State boundary surface of natural and reconstituted clay

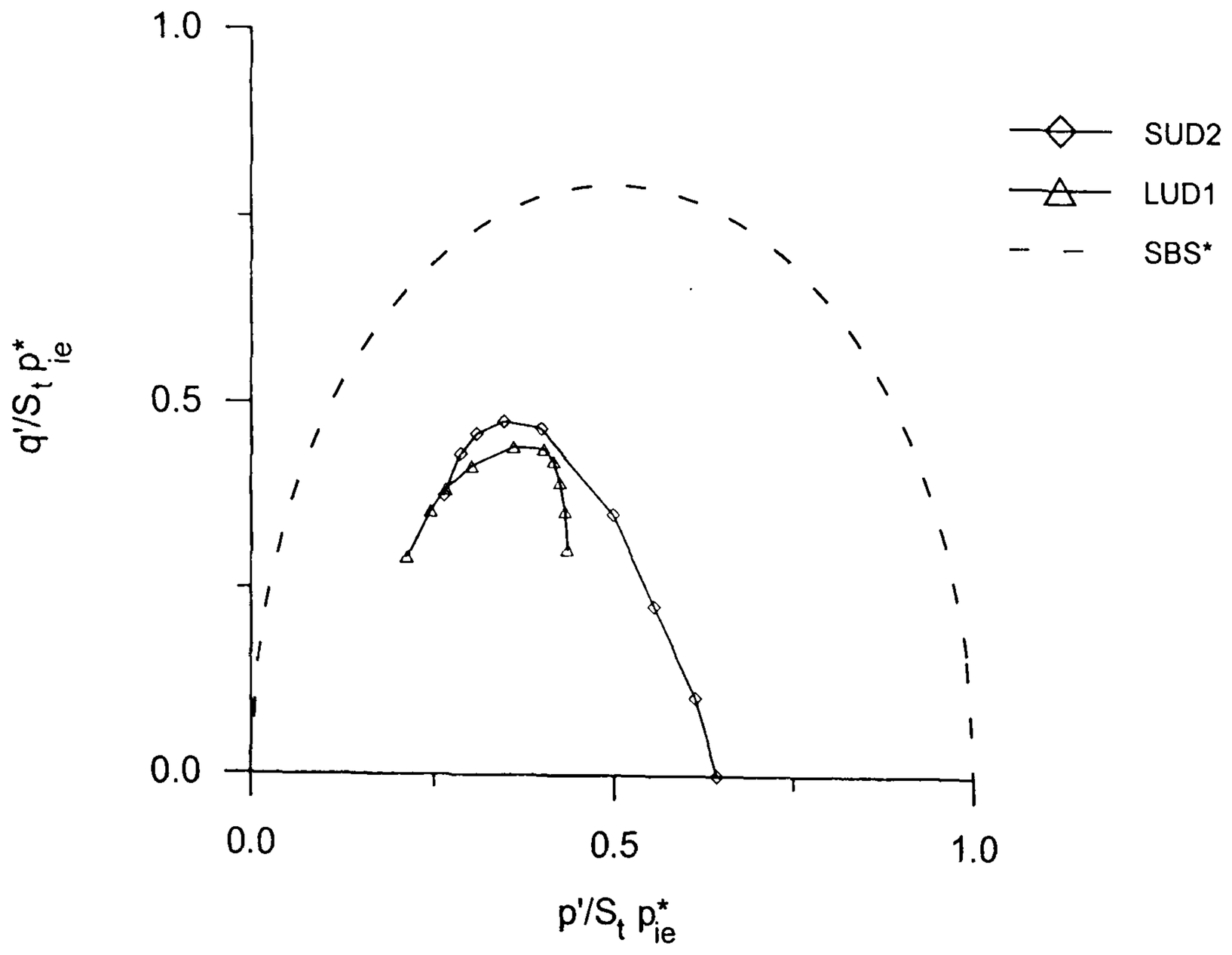

Figure 3.3.5 Consolidated undrained shear tests on Bothkennar clay samples normalised for volume and initial degree of structure, St, computed from the recompression stage (data from Smith, 1992)

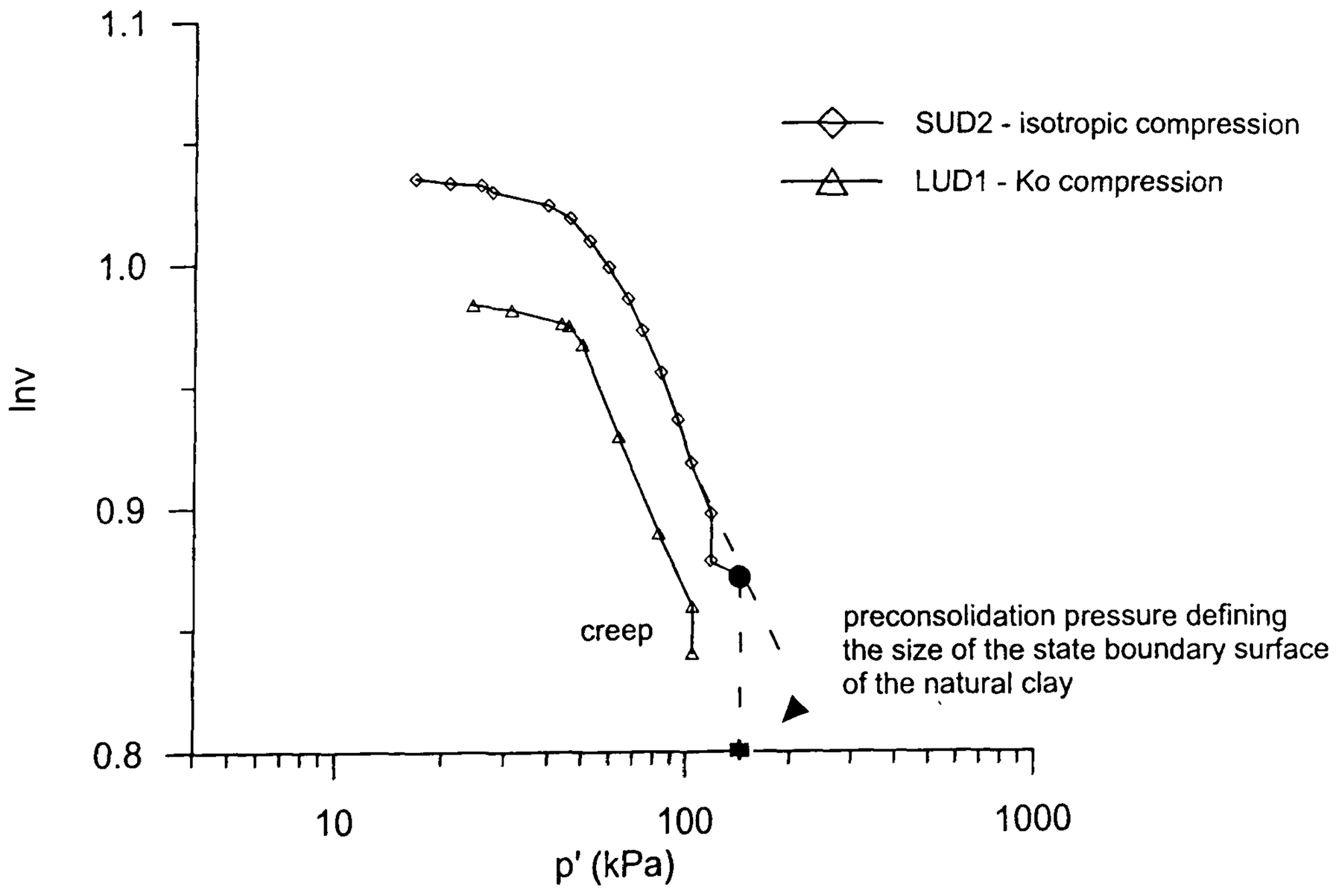

Figure 3.3.6 Recompression stage: isotropic and one-dimensional compression curves obtained for Bothkennar clay samples (data from Smith, 1992)

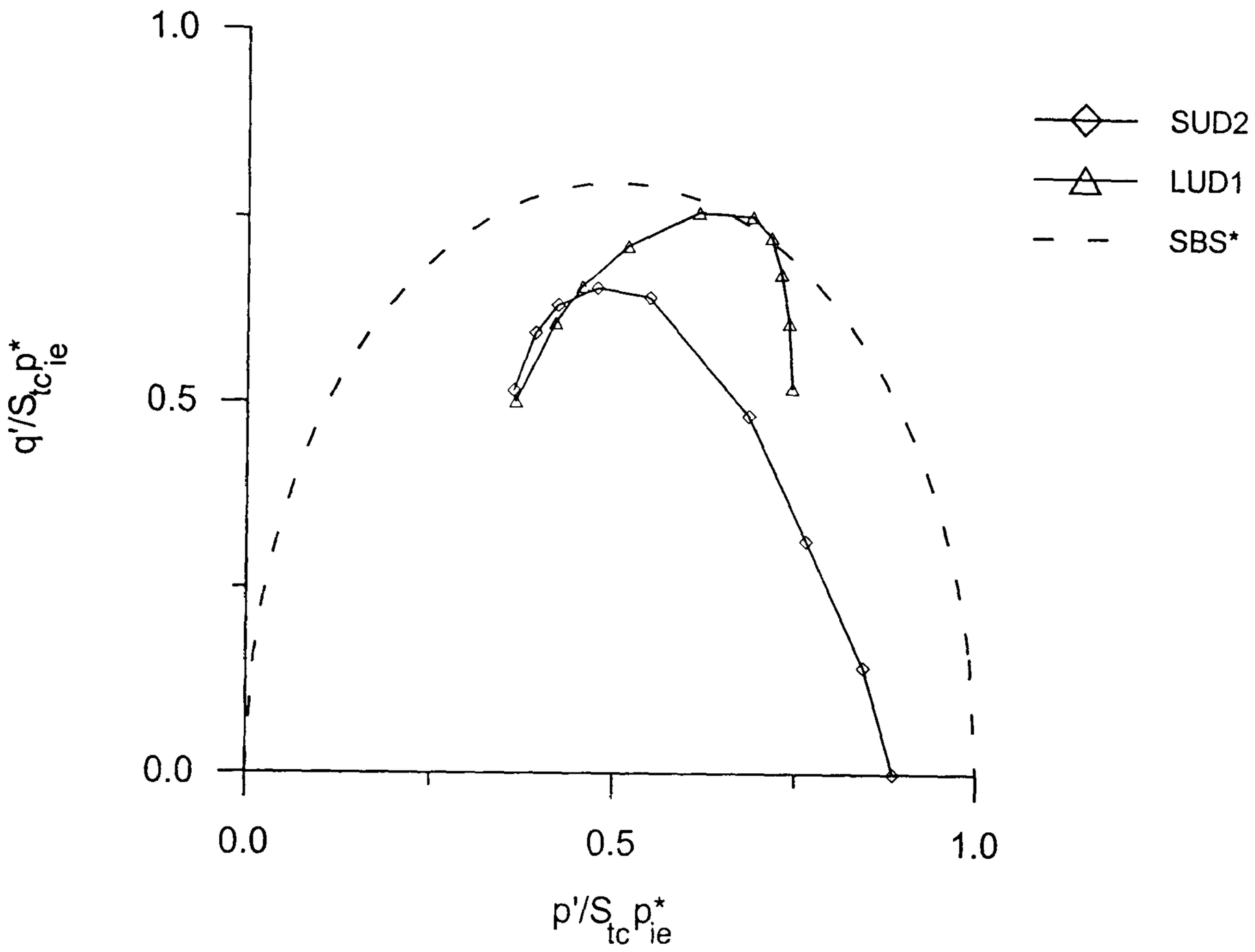

Figure 3.3.7 Consolidated undrained shear tests on Bothkennar clay samples normalised for volume and degree of structure at the end of consolidation, S_{tc} (data from Smith, 1992)

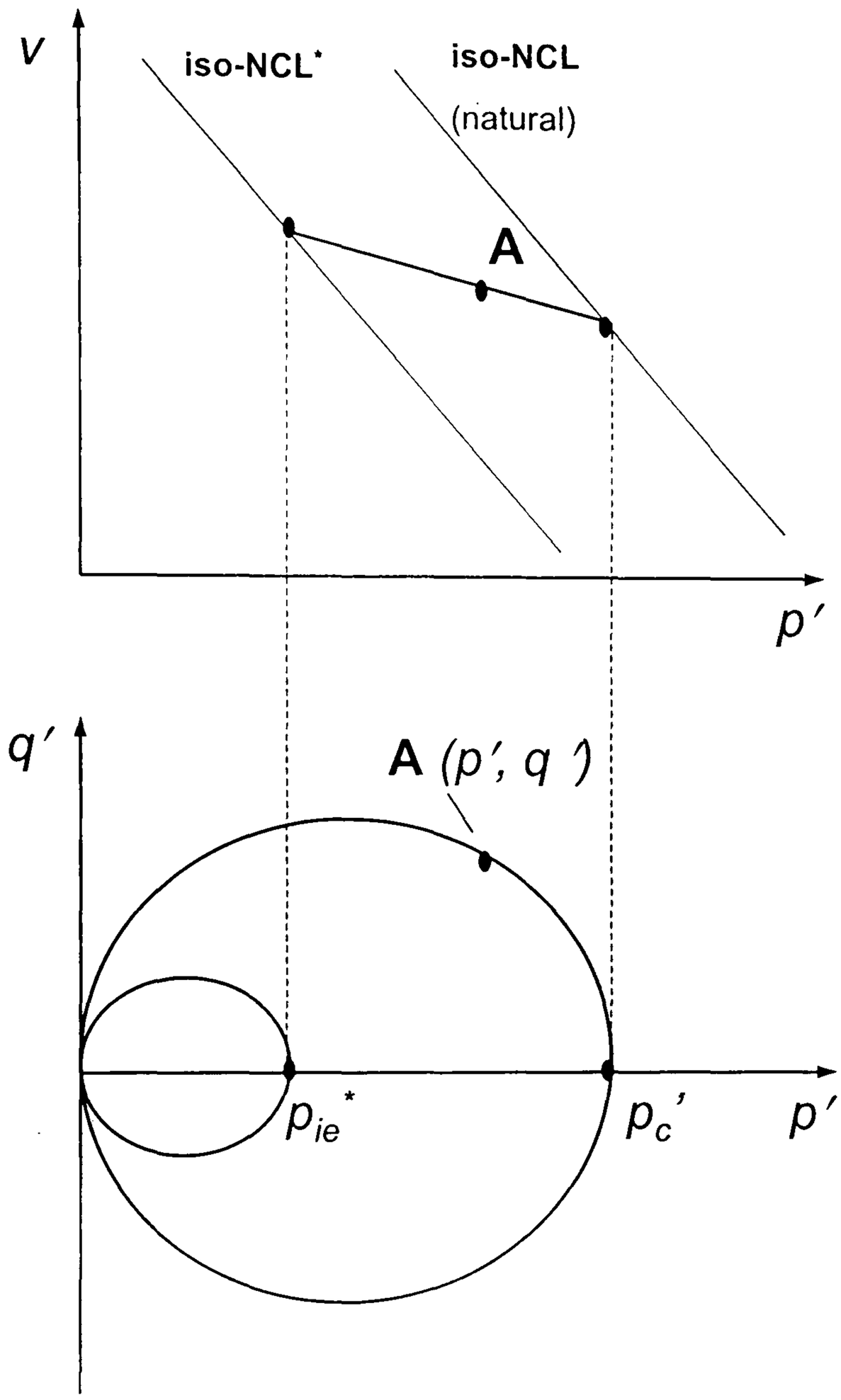

Figure 3.3.8 Schematic diagrams describing the determination of current sensitivity

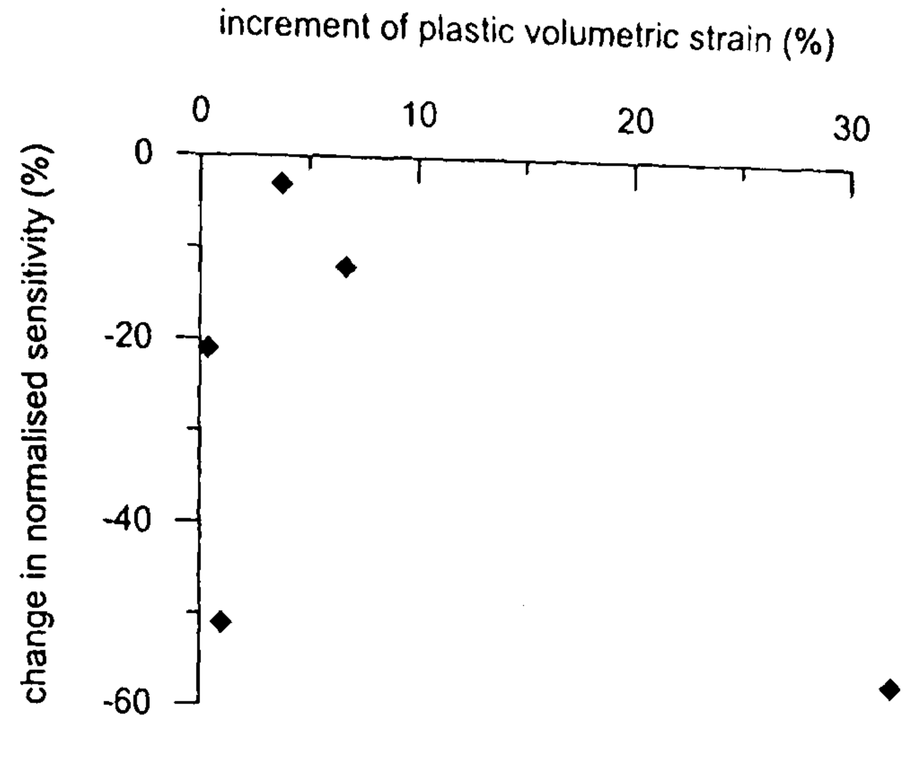

(a)

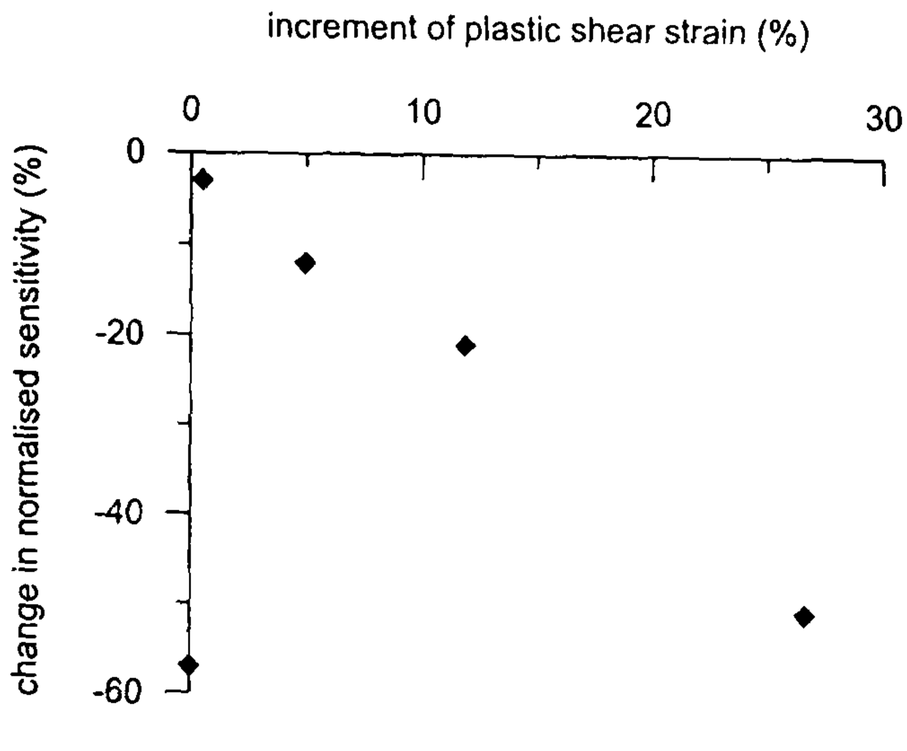

(b)

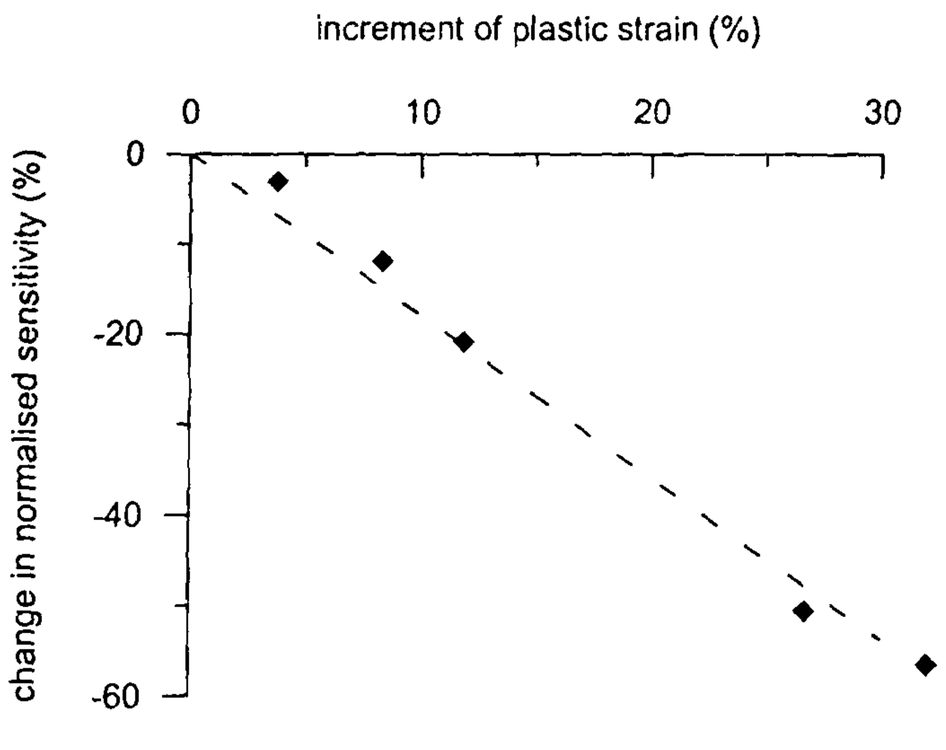

(c)

Figure 3.3.9 Pisa clay: rate of change in normalised sensitivity with increment of (a) plastic volumetric strain (b) plastic shear strain (c) plastic strain (data from Callisto, 1996; Rampello *et al.*, 1996))

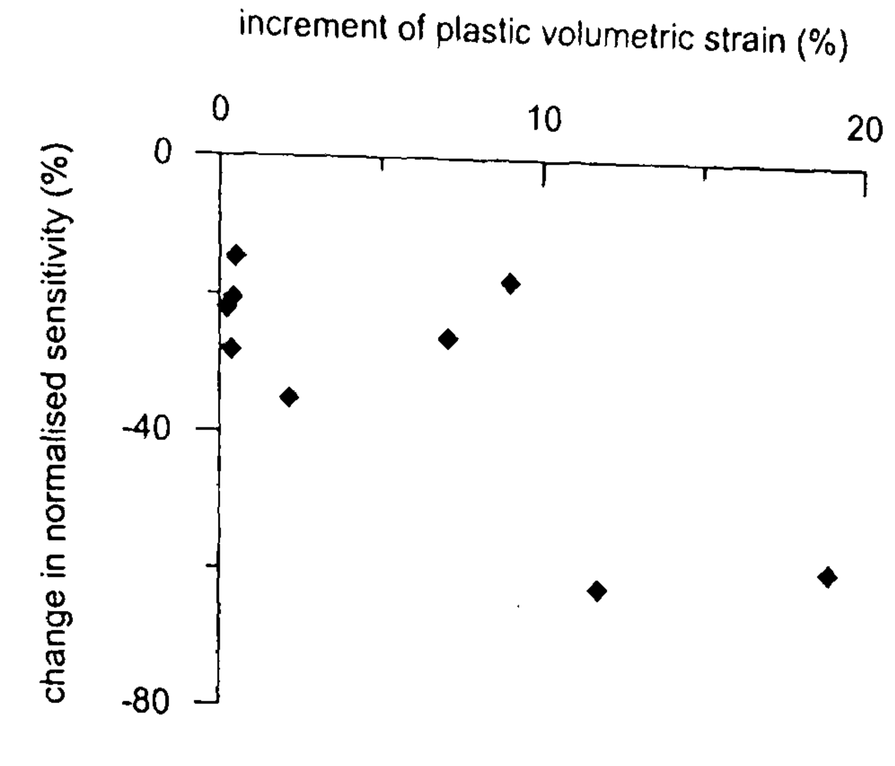

(a)

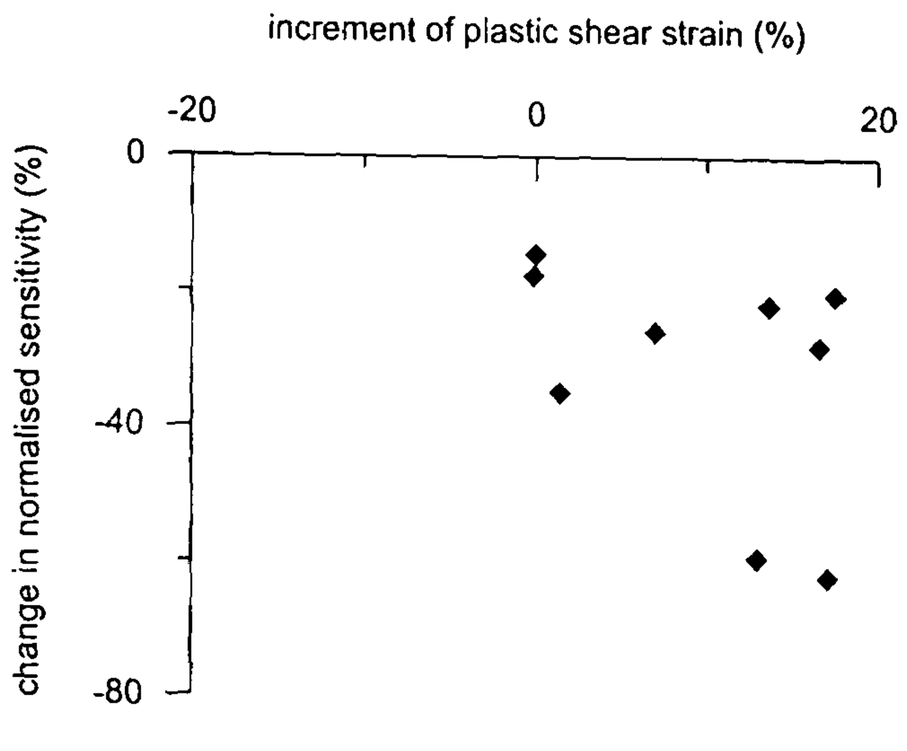

(b)

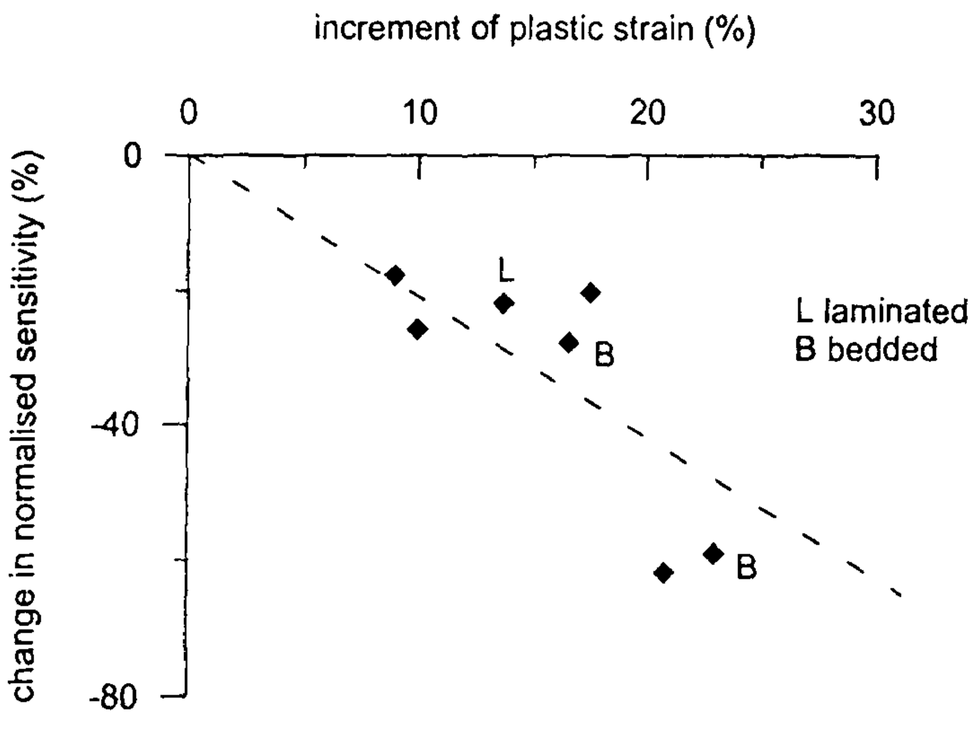

(c)

Figure 3.3.10 Bothkennar clay: rate of change in normalised sensitivity with increment of (a) plastic volumetric strain (b) plastic shear strain (c) plastic strain (data from Allman, 1992; Smith, 1992))

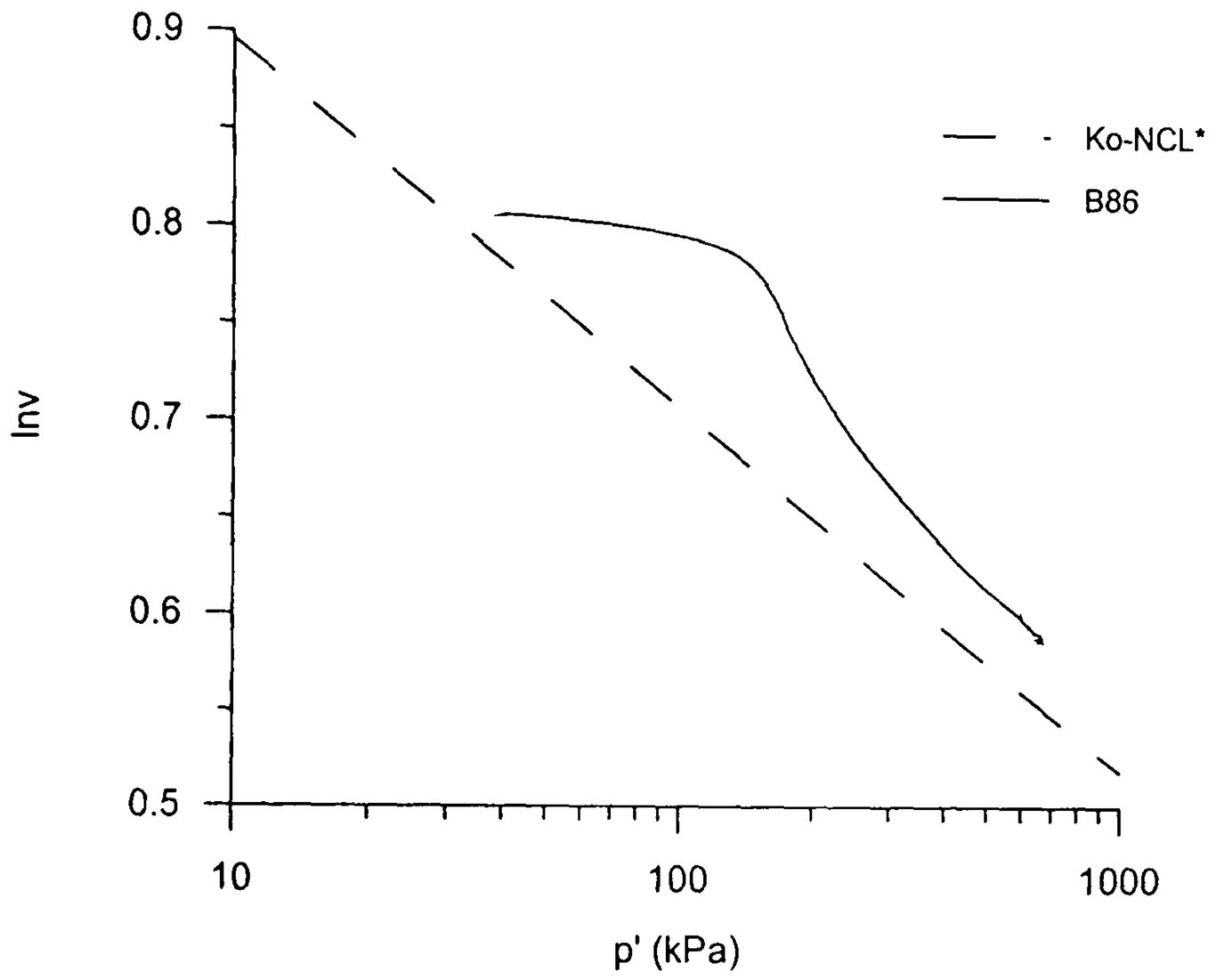

Figure 3.3.11 Effects of fabric on one-dimensional compression curve obtained for Bothkennar clay sample from the bedded facies (data from Allman, 1992)

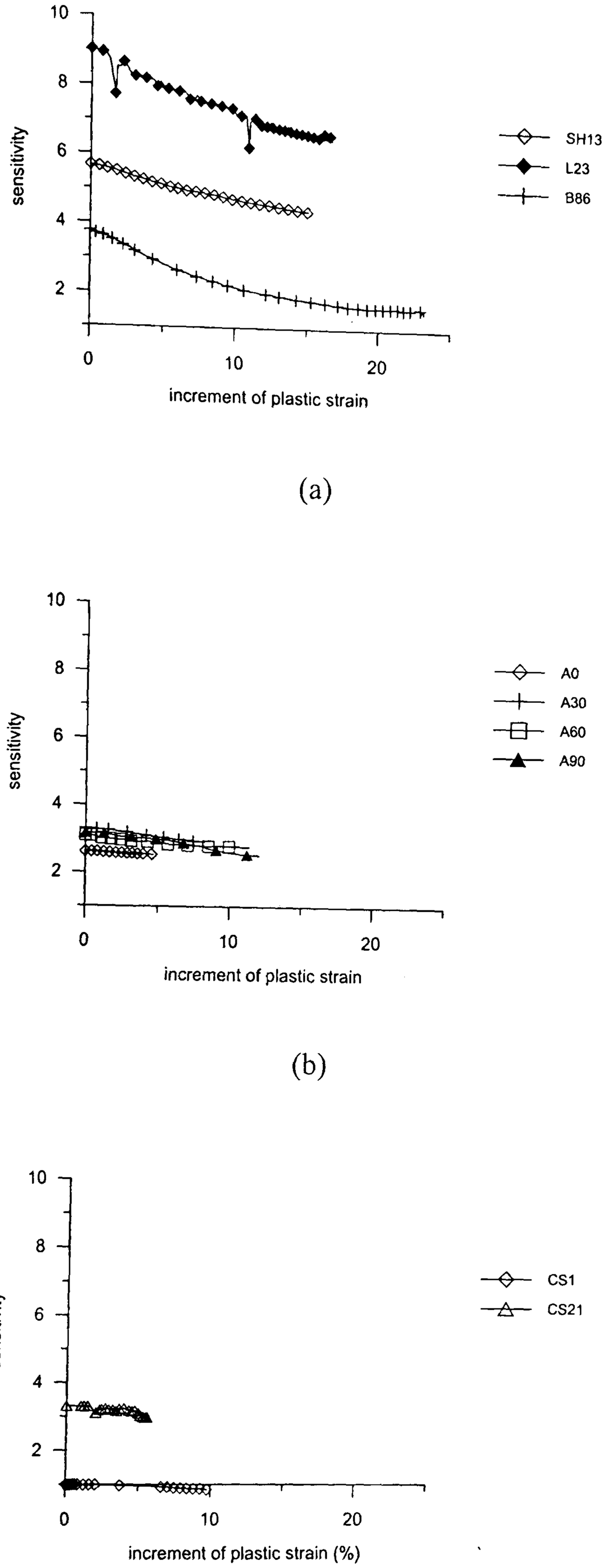

Figure 3.3.12 Effects of fabric on the change in sensitivity with plastic strain increment in (a) Bothkennar clay (data from Allman, 1992) (b) Pisa clay (data from Callisto, 1996) (c) Sibari clay (data from Coop & Cotecchia, 1995)

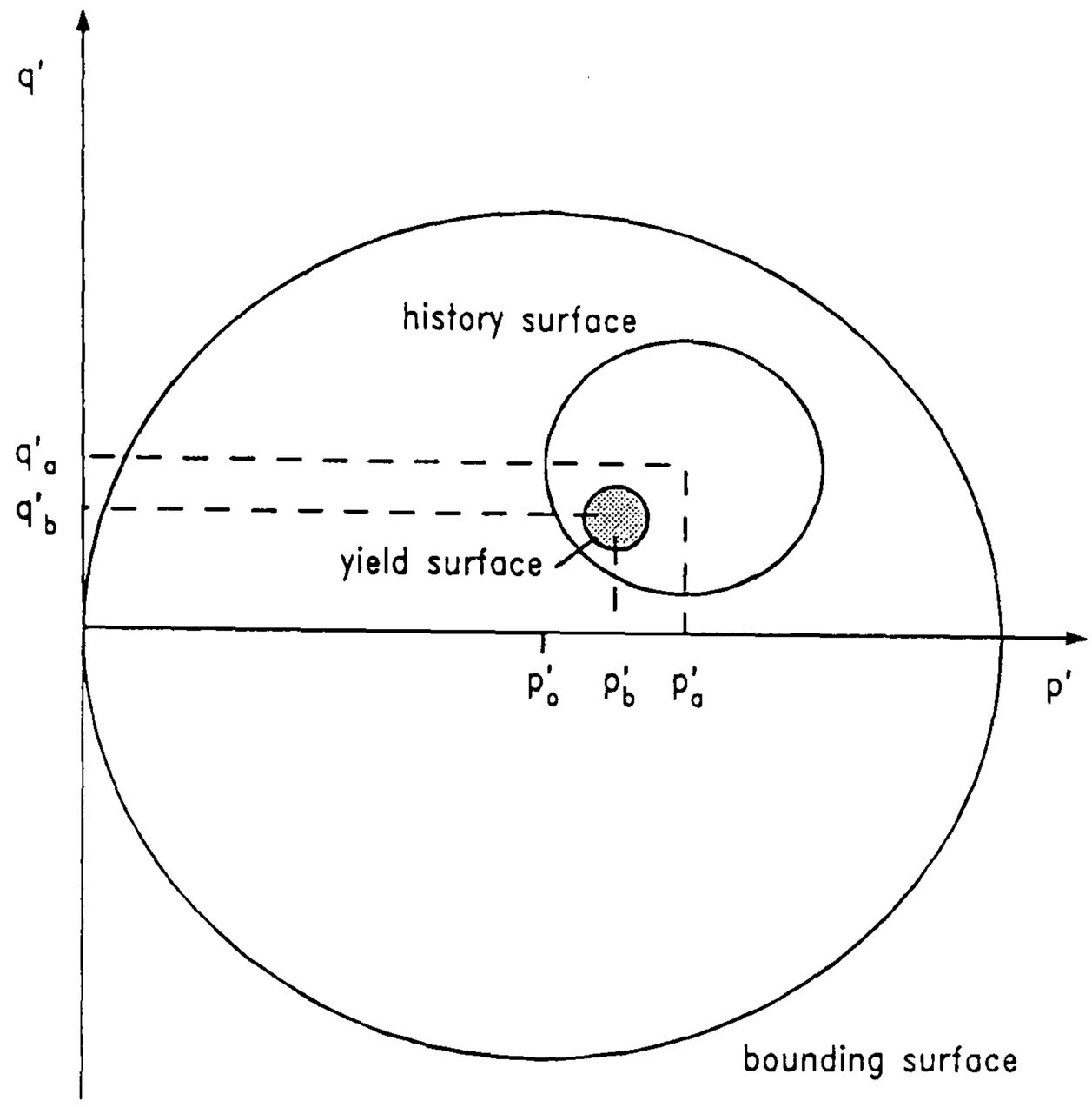

Figure 4.2.1 Diagram showing the three yield surfaces that constitute the 3-SKH model, defined in stress space (after Stallebrass, 1990)

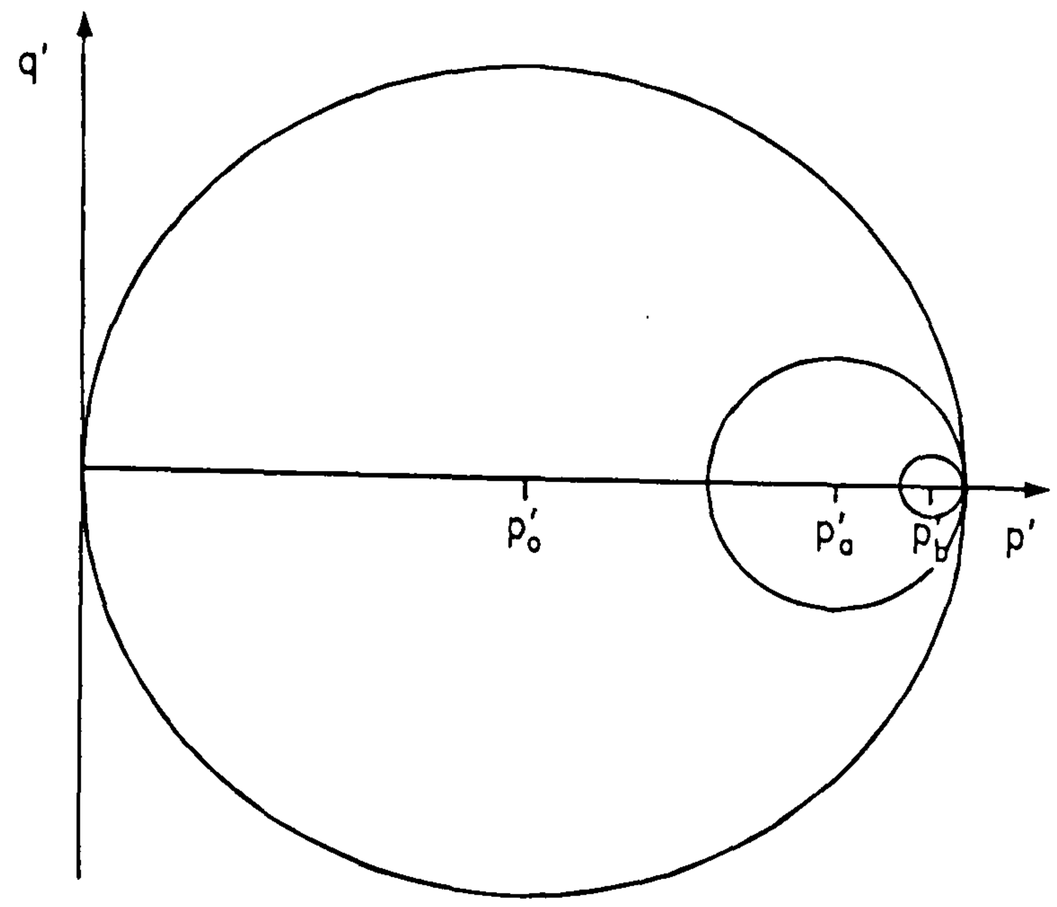

Figure 4.2.2 Diagram showing the position of the surfaces in the 3-SKH model when b_1 and b_2 are at a maximum (after Stallebrass, 1990)

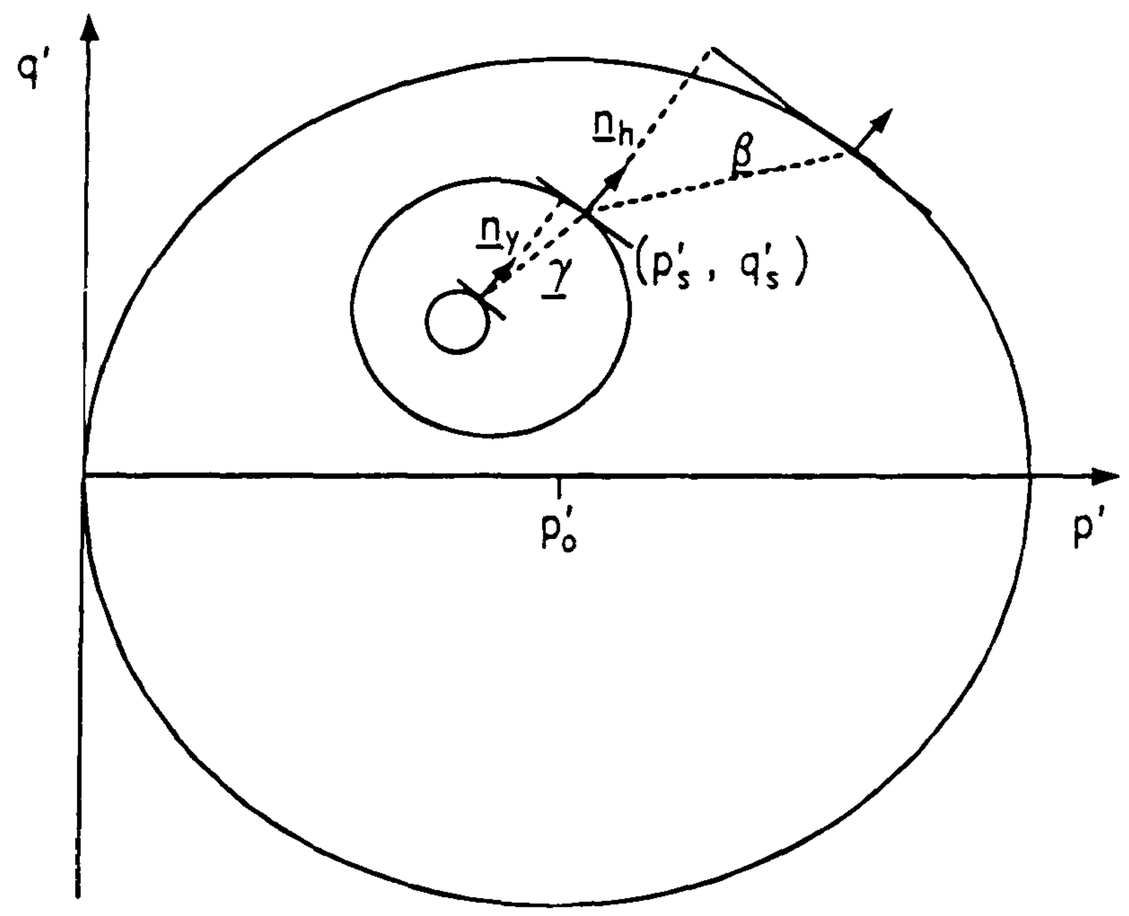

Figure 4.2.3 Diagram defining the main components of the parameters b_1 and b_2 for the 3-SKH model (after Stallebrass, 1990)

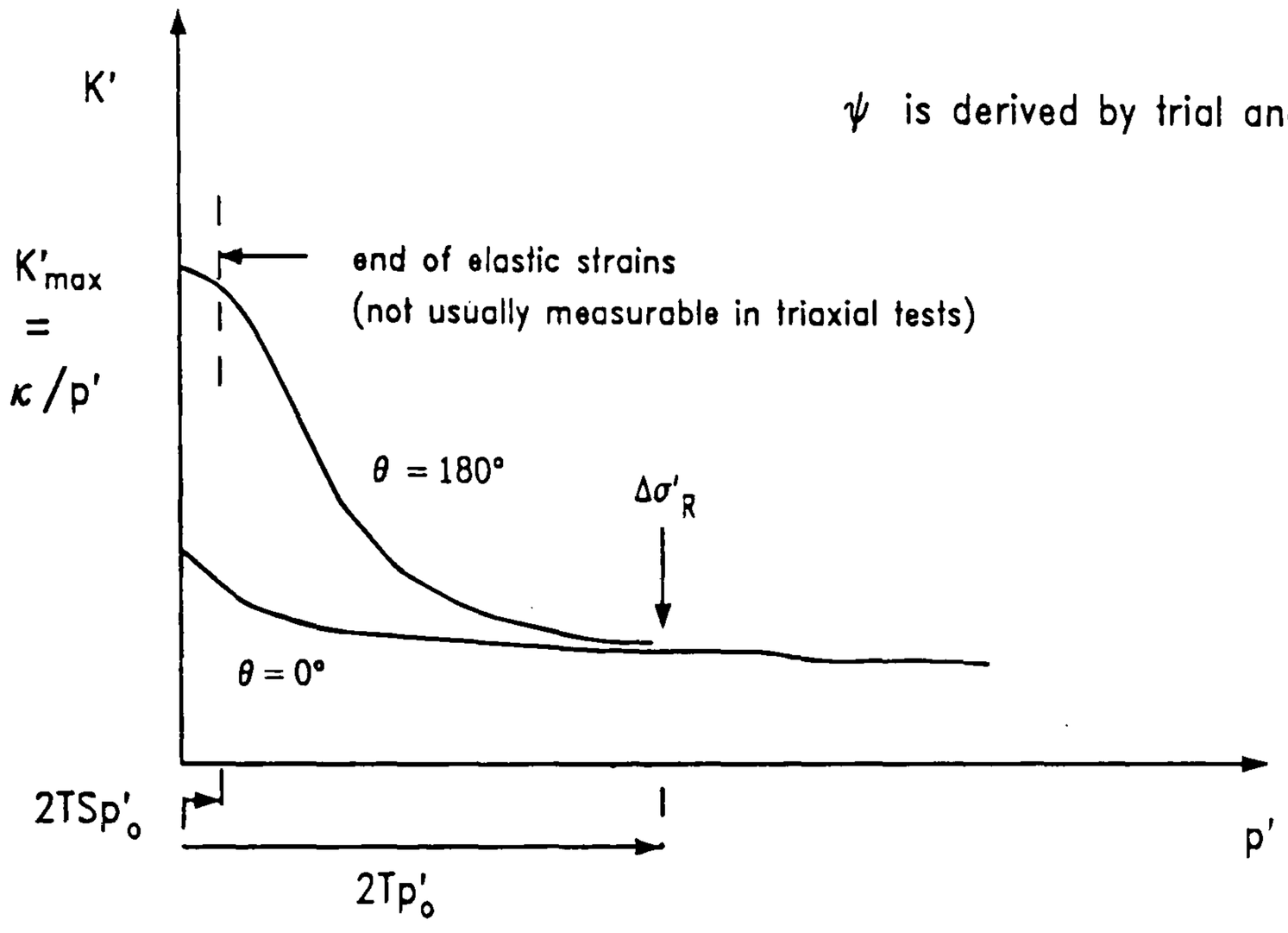

Figure 4.2.4 Diagram showing how the 3-SKH model parameters can be obtained from typical stiffness curves for a constant q′ compression path with two recent stress histories 0 and 180 degrees (after Stallebrass, 1990)

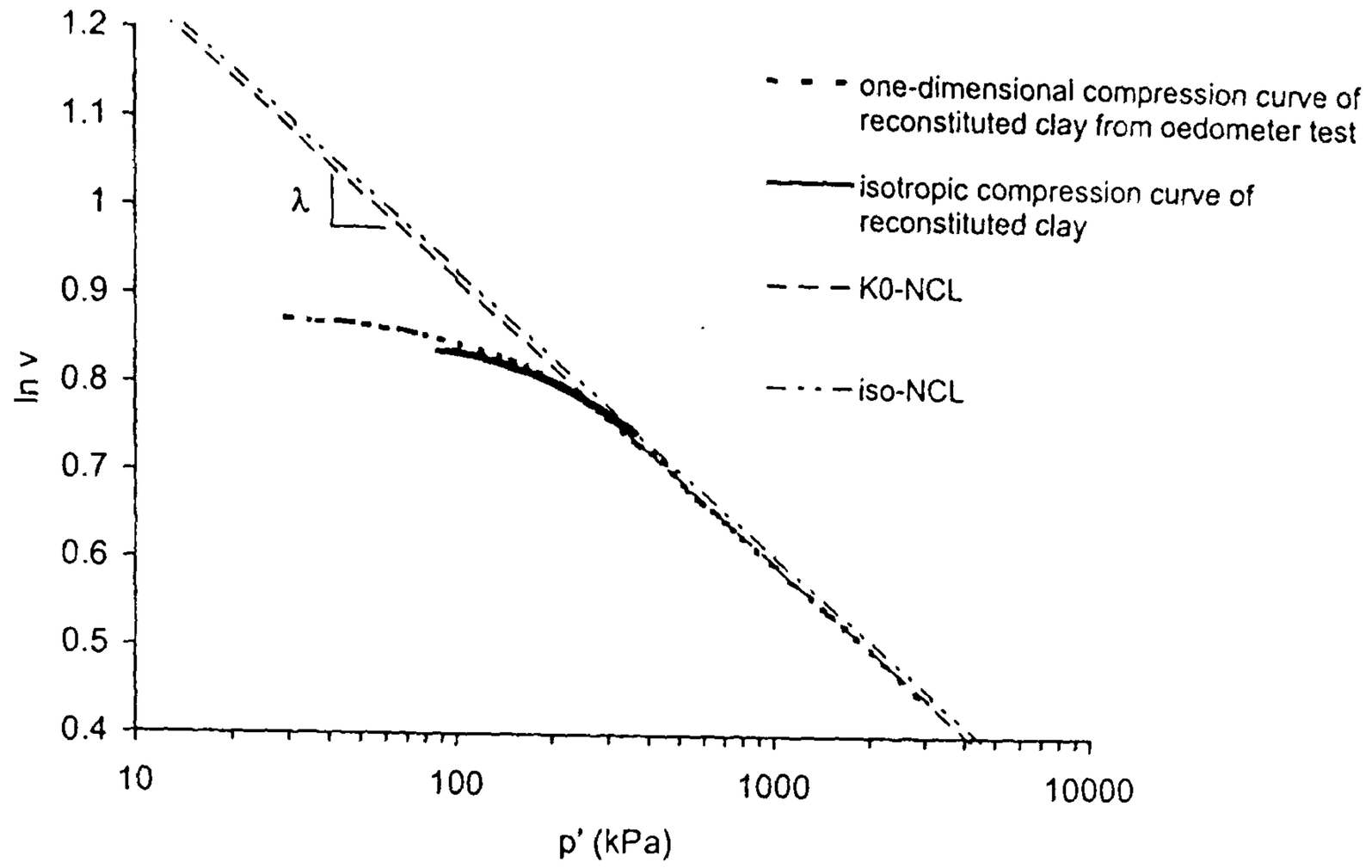

Figure 4.2.5 Determination of compression parameters for Pisa clay (data from Callisto, 1996)

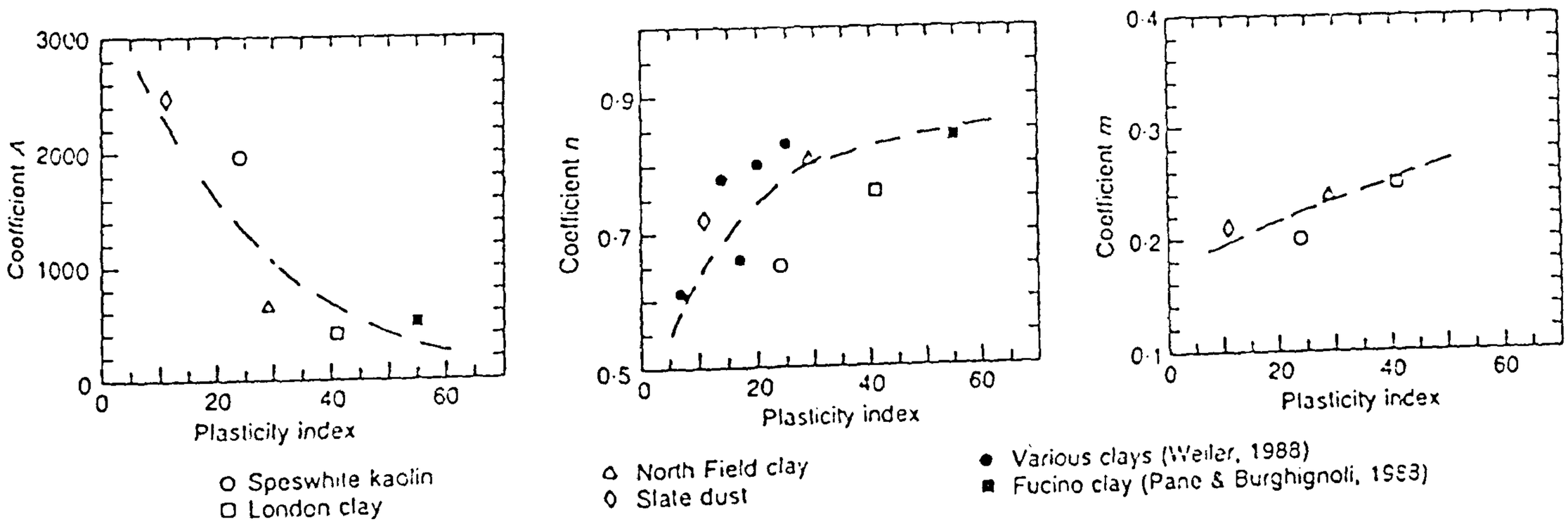

Figure 4.2.6 Variation of stiffness constants for G_e' with plasticity index (after Viggiani & Atkinson, 1995)

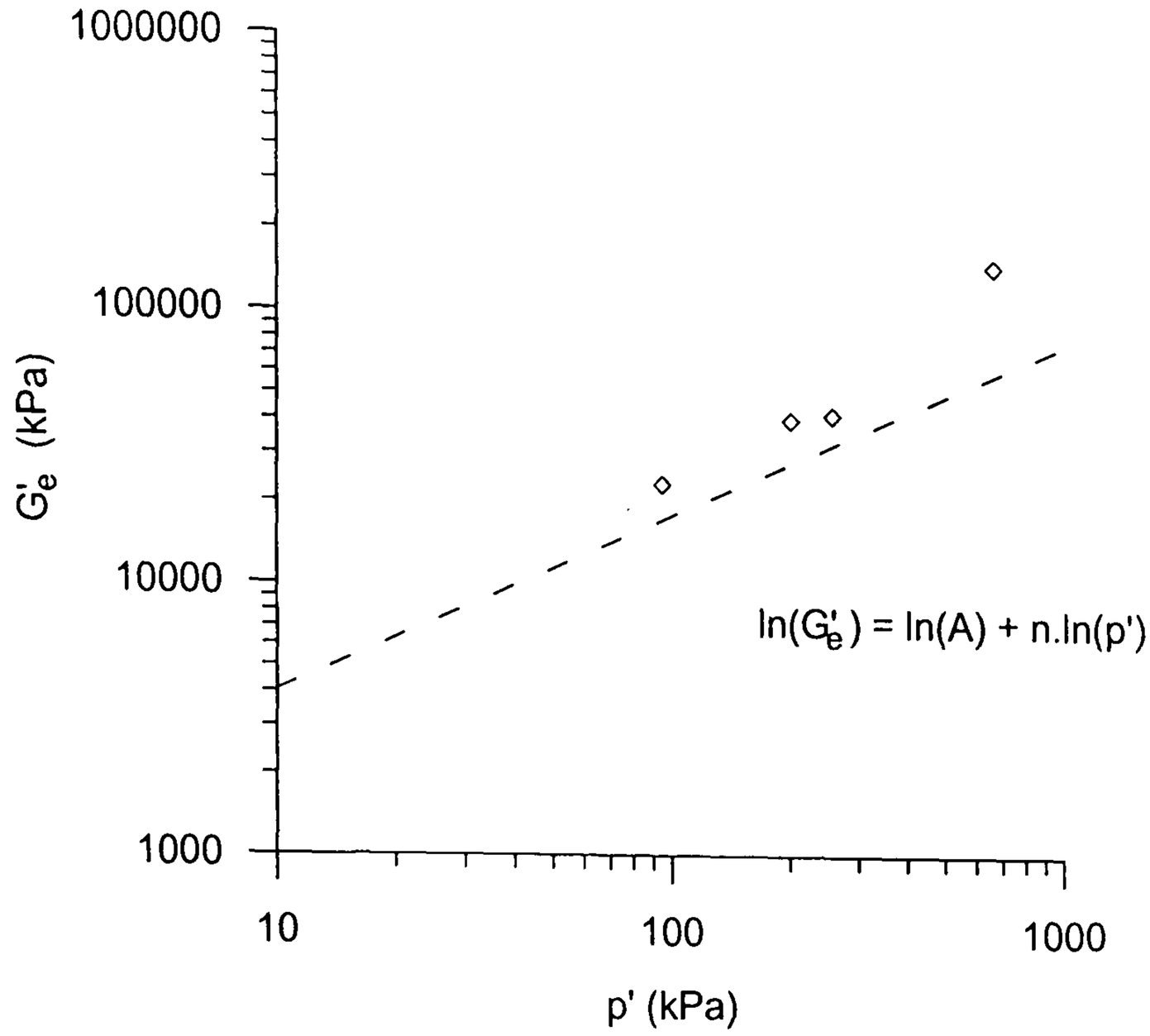

Figure 4.2.7 Variation of elastic stiffness of reconstituted Bothkennar clay determined in bender element tests with mean effective stress (data from Coop, 1998)

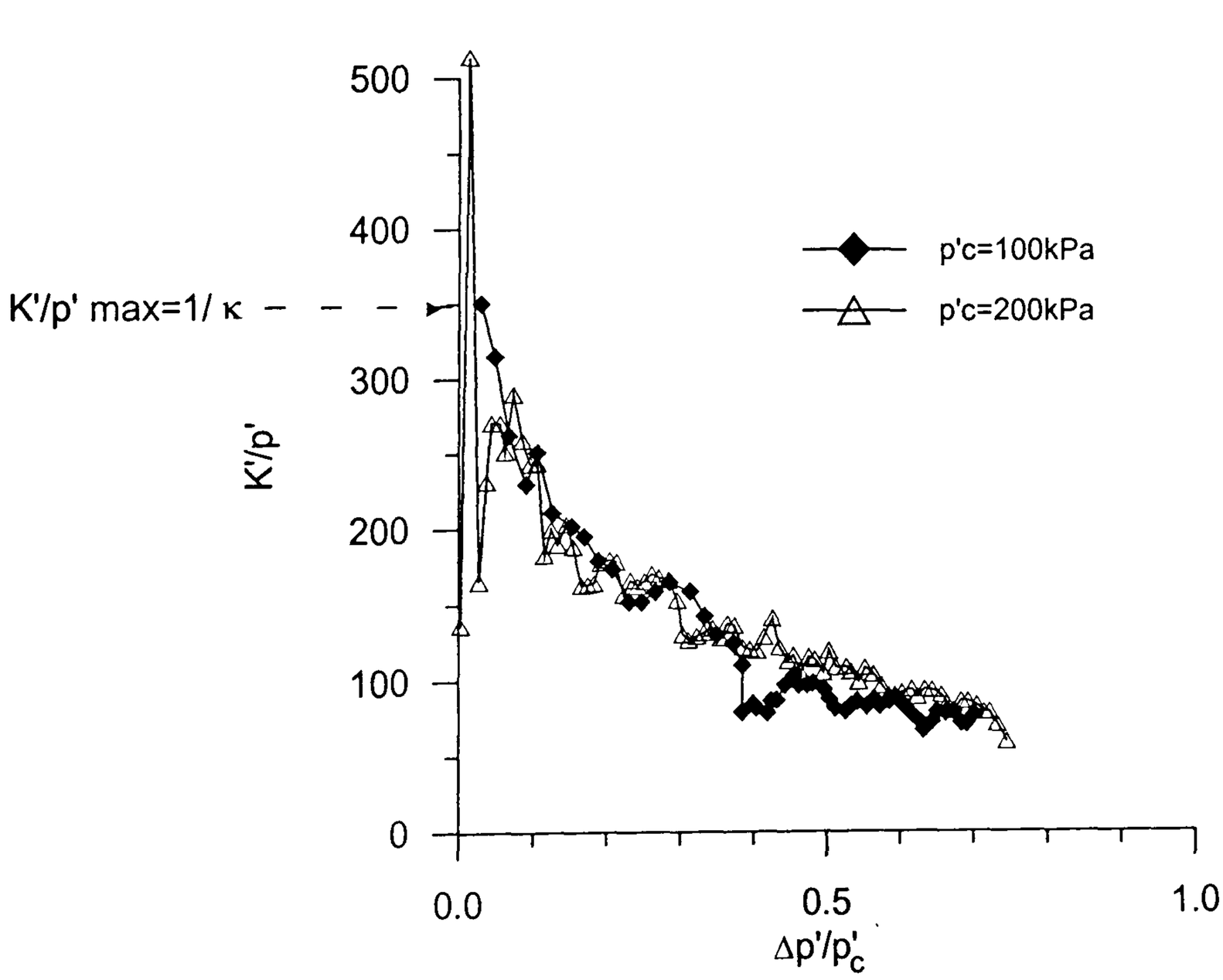

Figure 4.2.8 Normalised stiffness curves for isotropic swelling on reconstituted Bothkennar clay (data from Allman, 1992)

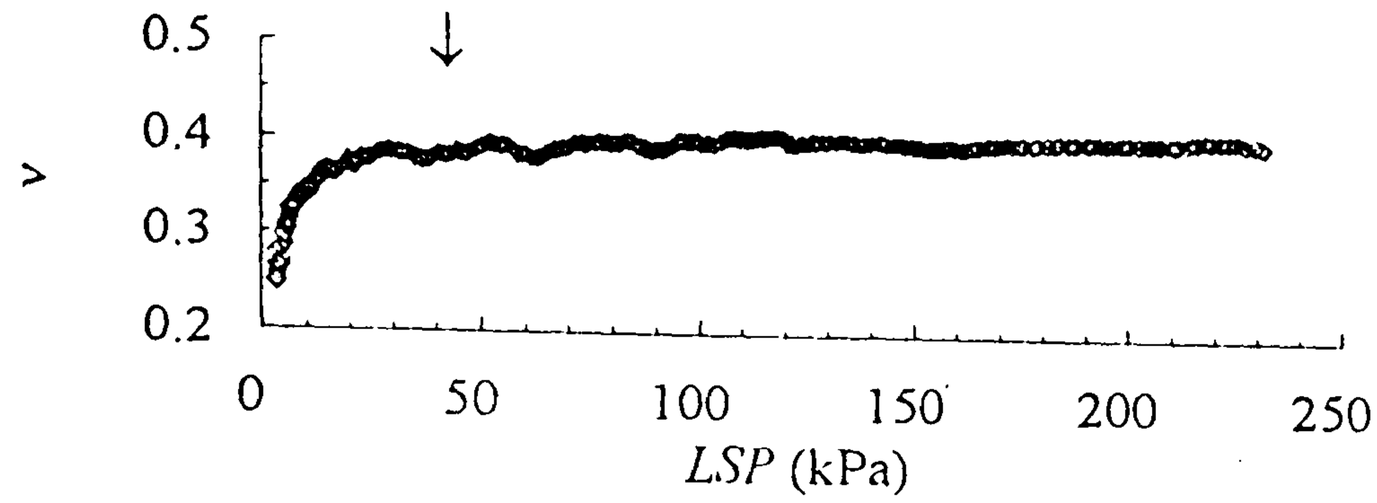

(a)

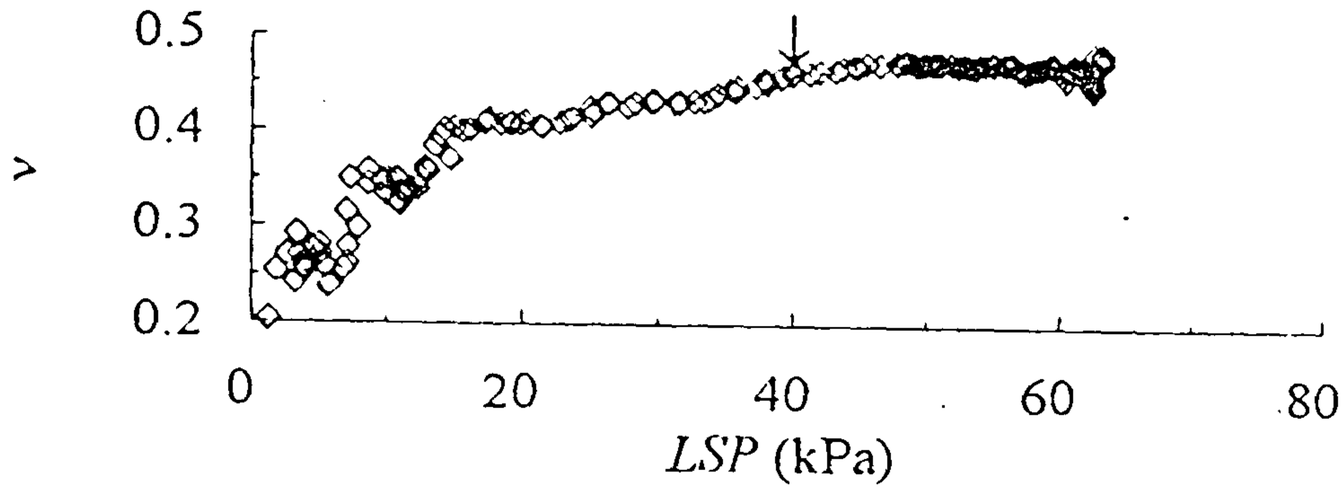

(b)

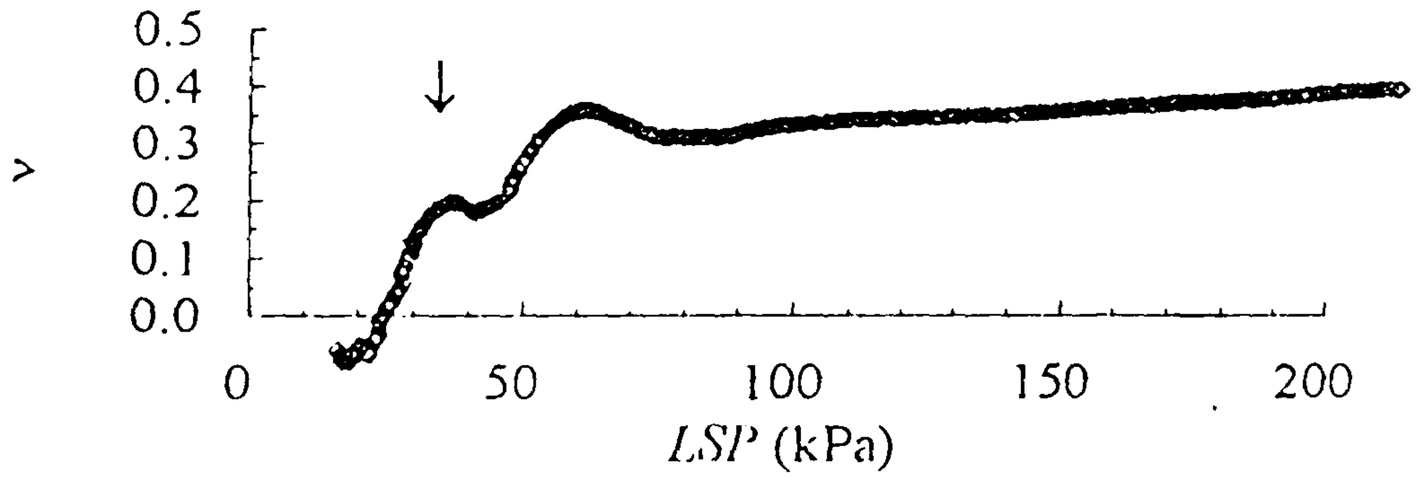

(c)

Figure 4.2.9 Poisson's ratio calculated from shear and bulk modulus of Pisa clay during drained probes (a) R30 (b) R60 (c) R315 (after Callisto, 1996)

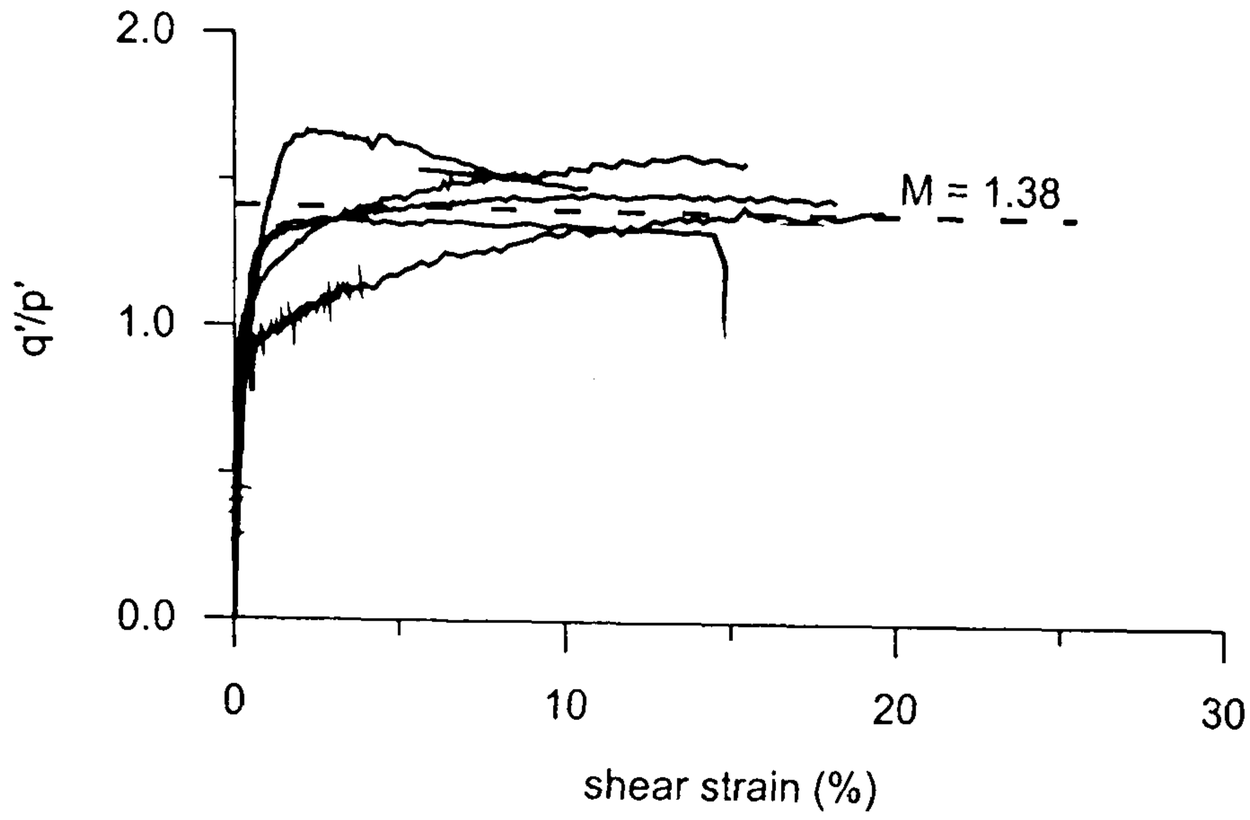

(a)

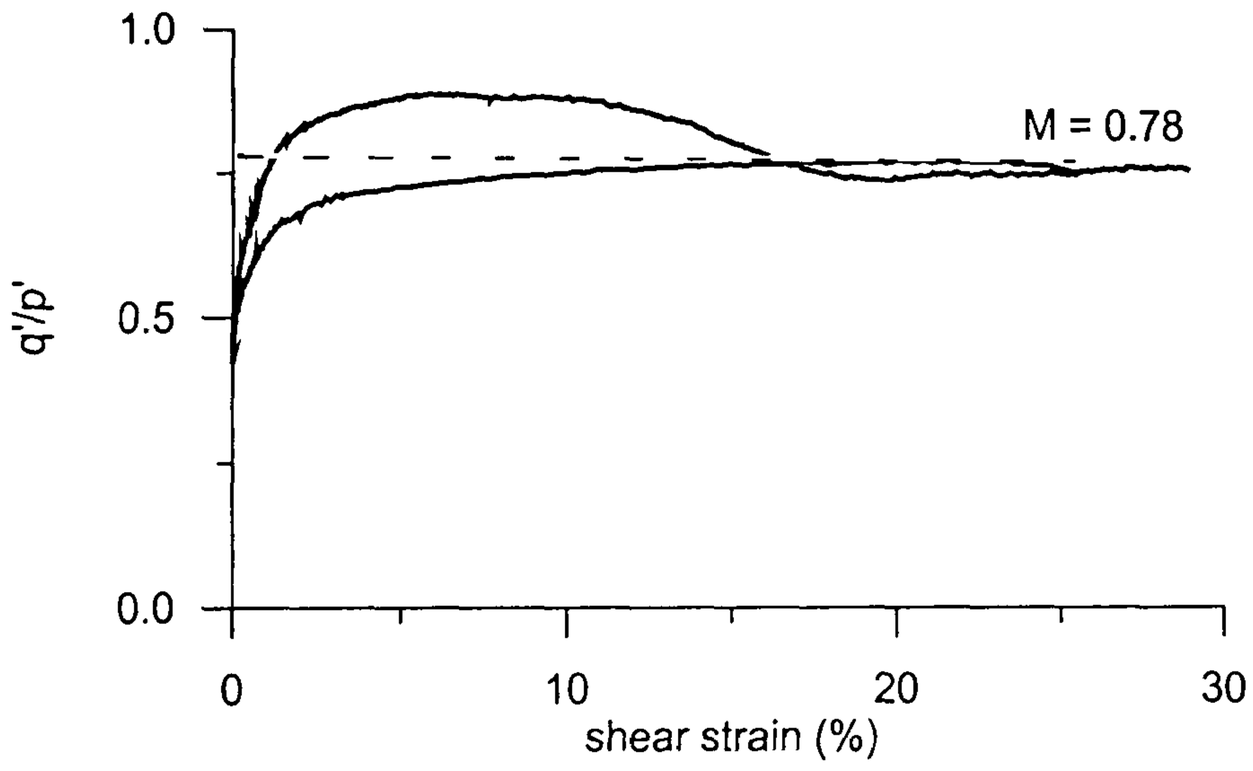

(b)

Figure 4.2.10 Friction coefficient M for (a) Bothkennar clay (data from Atkinson & Allman, 1992) (b) Pisa clay (data from Callisto, 1996)

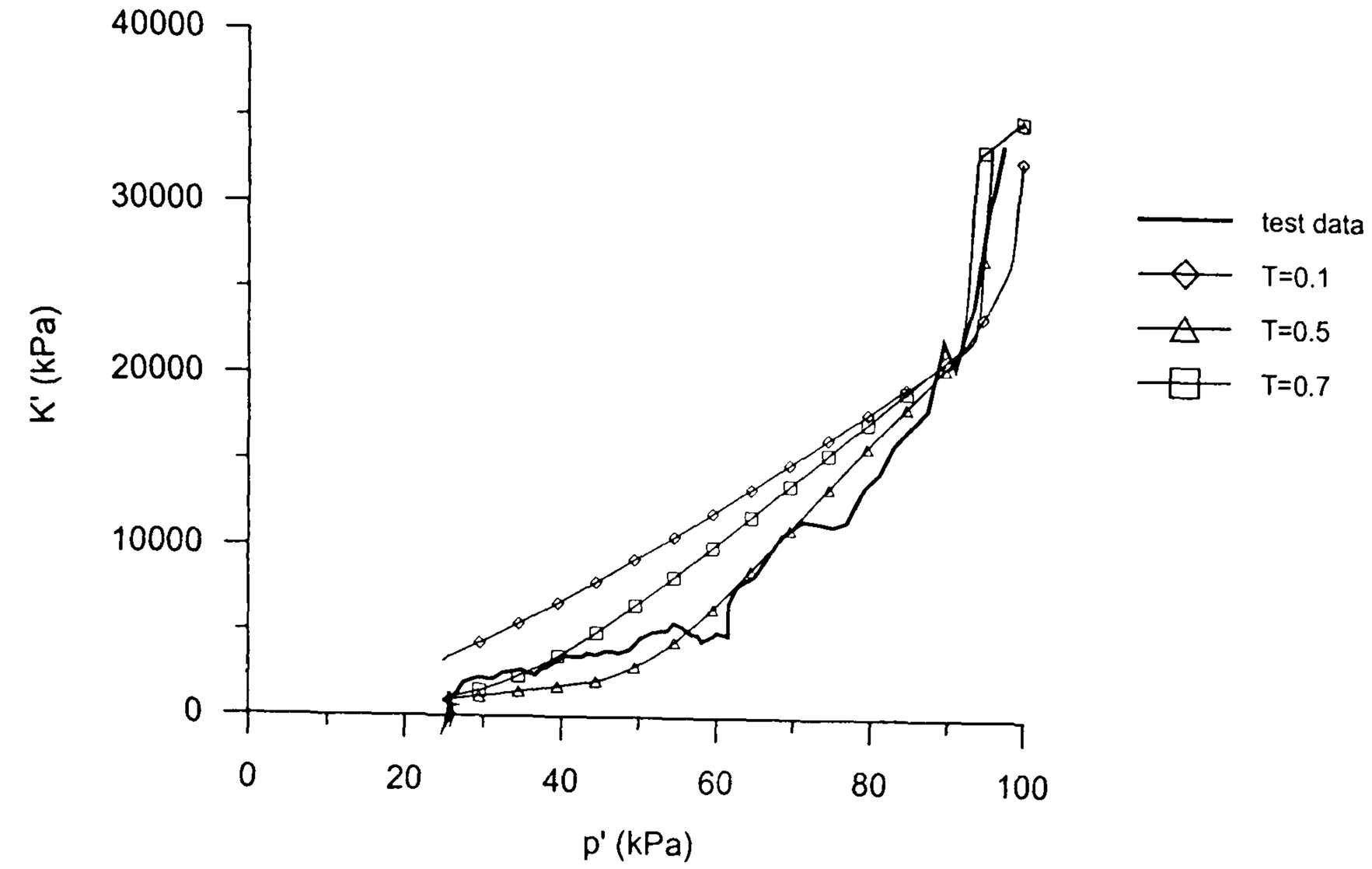

(a)

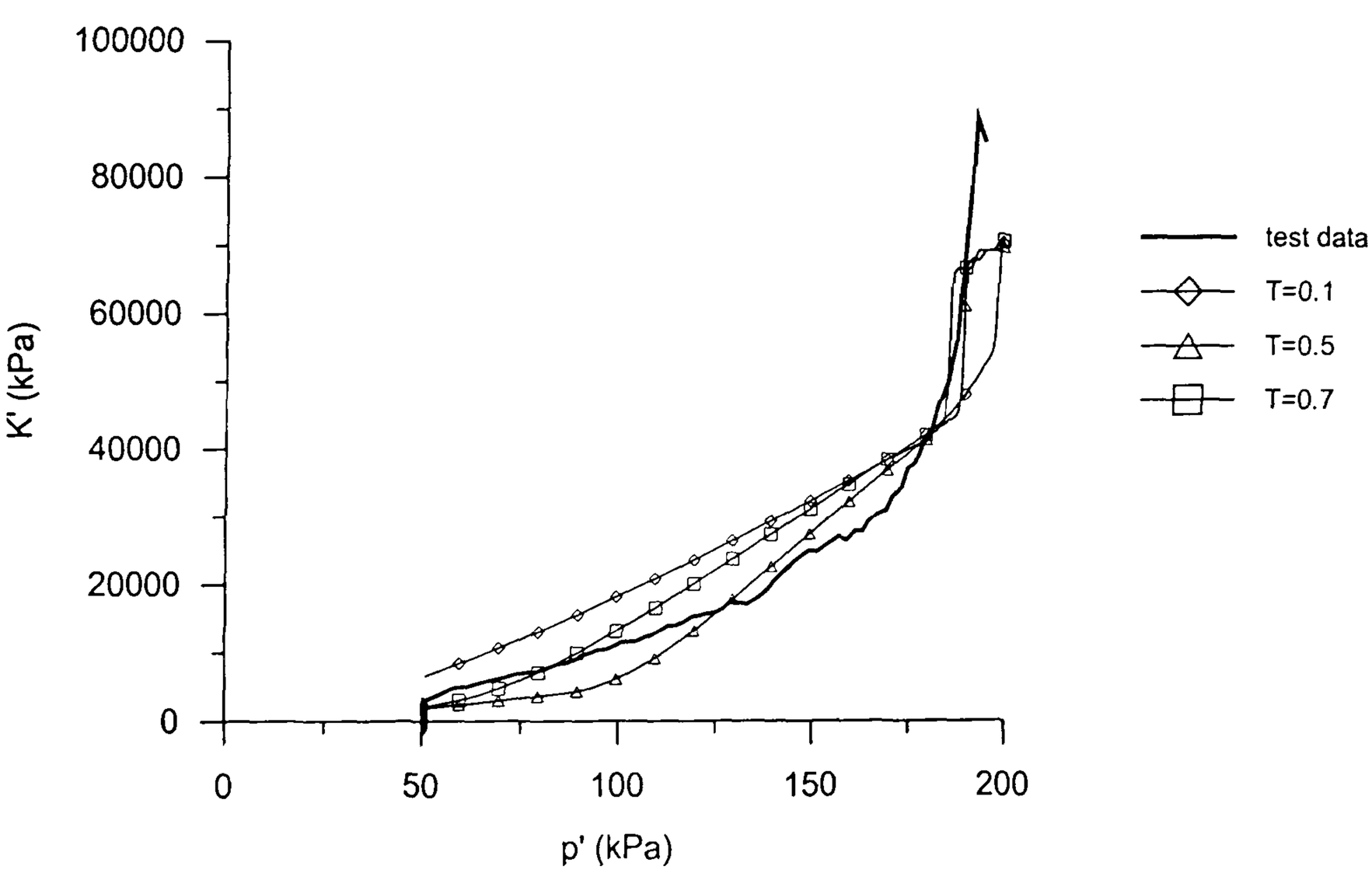

(b)

Figure 4.2.11 Effect of varying T on the predicted value of bulk modulus during isotropic swelling of Bothkennar clay from (a) p_c'=100kPa (b) p_c'=200kPa (test data from Allman, 1992)

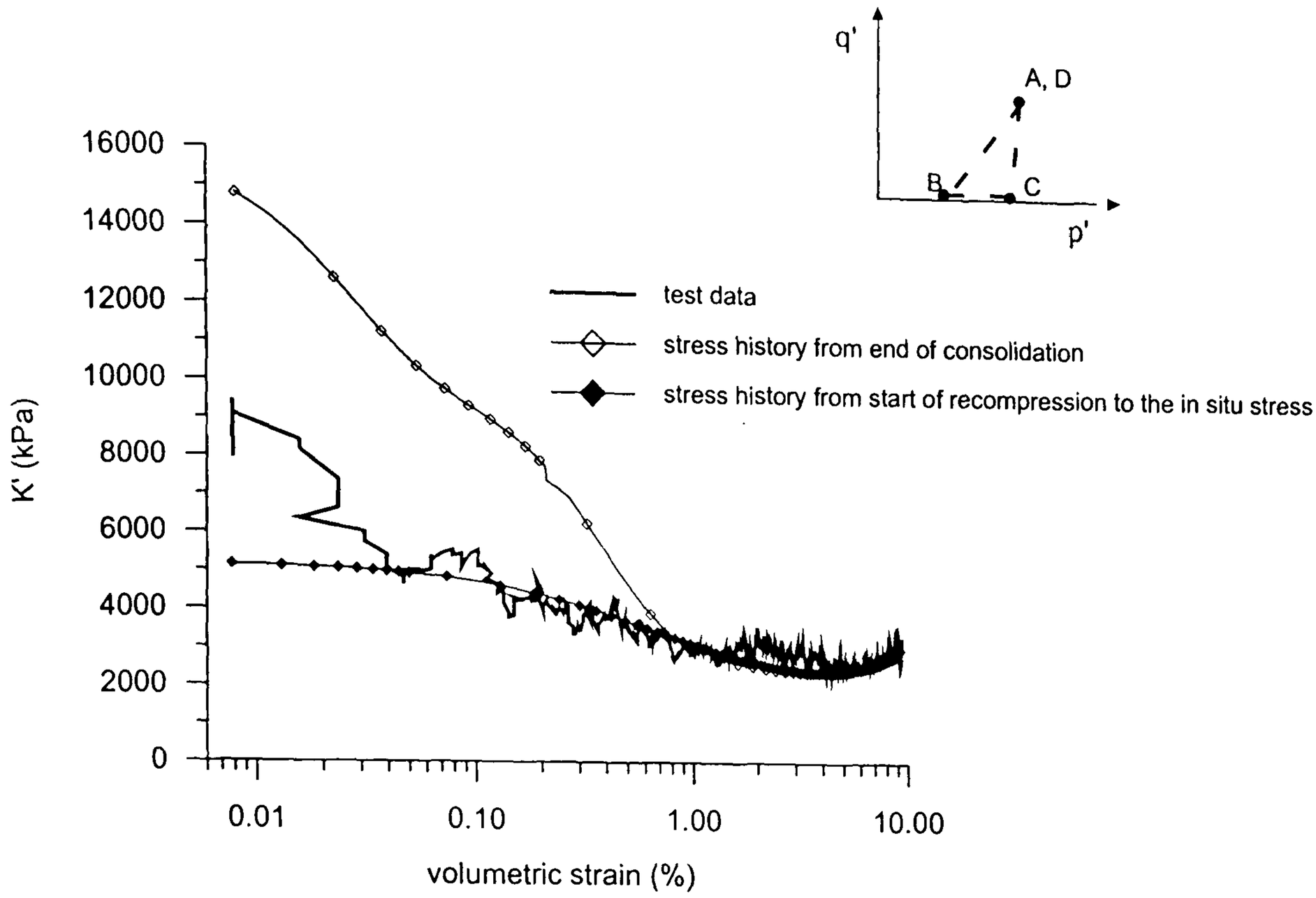

(a)

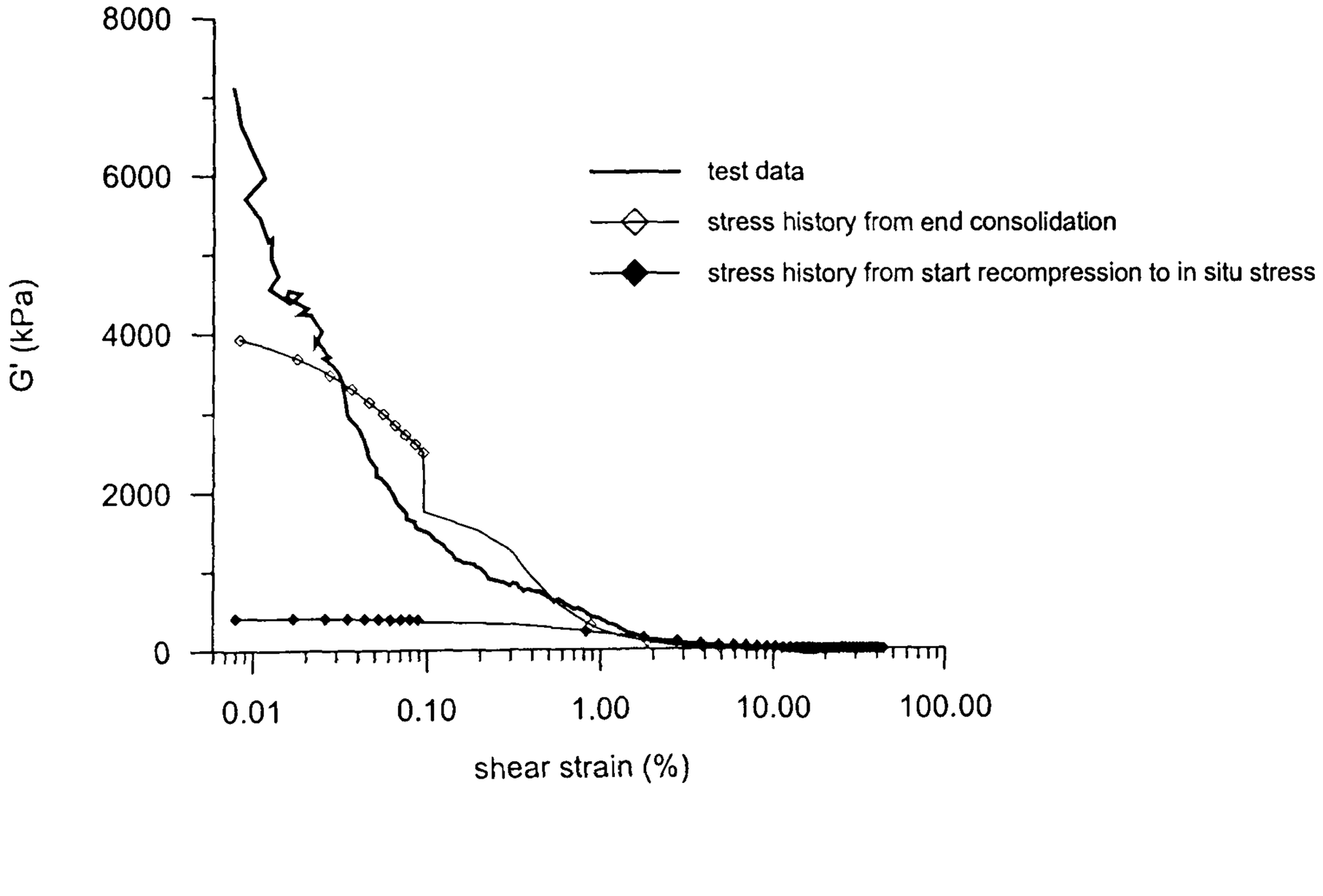

(b)

Figure 4.2.12 Effect of modelling the stress history back to the end of consolidation in the oedometer, on the prediction of stiffness during drained probes on reconstituted Pisa clay samples (a) R0 (b) R90 (test data from Callisto, 1996)

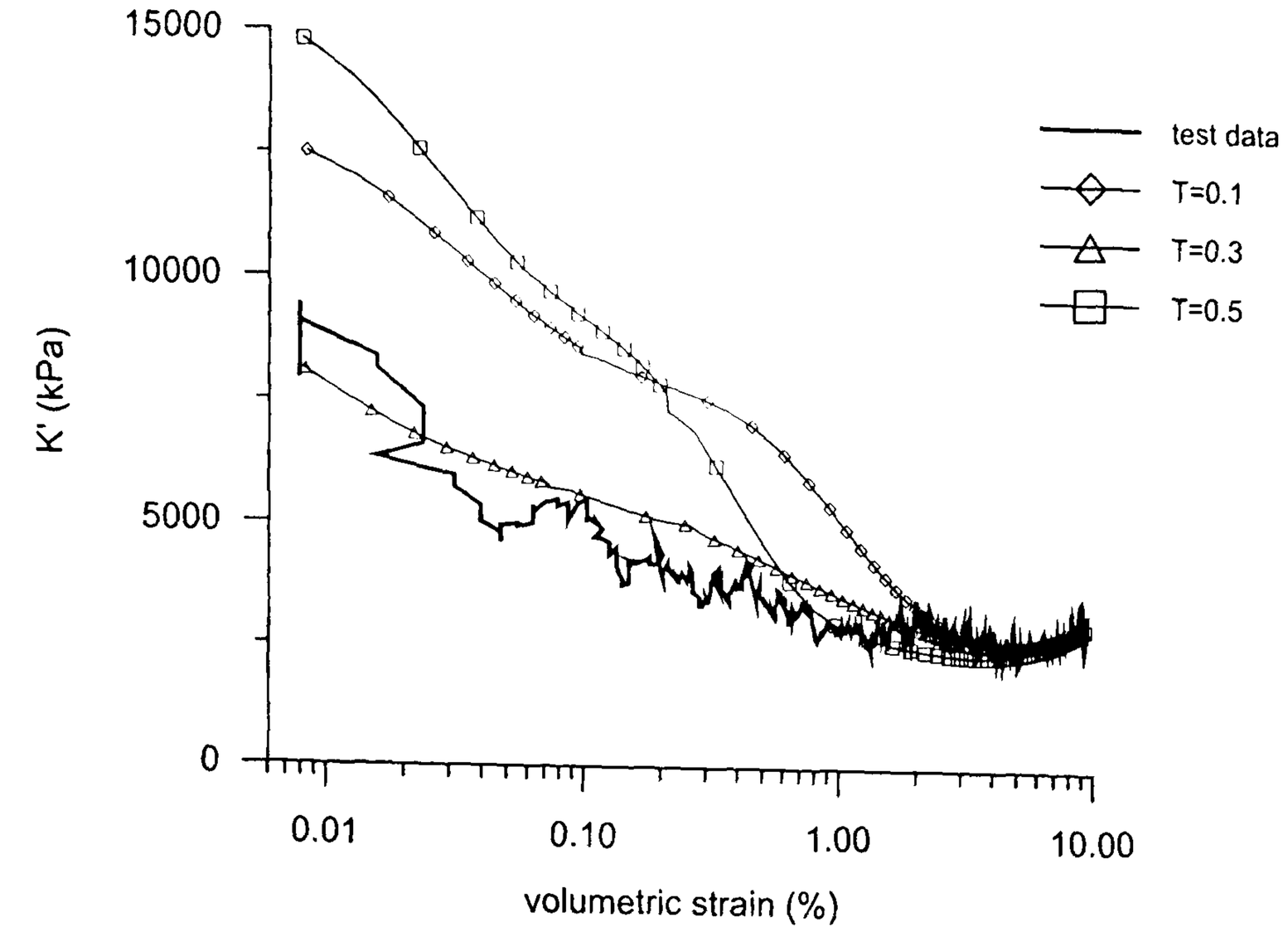

(a)

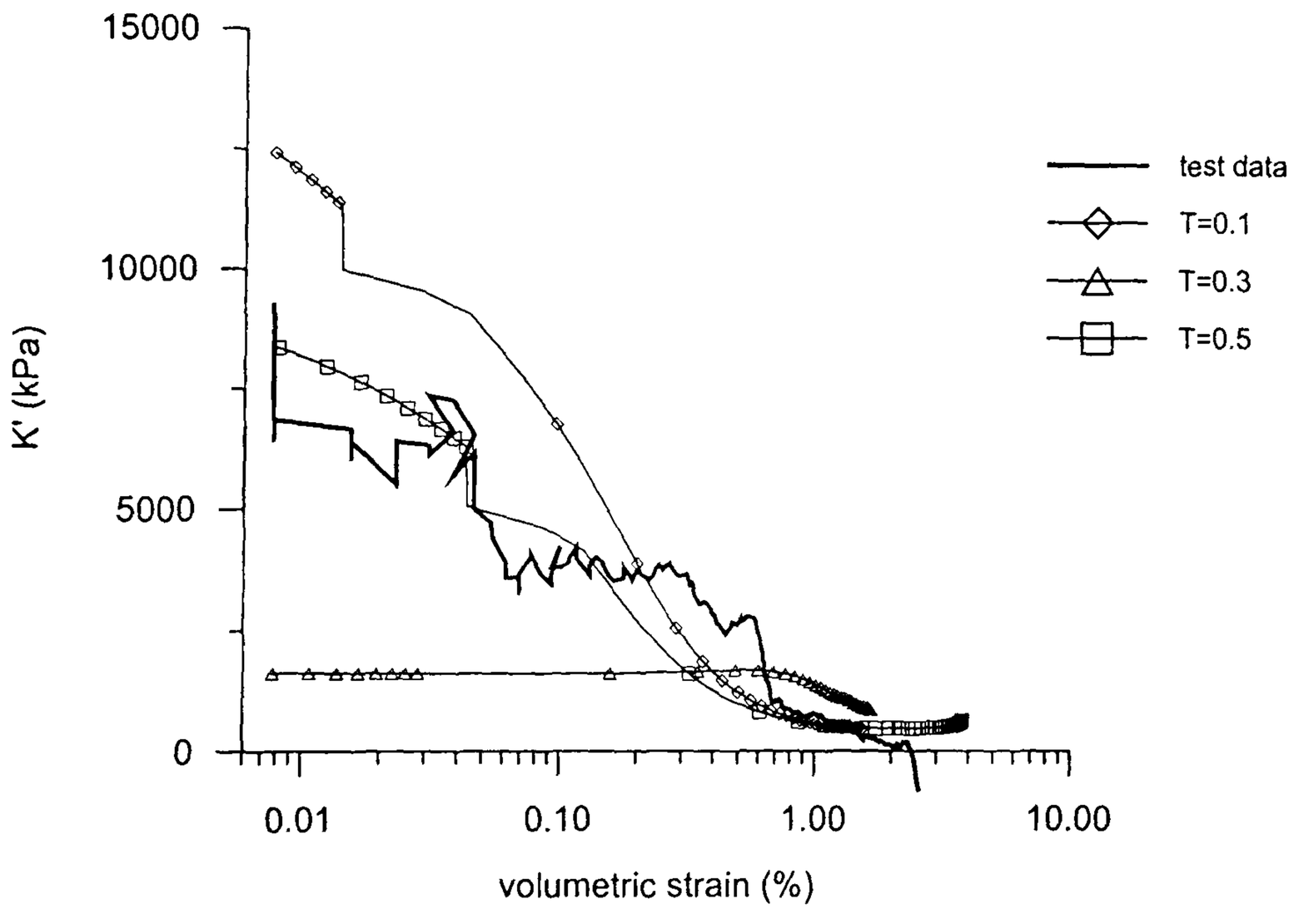

(b)

Figure 4.2.13 Effect of varying T on the predicted value of bulk modulus during drained probes on Pisa clay samples (a) R0 (b) R60 (test data from Callisto, 1998)

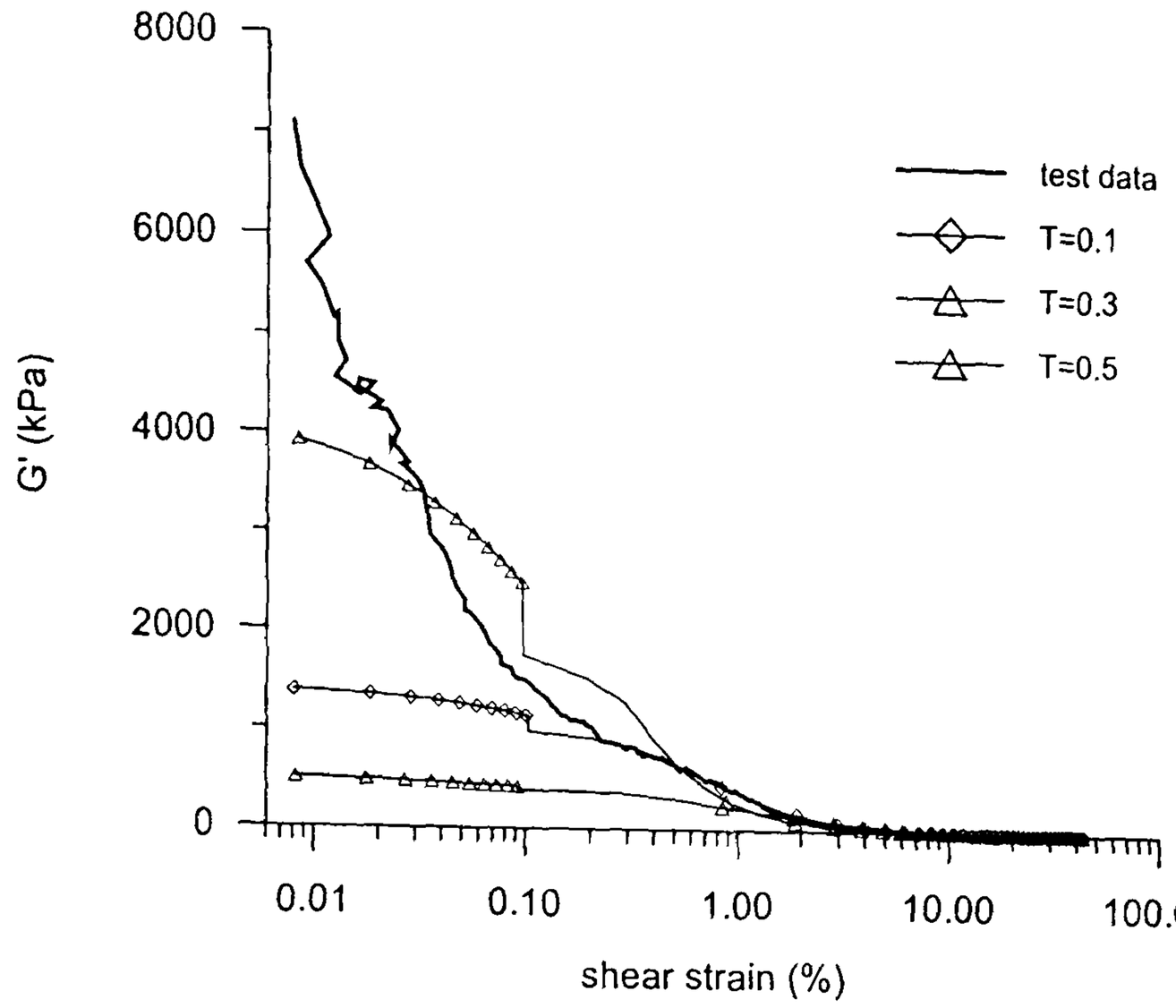

(a)

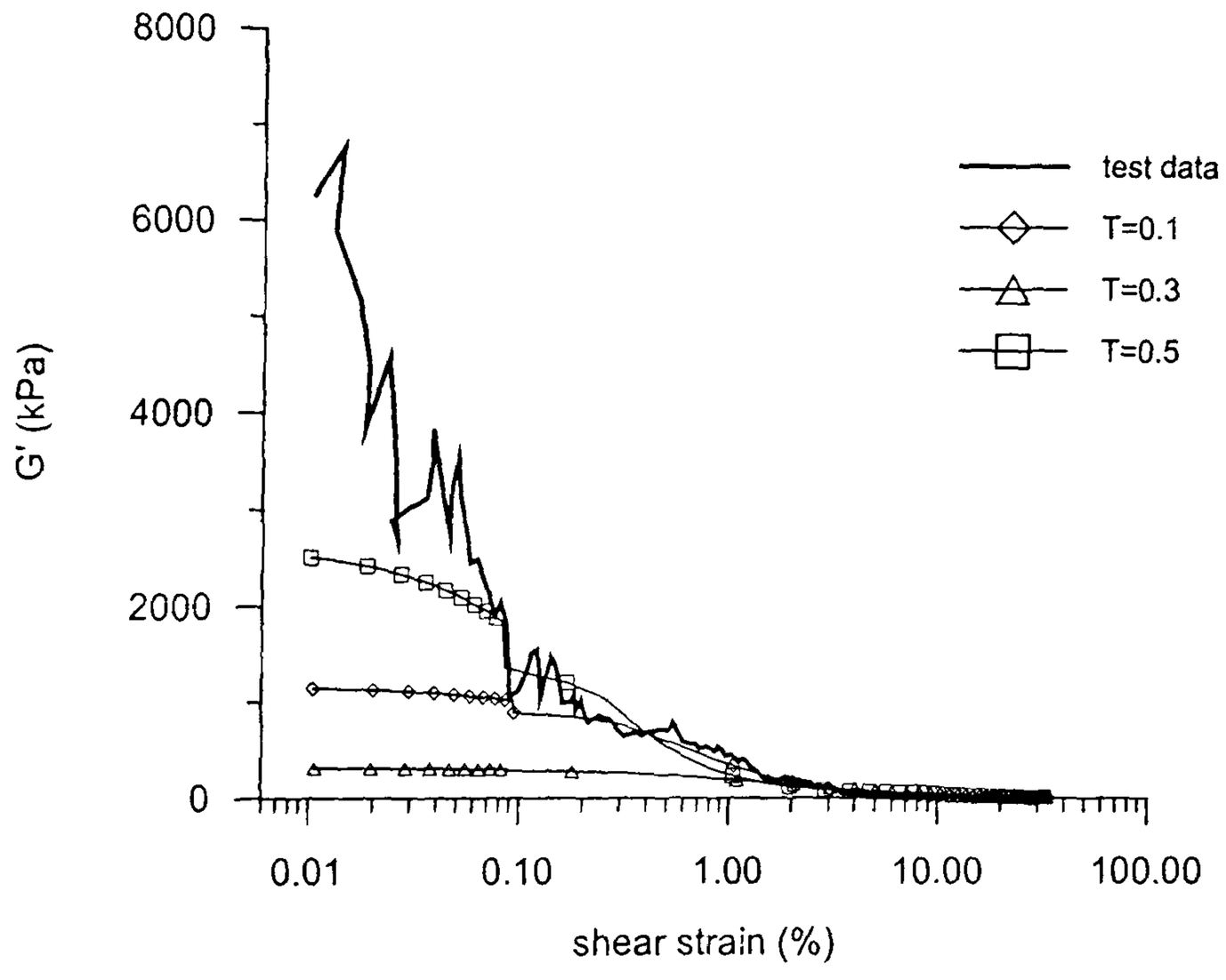

(b)

Figure 4.2.14 Effect of varying T on the predicted value of shear modulus during drained probes on Pisa clay samples (a) R90 (b) R60 (test data from Callisto, 1998)

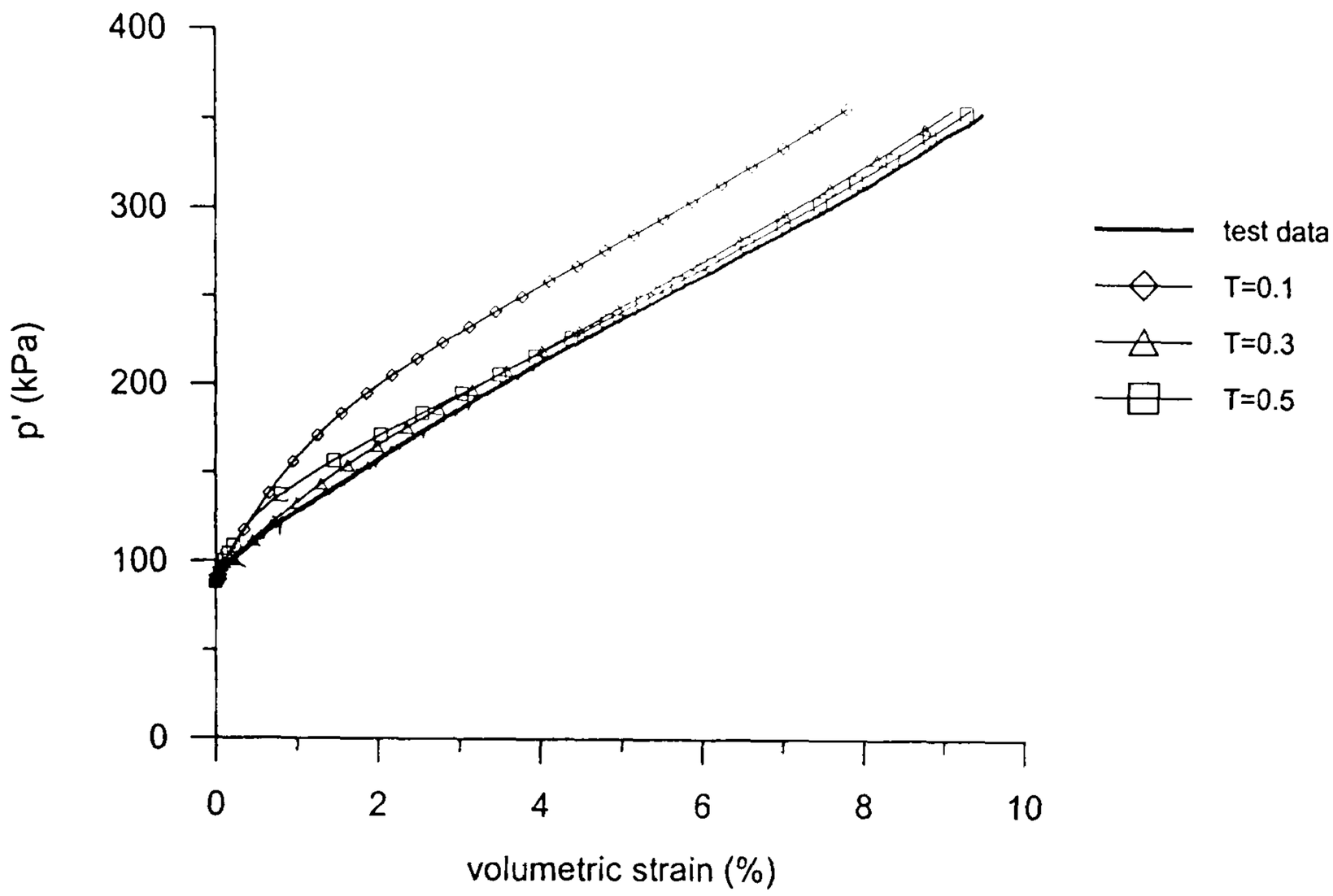

Figure 4.2.15 Effect of T on the predicted large strain behaviour during drained probe on Pisa clay sample R0 (test data from Callisto, 1996)

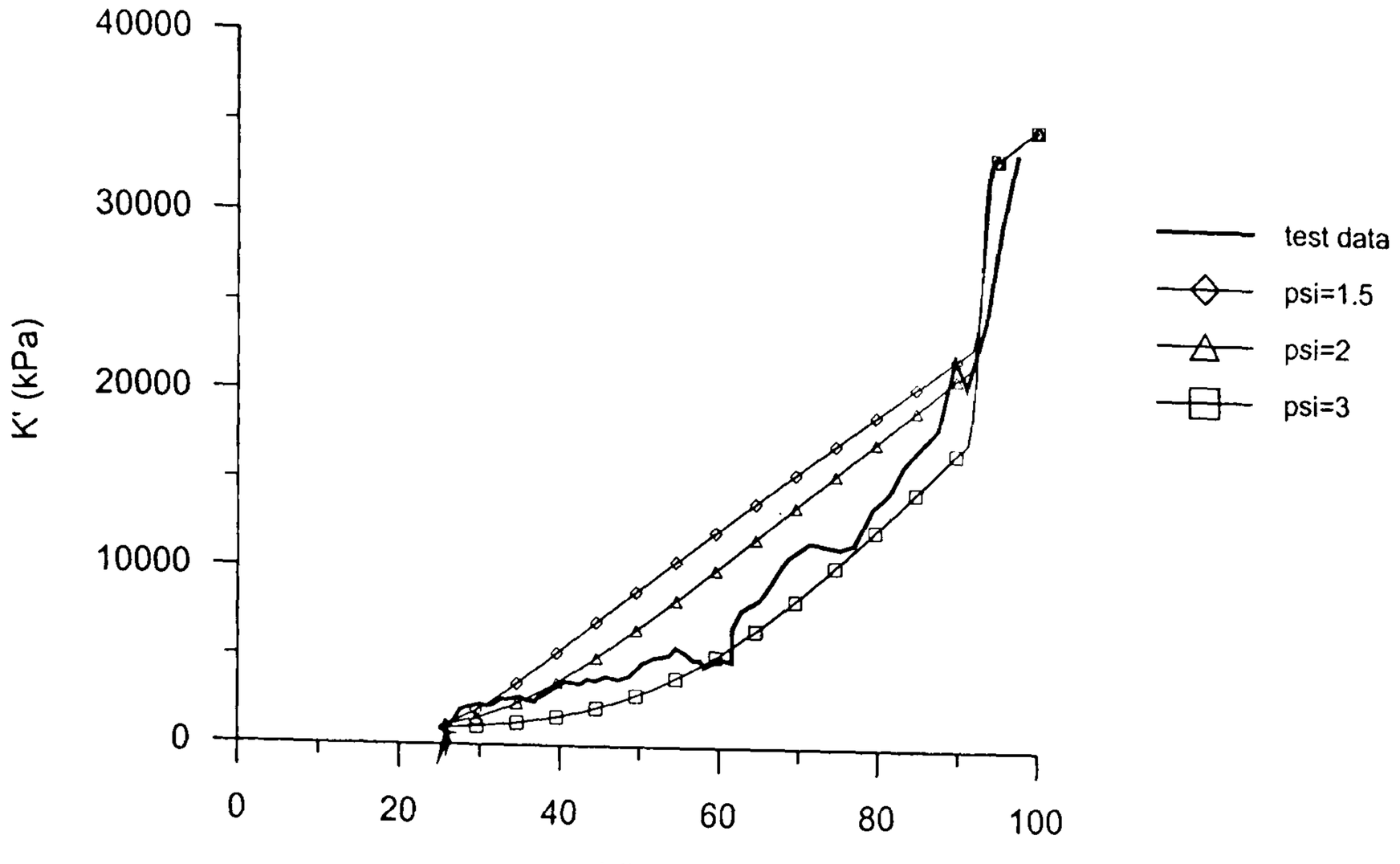

(a)

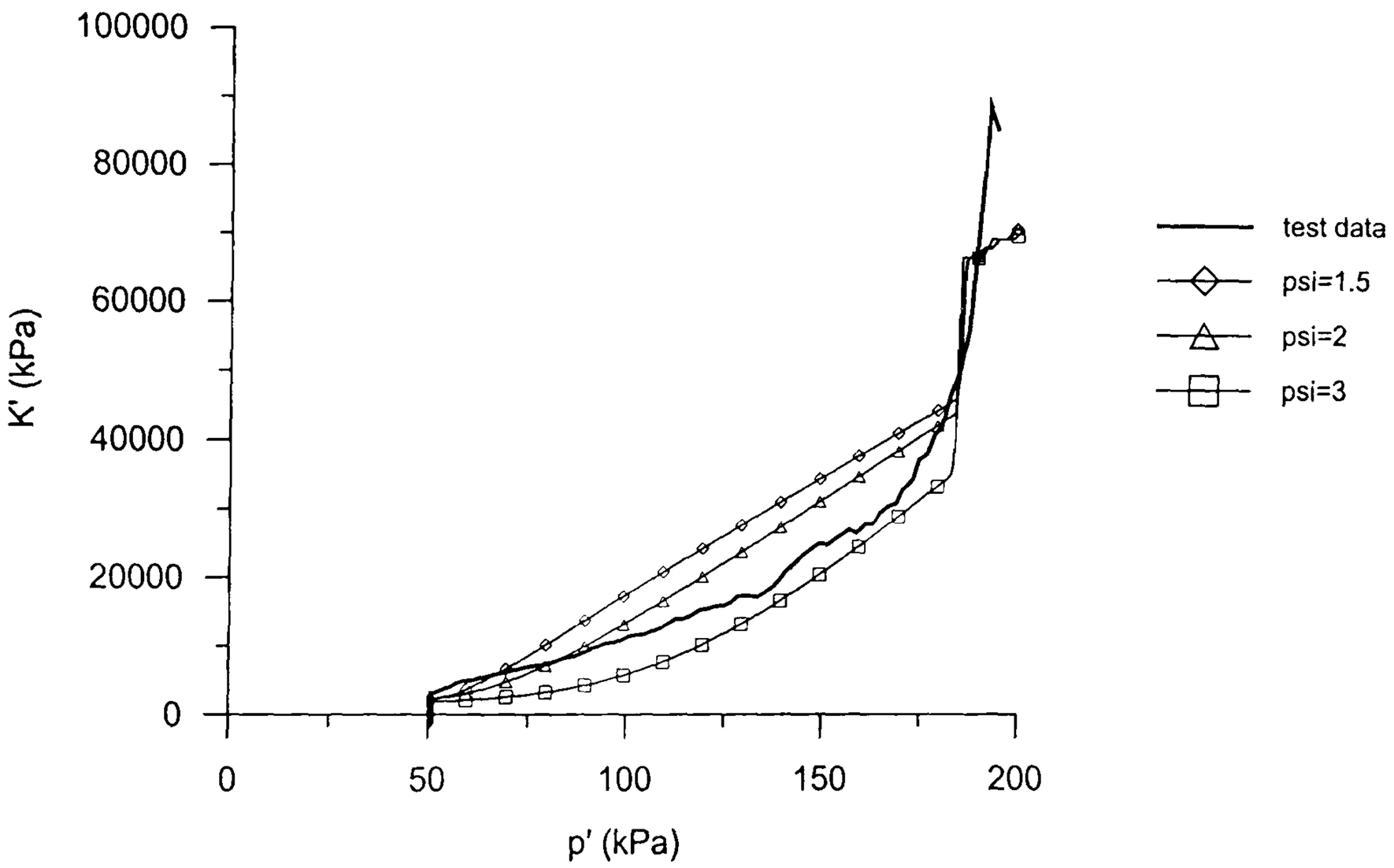

(b)

Figure 4.2.16 Effect of varying ψ on the predicted value of bulk modulus during isotropic swelling of Bothkennar clay from (a) p_c'=100kPa (b) p_c'=200kPa (test data from Allman, 1992)

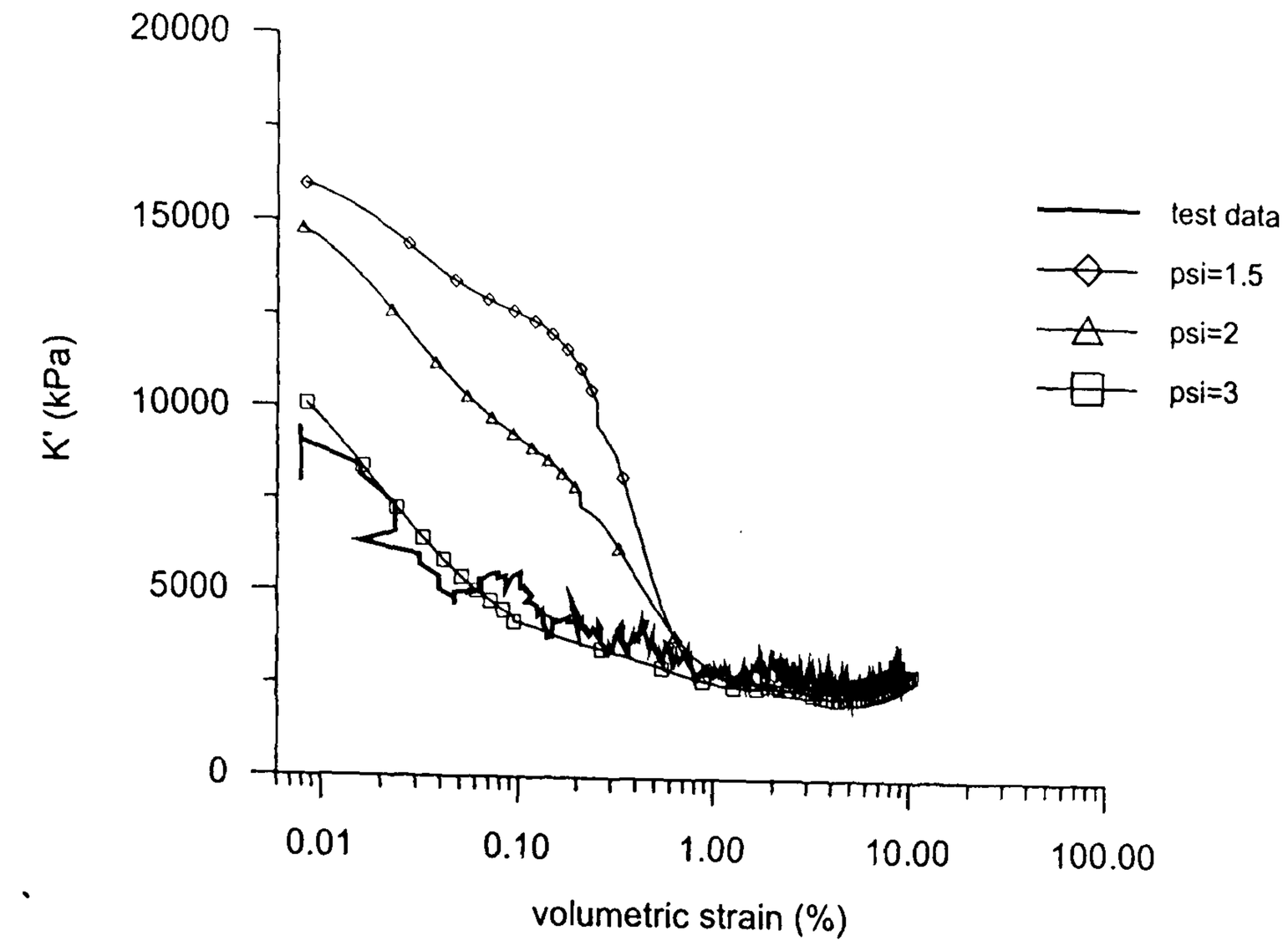

(a)

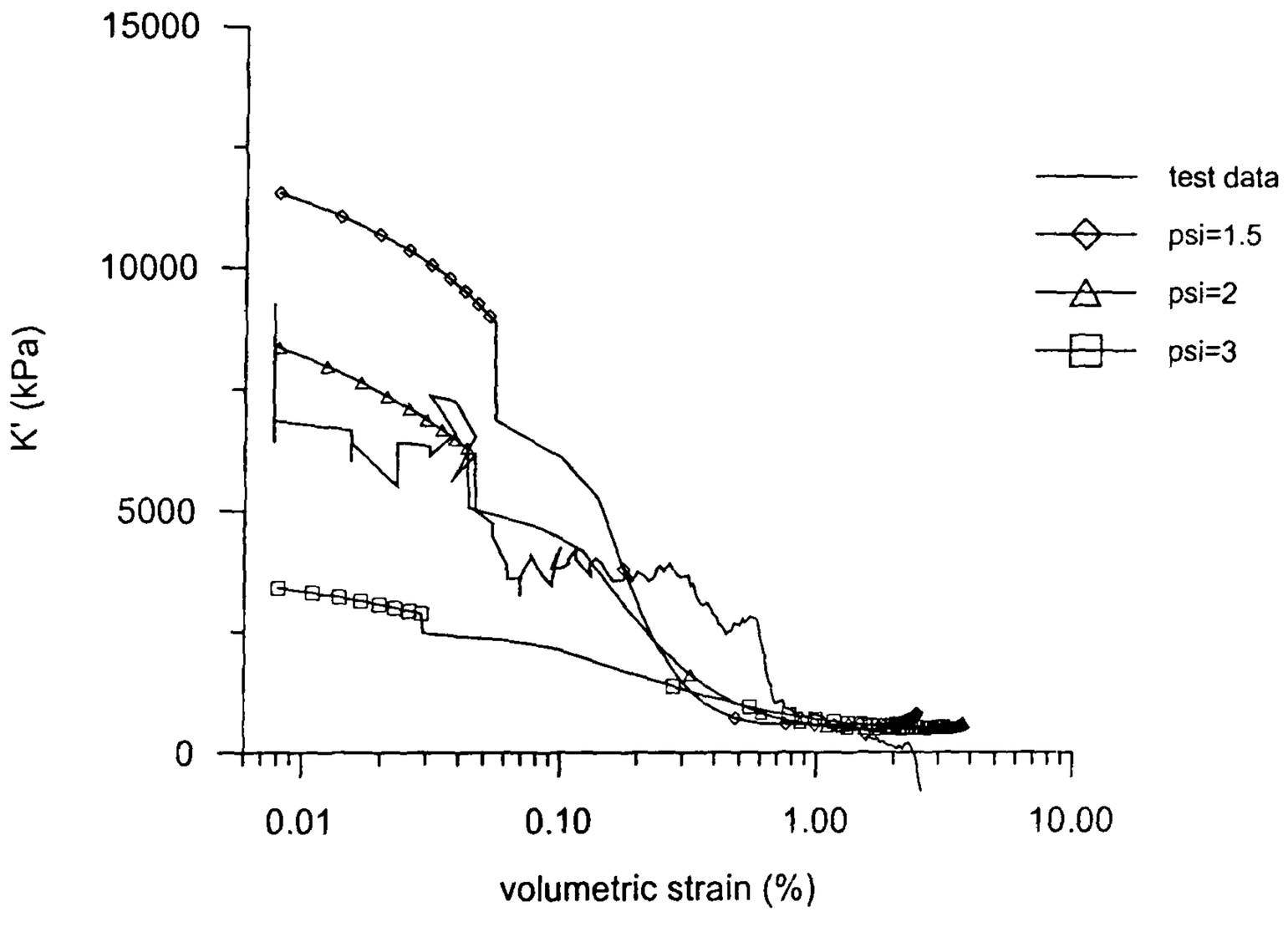

(b)

Figure 4.2.17 Effect of varying ψ on the predicted value of bulk modulus during drained probes on Pisa clay samples (a) R0 (b) R60 (test data from Callisto, 1998)

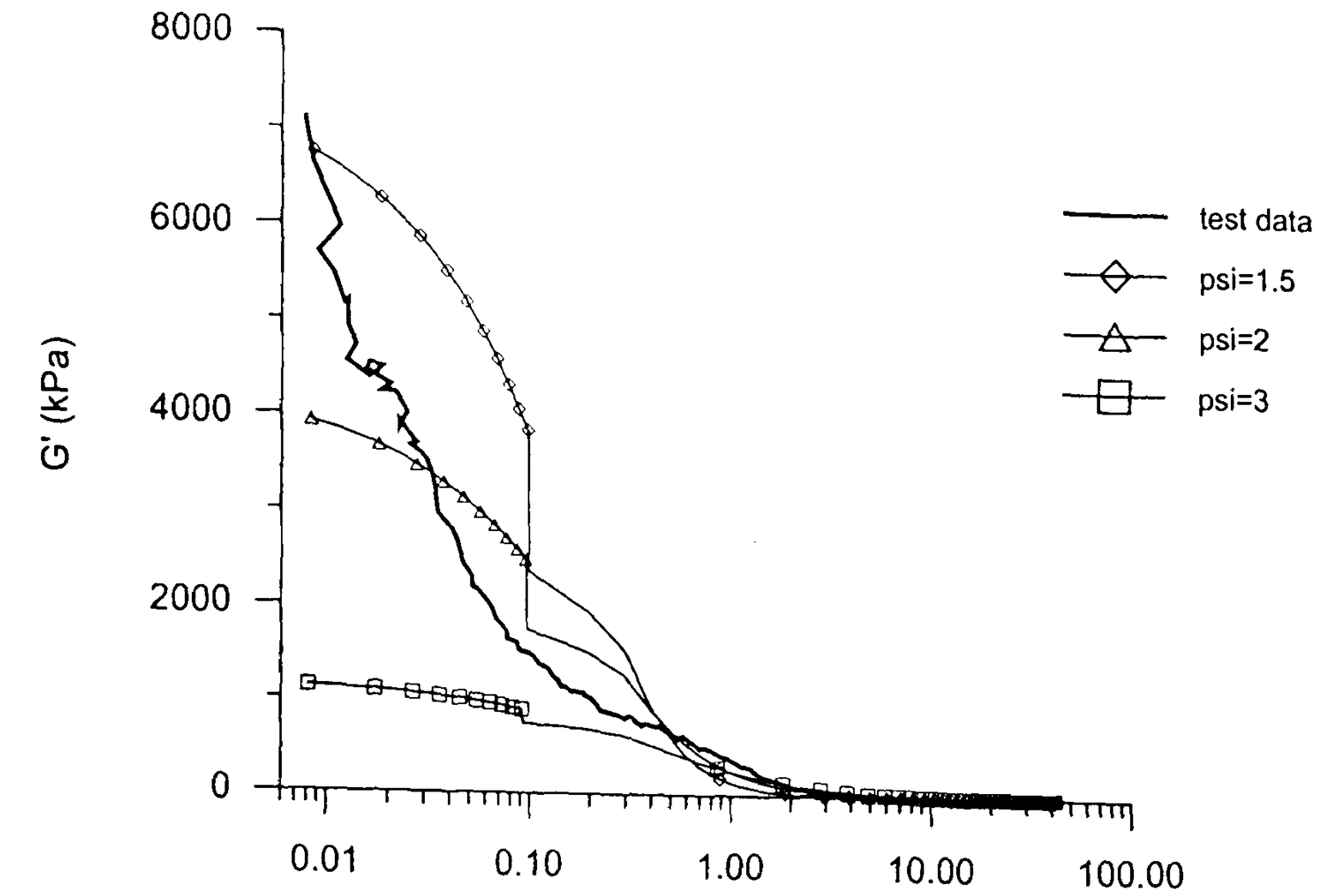

(a)

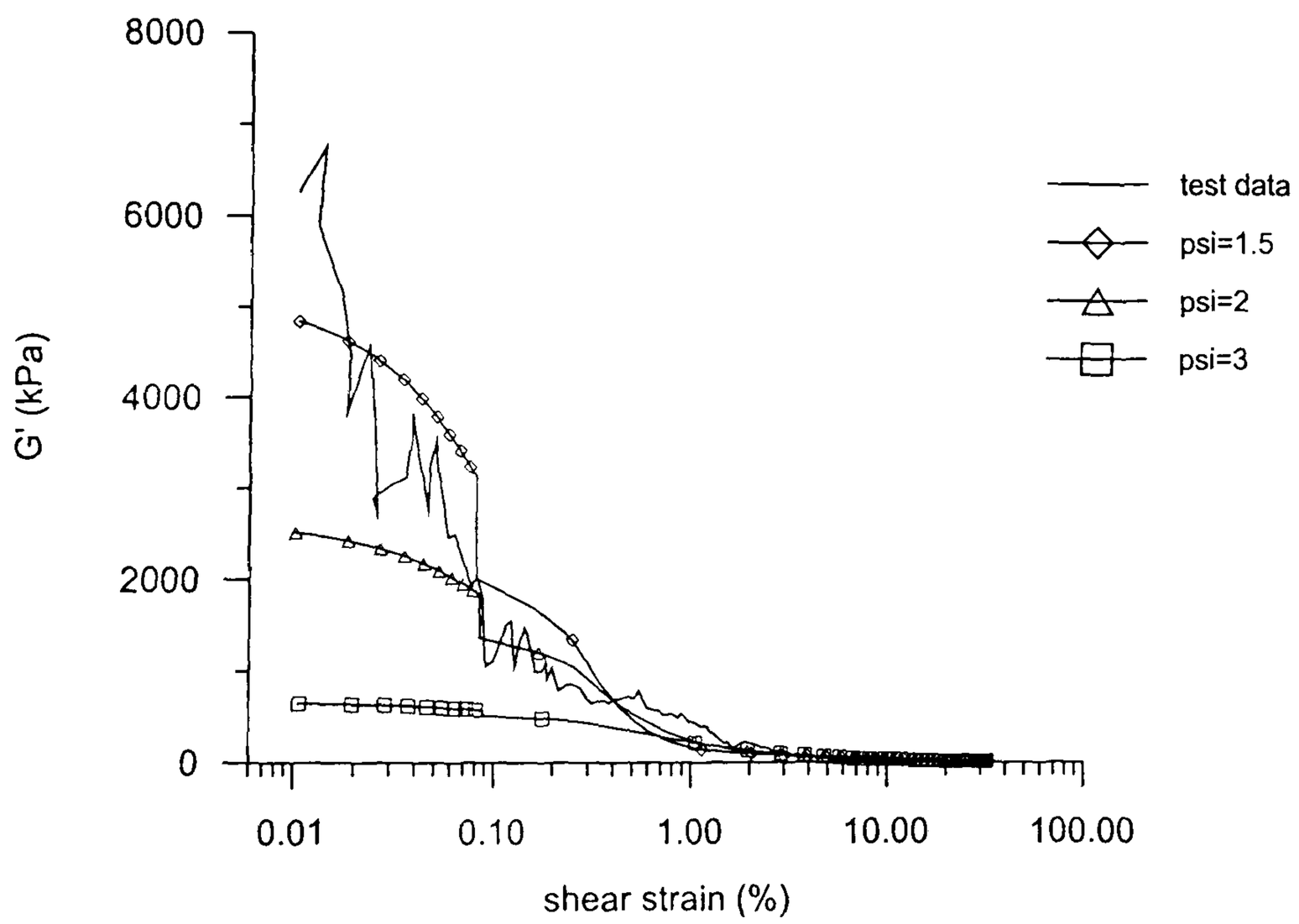

(b)

Figure 4.2.18 Effect of varying ψ on the predicted value of shear modulus during drained probes on Pisa clay samples (a) R90 (b) R60 (test data from Callisto, 1998)

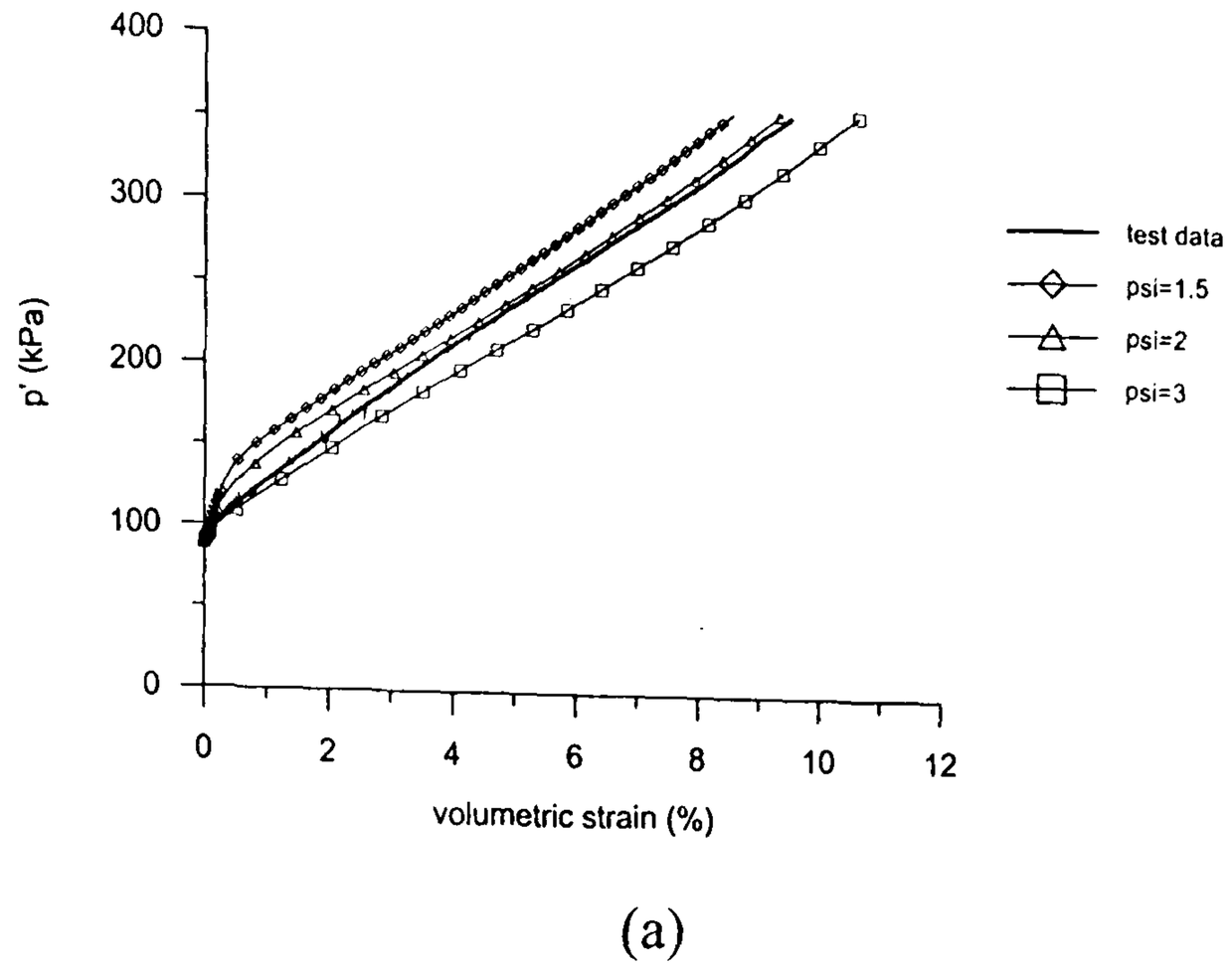

(a)

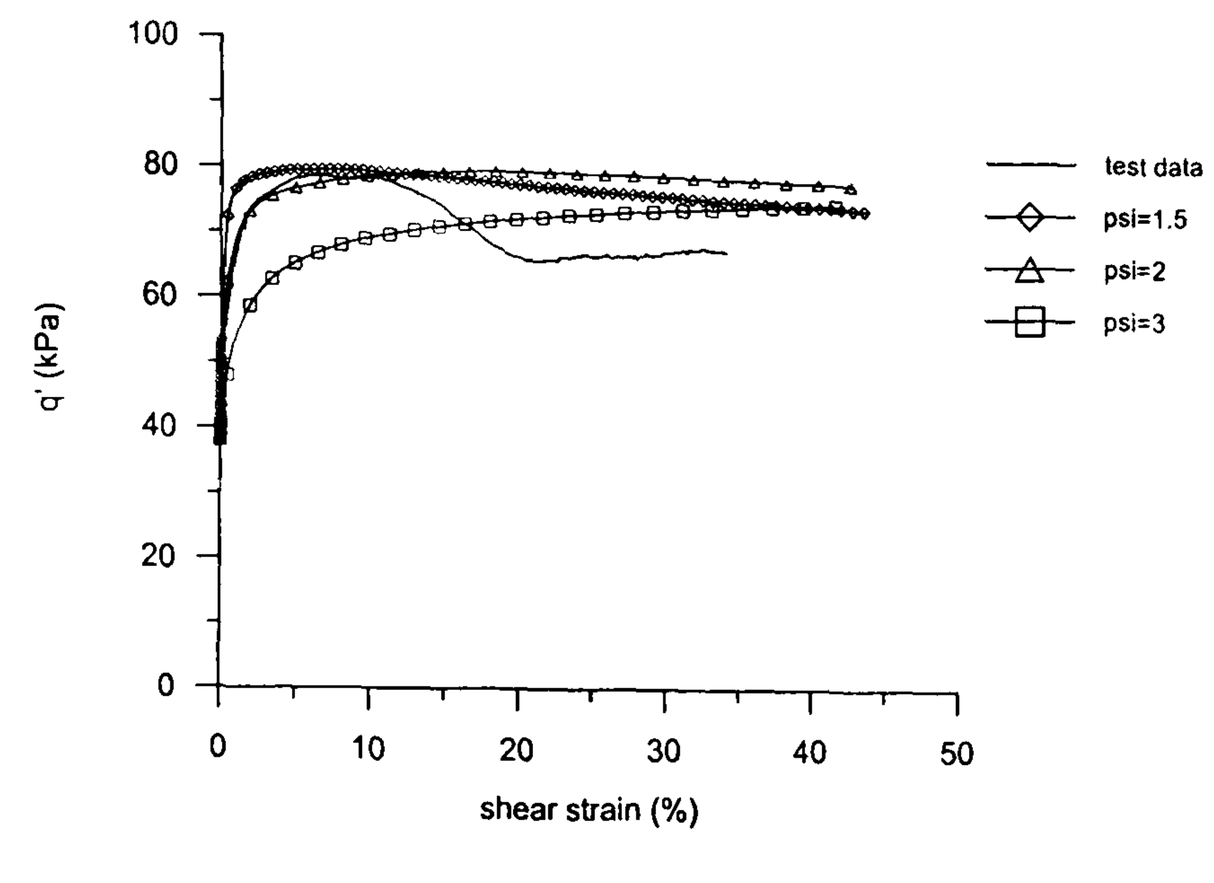

(b)

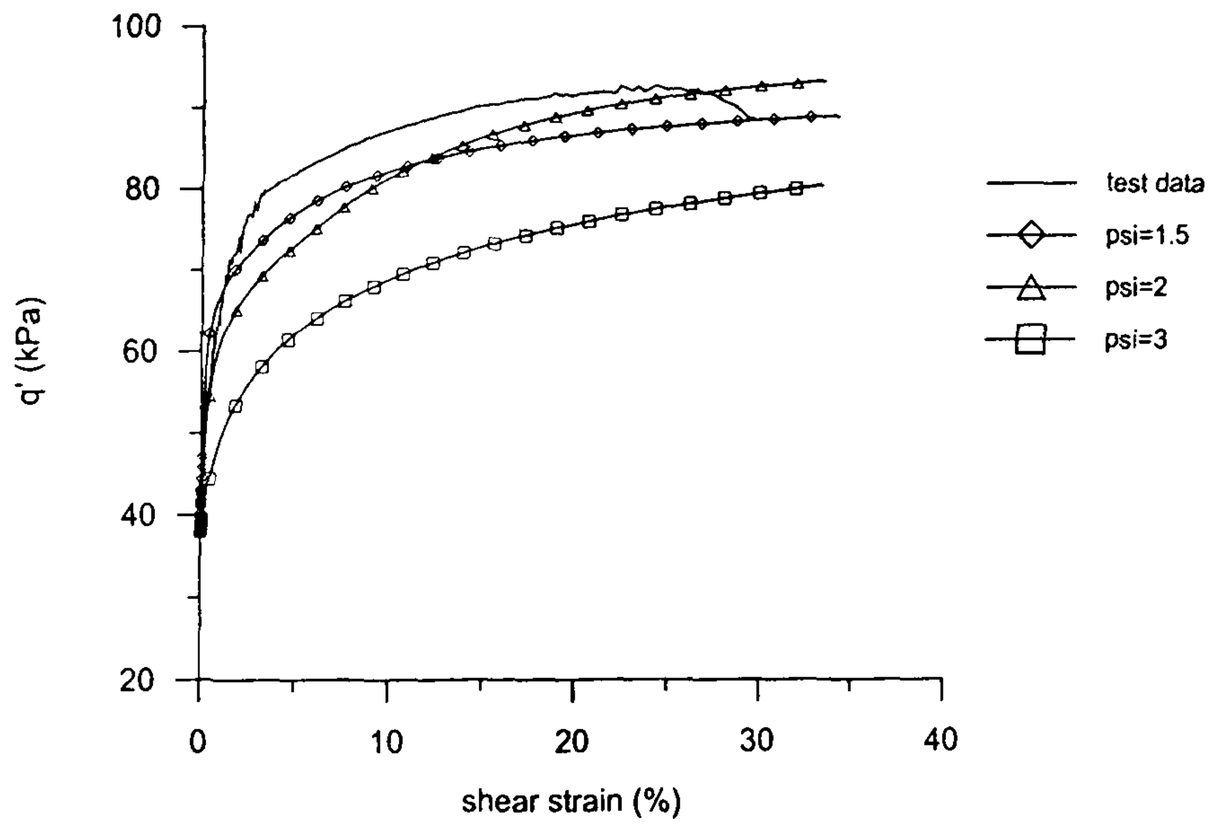

(c)

Figure 4.2.19 Effect of varying ψ on predicted large strain behaviour during drained probes on Pisa clay reconstituted samples (a) R0 (b) R90 (c) R60 (test data from Callisto, 1996)

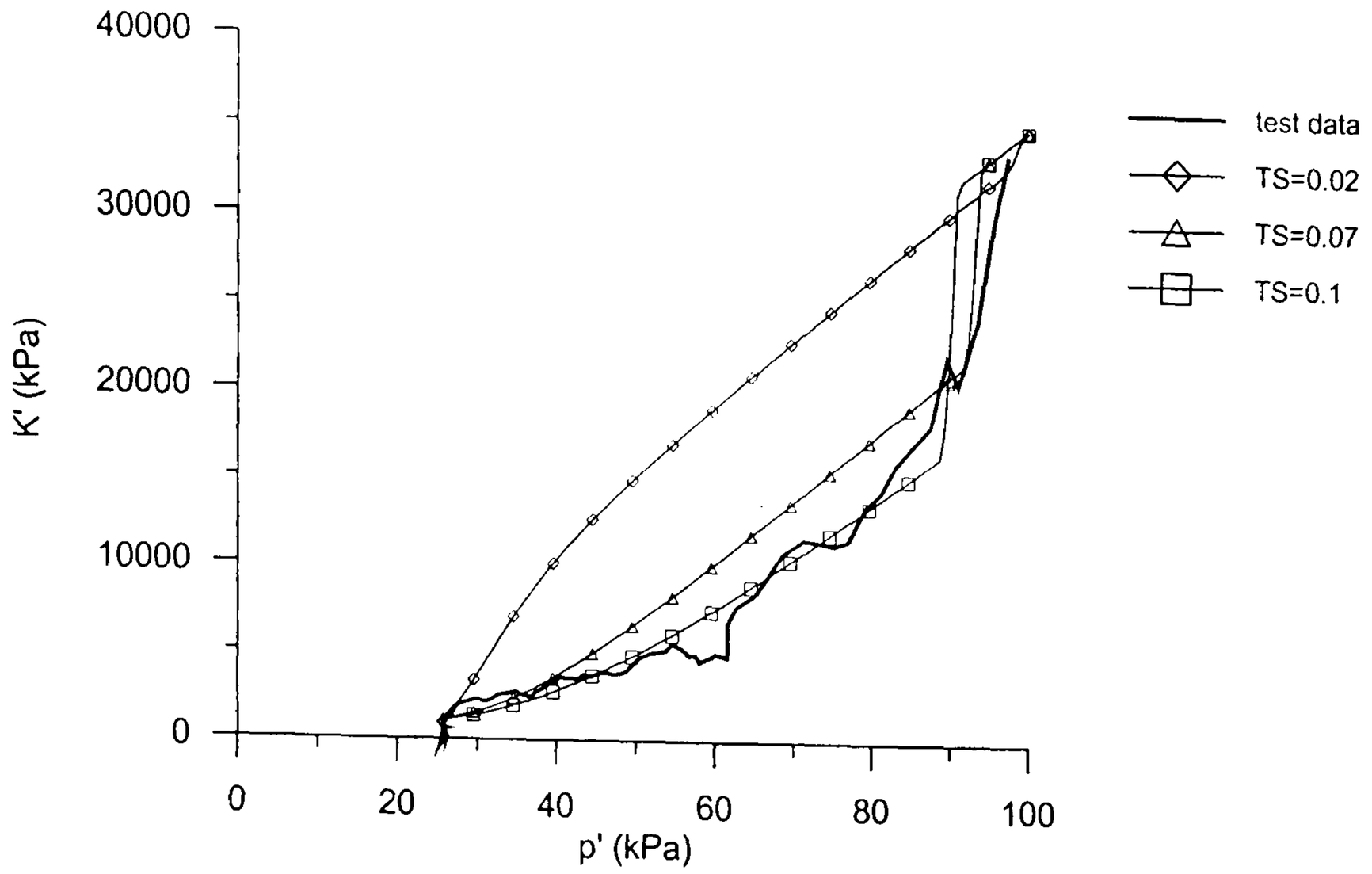

(a)

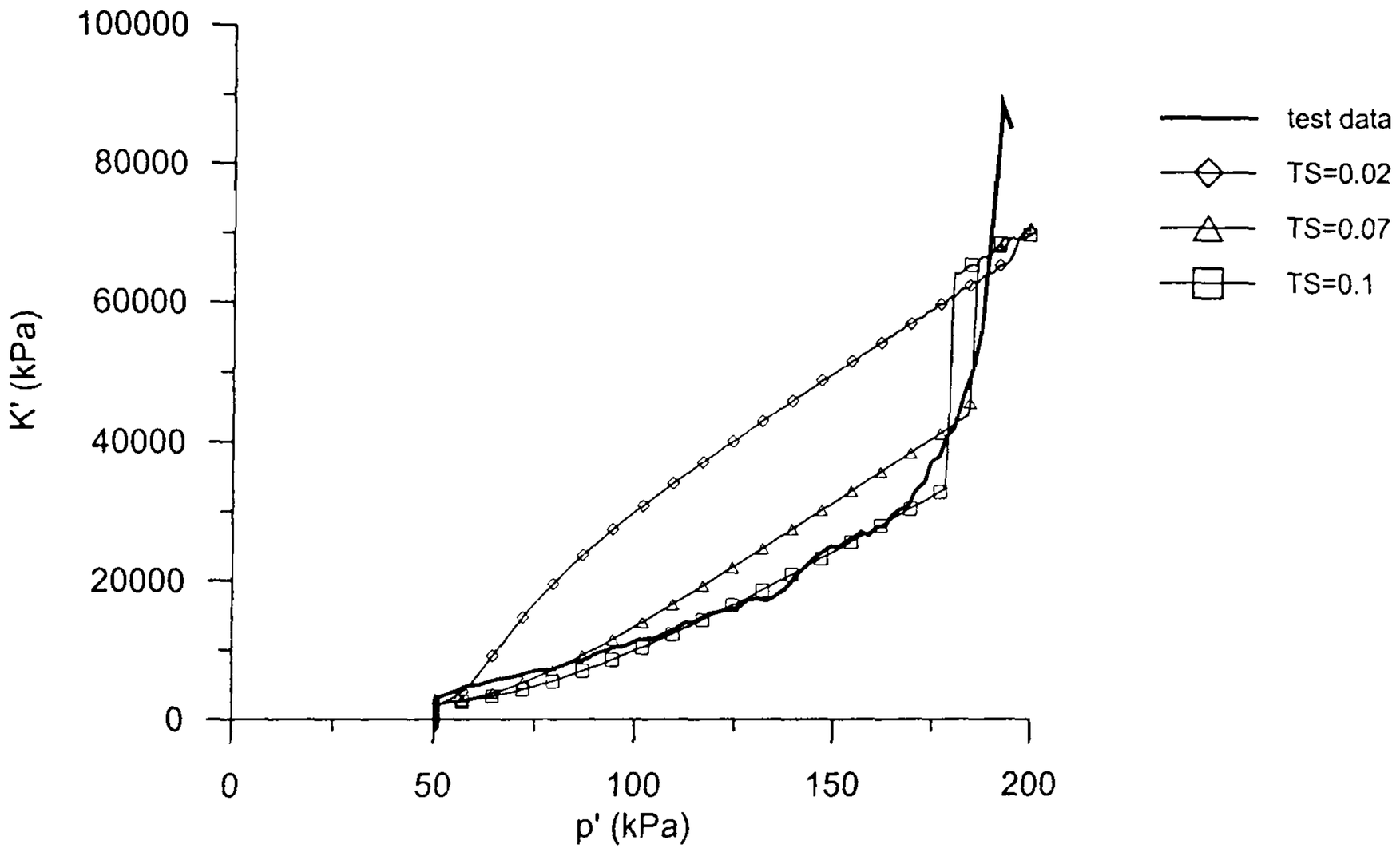

(b)

Figure 4.2.20 Effect of varying TS on the predicted value of bulk modulus during isotropic swelling of Bothkennar clay from (a) p_c'=100kPa (b) p_c'=200kPa (test data from Allman, 1992)

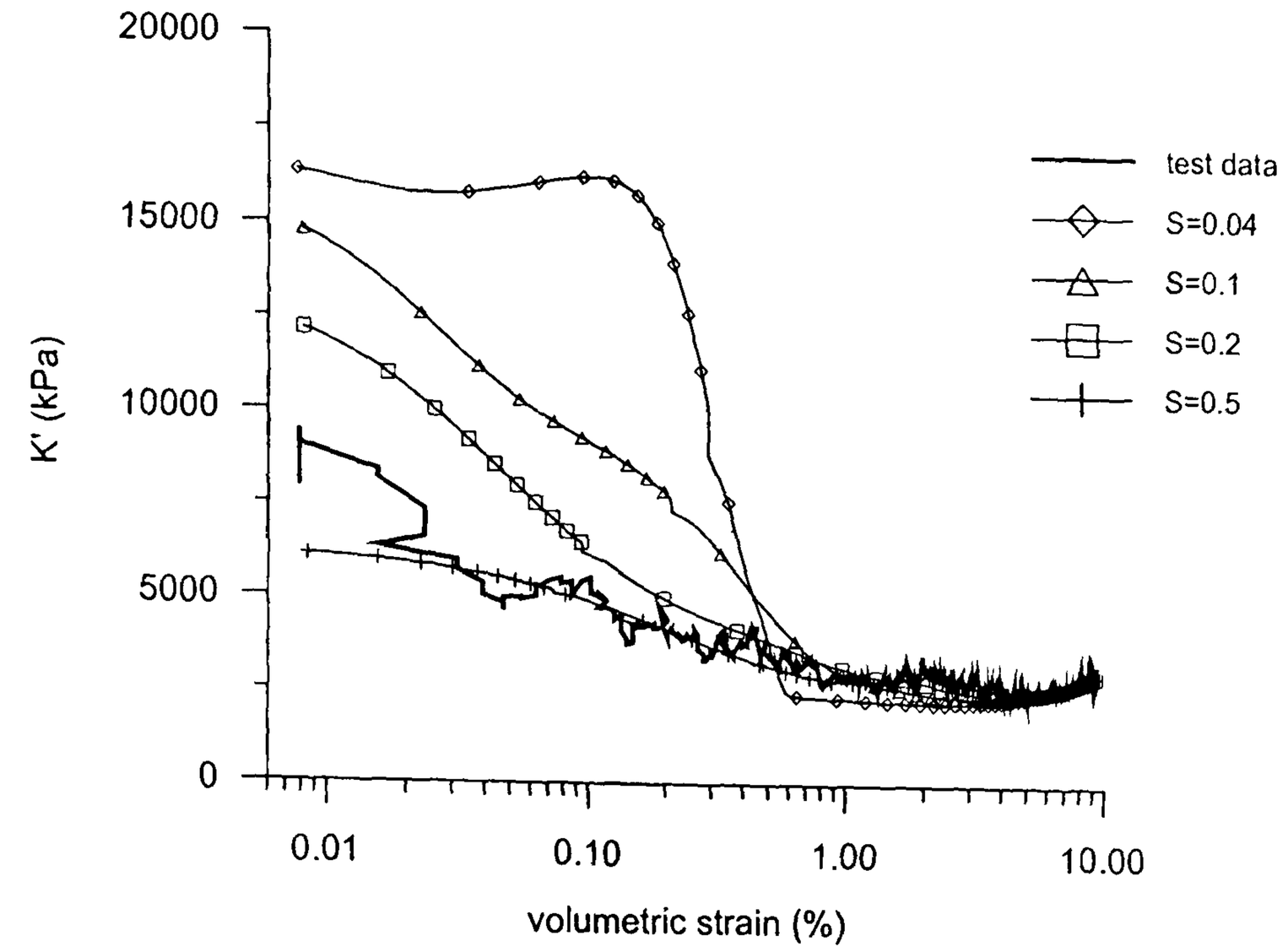

(a)

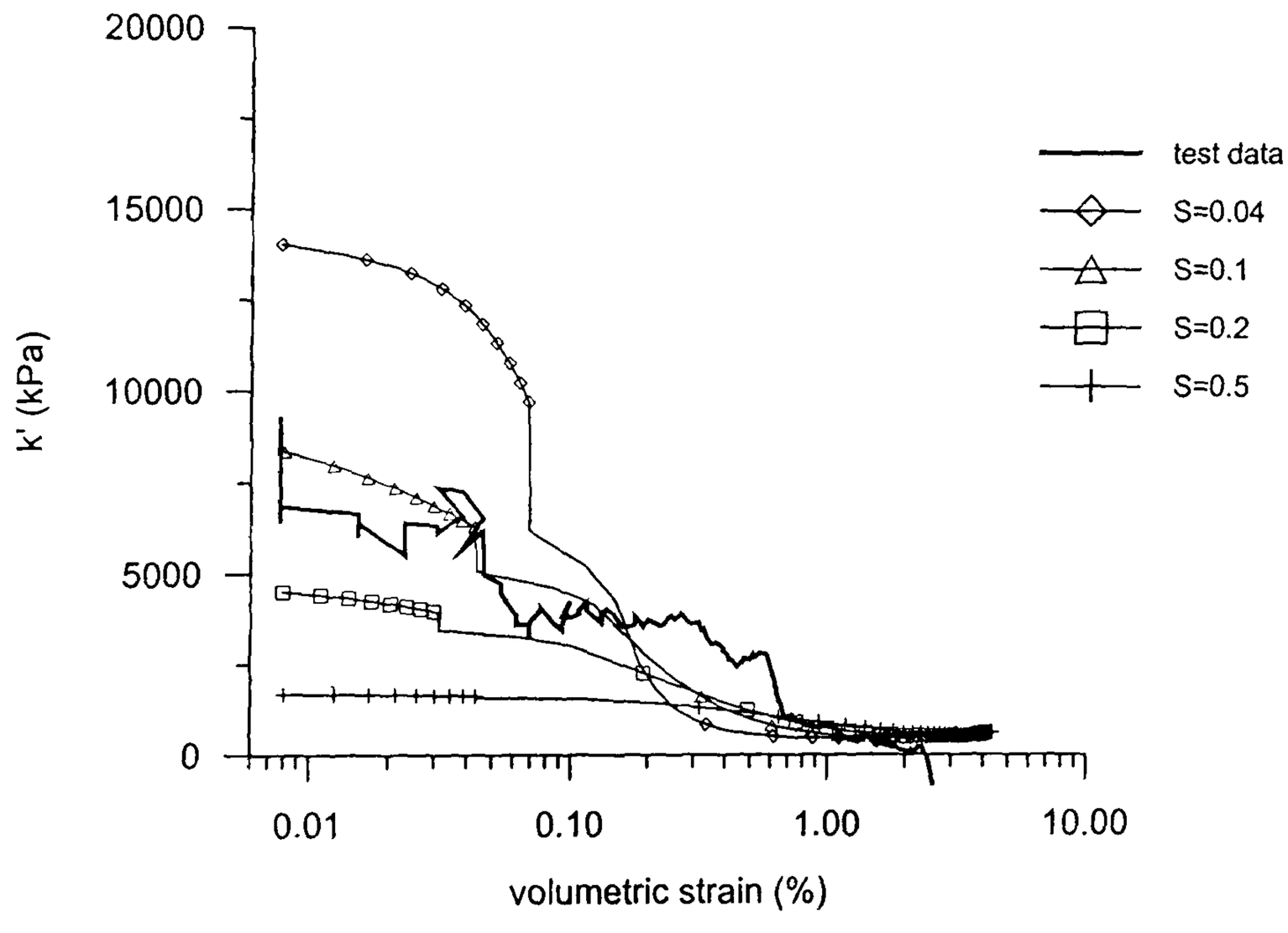

(b)

Figure 4.2.21 Effect of varying S on the predicted value of bulk modulus during drained probes on Pisa clay samples (a) R0 (b) R60 (test data from Callisto, 1998)

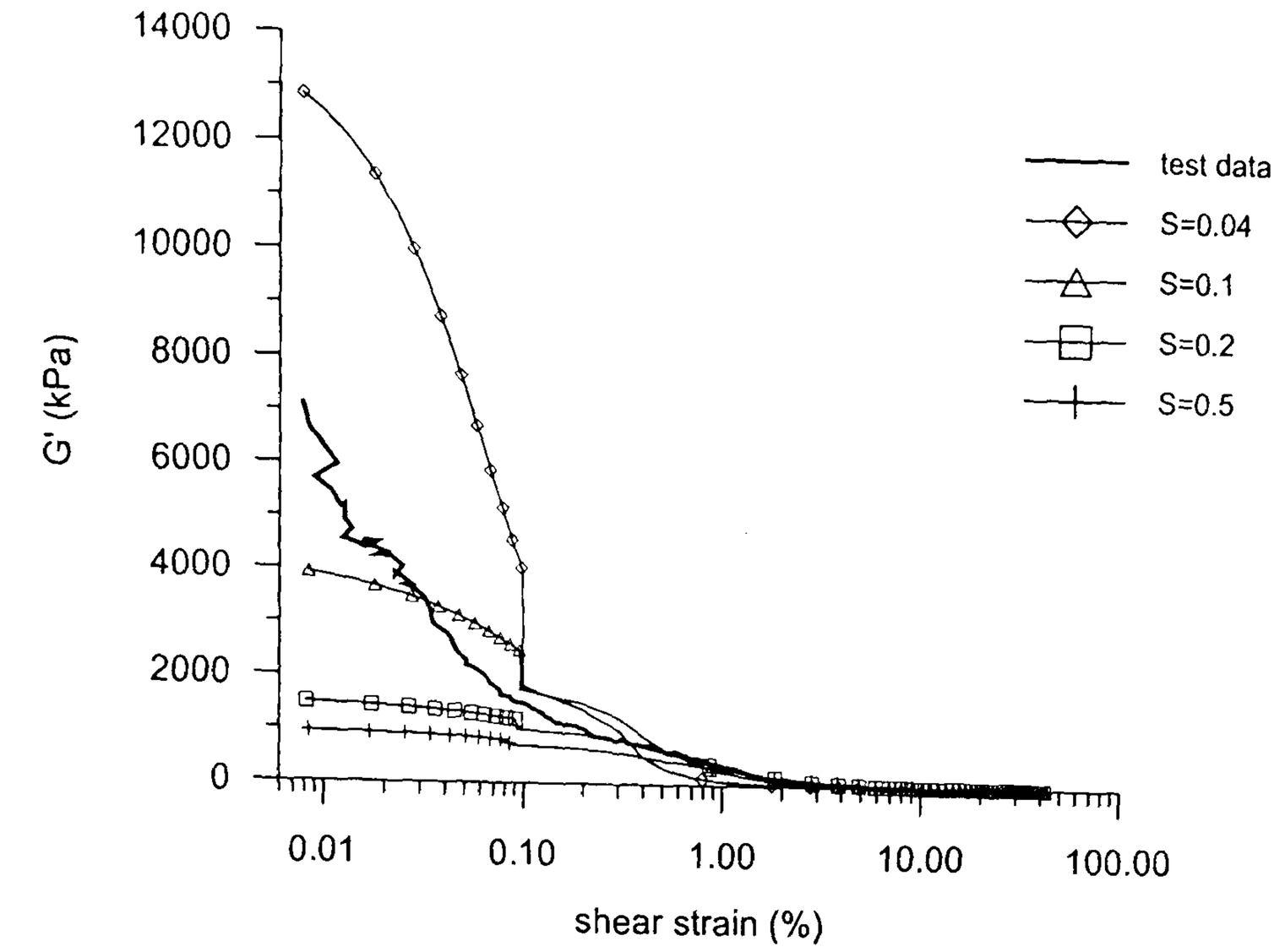

(a)

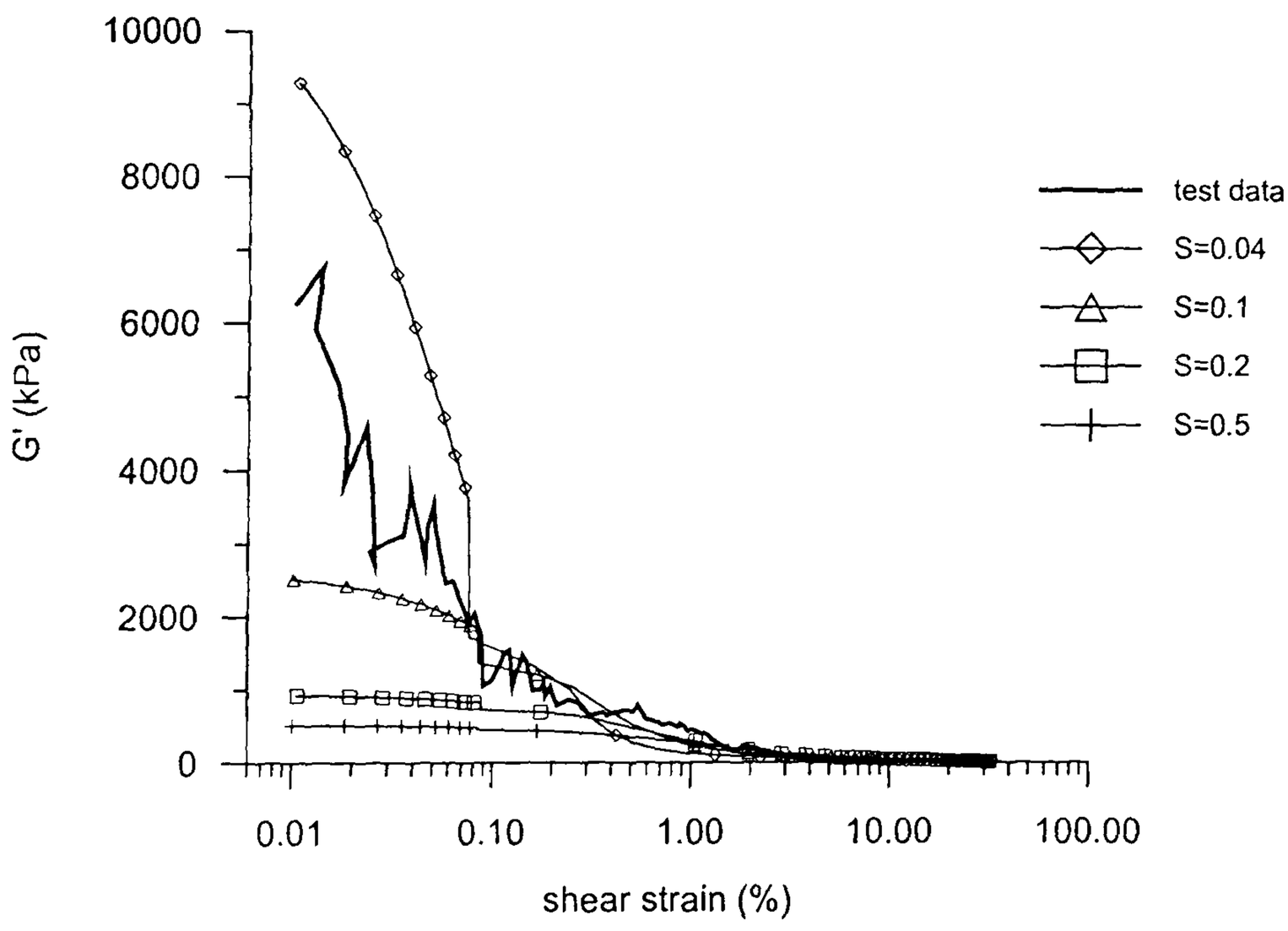

(b)

Figure 4.2.22 Effect of varying S on the predicted value of shear modulus during drained probes on Pisa clay samples (a) R90 (b) R60 (test data from Callisto, 1998)

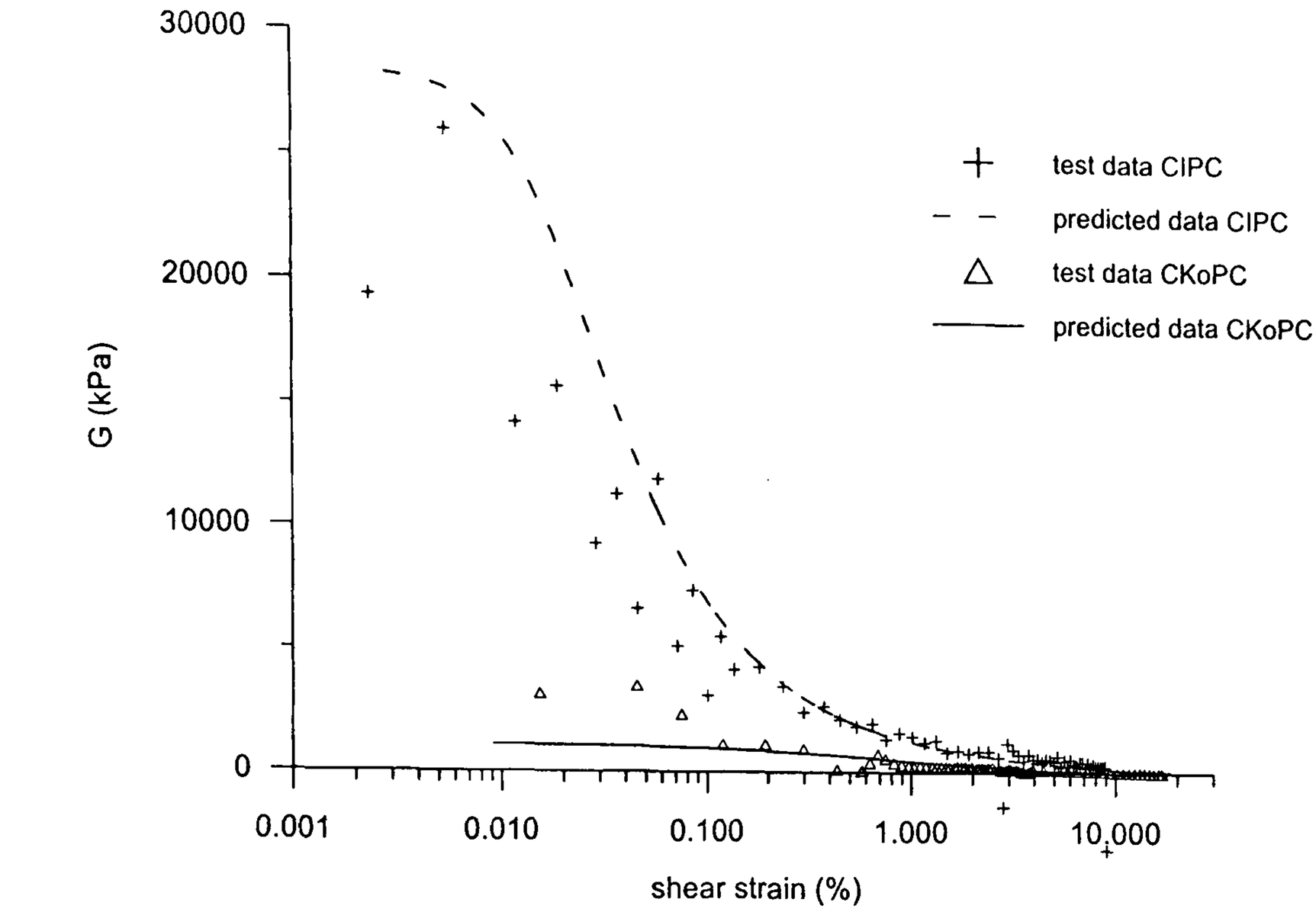

Figure 4.2.23 Comparison of 3-SKH model prediction and experimental results for drained triaxial compression tests on isotropically and anisotropically consolidated Bothkennar clay (test data from Allman, 1992)

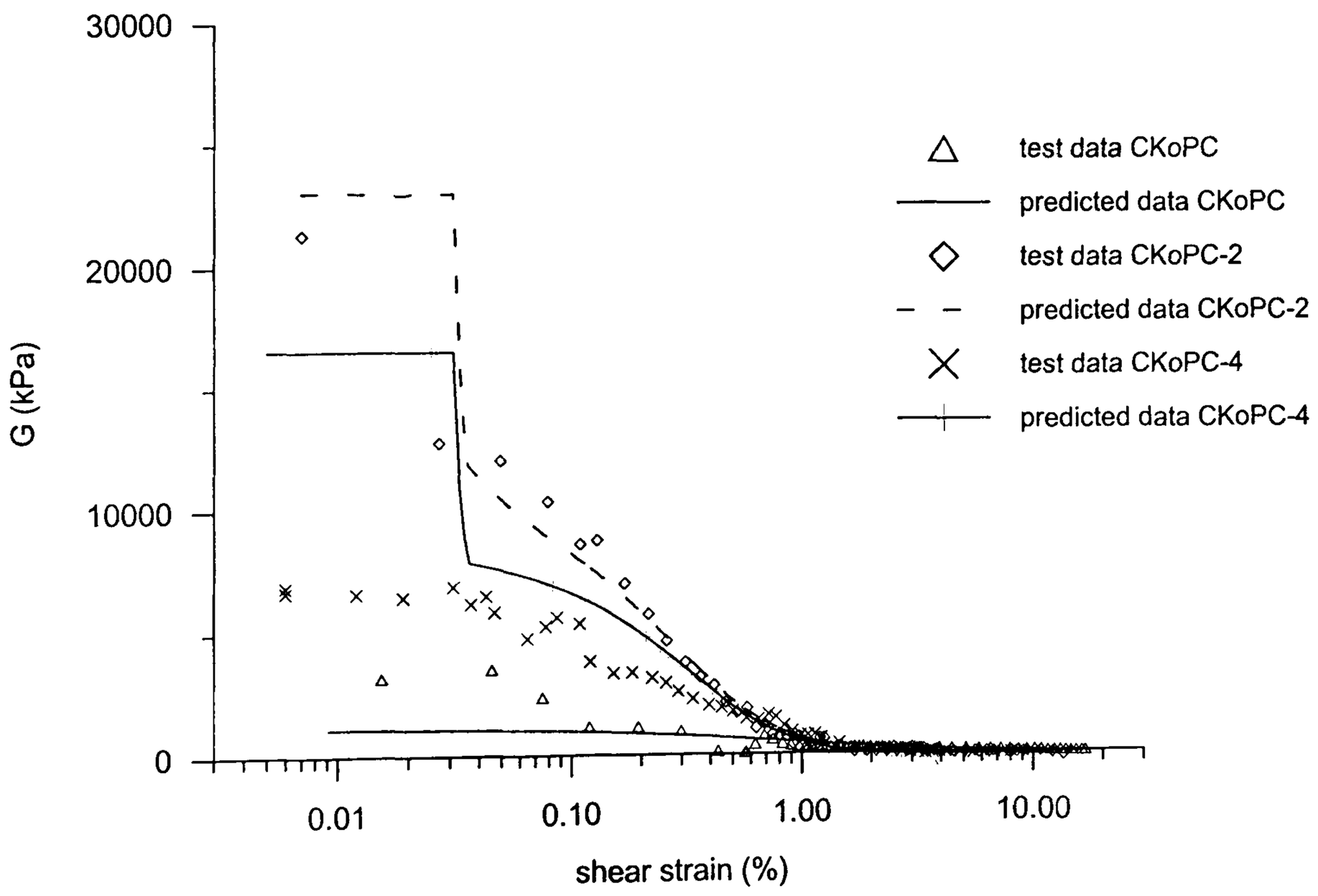

Figure 4.2.24 Comparison of 3-SKH model prediction and experimental results for drained triaxial compression tests on overconsolidated Bothkennar clay (test data from Allman, 1992)

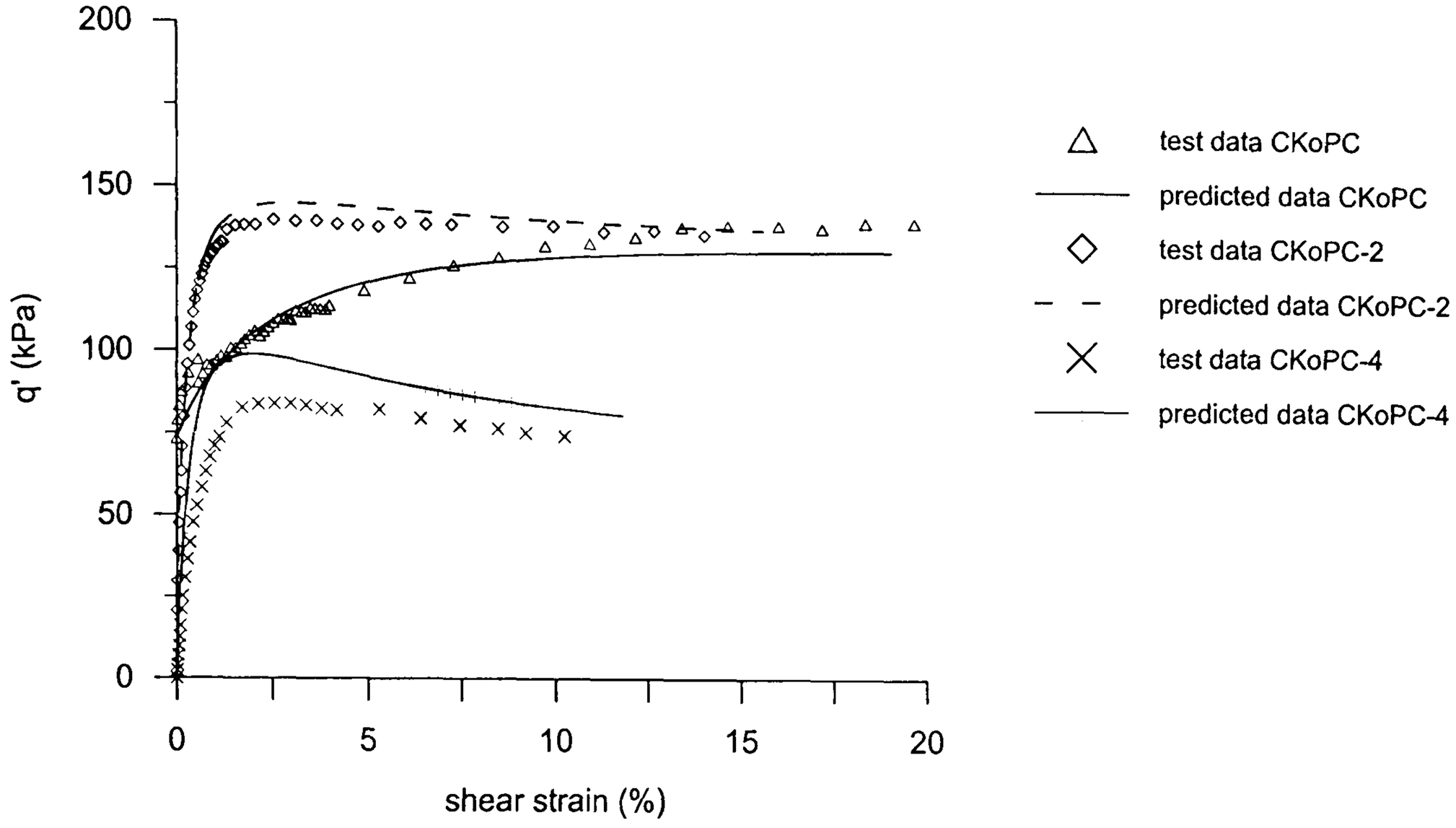

Figure 4.2.25 Comparison of 3-SKH model prediction and experimental results of stress-strain response during drained triaxial compression tests on overconsolidated Bothkennar clay (test data from Allman, 1992)

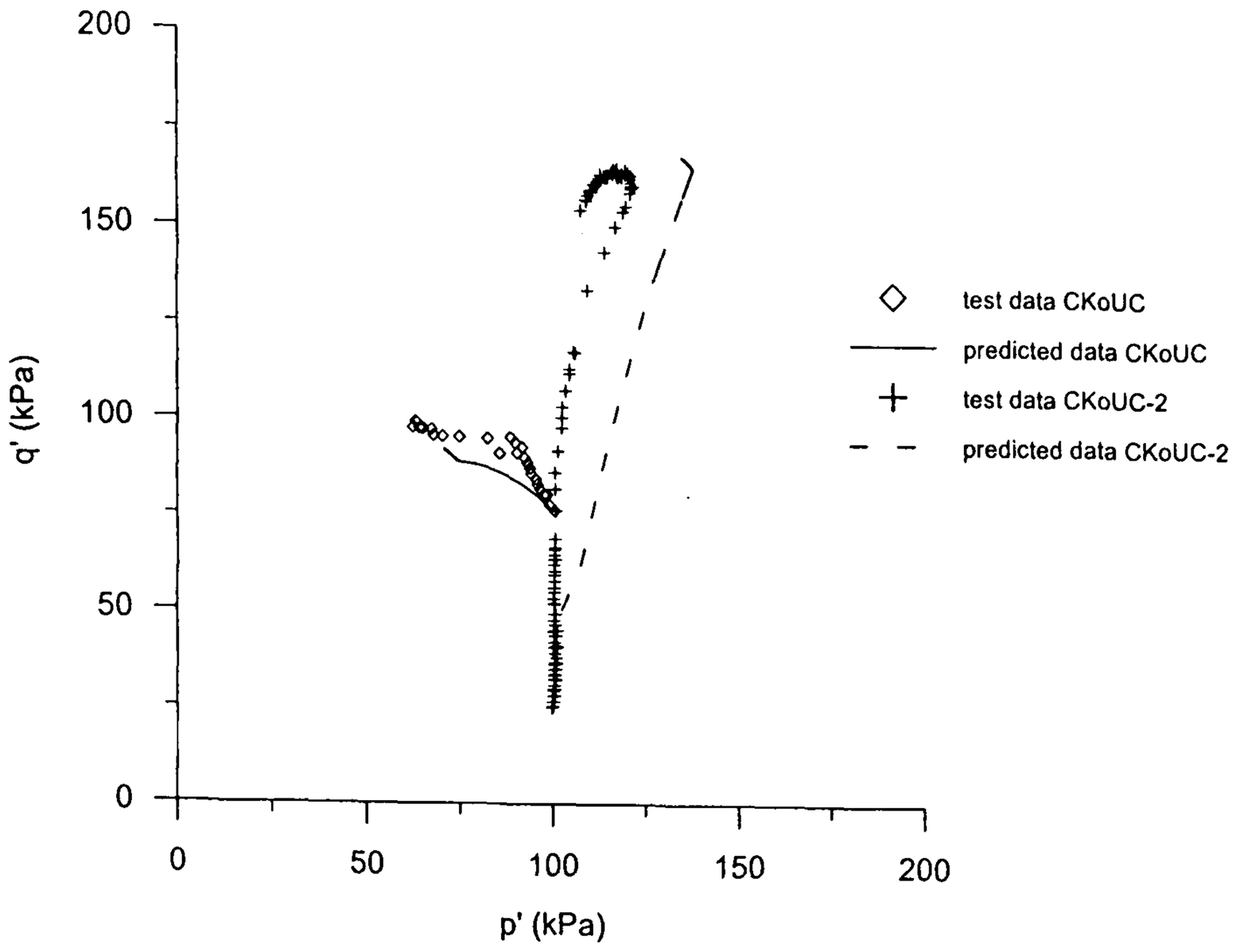

Figure 4.2.26 Comparison of 3-SKH model prediction and experimental results for undrained triaxial compression tests on anisotropically normally and overconsolidated Bothkennar clay (test data from Allman, 1992)

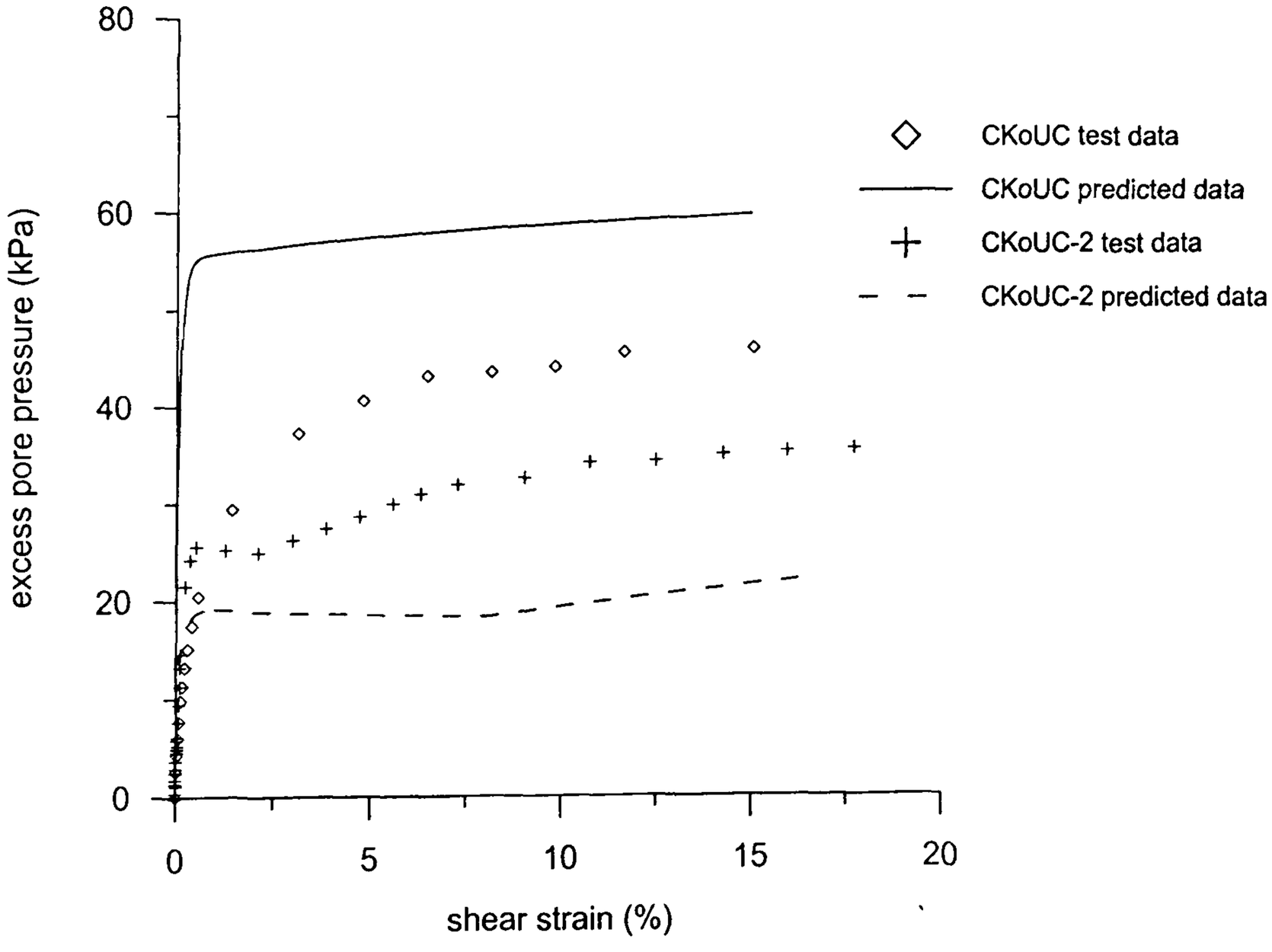

Figure 4.2.27 Comparison of 3-SKH model prediction and experimental results of excess pore pressure in undrained triaxial compression tests on anisotropically normally and overconsolidated Bothkennar clay (test data from Allman, 1992)

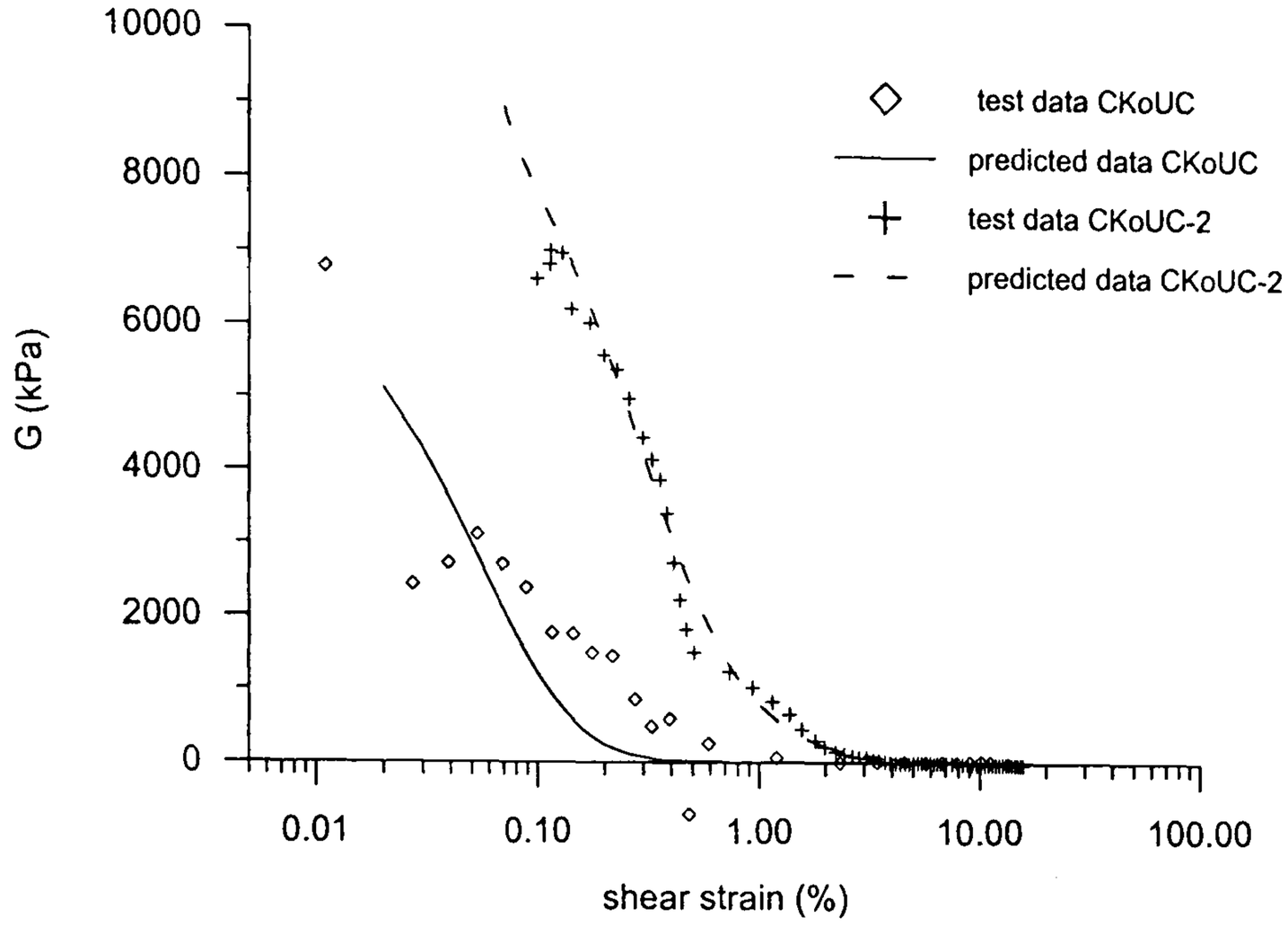

Figure 4.2.28 Comparison of predicted and experimental values of shear modulus during undrained triaxial compression tests on anisotropically normally and overconsolidated Bothkennar clay (test data from Allman, 1992)

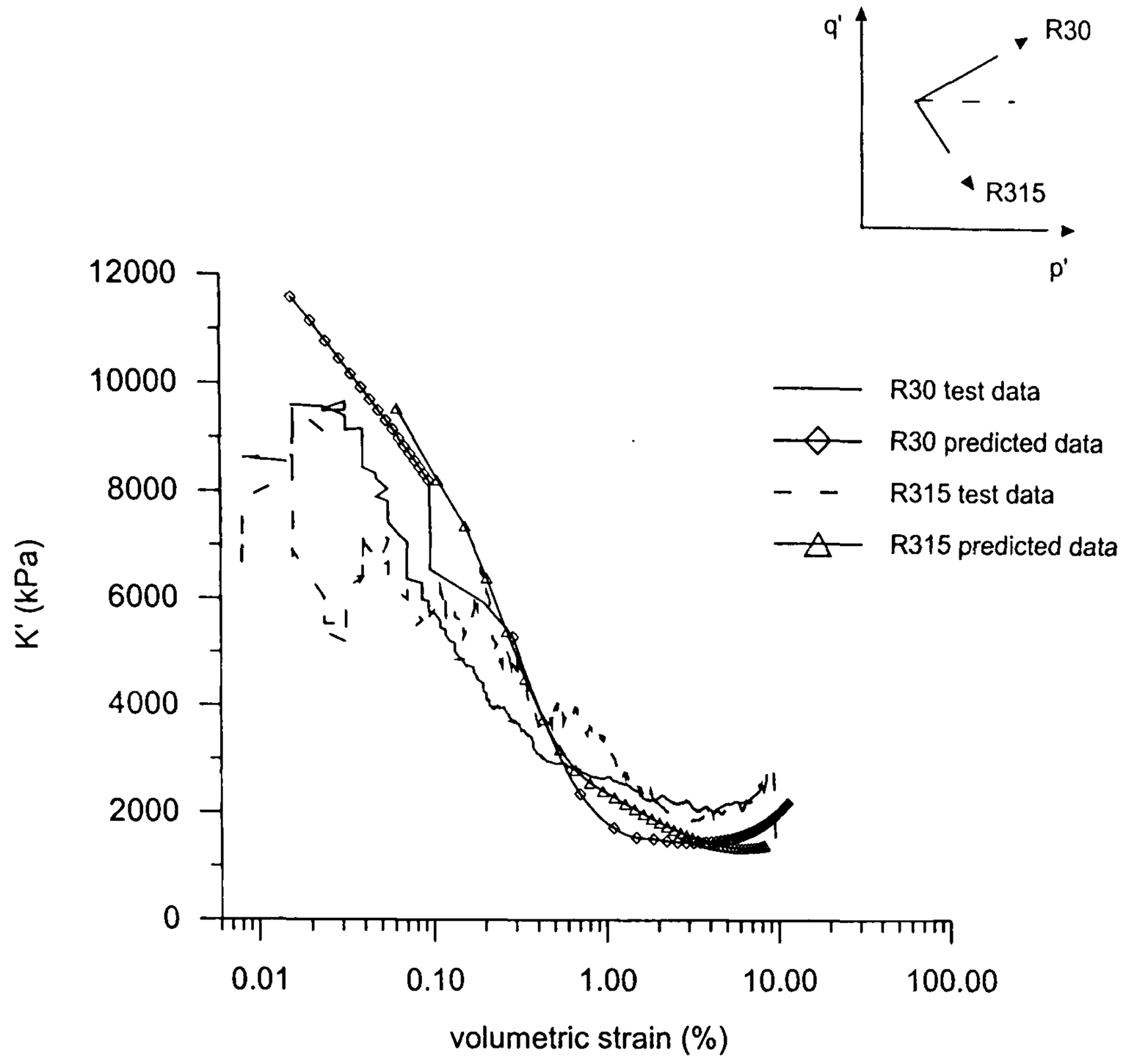

Figure 4.2.29 Comparison of 3-SKH model prediction and experimental results for values of bulk modulus during drained probes on reconstituted Pisa clay samples (data from Callisto, 1996)

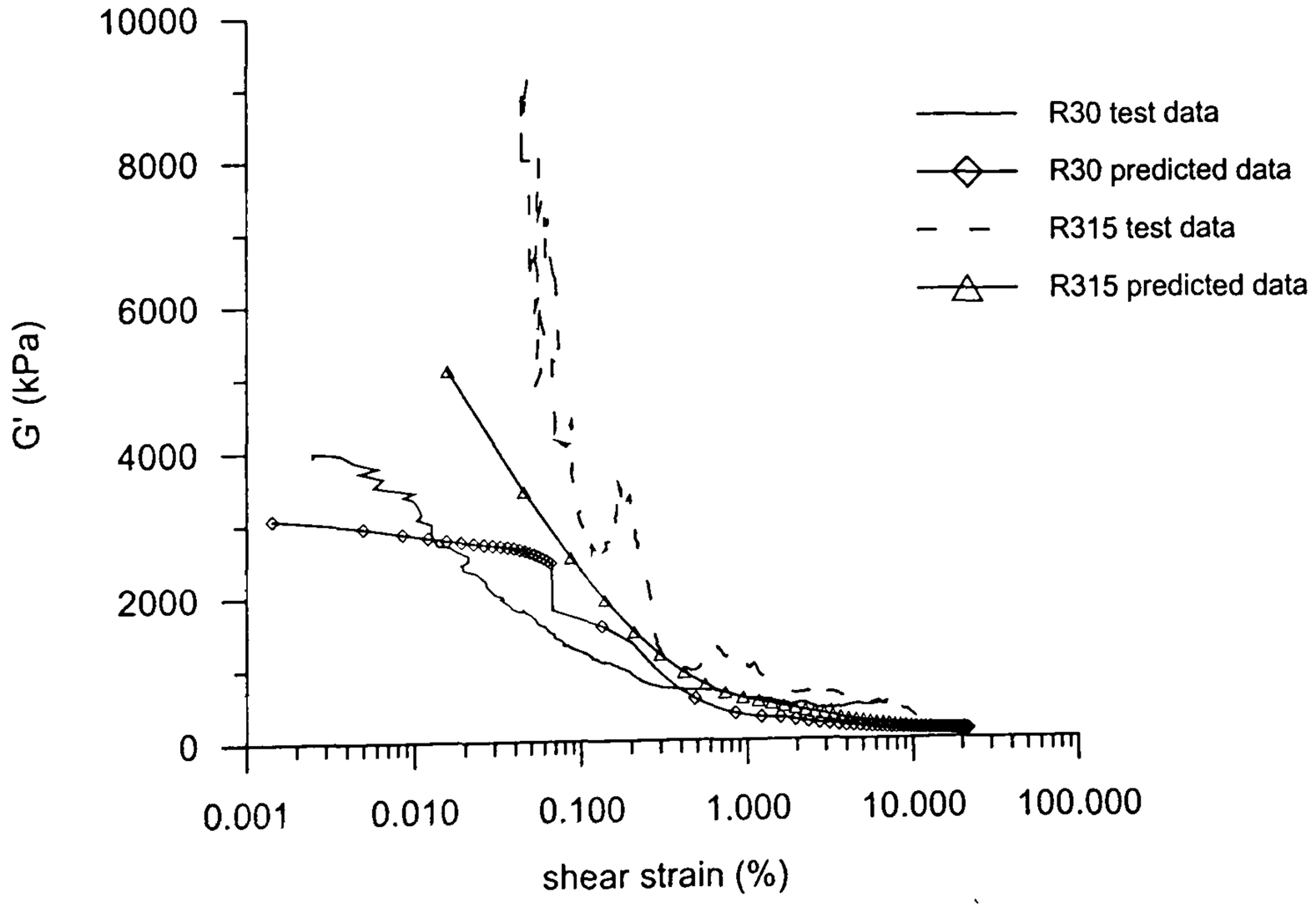

Figure 4.2.30 Comparison of 3-SKH model prediction and experimental results for values of shear modulus during drained probes on reconstituted Pisa clay samples (data from Callisto, 1996)

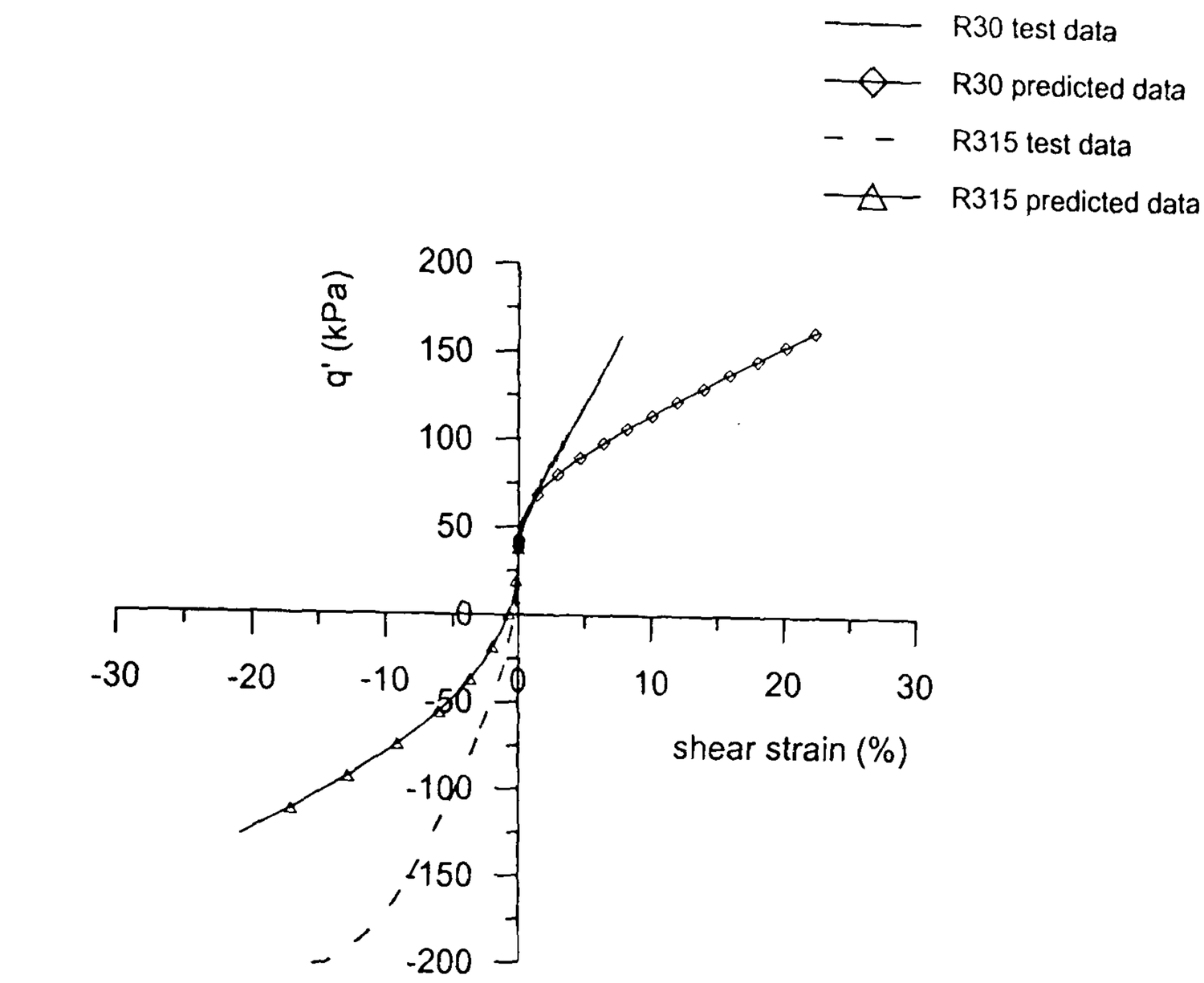

Figure 4.2.31 Comparison of 3-SKH model prediction and experimental results for the stress-strain response during drained probes on reconstituted Pisa clay samples (data from Callisto, 1996)

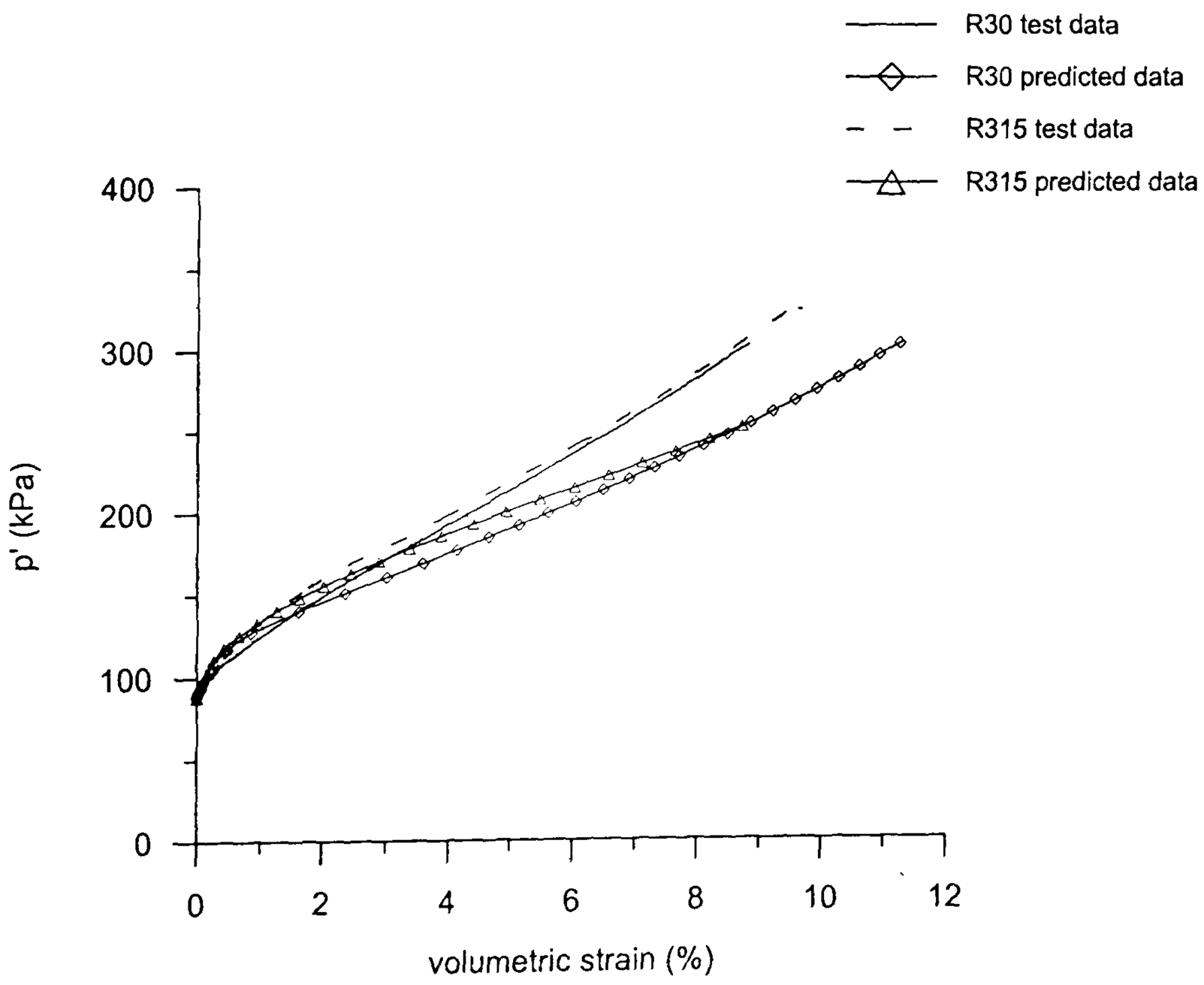

Figure 4.2.32 Comparison of 3-SKH model prediction and experimental results for the volumetric response during drained probes on reconstituted Pisa clay samples (data from Callisto, 1996)

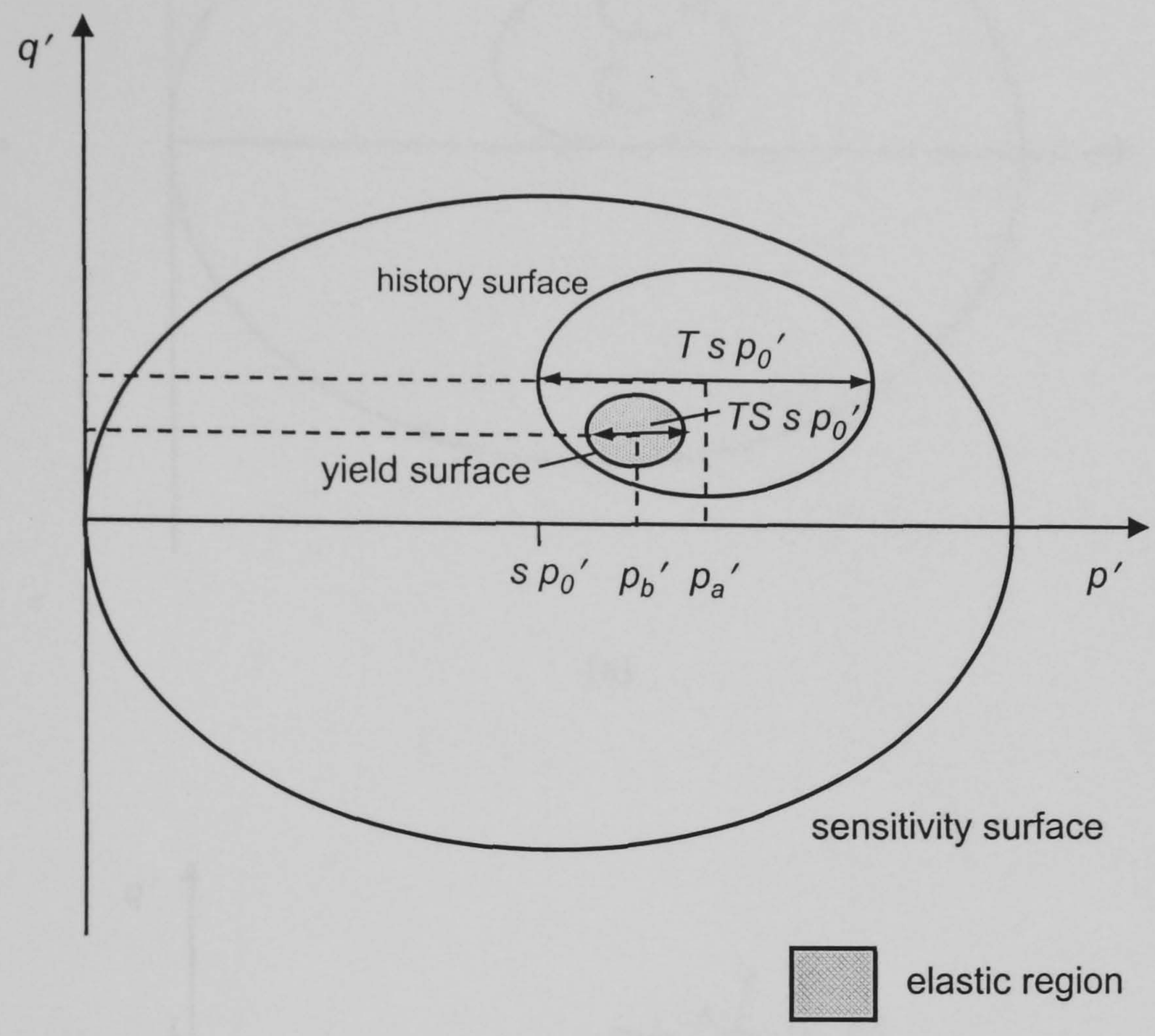

Figure 4.3.1 Diagram showing the three surfaces that constitute the S3-SKH model, in stress space

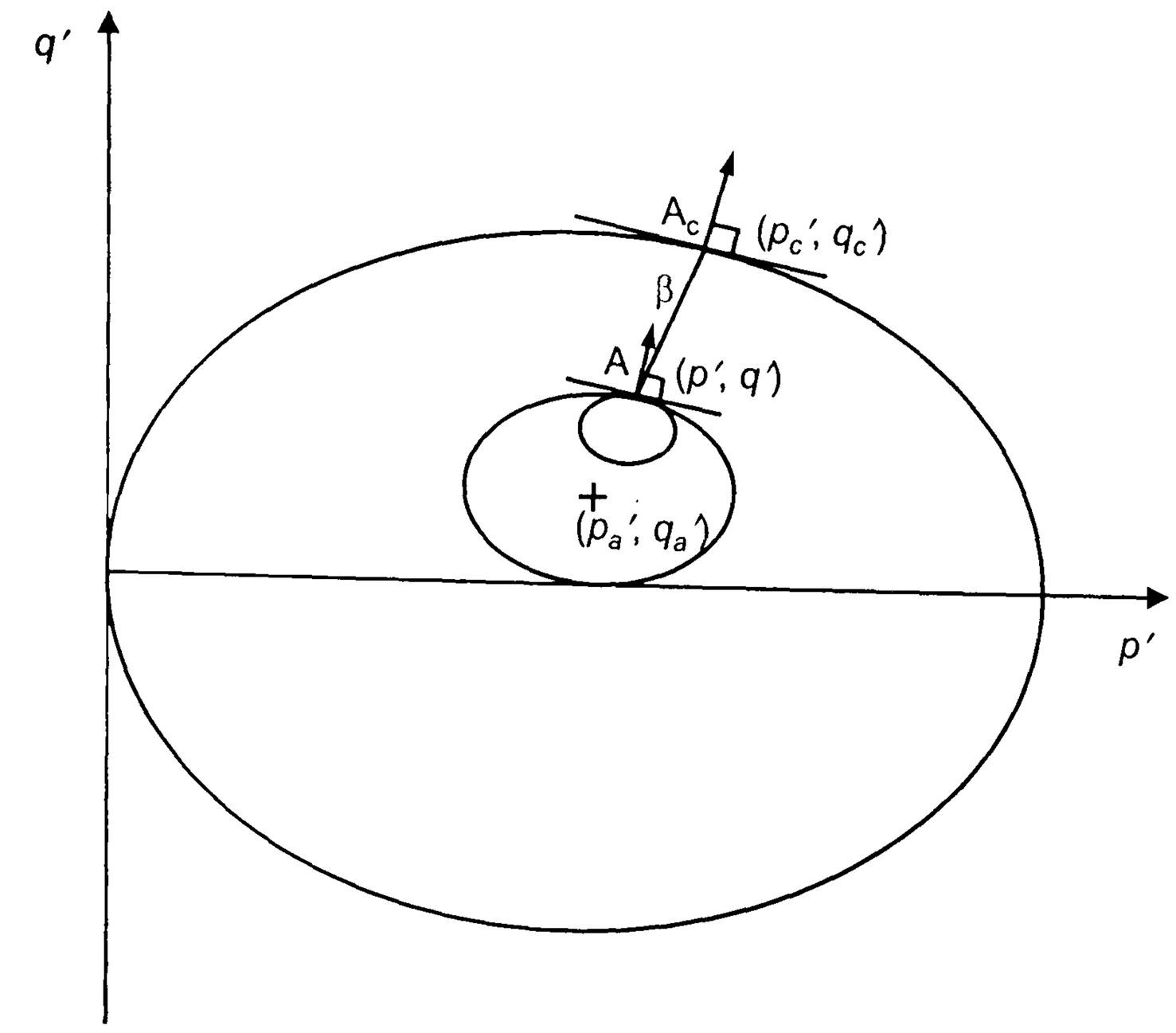

(a)

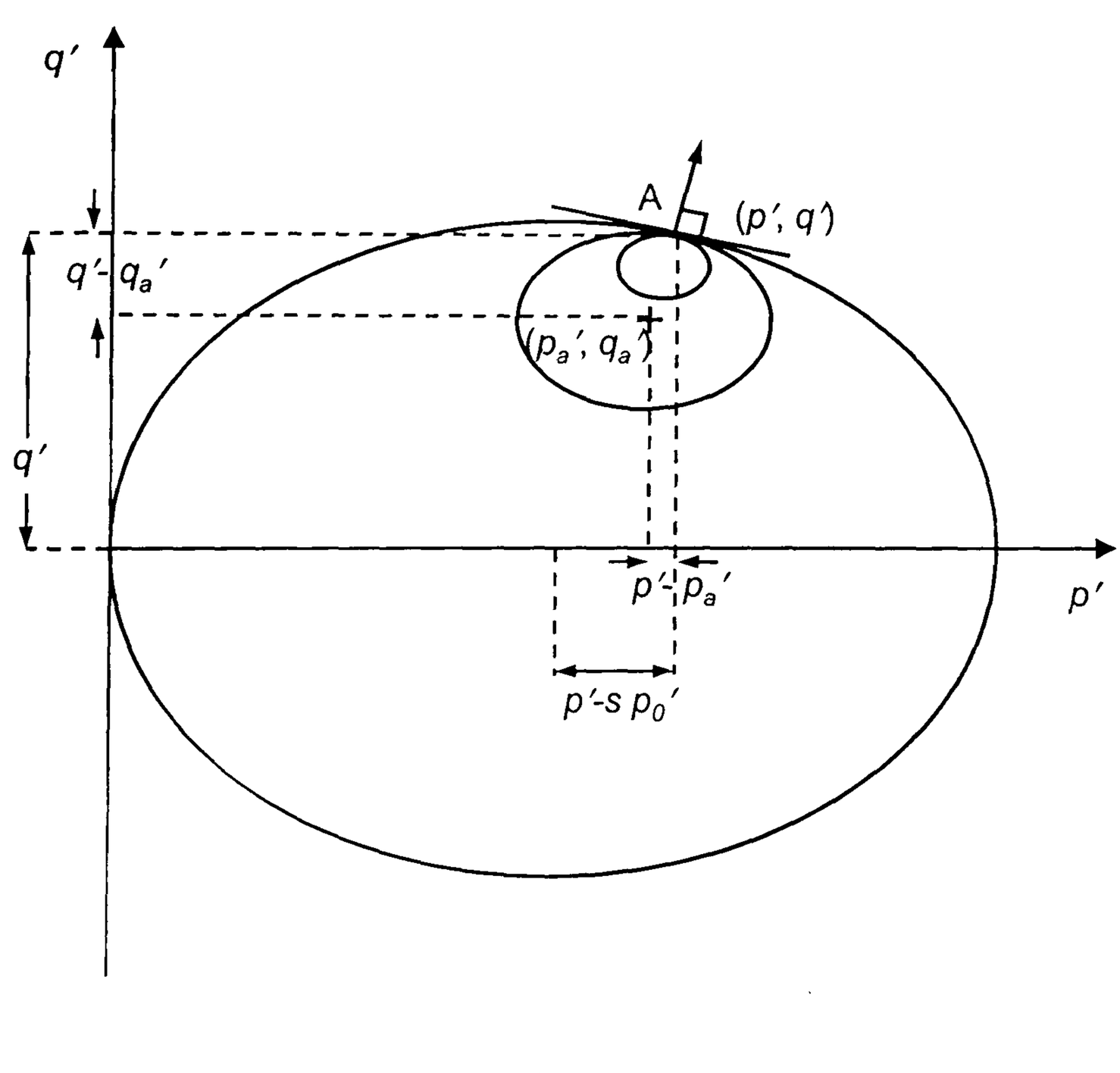

(b)

Figure 4.3.2 Diagrams illustrating (a) the definition of a conjugate point and the vector β (b) the geometry of the surfaces when they are in contact

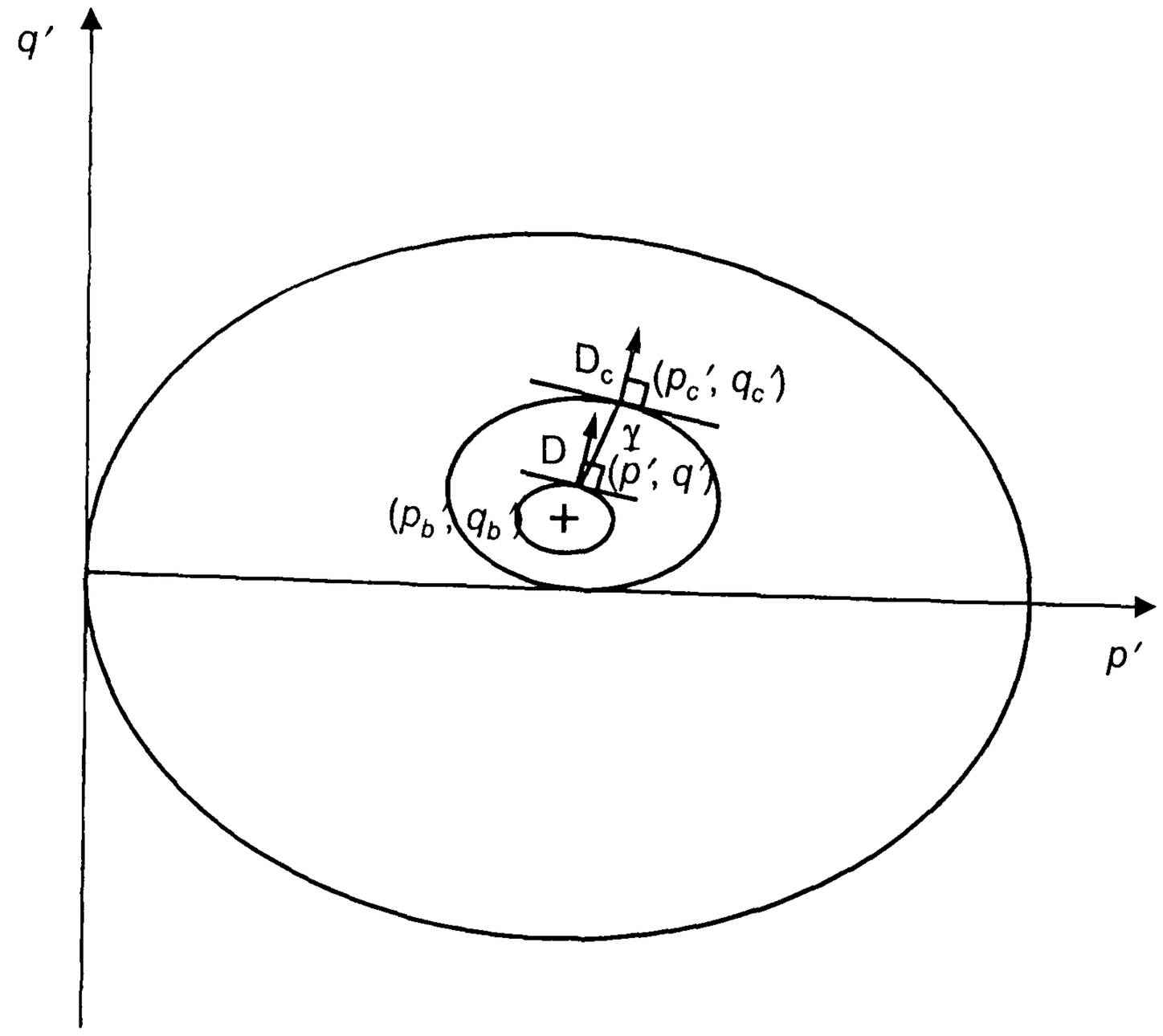

(a)

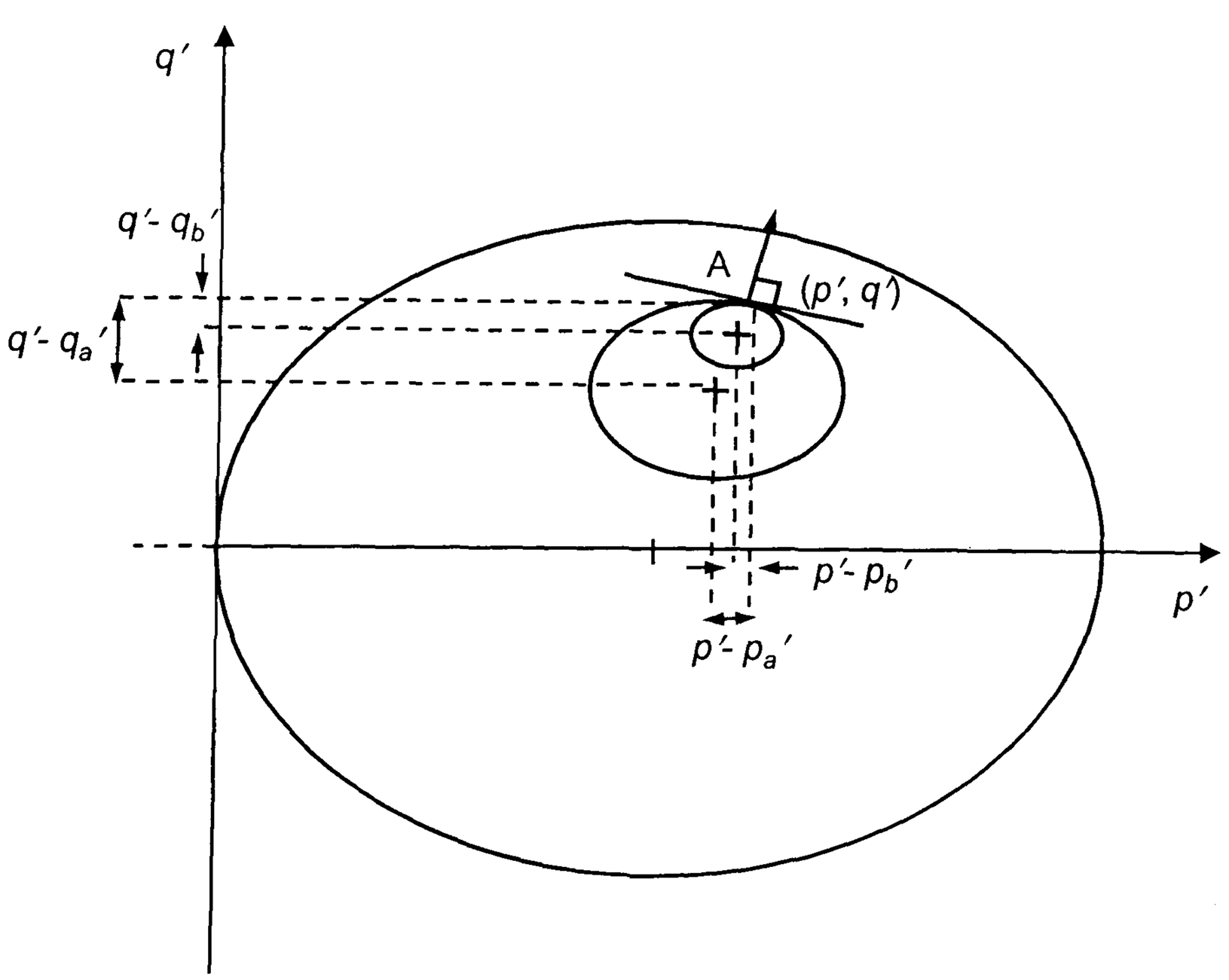

(b)

Figure 4.3.3 Diagrams illustrating (a) the definition of a conjugate point and the vector γ (b) the geometry of the surfaces when they are in contact

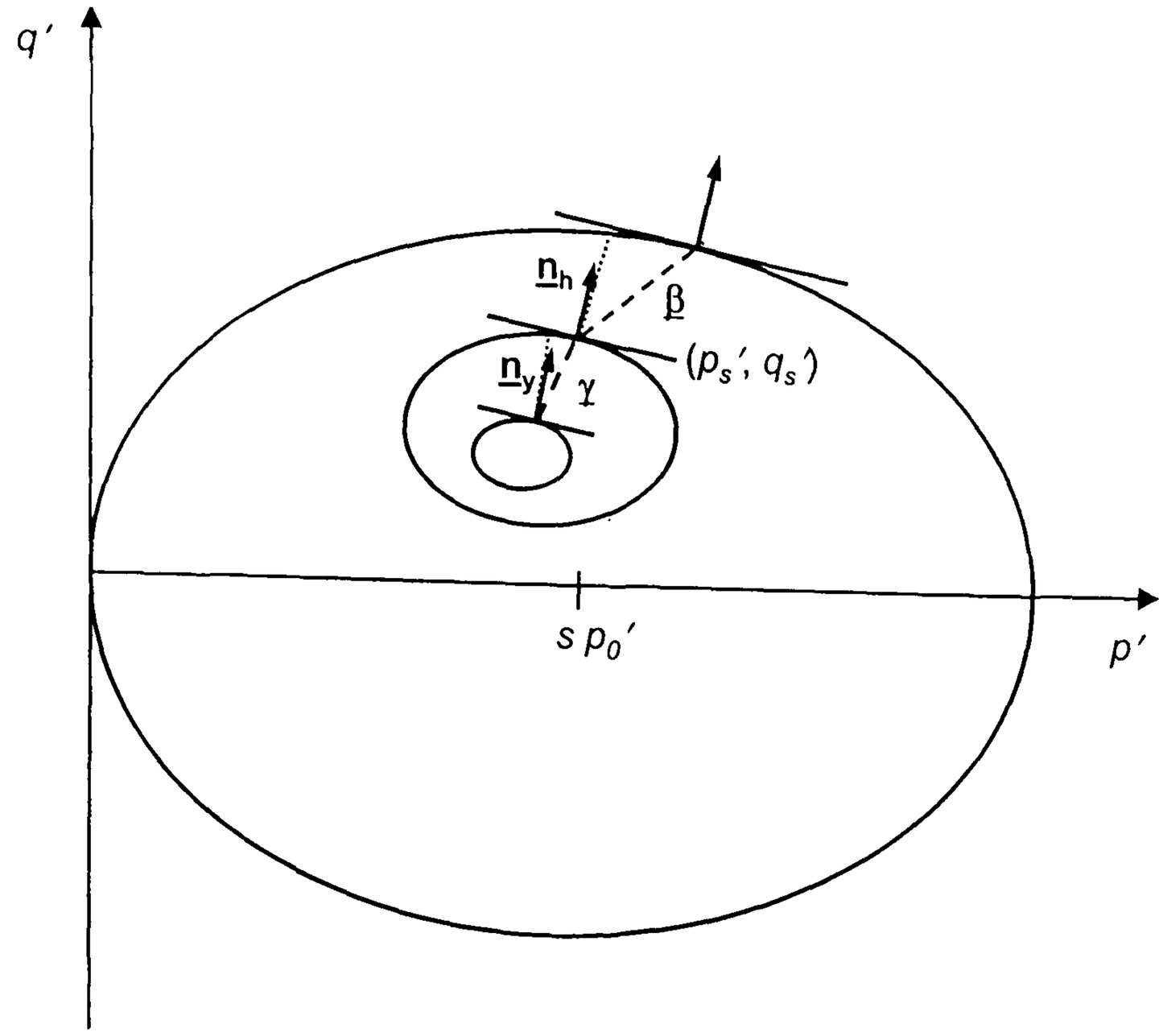

Figure 4.3.4.Diagram defining the main component of the parameters b_1 and b_2

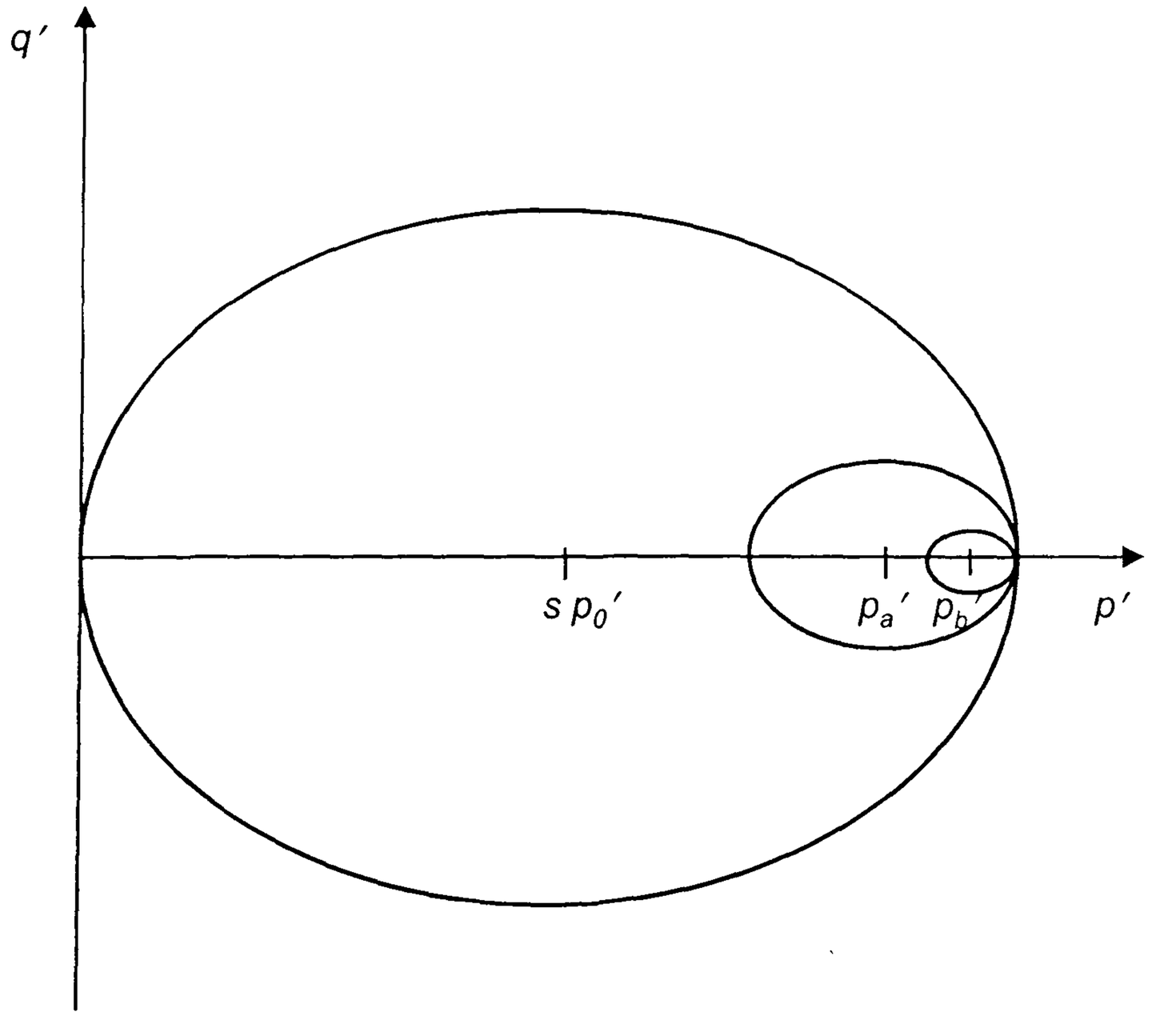

Figure 4.3.5 Diagram showing the position of the surfaces when b_1 and b_2 are at a maximum

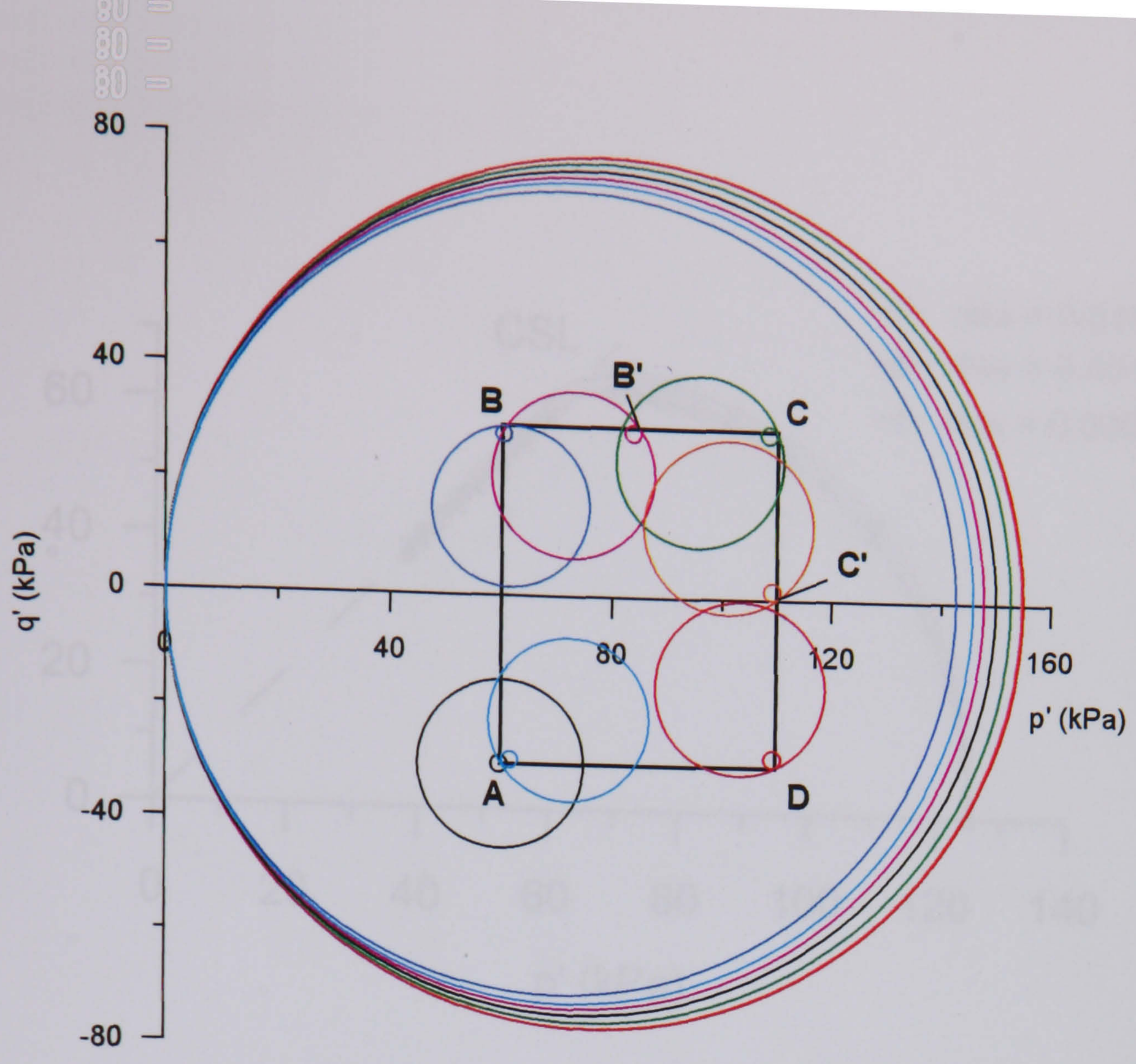

Figure 4.3.6 Diagram showing the position of the kinematic surfaces along a drained stress path

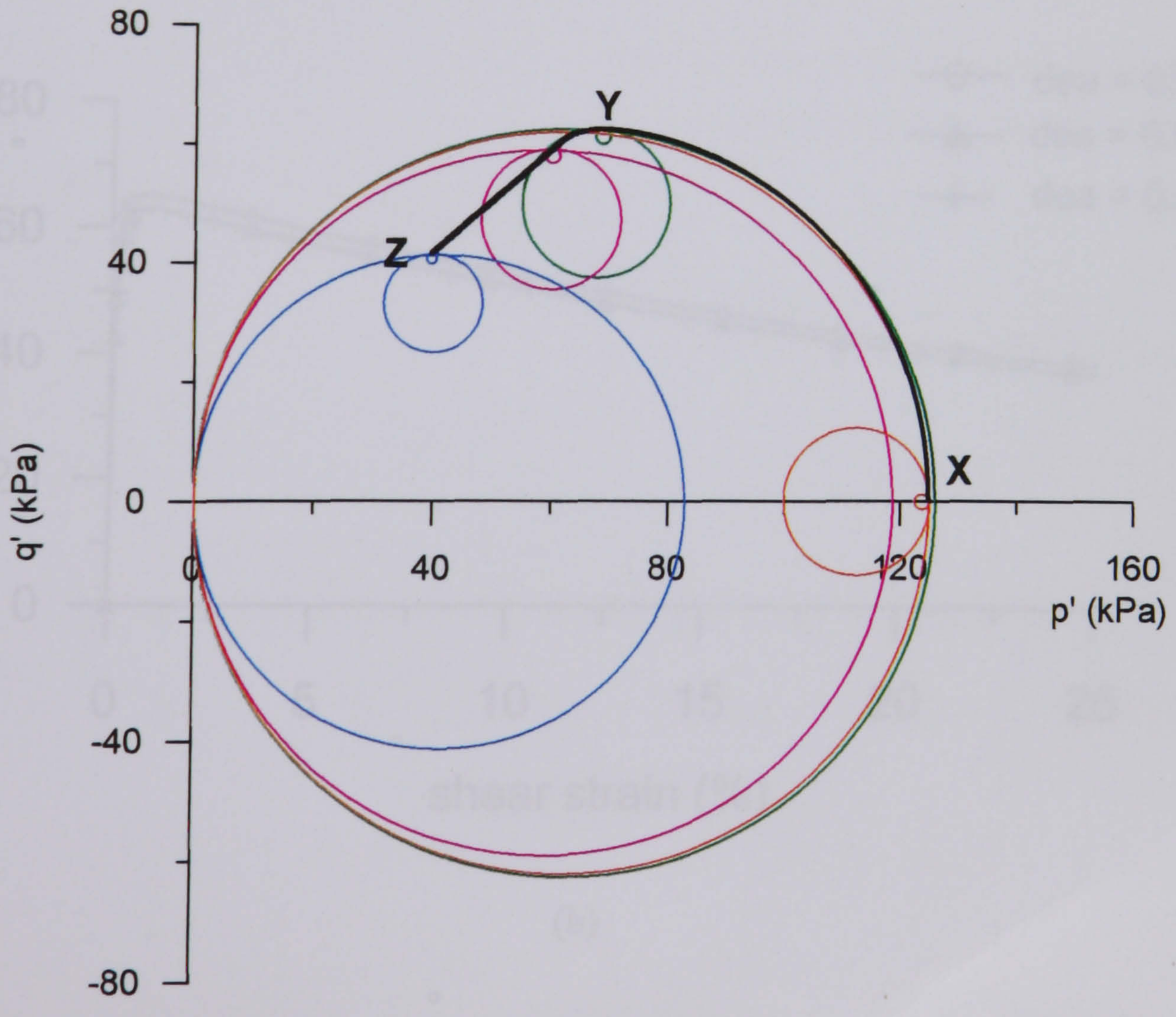

Figure 4.3.7 Diagram showing the position of the kinematic surfaces along an undrained stress path

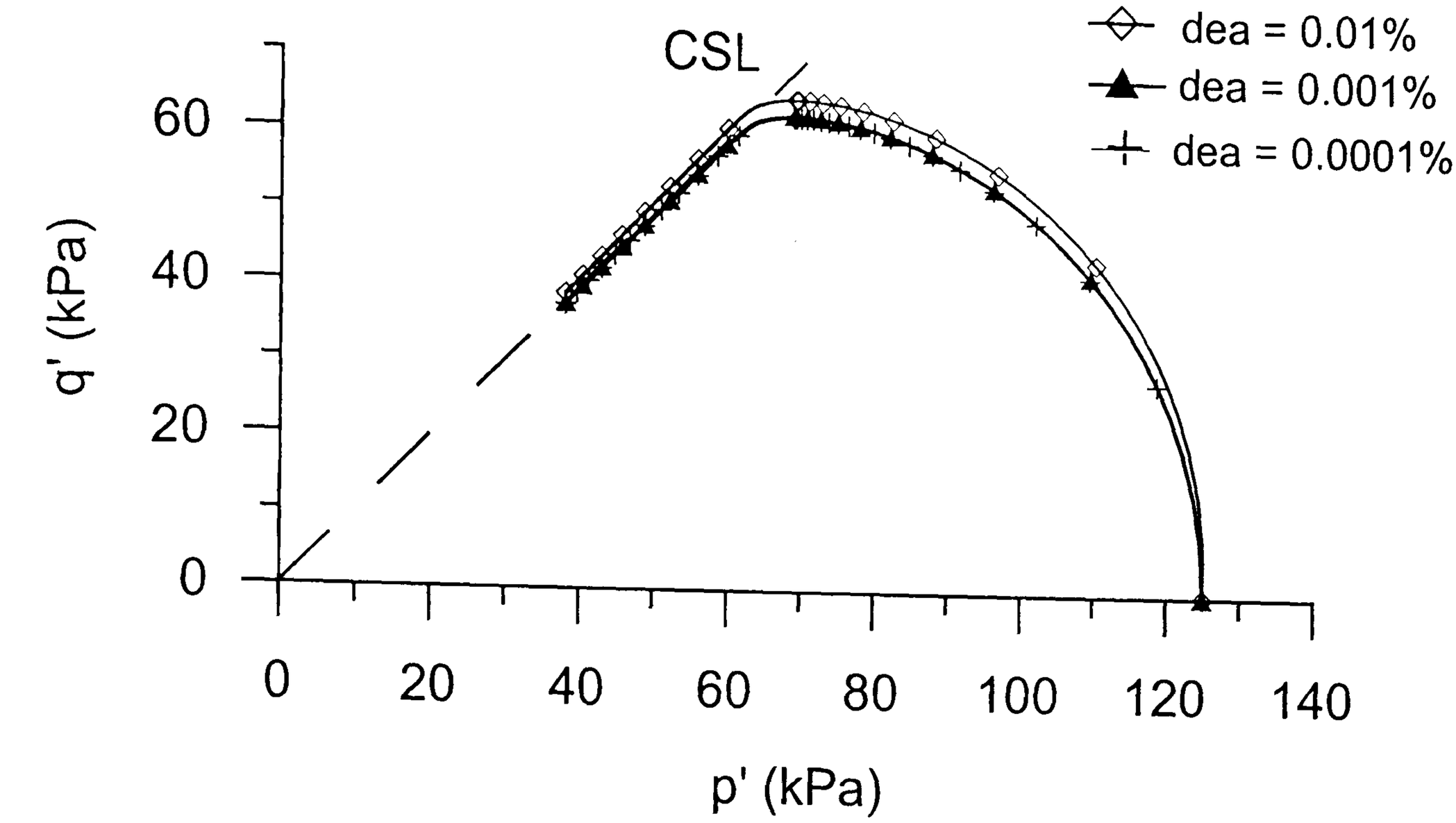

(a)

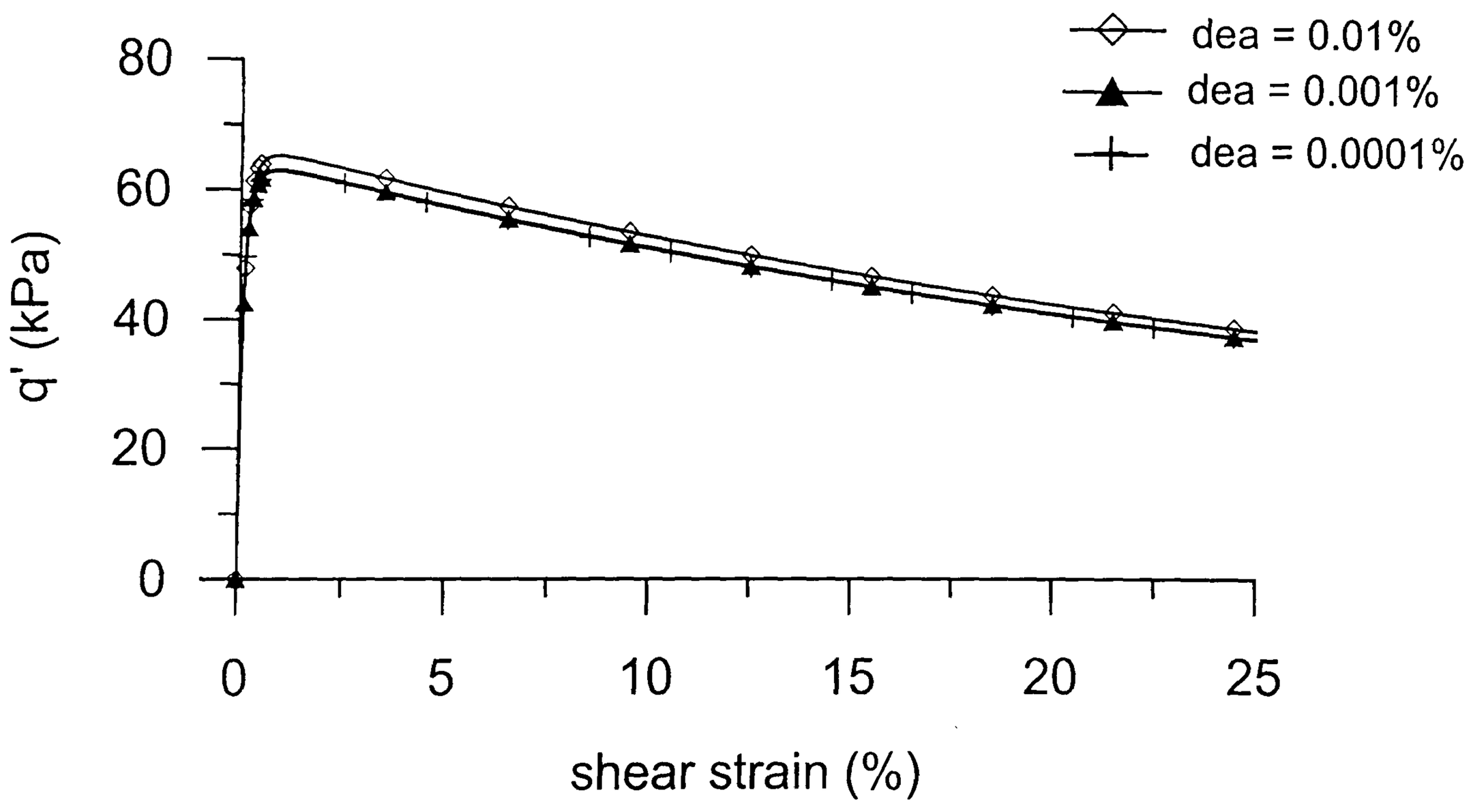

(b)

Figure 4.3.8 Comparison of numerical simulations of undrained compression for different increments of strain using double precision variables
(a) stress path (b) stress-strain curve q'-ε_s

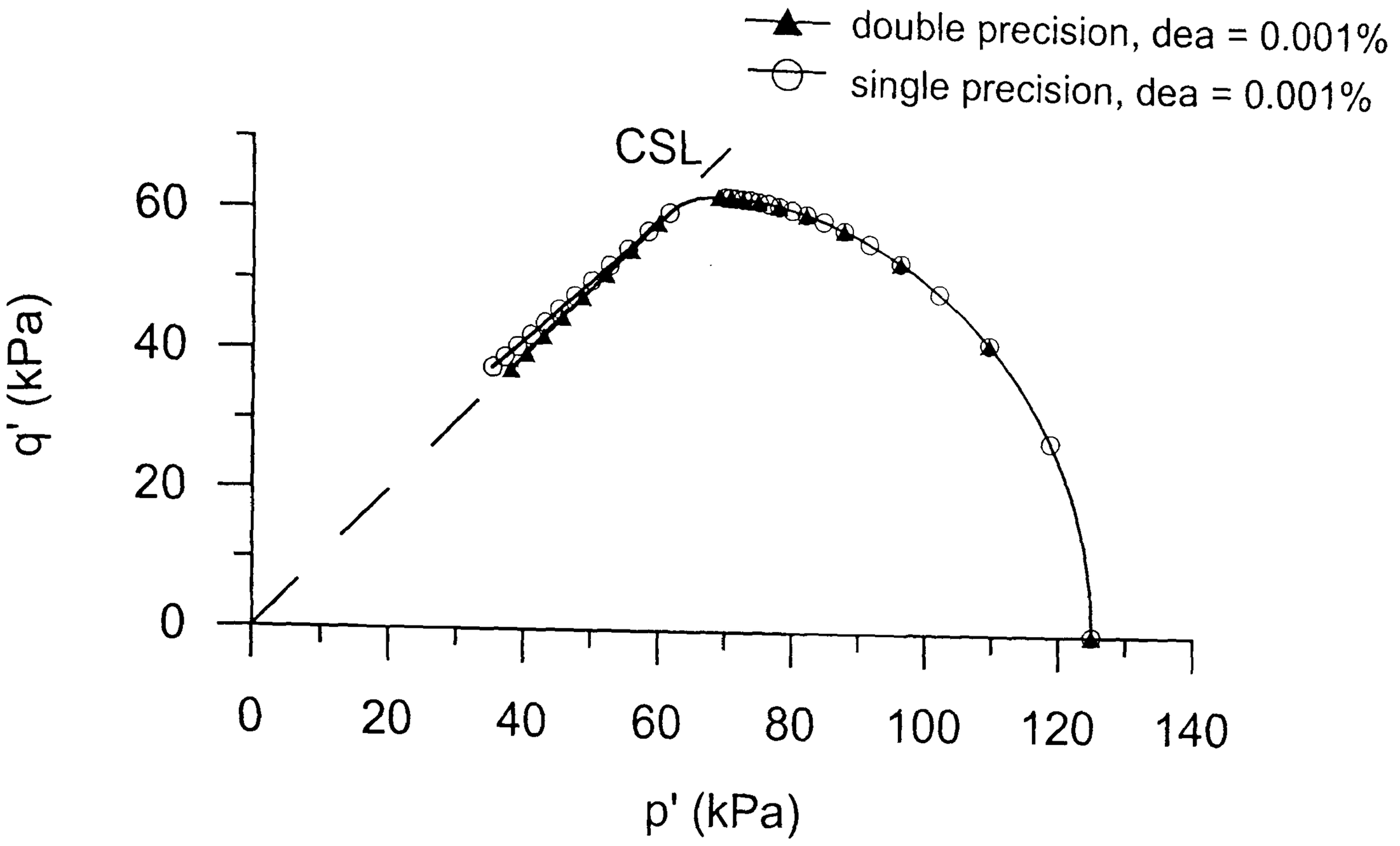

(a)

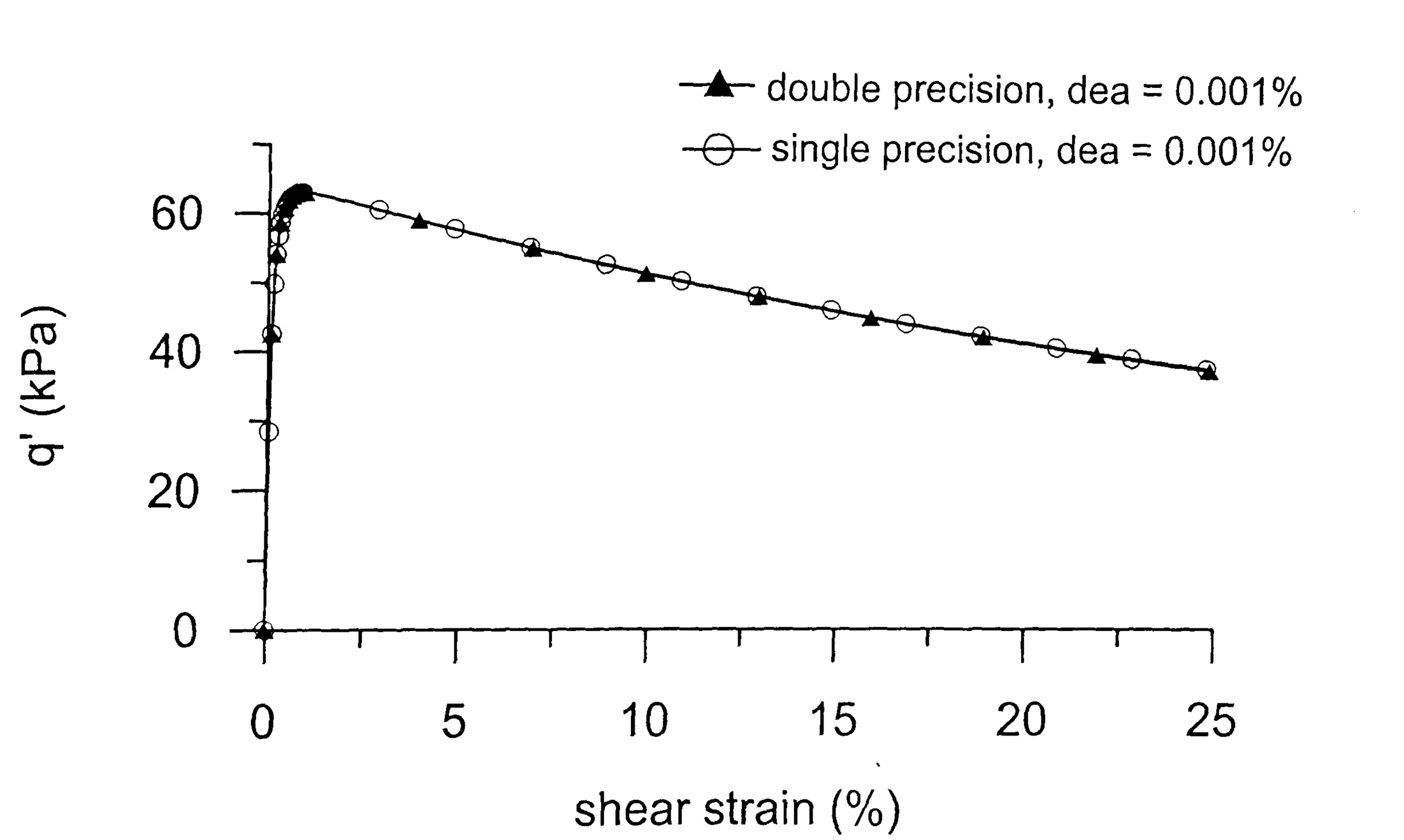

(b)

Figure 4.3.9 Comparison of numerical simulations of undrained compression for an increment of strain dea = 0.001% using single and double precision variables (a) stress path (b) stress-strain curve q'-ε_s

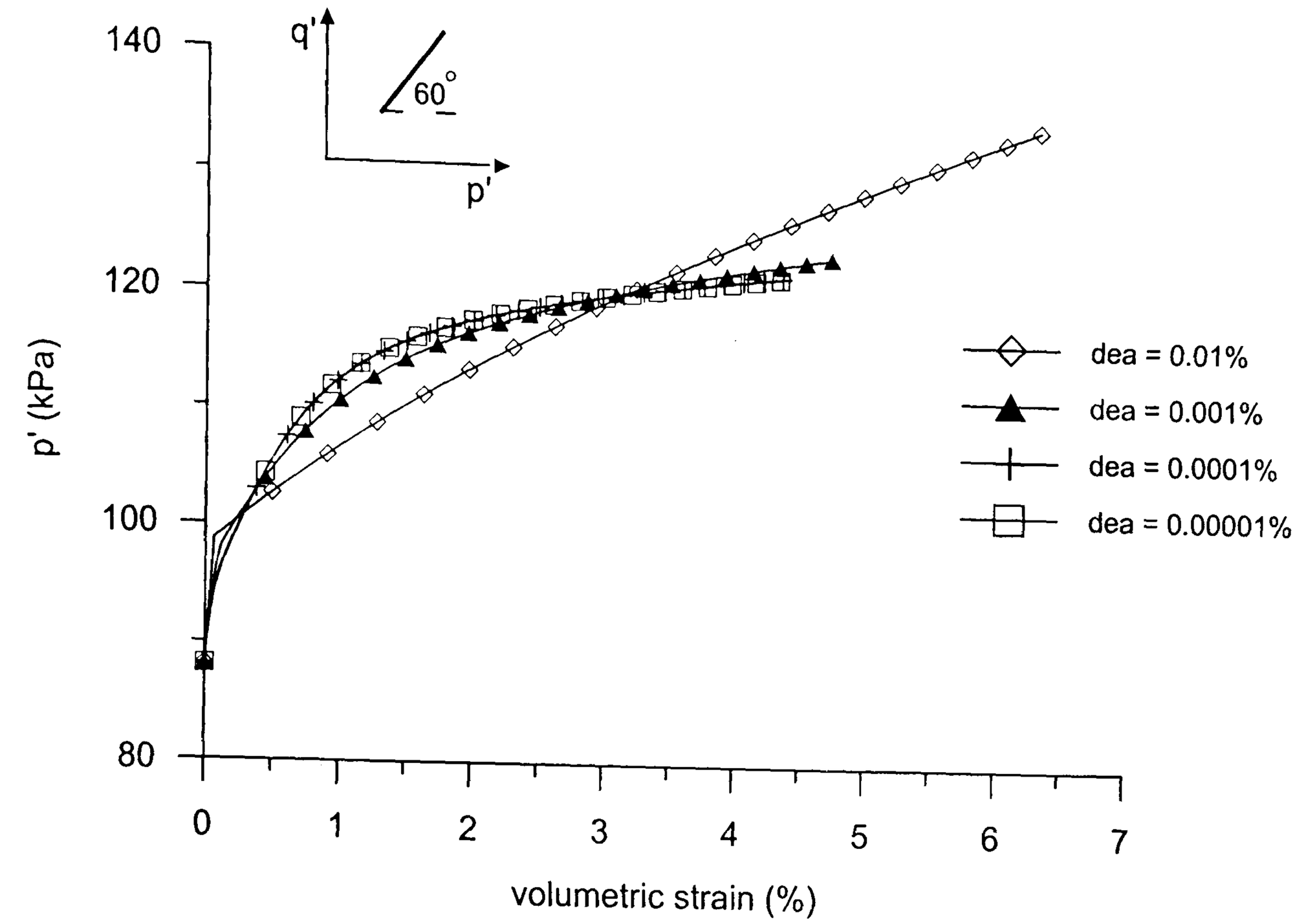

(a)

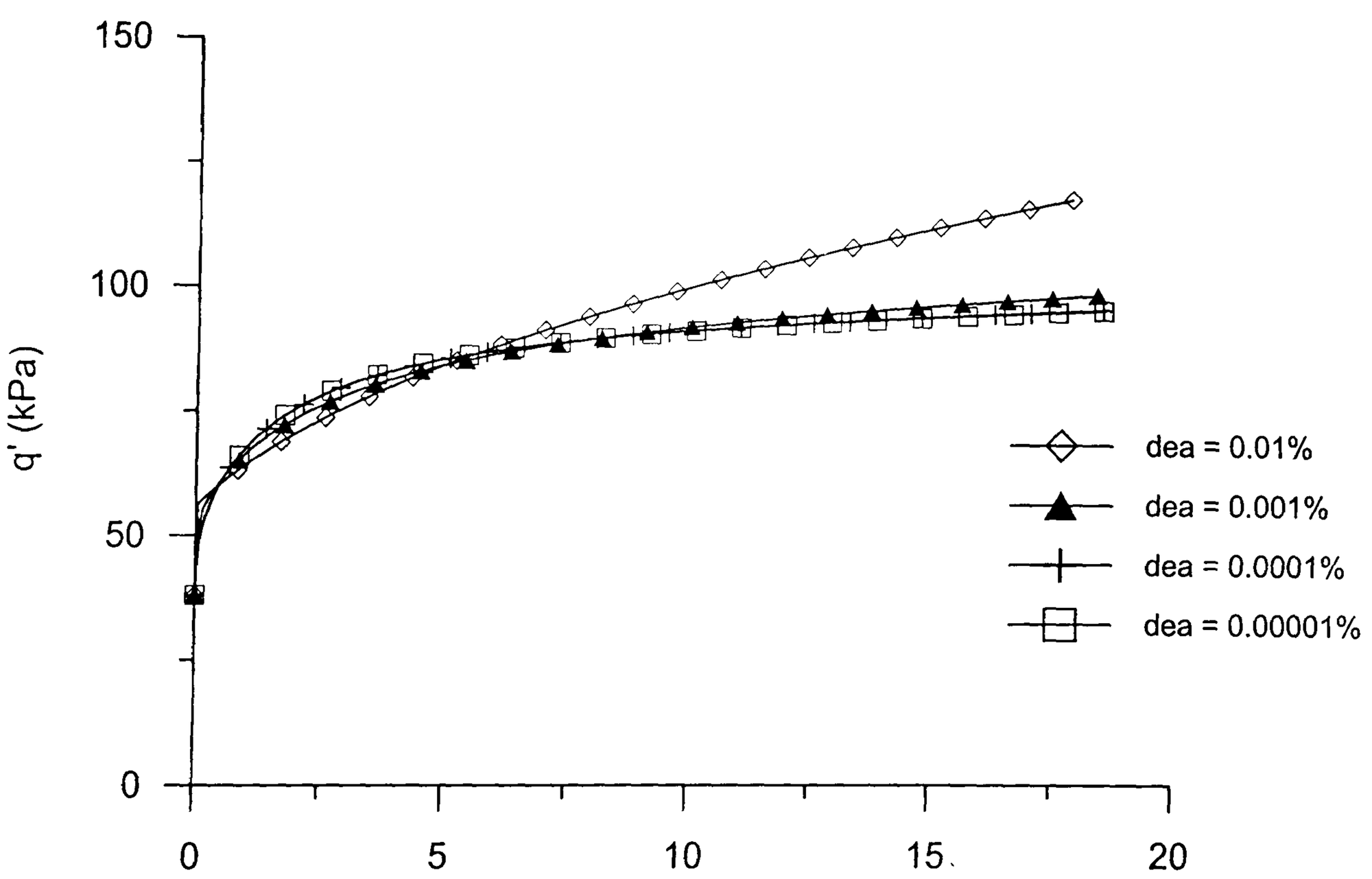

(b)

Figure 4.3.10 Comparison of stress-strain curves obtained in analyses simulating a drained probing test for different increments of strain using double precision variables (a) p'-ε_v (b) q'-ε_s

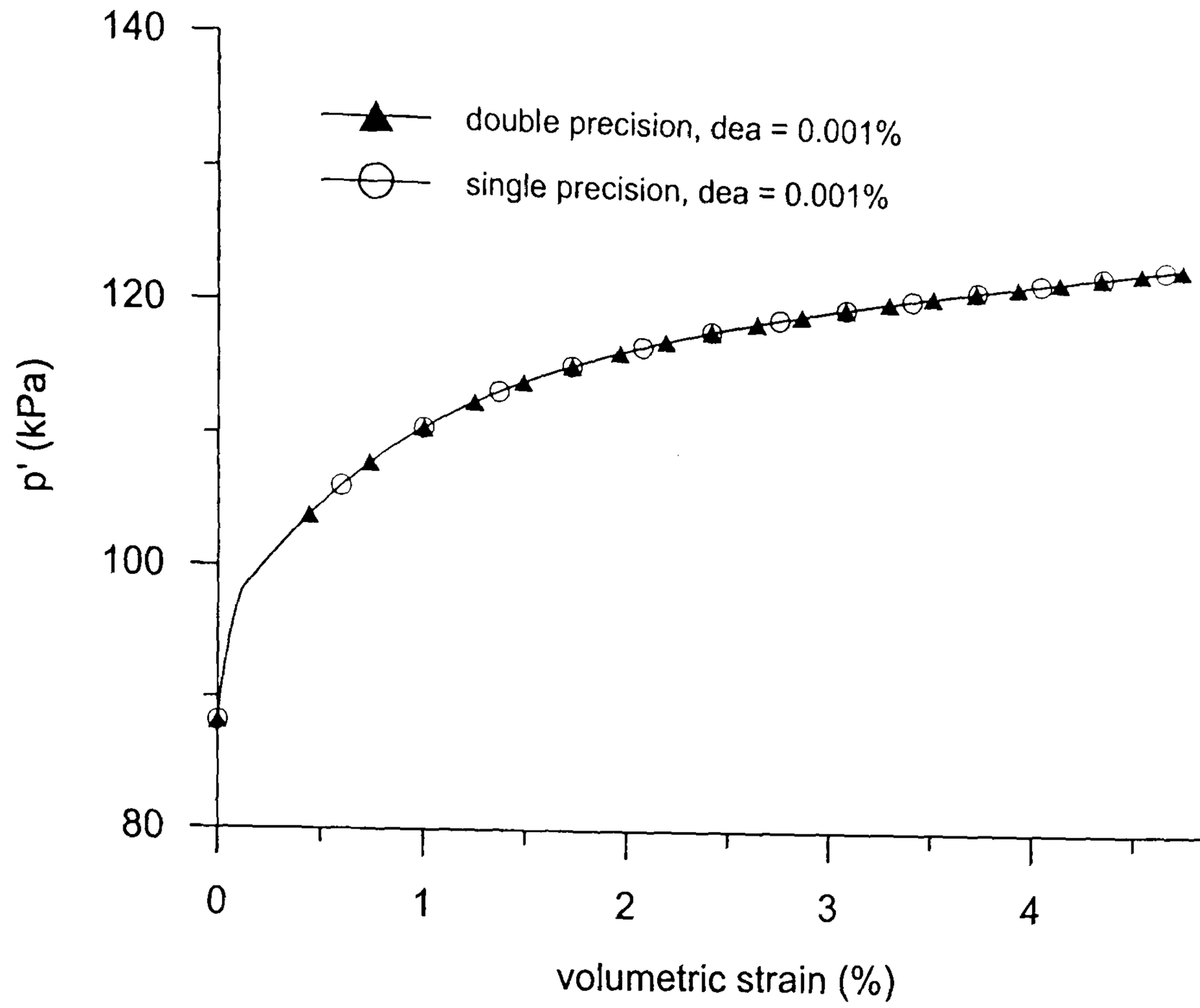

(a)

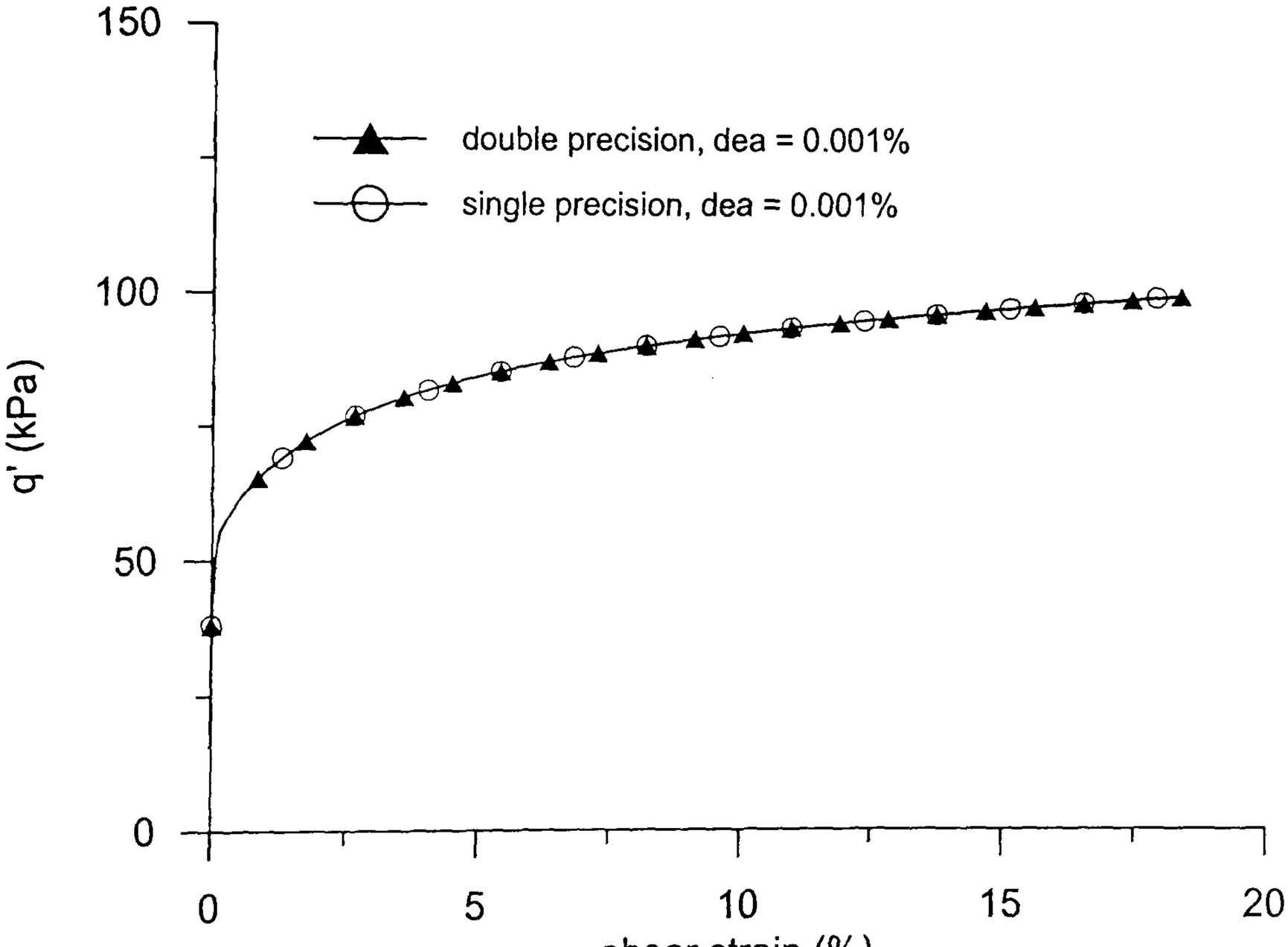

(b)

Figure 4.3.11 Comparison of stress-strain curves obtained in analyses simulating a drained probing test for an increment of strain dea = 0.001% using single and double precision variables (a) p'-ε_v (b) q'-ε_s

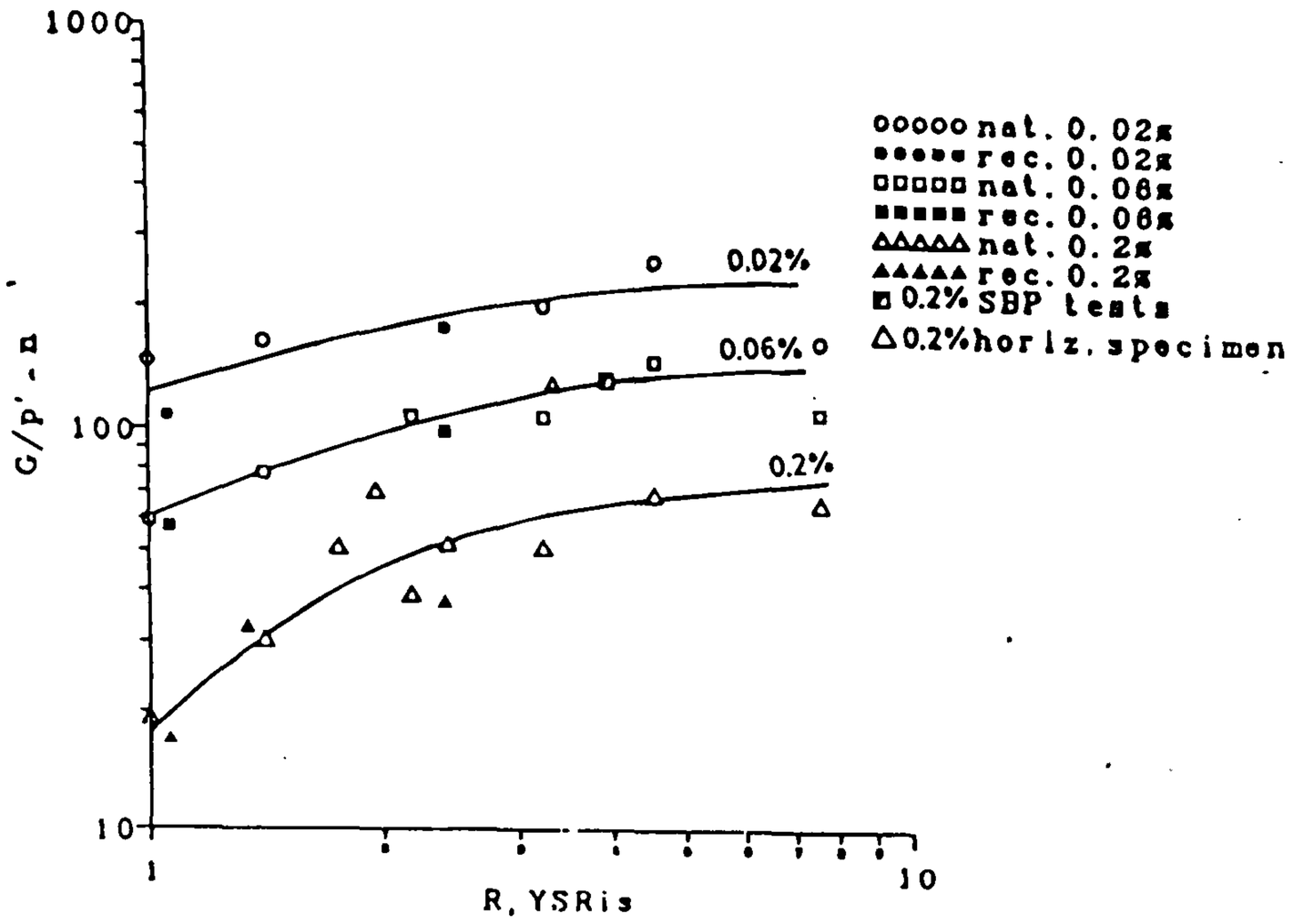

Figure 4.4.1 Variation of stiffness in natural and reconstituted Pappadai clay samples, normalised by p'^{n}, with overconsolidation ratio and yield stress ratio (after Cotecchia, 1996)

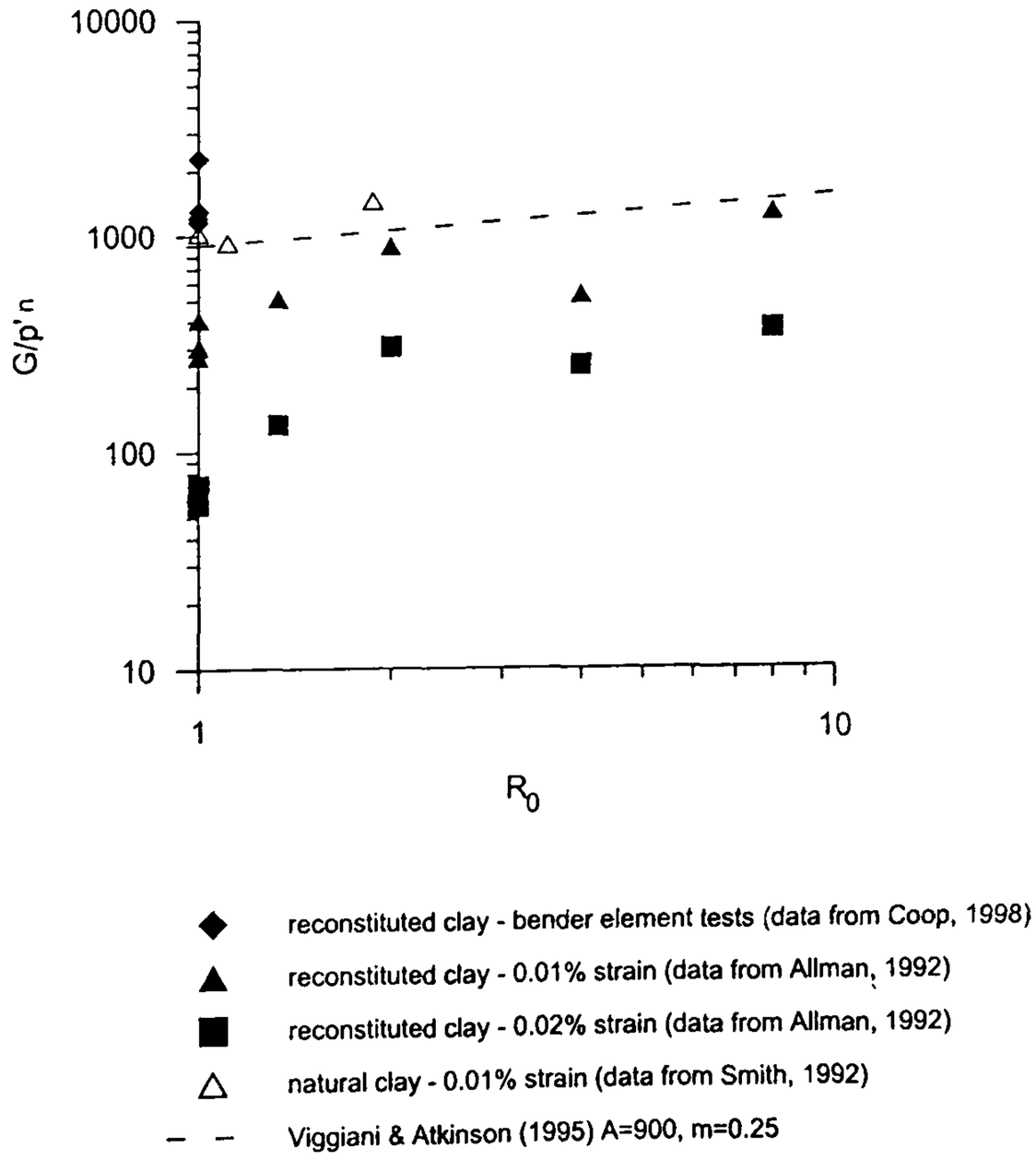

Figure 4.4.2 Variation of stiffness in natural and reconstituted Bothkennar clay samples, normalised by p'^{n}, with overconsolidation ratio (data from Allman, 1992; Coop, 1998; Smith, 1992)

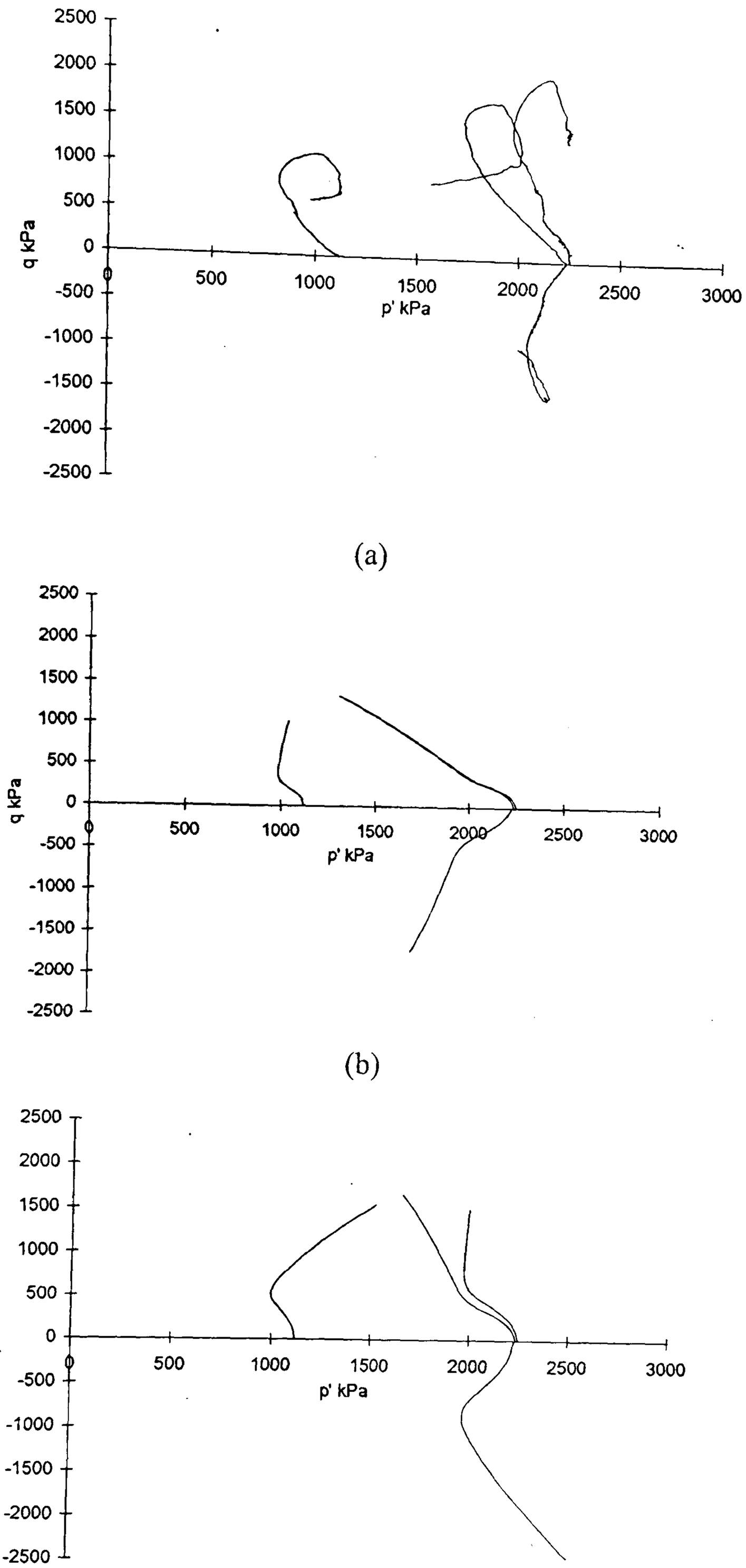

Figure 4.4.3 Comparison of (a) undrained stress paths for natural samples of Boom clay and 3-SKH model prediction using an initial state boundary surface computed from (b) the reconstituted compression behaviour (c) the natural compression behaviour (after Ingram, 2000)

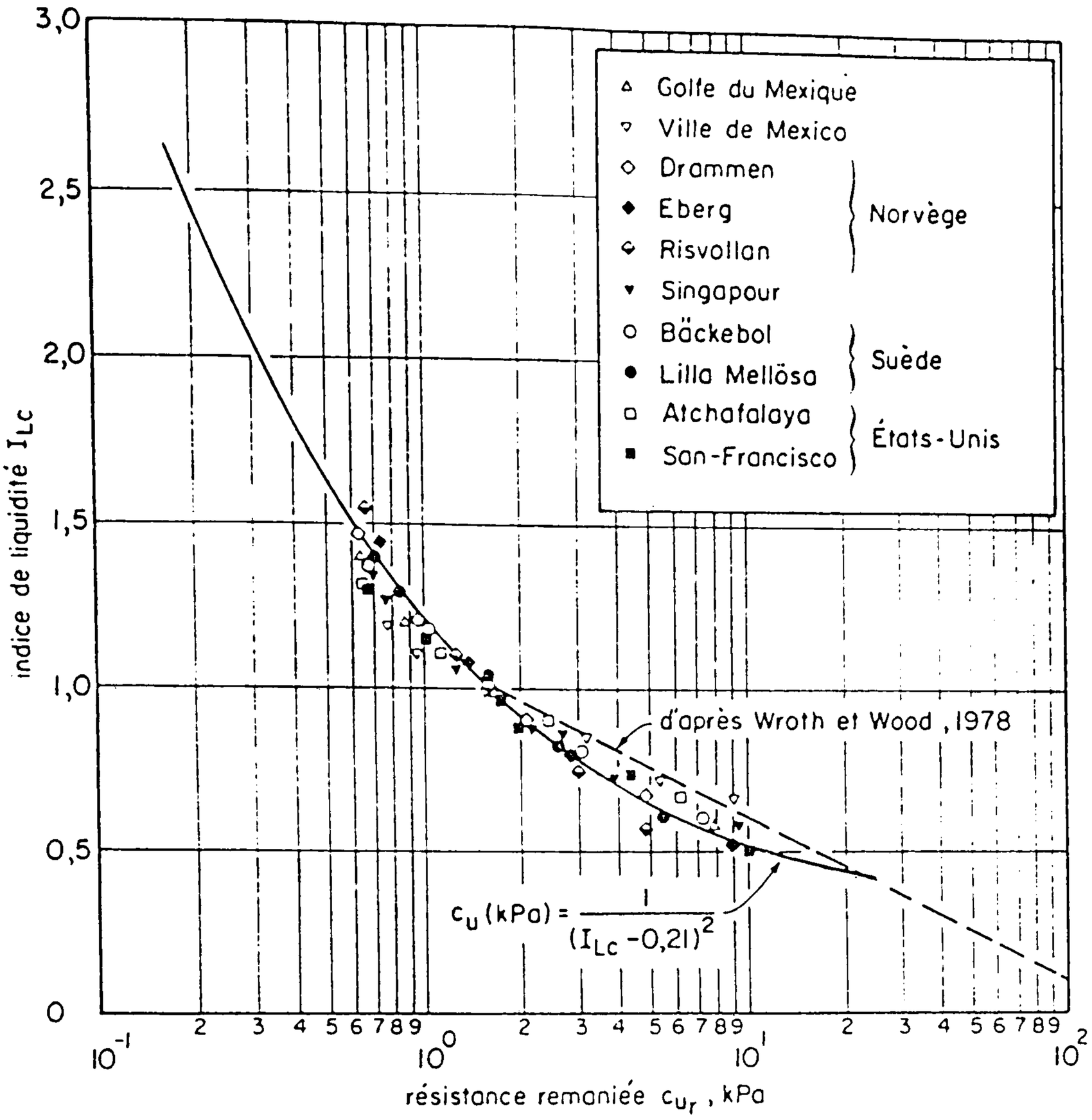

(a)

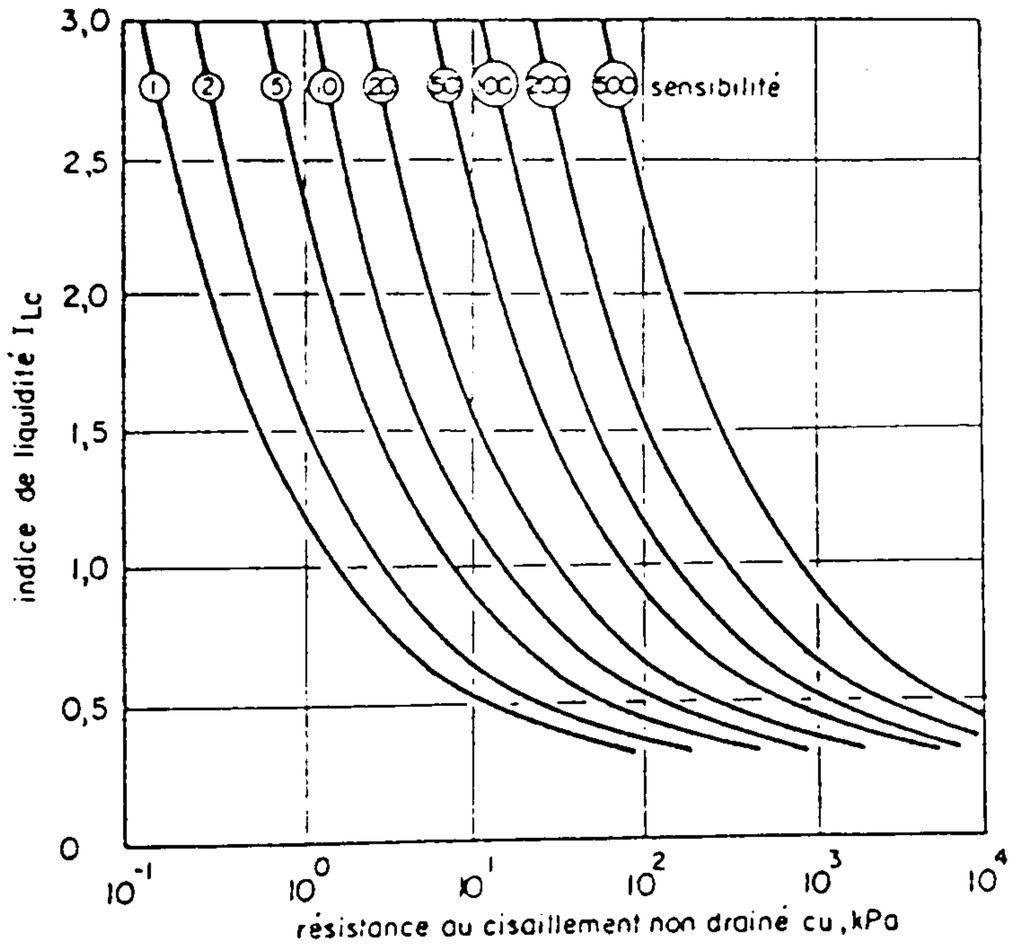

(b)

Figure 4.4.4 Relationship between (a) undrained shear strength of the reconstituted clay, C_{ur}, and liquidity index, I_{LC}, determined in a BS fall cone test (b) undrained shear strength of the natural clay, liquidity index and sensitivity (after Leroueil et al., 1983)

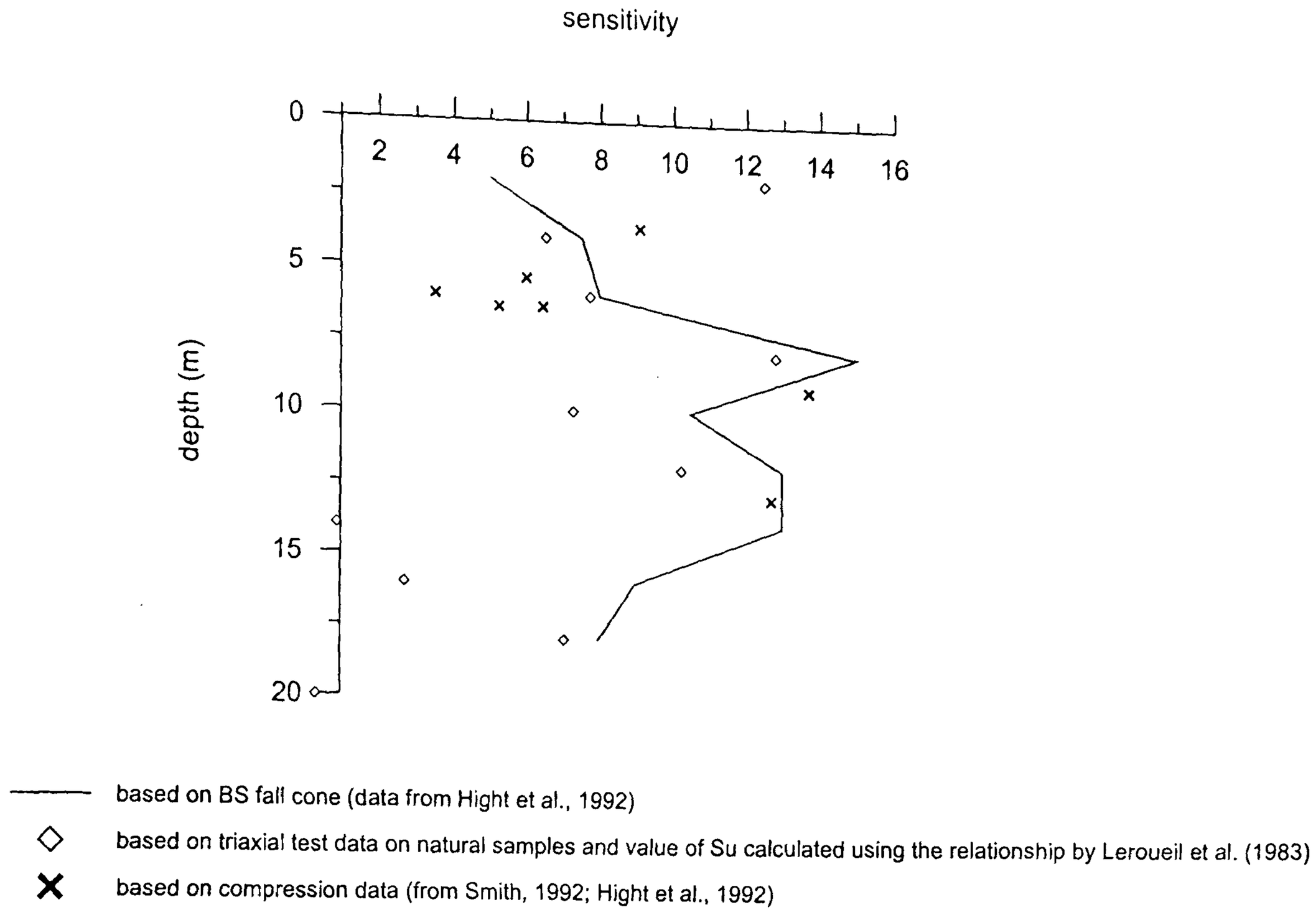

Figure 4.4.5 Profile of sensitivity against depth in Bothkennar clay, computed using different methods

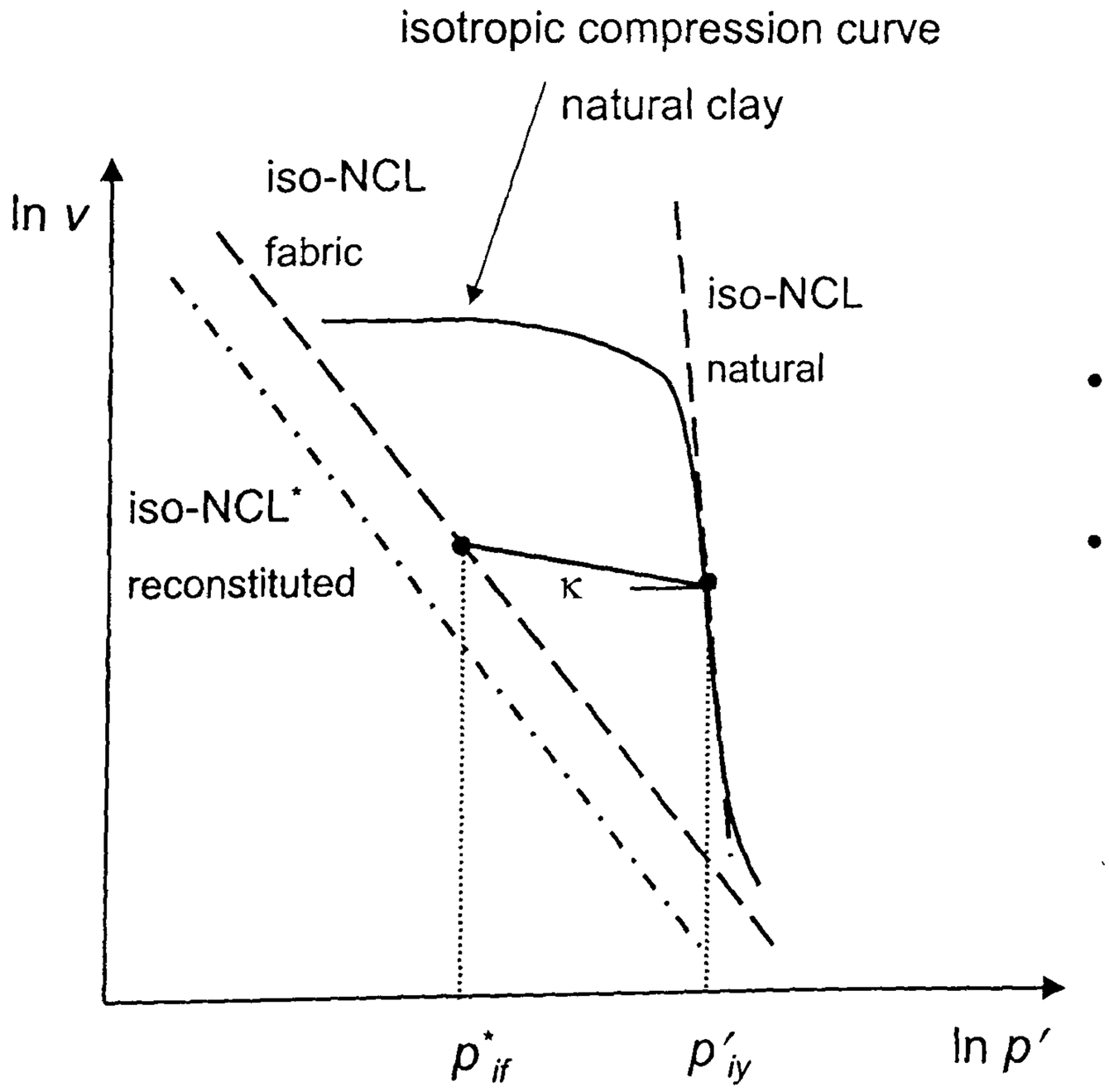

- **iso-NCL fabric**

  $\ln v = N - \lambda \ln p'$

- **iso-NCL natural**

  $\ln v = N_n - \lambda_n \ln p'$

Figure 4.4.6 Diagram showing the isotropic normal compression lines of natural soil and the isotropic compression line representing the degree of fabric used in the derivation of the parameter *k*

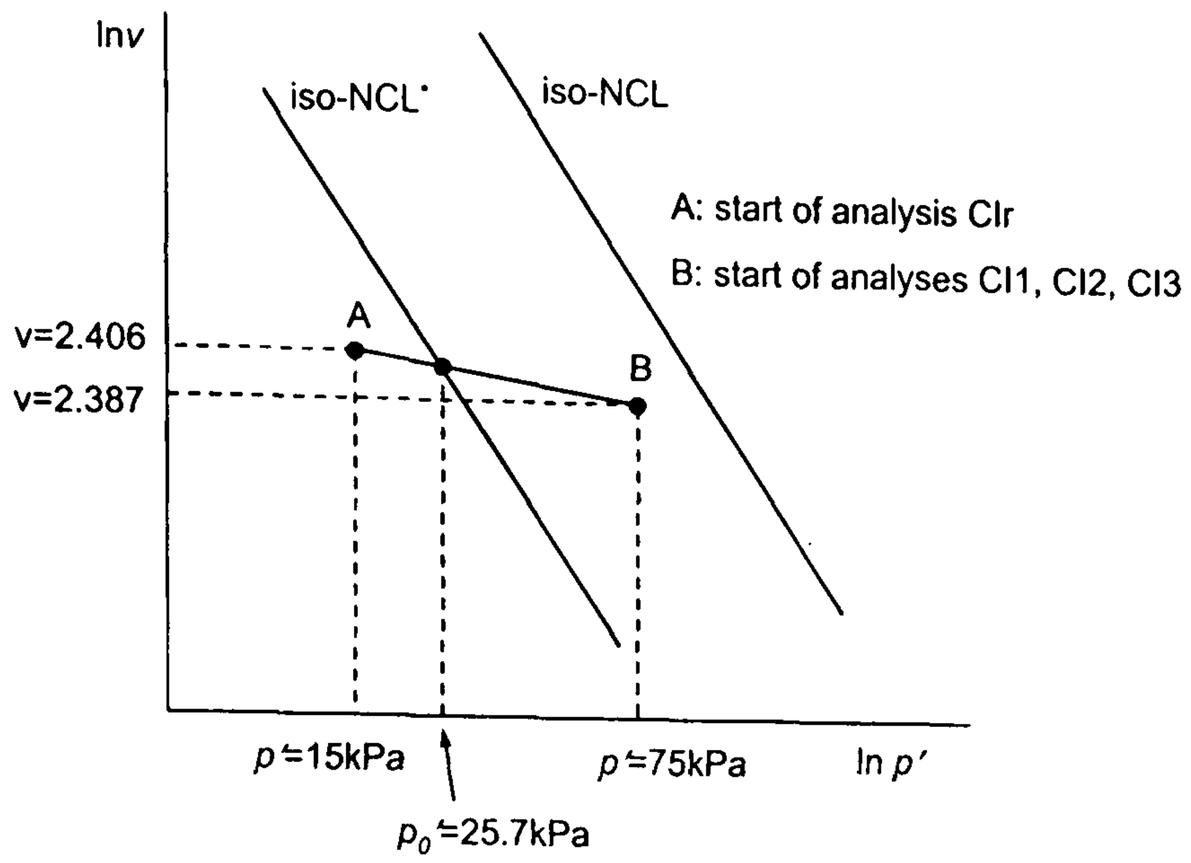

(a)

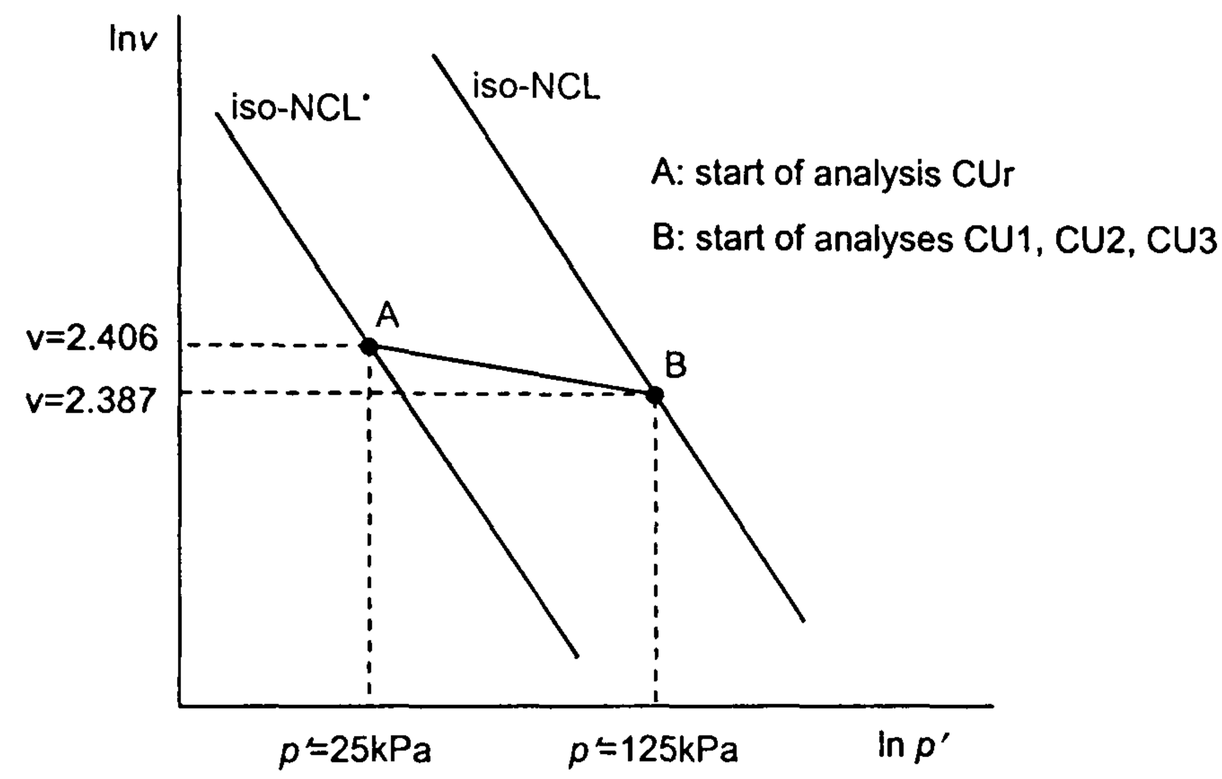

(b)

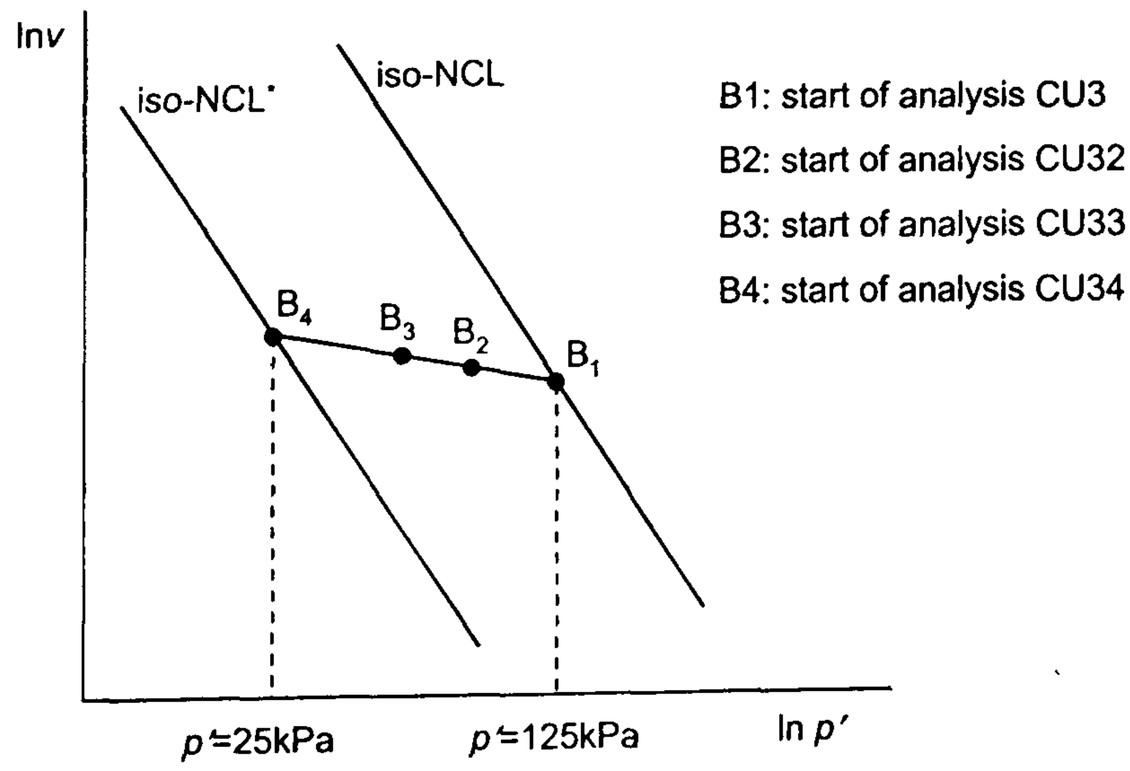

(c)

Figure 5.2.1 Diagrams showing the state of the samples at the start of the tests

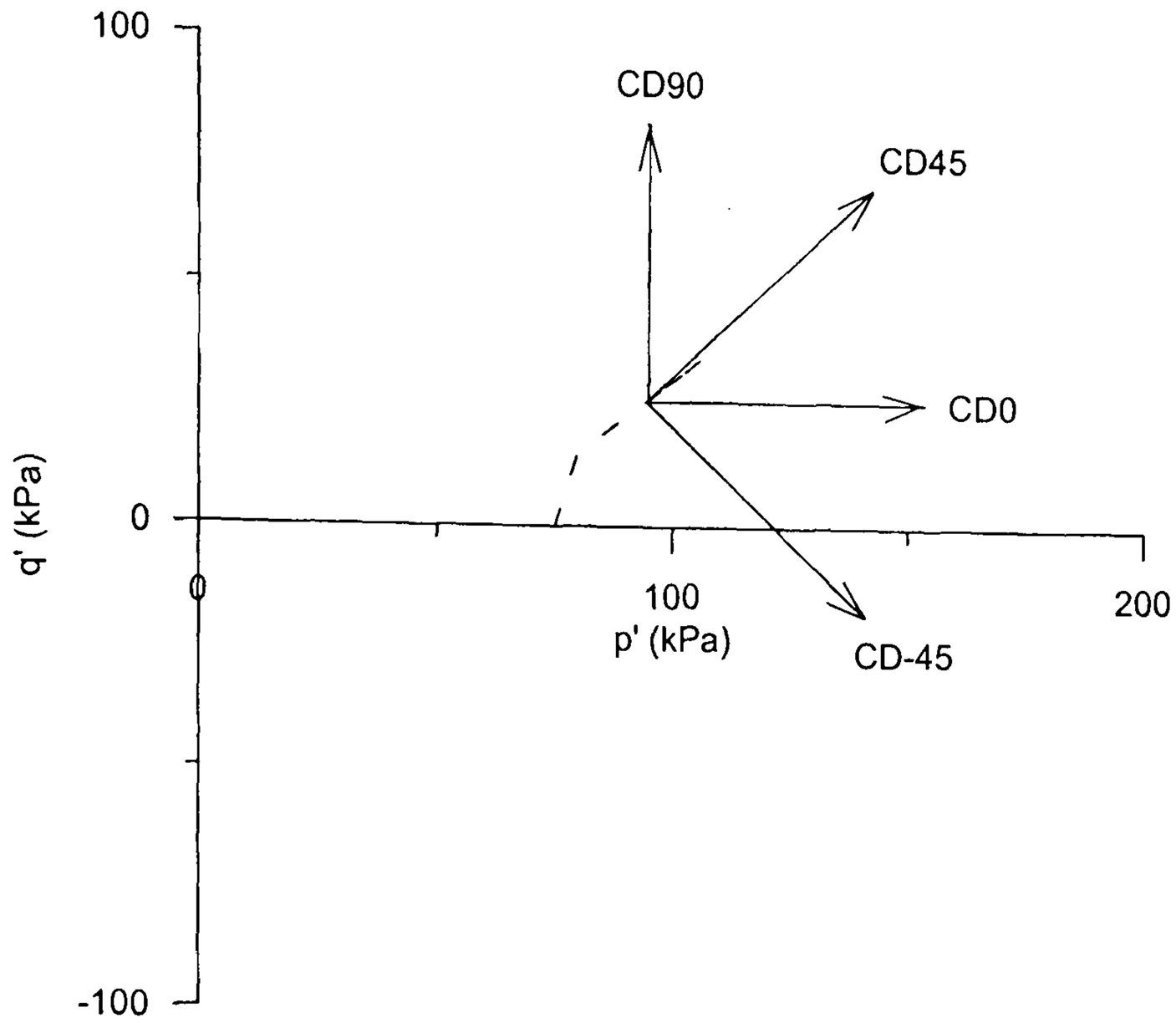

Figure 5.2.2 Diagram showing the stress paths followed to simulate drained probes

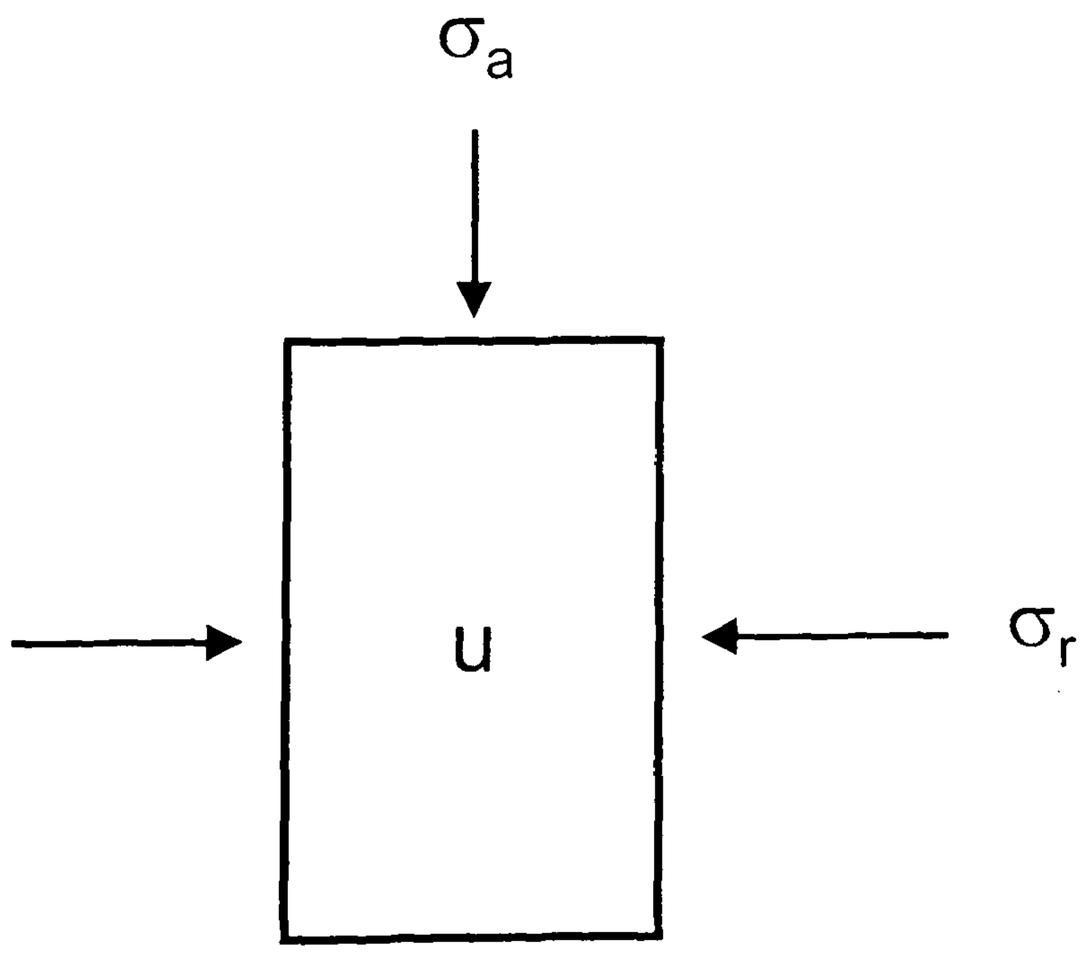

Figure 5.2.3 Diagram showing a single element used in the computations

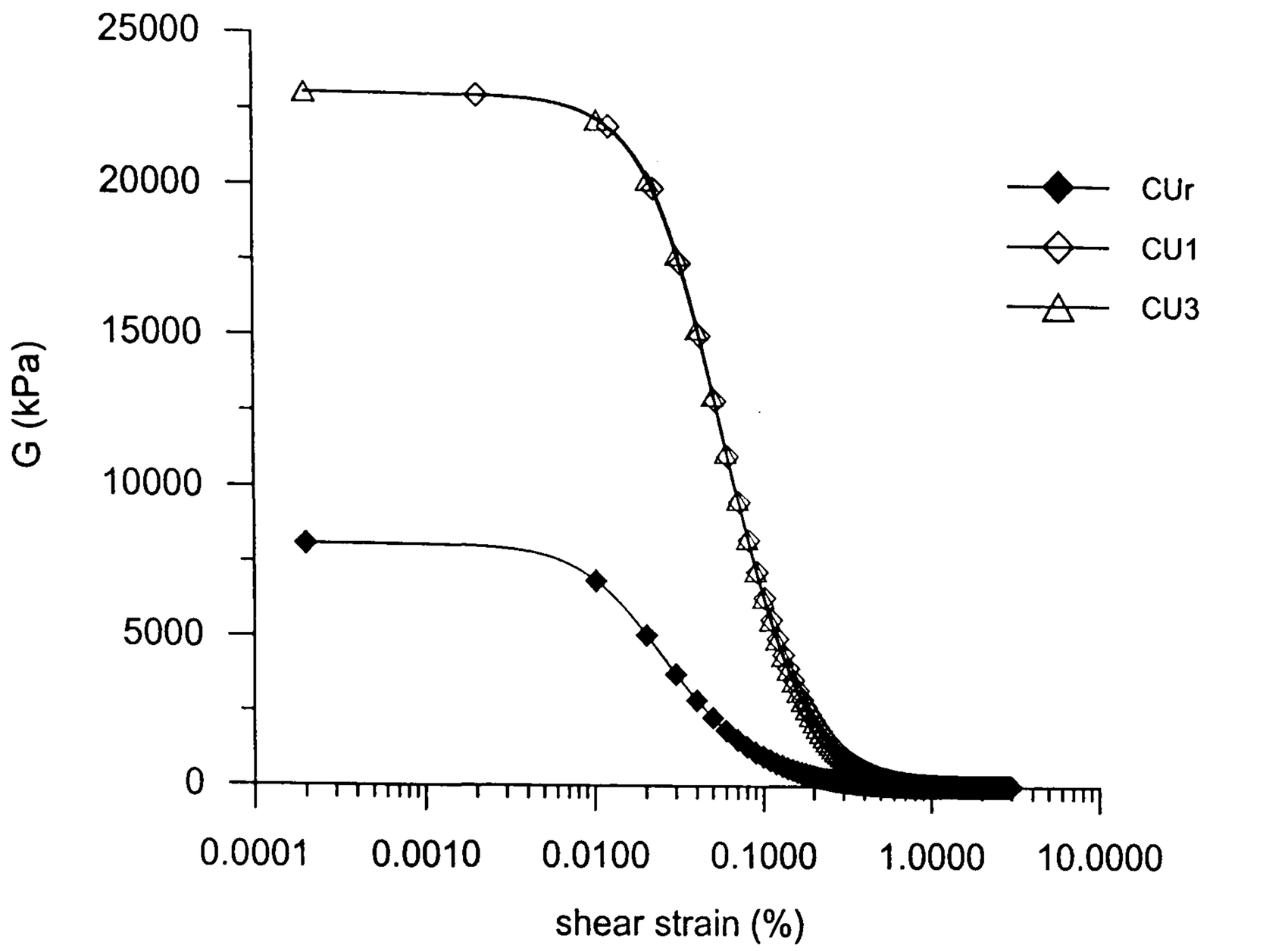

Figure 5.2.4 Model prediction of stiffness curve for an undrained triaxial compression test on a natural and reconstituted sample

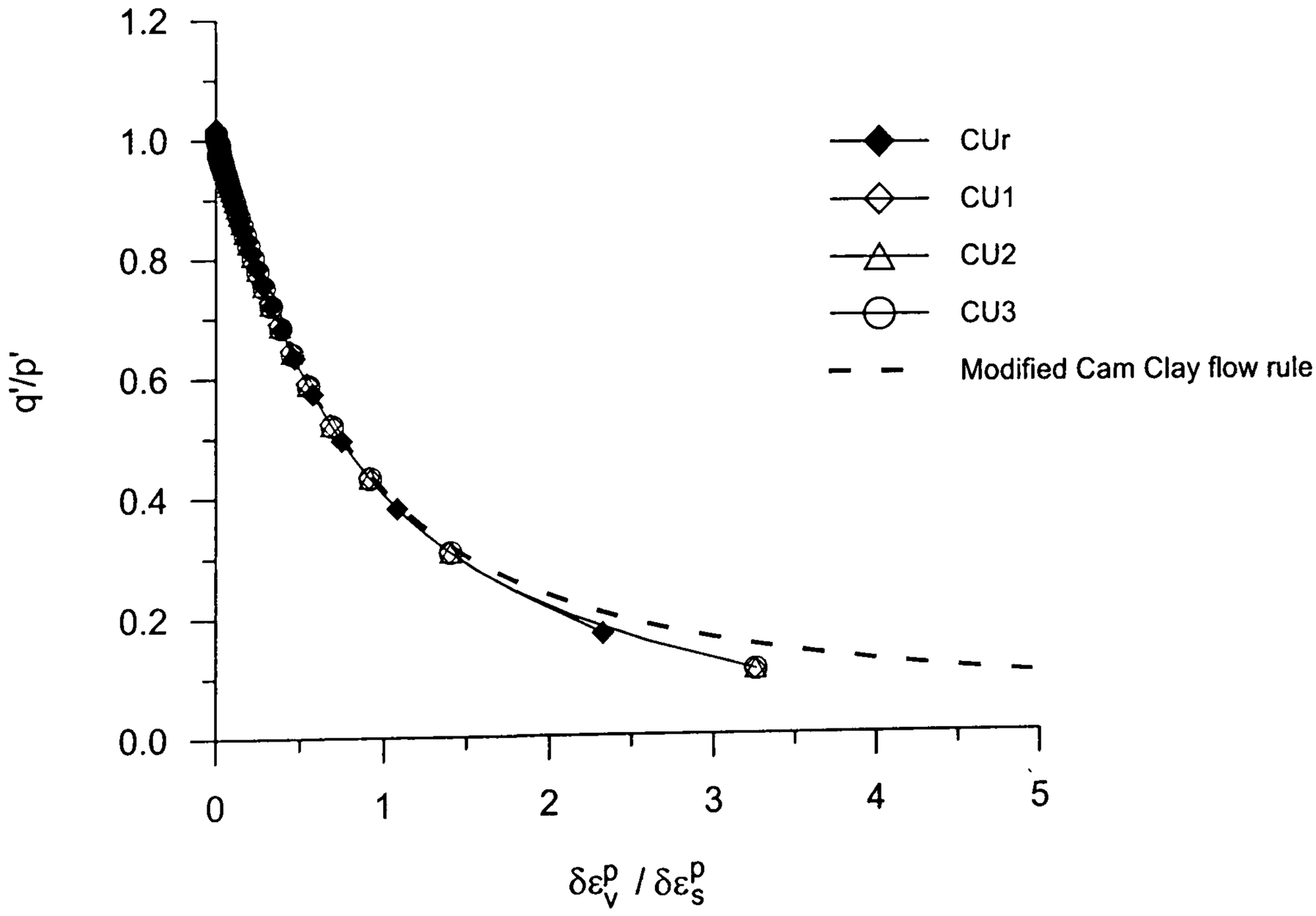

Figure 5.2.5 Model prediction of stress-dilatancy for an undrained triaxial compression test on a natural and reconstituted sample

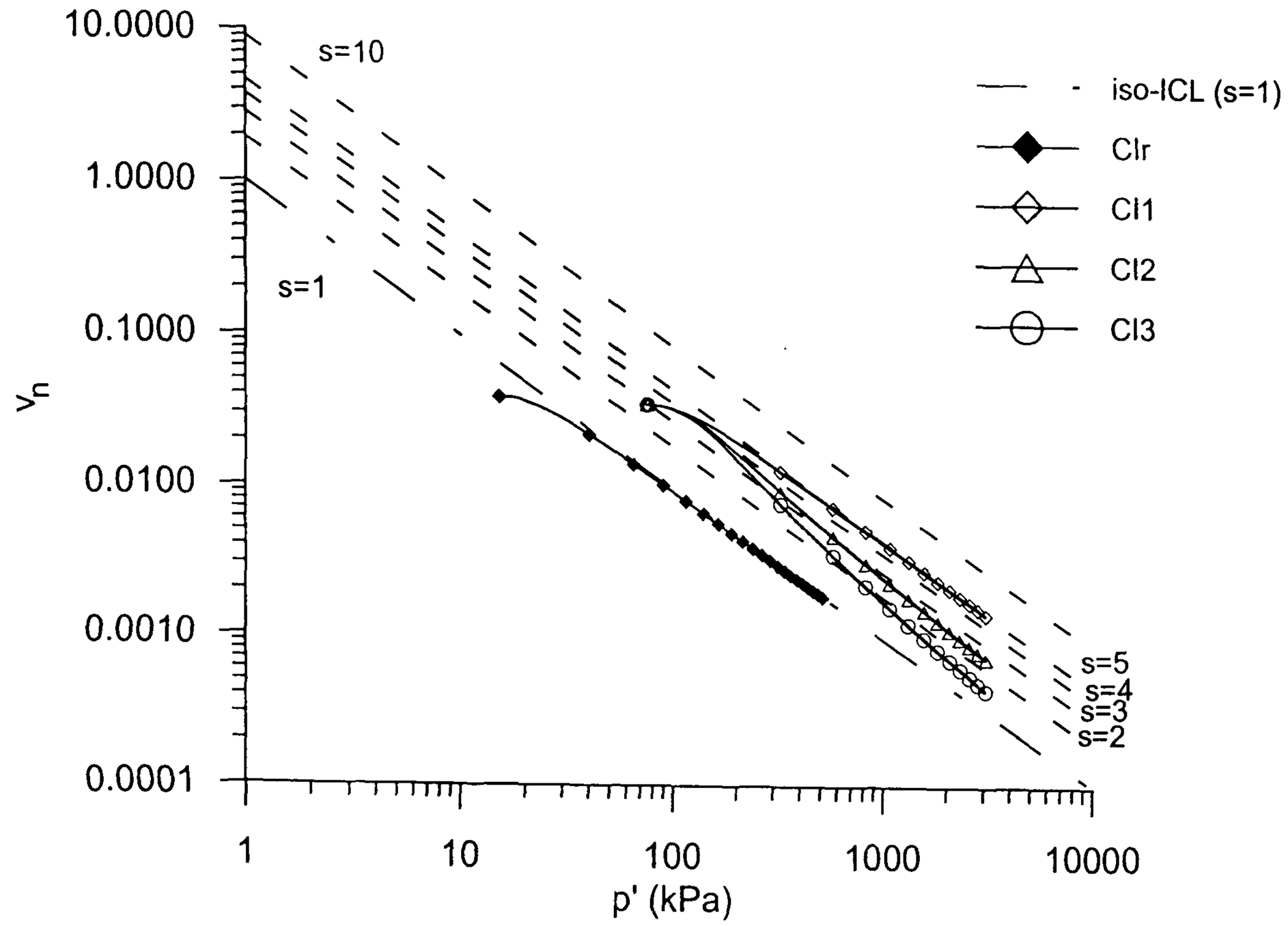

Figure 5.2.6 Effect of varying the value of ultimate sensitivity on predicted volumetric response during isotropic compression

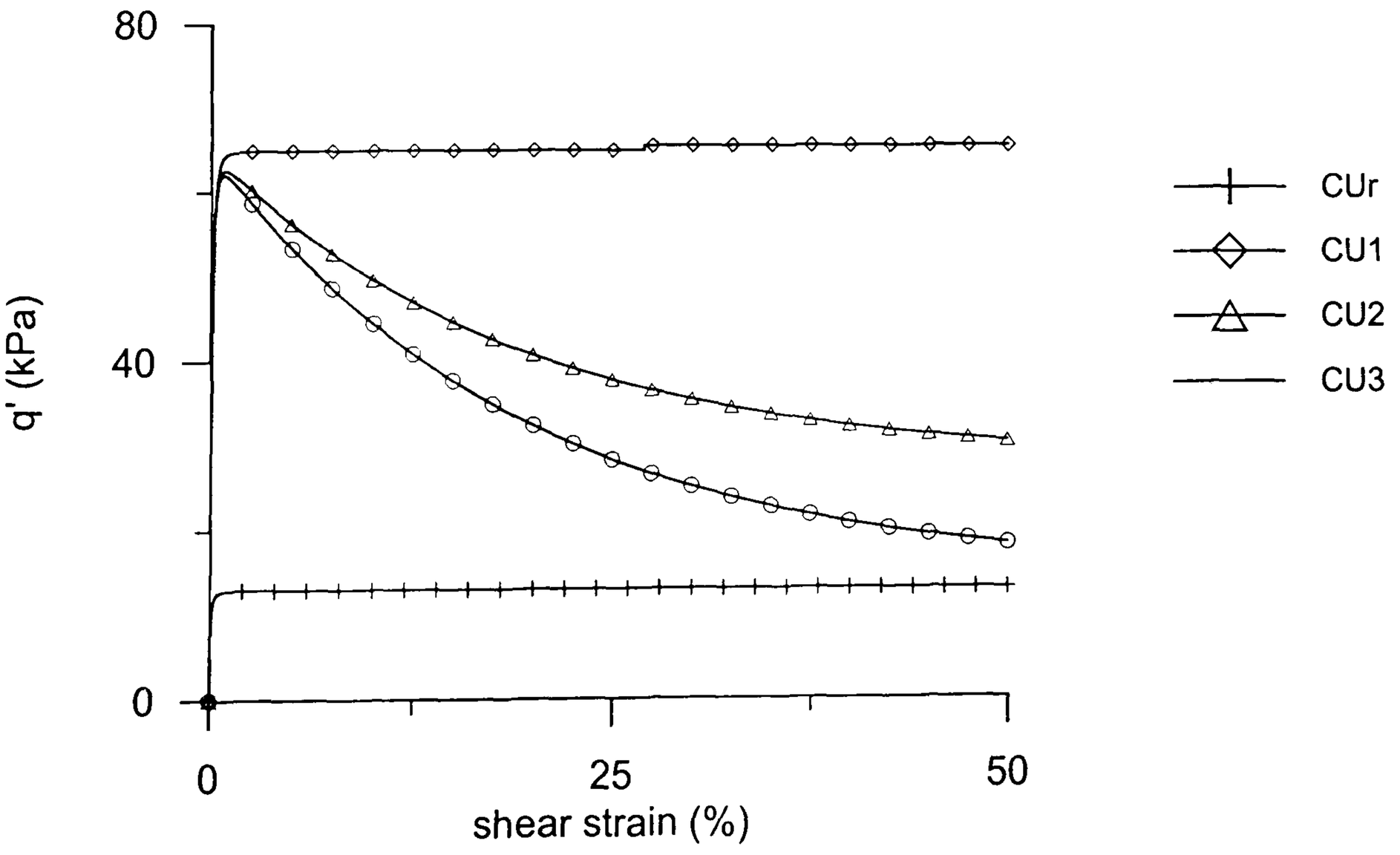

Figure 5.2.7 Effect of varying the value of ultimate sensitivity on predicted stress-strain response during undrained triaxial compression

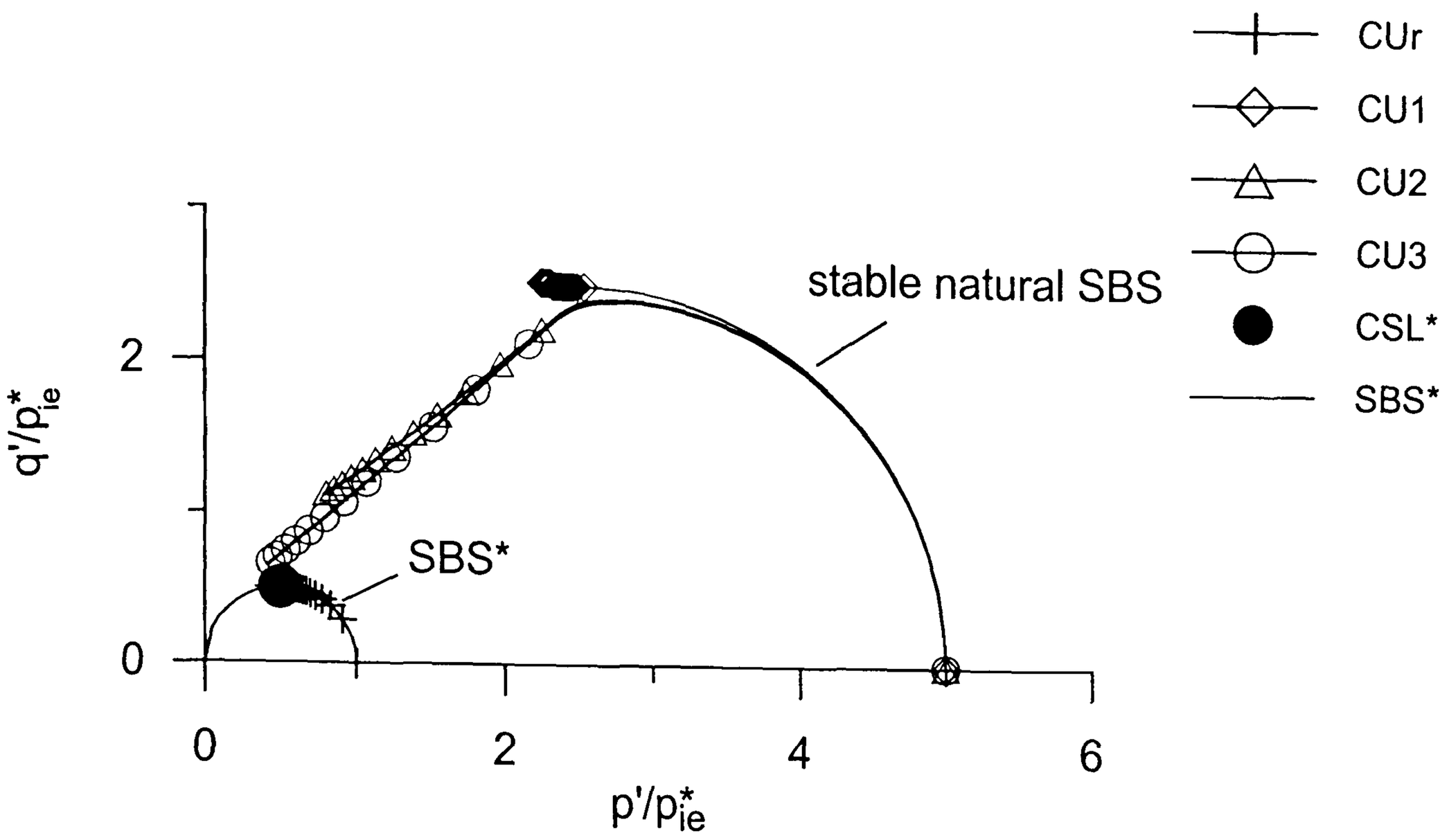

Figure 5.2.8 Predicted stress paths during undrained triaxial compression of natural and reconstituted samples, normalised for volume

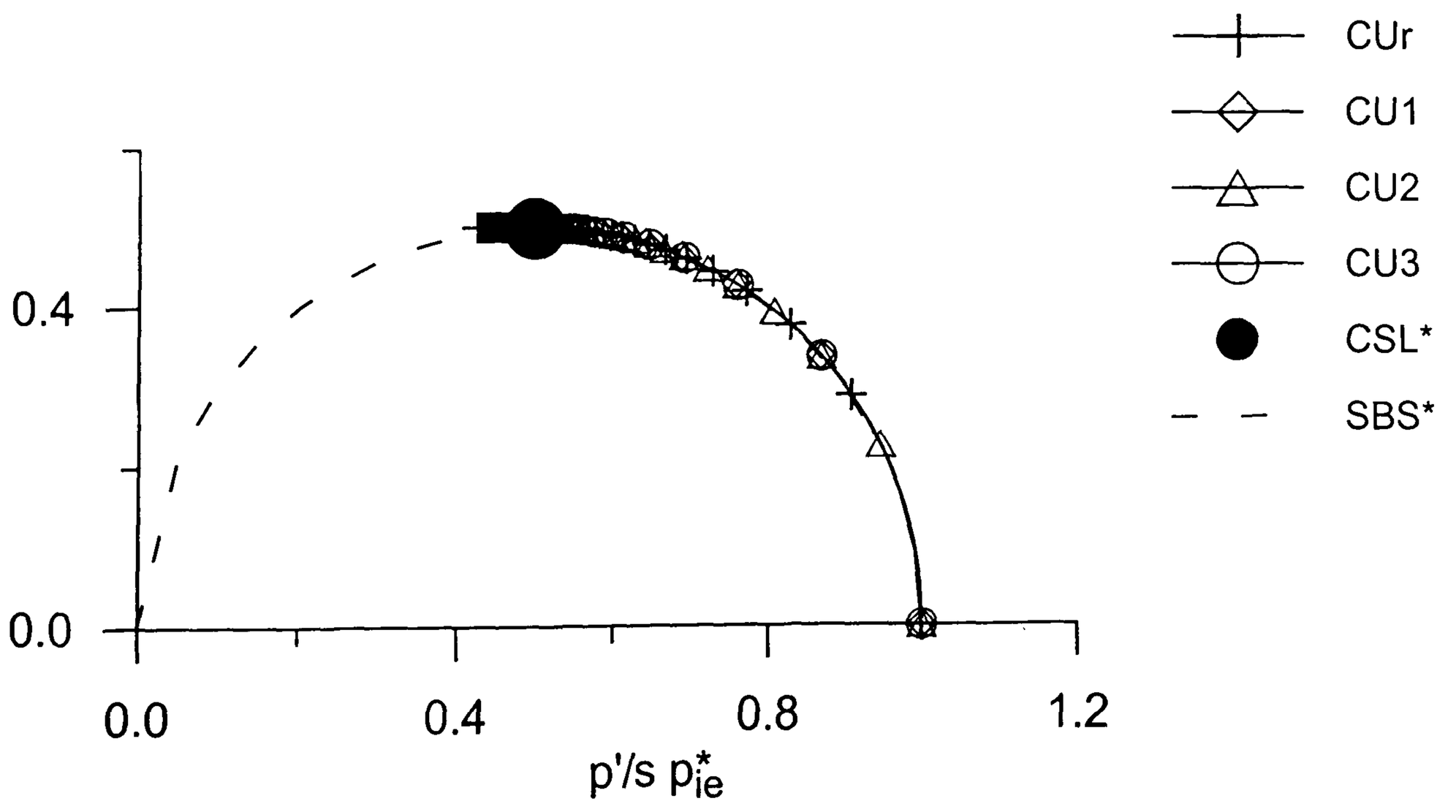

Figure 5.2.9 Predicted stress paths during undrained triaxial compression of natural and reconstituted samples, normalised for volume and current structure

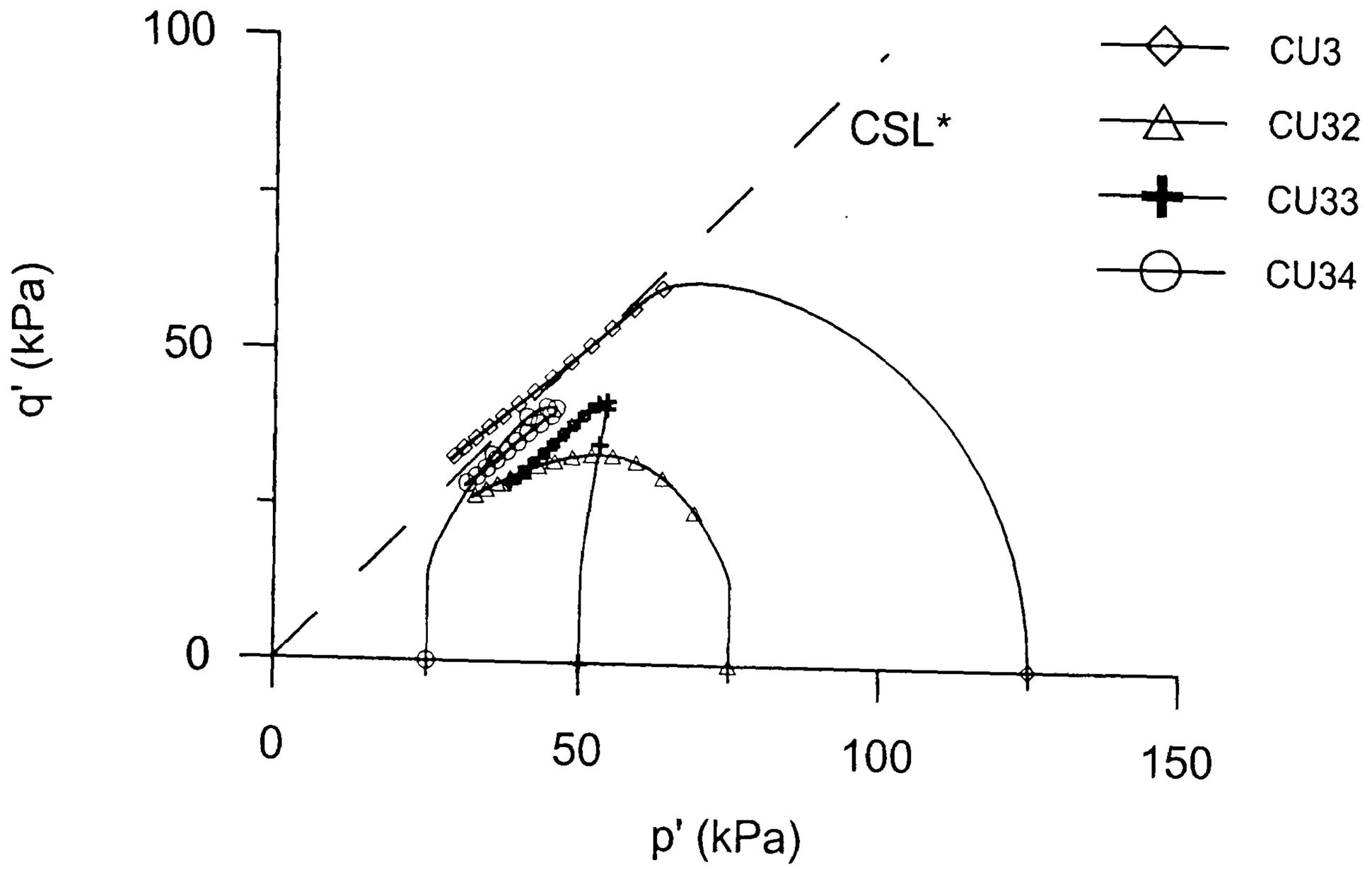

Figure 5.2.10 Predicted stress paths during undrained triaxial compression of natural samples sheared at different levels of overconsolidation

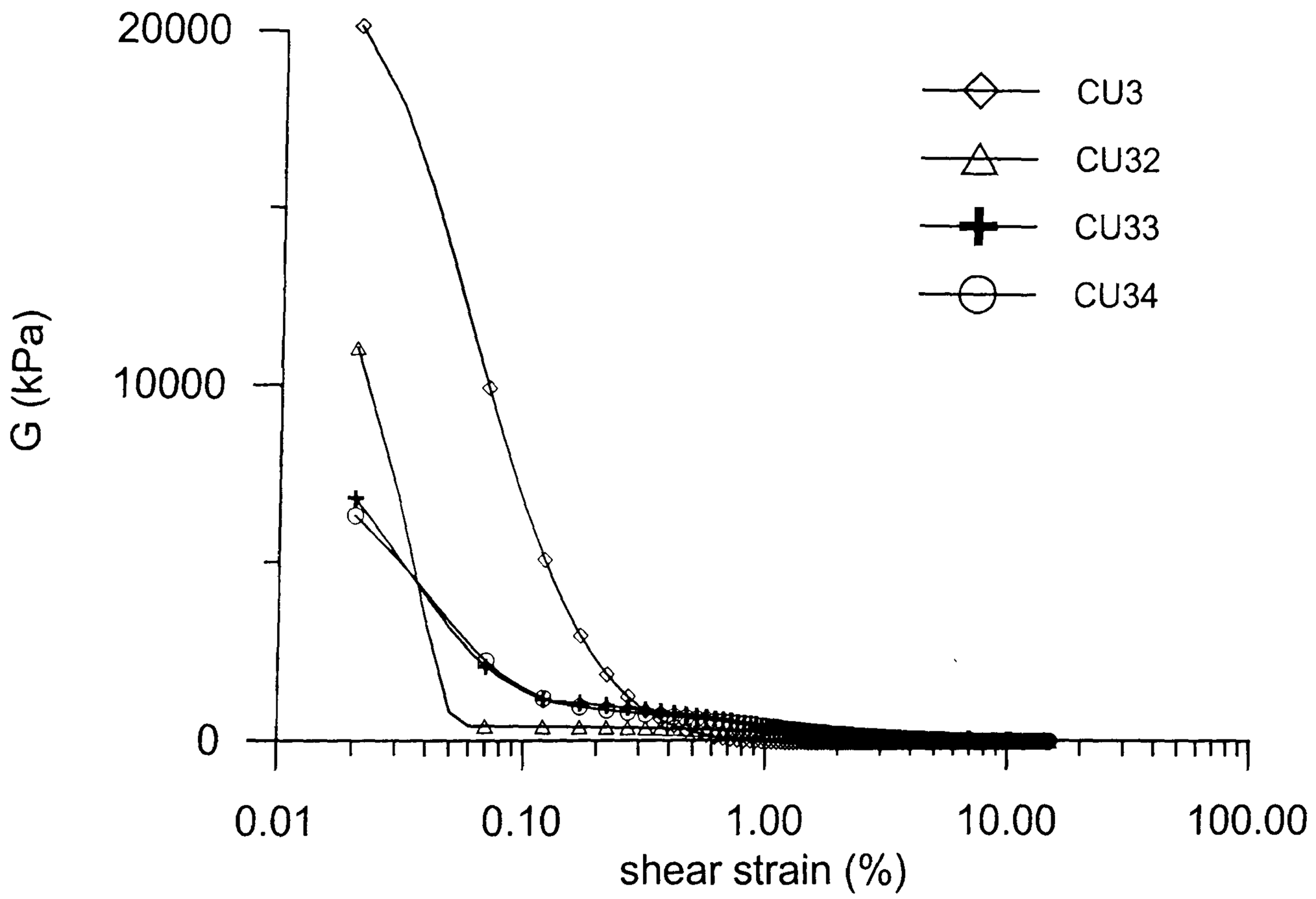

Figure 5.2.11 Predicted stiffness curves during undrained triaxial compression of natural samples sheared from different levels of overconsolidation

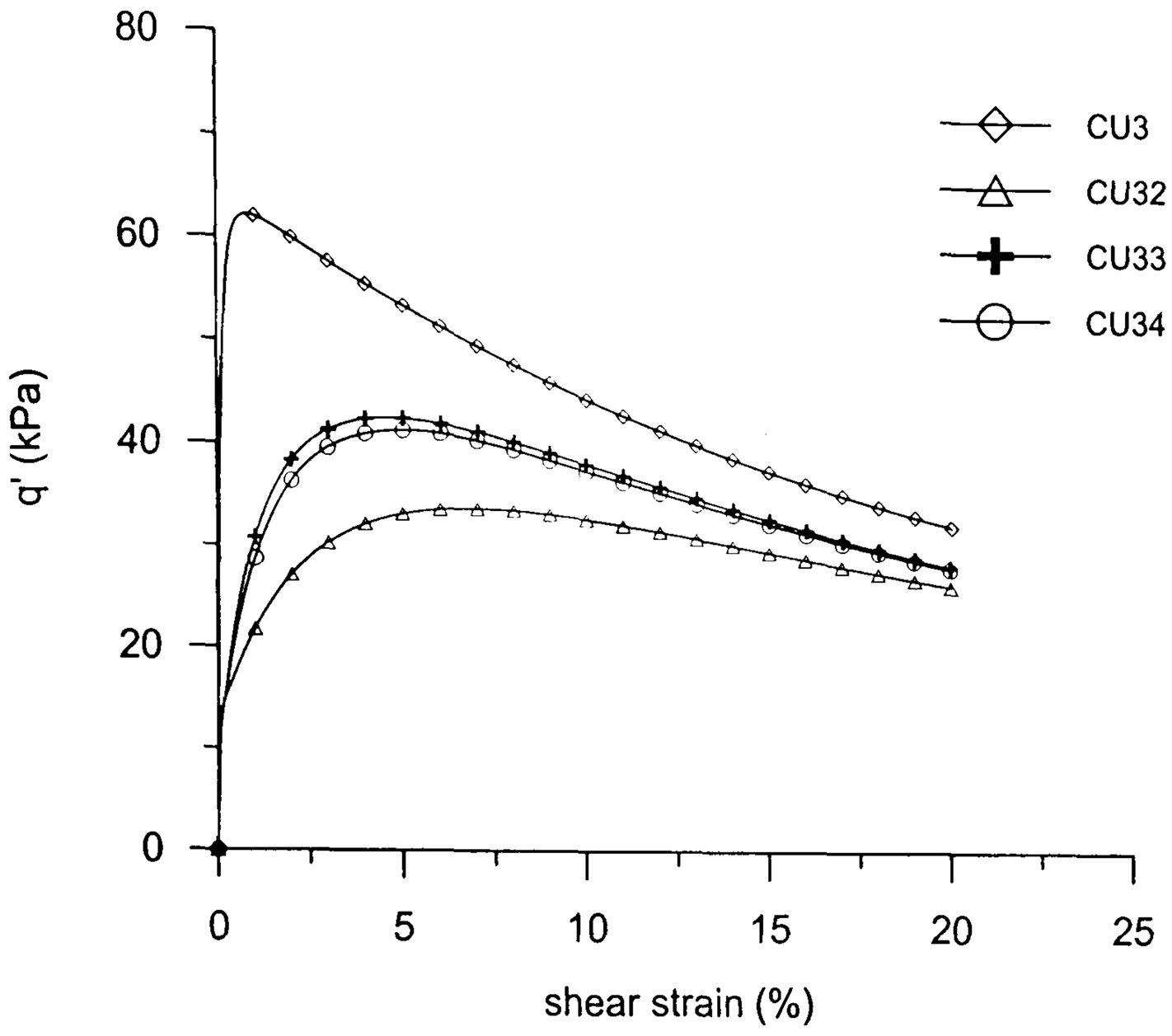

Figure 5.2.12 Predicted stress-strain response during undrained triaxial compression on natural samples started shearing at different levels of overconsolidation

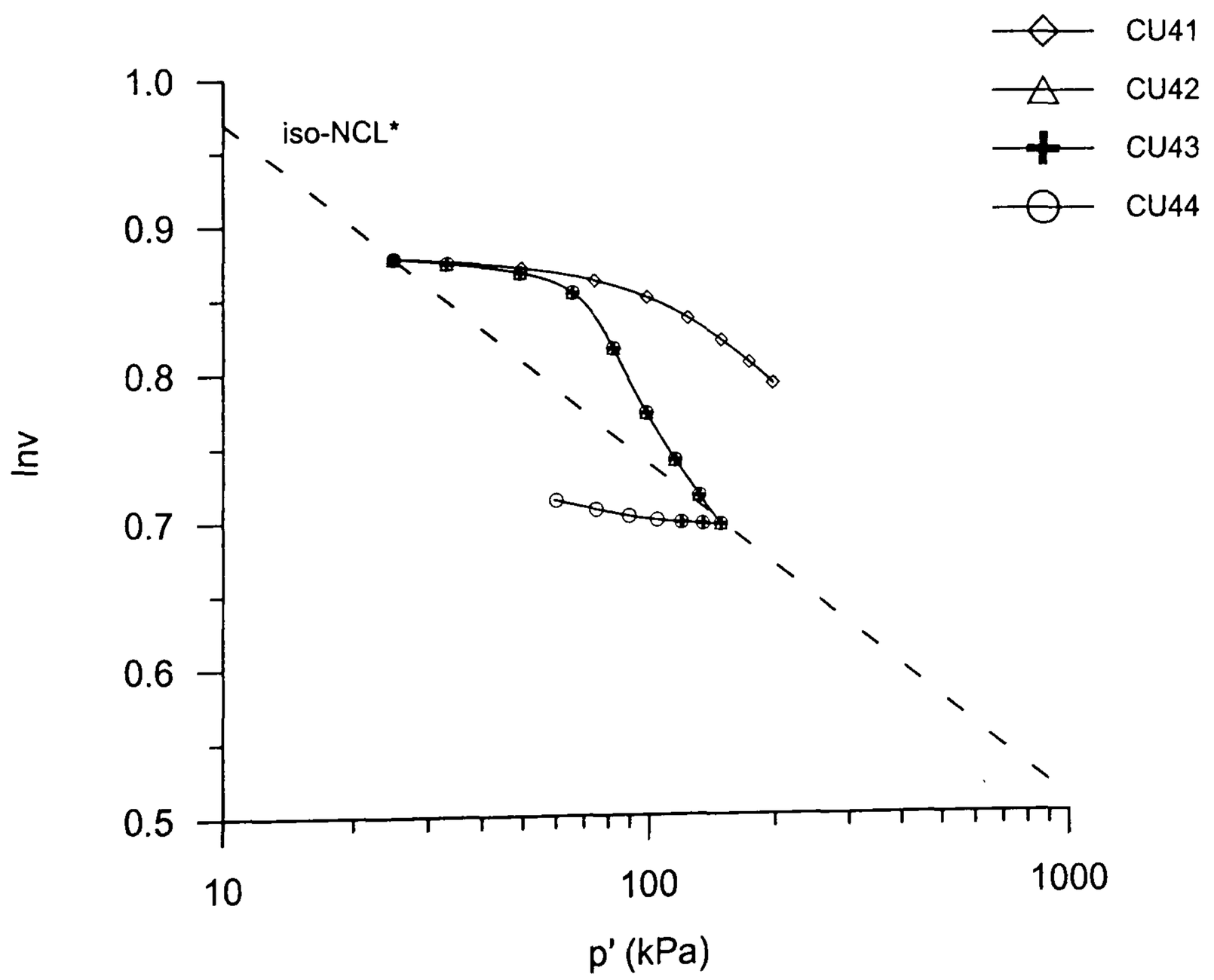

Figure 5.2.13 Predicted volumetric response during isotropic and anisotropic compression beyond gross yield, prior to shearing undrained

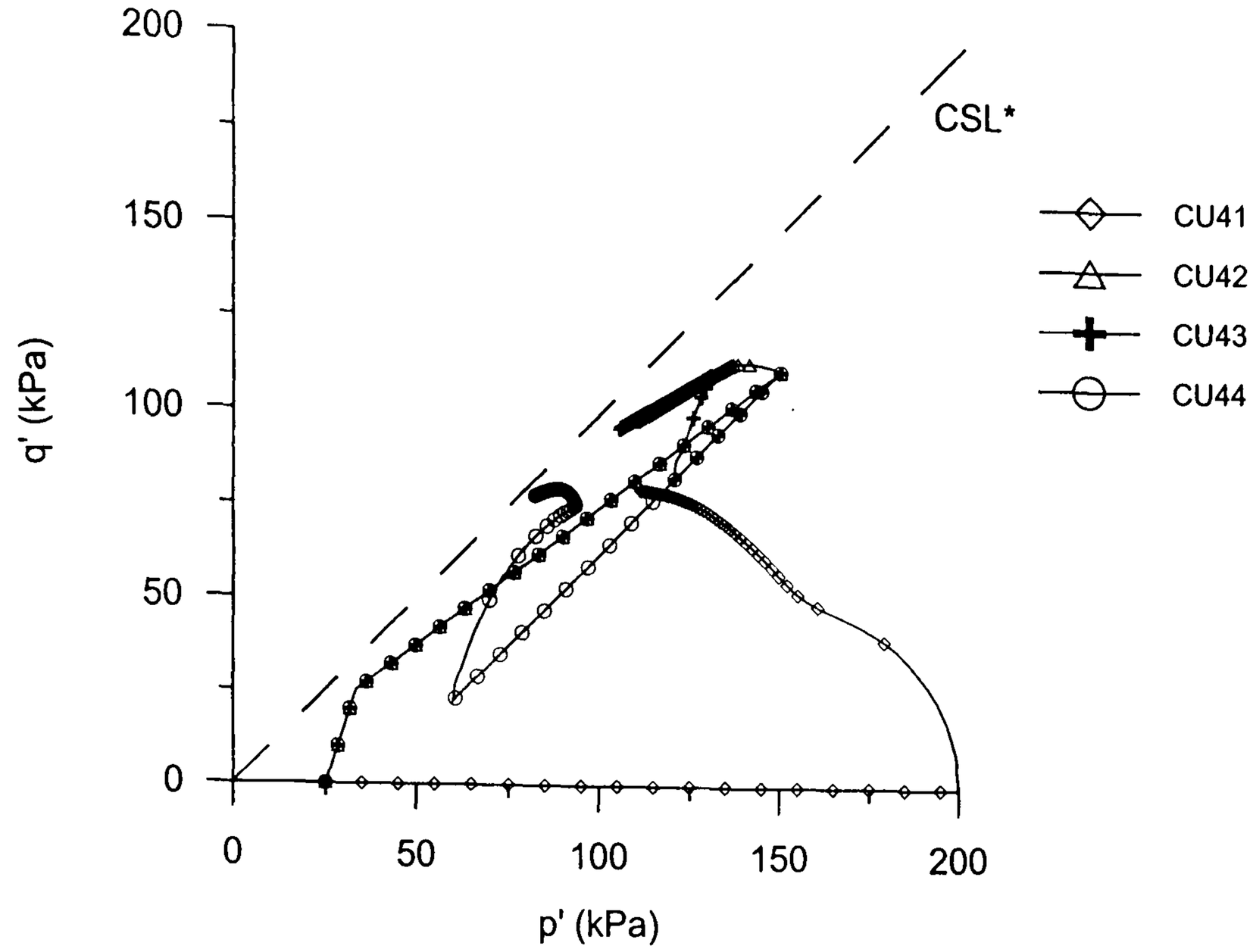

Figure 5.2.14 Predicted stress-strain response during undrained triaxial compression on natural samples compressed beyond gross yield before shearing

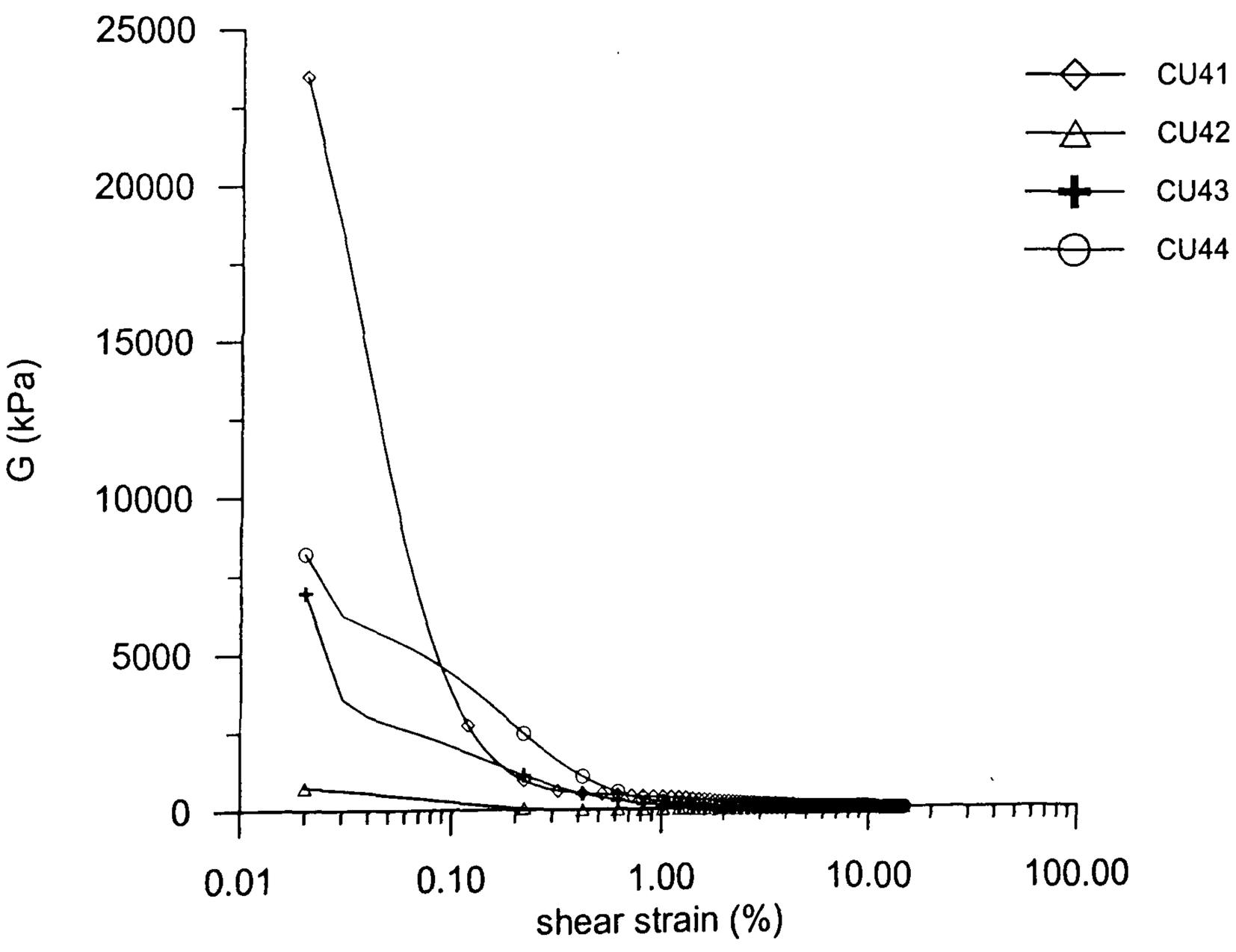

Figure 5.2.15 Predicted stiffness curve during undrained triaxial compression on natural samples compressed beyond yield before shearing

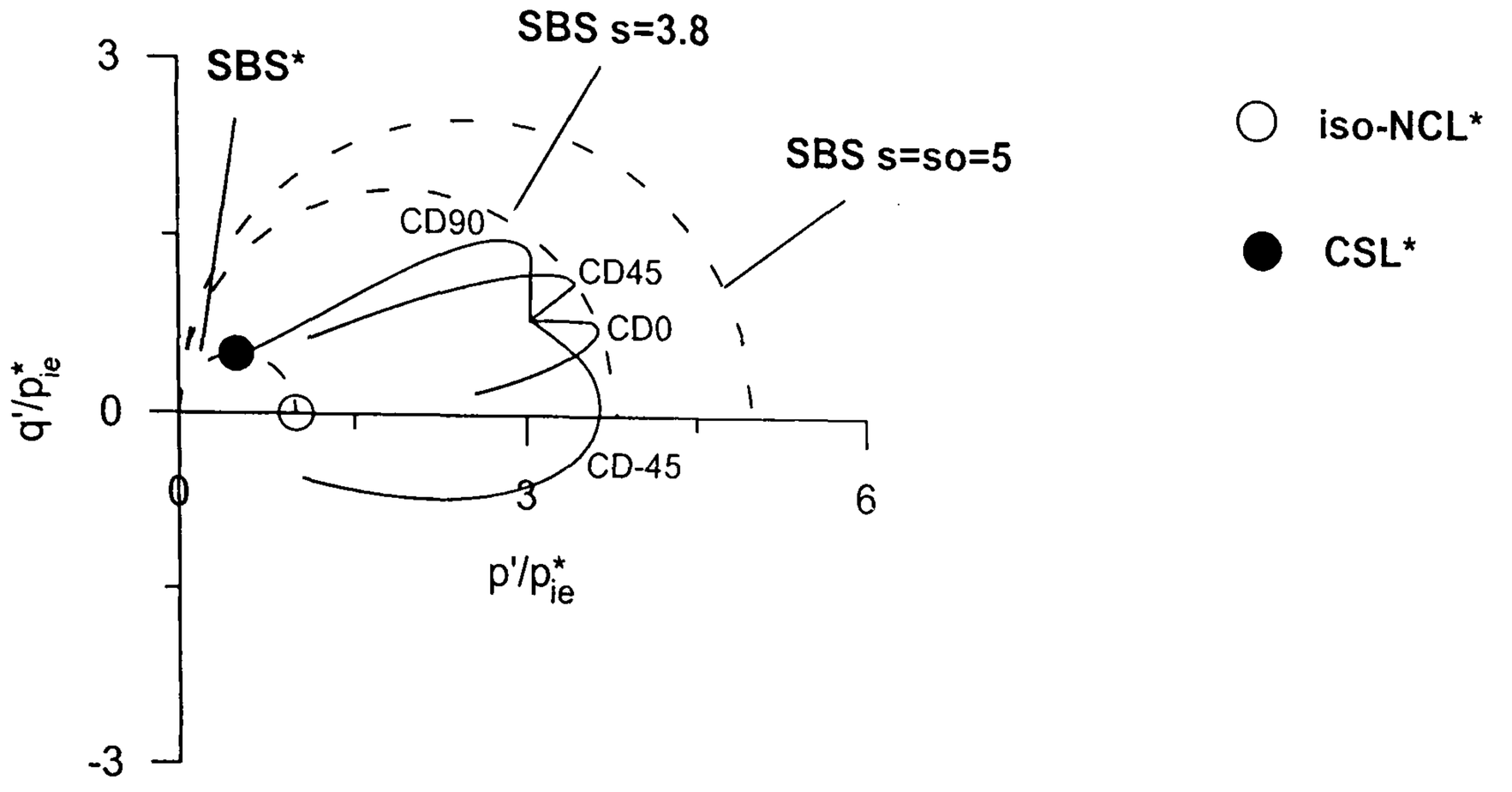

Figure 5.2.16 Predicted stress paths during drained probes on natural samples, normalised for volume

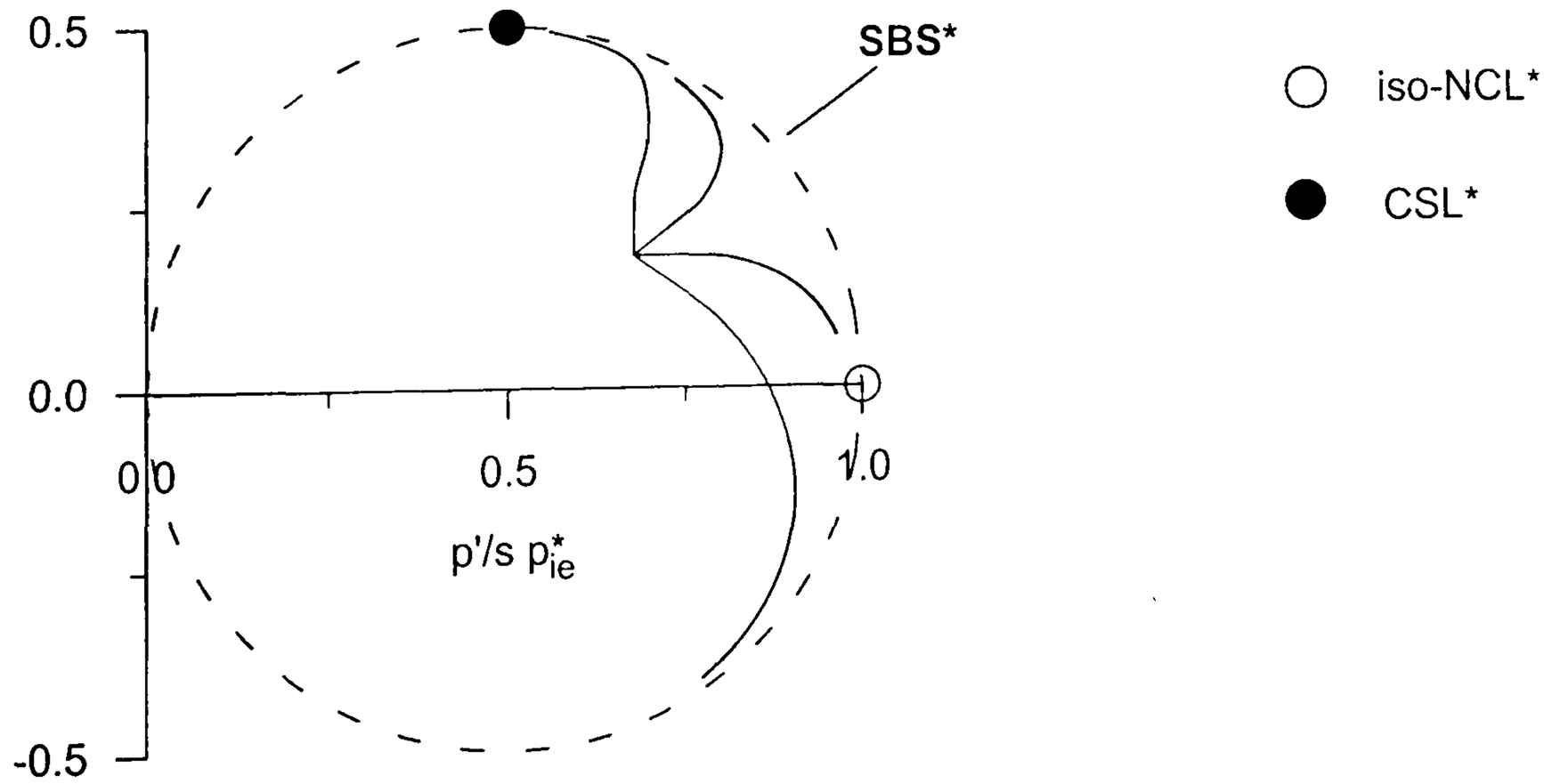

Figure 5.2.17 Predicted stress paths during drained probes on natural samples, normalised for volume and current structure

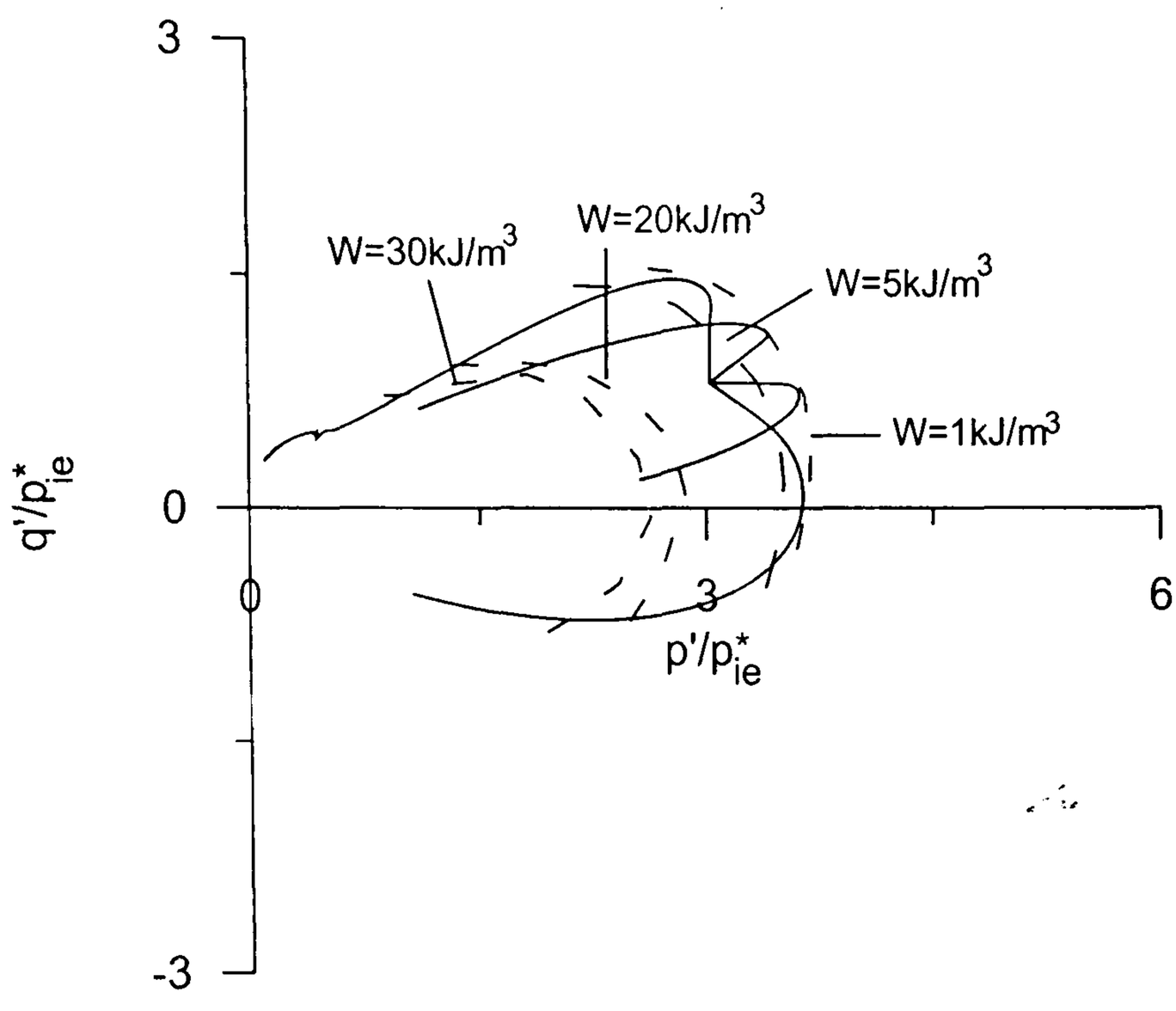

Figure 5.2.18 Predicted contours of strain energy and stress paths during drained probes on natural samples, normalised for volume

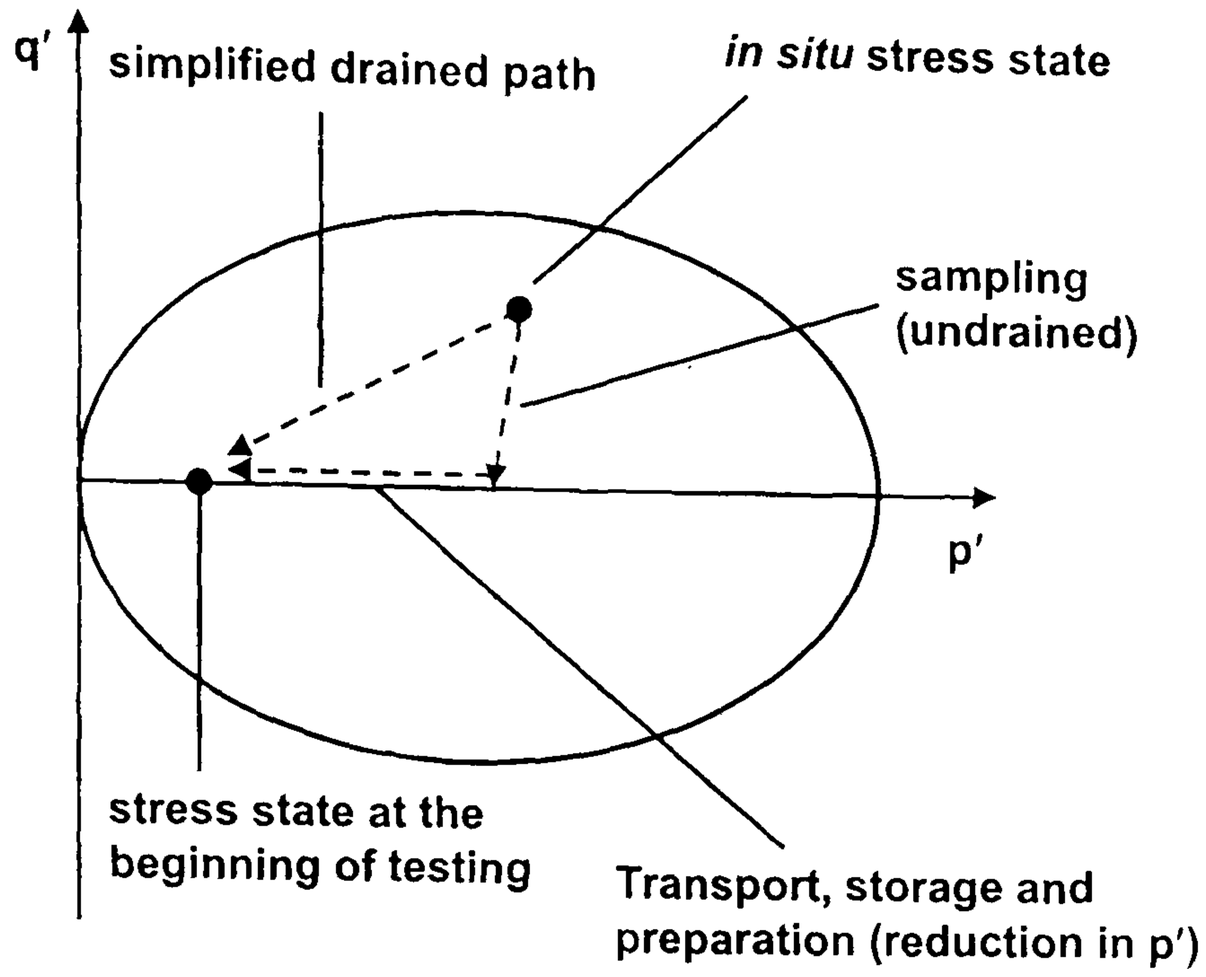

Figure 5.3.1 Diagram showing the stress path followed by a sample during sampling and preparation, and a proposed simplified drained path for modelling

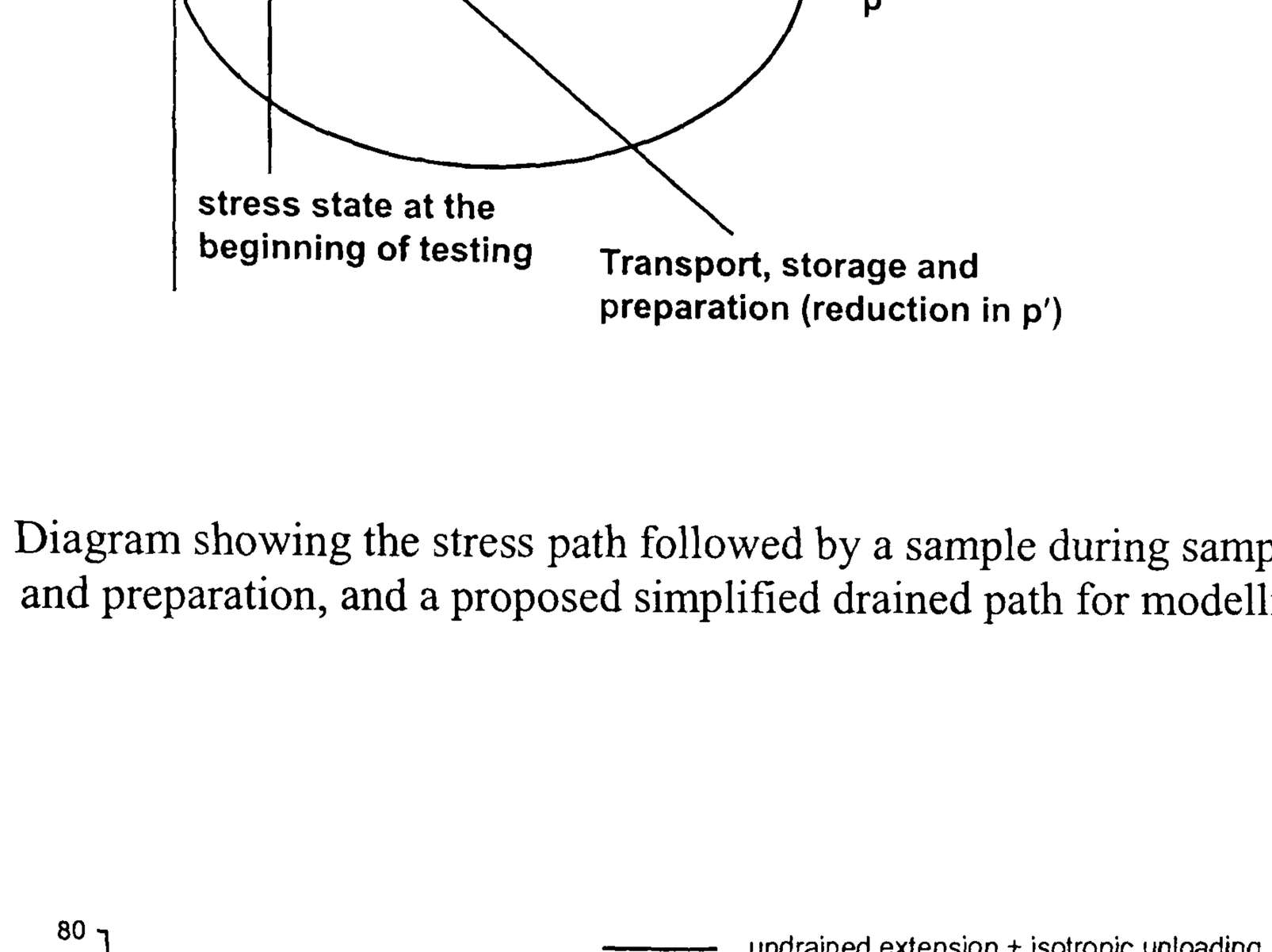

Figure 5.3.2 Diagram showing the configuration of the surfaces after simulating the estimated stress path during sampling and preparation of the sample, and after simulating the proposed simplified drained path

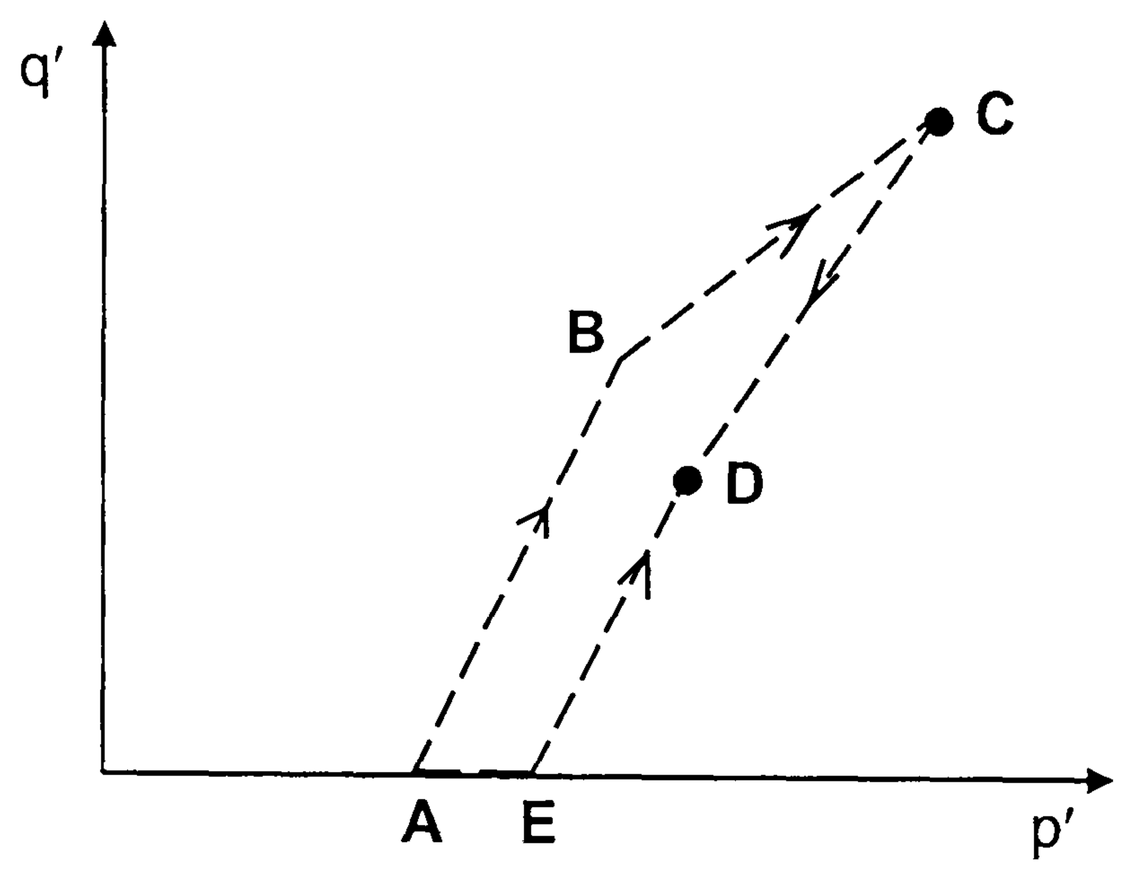

Figure 5.3.3 Diagram showing the different stress paths followed during recompression to *in situ* stress

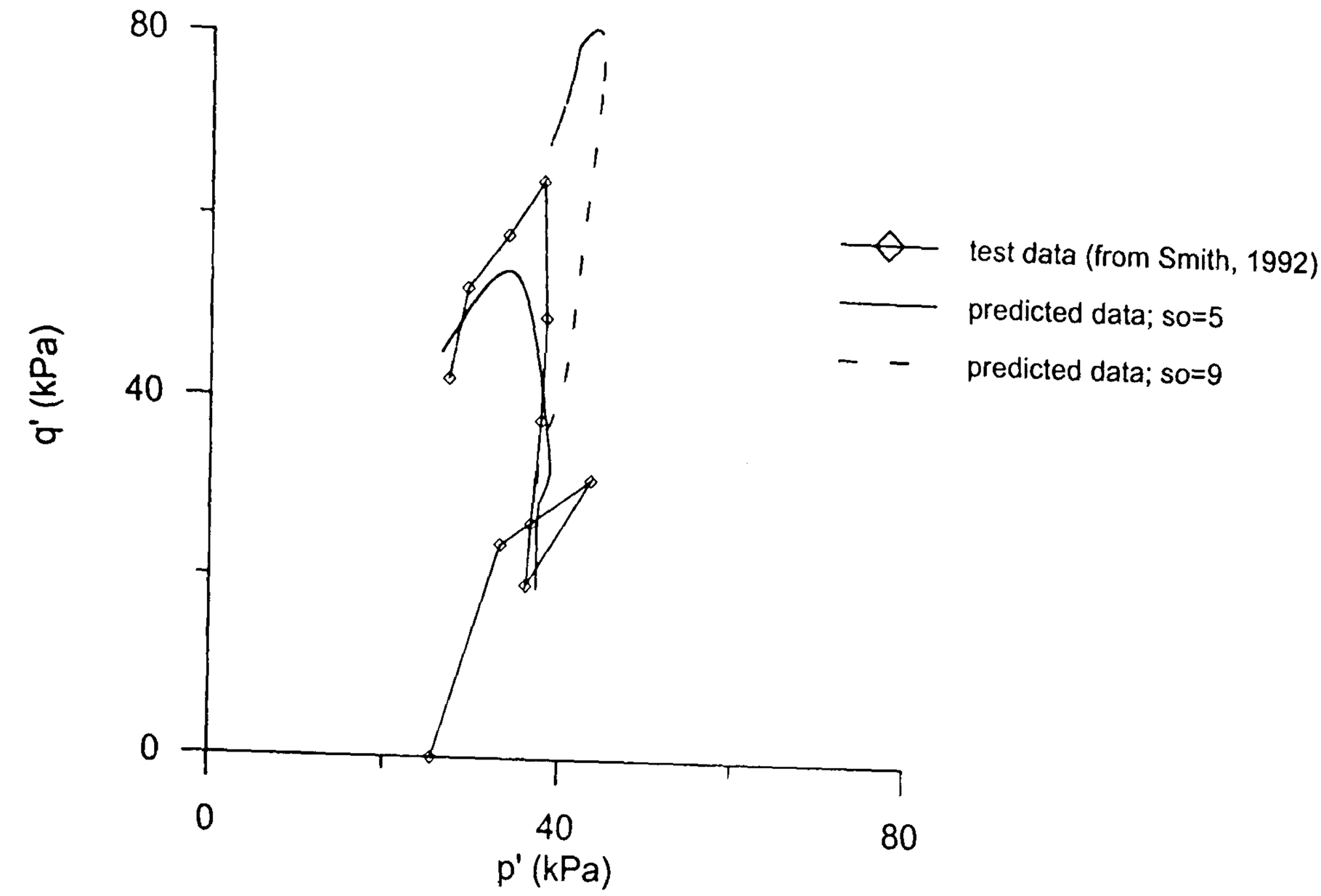

(a)

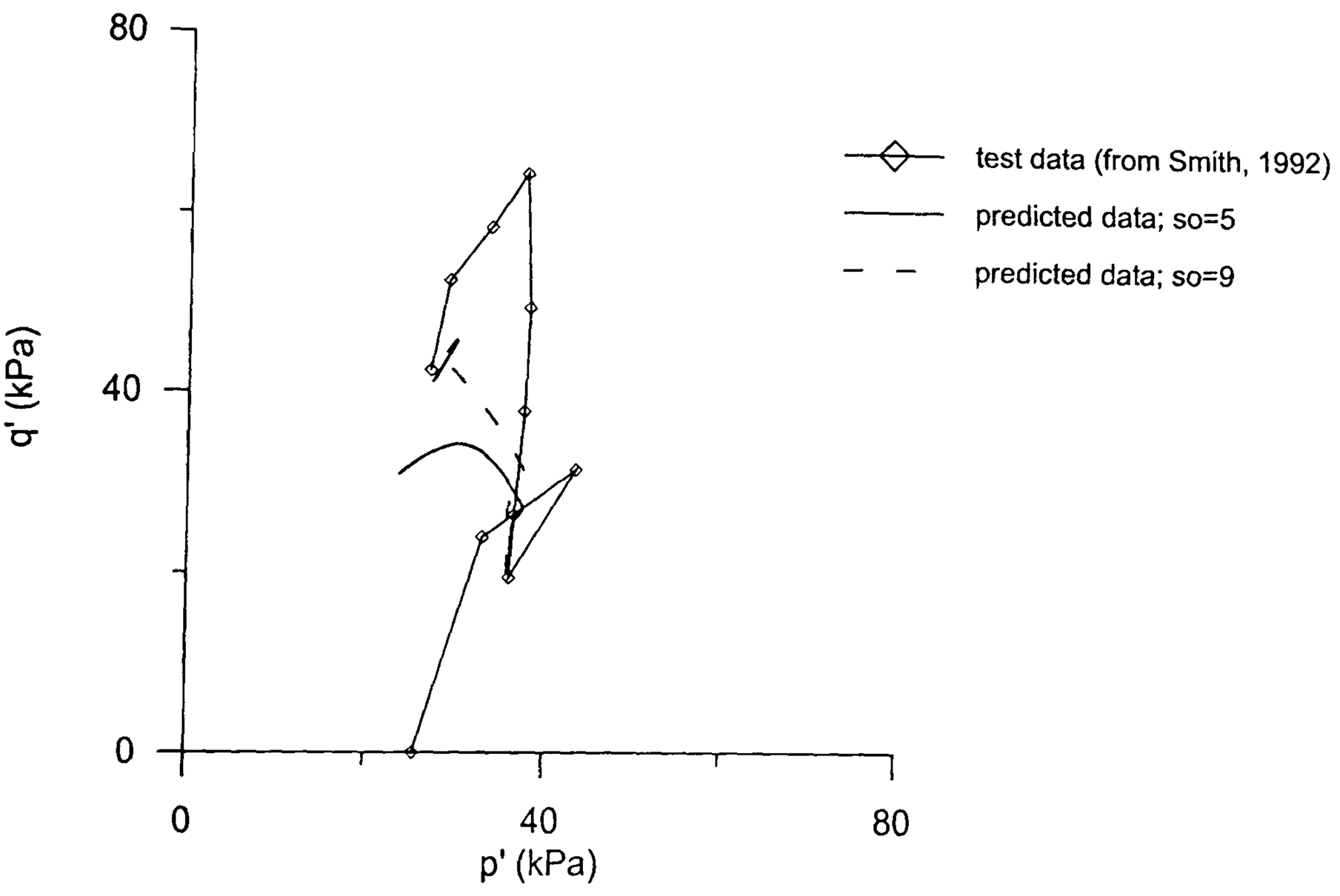

(b)

Figure 5.3.4 Comparison between model prediction and experimental results obtained for undrained triaxial compression test on natural Bothkennar clay sample SCU1 when (a) the full stress history is simulated (sampling, preparation and recompression) and (b) only recompression is simulated

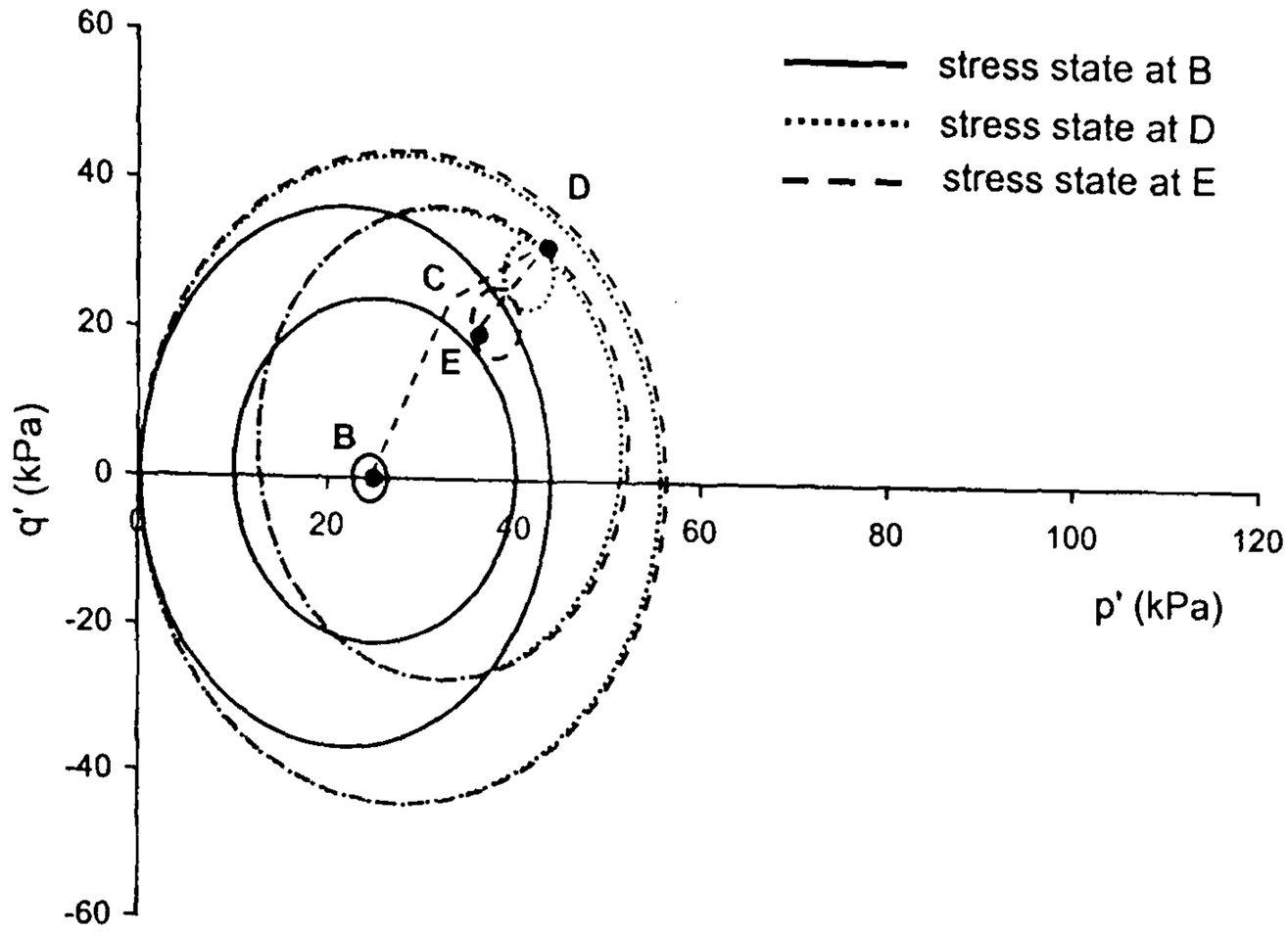

Figure 5.3.5 Diagram showing the configuration of the surfaces when only the recompression history has been simulated

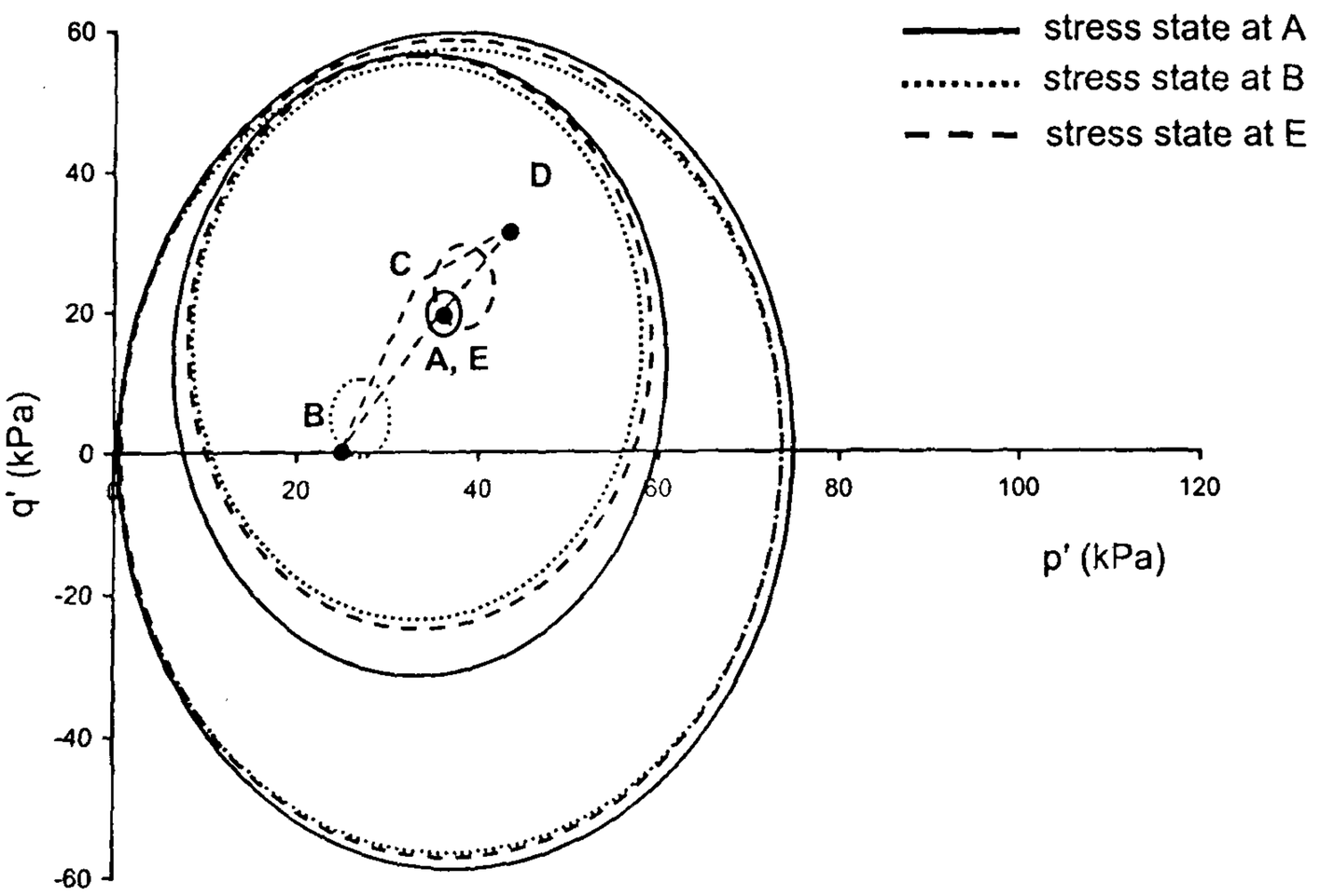

Figure 5.3.6 Diagram showing the configuration of the surfaces when the full stress history has been simulated (sampling, preparation and recompression)

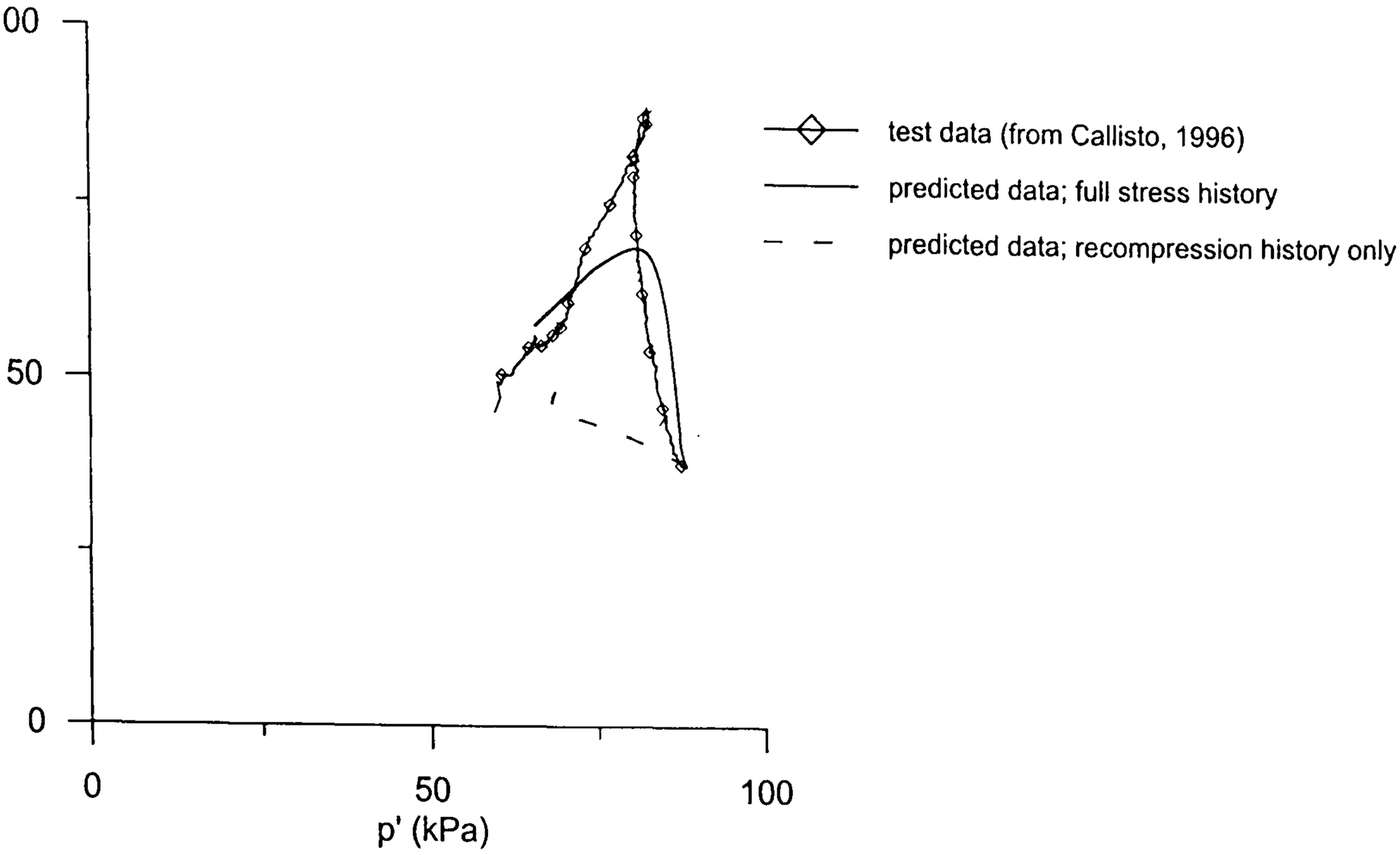

Figure 5.3.7 Comparison between model prediction when the full stress history is simulated and when only recompression is simulated, and experimental results for undrained triaxial compression test AUC on natural Pisa clay

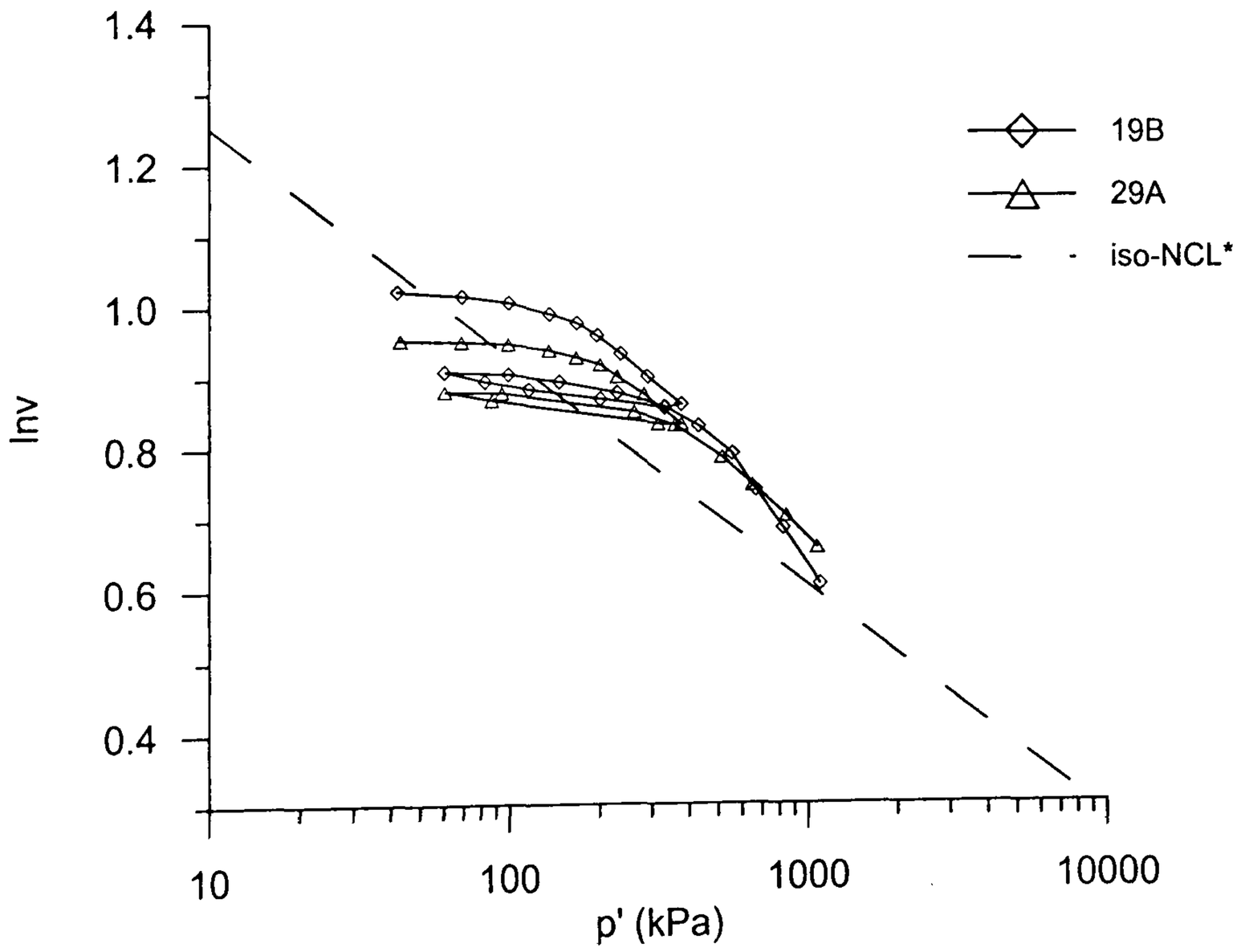

Figure 5.3.8 Isotropic compression curves obtained from tests on natural Pisa clay samples 19B and 29A (test data from Rampello, 1993)

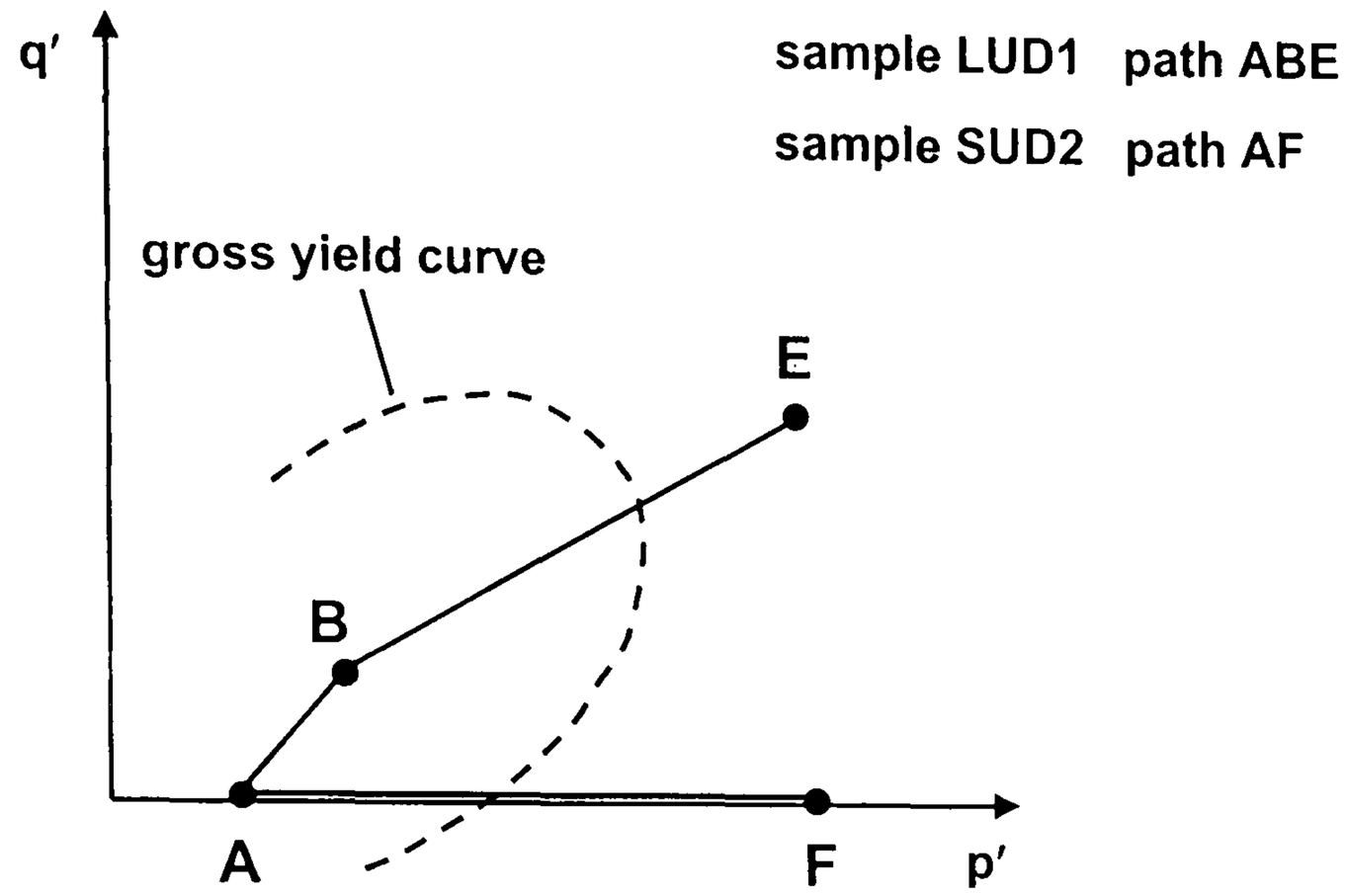

Figure 5.3.9 Diagram showing compression stress paths followed by natural Bothkennar clay samples SUD2 and LUD1 prior to shearing

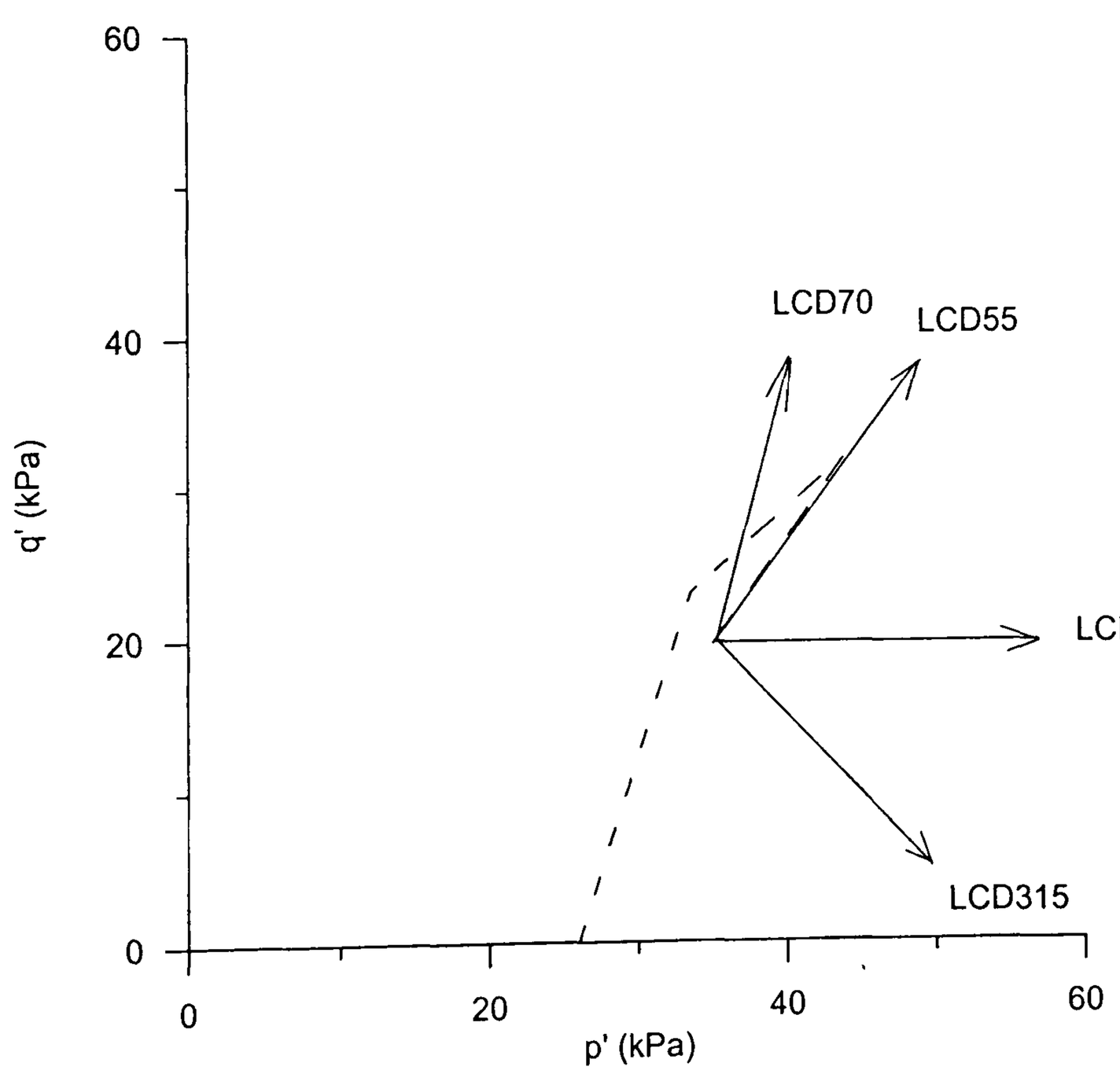

Figure 5.3.10 Diagram showing stress paths followed during drained probes on natural Bothkennar clay samples

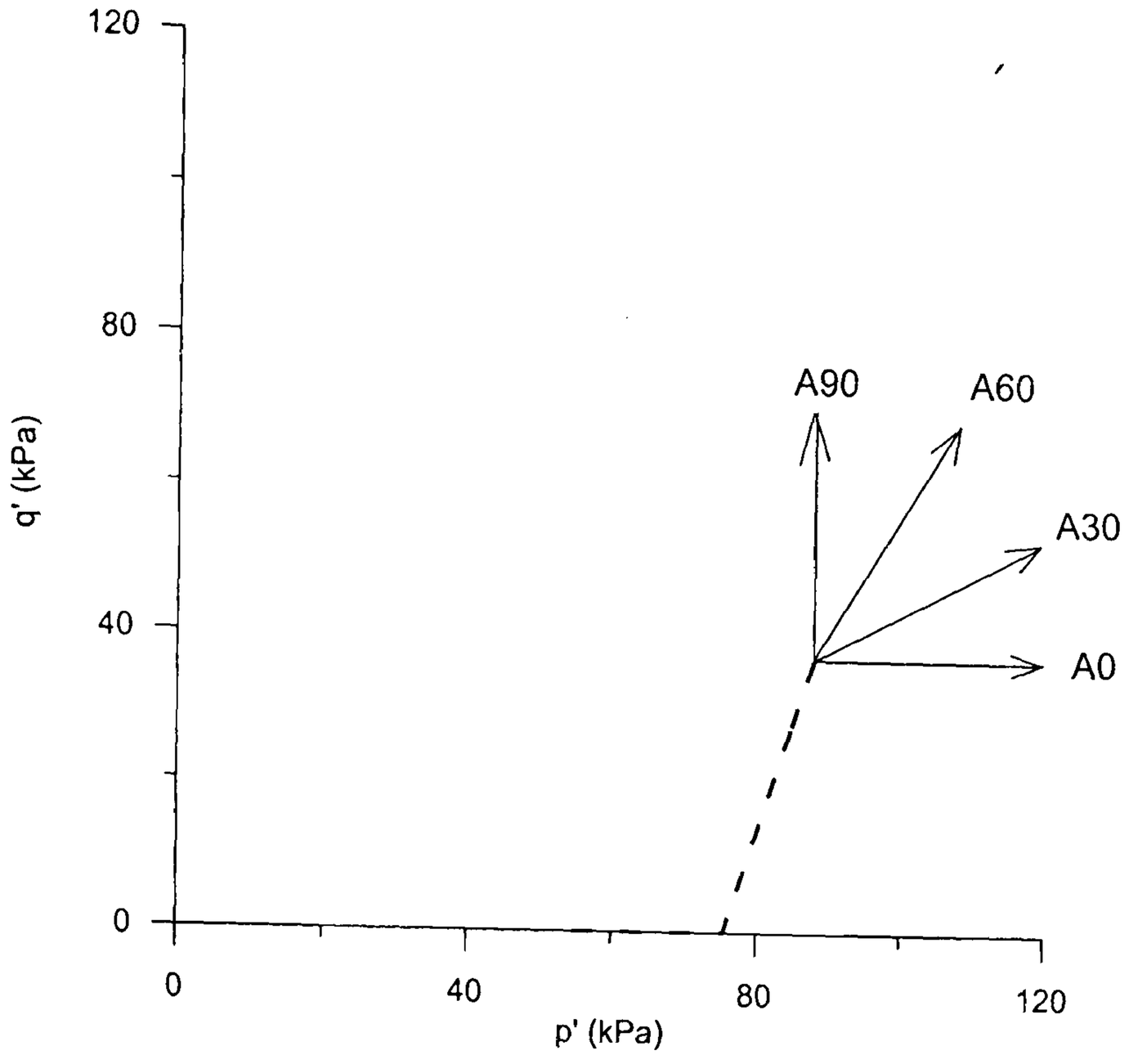

Figure 5.3.11 Diagram showing stress paths followed during drained probes on natural Pisa clay samples

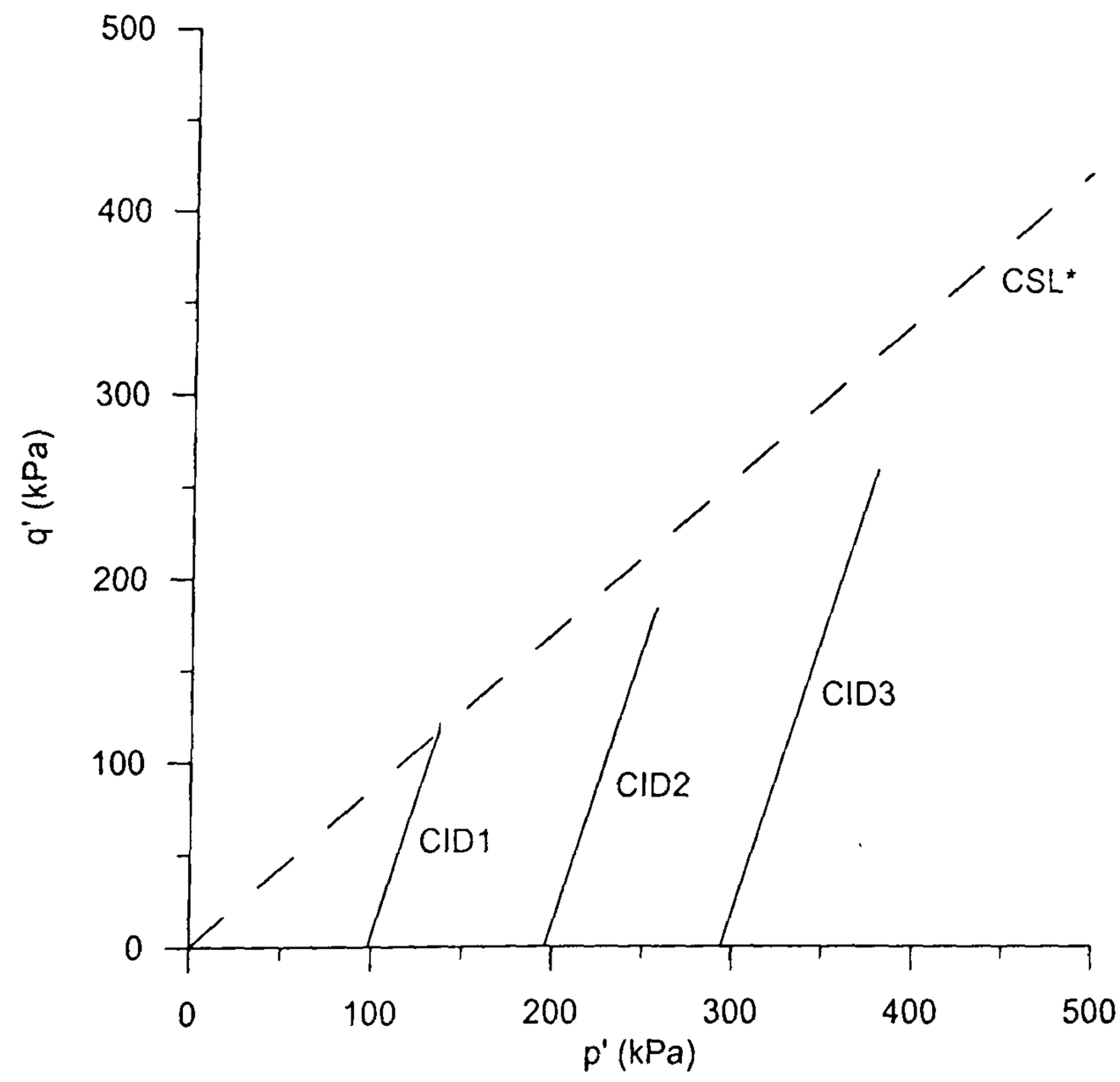

Figure 5.3.12 Diagram showing stress paths followed during drained tests on natural Pisa clay samples

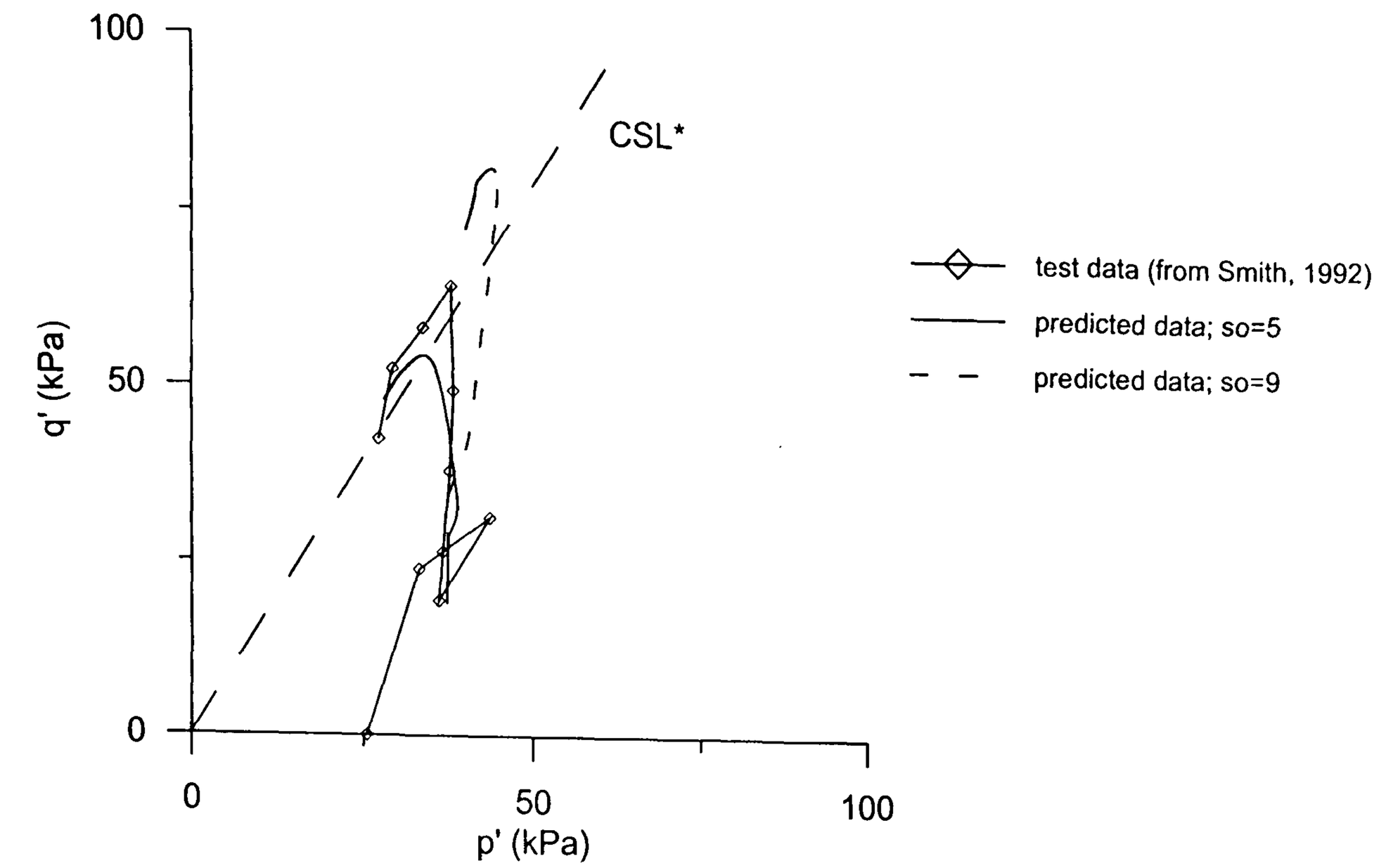

Figure 5.3.13 Comparison between model prediction and experimental results for stress paths obtained from undrained triaxial compression test on Bothkennar clay sample SCU1

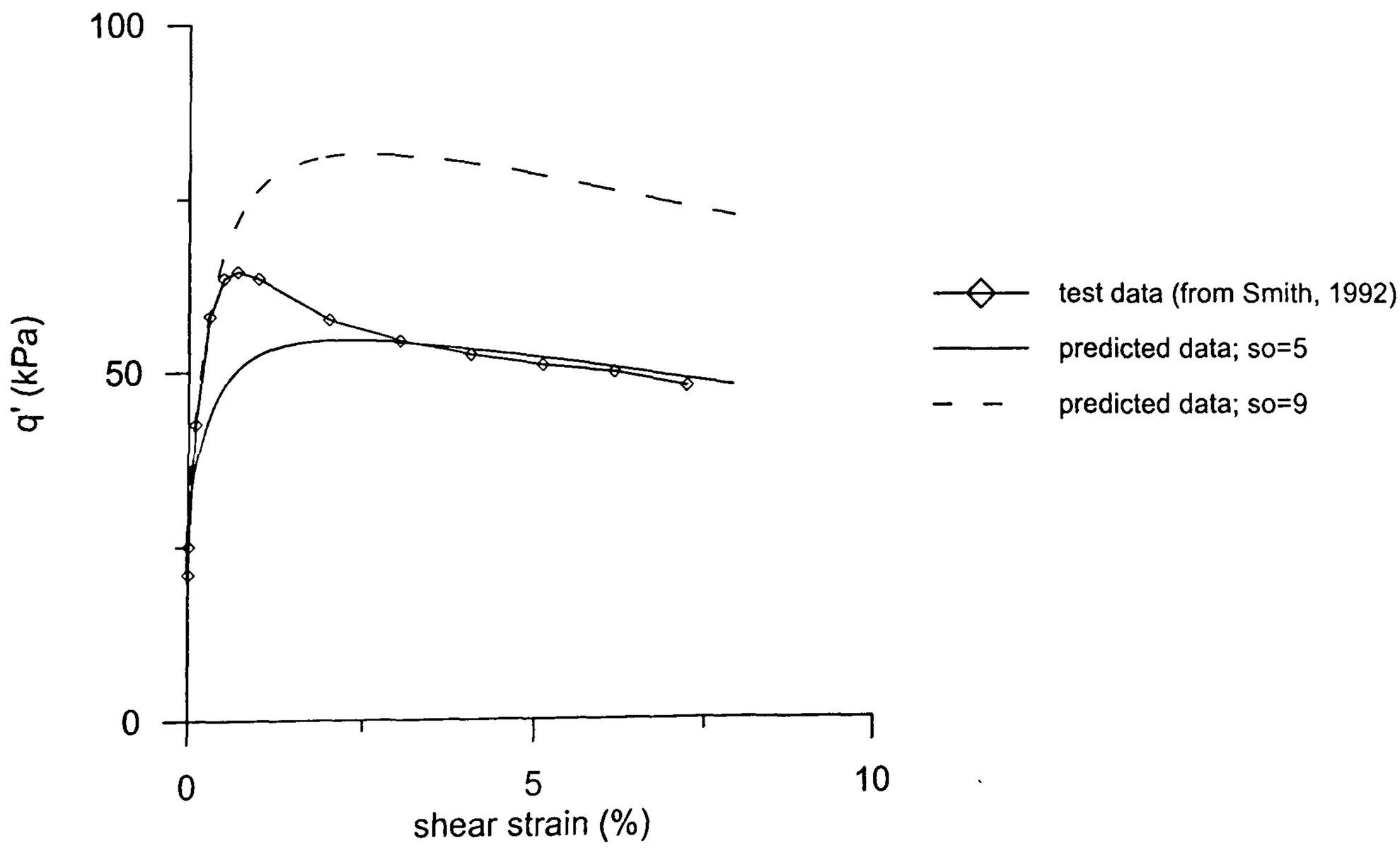

Figure 5.3.14 Comparison between model prediction and experimental results for stress-strain curves obtained from undrained triaxial compression test on Bothkennar clay sample SCU1

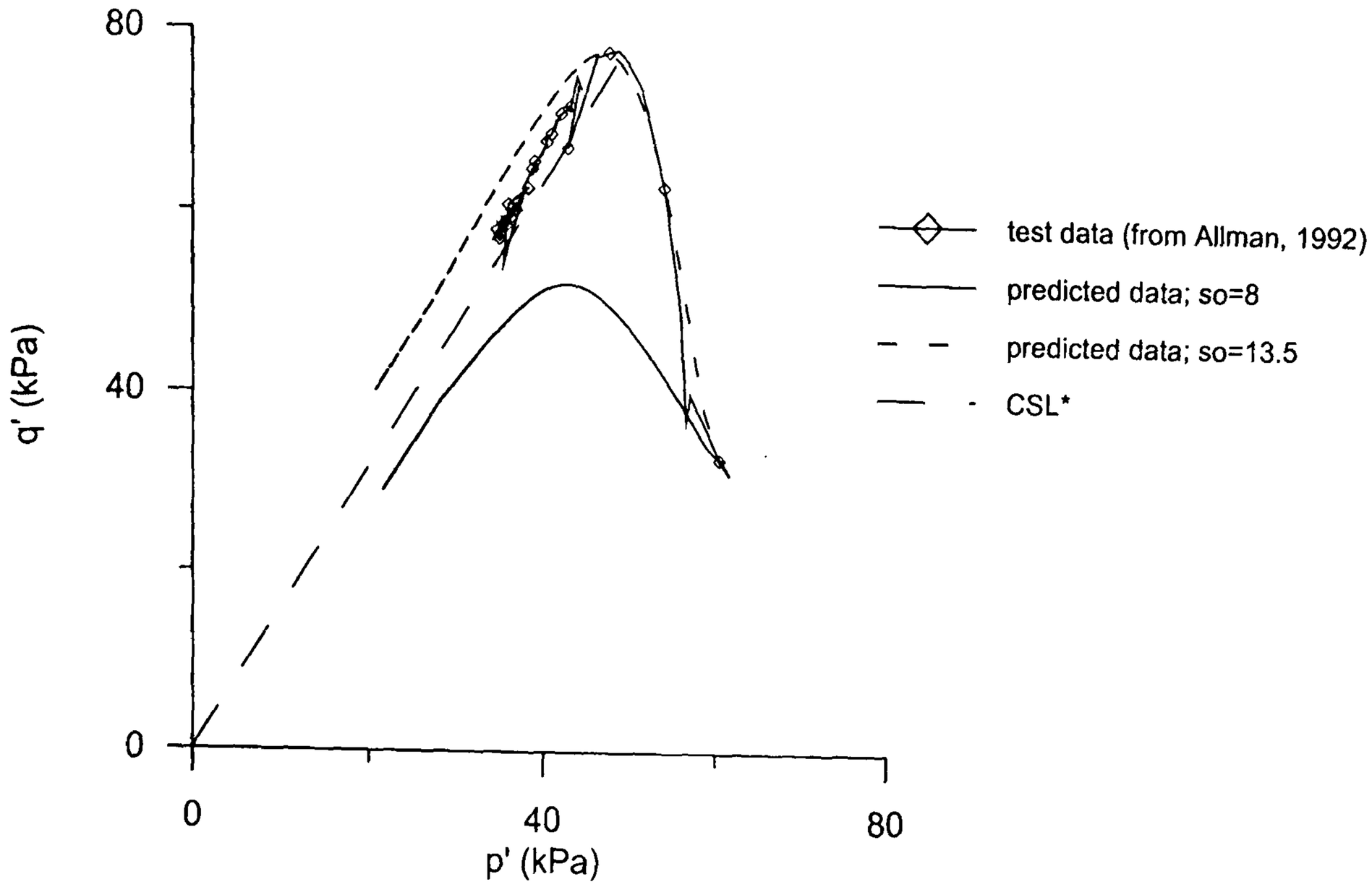

Figure 5.3.15 Comparison between model prediction and experimental results for stress paths obtained from undrained triaxial compression test on Bothkennar clay sample L23

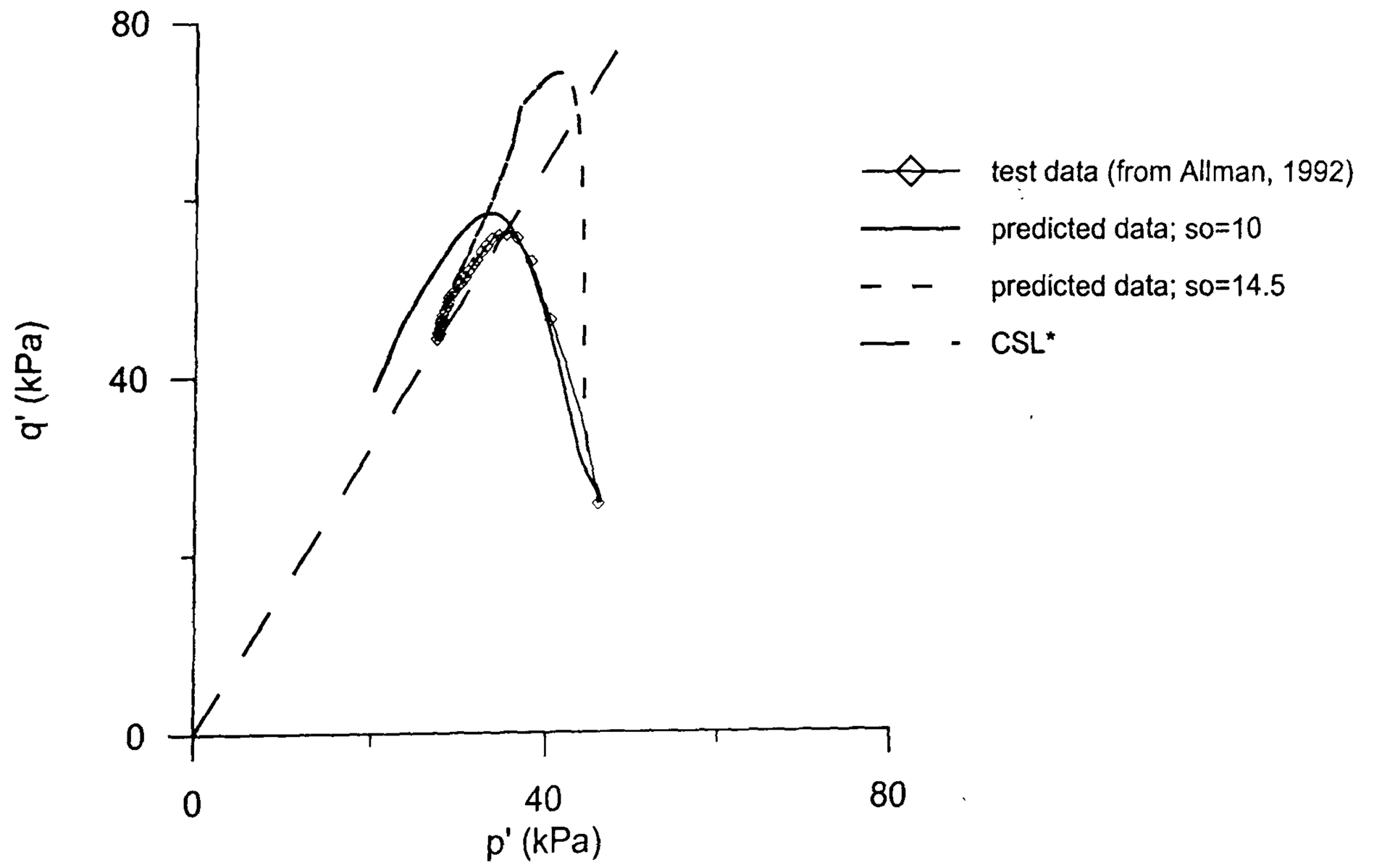

Figure 5.3.16 Comparison between model prediction and experimental results for stress paths obtained from undrained triaxial compression test on Bothkennar clay sample SH13

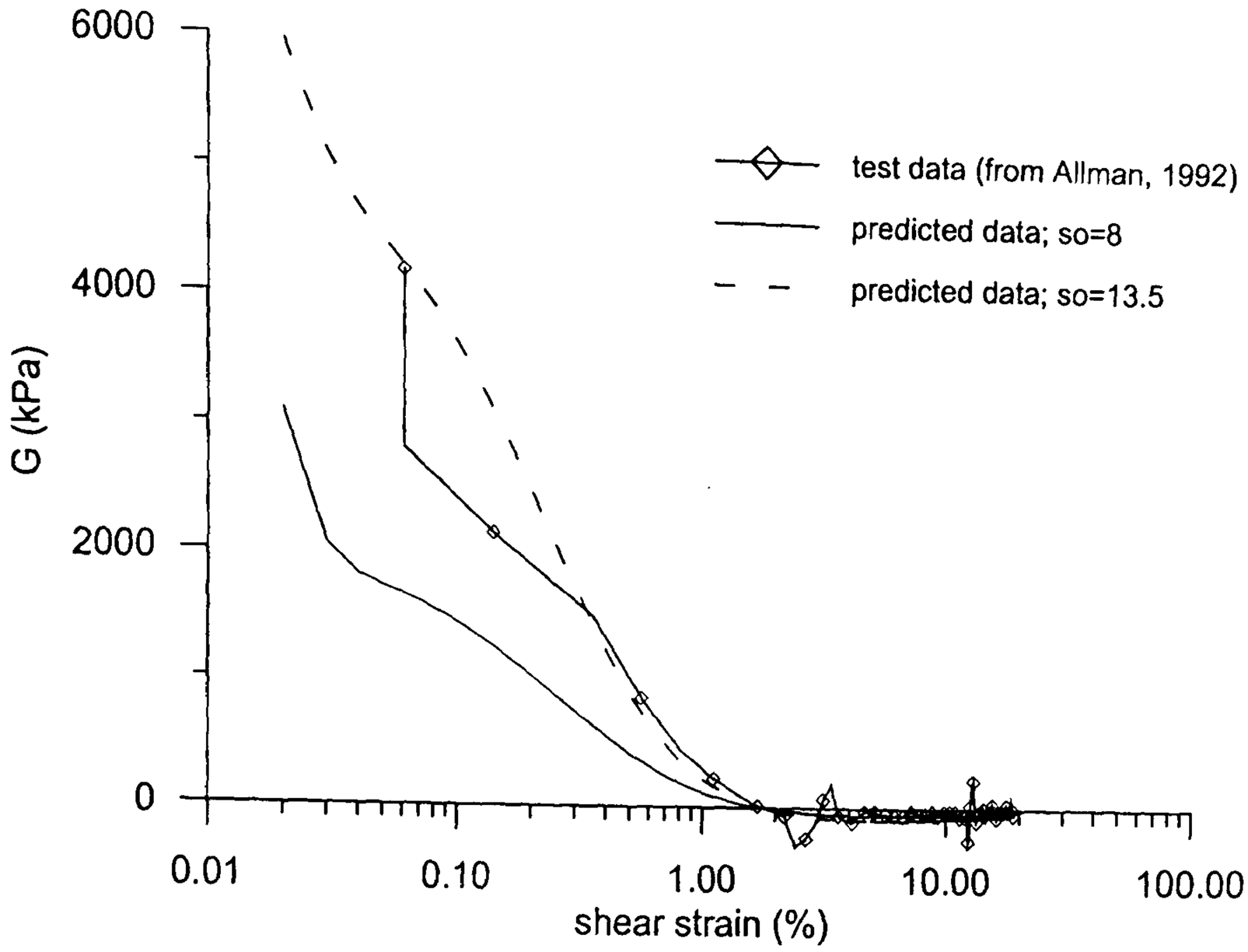

Figure 5.3.17 Comparison between model prediction and experimental results for stiffness curves obtained from undrained triaxial compression test on Bothkennar clay sample L23

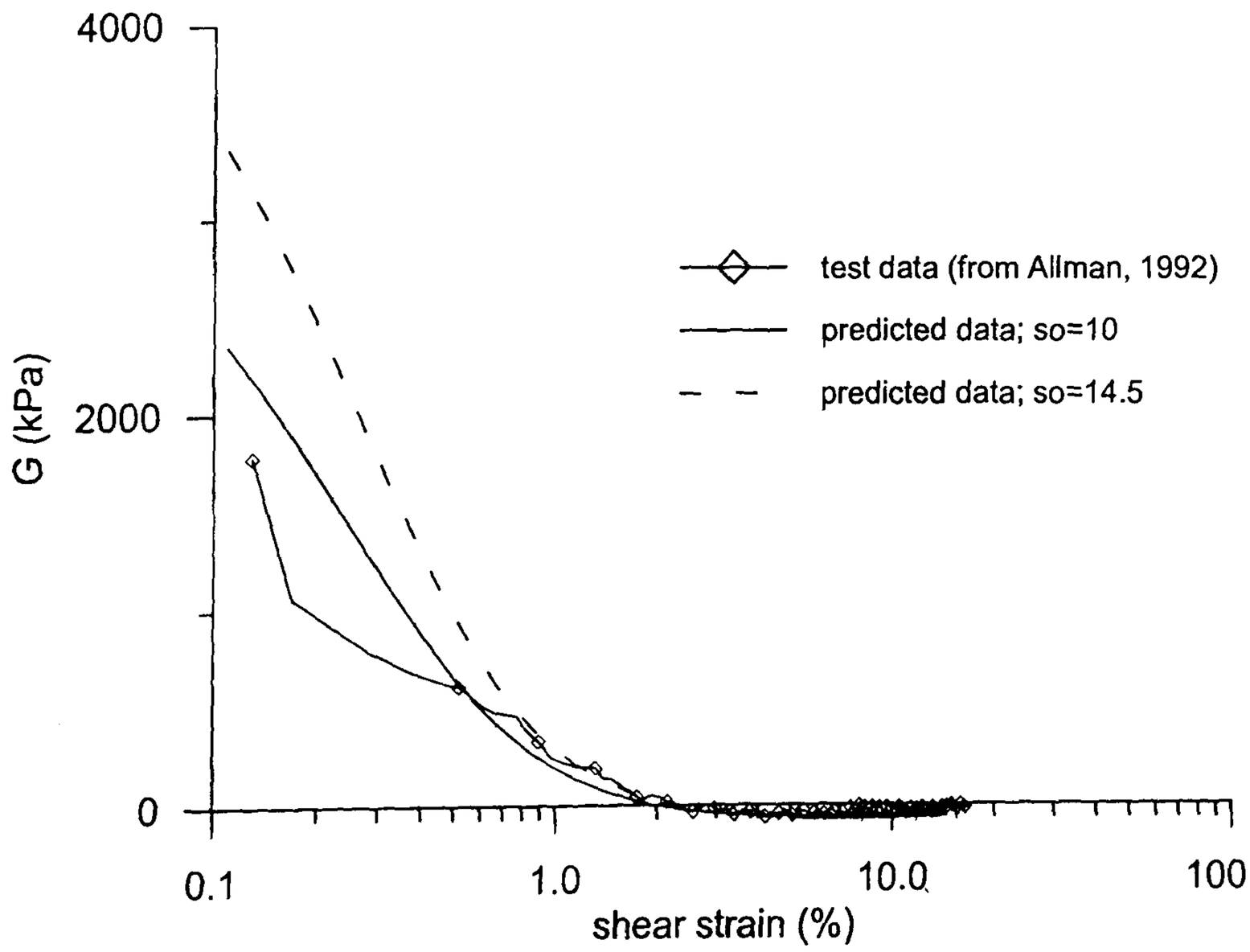

Figure 5.3.18 Comparison between model prediction and experimental results for stiffness curves obtained from undrained triaxial compression test on Bothkennar clay sample SH13

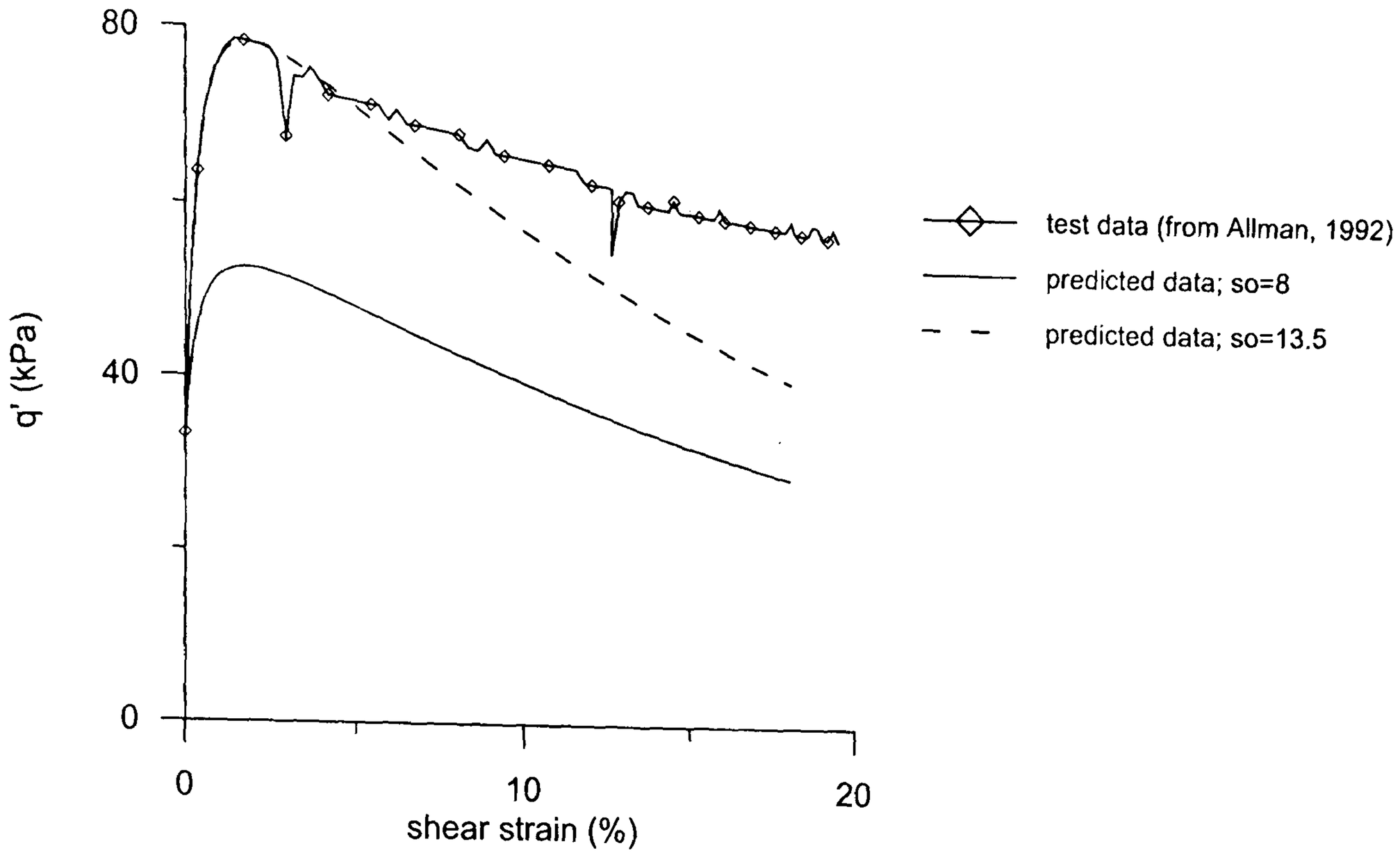

Figure 5.3.19 Comparison between model prediction and experimental results for stress-strain curves obtained from undrained triaxial compression test on Bothkennar clay sample L23

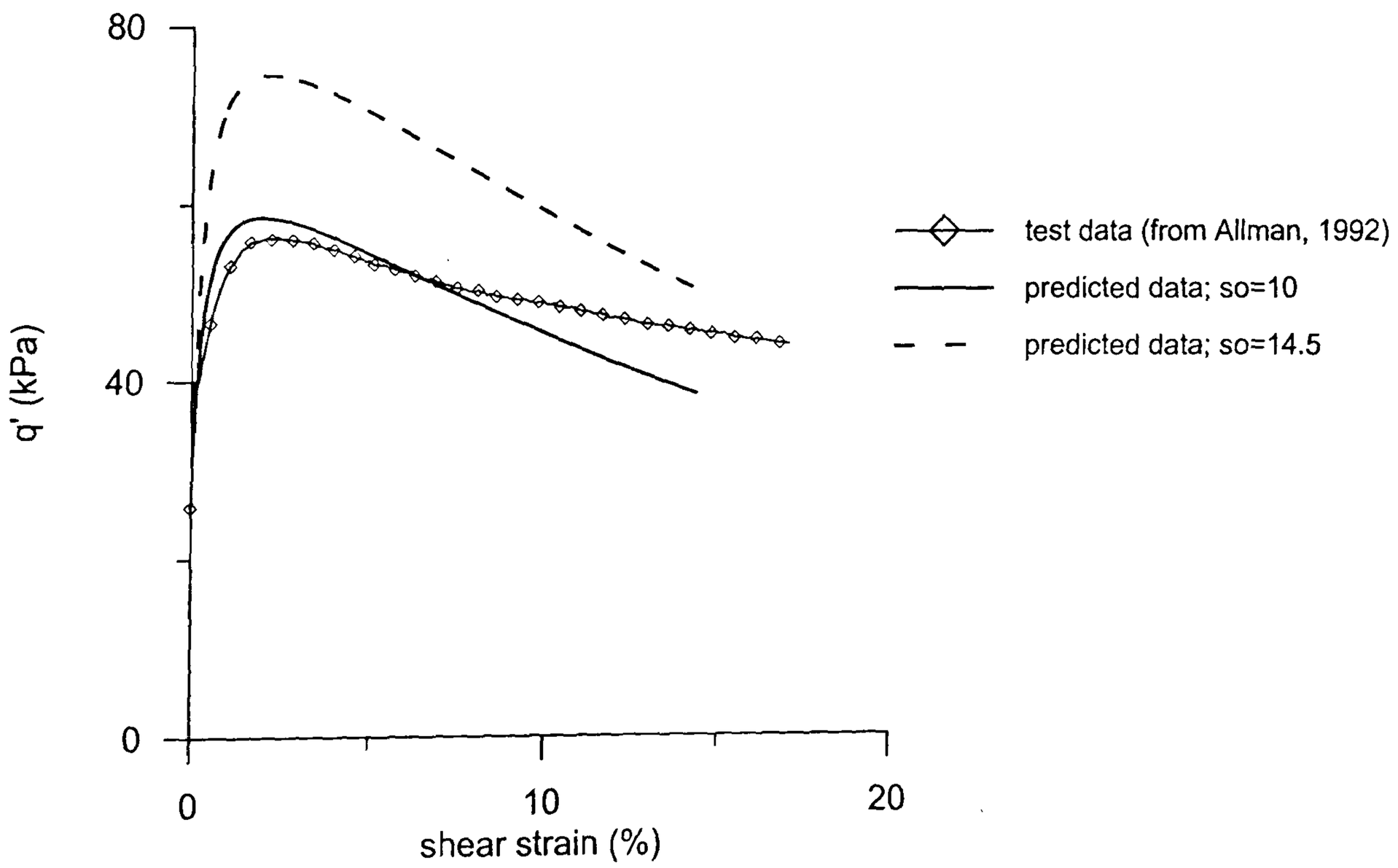

Figure 5.3.20 Comparison between model prediction and experimental results for stress-strain curves obtained from undrained triaxial compression test on Bothkennar clay sample SH13

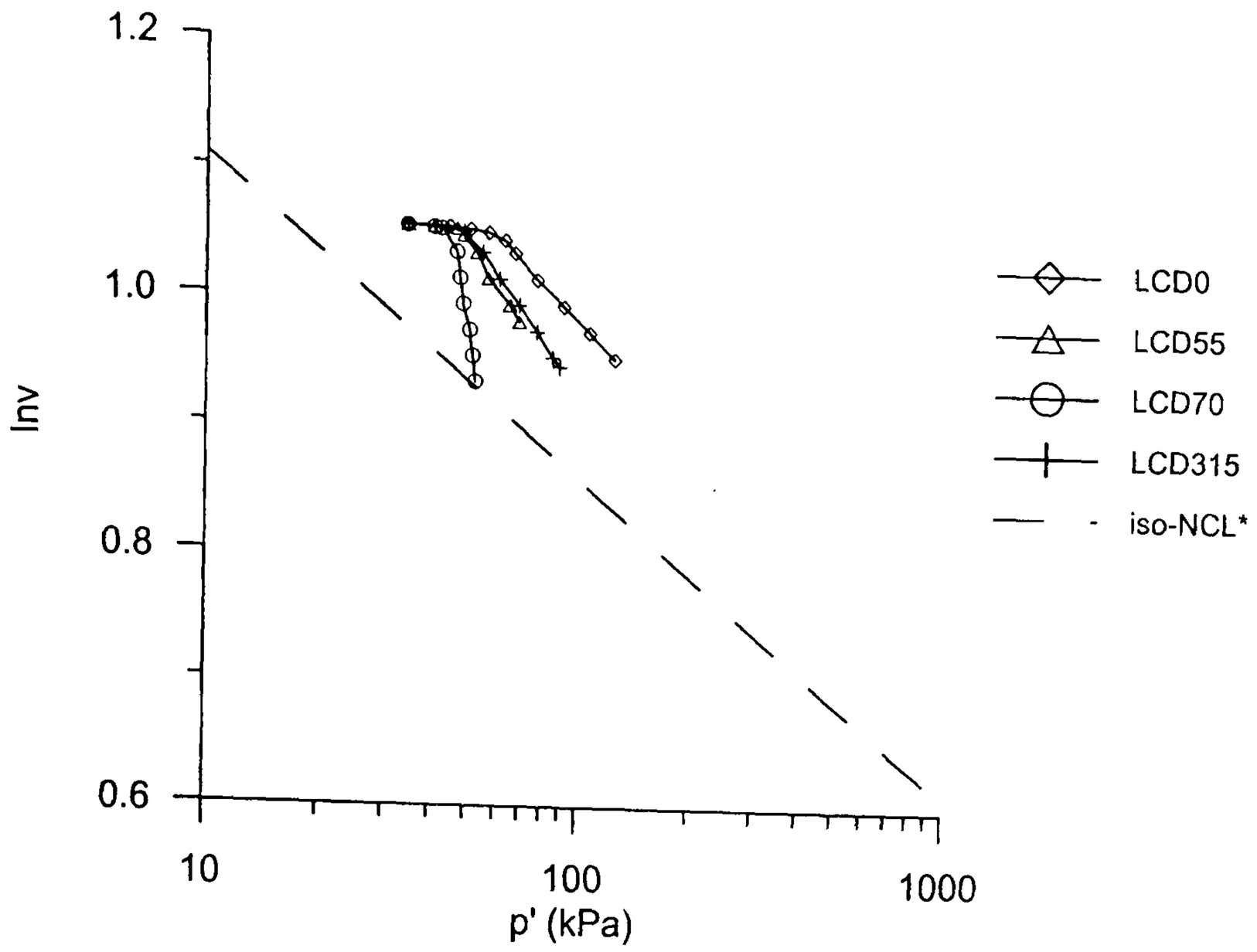

(a)

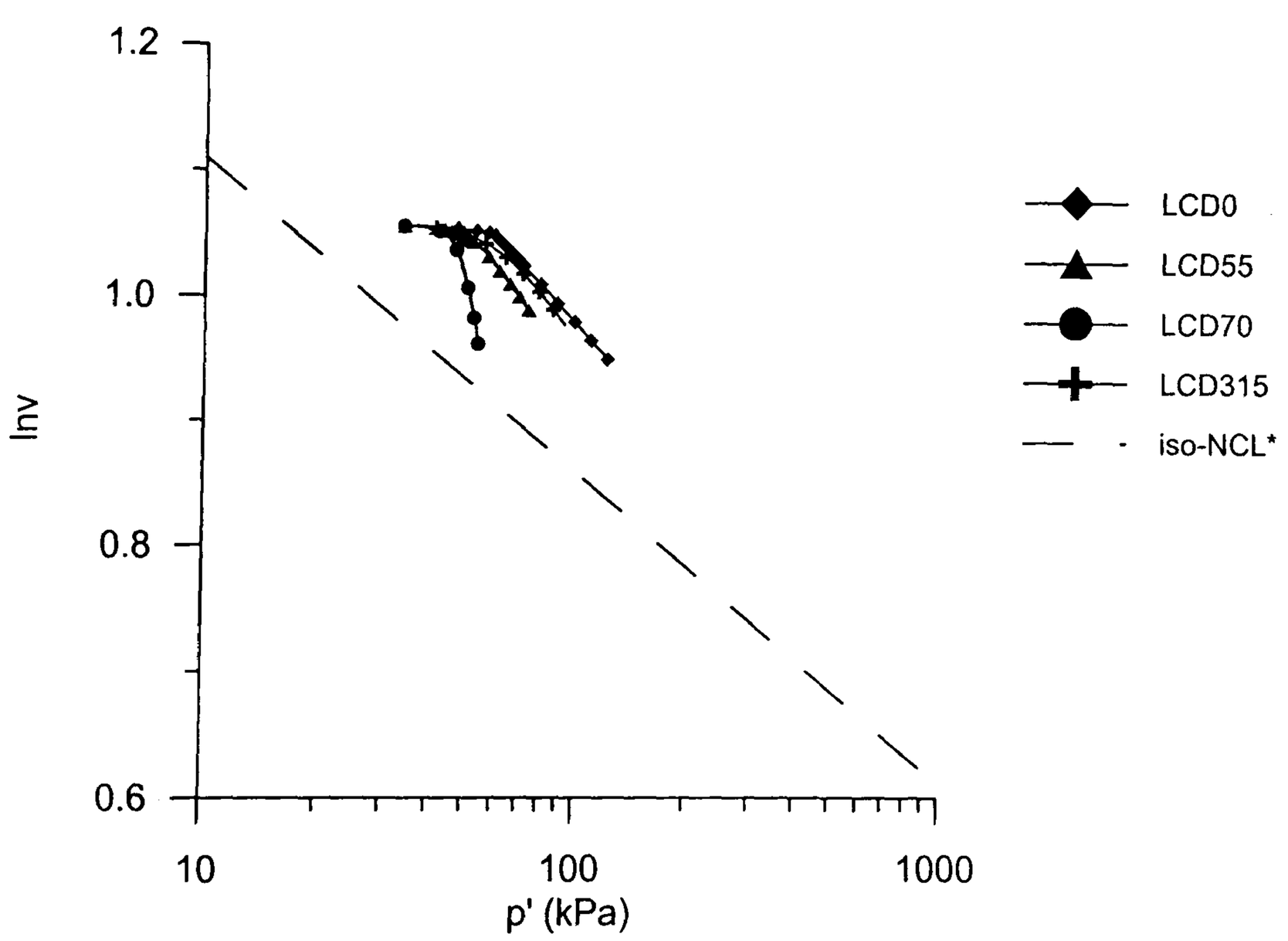

(b)

Figure 5.3.21 Volumetric response obtained during drained probes on natural Bothkennar clay samples (a) experimental results (test data from Smith, 1992) (b) model prediction

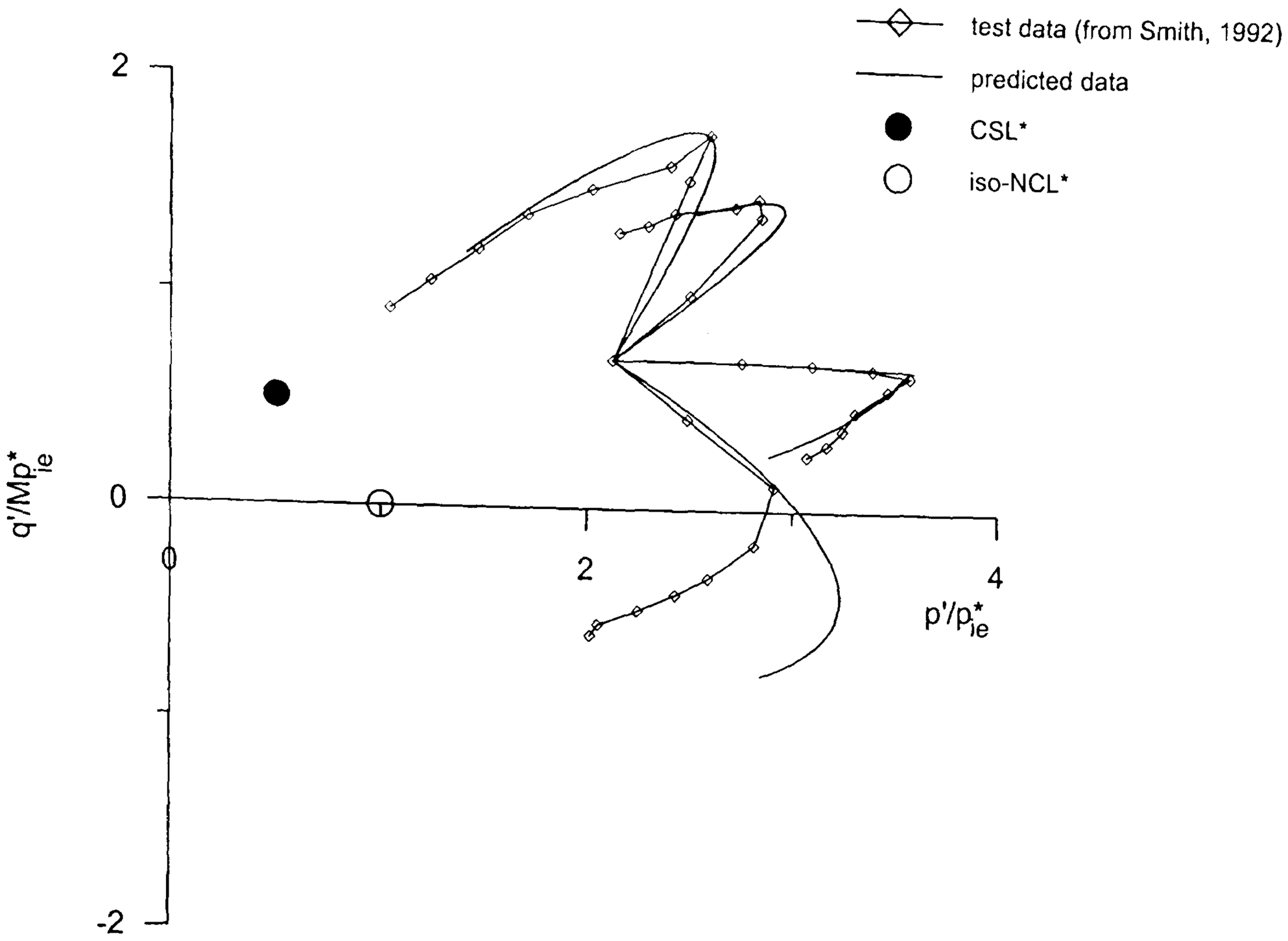

Figure 5.3.22 Comparison between model prediction and experimental results for normalised stress paths obtained from drained probes on Bothkennar clay samples

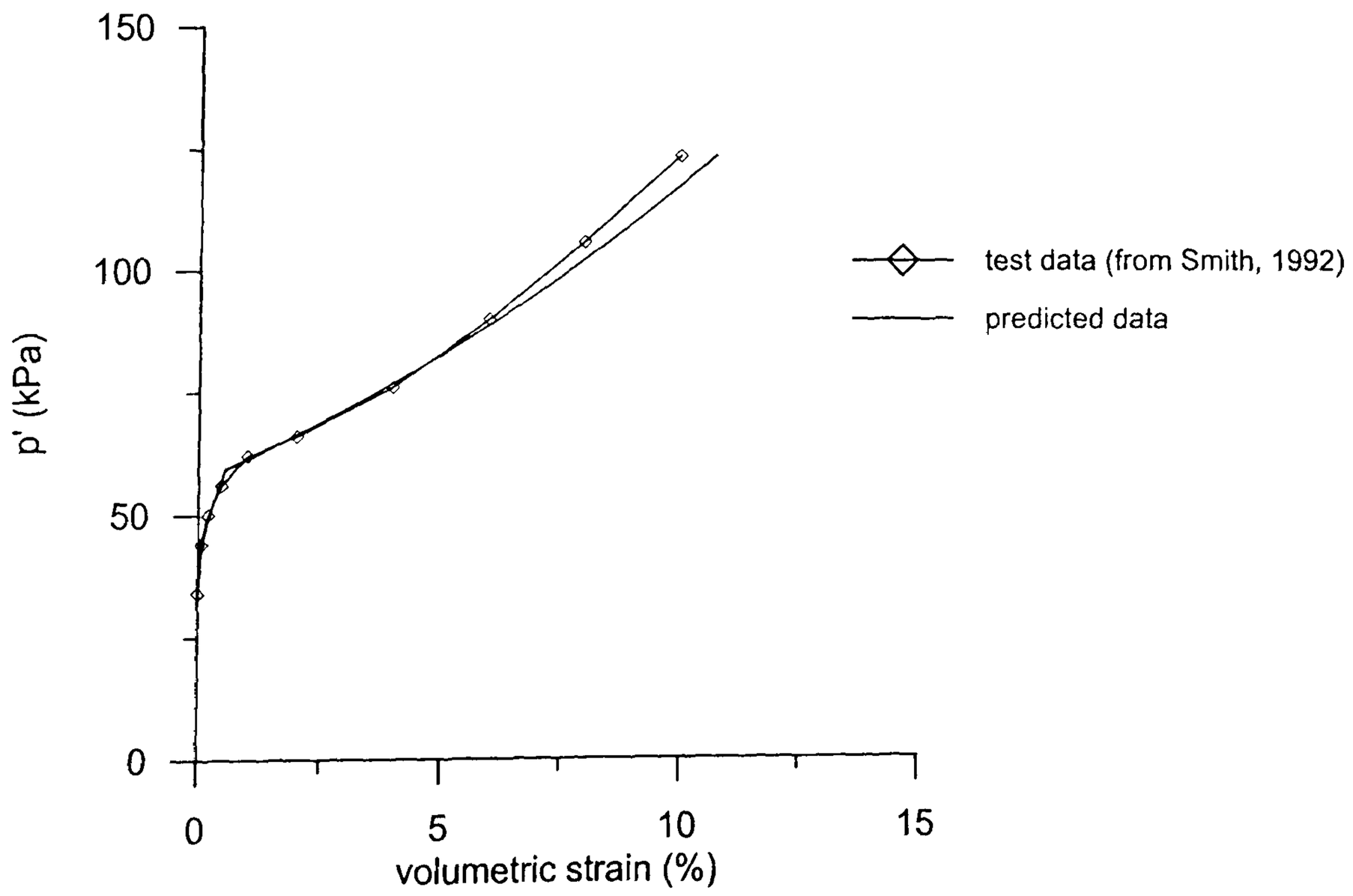

Figure 5.3.23 Comparison between model prediction and experimental results for volumetric stress-strain curve obtained from drained probe LCD0 on Bothkennar clay

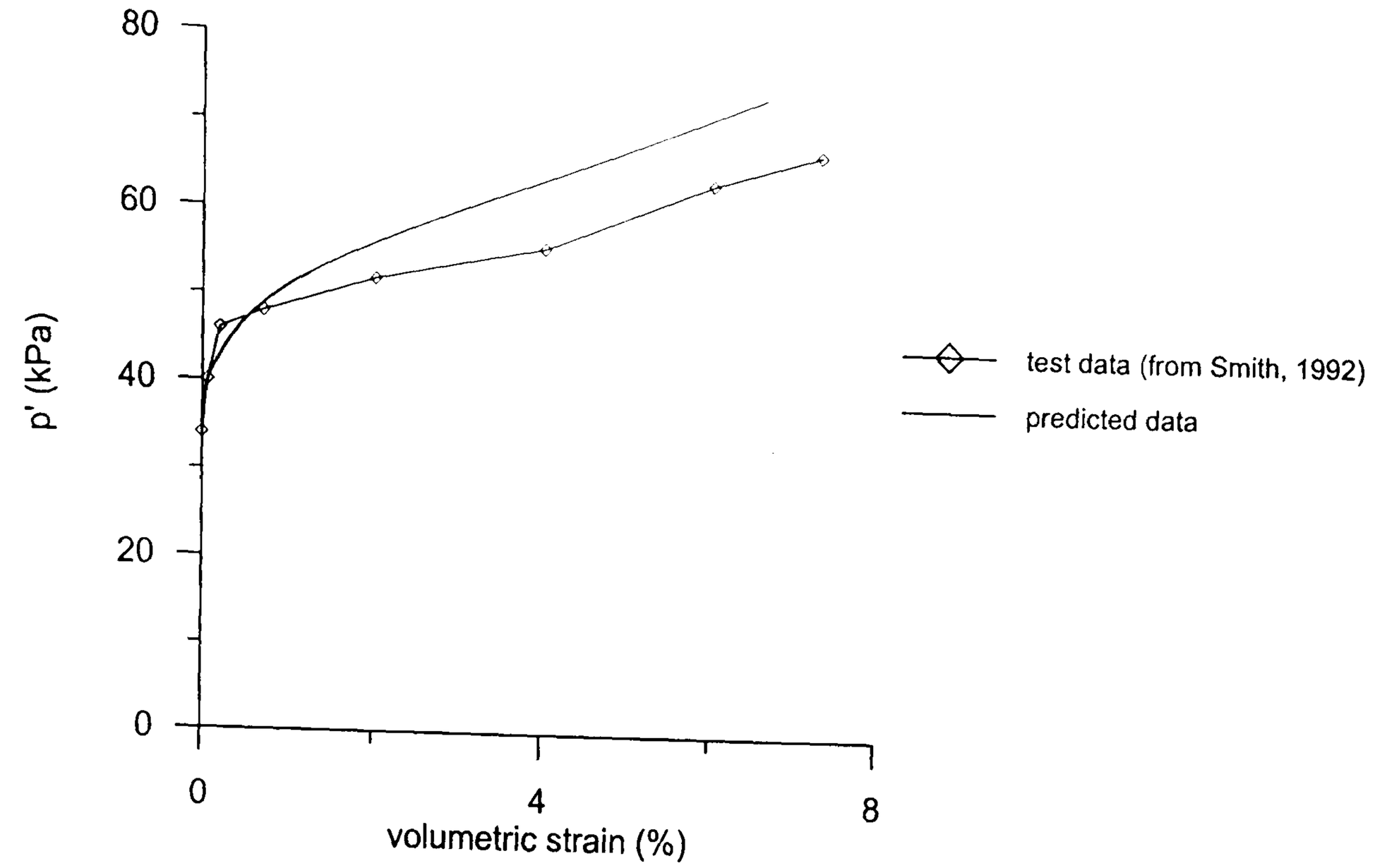

(a)

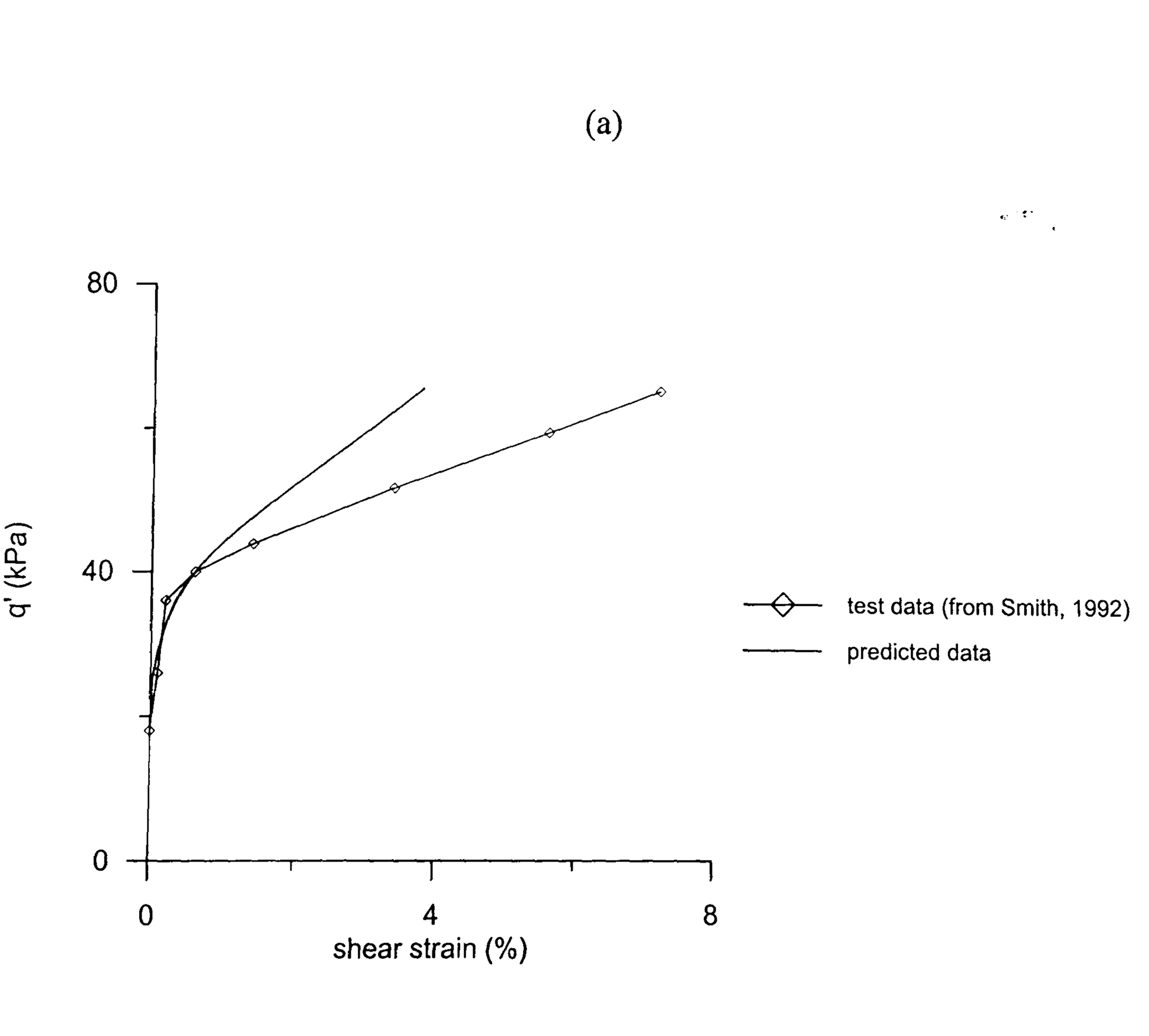

(b)

Figure 5.3.24 Comparison between model prediction and experimental results for stress-strain curves obtained from drained probe LCD55 on Bothkennar clay (a) volumetric response (b) deviatoric response

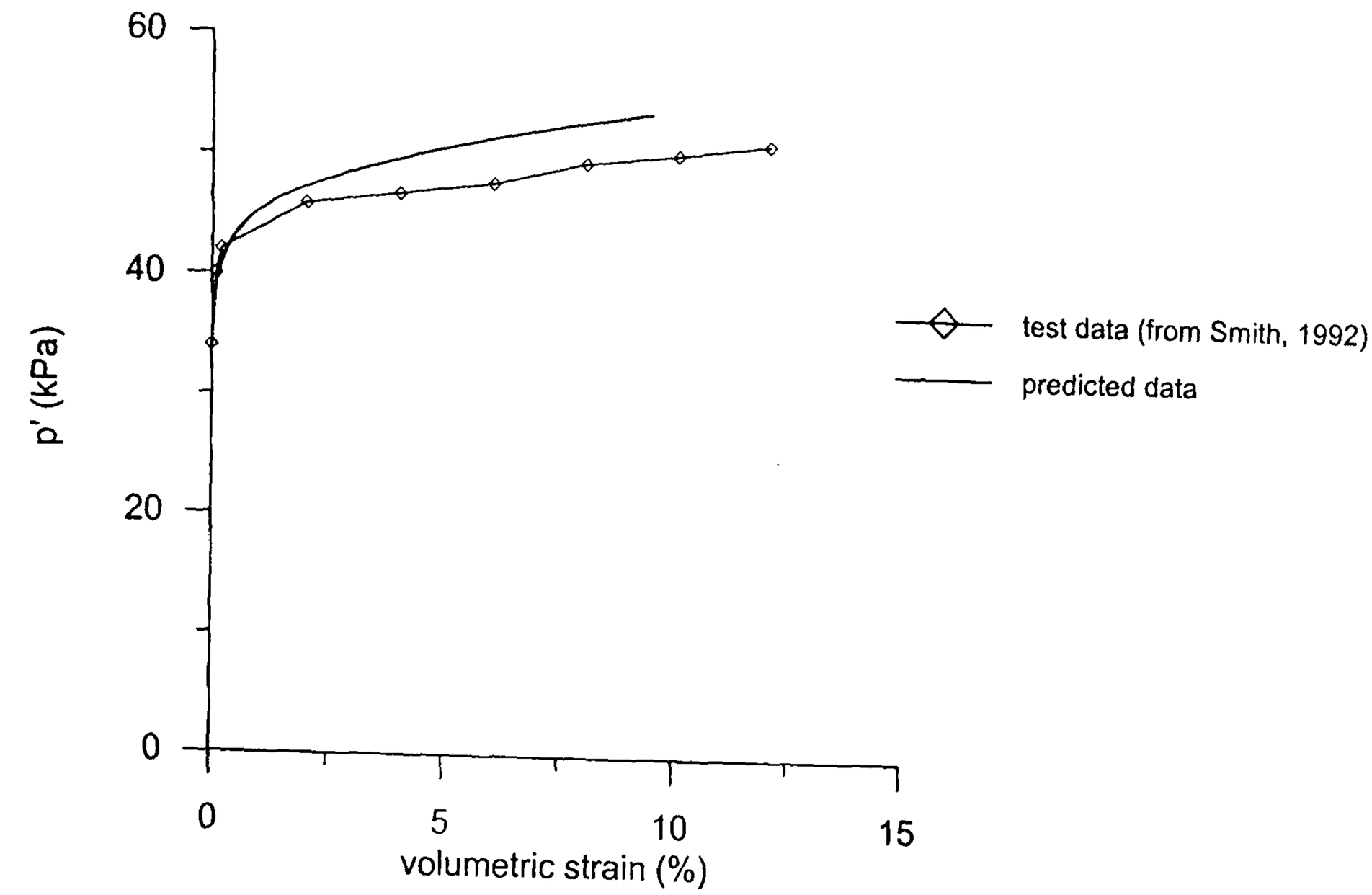

(a)

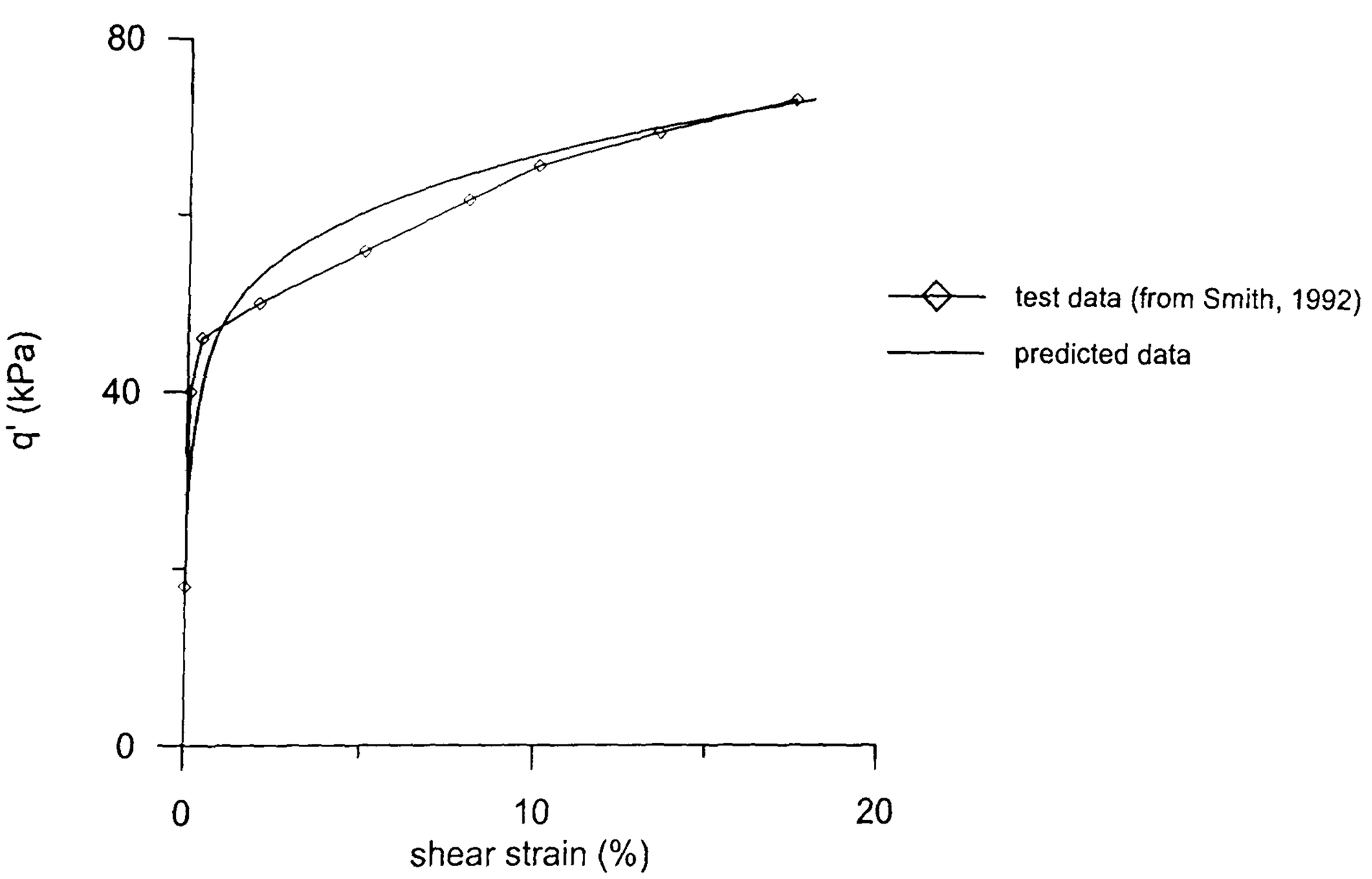

(b)

Figure 5.3.25 Comparison between model prediction and experimental results for stress-strain curves obtained from drained probe LCD70 on Bothkennar clay (a) volumetric response (b) deviatoric response

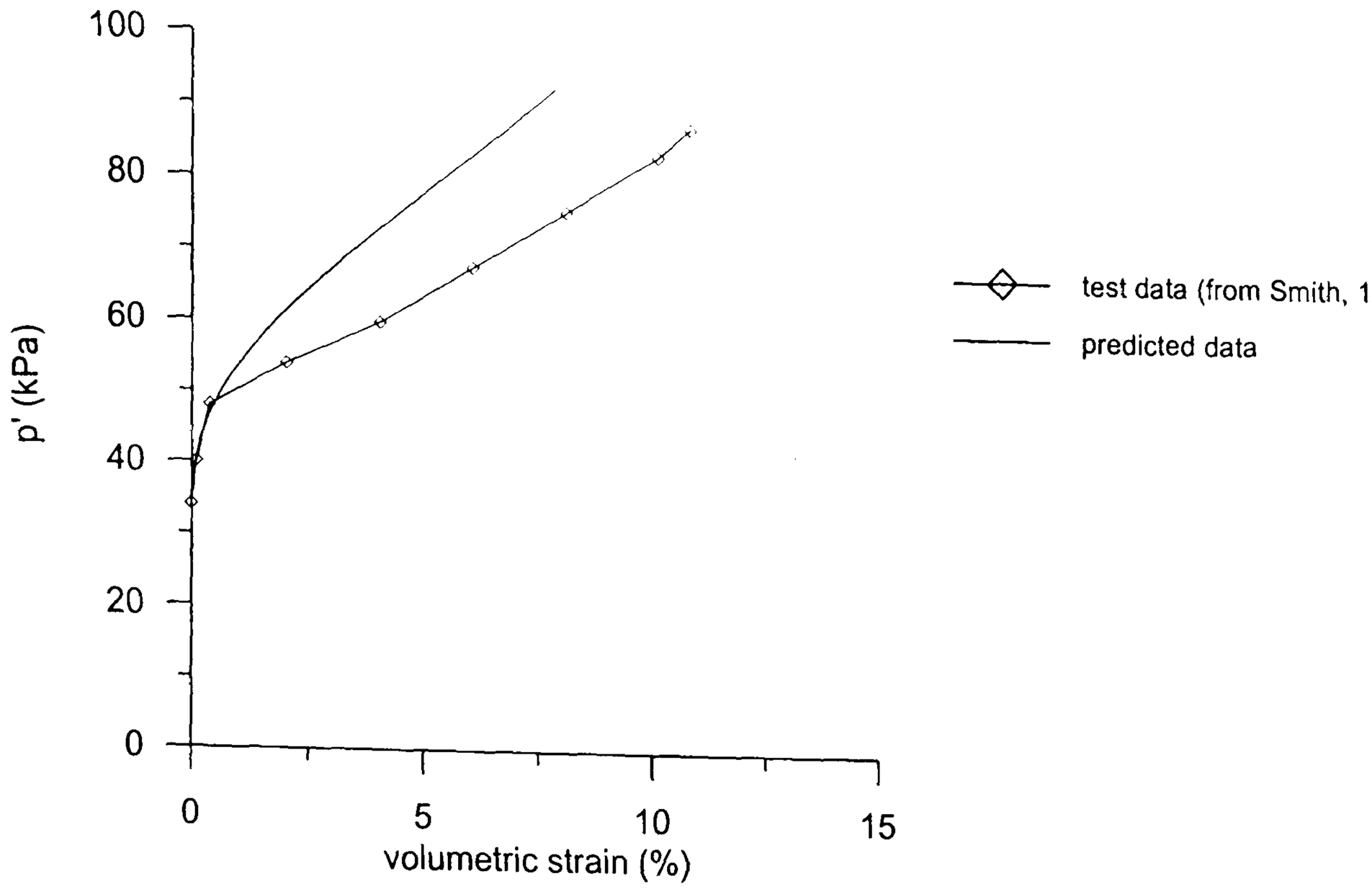

(a)

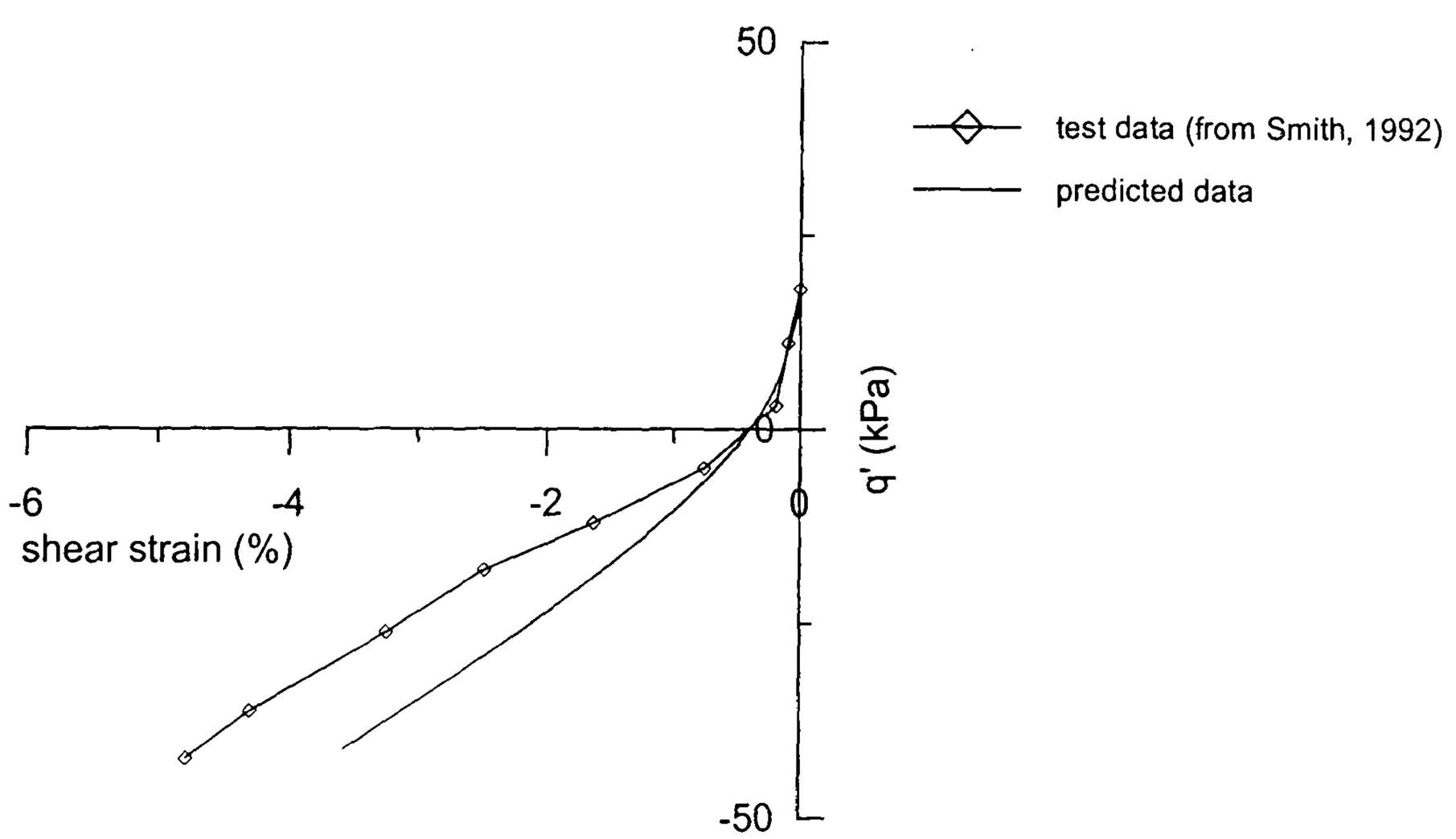

(b)

Figure 5.3.26 Comparison between model prediction and experimental results for stress-strain curves obtained from drained probe LCD315 on Bothkennar clay (a) volumetric response (b) deviatoric response

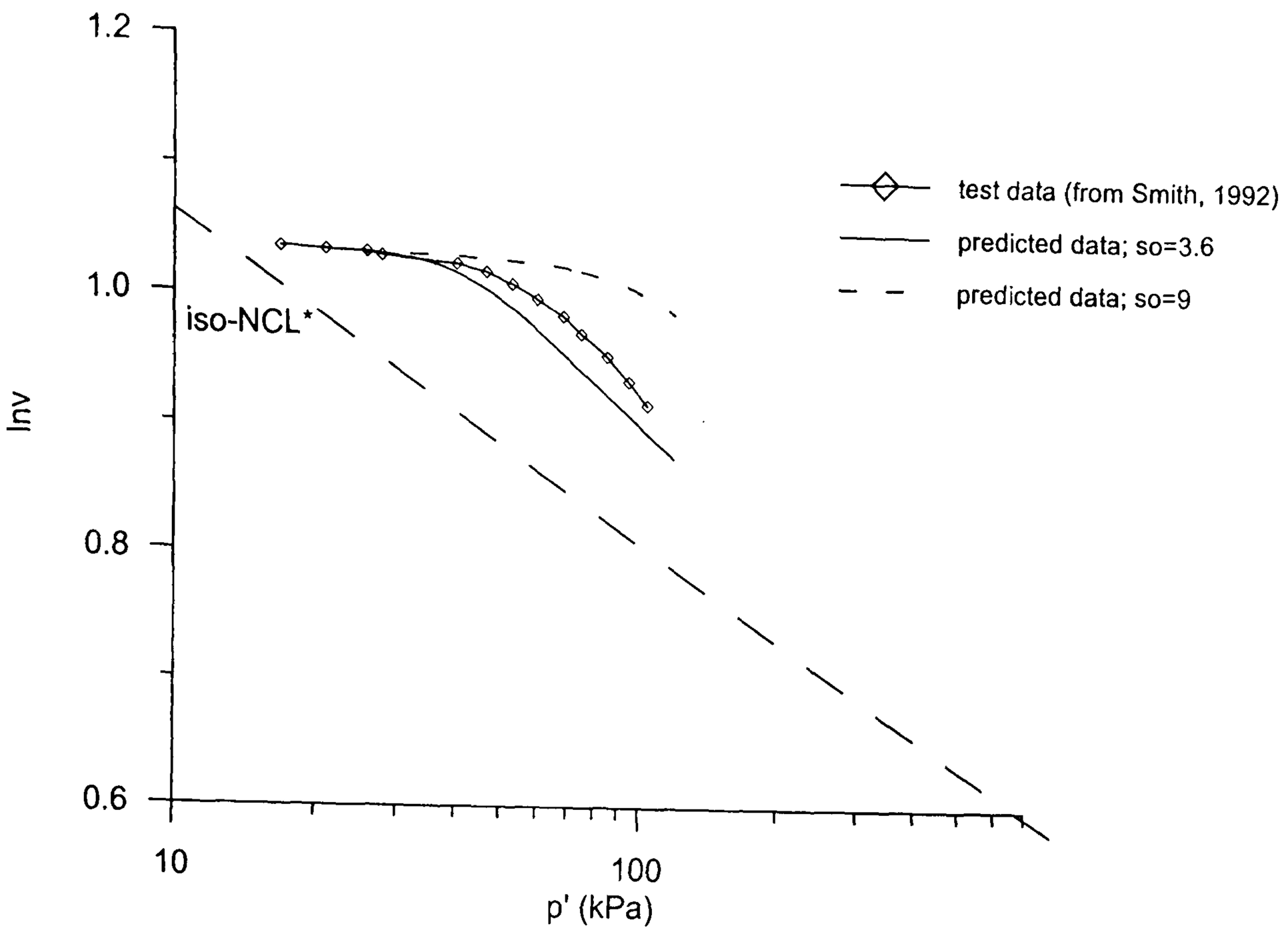

(a)

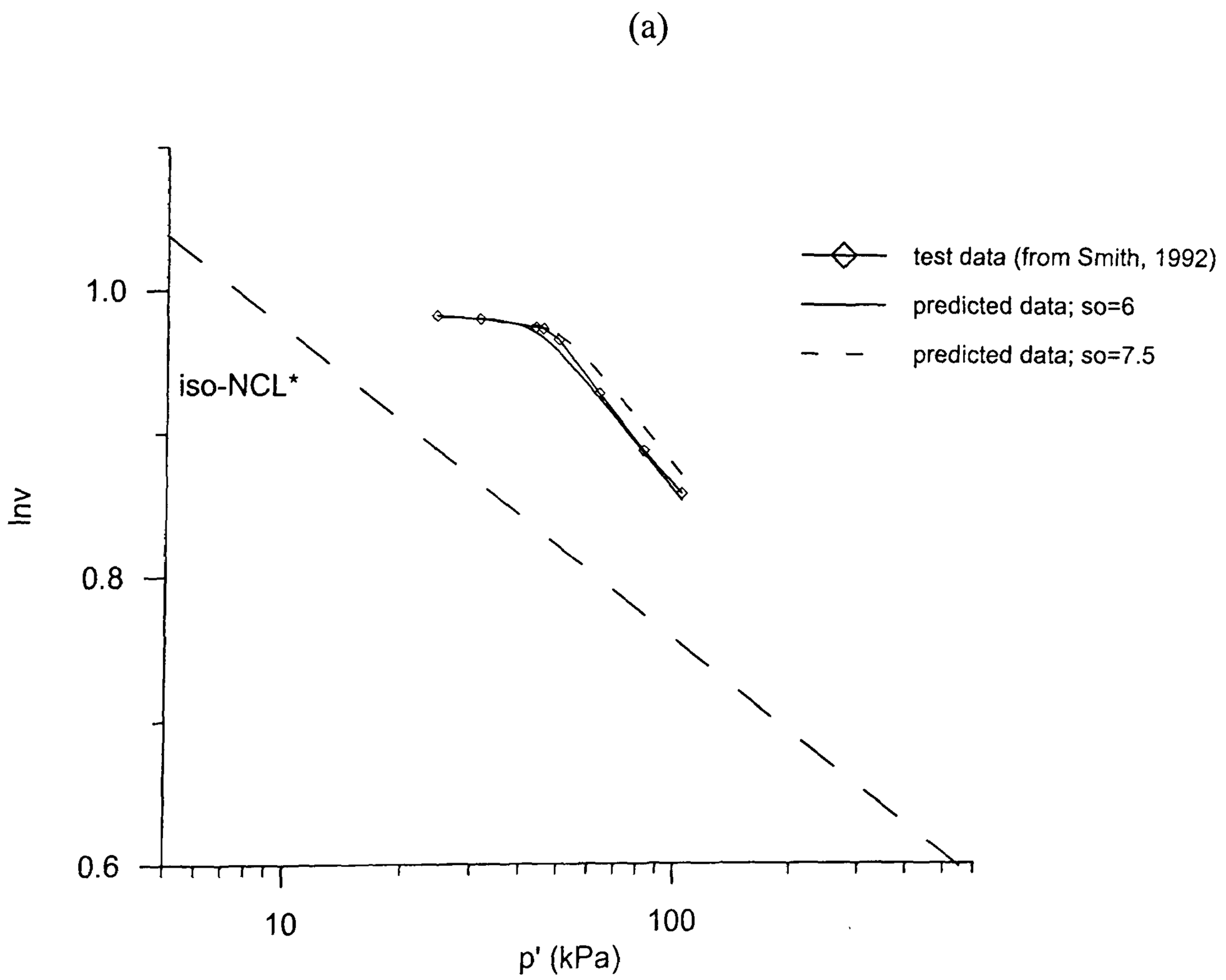

(b)

Figure 5.3.27 Comparison between model prediction and experimental results obtained from volumetric compression on Bothkennar clay samples (a) SUD2 (b) LUD1

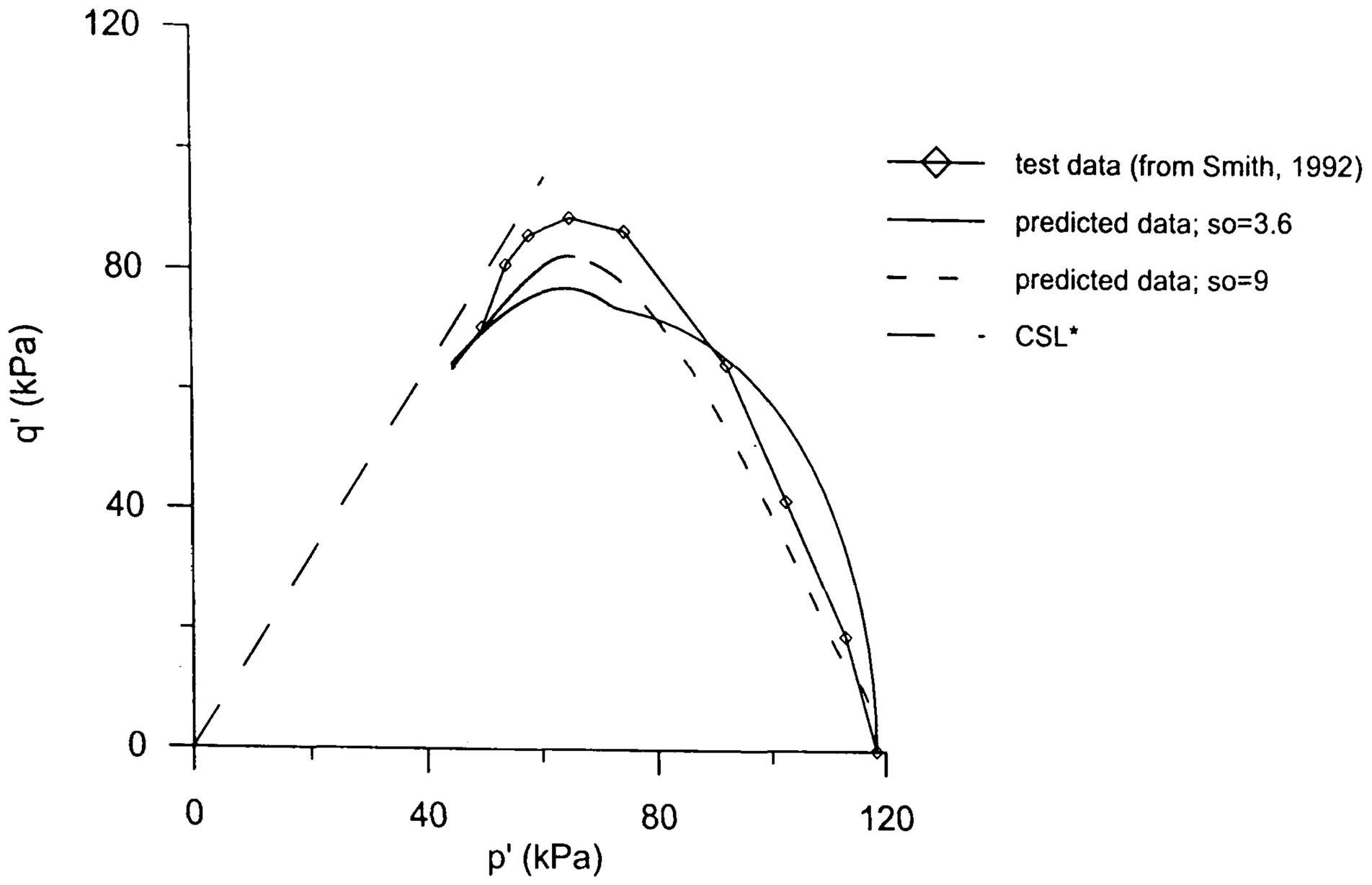

Figure 5.3.28 Comparison between model prediction and experimental results for stress path obtained from undrained triaxial compression test on Bothkennar clay sample SUD2

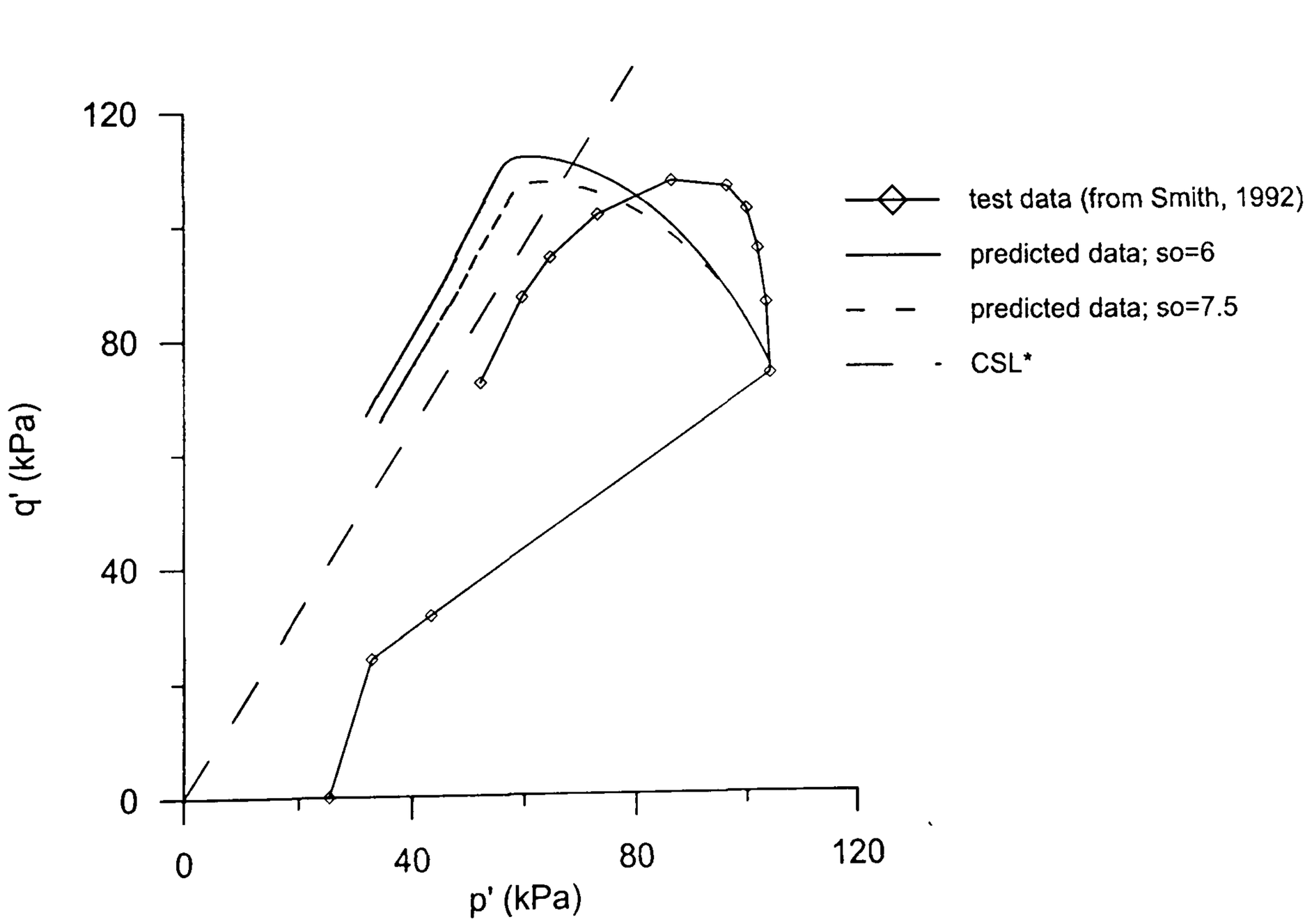

Figure 5.3.29 Comparison between model prediction and experimental results for stress path obtained from undrained triaxial compression test on Bothkennar clay sample LUD1

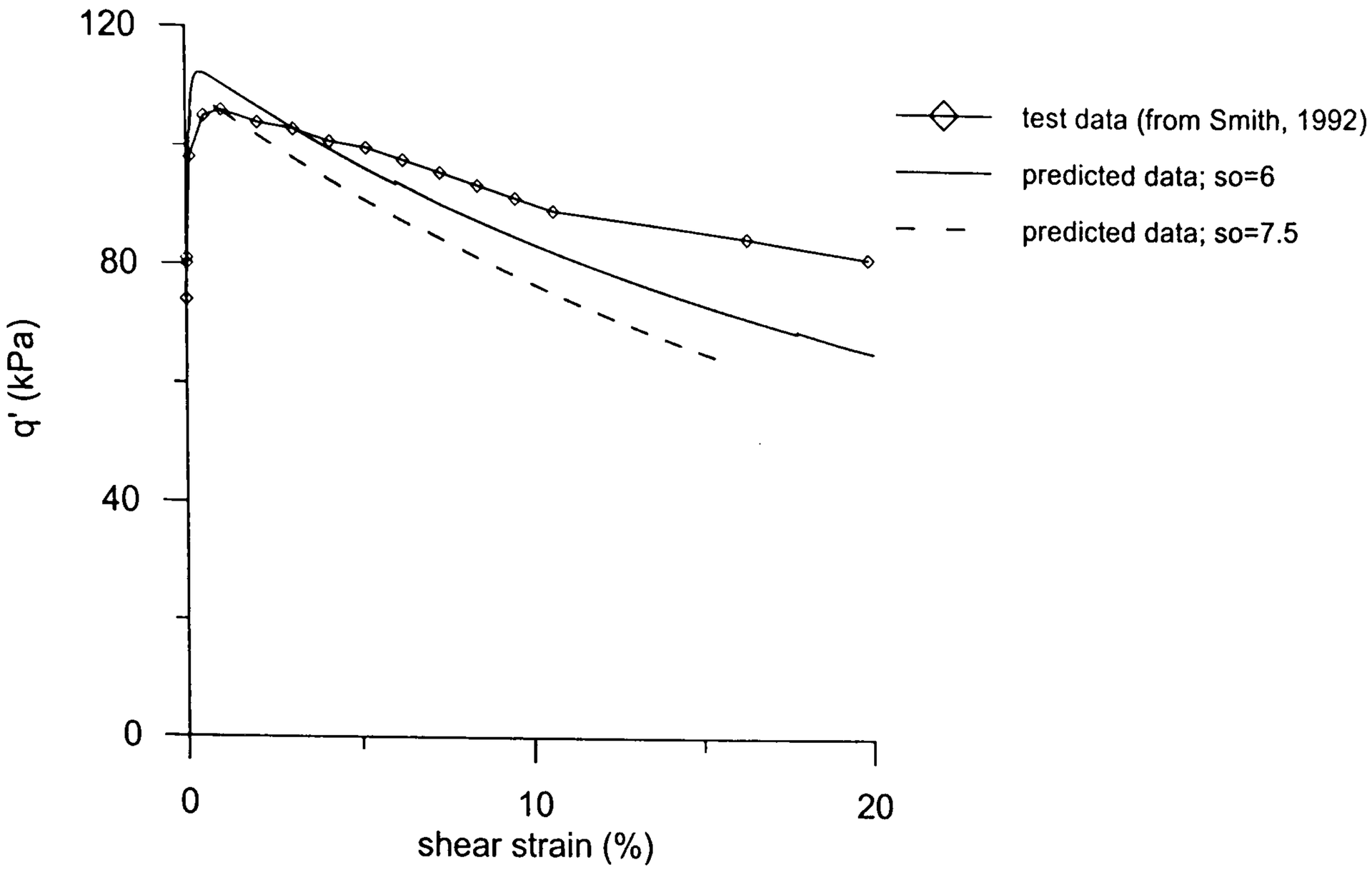

Figure 5.3.30 Comparison between model prediction and experimental results for stress-strain curve obtained from undrained triaxial compression test on Bothkennar clay sample LUD1

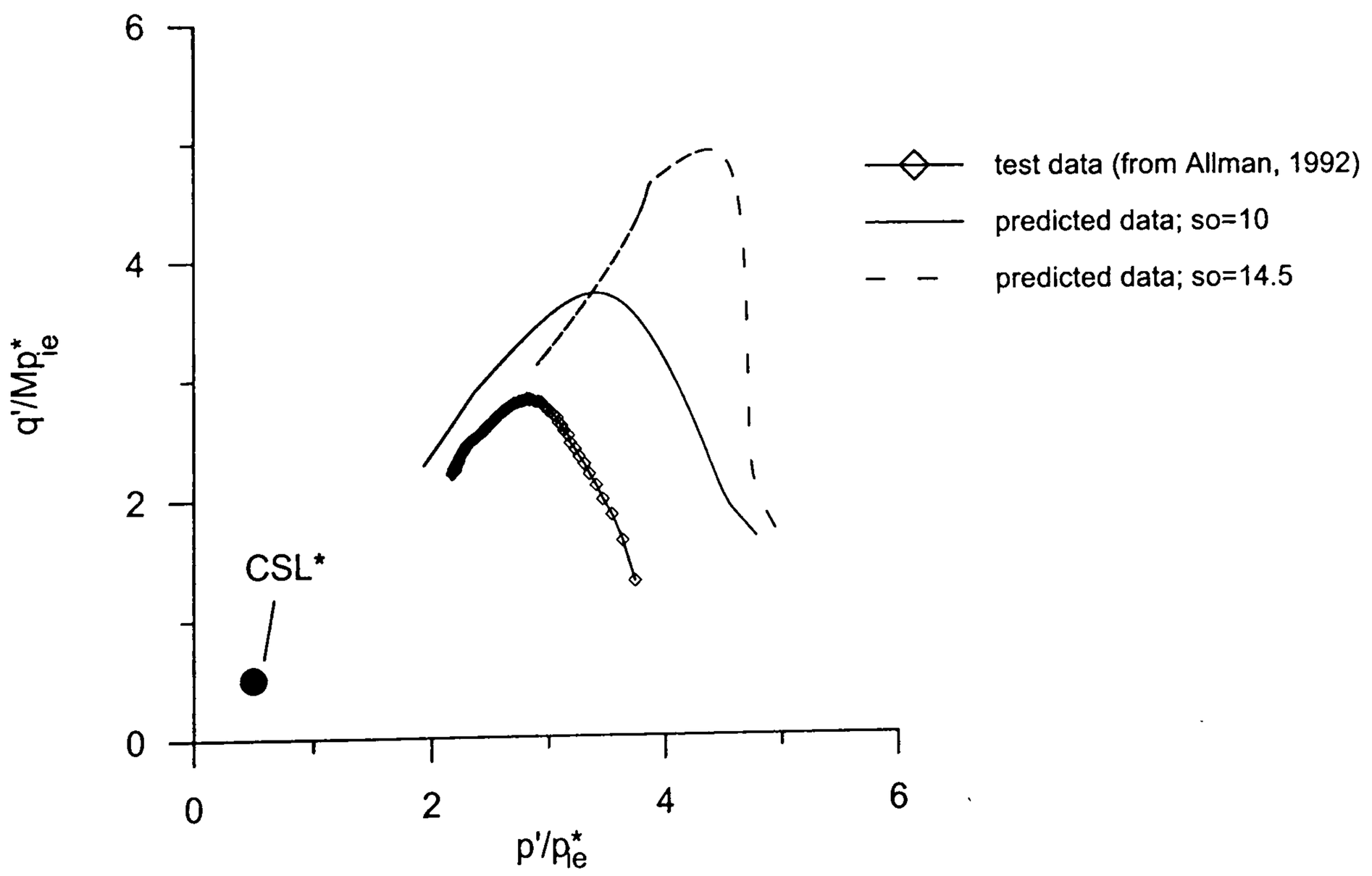

Figure 5.3.31 Comparison between model prediction and experimental results for stress paths normalised for volume, obtained from undrained triaxial compression test on Bothkennar clay sample SH13

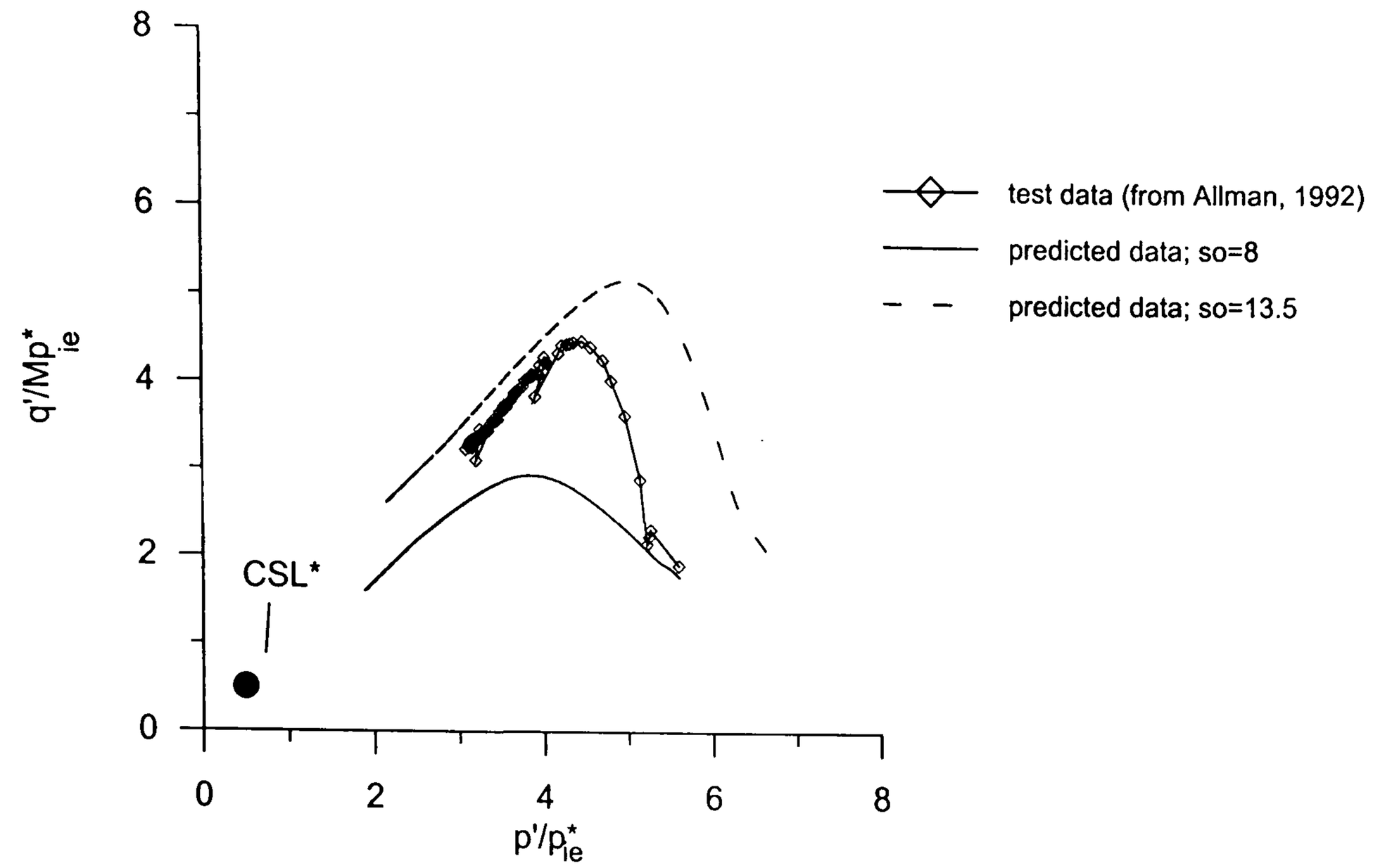

Figure 5.3.32 Comparison between model predictions and experimental results for the stress path normalised for volume, obtained from an undrained triaxial compression test on Bothkennar clay sample L23

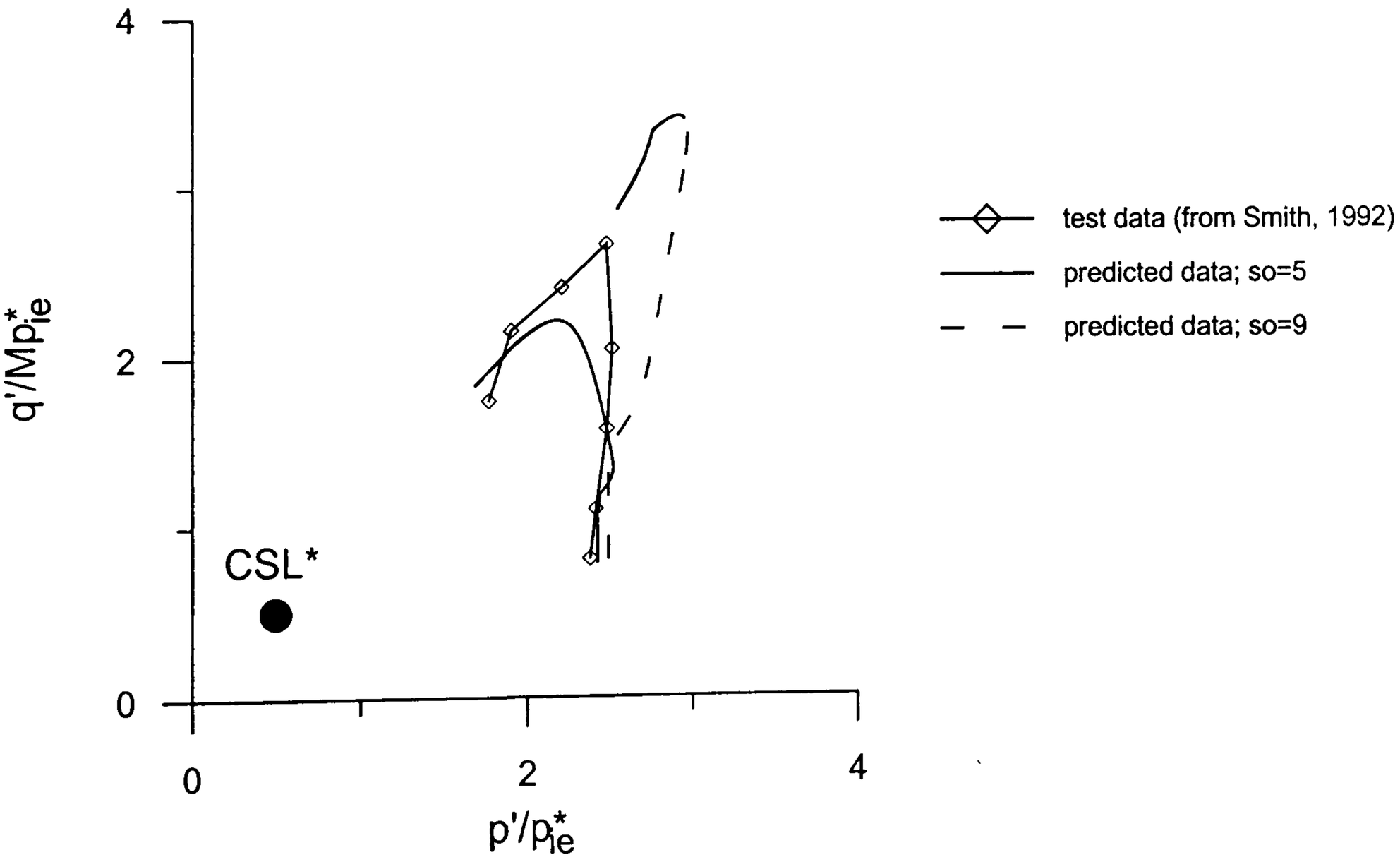

Figure 5.3.33 Comparison between model predictions and experimental results for the stress path normalised for volume, obtained from an undrained triaxial compression test on Bothkennar clay sample SCU1

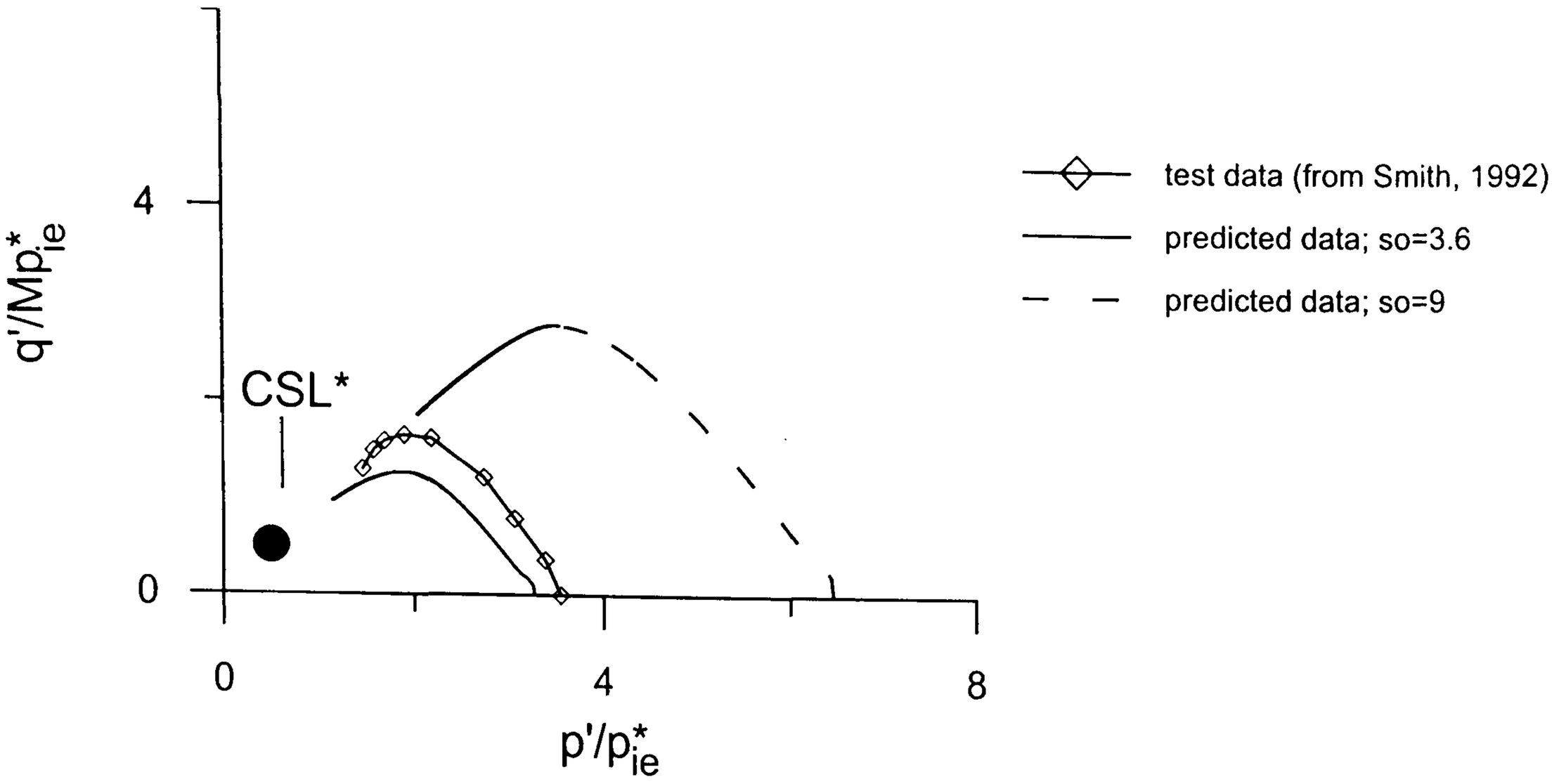

Figure 5.3.34 Comparison between model prediction and experimental results for stress paths normalised for volume, obtained from undrained triaxial compression test on Bothkennar clay sample SUD2

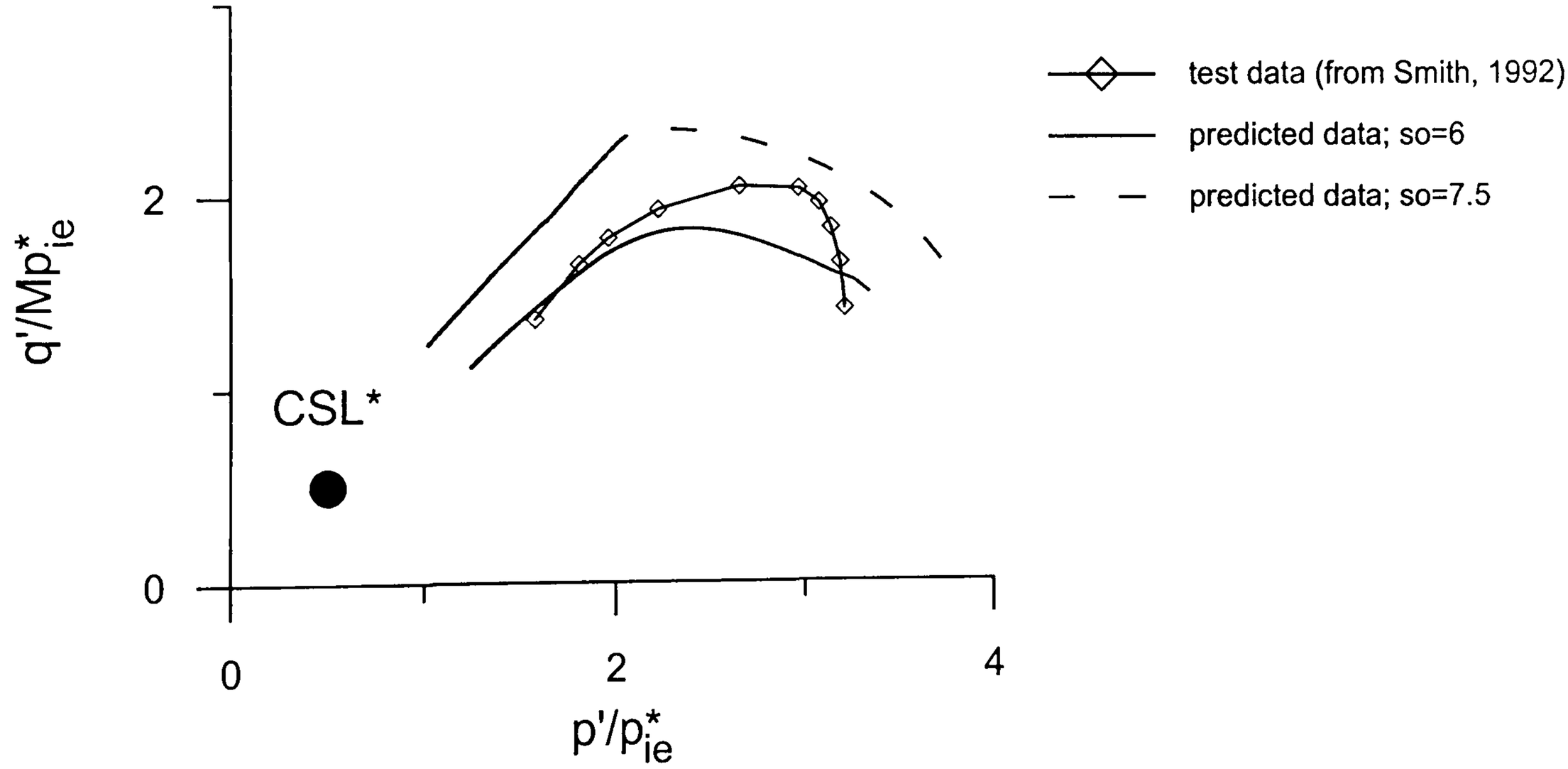

Figure 5.3.35 Comparison between model prediction and experimental results for stress paths normalised for volume, obtained from undrained triaxial compression test on Bothkennar clay sample LUD1

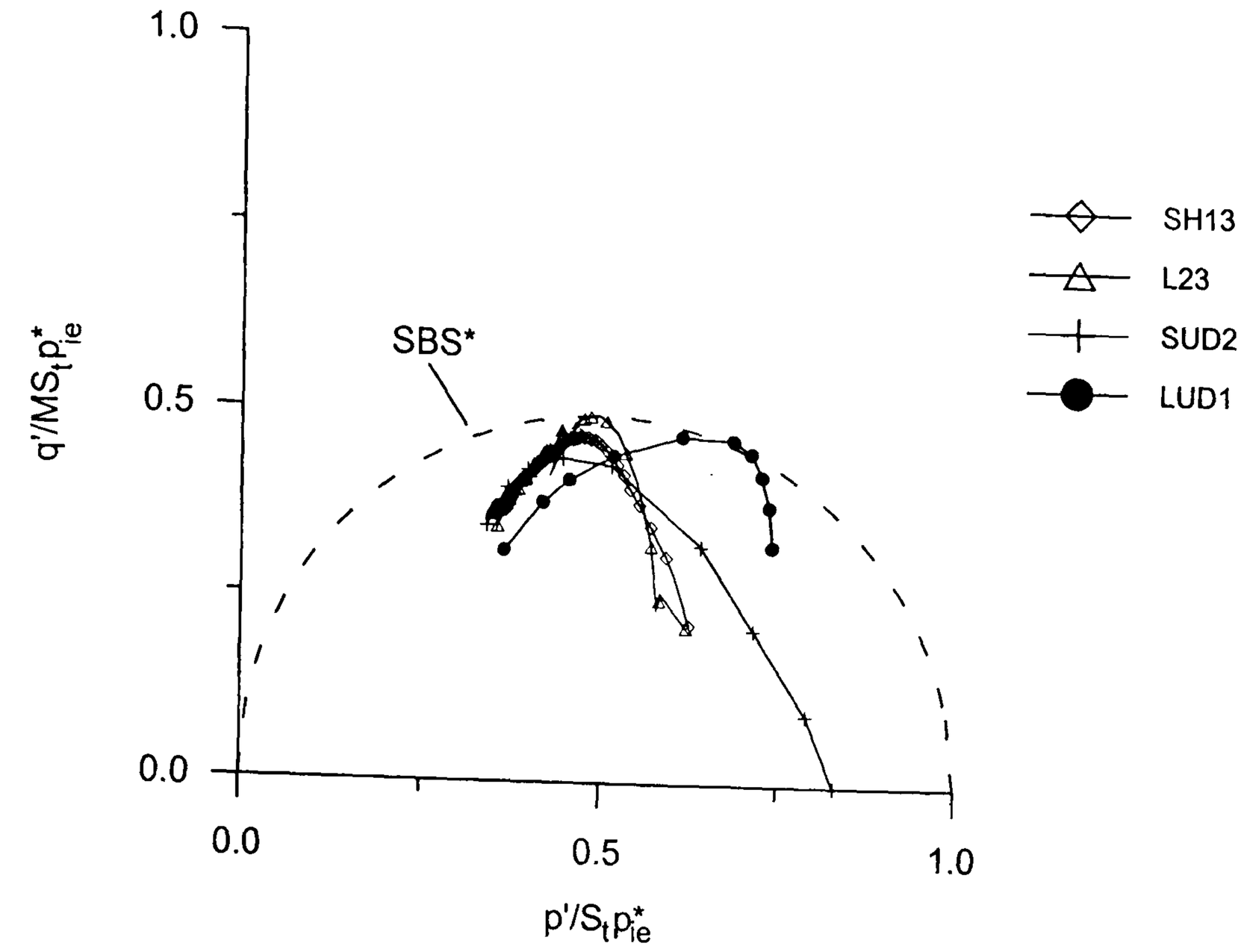

(a)

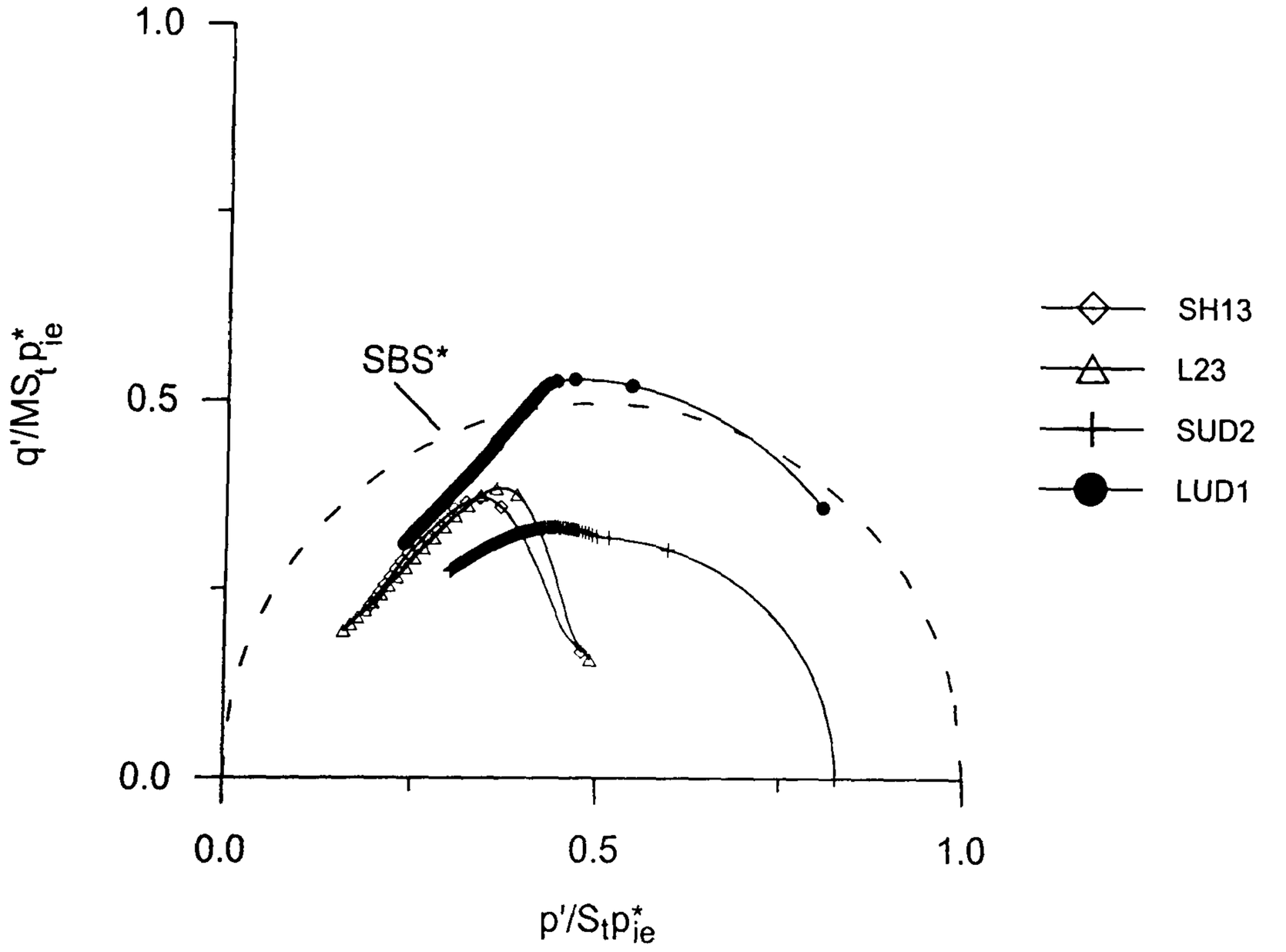

(b)

Figure 5.3.36 Comparison between model predictions and experimental results for stress paths normalised for volume and initial structure, obtained from undrained triaxial compression tests on Bothkennar clay (a) test data (from Allman, 1992; Smith, 1992) (b) model predictions

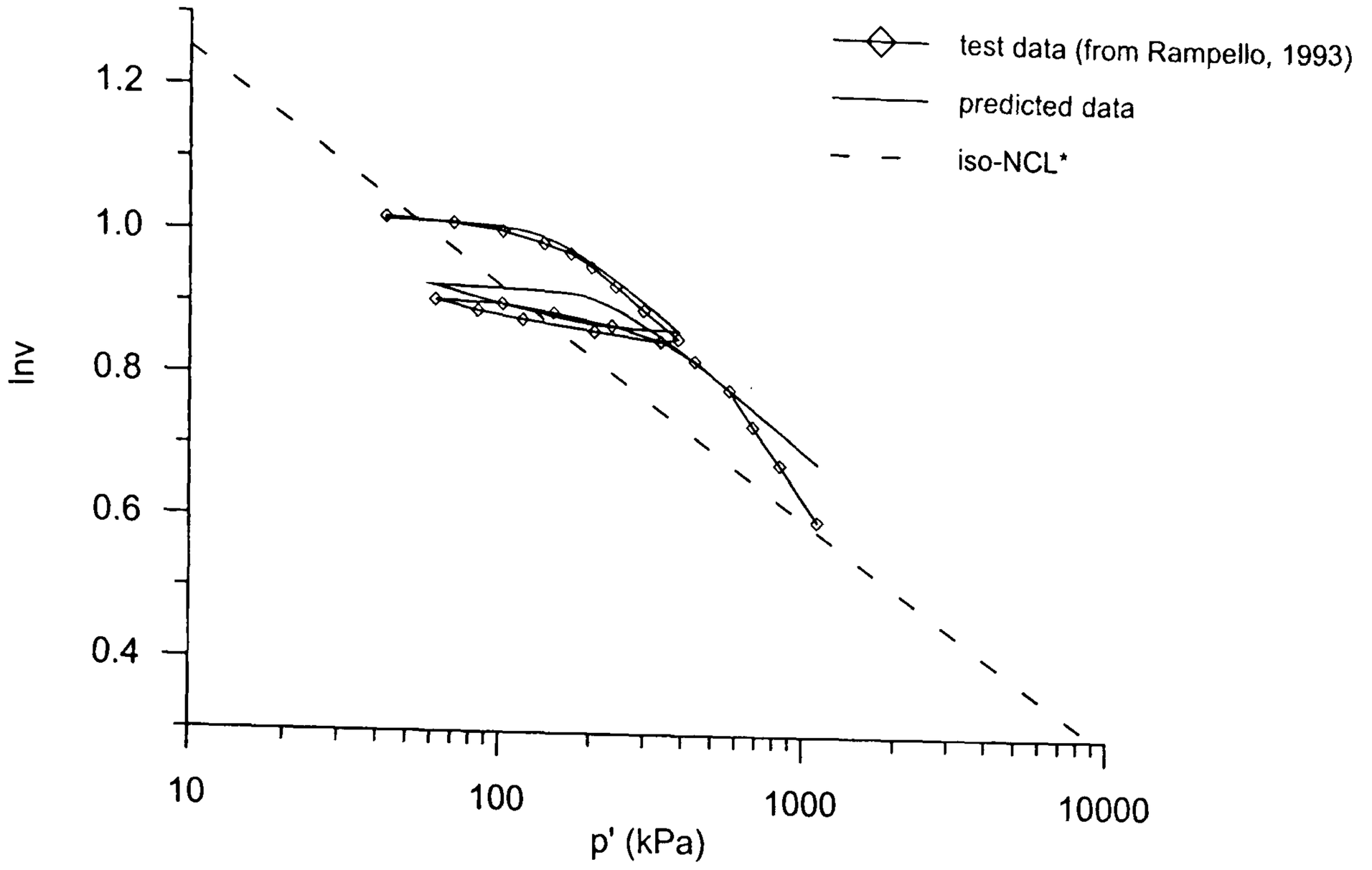

(a)

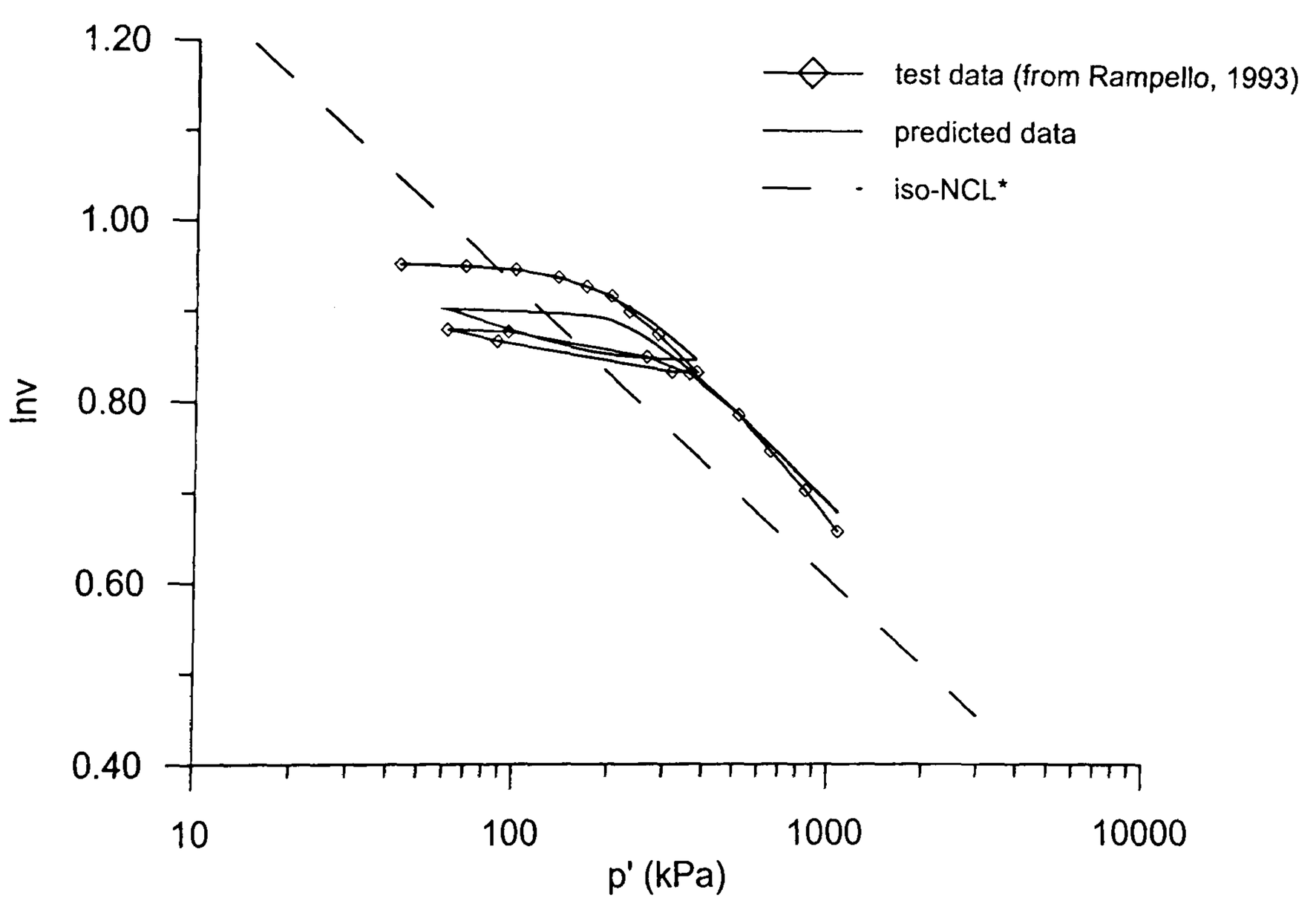

(b)

Figure 5.3.37 Comparison between model prediction and experimental results obtained from isotropic compression tests on Pisa clay samples (a) 19B (b) 29A

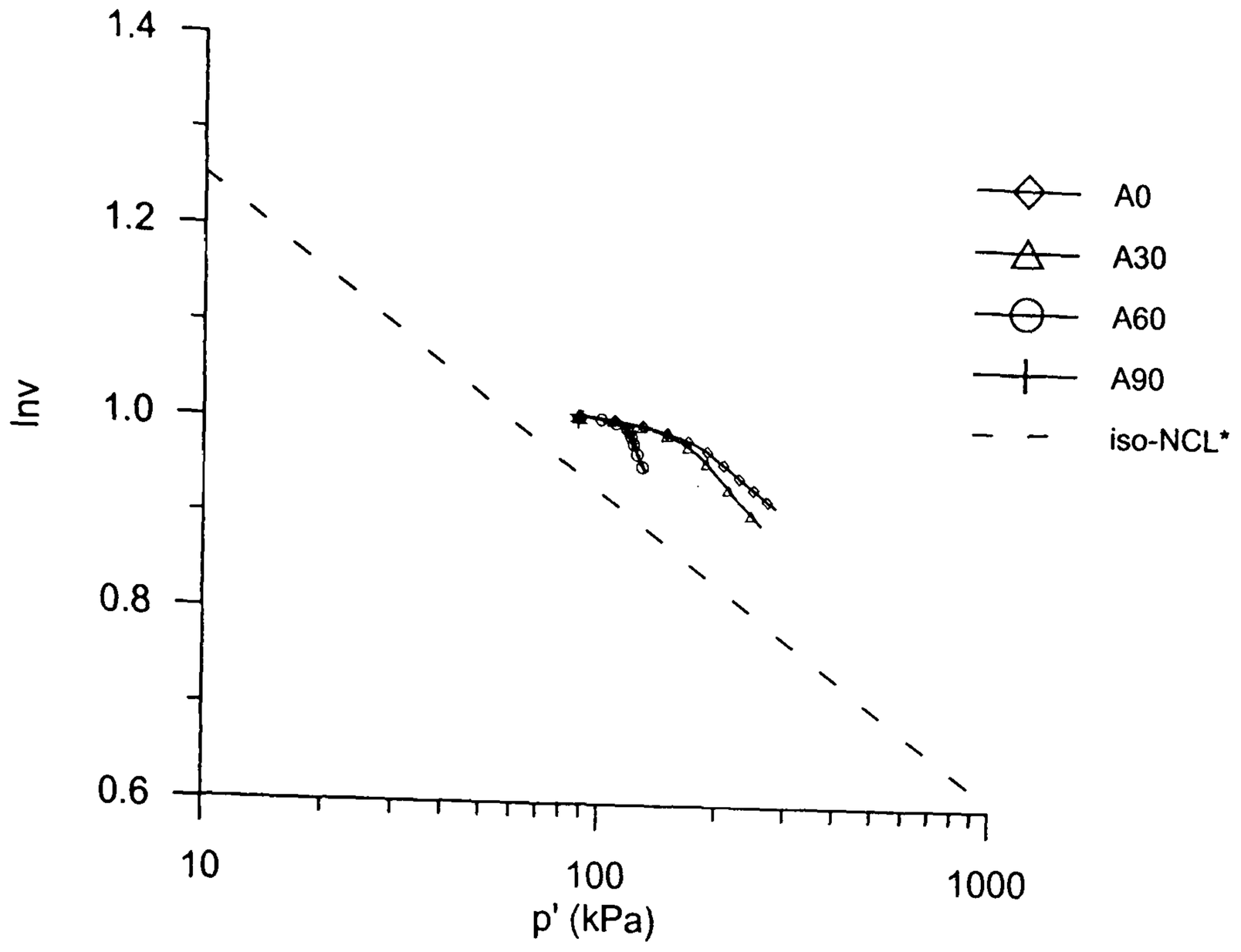

(a)

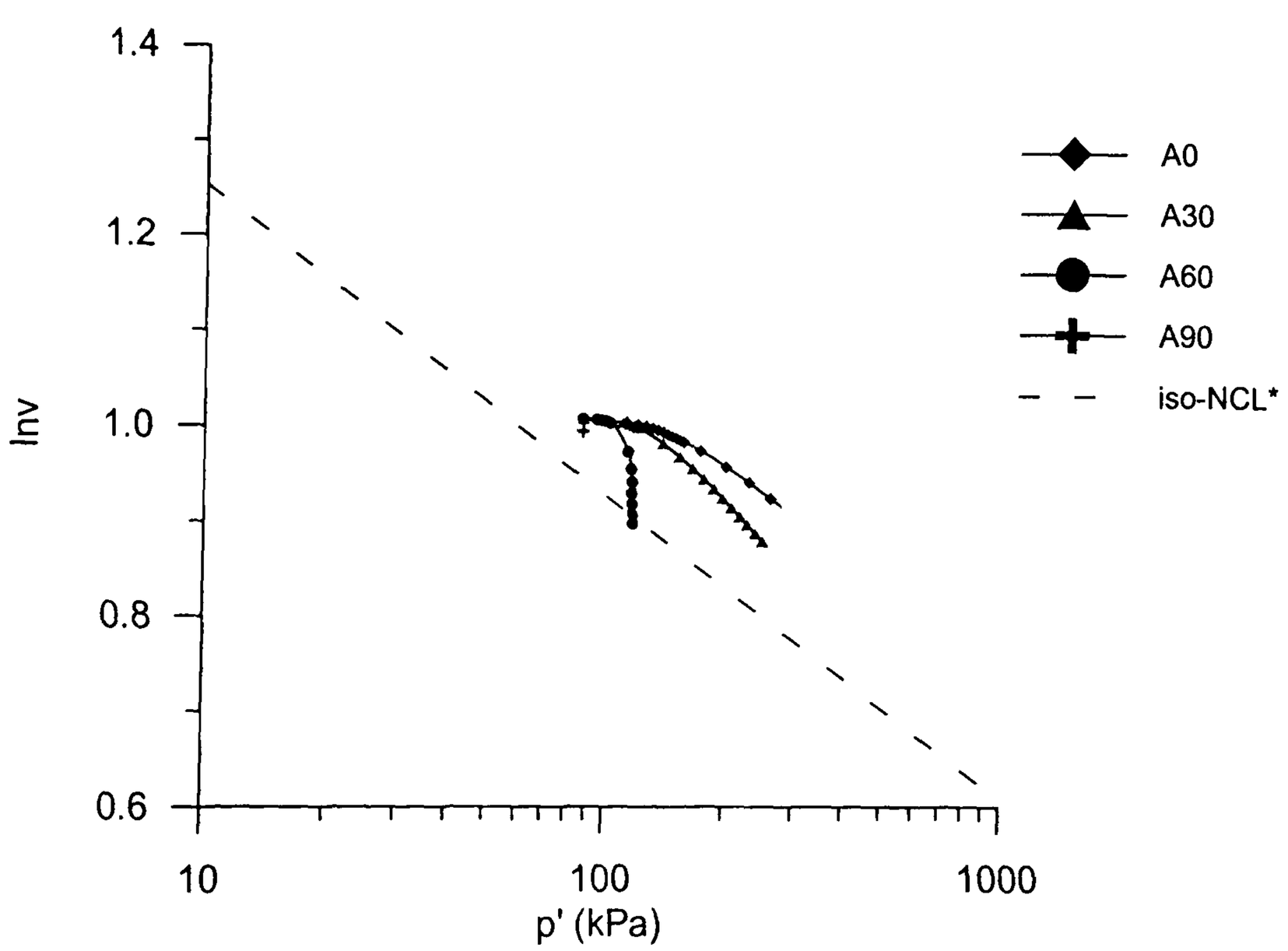

(b)

Figure 5.3.38 Volumetric response obtained during drained probes on natural Pisa clay samples (a) experimental results (test data from Callisto, 1996) (b) model prediction

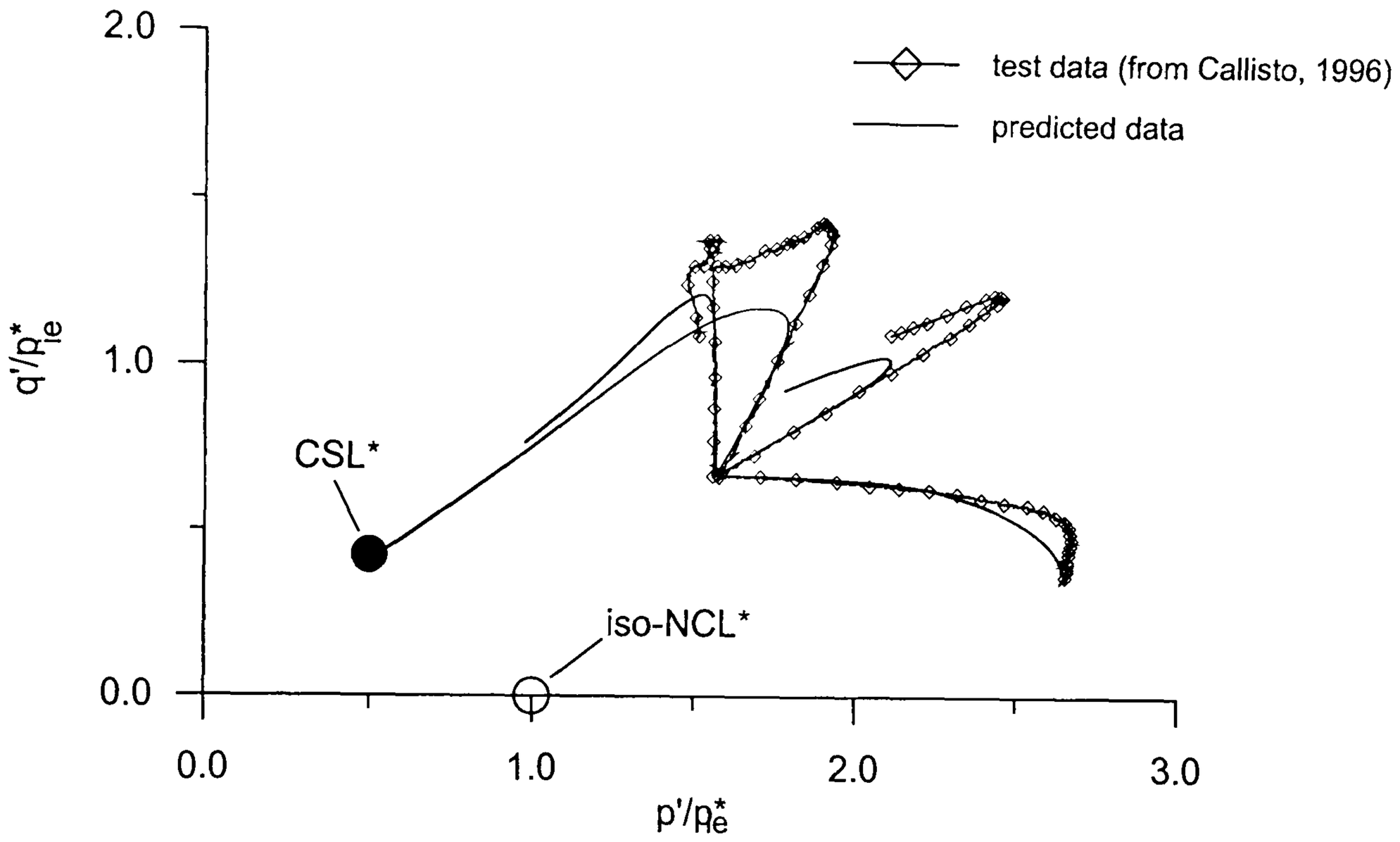

Figure 5.3.39 Comparison between model prediction and experimental results for normalised stress paths obtained from drained probes on Pisa clay samples

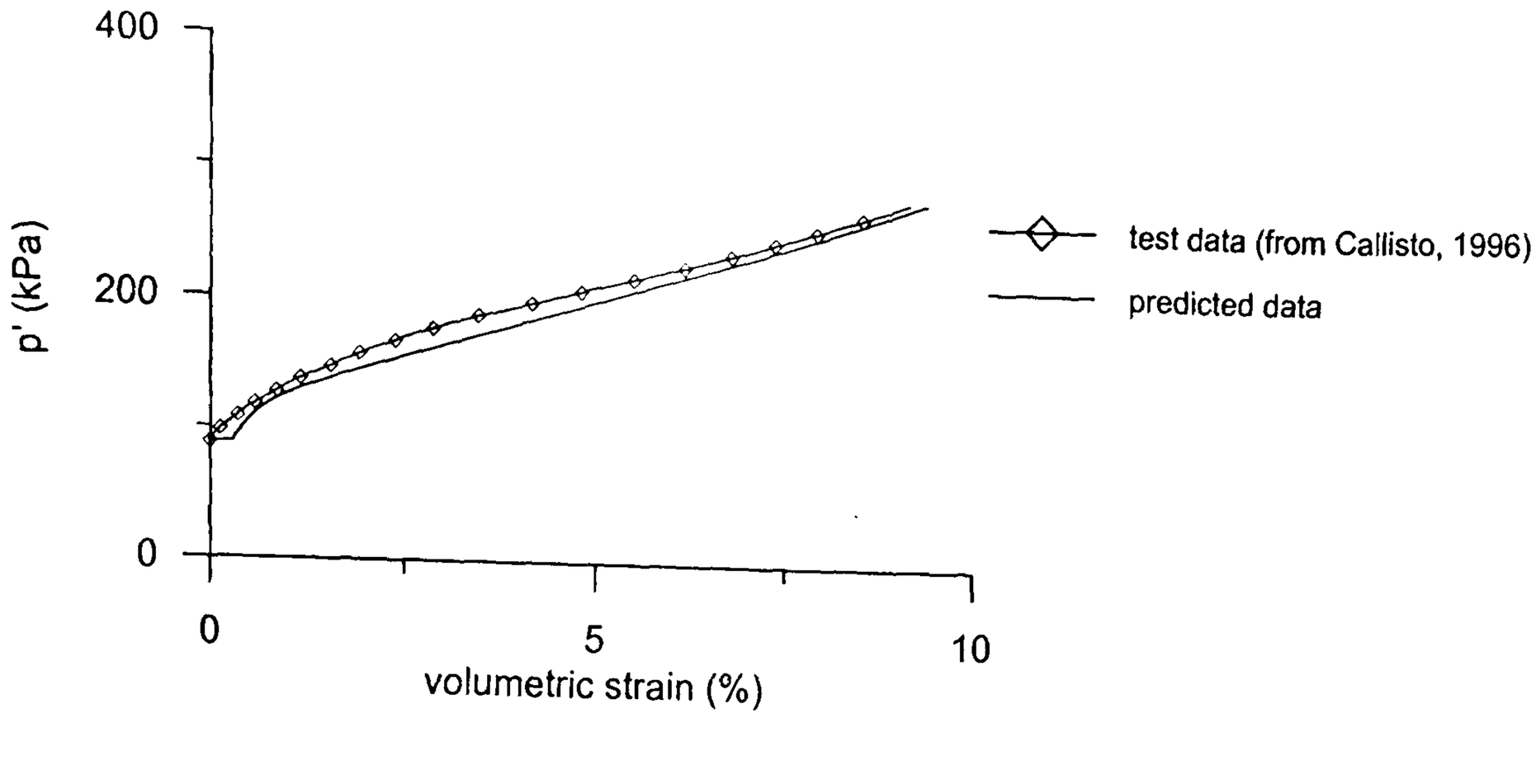

(a)

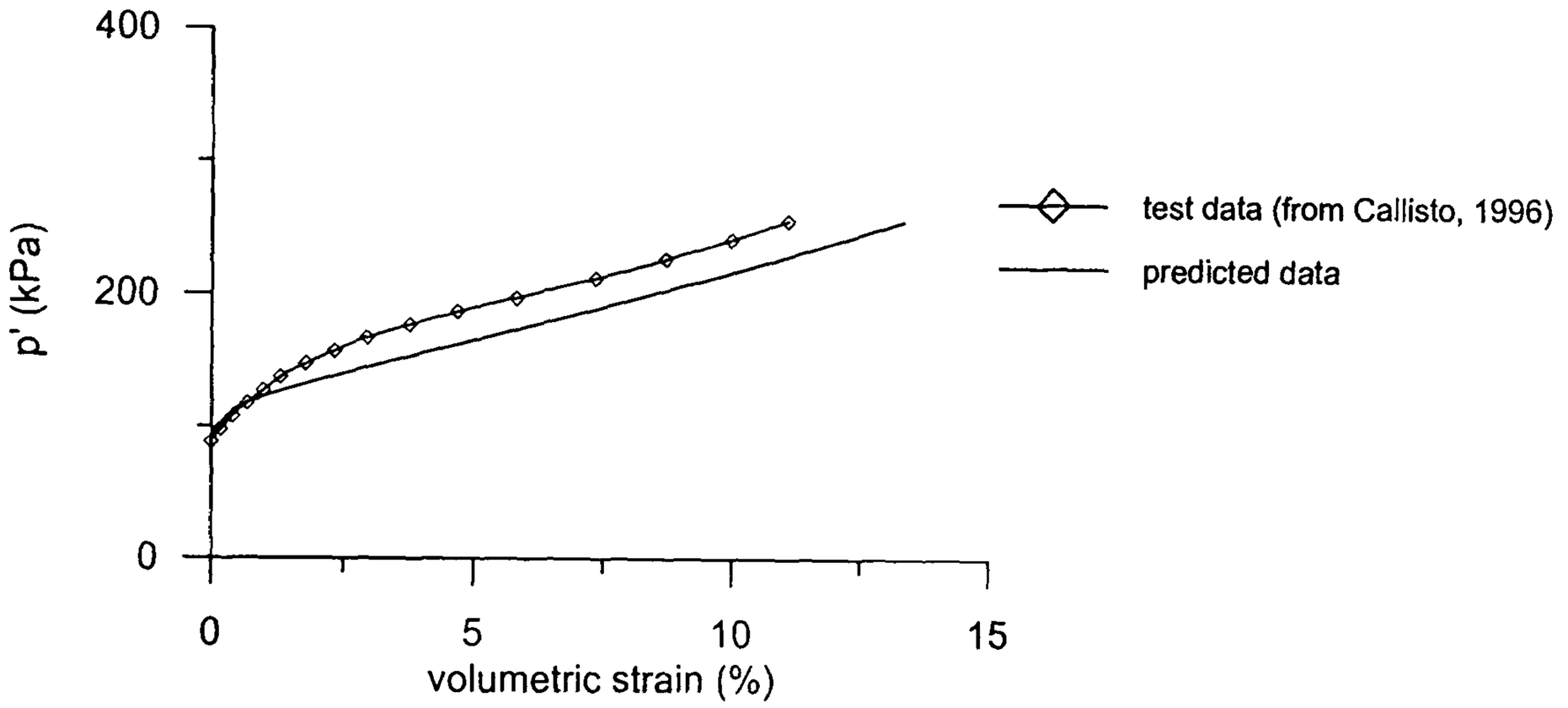

(b)

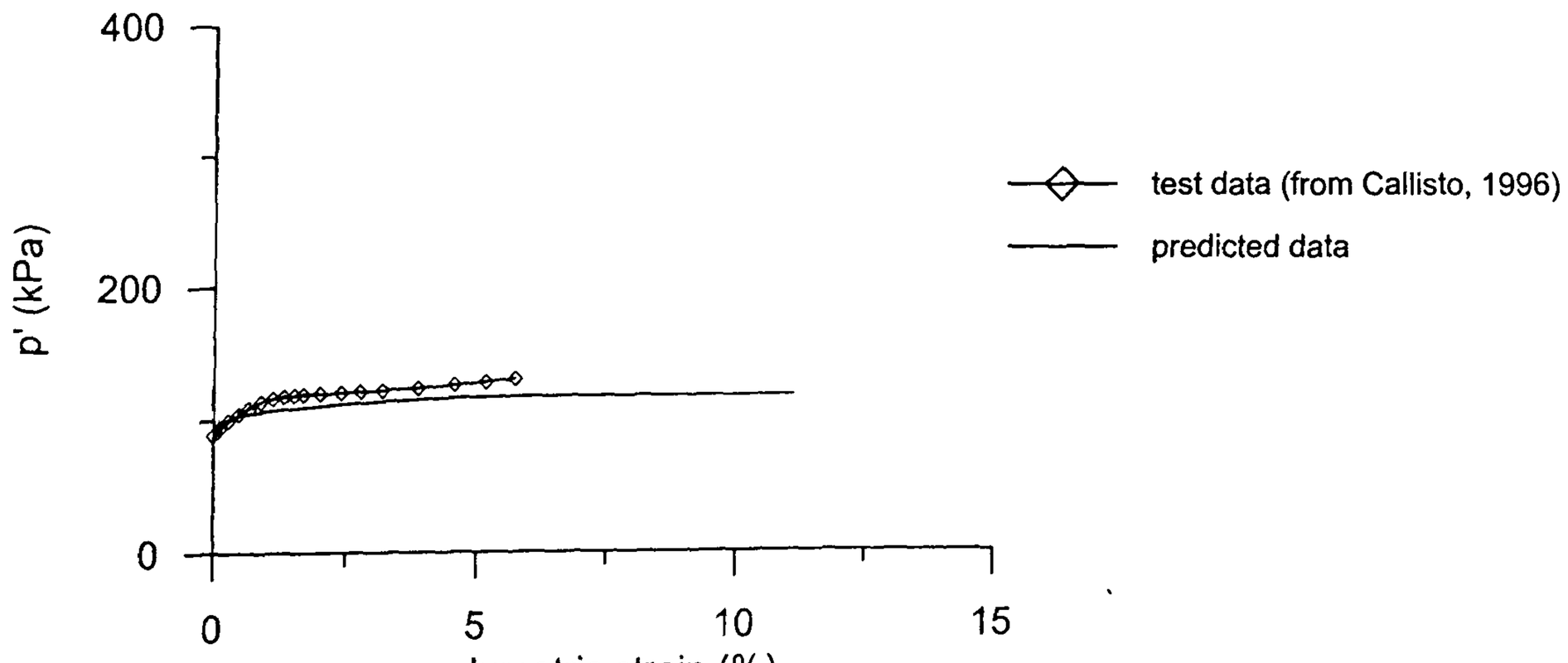

(c)

Figure 5.3.40 Comparison between model prediction and experimental results for volumetric stress-strain curves obtained from drained probes (a) A0 (b) A30 (c) A60 on Pisa clay samples

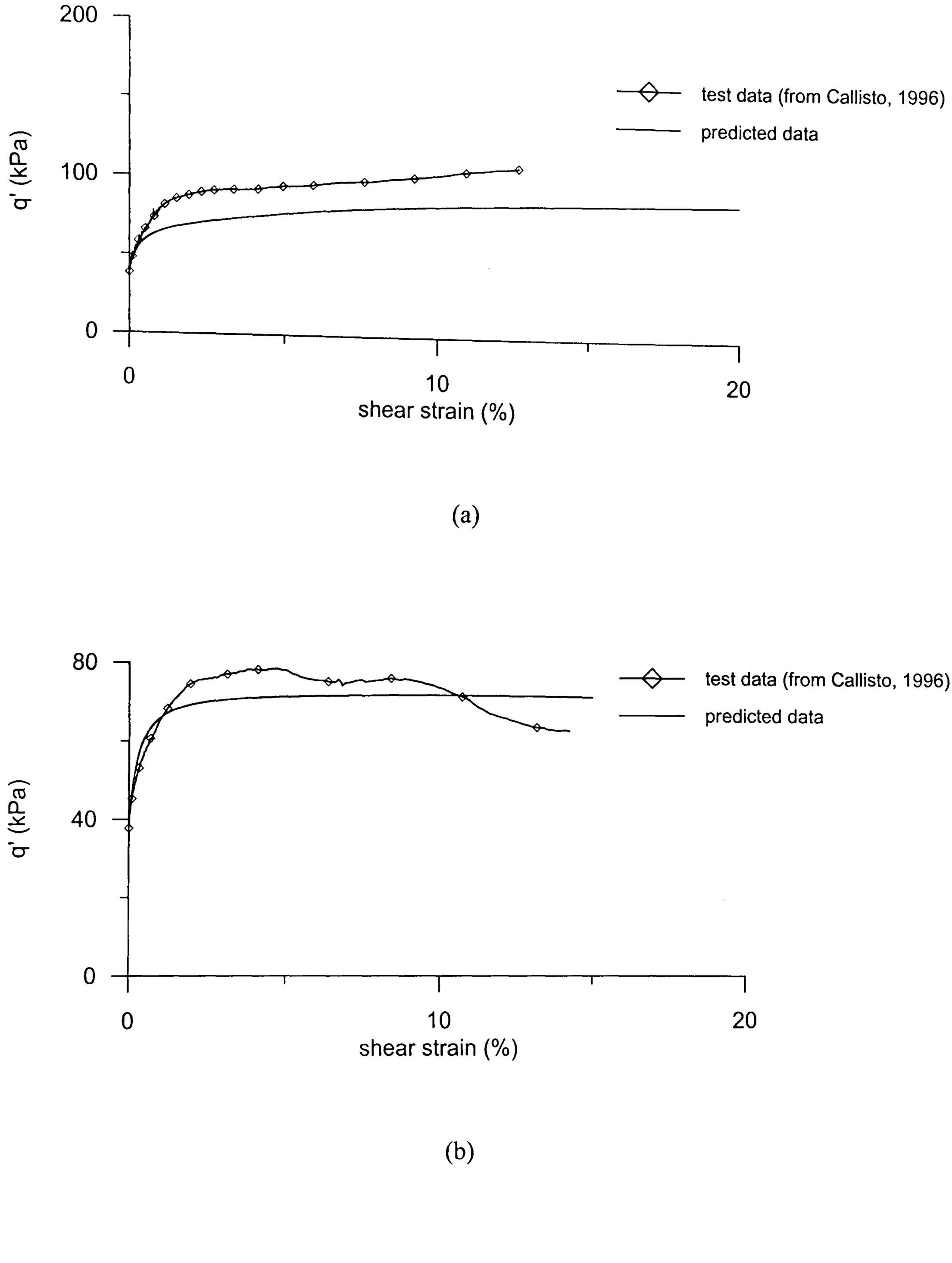

Figure 5.3.41 Comparison between model prediction and experimental results for deviatoric stress-strain curves obtained from drained probes (a) A60 (b) A90 on Pisa clay samples

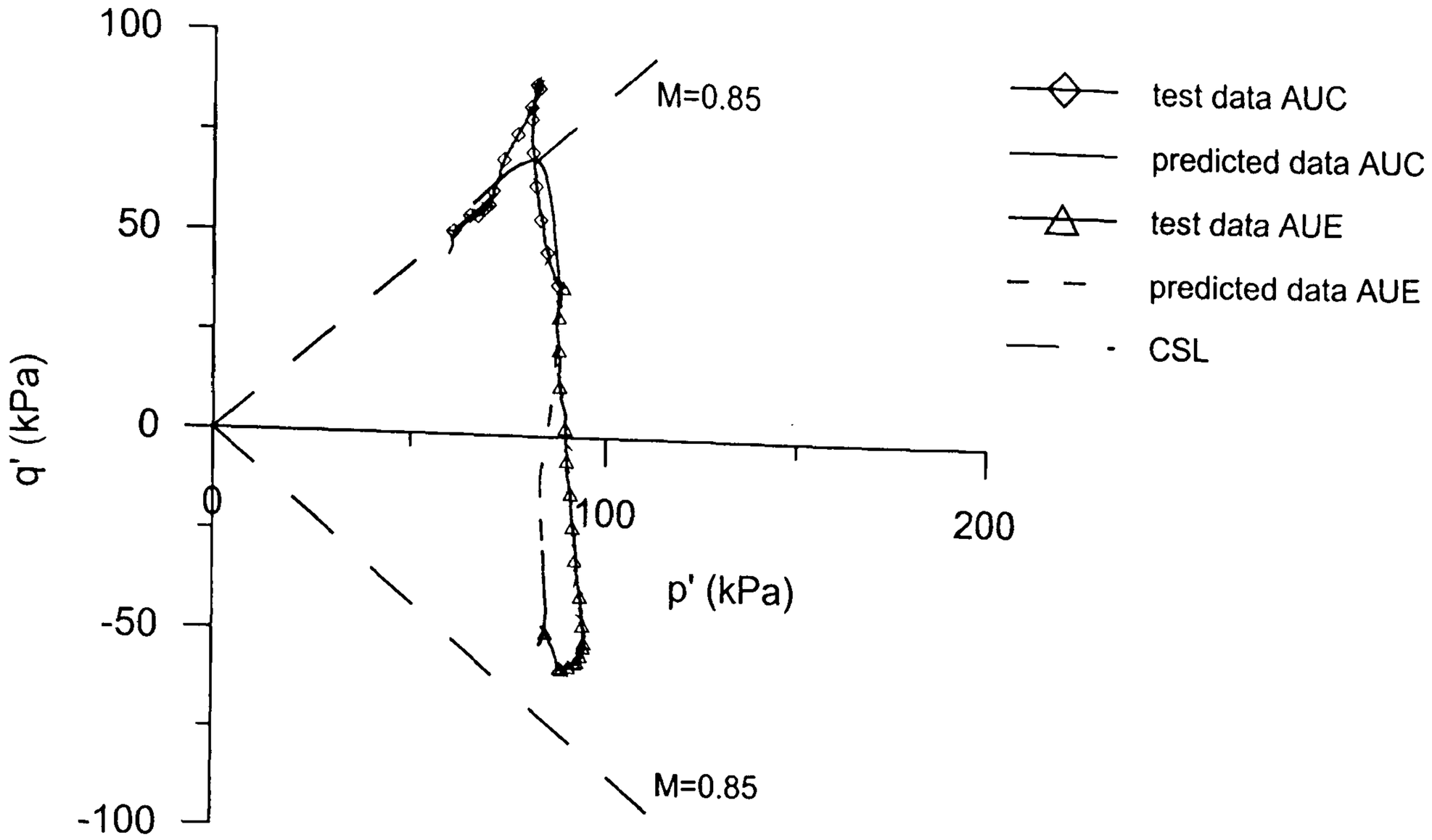

Figure 5.3.42 Comparison between model prediction and experimental results for stress paths obtained from undrained triaxial compression and extension tests, AUC and AUE, on Pisa clay samples (test data from Callisto, 1996)

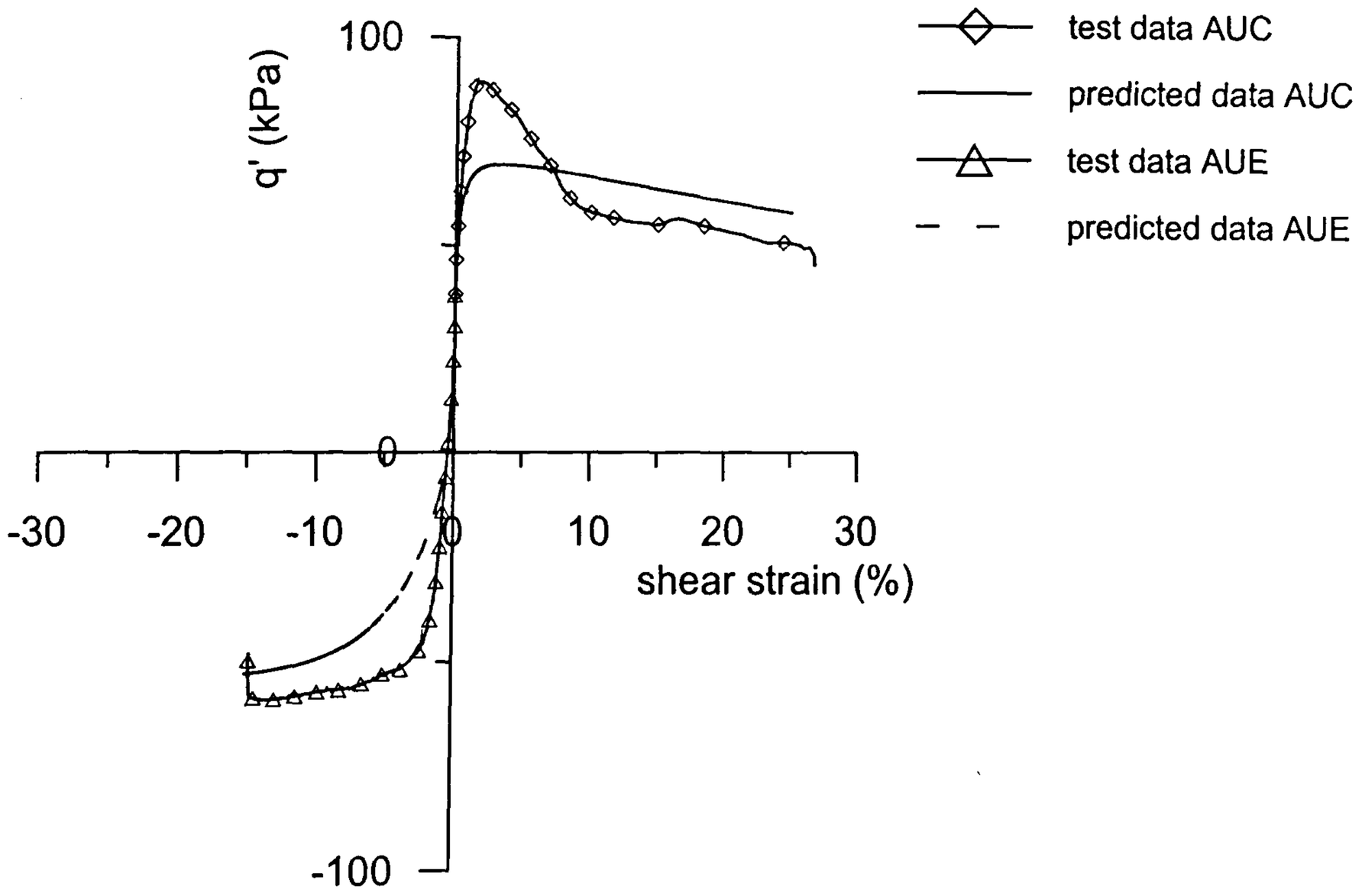

Figure 5.3.43 Comparison between model prediction and experimental results for stress-strain curves obtained from undrained triaxial compression and extension tests AUC and AUE on Pisa clay samples (test data from Callisto, 1996)

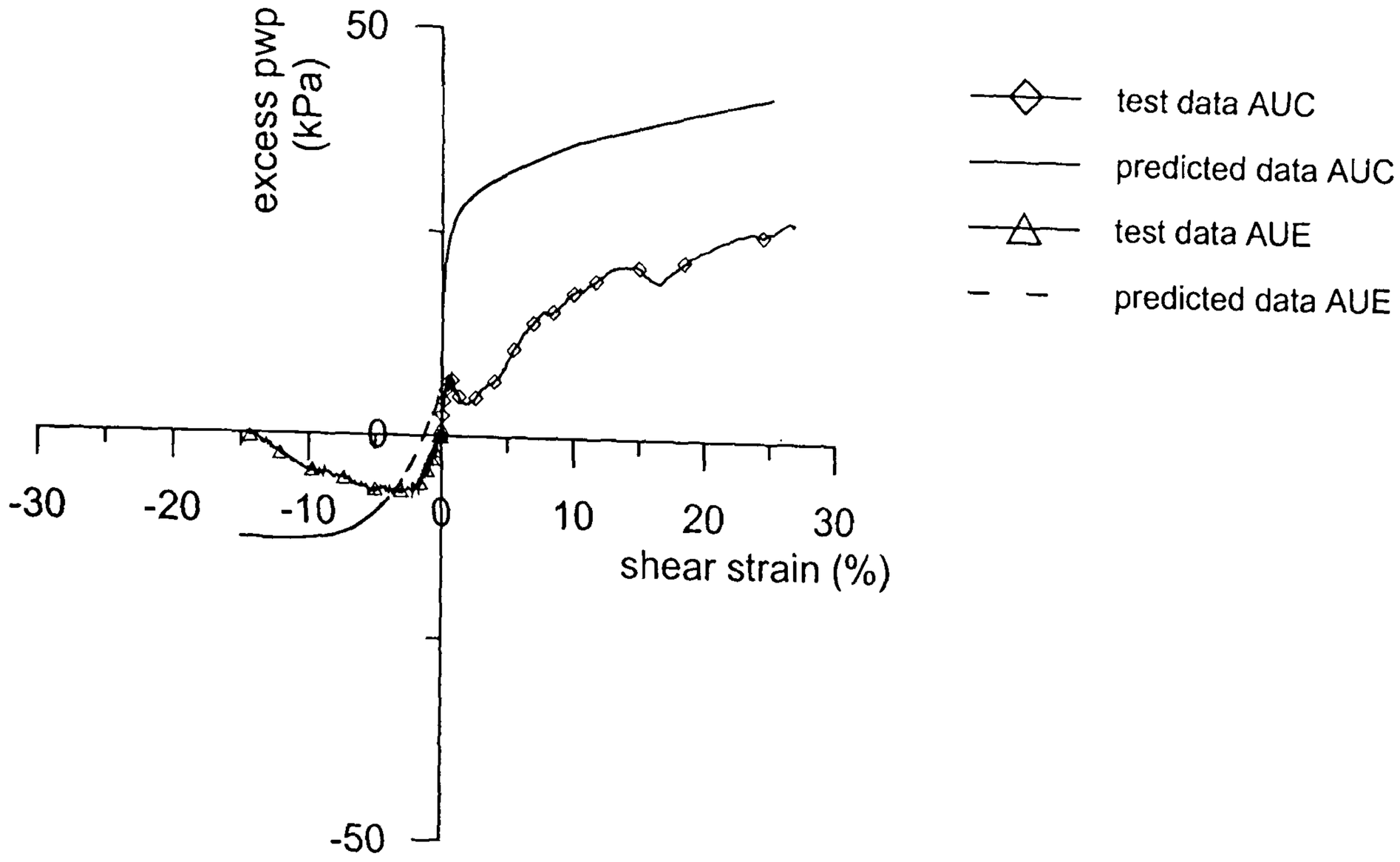

Figure 5.3.44 Comparison between model prediction and experimental results for excess pore water pressure obtained from undrained triaxial compression and extension tests AUC and AUE on Pisa clay samples (test data from Callisto, 1996)

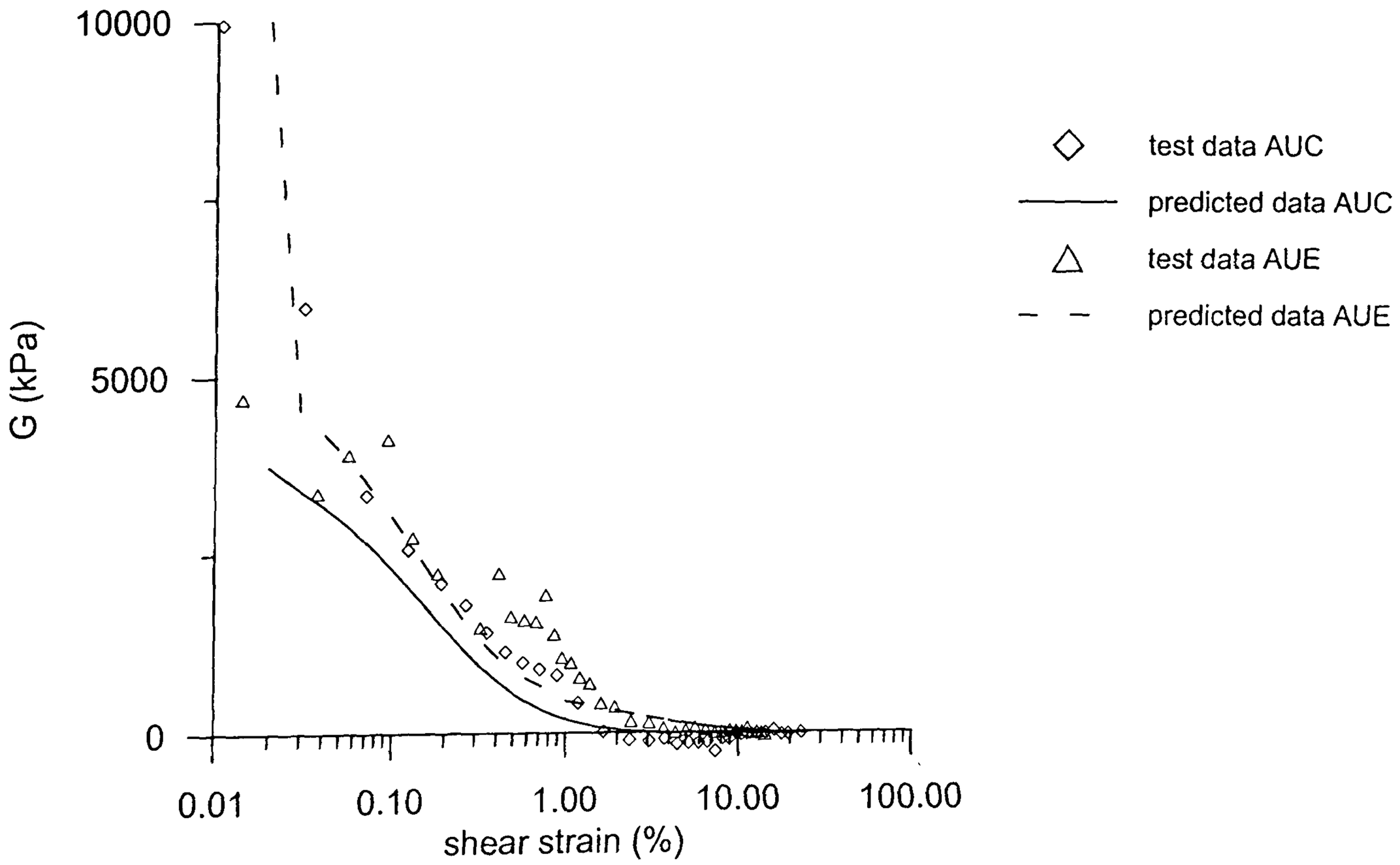

Figure 5.3.45 Comparison between model prediction and experimental results for stiffness curves obtained from undrained triaxial compression and extension tests AUC and AUE on Pisa clay samples (test data from Callisto, 1996)

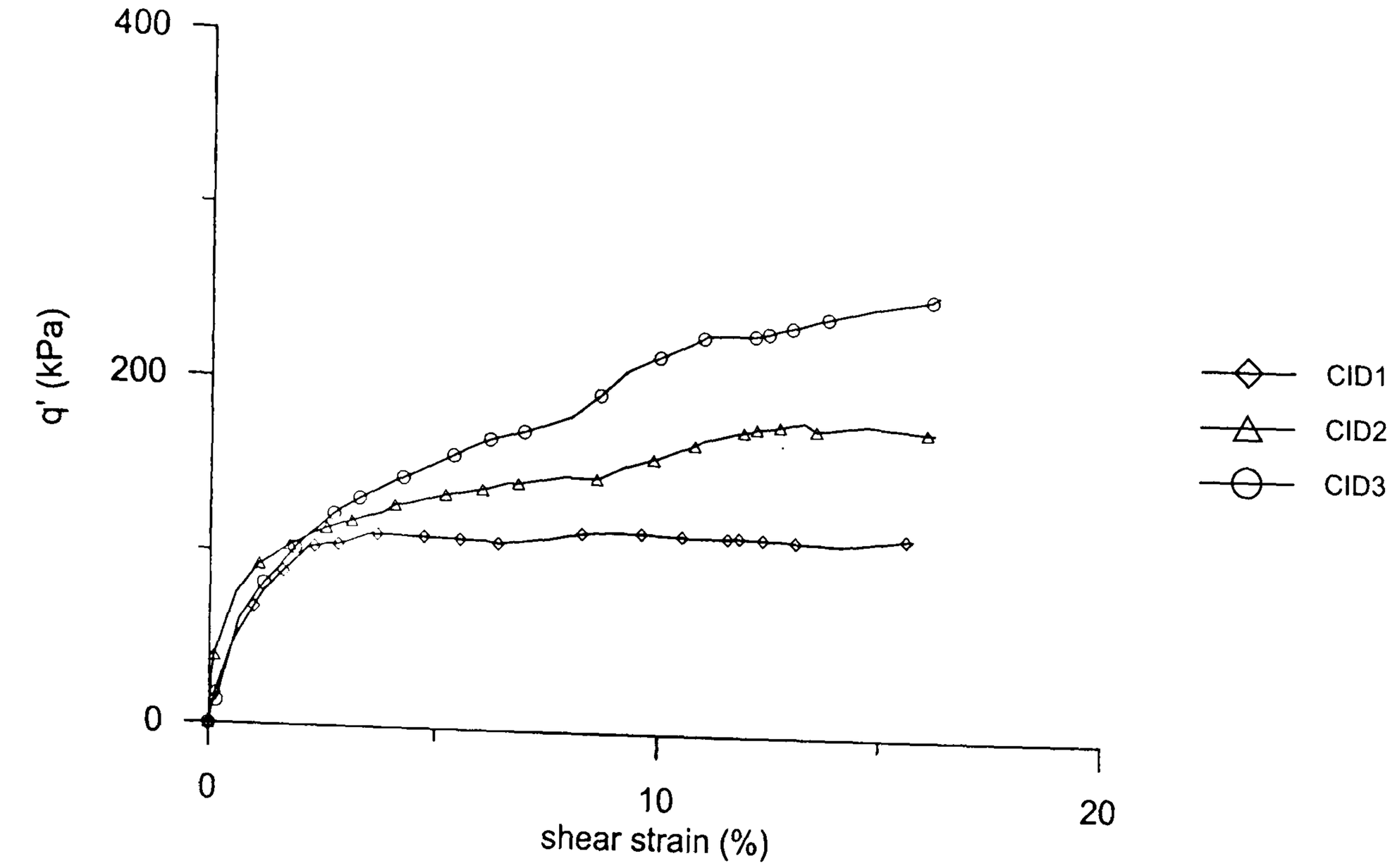

(a)

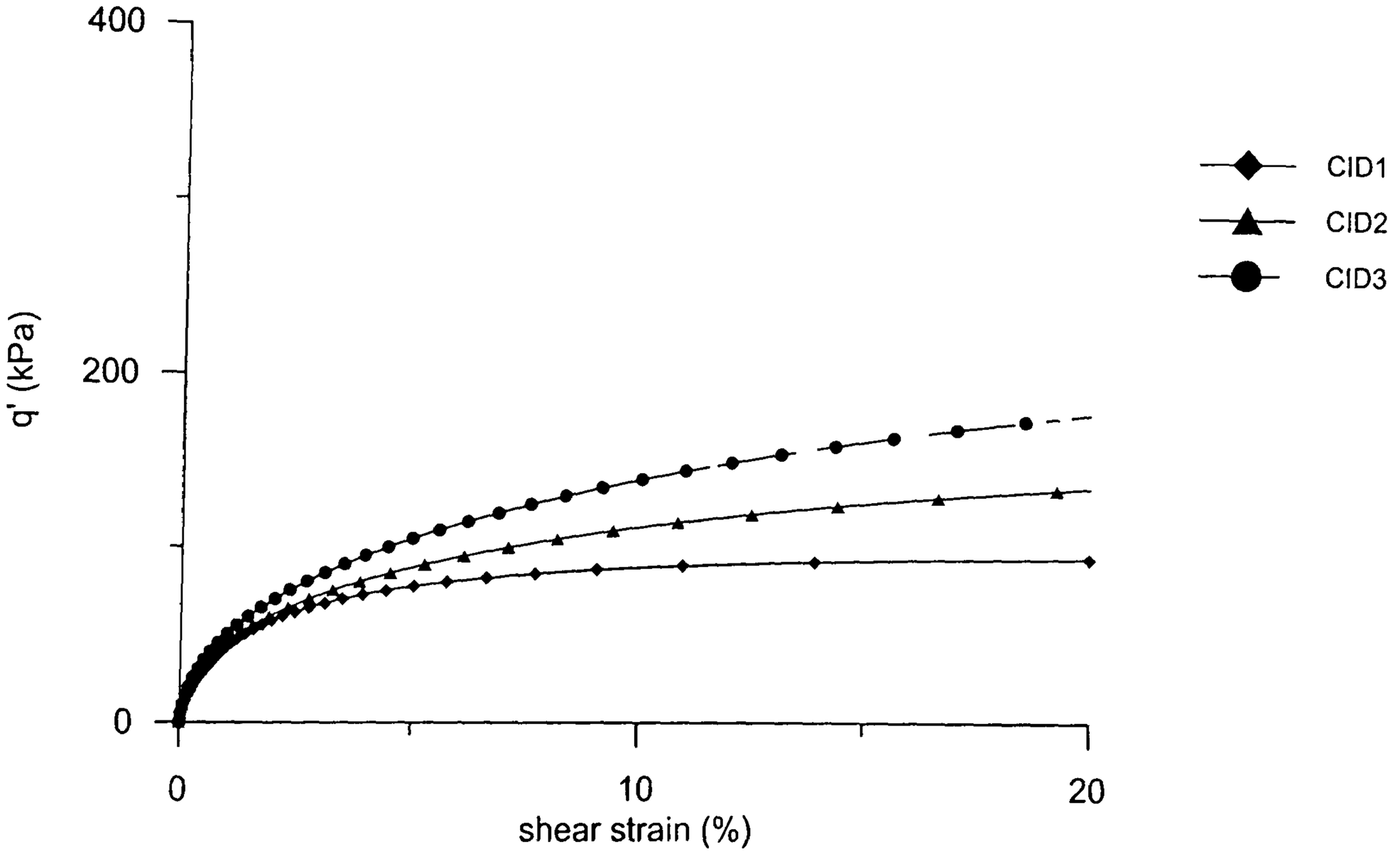

(b)

Figure 5.3.46 Stress-strain response during isotropically consolidated drained tests on Pisa clay samples (a) test data (from Rampello, 1993) (b) model prediction

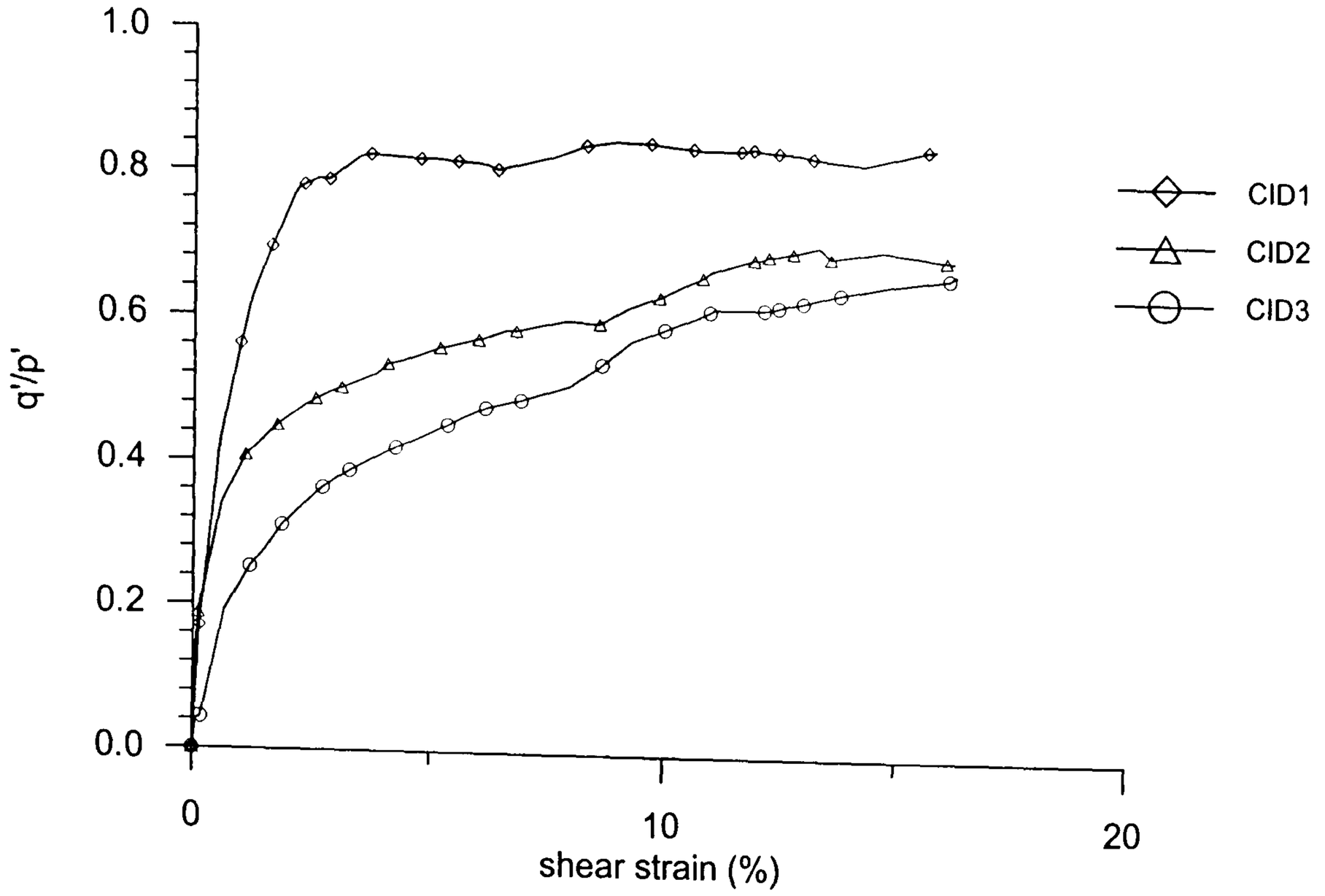

(a)

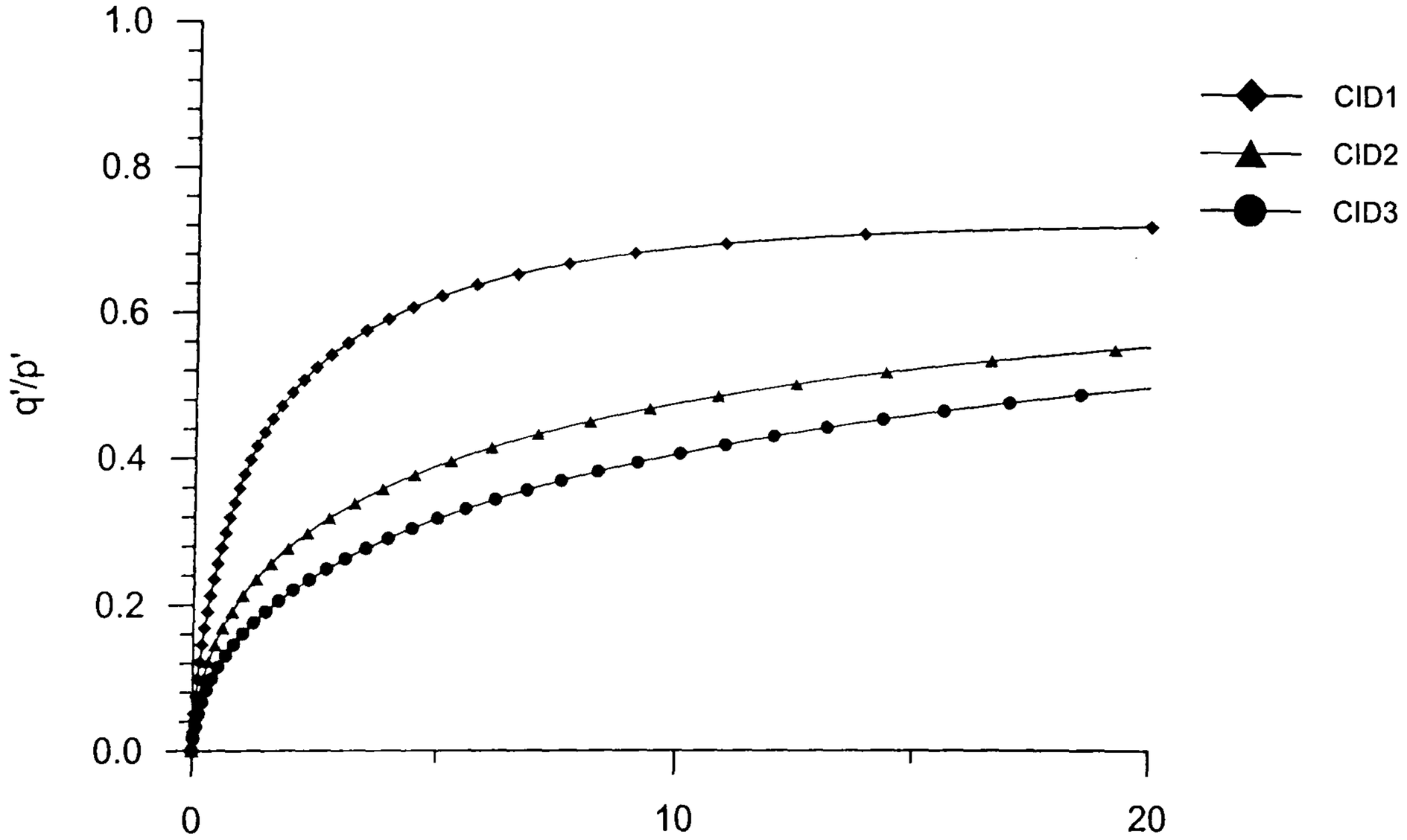

(b)

Figure 5.3.47 Variation of stress ratio with shear strain during isotropically consolidated drained tests on Pisa clay samples (a) test data (from Rampello, 1993) (b) model prediction

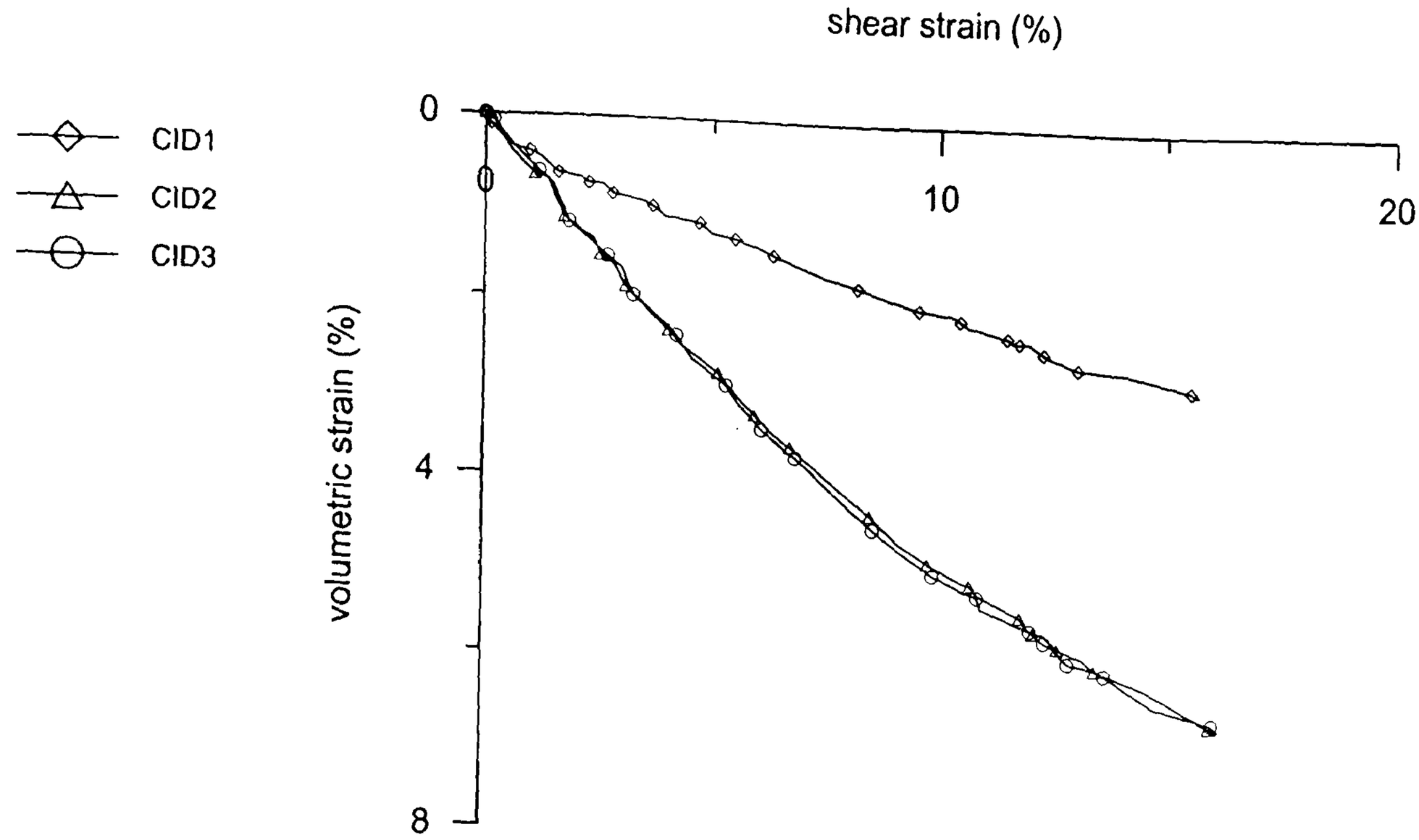

(a)

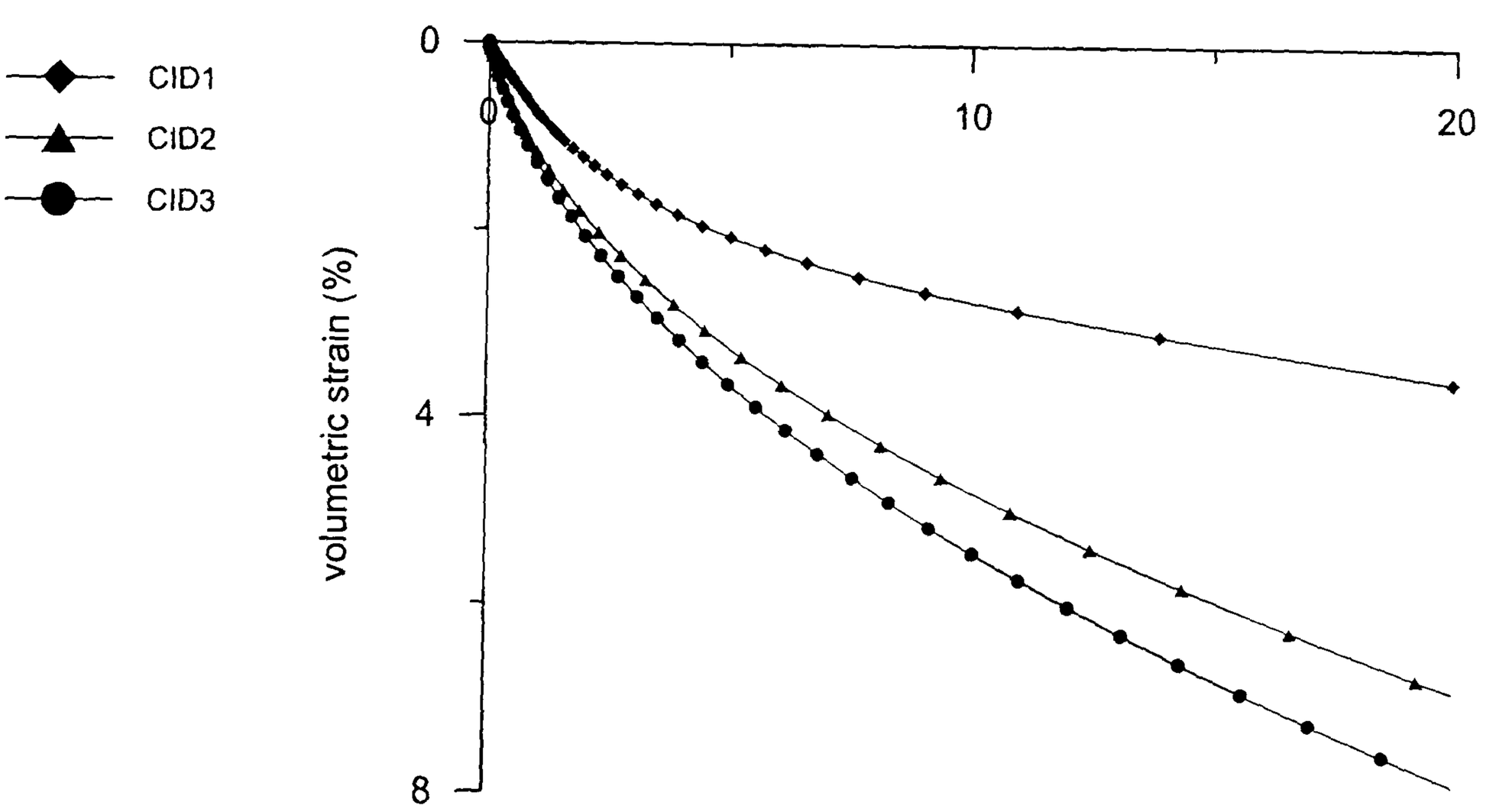

(b)

Figure 5.3.48 Volumetric response during isotropically consolidated drained tests on Pisa clay samples (a) test data (from Rampello, 1993) (b) model prediction

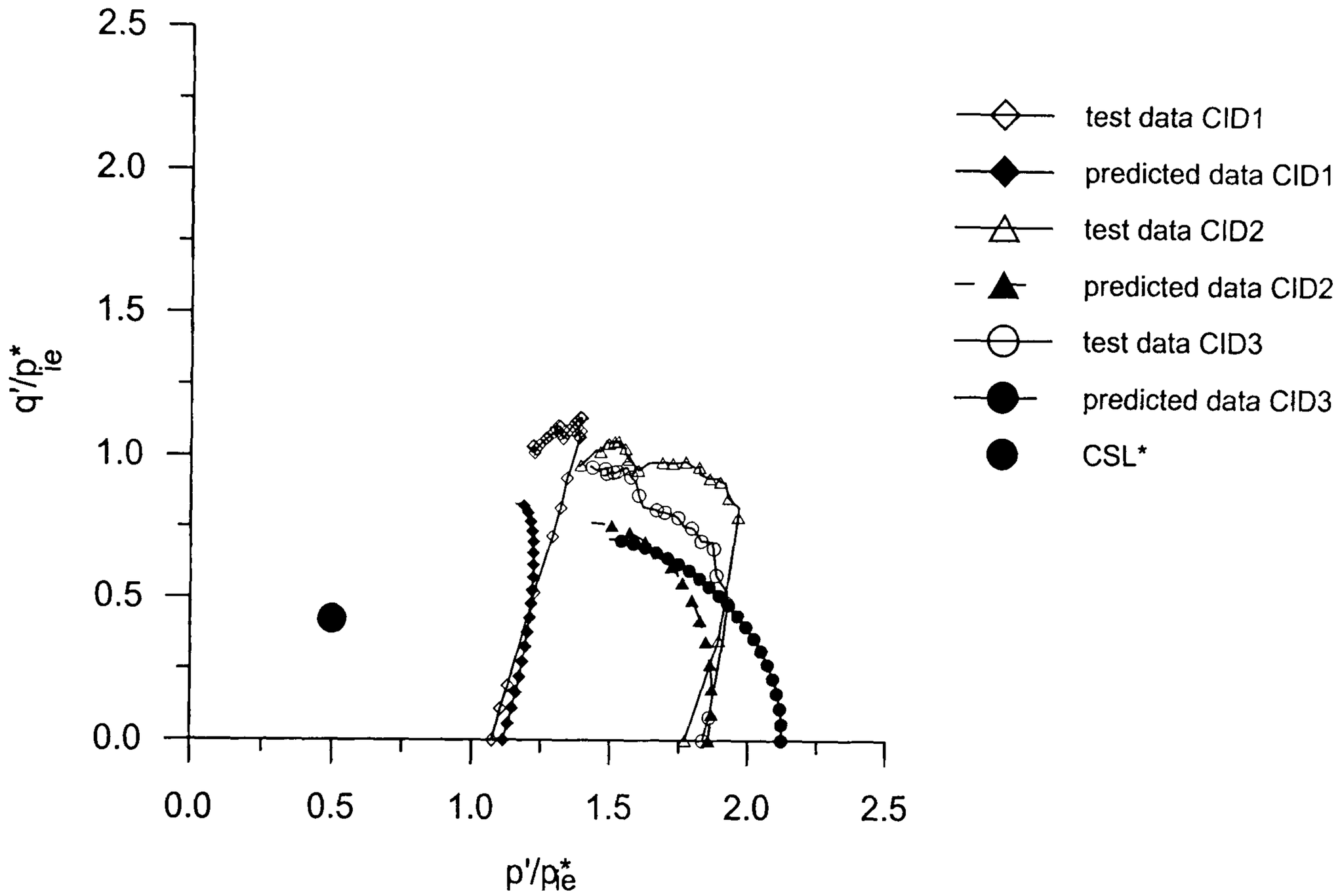

Figure 5.3.49 Comparison between model prediction and experimental results for normalised stress paths obtained from isotropically consolidated drained tests on Pisa clay samples (test data from Rampello, 1993)

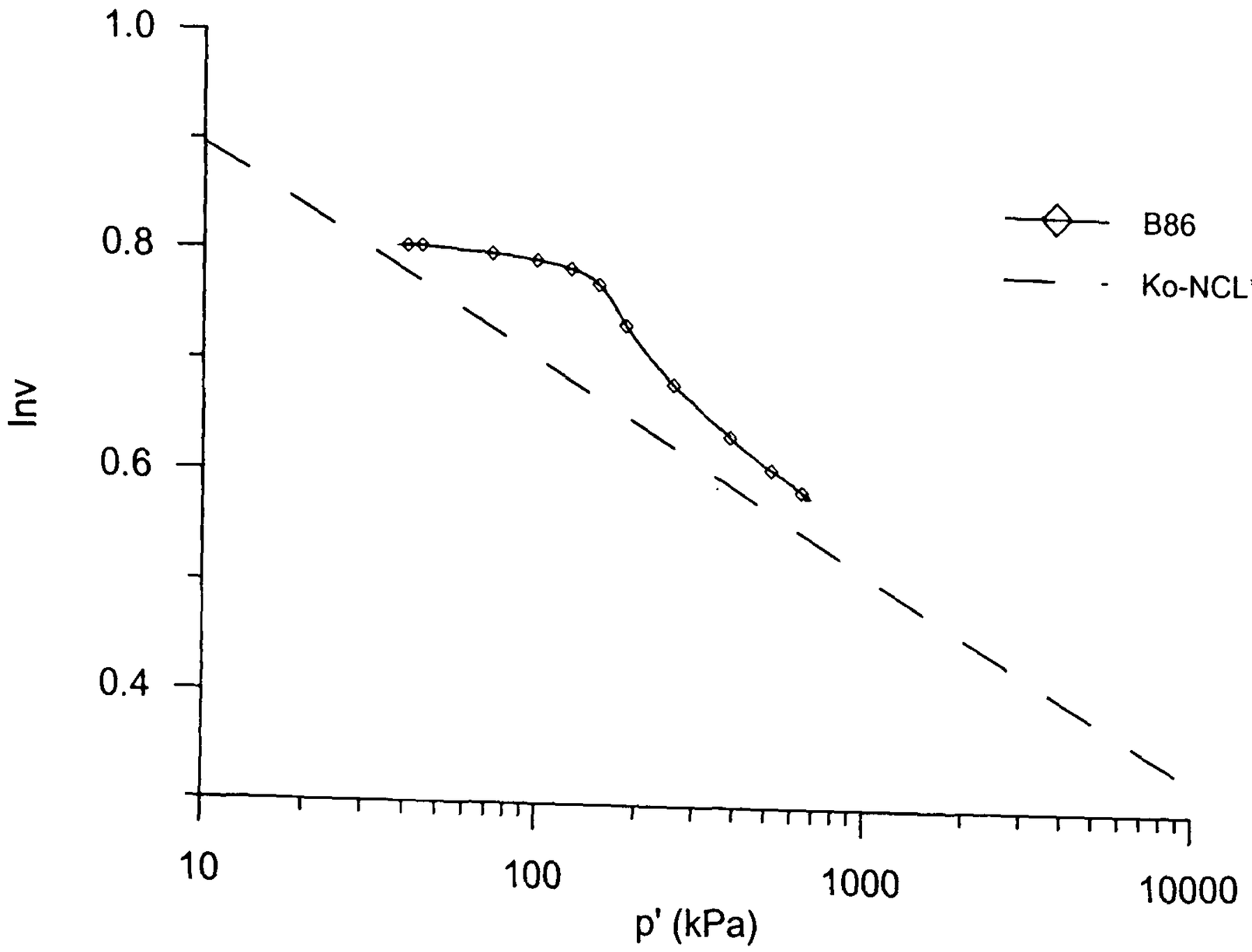

(a)

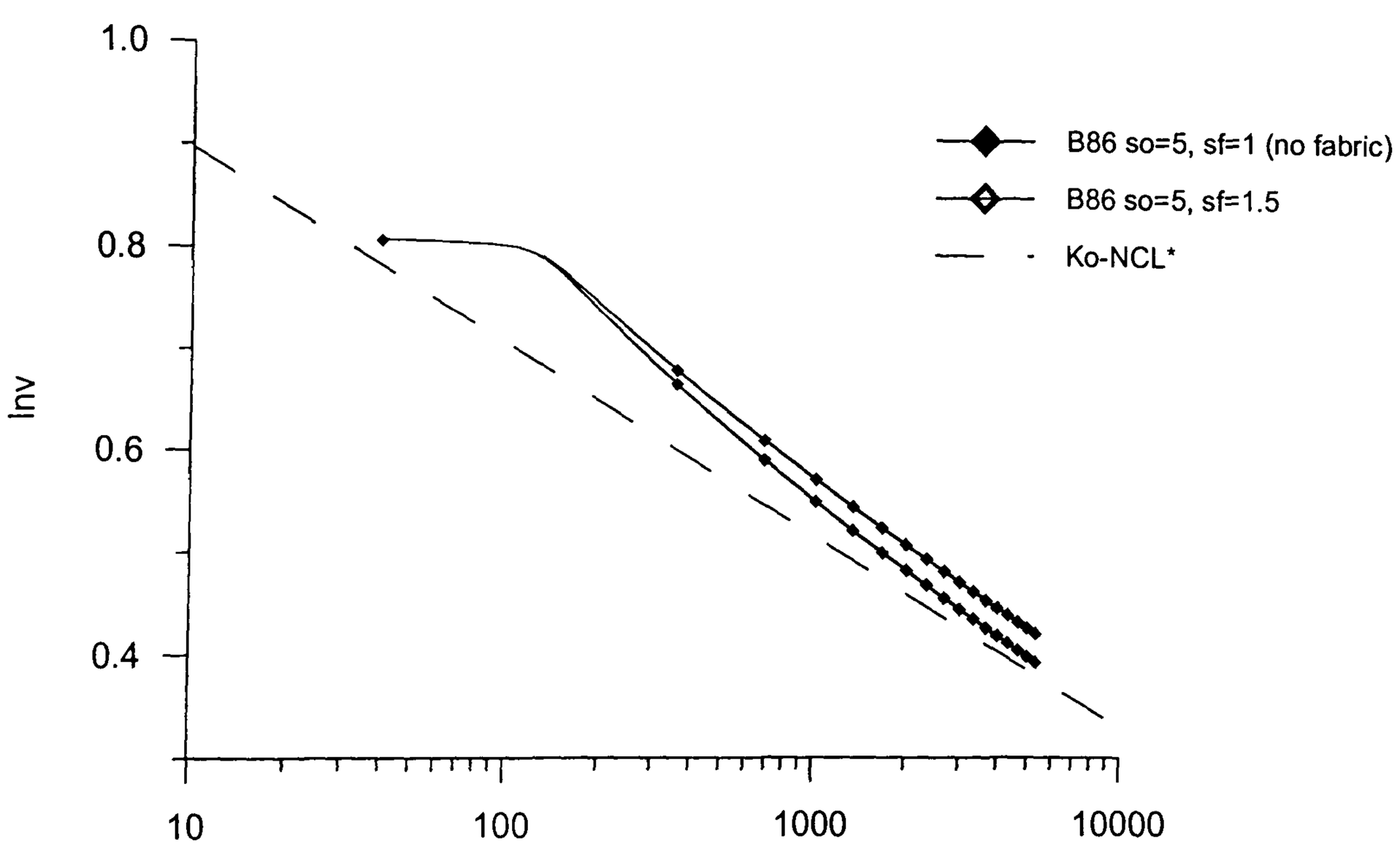

(b)

Figure 5.3.50 Effect of including fabric in analysis simulating one-dimensional compression on Bothkennar clay sample B86 (a) test data (from Allman, 1992) (b) model prediction

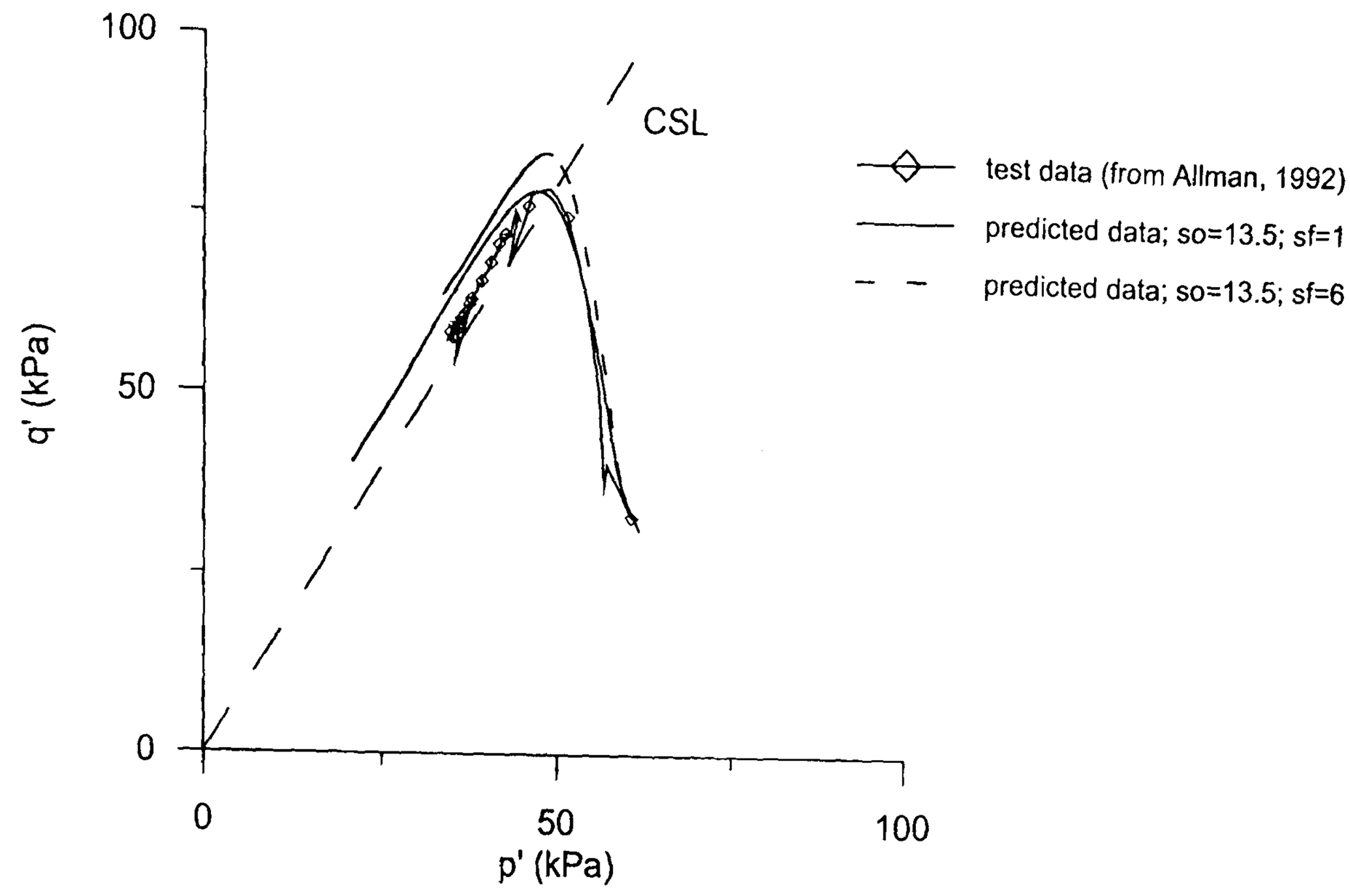

Figure 5.3.51 Effect of including fabric on stress paths obtained from an analysis simulating undrained triaxial compression of Bothkennar clay sample L23 from the bedded facies

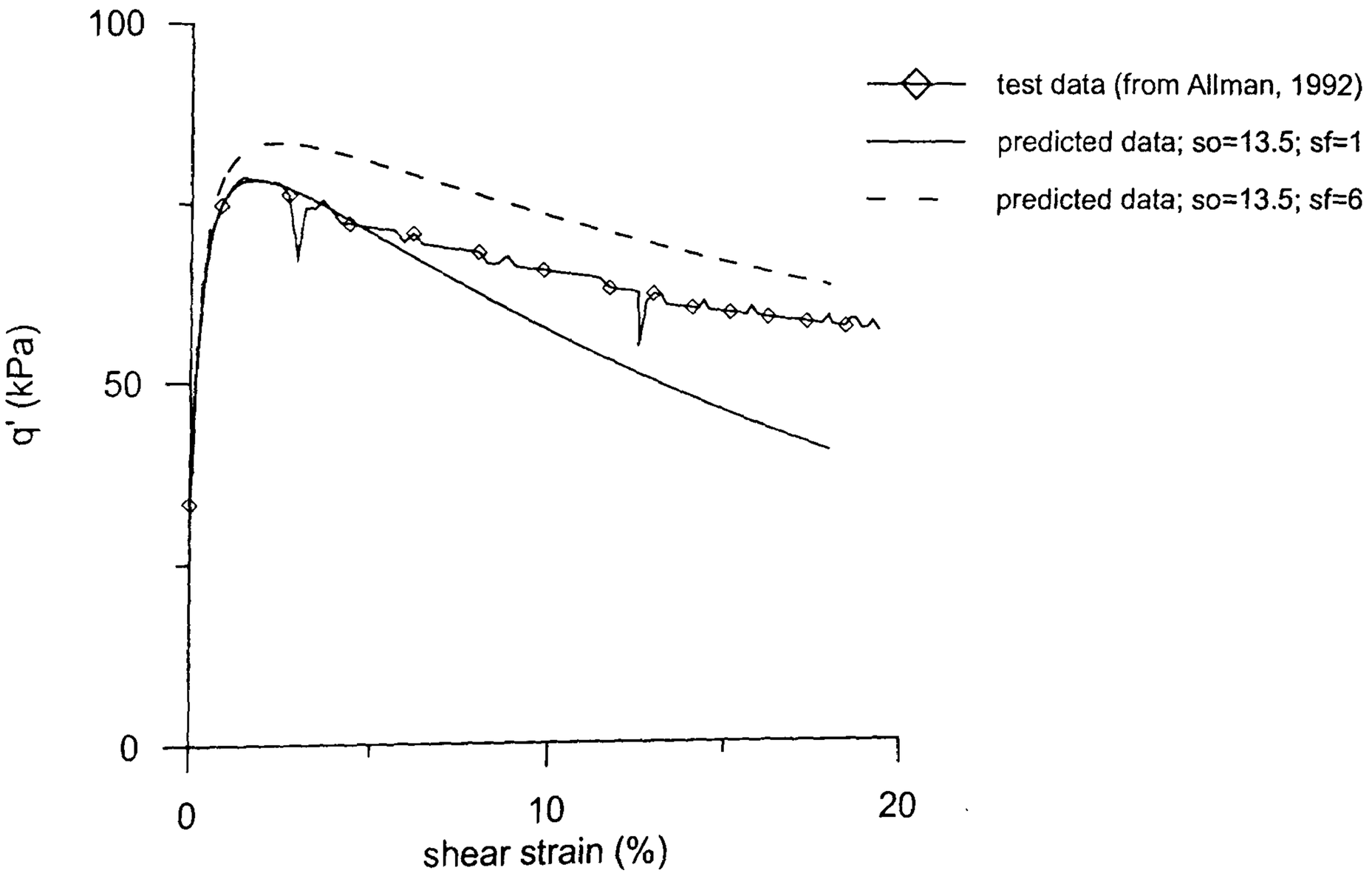

Figure 5.3.52 Effect of including fabric on stress-strain curve obtained from an analysis simulating undrained triaxial compression of Bothkennar clay sample L23 from the bedded facies

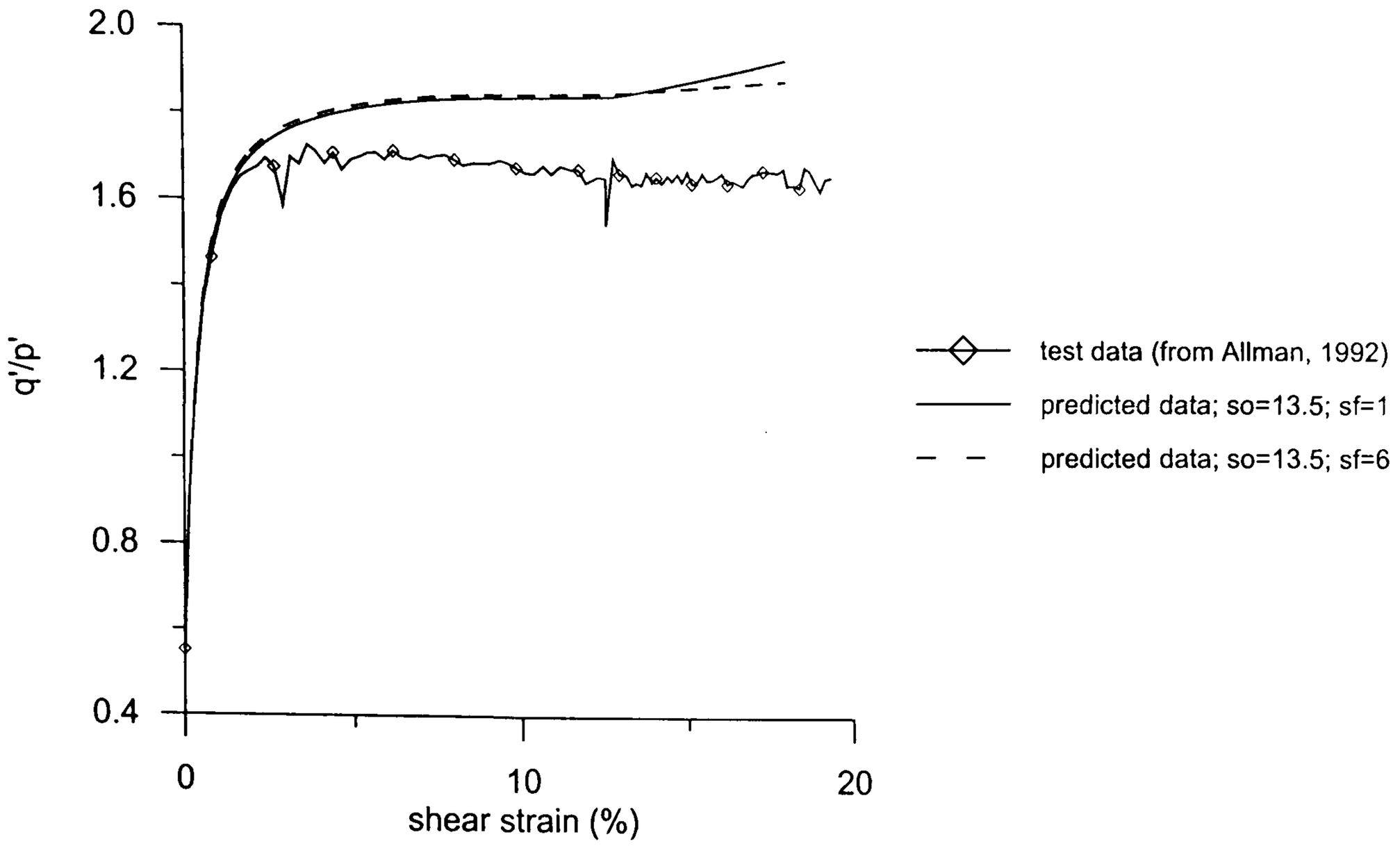

Figure 5.3.53 Effect of including fabric on variation in stress ratio with shear strain obtained from analysis simulating undrained triaxial compression on Bothkennar clay sample L23 from the bedded facies

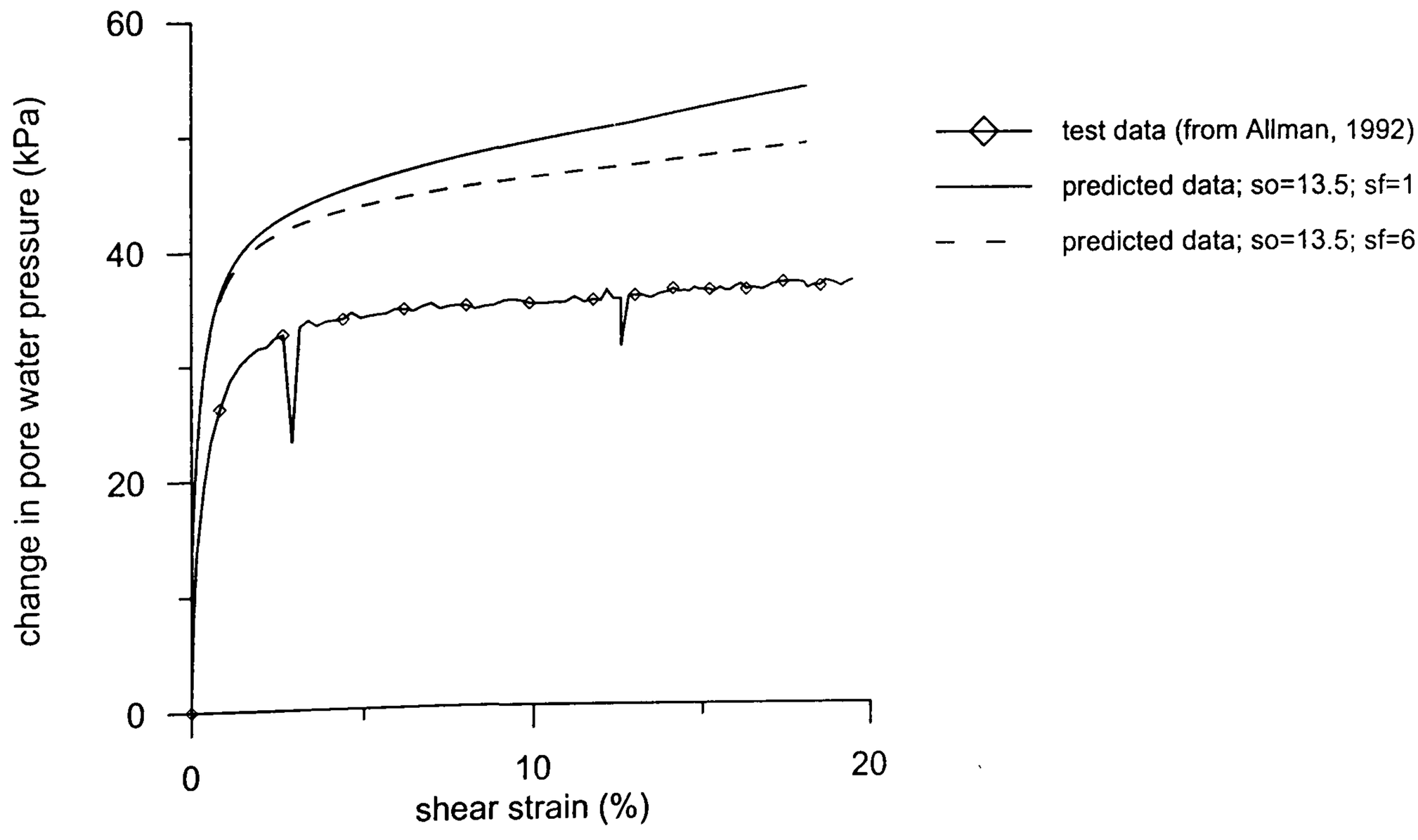

Figure 5.3.54 Effect of including fabric on change in excess pore pressure obtained from analysis simulating undrained triaxial compression on Bothkennar clay sample L23 from the bedded facies